EVALUATION OF PROBING TOOLS IMPLEMENTED IN CAMx

CRC Project A-37-1

Prepared by

Yang Zhang, Krish Vijayaraghavan and Christian Seigneur
Atmospheric & Environmental Research, Inc.
2682 Bishop Drive, Suite 120, San Ramon, CA 94583

Gail Tonnesen
University of California at Riverside, Riverside, CA.

Document Number CP099-1-2
August 2002

Prepared for
Coordinating Research Council, Inc.
Alpharetta, Georgia

TABLE OF CONTENTS

Executive Summary E-1

E.1 Background E-1

E.2 Consistency between DDM and OSAT E-3

E.3 Complimentarity among DDM, OSAT and PA E-7

E.4 Stretchability E-11

E.5 Comparison of the Results from CRC projects A-29 and A-37 ..... E-12

E.6 Computational Requirements E-14

E.7 Recommendations E-14

Technical Summary T-1

T.1 The Probing Tools T-3

T.2 Consistency T-5

T.3 Complementarity T-16

T.4 Stretchability T-20

T.5 Comparison of the Results from CRC projects A-29 and A-37 ..... T-23

T.6 Computational/Implementation Requirements T-24

1. Introduction 1-1

2. Modeling Domain and Episode 2-1

3. Selection of Receptors 3-1

4. Design of Base and Sensitivity Simulations 4-1

5. Post-Processing of the Simulation Results 5-1

TABLE OF CONTENTS (continued)

6. Evaluation of DDM, OSAT and PA 6-1

6.1 Consistency 6-1

6.1.1 Ranking of O_3 Sensitivities and Contributions 6-3

6.1.1.1 Ranking of DDM Sensitivities with Respect to NO_x and VOC Emissions from 11 Core Source Areas 6-5

6.1.1.2 Comparison of the DDM and OSAT Rankings of O_3 Contributors from the 11 Core Source Areas 6-30

6.1.1.3 Ranking of DDM Sensitivities with Respect to Total NO_x and VOC Emissions from Six Boundary Source Areas 6-54

6.1.1.4 Comparison of the DDM and OSAT Rankings of O_3 Contributors from the Six Boundary Source Areas 6-58

6.1.2 NO_x- or VOC-sensitivity 6-58

6.1.2.1 Spatial Distribution of NO_x- or VOC-Sensitivity of O_3 Chemistry 6-71

6.1.2.2 Comparison of the NO_x- or VOC-Sensitivity Predicted at Four Receptors by DDM and OSAT 6-78

6.1.2.3 Comparison of NO_x- or VOC-sensitivity Predicted at the Four Receptors by PA, DDM, and PA 6-91

6.1.3 Photochemical reactivity of VOCs 6-99

6.1.3.1 Comparison Between the Incremental Reactivity from DDM and the O_3 Productivity from OSAT 6-105

TABLE OF CONTENTS (continued)

6.2 Complementarity 6-114

6.2.1 Source Apportionment 6-114

6.2.1.1 Domain-wide O_3 Sensitivities and Source Contributions from Four Source Categories 6-116

6.2.1.2 Receptor-Wide O_3 Sensitivities and Source Contributions from Four Source Categories 6-123

6.2.1.3 The Relationship Between DDM Sensitivities and OSAT Source Contributions 6-127

6.2.1.4 Comparisons with OSAT-DDM relationship predicted by CRC Project A-29 6-139

6.2.2 Relative Importance of Chemistry and Transport 6-141

6.2.3 Detailed Chemical Analysis 6-162

6.2.4 Model Responses to Changes in ICs, BCs, and Emissions 6-178

6.2.5 Other differences among the three probing tools 6-179

6.3 Stretchability 6-180

6.3.1 Accuracy of DDM and OSAT Results under Small and Large Perturbations 6-181

6.3.1.1 O_3 Concentrations Predicted by the DDM Sensitivities under Different Emission Scenarios 6-181

6.3.1.2 Validity of the OSAT Source Attribution Results under Different Emission Scenarios 6-187

6.3.2 Consistency in Predicting NO_x- vs. VOC-sensitivity under Different Emission Reduction Scenarios 6-203

6.3.3 Changes in Chemical Signatures in the Four Receptors under a 75% Reduction in Anthropogenic NO_x Emissions 6-213

6.4 Computational/Implementation Requirements 6-218

7. References 7-1

LIST OF TABLES

Table 1-1. Chemical process analysis outputs in CAMx for the CBM-IV mechanism 1-5

Table 4-1. Description of base and sensitivity simulations with CAMx and probing tools. 4-2

Table 6-1. The top 10 O_3 sensitivities by source area and by source group for stratified 1-hr O_3 levels for the whole receptor region in Atlanta. 6-6

Table 6-2. The top 10 O_3 sensitivities by source area and by source group for stratified 8-hr O_3 levels for the whole receptor region in Atlanta. 6-7

Table 6-3. The top 2 contributors to O_3 formation by source area and by source group predicted by DDM for stratified 1-hr O_3 levels for 9 subareas in Atlanta. 6-10

Table 6-4. The top 2 contributors to O_3 formation by source area and by source group predicted by DDM for stratified 8-hr O_3 levels for 9 subareas in Atlanta. 6-11

Table 6-5. The top 10 O_3 sensitivities by source area and by source group for stratified 1-hr O_3 levels for the whole receptor region in Chicago. 6-13

Table 6-6. The top 10 O_3 sensitivities by source area and by source group for stratified 8-hr O_3 levels for the whole receptor region in Chicago. 6-14

Table 6-7. The top 2 contributors to O_3 formation by source area and by source group predicted by DDM for stratified 1-hr O_3 levels for 9 subareas in Chicago. 6-15

Table 6-8. The top 2 contributors to O_3 formation by source area and by source group predicted by DDM for stratified 8-hr O_3 levels for 9 subareas in Chicago. 6-16

Table 6-9. The top 10 O_3 sensitivities by source area and by source group for stratified 1-hr O_3 levels for the whole receptor region in New York City. 6-19

Table 6-10. The top 10 O_3 sensitivities by source area and by source group for stratified 8-hr O_3 levels for the whole receptor region in New York City.

.....6-20
Table 6-11. The top 2 contributors to O_3 formation by source area and by source group predicted by DDM for stratified 1-hr O_3 levels for 9 subareas in New York City.....6-21
Table 6-12. The top 2 contributors to O_3 formation by source area and by source group predicted by DDM for stratified 8-hr O_3 levels for 9 subareas in New York City.....6-22
Table 6-13. The top 10 O_3 sensitivities by source area and by source group for stratified 1-hr O_3 levels for the whole receptor region in Altoona. 6-26
Table 6-14. The top 10 O_3 sensitivities by source area and by source group for stratified 8-hr O_3 levels for the whole receptor region in Altoona. 6-27
Table 6-15. The top 2 contributors to O_3 formation by source area and by source group predicted by DDM for stratified 1-hr O_3 levels for 9 subareas in Altoona. 6-28
Table 6-16. The top 2 contributors to O_3 formation by source area and by source group predicted by DDM for stratified 8-hr O_3 levels for 9 subareas in Altoona. 6-29
Table 6-17. The top 10 O_3 contributors by source area and by source group predicted by OSAT for stratified 1-hr O_3 levels for the whole receptor region in Atlanta. 6-34
Table 6-18. The top 10 O_3 contributors by source area and by source group predicted by OSAT for stratified 8-hr O_3 levels for the whole receptor region in Atlanta. 6-35
Table 6-19. The top 2 contributors to O_3 concentrations by source area and by source group predicted by OSAT for stratified 1-hr O_3 levels for 9 subareas in Atlanta. 6-36
Table 6-20. The top 2 contributors to O_3 concentrations by source area and by source group predicted by OSAT for stratified 8-hr O_3 levels for subareas in Atlanta. 6-37

Table 6-21. The top 10 O_3 contributors by source area and by source group predicted by OSAT for stratified 1-hr O_3 levels for the whole receptor region in Chicago..... 6-39
Table 6-22. The top 10 O_3 contributors by source area and by source group predicted by OSAT for stratified 8-hr O_3 levels for the whole receptor region in Chicago..... 6-40
Table 6-23. The top 2 contributors to O_3 concentrations by source area and by source group predicted by OSAT for stratified 1-hr O_3 levels for 9 subareas in Chicago..... 6-41
Table 6-24. The top 2 contributors to O_3 concentrations by source area and by source group predicted by OSAT for stratified 8-hr O_3 levels for 9 subareas in Chicago..... 6-42
Table 6-25. The top 10 O_3 contributors by source area and by source group predicted by OSAT for stratified 1-hr O_3 levels for the whole receptor region in New York City..... 6-45
Table 6-26. The top 10 O_3 contributors by source area and by source group predicted by OSAT for stratified 8-hr O_3 levels for the whole receptor region in New York City..... 6-46
Table 6-27. The top 2 contributors to O_3 concentrations by source area and by source group predicted by OSAT for stratified 1-hr O_3 levels for 9 subareas in New York City..... 6-47
Table 6-28. The top 2 contributors to O_3 concentrations by source area and by source group predicted by OSAT for stratified 8-hr O_3 levels for 9 subareas in New York City..... 6-48
Table 6-29. The top 10 O_3 contributors by source area and by source group predicted by OSAT for stratified 1-hr O_3 levels for the whole receptor region in Altoona..... 6-50
Table 6-30. The top 10 O_3 contributors by source area and by source group predicted by OSAT for stratified 8-hr O_3 levels for the whole receptor region in Altoona..... 6-51

Table 6-31. The top 2 contributors to O_3 concentrations by source area and by source group predicted by OSAT for stratified 1-hr O_3 levels for 9 subareas in Altoona. 6-52
Table 6-32. The top 2 contributors to O_3 concentrations by source area and by source group predicted by OSAT for stratified 8-hr O_3 levels for 9 subareas in Altoona. 6-53
Table 6-33. The top 2 O_3 sensitivities by source area to the total NO_x and VOC emissions from the 6 boundary source areas predicted by DDM for stratified 1-hr O_3 levels in Atlanta, Chicago, New York City, and Altoona. 6-55
Table 6-34. The top 2 O_3 sensitivities by source area to the total NO_x and VOC emissions from the 6 boundary source areas predicted by DDM for stratified 8-hr O_3 levels in Atlanta, Chicago, New York City, and Altoona. 6-56
Table 6-35. The top 2 O_3 contributors by source area from the total NO_x and VOC emissions from the 6 boundary source areas predicted by OSAT for stratified 1-hr O_3 levels in Atlanta, Chicago, New York City, and Altoona. 6-59
Table 6-36. The top 2 O_3 contributors by source area from the total NO_x and VOC emissions from the 6 boundary source areas predicted by OSAT for stratified 8-hr O_3 levels in Atlanta, Chicago, New York City, and Altoona. 6-60
Table 6-37. NO_x- vs. VOC-limited O_3 concentration in 9 subareas in Atlanta predicted by DDM and OSAT under the EPA 2007 base emission scenario..... 6-79
Table 6-38. NO_x- vs. VOC-limited O_3 concentration in 9 subareas in Chicago predicted by DDM and OSAT under the EPA 2007 base emission scenario..... 6-80
Table 6-39. NO_x- vs. VOC-limited O_3 concentration in 9 subareas in New York City predicted by DDM and OSAT under the EPA 2007 base emission scenario..... 6-81

Table 6-40. NO_x- vs. VOC-limited O_3 concentration in 9 subareas in Altoona predicted by DDM and OSAT under the EPA 2007 base emission scenario..... 6-82

Table 6-41. NO_x- vs. VOC-limited O_3 concentration at four receptors predicted by DDM and OSAT under the EPA 2007 base emission scenario. 6-84

Table 6-42. O_3 sensitivities to contributions of NO_x and VOC emissions from 6 most influential source areas at peak hourly O_3 time in New York City. 6-87

Table 6-43. O_x production sensitivity to precursors at four receptors predicted by PA under the EPA 2007 base emission scenario. The sensitivity was determined using the ratio of $P(H_2O_2)/P(HNO_3)$. 6-92

Table 6-44. The technical capabilities of DDM, OSAT, and PA implemented in CAMx..... 6-115

Table 6-45. NO_x- vs. VOC-limited O_3 concentration at four receptors predicted by DDM and OSAT under the 25% anthropogenic VOC emission reduction scenario..... 6-204

Table 6-46. NO_x- vs. VOC-limited O_3 concentration at four receptors predicted by DDM and OSAT under the 25% anthropogenic NO_x emission reduction scenario..... 6-205

Table 6-47. NO_x- vs. VOC-limited O_3 concentration at four receptors predicted by DDM and OSAT under the 75% anthropogenic NO_x emission reduction scenario..... 6-206

Table 6-48. O_x production sensitivity to precursors at four receptors predicted by PA under 75% anthropogenic NO_x emission reduction scenario. The sensitivity was determined using the ratio of $P(H_2O_2)/P(HNO_3)$. 6-209

Table 6-49. Process analysis outputs at four receptors on July 14 under the EPA 2007 base emission scenario (PA base run B4) and the 75% anthropogenic NO_x emission reduction scenario (PA sensitivity run S9). 6-214/215

Table 6-50. The memory and computational requirements for CAMx base model and CAMx with a probing tool. 6-219

LIST OF FIGURES

Figure T-1. Overview of technical components for evaluation of probing tools..... T-2

Figure T-2. The geographic source areas for application of OSAT and DDM probing tools in the OTAG modeling domain..... T-6

Figure 1-1. Process diagram illustrating important diagnostics for characterizing photochemical production of O_3..... 1-3

Figure 2-1. The geographic source areas for application of OSAT and DDM probing tools in the OTAG modeling domain..... 2-2

Figure 5-1. Nine subareas in the receptor region defined for data analyses. The subarea indices start from the NW corner of each receptor and proceed row-wise. Each subarea consists of 9 fine grid cells..... 5-3

Figure 6-1. Overview of technical components for evaluation of probing tools..... 6-2

Figure 6-2. The agreeable number of O_3 contributors between the DDM and OSAT rankings by source area in the top 10 contributors for (a) 1-hr and (b) 8-hr stratified O_3 concentration levels at four receptors under the EPA 2007 base emission scenario (DDM base runs B2 and OSAT base run B1).. 6-31

Figure 6-3. The agreeable number of O_3 contributors between the DDM and OSAT rankings by source group in the top 10 contributors for (a) 1-hr and (b) 8-hr stratified O_3 concentration levels at four receptors under the EPA 2007 base emission scenario (DDM base runs B2 and OSAT base run B1).. 6-32

Figure 6-4. The spatial distribution of the differences in (a) the O_3 sensitivities to total NO_x and VOC predicted by DDM at 2 p.m. on July 11, (b) the O_3 contributions from total NO_x and VOC predicted by OSAT at 2 p.m. on July 11, and (c) the accumulative daily total Ox production under NO_x- and VOC-limited conditions predicted by PA on July 11. All results were obtained under the EPA 2007 base emission scenario (DDM base run B7, OSAT base run B1, and PA base run B4)..... 6-72

Figure 6-5. The spatial distribution of the differences in (a) the O_3 sensitivities to total NO_x and VOC predicted by DDM at 2 p.m. on July 12, (b) the O_3 contributions from total NO_x and VOC predicted by OSAT at 2 p.m. on

July 12, and (c) the accumulative daily total O_x production under NO_x- and VOC-limited conditions predicted by PA on July 12. All results were obtained under the EPA 2007 base emission scenario (DDM base run B7, OSAT base run B1, and PA base run B4). 6-73

Figure 6-6. The spatial distribution of the differences in (a) the O_3 sensitivities to total NO_x and VOC predicted by DDM at 2 p.m. on July 13, (b) the O_3 contributions from total NO_x and VOC predicted by OSAT at 2 p.m. on July 13, and (c) the accumulative daily total O_x production under NO_x- and VOC-limited conditions predicted by PA on July 13. All results were obtained under the EPA 2007 base emission scenario (DDM base run B7, OSAT base run B1, and PA base run B4). 6-74

Figure 6-7. The spatial distribution of the differences in (a) the O_3 sensitivities to total NO_x and VOC predicted by DDM at 2 p.m. on July 14, (b) the O_3 contributions from total NO_x and VOC predicted by OSAT at 2 p.m. on July 14, and (c) the accumulative daily total O_x production under NO_x- and VOC-limited conditions predicted by PA on July 14. All results were obtained under the EPA 2007 base emission scenario (DDM base run B7, OSAT base run B1, and PA base run B4). 6-75

Figure 6-8. The spatial distribution of the differences in (a) the O_3 sensitivities to total NO_x and VOC predicted by DDM at 2 p.m. on July 15, (b) the O_3 contributions from total NO_x and VOC predicted by OSAT at 2 p.m. on July 15, and (c) the accumulative daily total O_x production under NO_x- and VOC-limited conditions predicted by PA on July 15. All results were obtained under the EPA 2007 base emission scenario (DDM base run B7, OSAT base run B1, and PA base run B4). 6-76

Figure 6-9. A correlation between the VOC-limited fractions of O_3 concentrations predicted by DDM and the differences in the predicted VOC-limited fractions of O_3 concentrations by DDM and OSAT in New York City under the EPA 2007 base emission scenario (DDM base run B2 and OSAT base run B1). 6-90

Figure 6-10. The receptor average O_x production in VOC-sensitive (top) and NO_x-sensitive (bottom) regimes for layers 1 to 4 in Atlanta on July 14 (a total O_x production up to 16:00 EST) under the EPA 2007 base emission scenario (PA base run B4). The VOC-sensitive plot includes O_x produced for equally-sensitive conditions. 6-95

Figure 6-11. The receptor average O_x production in VOC-sensitive (top) and NO_x-sensitive (bottom) regimes for layers 1 to 4 in Chicago on July 14 (a total O_x production up to 16:00 EST) under the EPA 2007 base emission scenario (PA base run B4). The VOC-sensitive plot includes O_x produced for equally-sensitive conditions. 6-96

Figure 6-12. The receptor average O_x production in VOC-sensitive (top) and NO_x-sensitive (bottom) regimes for layers 1 to 4 in New York City on July 14 (a total O_x production up to 16:00 EST) under the EPA 2007 base emission scenario (PA base run B4). The VOC-sensitive plot includes O_x produced for equally-sensitive conditions. 6-97

Figure 6-13. The receptor average O_x production in VOC-sensitive (top) and NO_x-sensitive (bottom) regimes for layers 1 to 4 in Altoona on July 14 (a total O_x production up to 16:00 EST) under the EPA 2007 base emission scenario (PA base run B4). The VOC-sensitive plot includes O_x produced for equally-sensitive conditions. 6-98

Figure 6-14. The top 5 incremental reactivities and O_3 productivities of VOC emission groups derived from the DDM and OSAT results at the time of peak O_3 concentration on July 11-15, 1995 in Atlanta under the EPA 2007 base emission scenario (DDM base run B2 and OSAT base run B1). 6-106

Figure 6-15. The top 5 incremental reactivities and O_3 productivities of VOC emission groups derived from the DDM and OSAT results at the time of peak O_3 concentration on July 11-15, 1995 in Chicago under the EPA 2007 base emission scenario (DDM base run B2 and OSAT base run B1). 6-107

Figure 6-16. The top 5 incremental reactivities and O_3 productivities of VOC emission groups derived from the DDM and OSAT results at the time of peak O_3

concentration on July 11-15, 1995 in New York City under the EPA 2007 base emission scenario (DDM base run B2 and OSAT base run B1).. 6-108

Figure 6-17. The top 5 incremental reactivities and O_3 productivities of VOC emission groups derived from the DDM and OSAT results at the time of peak O_3 concentration on July 11-15, 1995 in Altoona under the EPA 2007 base emission scenario (DDM base run B2 and OSAT base run B1). 6-109

Figure 6-18. The spatial distribution of O_3 sensitivities predicted by DDM at 2 p.m. on July 15 under the EPA 2007 base emission scenario (DDM base run B7) for emissions from (a) biogenic VOC, (b) on-road mobile VOC, (c) other surface anthropogenic VOC, and (d) elevated anthropogenic VOC, (e) biogenic NO_x, (f) on-road mobile NO_x, (g) other surface anthropogenic NO_x, and (h) elevated anthropogenic NO_x. 6-117/118

Figure 6-19. The spatial distribution of O_3 contributions predicted by OSAT at 2 p.m. on July 15 under the EPA 2007 base emission scenario (OSAT base run B1) for emissions from (a) biogenic VOC, (b) on-road mobile VOC, (c) other surface anthropogenic VOC, and (d) elevated anthropogenic VOC, (e) biogenic NO_x, (f) on-road mobile NO_x, (g) other surface anthropogenic NO_x, and (h) elevated anthropogenic NO_x. 6-119/120

Figure 6-20. The O_3 sensitivities to total NO_x and VOC emissions from four source categories, ICs, and BCs predicted by DDM at 3 p.m. on July 15 under the EPA 2007 base emission scenario (DDM base run B7) in (a) Atlanta, (b) Chicago, (c) New York City, and (d) Altoona. 6-124

Figure 6-21. The O_3 contributions of total NO_x and VOC emissions from four source categories, ICs, and BCs predicted by OSAT at 3 p.m. on July 15 under the EPA 2007 base emission scenario (OSAT base run B1) in (a) Atlanta, (b) Chicago, (c) New York City, and (d) Altoona. 6-125

Figure 6-22. The DDM sensitivities versus the OSAT source contributions of VOC emissions from (a) biogenic, (b) on-road mobile, (c) other surface anthropogenic, and (d) elevated anthropogenic sources in Atlanta. The data shown only include the DDM and OSAT results for all fine grid cells

with an O_3 concentration > 80 ppb at 3 p.m. on July 11-15 under the EPA 2007 base emission scenario (DDM base run B7 and OSAT base run B1).. 6-128

Figure 6-23. The DDM sensitivities versus the OSAT source contributions of NO_x emissions from (a) biogenic, (b) on-road mobile, (c) other surface anthropogenic, and (d) elevated anthropogenic sources in Atlanta. The data shown only include the DDM and OSAT results for all fine grid cells with an O_3 concentration > 80 ppb at 3 p.m. on July 11-15 under the EPA 2007 base emission scenario (DDM base run B7 and OSAT base run B1). 6-129

Figure 6-24. The DDM sensitivities versus the OSAT source contributions of VOC emissions from (a) biogenic, (b) on-road mobile, (c) other surface anthropogenic, and (d) elevated anthropogenic sources in Chicago. The data shown only include the DDM and OSAT results for all fine grid cells with an O_3 concentration > 80 ppb at 3 p.m. on July 11-15 under the EPA 2007 base emission scenario (DDM base run B7 and OSAT base run B1).. 6-130

Figure 6-25. The DDM sensitivities versus the OSAT source contributions of NO_x emissions from (a) biogenic, (b) on-road mobile, (c) other surface anthropogenic, and (d) elevated anthropogenic sources in Chicago. The data shown only include the DDM and OSAT results for all fine grid cells with an O_3 concentration > 80 ppb at 3 p.m. on July 11-15 under the EPA 2007 base emission scenario (DDM base run B7 and OSAT base run B1). 6-131

Figure 6-26. The DDM sensitivities versus the OSAT source contributions of VOC emissions from (a) biogenic, (b) on-road mobile, (c) other surface anthropogenic, and (d) elevated anthropogenic sources in New York City. The data shown only include the DDM and OSAT results for all fine grid cells with an O_3 concentration > 80 ppb at 3 p.m. on July 11-15 under the EPA 2007 base emission scenario (DDM base run B7 and OSAT base run B1)..... 6-132

Figure 6-27. The DDM sensitivities versus the OSAT source contributions of NO_x emissions from (a) biogenic, (b) on-road mobile, (c) other surface anthropogenic, and (d) elevated anthropogenic sources in New York City. The data shown only include the DDM and OSAT results for all fine grid cells with an O_3 concentration > 80 ppb at 3 p.m. on July 11-15 under the EPA 2007 base emission scenario (DDM base run B7 and OSAT base run B1)..... 6-133

Figure 6-28. The DDM sensitivities versus the OSAT source contributions of VOC emissions from (a) biogenic, (b) on-road mobile, (c) other surface anthropogenic, and (d) elevated anthropogenic sources in Altoona. The data shown only include the DDM and OSAT results for all fine grid cells with an O_3 concentration > 80 ppb at 3 p.m. on July 11-15 under the EPA 2007 base emission scenario (DDM base run B7 and OSAT base run B1).. 6-134

Figure 6-29. The DDM sensitivities versus the OSAT source contributions of NO_x emissions from (a) biogenic, (b) on-road mobile, (c) other surface anthropogenic, and (d) elevated anthropogenic sources in Altoona. The data shown only include the DDM and OSAT results for all fine grid cells with an O_3 concentration > 80 ppb at 3 p.m. on July 11-15 under the EPA 2007 base emission scenario (DDM base run B7 and OSAT base run B1).. 6-135

Figure 6-30. The (a) O_3 sensitivities to total NO_x and VOC emissions from 17 source areas, ICs, and BCs predicted by DDM and (b) O_3 contributions of total NO_x and VOC emissions from 17 source areas, ICs, and BCs predicted by OSAT at 3 p.m. on July 15 under the EPA 2007 base emission scenario (DDM base runs B2 and B3 and OSAT base run B1) in Atlanta. 6-142

Figure 6-31. The (a) O_3 sensitivities to total NO_x and VOC emissions from 17 source areas, ICs, and BCs predicted by DDM and (b) O_3 contributions of total NO_x and VOC emissions from 17 source areas, ICs, and BCs predicted by OSAT at 3 p.m. on July 15 under the EPA 2007 base emission scenario (DDM base runs B2 and B3 and OSAT base run B1) in Chicago. 6-143

Figure 6-32. The (a) O_3 sensitivities to total NO_x and VOC emissions from 17 source areas, ICs, and BCs predicted by DDM and (b) O_3 contributions of total NO_x and VOC emissions from 17 source areas, ICs, and BCs predicted by OSAT at 3 p.m. on July 15 under the EPA 2007 base emission scenario (DDM base runs B2 and B3 and OSAT base run B1) in New York City..... 6-144

Figure 6-33. The (a) O_3 sensitivities to total NO_x and VOC emissions from 17 source areas, ICs, and BCs predicted by DDM and (b) O_3 contributions of total NO_x and VOC emissions from 17 source areas, ICs, and BCs predicted by OSAT at 3 p.m. on July 15 under the EPA 2007 base emission scenario (DDM base runs B2 and B3 and OSAT base run B1) in Altoona..... 6-145

Figure 6-34. The O_3 sensitivities to total NO_x and VOC emissions from 3 source categories and 17 source areas predicted by DDM at 3 p.m. on July 15 under the EPA 2007 base emission scenario (DDM base runs B2 and B3) in Atlanta. 6-146

Figure 6-35. The O_3 contributions of total NO_x and VOC emissions from 3 source categories and 17 source areas predicted by OSAT at 3 p.m. on July 15 under the EPA 2007 base emission scenario (OSAT base run B1) in Atlanta. 6-147

Figure 6-36. The O_3 sensitivities to total NO_x and VOC emissions from 3 source categories and 17 source areas predicted by DDM at 3 p.m. on July 15 under the EPA 2007 base emission scenario (DDM base runs B2 and B3) in Chicago..... 6-148

Figure 6-37. The O_3 contributions of total NO_x and VOC emissions from 3 source categories and 17 source areas predicted by OSAT at 3 p.m. on July 15 under the EPA 2007 base emission scenario (OSAT base run B1) in Chicago..... 6-149

Figure 6-38. The O_3 sensitivities to total NO_x and VOC emissions from 3 source categories and 17 source areas predicted by DDM at 3 p.m. on July 15 under the EPA 2007 base emission scenario (DDM base runs B2 and B3) in New York City..... 6-150

Figure 6-39. The O_3 contributions of total NO_x and VOC emissions from 3 source categories and 17 source areas predicted by OSAT at 3 p.m. on July 15 under the EPA 2007 base emission scenario (OSAT base run B1) in New York City. 6-151

Figure 6-40. The O_3 sensitivities to total NO_x and VOC emissions from 3 source categories and 17 source areas predicted by DDM at 3 p.m. on July 15 under the EPA 2007 base emission scenario (DDM base runs B2 and B3) in Altoona. 6-152

Figure 6-41. The O_3 contributions of total NO_x and VOC emissions from 3 source categories and 17 source areas predicted by OSAT at 3 p.m. on July 15 under the EPA 2007 base emission scenario (OSAT base run B1) in Altoona. 6-153

Figure 6-42. The change in hourly O_3 concentration in ppb caused by different processes as a function of time in Atlanta. The data shown were obtained by taking an average over the 81 fine grid cells for layers 1 to 7 in the receptor region. Lateral boundary inflow/outflow has been aggregated to a single net term. 6-157

Figure 6-43. The change in hourly O_3 concentration in ppb caused by different processes as a function of time in Chicago. The data shown were obtained by taking an average over the 81 fine grid cells for layers 1 to 7 in the receptor region. Lateral boundary inflow/outflow has been aggregated to a single net term. 6-158

Figure 6-44. The change in hourly O_3 concentration in ppb caused by different processes as a function of time in New York City. The data shown were obtained by taking an average over the 81 fine grid cells for layers 1 to 7 in the receptor region. Lateral boundary inflow/outflow has been aggregated to a single net term. 6-159

Figure 6-45. The change in hourly O_3 concentration in ppb caused by different processes as a function of time in Altoona. The data shown were obtained by taking an average over the 81 fine grid cells for layers 1 to 7 in the

receptor region. Lateral boundary inflow/outflow has been aggregated to a single net term. 6-160
Figure 6-46. The daily O_x production predicted by PA under the EPA 2007 base emission scenario (PA base run B4) on July 11 (top) and July 14 (bottom). 6-163
Figure 6-47. The daily O_x photochemical destruction predicted by PA under the EPA 2007 base emission scenario (PA base run B4) on July 11 (top) and July 14 (bottom). 6-164
Figure 6-48. The daily OH initiation from O^1D predicted by PA under the EPA 2007 base emission scenario (PA base run B4) on July 11 (top) and July 14 (bottom). 6-165
Figure 6-49. The daily HO_2 initiation predicted by PA under the EPA 2007 base emission scenario (PA base run B4) on July 11 (top) and July 14 (bottom). 6-166
Figure 6-50. The daily OH reacted with CO and CH_4 predicted by PA under the EPA 2007 base emission scenario (PA base run B4) on July 11 (top) and July 14 (bottom). 6-167
Figure 6-51. The daily OH reacted with all VOC species including CO and CH_4 but excluding biogenic VOC predicted by PA under the EPA 2007 base emission scenario (PA base run B4) on July 11 (top) and July 14 (bottom). 6-168
Figure 6-52. The daily OH reacted with isoprene predicted by PA under the EPA 2007 base emission scenario (PA base run B4) on July 11 (top) and July 14 (bottom). 6-169
Figure 6-53. The daily HNO_3 production from $OH+NO_2$ predicted by PA under the EPA 2007 base emission scenario (PA base run B4) on July 11 (top) and July 14 (bottom). 6-170
Figure 6-54. The daily HNO_3 production from N_2O_5 predicted by PA under the EPA 2007 base emission scenario (PA base run B4) on July 11 (top) and July 14 (bottom). 6-171

Figure 6-55. The percent conversion of HO_2 to NO predicted by PA under the EPA 2007 base emission scenario (PA base run B4) on July 11 (top) and July 14 (bottom). 6-172

Figure 6-56. The percent of OH reacting in radical propagation reactions predicted by PA under the EPA 2007 base emission scenario (PA base run B4) on July 11 (top) and July 14 (bottom). 6-173

Figure 6-57. The indicator ratio of $P(H_2O_2)/P(HNO_3)$ predicted by PA under the EPA 2007 base emission scenario (PA base run B4) on July 11 (top) and July 14 (bottom). 6-174

Figure 6-58. The production efficiency of O_x per NO_x converted to HNO_3 predicted by PA under the EPA 2007 base emission scenario (PA base run B4) on July 11 (top) and July 14 (bottom). 6-175

Figure 6-59. (a) The percent differences and (b) absolute differences in the calculated O_3 concentrations using the O_3 concentrations and sensitivities predicted from DDM base run B7 and the simulated O_3 concentrations from DDM sensitivity runs S2, S5, and S8 in all 81 fine grid cells in Atlanta at 3 p.m. on July 15, 1995. Labels on the x-axis correspond to fine grid cell indices for each receptor starting from the NW corner and proceeding row-wise. 6-182

Figure 6-60. (a) The percent differences and (b) absolute differences in the calculated O_3 concentrations using the O_3 concentrations and sensitivities predicted from DDM base run B7 and the simulated O_3 concentrations from DDM sensitivity runs S2, S5, and S8 in all 81 fine grid cells in Chicago at 3 p.m. on July 15, 1995. Labels on the x-axis correspond to fine grid cell indices for each receptor starting from the NW corner and proceeding row-wise. 6-183

Figure 6-61. (a) The percent differences and (b) absolute differences in the calculated O_3 concentrations using the O_3 concentrations and sensitivities predicted from DDM base run B7 and the simulated O_3 concentrations from DDM sensitivity runs S2, S5, and S8 in all 81 fine grid cells in New York City at 3 p.m. on July 15, 1995. Labels on the x-axis correspond to fine grid cell

indices for each receptor starting from the NW corner and proceeding row-wise.
..... 6-184

Figure 6-62. (a) The percent differences and (b) absolute differences in the calculated O_3 concentrations using the O_3 concentrations and sensitivities predicted from DDM base run B7 and the simulated O_3 concentrations from DDM sensitivity runs S2, S5, and S8 in all 81 fine grid cells in Altoona at 3 p.m. on July 15, 1995. Labels on the x-axis correspond to fine grid cell indices for each receptor starting from the NW corner and proceeding row-wise.
..... 6-185

Figure 6-63. The spatial distribution of O_3 contributions predicted by OSAT at 2 p.m. on July 15 under the 25% anthropogenic VOC emissions reduction scenario (DDM sensitivity run S1) for emissions from (a) biogenic VOC, (b) on-road mobile VOC, (c) other surface anthropogenic VOC, and (d) elevated anthropogenic VOC, (e) biogenic NO_x, (f) on-road mobile NO_x, (g) other surface anthropogenic NO_x, and (h) elevated anthropogenic NO_x..... 6-188/189

Figure 6-64. The spatial distribution of O_3 contributions predicted by OSAT at 2 p.m. on July 15 under the 25% anthropogenic NO_x emissions reduction scenario (DDM sensitivity run S4) for emissions from (a) biogenic VOC, (b) on-road mobile VOC, (c) other surface anthropogenic VOC, and (d) elevated anthropogenic VOC, (e) biogenic NO_x, (f) on-road mobile NO_x, (g) other surface anthropogenic NO_x, and (h) elevated anthropogenic NO_x.
..... 6-190/191

Figure 6-65. The spatial distribution of O_3 contributions predicted by OSAT at 2 p.m. on July 15 under the 75% anthropogenic NO_x emissions reduction scenario (DDM sensitivity run S7) for emissions from (a) biogenic VOC, (b) on-road mobile VOC, (c) other surface anthropogenic VOC, and (d) elevated anthropogenic VOC, (e) biogenic NO_x, (f) on-road mobile NO_x, (g) other surface anthropogenic NO_x, and (h) elevated anthropogenic NO_x..... 6-192/193

Figure 6-66. The O_3 contributions of total NO_x and VOC emissions from four source categories, ICs, and BCs predicted by OSAT at 3 p.m. on July 15 under the 25% anthropogenic VOC emissions reduction scenario (OSAT sensitivity run S1) in (a) Atlanta, (b) Chicago, (c) New York City, and (d) Altoona. 6-195

Figure 6-67. The O_3 contributions of total NO_x and VOC emissions from four source categories, ICs, and BCs predicted by OSAT at 3 p.m. on July 15 under the 25% anthropogenic NO_x emissions reduction scenario (OSAT sensitivity run S4) in (a) Atlanta, (b) Chicago, (c) New York City, and (d) Altoona. 6-196

Figure 6-68. The O_3 contributions of total NO_x and VOC emissions from four source categories, ICs, and BCs predicted by OSAT at 3 p.m. on July 15 under the 75% anthropogenic NO_x emissions reduction scenario (OSAT sensitivity run S7) in (a) Atlanta, (b) Chicago, (c) New York City, and (d) Altoona. 6-197

Figure 6-69. (a) The percent differences and (b) absolute differences in the calculated O_3 concentrations using the O_3 concentrations and source contributions predicted from OSAT base run B1 and the simulated O_3 concentrations from OSAT sensitivity runs S1, S4, and S7 in all 81 fine grid cells in Atlanta at 3 p.m. on July 15, 1995. Labels on the x-axis correspond to fine grid cell indices for each receptor starting from the NW corner and proceeding row-wise. 6-199

Figure 6-70. (a) The percent differences and (b) absolute differences in the calculated O_3 concentrations using the O_3 concentrations and source contributions predicted from OSAT base run B1 and the simulated O_3 concentrations from OSAT sensitivity runs S1, S4, and S7 in all 81 fine grid cells in Chicago at 3 p.m. on July 15, 1995. Labels on the x-axis correspond to fine grid cell indices for each receptor starting from the NW corner and proceeding row-wise. 6-200

Figure 6-71. (a) The percent differences and (b) absolute differences in the calculated O_3 concentrations using the O_3 concentrations and source contributions predicted from OSAT base run B1 and the simulated O_3 concentrations from OSAT sensitivity runs S1, S4, and S7 in all 81 fine grid cells in New York City at 3 p.m. on July 15, 1995. Labels on the x-axis correspond to fine grid cell indices for each receptor starting from the NW corner and proceeding row-wise. 6-201

Figure 6-72. (a) The percent differences and (b) absolute differences in the calculated O_3 concentrations using the O_3 concentrations and source contributions predicted from OSAT base run B1 and the simulated O_3 concentrations from OSAT sensitivity runs S1, S4, and S7 in all 81 fine grid cells in Altoona at 3 p.m. on July 15, 1995. Labels on the x-axis correspond to fine grid cell indices for each receptor starting from the NW corner and proceeding row-wise. 6-202

Figure 6-73. The receptor average O_x production in VOC-sensitive (top) and NO_x-sensitive (bottom) regimes for layers 1 to 4 in Atlanta on July 14 (a total O_x production up to 16:00 EST) under 75% anthropogenic NO_x emission reduction scenario (PA sensitivity run S9). The VOC-sensitive plot includes O_x produced for equally-sensitive conditions. 6-210

Figure 6-74. The receptor average O_x production in VOC-sensitive (top) and NO_x-sensitive (bottom) regimes for layers 1 to 4 in Chicago on July 14 (a total O_x production up to 16:00 EST) under 75% anthropogenic NO_x emission reduction scenario (PA sensitivity run S9). The VOC-sensitive plot includes O_x produced for equally-sensitive conditions. 6-211

Figure 6-75. The receptor average O_x production in VOC-sensitive (top) and NO_x-sensitive (bottom) regimes for layers 1 to 4 in New York City on July 14 (a total O_x production up to 16:00 EST) under 75% anthropogenic NO_x emission reduction scenario (PA sensitivity run S9). The VOC-sensitive plot includes O_x produced for equally-sensitive conditions. 6-212

ACKNOWLEDGMENTS

This work was supported by CRC under contract A-37-1. Thanks are due to Drs. Greg Yarwood and Ralph Morris, ENVIRON International Corporation, for conducting all simulations, preparing a suite of preliminary figures and tables, and for helpful discussions regarding the three probing tools implemented in CAMx. Thanks are also due to Dr. Alan Dunker, GM, and Dr. Dan Baker, Equilon, for their constructive inputs for the program planning.

LEGAL NOTICE

EXECUTIVE SUMMARY

E.1 Background

Probing techniques such as mass balance analysis and sensitivity analysis are useful to provide diagnostic evaluations of air quality models and to indicate the possible effects of changes in emissions of nitrogen oxides (NO_x) and volatile organic compounds (VOC) on ozone (O_3) concentrations.

Mass balance analysis provides quantitative information on the contribution of the various processes (e.g., transport and chemical reactions) to the modeled ambient concentrations, whereas sensitivity analysis, in general, provides quantitative information on the response of these concentrations to changes in the air pollution system. However, as will be shown in this project, the two types of analyses are related and can be roughly compared, especially when considering small to moderate changes in emissions. Since O_3 concentrations are a non-linear function of their precursors, mass balance analysis and sensitivity analysis will provide different types of information on the air quality modeling system.

Three probing techniques have been incorporated into CAMx: the Decoupled Direct Method (DDM), the Ozone Source Attribution Technology (OSAT), and Process Analysis (PA).

DDM is a sensitivity analysis technique that uses first-order derivatives to characterize, in CAMx, the response of the O_3 concentrations to changes in emission levels and boundary conditions. Because it uses first-order derivatives, DDM is accurate only to characterize small perturbations in the model inputs (up to about 40% perturbations, Dunker et al., 2002a). Also, the sum of the first-order derivatives characterize only a fraction of the O_3 concentration (typically, 60 to 65%). Higher-order derivatives would be required to represent large perturbations and characterize the total O_3 concentration. DDM is, therefore, a suitable technique to assess the effect on O_3 concentrations of changes in NO_x or VOC emissions that do not exceed about 40%. Such conditions may be appropriate for emission control scenarios designed to address many non-attainment issues (i.e., when the exceedance concentration and the regulatory

standard concentration fall within the linear response range, then sensitivity analysis can be used to address attainment issues).

OSAT is a mass balance analysis technique that tracks NO_x and VOC emissions/boundary conditions, using DDM sensitivity coefficients to attribute O_3 formation to either NO_x or VOC emissions/boundary conditions (note that CO was included in VOC in this project). As O_3 formation is simulated within CAMx, it is attributed to its precursors, NO_x and/or VOC. There are two versions of OSAT, which differ primarily in their methods used to attribute O_3 formation to NO_x and VOC. The original OSAT uses the ratio of the actual instantaneous production rates of H_2O_2 and HNO_3 (P_{H2O2}/P_{HNO3}) as an indicator of NO_x- or VOC-sensitive chemistry. In the updated OSAT, DDM is used to quantify the attribution between NO_x and VOC of the incremental O_3 being formed. Note that this use of DDM is approximate since DDM does not apply, in theory, to the whole O_3 amount but only to the fraction explained by the first-order derivatives (see above). Moreover, negative sensitivities calculated by DDM are interpreted as zero contributions in the OSAT formulation. Such negative sensitivities result from the titration of O_3 concentrations and inhibition of O_3 formation by NO_x and, in some cases, VOC. Therefore, the updated OSAT does not account for such inhibitions and will tend to overestimate the contribution of the precursor with a negative sensitivity and underestimate the contribution of the other precursor. The updated OSAT is evaluated in this project.

PA is also a mass balance analysis technique. In its CAMx implementation, PA provides a comprehensive analysis of the contribution of both chemical transformation and physical transport processes to O_3 concentrations at a given location (grid cell or cells) and time. As implemented in grid models such as CAMx, PA does not maintain a record of the contribution of chemistry and transport processes within air parcels as they are transported across the model grid cells. Therefore, information on the earlier "history" of O_3 formation along the air parcel back trajectory is not available and PA provides only local information. By contrast, DDM and OSAT account for the history of O_3 formation.

The three probing tools, DDM, OSAT, and PA, are evaluated in this project, for illustrative purposes, using the July 7-15, 1995 O_3 episode over the eastern United States

(OTAG domain). Four receptor areas were selected according to various selection criteria: Chicago, Atlanta, New York City, and a rural area, Altoona, in central Pennsylvania. The entire modeling domain was divided into 17 source areas including the four receptor areas (i.e., local sources).

It is important to note at the outset of this analysis that the three probing tools are significantly different in their design and, as a result, we cannot expect these probing tools to give exactly the same answers. However, these tools will be used to understand the processes that lead to the O_3 concentrations simulated by the air quality model. In particular, DDM and OSAT are likely to be used to provide information on the source areas or source categories that influence most or contribute most to the simulated O_3 concentrations. The objective of this analysis is, therefore, to evaluate the extent to which these three distinct probing tools give results that are consistent among them, to identify the possible discrepancies and, if warranted, to reconcile those discrepancies.

E.2 Consistency between DDM and OSAT

Our evaluation of consistency focuses on DDM and OSAT since both techniques provide quantitative information that can be used to indicate the source areas and/or source categories that contribute most to O_3 concentrations. We address first the ranking of source areas in terms of the sensitivity coefficient for DDM and the O_3 contribution for OSAT (hereafter, referred to as ranking of O_3 contributors for simplicity). Next, we address the issue of NO_x- versus VOC-sensitivity of O_3 concentrations. Finally, we address VOC reactivity.

Source ranking comparison

DDM and OSAT agree well on the set of top ten O_3 contributors by source area (out of a total of twenty-two contributors) and the set of top ten O_3 contributors by source group (out of a total of sixty-six source groups), however, they predict different rankings among those sets of top ten contributors for each of the four receptor regions.

In Atlanta, DDM and OSAT predict a similar ranking for some of the most influential contributors but a different ranking for other top ten contributors. Both DDM

and OSAT predict that NO_x and VOC emissions from local and surrounding source areas are the most influential contributors and NO_x and VOC emissions from upwind source areas are the second most influential contributors. For the highest 1-hour average O_3 concentrations (110 to 120 ppb), DDM gives greater importance to VOC emissions from upwind areas whereas OSAT gives greater importance to NO_x emissions from these upwind areas. For O_3 concentrations in the 90 to 110 ppb range, DDM shows slightly greater importance of biogenic VOC emissions from local and upwind source areas, whereas OSAT shows slightly greater importance of surface/elevated NO_x and surface anthropogenic VOC emissions from local and upwind source areas.

Similarly, in Chicago, both DDM and OSAT predict that NO_x and VOC emissions from surrounding and local source areas are the most influential contributors, and NO_x and VOC emissions from upwind source areas are the second most influential contributors. For high O_3 concentrations (> 90 ppb), DDM gives more importance to local surface NO_x emissions (but with a negative sensitivity) and biogenic VOC emissions from local, surrounding and other upwind areas. OSAT gives more weight to NO_x emissions from local, surrounding and upwind source areas.

In New York, both DDM and OSAT predict that the most influential contributors are NO_x and VOC emissions from the immediate upwind source areas, followed by NO_x emissions from surrounding source areas and NO_x and VOC emissions from local and distant upwind source areas. DDM gives greater importance to biogenic VOC emissions from local, surrounding and other upwind source areas for high O_3 concentrations (> 90 ppb) whereas OSAT gives greater importance to NO_x emissions from those source areas.

In Altoona, both DDM and OSAT predict that NO_x and/or VOC emissions from surrounding and upwind source areas are the most influential contributors. For high O_3 concentrations (> 90 ppb), DDM gives greater importance to upwind biogenic VOC emissions whereas OSAT gives greater importance to NO_x emissions from local and upwind source areas.

Results obtained for the 8-hour average O_3 concentrations (> 80 ppb) differ from those obtained for the 1-hour average O_3 concentrations in Atlanta and Chicago, thereby suggesting that different emission control strategies may be needed for 1-hour and 8-hour

average O_3 concentrations. On the other hand, results are similar for 1-hour and 8-hour average O_3 concentrations in New York City and Altoona.

When results were analyzed for subareas within each receptor region (nine subareas per receptor region), the rankings of the top two O_3 contributors varied among subareas for a given receptor region, for both DDM and OSAT. This variability indicates the difficulty of designing emission control strategies that are both simple, yet effective over an entire airshed.

NO_x-versus VOC-sensitivity of O_3 chemistry

In Atlanta and Altoona, DDM tends to predict NO_x-sensitive O_3 concentrations, OSAT shows that O_3 concentrations are primarily contributed by NO_x emissions, and PA shows that local O_x production under the NO_x-limited conditions is greater than that under the VOC-limited conditions. Therefore, all three probing tools provide results that are qualitatively consistent in Atlanta and Altoona. In addition, all three probing tools predict a spatial variability in the O_3 sensitivity to VOC and NO_x emissions among the individual grid cells and subareas in Chicago, New York City, and Altoona. However, in Chicago and New York City, these tools differ significantly in their assessment of the NO_x- versus VOC-sensitivity of O_3 chemistry. DDM tends to predict VOC-limited O_3 concentrations. As discussed above, OSAT does not account for the NO_x inhibition of O_3 formation in the urban areas and as a result tends to predict greater NO_x contributions than VOC contributions in most cases. The discrepancy between DDM and OSAT increases as the DDM VOC-sensitivity increases. Therefore, in its present formulation, OSAT should not be used to infer VOC-versus NO_x-sensitivity of O_3 chemistry in areas where negative sensitivities are likely to play a major role. PA, on the other hand, predicts that local O_x production is VOC-sensitive for some days and NO_x-sensitive for other days in Chicago and New York City. The PA results also identify the particular grid cells for which O_x production is inhibited by high NO_x concentrations. The results of PA and DDM differ in terms of sensitivity to VOC and NO_x because DDM predicts the effects of changes in emissions along the air parcel trajectories, whereas PA provides a mass budget explanation of the sensitivity of O_x production in the receptor region. However, the PA predictions of NO_x inhibited O_3 photochemistry in the base case for

Chicago and New York are qualitatively consistent with the DDM predictions of NO_x disbenefits for these regions.

Photochemical reactivity of VOC source groups

Both DDM and OSAT provide quantitative information on VOC reactivities that, to some extent, can be compared. The top three photochemical reactivities predicted by DDM and OSA are generally consistent in Chicago but are quite different in other receptor regions.

These large discrepancies occur when DDM predicts negative reactivities for some VOC source groups. Those VOC source groups may contain some anthropogenic VOC species such as xylenes, toluene, acetaldehyde and higher molecular aldehydes (ALD2), and a few biogenic VOC species such as olefins that may inhibit O_3 formation. In such cases, however, OSAT predicts large positive O_3 productivities for those VOC source groups. The discrepancy in DDM and OSAT predictions is due to the fact that the inhibition effect of those VOC emission groups on O_3 formation was accounted for by DDM but not by OSAT. The reactivity of VOC source groups may vary in magnitudes and mathematical signs with the levels of perturbations in VOC emissions (e.g., a small decrease in toluene emissions may increase O_3 formation due to less organic nitrate formation whereas a large decrease in toluene emissions may decrease O_3 formation due to lower precursor levels). The DDM predictions of the VOC reactivity are only accurate for small perturbations and may not be representative of large perturbations. The accuracy of the DDM and OSAT predictions of VOC reactivity for large perturbations (e.g., 75% reduction in VOC emissions) was not evaluated in this project and is recommended for future investigation.

E.3 Complementarity among DDM, OSAT, and PA

The three probing techniques considered here provide results that are different because of the design of the individual techniques but can be seen as complementary if they are used and interpreted properly. We discuss below the complementarity of these three techniques to address source attribution, the relative importance of local chemistry and long-range transport, detailed chemical analysis, and the model responses to changes in emission levels.

Source apportionment

Both OSAT (directly) and DDM (approximately through linear sensitivities) can attribute O_3 to source groups based on geographic area and emissions category, whereas PA provides no source category specific information. While OSAT attributes total O_3 concentration to all source groups, DDM provides first-order sensitivity of O_3 to all source groups. OSAT can track a larger number of source groups than DDM because OSAT uses reactivity-weighted tracers, whereas the number of source groups and geophysical regions treated with DDM is limited by the associated computational burden. OSAT results are naturally interpretable as source apportionments because they are based on the proportional contribution of emissions to the O_3 forming process; namely, the sum of O_3 contributions from all source groups always equals the predicted O_3 concentration. However, OSAT may overestimate the contribution of some sources (e.g., surface anthropogenic sources) and underestimate the contribution of other sources (e.g., biogenic sources) because it does not account for the titration/inhibition effect of NO_x (or VOC) on O_3 chemistry. On the other hand, DDM correctly accounts for the negative sensitivities, but DDM sensitivities cannot be strictly interpreted as source apportionments because the sum of all first-order sensitivities will not account for all of the O_3 concentration (it usually accounts for 60-65% of the total O_3 concentration); therefore, DDM provides source contribution to a fraction of the O_3 concentration (60-65%). Note that it is this fraction that will be mainly affected by small to moderate changes in emission levels. Although the source contributions expressed in terms of the percentage of the sum of the first-order sensitivity of O_3 predicted by DDM are not equivalent to those expressed in terms of the percentage of total O_3 concentration predicted by OSAT, a qualitative comparison between the DDM and OSAT source contributions was conducted to provide the relative importance of all source groups.

The source contributions predicted by DDM and OSAT are very similar in Atlanta, but somewhat different in New York City and Altoona and significantly different in Chicago. The major differences in the DDM and OSAT predictions are that DDM predicts negative source contributions whereas OSAT always predicts positive contributions. In particular, DDM predicts a negative contribution for on-road mobile source and a relatively smaller contribution of other surface and elevated anthropogenic

sources than OSAT does in Chicago. This results in a much higher contribution from biogenic emissions predicted by DDM than OSAT in Chicago; i.e., 71% of O_3 first-order sensitivity in DDM (which is equivalent to 43% of total O_3 concentration) vs. 33% of total O_3 concentration in OSAT.

Relative importance of chemistry and transport

The relative importance of chemistry and transport predicted by DDM and OSAT in the four receptor regions is generally consistent. Atlanta is mostly affected by local photochemistry. The local and surrounding sources in Atlanta are overwhelmingly more important than upwind sources, contributing to 90% of the O_3 sensitivity by DDM and 86% of the O_3 concentration by OSAT. New York City and Altoona are strongly influenced by long-range transport of pollutants. In New York City, the local/surrounding and upwind sources contribute to 40% and 52% of the O_3 sensitivity by DDM and 37% and 52% of the O_3 concentration by OSAT, respectively. In Altoona, the upwind emissions contribute to 57% of the O_3 sensitivity by DDM and 58% of the O_3 concentration by OSAT. Both transport and local photochemistry could be important to O_3 formation in Chicago. DDM predicts that both surrounding and upwind emissions are the most important sources, contributing to 38% and 40% of the O_3 sensitivity, respectively, while OSAT predicts that the local, surrounding, and upwind emissions, contribute to 34%, 28% and 27% of the O_3 concentration, respectively.

PA, on the other hand, provides the relative importance of various processes including chemistry, lateral boundary transport, top boundary transport, and deposition to the local and instantaneous O_3 production. The PA results are qualitatively consistent with those of DDM and OSAT for cases where local emissions dominate O_3 formation (e.g., in Atlanta) but inconsistent with the DDM and OSAT results for cases where transport is important to local O_3 formation (e.g., Chicago, New York City, and Altoona). This is due to the fact that DDM and OSAT account for the time history of the air parcels whereas PA provides local information.

Detailed chemical analysis

PA is the only tool that provides detailed chemical analysis among the three probing tools implemented in CAMx. The Integrated Reaction Rate (IRR) component of PA is designed to elucidate important chemical pathways and to identify key chemical characteristics. The chemical process analysis outputs in CAMx provide information on odd oxygen (O_x) (defined as $O_x = O_3 + NO_2 + O(^3P) + O(^1D) + 2\ NO_3 + 3\ N_2O_5 + PAN + HNO_4$) and NO_x budgets and radical initiation, propagation, and termination. This information is particularly useful for investigating mechanistic differences under different chemical regimes or between different mechanisms. It is also useful to assess the spatial and temporal variability in the sensitivity of O_x and O_3 production to precursors and to investigate the relationships between O_3 and its precursors. A detailed chemical analysis was conducted for the base case simulation with the EPA 2007 emission inventory.

Model response to emission changes

Both OSAT and DDM can be used to predict model responses to changes in input parameters or variables such as initial conditions, boundary conditions, and emissions, whereas PA does not have this capability. However, there is a major difference in characterizing the model responses to perturbations in inputs between OSAT and DDM. DDM is more directly applicable to predicting the response to changes in emissions because the sensitivity coefficients directly address this issue. This information is particularly useful in developing emission control strategies for many non-attainment areas in the U.S. The main limitation of DDM is that first-order sensitivities are only representative of small changes for non-linear systems, and are not expected to be accurate for large changes that require higher-order derivatives to characterize the model response.

OSAT is less applicable to quantitative prediction of the response to changes in emissions because OSAT does not calculate sensitivity coefficients and the extrapolation of the OSAT results to a different emission scenario involves some assumptions by the user. The most likely assumption that the user will make is linearity, i.e., that OSAT source contributions will scale proportionately with emissions. Our evaluation shows that applying linear scaling to the OSAT results is reasonably accurate for small

perturbations in VOC emission levels but less accurate for both small and large perturbations in NO_x emissions (see more detailed results in the next section). Therefore caution should be taken when using the OSAT results to extrapolate from a base simulation to an emission scenario with a perturbation in NO_x emissions.

E.4 Stretchability

The applicability of the probing tools to moderate (25%) and large (75%) emission changes was tested for both DDM and OSAT. Our test results for DDM and OSAT show that both DDM and OSAT predict accurate model responses under the 25% VOC emission reduction scenario. For the 25% NO_x emission reduction scenario, DDM predicts accurate model responses, whereas OSAT predicts inaccurate model responses due to the fact that OSAT does not account for the effect of NO_x titration on O_3 formation. For the 75% NO_x emission reduction scenario, both DDM and OSAT predict inaccurate model responses, with less errors in the OSAT predictions than the DDM predictions.

For DDM, we tested whether the sensitivity coefficients can be used to predict the change in O_3 concentrations due to changes in emissions. The DDM results from the base case were used to estimate the O_3 concentration for an emission control case. The estimated O_3 concentration was then compared to the O_3 concentration simulated with the emission change. DDM showed the ability to predict O_3 concentrations due to 25% changes in VOC and NO_x emission levels within 10%. However, large errors (up to 98.2%) in estimated O_3 concentrations were obtained for 75% changes in precursor emissions.

For OSAT, we tested both the sensitivity of the source contributions to changes in emission levels and the ability of OSAT to predict model response. In particular, we evaluated the validity of applying linear scaling to the OSAT source attribution results under different emission scenarios. As compared to the base case, the differences in the source contributions of different source categories were within 4% for 25% NO_x or VOC emission reduction scenarios and within 11% for 75% NO_x emission reduction scenario. Those results show that the OSAT source attribution results are relatively stable for

emission scenarios with a small perturbation (e.g., a 25% reduction in anthropogenic NO_x and VOC emissions) but different (as expected) for emission scenarios with a large perturbation (e.g., a 75% emission reduction). OSAT showed the ability to predict O_3 concentrations due to 25% changes in VOC emission levels within 10%. However, large errors in estimated O_3 concentrations were obtained for 25% and 75% changes in NO_x emissions (up to -31.9% and -45.3%, respectively) due to the fact that OSAT does not account for the effect of NO_x titration on O_3 formation.

E.5 Comparison of the Results from CRC Projects A-29 and A-37

In a separate CRC project A-29, the results of DDM and the original version of OSAT were compared in terms of the ranking of the top 5 O_3 contributors, the correlation between the two sets of results, the relative importance of the source categories, and the spatial distributions of DDM sensitivities and OSAT source contributions for the Lake Michigan region for the O_3 episode of July 7-13, 1995 (Dunker et al., 2002b). The comparison between the results of DDM and the updated version of OSAT conducted in this project included all aforementioned components and was more comprehensive than that of CRC project A-29. The results from this project are generally consistent with those from CRC project A-29 in terms of the ranking of the top 5 O_3 contributors and the spatial distributions of DDM sensitivities and OSAT source contributions. There are three major differences in the results from the two projects:

- CRC Project A-29 reported that the original version of OSAT predicted a small and positive source contribution (0.3-2.6 ppb) for receptors where DDM predicted a large negative sensitivity (-33 ppb) to anthropogenic area-source NO_x emissions (e.g.,Chicago area). However, it was found in this project that in those regions where NO_x significantly inhibited O_3 formation (with negative sensitivities of -40 to -10 ppb), the updated version of OSAT predicted much larger positive source contributions (10 to 25 ppb) than those reported in CRC Project A-29.

- A consistently good relation between the DDM sensitivities and OSAT source contributions for all the cases (with R^2 values of 0.8-0.98) was found in CRC Project A-29, whereas, in this project, poor correlation (with R^2 values as low as 0.02 to 0.33) was found for some source categories (e.g., on-road mobile, other surface anthropogenic, and elevated anthropogenic NO_x emissions) at some receptors (e.g., Chicago) where the titration/inhibition effect of NO_x is important (i.e., there are large negative sensitivities for those source groups).
- There are some inconsistencies or even conflicts regarding the relative importance of some source categories (e.g., biogenic VOC, elevated point-source NO_x emissions) predicted by DDM and OSAT between the two projects. For example, CRC project A-29 predicted that the original version of OSAT ascribes greater importance to biogenic VOC emissions than does DDM and DDM ascribes greater importance to point-source NO_x emissions than does OSAT. The relative importance of biogenic VOC and point-source NO_x emissions predicted by DDM and the updated version of OSAT in this project was just the opposite of that predicted from CRC project A-29, namely, DDM ascribes greater importance to biogenic VOC emissions than does OSAT and OSAT ascribes greater importance to point-source NO_x emissions than does DDM.

Several important factors may be responsible for the inconsistencies between the results in Projects A-29 and A-37. First, the versions of OSAT used in the two projects are substantially different (see Chapter 1 for major differences between the original and the updated versions of OSAT). Second, Project A-37 used an emission inventory for 2007 whereas Project A-29 used an inventory for 1995. These inventories could be quite different both in absolute amount of emissions and in the relative proportions of mobile, point-source, other anthropogenic, and biogenic emissions. Furthermore, the results were analyzed differently in the two projects. For example, for the scatter plots in Project A-29, sensitivities and source contributions were averaged across receptor regions but not across geographic source regions. In the scatter plots in this poject (e.g., Figures 6-22 to 6-29), sensitivities and source contributions were plotted for individual grid cells in the receptor regions, but there was only one geographic source region. The different

averaging procedures employed in the two studies may affect the comparison between DDM and OSAT. Nevertherless, The inconsistencies in the results in Projects A-29 and A-37 indicate that the predicted contributions and relative importance of the source categories are sensitive to the selected locations of receptors and the episode simulated and may be different from case to case.

E.6 Computational Requirements

The simulations with CAMx and PA impose minimal computational burden on the top of the base case CAMx simulation, whereas the simulations with CAMx and OSAT and DDM require a significant increase in memory and CPU time. In particular, a single DDM run to provide sensitivity information that is comparable to that from OSAT requires much more memory (about 2.3 GigaBytes vs. 325 MegaBytes) and CPU times (greater by a factor of 3-6) than the OSAT run and has to be split into several small runs.

The development and implementation of each of the three probing tools impose several challenges that are either common (e.g., accuracy, CPU cost, and interface) or unique (e.g., the size of the outputs for PA, the source-receptor relationships for OSAT, and the optimization of the efficiency and accuracy of the sensitivity calculation for DDM) to those tools.

E.7 Recommendations

The three probing tools currently implemented in CAMx can provide useful information regarding O_3 formation. However, each of those tools has limitations that the user must understand in order to avoid any misinterpretation of the results.

DDM provides accurate information on the response of O_3 to changes in NO_x and VOC emissions up to about 40%. Such information may be appropriate for the development of the emission control strategies for many non-attainment areas.

OSAT provides source attribution of O_3 to NO_x and VOC emissions but does not account for the O_3 inhibition effects of NO_x and VOC. Consequently, OSAT may provide misleading information in areas where strong inhibitions occur (e.g., NO_x

titration/inhibition of O_3 in VOC-sensitive urban areas). This limitation of OSAT could be minimized if the technique were modified to account for such negative contributions of NO_x and VOC species.

PA provides useful information on the local aspects of O_3 formation and of the O_3 budget (i.e., local formation versus transport). As such, it can complement the DDM and OSAT analyses. Specifically, PA may be useful for targeting controls to particular grid cells where local production of O_x is identified as either VOC- or NO_x-sensitive.

The three probing techniques evaluated here provide valuable information on the possible responses of O_3 concentrations to NO_x and VOC emissions and/or the processes leading to those O_3 concentrations**.** Application of these techniques can guide and focus the development of emissions control strategies. Thoughtful interpretation of the results, supported by development of post-processing tools, and increasing familiarity should ultimately reduce the overall burden on air quality planners. Nevertheless, the effect of well-crafted multi-pollutant emission scenarios should be assessed by simulating these actual scenarios.

TECHNICAL SUMMARY

The three probing tools, the Decoupled Direct Method (DDM), the Ozone Source Attribution Technology (OSAT) and Process Analysis (PA), implemented in CAMx are evaluated systematically with a number of base and sensitivity simulation results for the July 7-15, 1995, O_3 episode in the OTAG domain – an episode chosen for illustrative purposes. It is important to note at the outset of this analysis that the three probing tools are significantly different in their design and, as a result, we cannot expect these probing tools to give exactly the same answers. However, these tools will be used to understand the processes that lead to the ozone (O_3) concentrations simulated by the air quality model. In particular, DDM and OSAT are likely to be used to provide information on the source areas or source categories that influence most or contribute most to the simulated O_3 concentrations, particularly concentrations at or above a regulatory standard concentration. The objective of this analysis is, therefore, to evaluate the extent to which these three distinct probing tools give results that are consistent among each other, to identify the possible discrepancies and, if warranted, to reconcile those discrepancies.

First, we present below brief descriptions of the probing tools considered here and describe the framework used for their evaluation. Four components are considered in this evaluation: consistency, complementarity, stretchability, and computational and implementation requirements. The first component, consistency, refers to the ability of different probing techniques to provide consistent results for a specific application (e.g., O_3 sensitivity to NO_x or VOCs; relative reactivities of VOCs). The second component, complementarity, refers to the fact that some probing techniques can provide information that others cannot provide. The third component, stretchability, addresses the range over which a probing technique can be considered reliable. The fourth component, computational requirements, characterizes the practical aspects of the probing technique computations (e.g., a probing technique can in theory be able to provide very detailed and comprehensive information but it may not be feasible computationally). An overview of these components is provided in Figure T-1. A summary of the detailed evaluation of the three probing tools in terms of the four components follows the descriptions of the probing tools.

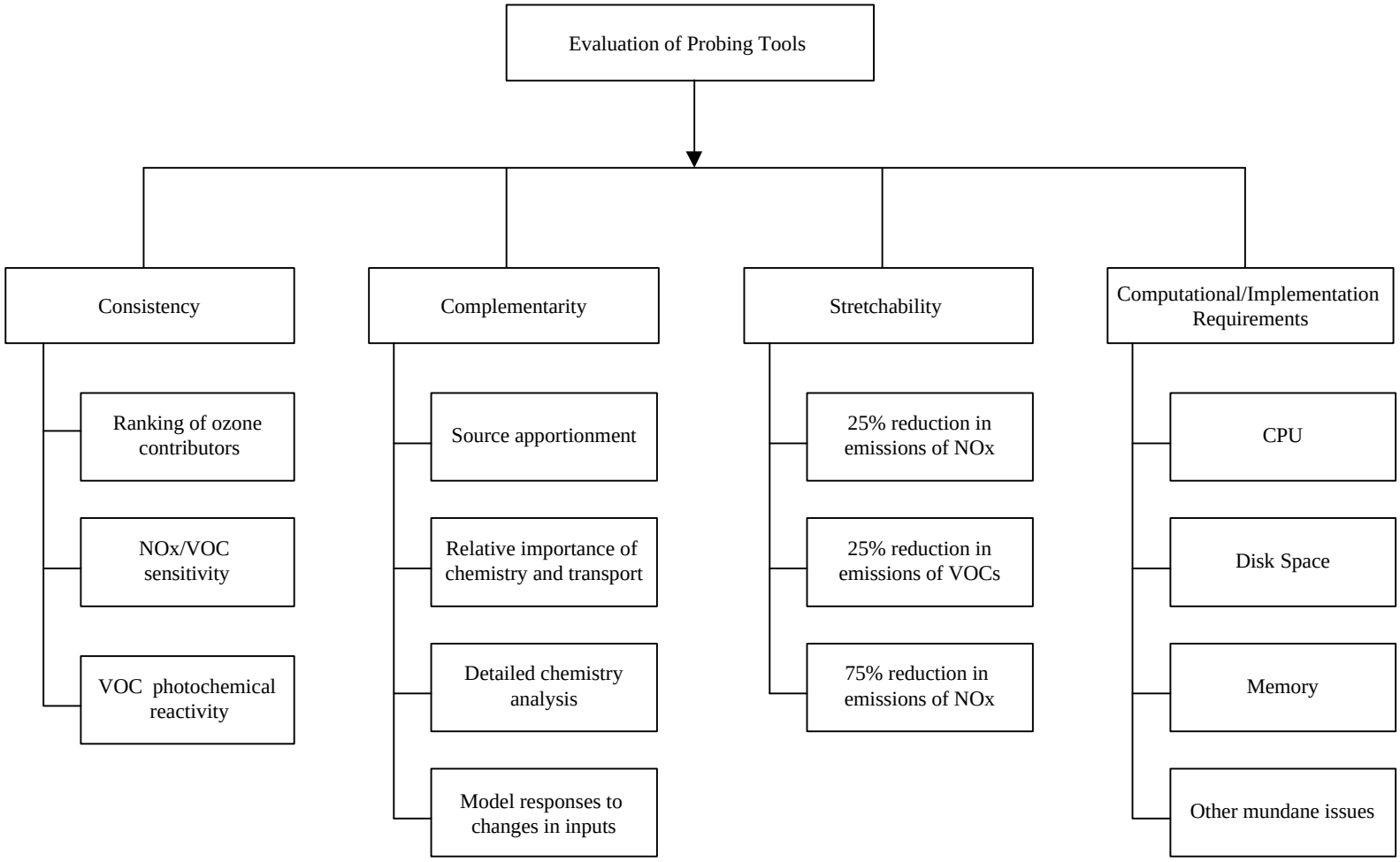

Figure T-1. Overview of technical components for evaluation of probing tools.

T.1 The Probing Tools

Probing tools can be organized into two major groups:

- Mass balance analysis techniques
- Sensitivity analysis techniques

Mass balance analysis provides quantitative information on the contribution of the various processes (e.g., transport and chemical reactions) to the modeled ambient concentrations, whereas sensitivity analysis provides quantitative information on the response of these concentrations to changes in the air pollution system. The latter technique is particularly useful in air quality planning when concentrations are at or above a regulatory standard concentration. Since ozone (O_3) concentrations are a non-linear function of their precursors, mass balance analysis and sensitivity analysis will provide different types of information on the air quality modeling system. However, as will be shown in this project, the two types of analyses are related and can be roughly compared, especially when considering small to moderate changes in emissions.

Mass balance techniques are appropriate for diagnostic evaluations of the air quality models (i.e., to identify which chemical transformation pathways and which physical transport processes govern O_3 concentrations). However, since mass balance analysis techniques cannot provide a quantitative measure of the response of O_3 concentrations to changes in emission levels unless that response is linear, it is not possible *a priori* to know how well a mass balance analysis technique can approximate the response of a non-linear system such as O_3 chemistry. Mass balance analysis techniques may be useful to identify which sources contribute to O_3 concentrations but are generally not accurate to characterize how these concentrations will respond to changes in emission levels. To obtain quantitative information on the response of O_3 concentrations to changes in the emission levels, sensitivity analysis techniques must be used. That information can be used to understand which model parameters and input variables (e.g., emission sources) influence the model output. The latter technique is

useful in air quality planning when concentrations are at or above a regulatory standard concentration.

DDM is a sensitivity analysis technique that uses first-order derivatives to characterize, in CAMx, the response of the O_3 concentrations to changes in emission levels and boundary conditions. Because it uses first-order derivatives, DDM is accurate only to characterize small perturbations in the model inputs (up to about 40% perturbations, Dunker et al., 2002a). Also, the sum of the first-order derivatives characterize only a fraction of the O_3 concentration (typically, 60 to 65%). Higher-order derivatives would be required to represent large perturbations and characterize the total O_3 concentration. DDM is, therefore, a suitable technique to assess the effect on O_3 concentrations of changes in nitrogen oxides (NO_x) or volatile organic compounds (VOC) emissions that do not exceed about 30%. Such conditions may be appropriate for emission control scenarios designed to address many non-attainment issues (i.e., when the exceedance concentration and the regulatory standard concentration fall within the linear response range, then sensitivity analysis can be used to address attainment issues).

OSAT is a mass balance analysis technique that tracks NO_x and VOC emissions/boundary conditions, using DDM sensitivity coefficients to attribute O_3 formation to either NO_x or VOC emissions/boundary conditions (note that CO was included in VOC in this project). As O_3 formation is simulated within CAMx, it is attributed to its precursors, NO_x and/or VOC. DDM is used to quantify the attribution between NO_x and VOC of the incremental O_3 being formed. Note that this use of DDM in OSAT is approximate since DDM does not apply, in theory, to the whole O_3 amount but only to the fraction explained by the first-order derivatives (see above). Moreover, negative sensitivities calculated by DDM are interpreted as zero contributions in the OSAT formulation. Such negative sensitivities result from the titration of O_3 concentrations and inhibition of O_3 formation by NO_x and, in some cases, VOC. Therefore, OSAT does not account for such inhibitions and will tend to overestimate the contribution of the precursor with a negative sensitivity and underestimate the contribution of the other precursor.

PA is also a mass balance analysis technique. In its CAMx implementation, PA provides a comprehensive analysis of the contribution of both chemical transformation

and physical transport processes to O_3 concentrations at a given location and time. As implemented in grid models such as CAMx, PA does not maintain a record of the contribution of chemistry and transport processes within air parcels as they are transported across the model grid cells. Therefore, information on the earlier "history" of O_3 formation along the air parcel back trajectory is not available and PA provides only local information. By contrast, DDM and OSAT account for the history of O_3 formation.

The modeling domain where the three probing tools were applied is presented in Figure T-2. Four receptor areas were selected according to various selection criteria in order to highlight features of the probing tools: Chicago (area 14), Atlanta (area 15), New York City (area 16) and a rural area, Altoona (area 17). The domain was divided into 17 emission source areas including the four receptor areas (i.e., local sources). We will refer to emission sources that correspond to the receptor regions as local. The emission sources located in an area surrounding a receptor region will be referred to as surrounding emissions (e.g., area 8 for Atlanta and area 4 for Chicago). Other emission sources that affect a receptor region are referred to as upwind sources. Areas that are distant from the western, northern or southern boundaries are referred to as the core source areas (there are 11 core source areas); the boundary source areas are source areas 1, 2, 3, 6, 9, and 10.

Each receptor region consists of 81 model fine-grid cells in the surface layer. Each receptor region is divided into 9 subareas (of 9 grid cells each). Most of our discussion focuses on receptor regions but we address also the variability among subareas within a given receptor region.

T.2 Consistency

Our evaluation of consistency focuses on DDM and OSAT since both techniques provide quantitative information that can be used to indicate the source areas and/or source categories that contribute most to O_3 concentrations. We address first the ranking of source areas in terms of their sensitivity coefficients for DDM and O_3 contribution for OSAT (hereafter, referred to as ranking of O_3 contributors for simplicity). Next, we address the issue of NO_x- versus VOC-sensitivity of O_3 concentrations. Finally, we address VOC reactivity.

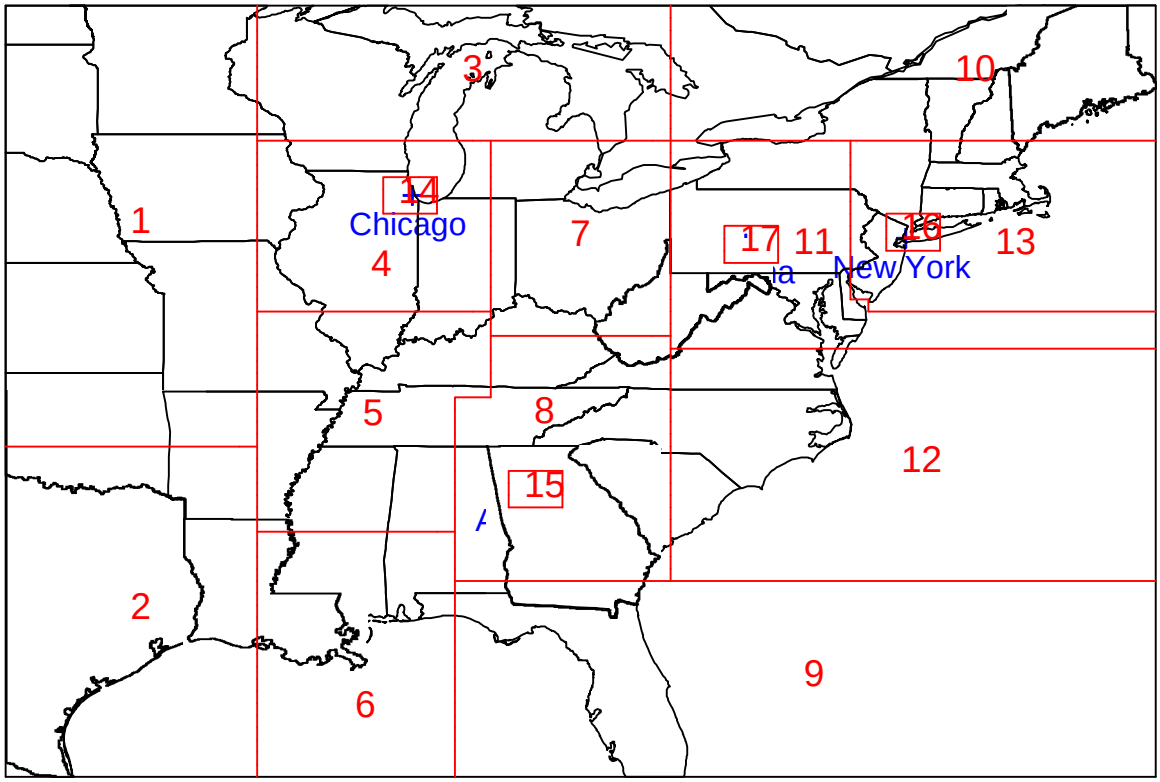

Figure T-2. The geographic source areas for application of OSAT and DDM probing tools in the OTAG modeling domain.

Source Ranking Comparison between DDM and OSAT

While PA does not provide any information on the contributions of precursors (NO_x and VOC) to O_3, both DDM and OSAT can provide rankings of the O_3 sensitivities/contributions to/of different source groups. Such rankings provide information on which source groups have the largest effects on O_3 formation in a particular receptor region and, therefore, are of most interest for the design of O_3 control strategies. In comparing the DDM and OSAT rankings, we ranked the set of top 10 O_3 contributors by source area (out of 22 contributors) and by source group (out of 66 contributors) at each receptor for 6 stratified O_3 levels with O_3 concentrations of < 80 ppb, 80-90 ppb, 90-100 ppb, 100-110 ppb, 110-120 ppb, and > 120 ppb using the DDM and OSAT predictions on July 11-15, 1995. The ranking was conducted for both the 1-hr and the 8-hr O_3 concentrations. The set of top two O_3 contributors by source area and by source group for these 1-hr and 8-hr O_3 concentration ranges in the nine subareas comprising each receptor region were also identified.

First, we summarize the contributions of the different source areas and source categories to the DDM sensitivities. Similarities and differences between the sensitivities of the 1-hour and 8-hour average O_3 concentrations are discussed[(1)]. Variability among subareas comprising each receptor region are also briefly addressed. Next, we compare the set of top 10 O_3 contributors predicted by DDM and OSAT.

Detailed analyses of the DDM sensitivities show that the high 1-hr O_3 concentrations (all levels > 90 ppb) are most sensitive to the local and surrounding NO_x and VOC emissions in Atlanta, indicating that a reduction in the local and surrounding emissions is likely to be the most effective O_3 control strategy for high 1-hr O_3 concentrations in this receptor region. The ranking and magnitude of 1-hr and 8-hr O_3 sensitivities differ for some high O_3 levels. Those differences suggest that different emission control strategies may be needed for 1-hr and 8-hr O_3 compliance in Atlanta.

In Chicago, both the 1-hr and 8-hr O_3 concentrations at all levels are most sensitive to the surrounding and local NO_x and/or VOC emissions and moderately

[(1)] Often in this discussion, not all 6 stratified O_3 concentration levels need to be retained, so several levels may be collapsed to facilitate easier presentation.

sensitive to the upwind emissions from source areas located east of the Mississippi. However, O_3 formation responds negatively to the changes in the local surface and elevated anthropogenic NO_x emissions due to the significant titration/inhibition effect of NO_x on O_3 formation in Chicago. Reduction of the surface and elevated anthropogenic NO_x emissions from the surrounding/upwind sources and the surface anthropogenic VOC emissions from the local and surrounding sources appear to be the most effective O_3 control strategies in Chicago. Since the ranking order of controllable source groups in the set of top 10 contributors is different for the highest 1-hr and 8-hr O_3 levels, different priorities in emission reductions may be needed to effectively reduce the maximum 1-hr or 8-hr O_3 in Chicago.

In New York City, the high 1-hr O_3 concentrations (all levels > 90 ppb) are most sensitive to the upwind NO_x and VOC emissions, the surrounding NO_x emissions, and the local VOC emissions. This indicates that both local photochemistry and long-range transport contribute to high O_3 concentrations in New York City. The differences in the 1-hr and 8-hr O_3 sensitivities for the O_3 levels > 80 ppb are small; this result suggests that the emission control strategies developed for the 1-hr O_3 concentrations should generally be applicable to the 8-hr O_3 concentrations in New York City.

In Altoona, a rural area, the O_3 concentrations at all levels are predominantly influenced by the surrounding and upwind NO_x and/or VOC emissions. The O_3 contribution of the local NO_x emissions is relatively small, indicating that high O_3 concentrations in this receptor region are mainly caused by regional transport across several states upwind. While the 1-hr O_3 concentrations were below the level of the 1-hr O_3 standard, the 8-hr maximum O_3 exceeded the new NAAQS of 80 ppb in Altoona during this high O_3 episode. Compared to the urban receptors discussed above, the elevated anthropogenic NO_x emissions play a more important role than the surface anthropogenic NO_x emissions for both 1-hr and 8-hr O_3 > 80 ppb in Altoona. These results suggest that reduction of the elevated and surface anthropogenic NO_x emissions from the upwind and surrounding sources should be the most effective control strategies for reduction of the peak 8-hr O_3 concentration in Altoona.

The effect of NO_x and/or VOC emissions from different source groups on O_3 formation in individual subareas comprising each receptor region is generally consistent

with the distribution of the local sources and vegetation in or nearby those receptor regions and the distribution of the point sources nearby or upwind. However, significant differences exist in the set of top two source contributors for all O_3 levels in all nine subareas in all four receptor regions, due to differences in the local and upwind emission sources and in the history of the air parcels across those subareas. The variability for subareas indicates the difficulty of designing emission control strategies that can be both simple, yet effective for an entire airshed. Different emission control strategies may be needed to reduce the maximum 1-hr or 8-hr O_3 concentrations for individual subareas or at the county-level.

Although DDM and OSAT agree well on the set of top 10 O_3 contributors from the 11 core source areas, they predict different rankings for those contributors in all receptor regions. In Atlanta, DDM and OSAT predict a similar ranking for some of the most influential contributors but a different ranking for other top ten contributors. Both DDM and OSAT predict that NO_x and VOC emissions from local and surrounding source areas are the most influential contributors and NO_x and VOC emissions from upwind source areas are the second most influential contributors. For low 1-hr and 8-hr O_3 level (< 80 ppb), OSAT gives greater importance to the local surface/elevated anthropogenic NO_x emissions and surrounding biogenic VOC emissions, whereas DDM gives greater importance to the upwind elevated/surface anthropogenic NO_x emissions and the local/upwind biogenic VOC emissions. For 1-hr and 8-hr O_3 levels in a mid-range of 80-90 ppb, 90-100 ppb, and 100-110 ppb, DDM and OSAT give similar rankings. For the highest 1-hr O_3 level of 110-120 ppb, OSAT gives greater importance to the upwind NO_x emissions; and DDM gives greater importance to the upwind VOC emissions. While the set of top two O_3 contributors for the 8-hr O_3 concentrations predicted by DDM and OSAT are quite similar, those for the 1-hr O_3 concentrations differ in many subareas in Atlanta.

Similarly, in Chicago, both DDM and OSAT predict that NO_x and VOC emissions from surrounding and local source areas are the most influential contributors, and NO_x and VOC emissions from upwind source areas are the second most influential contributors. For low 1-hr and 8-hr O_3 levels (< 80 ppb), DDM gives more weight to the local surface/elevated anthropogenic NO_x emissions and the upwind/local biogenic VOC

emissions; OSAT gives more weight to the surrounding NO_x emissions from all source categories and the upwind surface/elevated anthropogenic NO_x emissions. For intermediate and high 1-hr and 8-hr O_3 levels (> 80 ppb), DDM gives more weight to the local surface anthropogenic NO_x emissions and the biogenic VOC emissions from local, surrounding and upwind sources; OSAT gives more weight to the surrounding NO_x emissions from all source categories, the local elevated anthropogenic NO_x emissions. and the upwind surface anthropogenic NO_x emissions.

In New York City, both DDM and OSAT predict that the most influential contributors are NO_x and VOC emissions from the immediate upwind source areas, followed by NO_x emissions from surrounding source areas and NO_x and VOC emissions from local and distant upwind source areas. For low 1-hr and 8-hr O_3 levels (< 80 ppb), DDM gives more weight to the local surface/elevated anthropogenic NO_x and the upwind biogenic VOC; OSAT gives more weight to the upwind elevated anthropogenic NO_x emissions and the upwind/surrounding surface anthropogenic NO_x. For 1-hr and 8-hr O_3 levels in the mid-range of 80-90 ppb, DDM gives more weight to the upwind/local biogenic VOC and the local surface anthropogenic NO_x emissions; OSAT gives more weight to the surrounding/upwind surface anthropogenic NO_x emissions and the upwind/surrounding elevated anthropogenic NO_x emissions. For higher 1-hr and 8-hr O_3 levels (> 90 ppb), DDM gives more weight to the biogenic VOC emissions from the upwind, local and surrounding sources; OSAT gives more weight to the local/upwind surface anthropogenic NO_x and the upwind/surrounding elevated anthropogenic NO_x emissions.

In Chicago and New York City, DDM predicts a negative sensitivity to the local NO_x emissions for all O_3 levels, whereas OSAT, by design, always predicts a positive O_3 contribution from the local NO_x emissions. Therefore, the OSAT ranking of O_3 contributors may be misleading for the development of O_3 control strategies in regions where there is a large titration/inhibition effect of NO_x on O_3 formation.

In Altoona, both DDM and OSAT predict that NO_x and/or VOC emissions from surrounding and upwind source areas are the most influential contributors. For 1-hr and 8-hr low O_3 levels (< 80 ppb), DDM gives greater importance to the upwind/surrounding biogenic VOC emissions; OSAT gives greater importance to the upwind elevated

anthropogenic NO_x emissions and the local surface anthropogenic NO_x emissions. For 1-hr and 8-hr O_3 level of 80-90 ppb, DDM gives greater importance to the upwind/surrounding biogenic VOC emissions; OSAT gives greater importance to the upwind elevated/surface anthropogenic NO_x emissions, the upwind elevated anthropogenic VOC emissions, and the local surface anthropogenic NO_x emissions. For the 1-hr O_3 levels of 90-100 ppb and 100-110 ppb and the 8-hr O_3 level of 90-100 ppb, DDM gives more weight to the upwind biogenic VOC emissions; OSAT gives more weight to the upwind elevated/surface anthropogenic NO_x emissions for the 1-hr and 8-hr O_3 and the local surface anthropogenic NO_x emissions for the 1-hr O_3.

Significant differences exist in the set of top two O_3 contributors predicted by DDM and OSAT from the 11 core source areas for 1-hr O_3 levels in all nine subareas in Atlanta and for all 1-hr and 8-hr O_3 levels in all nine subareas in each of Chicago, New York City and Altoona receptor regions. In general, for low O_3 levels (< 80 ppb), DDM gives more weight to the local surface/elevated anthropogenic NO_x and the surrounding/upwind biogenic VOC emissions; whereas OSAT gives more weight to the surrounding surface anthropogenic/elevated anthropogenic/biogenic NO_x emissions and the upwind elevated anthropogenic NO_x emissions. For high O_3 levels (> 80 ppb), DDM gives more weight to the biogenic VOC emissions from the local, surrounding, and upwind sources; whereas OSAT gives more weight to the local surface anthropogenic VOC emissions, the local elevated anthropogenic NO_x emissions, the surrounding surface anthropogenic/elevated anthropogenic/biogenic NO_x emissions, and the upwind surface/elevated anthropogenic NO_x emissions.

The set of top two O_3 contributions by source area for the six boundary source areas predicted by DDM and OSAT are quite similar. The effect of the total emissions from the boundary source areas 1, 2, 3, and 9 on O_3 concentrations at the four receptors is either greater than or comparable to the effect of some source groups from the 11 core source areas. The effects of the six boundary source areas on 8-hr O_3 concentrations in the four receptor regions are almost identical to those for the 1-hr O_3 concentrations at all four receptors.

The NO_x- vs VOC-Sensitivity of O_3 Chemistry

Each of the three probing tools provides information that can be used to directly or indirectly determine the NO_x- or VOC-sensitivity of peak O_3 concentrations at a particular receptor. Such information may typically be used to identify the relative effectiveness of NO_x versus VOC emission reductions. However, the sensitivity of peak O_3 concentrations estimated by these tools is different, due to different characteristics of each tool and different quantity/approach used by these tools.

DDM and OSAT differ significantly in their assessment of the NO_x- versus VOC-sensitivity of O_3 chemistry. These differences result from the fact that OSAT does not account for negative contributions to O_3, whereas DDM accounts for negative sensitivities of O_3 to NO_x and VOC. As a result, OSAT tends to show discrepancies with DDM in cases where negative sensitivities play an important role. This is the case in areas that are VOC-sensitive because NO_x typically inhibits O_3 formation and O_3 shows a negative sensitivity to NO_x. In such cases, OSAT may even show a larger contribution of NO_x to O_3 compared to the VOC contribution because the NO_x contributions from upwind areas are not compensated by the NO_x inhibitions from local areas. Therefore, the cumulative contribution of NO_x to O_3 predicted by OSAT tends to be overestimated.

In Atlanta and Altoona, DDM tends to predict NO_x-sensitive O_3 concentrations, OSAT shows that O_3 concentrations are primarily contributed by NO_x emissions, and PA shows that O_x production under the NO_x-limited conditions is greater than that under the VOC-limited conditions. Therefore, all three probing tools provide results that are qualitatively consistent. It is expected that PA would predicte results that were consistent with those of DDM and OSAT in Atlanta and Altoona, because the effect of NO_x titration on O_3 formation was relatively small at both locations and the local emissions dominated O_3 chemistry in Atlanta. In addition, all three probing tools predict a spatial variability in the O_3 sensitivity to VOC and NO_x emissions among the individual grid cells and nine subareas in each of Chicago, New York City, and Altoona receptor regions.

In Chicago and New York City, DDM tends to predict VOC-limited O_3 concentrations. As discussed above, OSAT does not account for the NO_x inhibition of O_3 formation in the urban areas and as a result tends to predict greater NO_x contributions than VOC contributions in most cases. The discrepancy between DDM and OSAT

increases as the DDM VOC-sensitivity increases. Therefore, in its present formulation, OSAT should not be used to infer VOC-versus NO_x-sensitivity of O_3 chemistry in areas where negative sensitivities are likely to play a major role. OSAT could be modified to account for negative contributions (corresponding to negative sensitivities of DDM that are currently set to zero in the current OSAT formulation); one would expect that consistency between OSAT and DDM would then improve. In the updated version of OSAT, the apportionment of ozone production into VOC- and NO_x-sensitive portions is performed by defining:

$$F_{VOC} = \left[\frac{\partial O_3}{\partial VOC} + \left|\frac{\partial O_3}{\partial VOC}\right|\right] \Bigg/ \left[\frac{\partial O_3}{\partial VOC} + \left|\frac{\partial O_3}{\partial VOC}\right| + \frac{\partial O_3}{\partial NO_x} + \left|\frac{\partial O_3}{\partial NO_x}\right|\right]$$

$$F_{NOx} = \left[\frac{\partial O_3}{\partial NO_x} + \left|\frac{\partial O_3}{\partial NO_x}\right|\right] \Bigg/ \left[\frac{\partial O_3}{\partial VOC} + \left|\frac{\partial O_3}{\partial VOC}\right| + \frac{\partial O_3}{\partial NO_x} + \left|\frac{\partial O_3}{\partial NO_x}\right|\right] \qquad \text{(T-1)}$$

This can be modified to account for negative contributions as follows:

$$F_{VOC} = \left[\frac{\partial O_3}{\partial VOC}\right] \Bigg/ \left[\frac{\partial O_3}{\partial VOC} + \frac{\partial O_3}{\partial NO_x}\right]$$

$$F_{NOx} = \left[\frac{\partial O_3}{\partial NO_x}\right] \Bigg/ \left[\frac{\partial O_3}{\partial VOC} + \frac{\partial O_3}{\partial NO_x}\right] \qquad \text{(T-2)}$$

Alternative formulations would need to be tested for special cases where $\partial O_3/\partial VOC$ and $\partial O_3/\partial NO_x$ are equal or very close in magnitude but opposite in sign and where the net O_3 production equals zero or is very small.

PA, on the other hand, predicts that local O_x production is VOC-sensitive for some days but NO_x-sensitive for other days in Chicago and New York City. The PA results also identify the particular grid cells for which O_x production is inhibited by high NO_x concentrations. The results of PA and DDM differ in terms of sensitivity to VOC and NO_x because DDM predicts the effects of changes in emissions along the air parcel trajectories, whereas PA provides a mass budget explanation of the sensitivity of O_x production in the receptor region. However, the PA predictions of NO_x inhibited O_3 photochemistry in the base case for Chicago and New York are qualitatively consistent with the DDM predictions of NO_x disbenefits for these regions.

The Photochemical Reactivity of VOC Source Groups

Both DDM and OSAT provide quantitative information on VOC reactivities that, to some extent, can be compared. PA as implemented in CAMx, on the other hand, provides neither the incremental reactivity nor the O_3 productivity of VOC species or source groups.

The estimation of VOC photochemical reactivity from the OSAT results requires comparing O_3 contributions at different times (the peak O_3 hour and a "background" O_3 hour). In a 3-D simulation, changes in wind fields may result in significant changes in upwind source areas, thereby introducing uncertainties in the analysis. To assess this possible source of uncertainty, we used two distinct background O_3 hours and quantified the effect on the OSAT results. In most cases, the effect was negligible and our methodology was, therefore, justified. In some cases, the uncertainties were too significant for the methodology to hold, and we point those cases out below.

The set of top three photochemical reactivities predicted by DDM and OSAT are generally consistent in Chicago but are quite different in other receptor regions. In Atlanta, DDM predicts that the local biogenic emission group (i.e., B-15) has the largest incremental reactivity, while OSAT predicts that either the local surface or elevated anthropogenic emission group (i.e., S-15 or E-15) has the largest O_3 productivity. The ranking and magnitude of the O_3 productivity of the local elevated anthropogenic VOC group (i.e., E-15) are higher than its incremental reactivity. In Chicago, DDM predicts that the local biogenic source group (i.e., B-14) has the largest incremental reactivity while OSAT predicts that either the local biogenic or elevated anthropogenic or surface anthropogenic source group (i.e., B-14 or E-14 or S-14) has the largest O_3 productivity. In New York City, DDM predicts that either the local elevated anthropogenic or biogenic source group (i.e., E-16 or B-16) has the largest incremental reactivity while OSAT predicts that the local elevated anthropogenic source group (i.e., E-16) has the largest O_3 productivity. DDM predicts the upwind elevated anthropogenic VOC (i.e., E-11 or E-7) to be more reactive than the surrounding elevated anthropogenic VOC (i.e., E-13), whereas OSAT predicts just the opposite for all days except July 15. In Altoona, both DDM and OSAT predict that either the upwind or local elevated anthropogenic source

group (i.e., E-11 or E-17) has the largest incremental reactivity or O_3 productivity except for July 13 when OSAT predicts a negative O_3 productivity for the two VOC source groups. The O_3 productivity of local surface anthropogenic VOC source group (i.e., S-17) ranks higher than its incremental reactivity (e.g., the 2nd or 3rd by OSAT vs. the 6th or 7th by DDM).

Large discrepancies exist when either DDM or OSAT predicts negative reactivities. The negative O_3 productivities predicted by OSAT indicate that the air parcel trajectory changed significantly between midnight and the peak hourly O_3 time. For such cases, the calculated O_3 productivities may not be as accurate as for cases when the air parcel trajectory is similar between the reference time and the peak hourly O_3 time. When DDM predicts negative incremental reactivities, OSAT predicts large positive O_3 productivities. The discrepancy in DDM and OSAT predictions is due to the fact that the inhibition effect of some VOC emission groups on O_3 formation was accounted for by DDM but not by OSAT. Those VOC source groups may contain some anthropogenic VOC species such as xylenes, toluene, acetaldehyde and higher molecular aldehydes (ALD2), and a few biogenic VOC species such as olefins that may inhibit O_3 formation. The reactivity of VOC source groups may vary in magnitudes and mathematical signs with the levels of perturbations in VOC emissions (e.g., a small decrease in toluene emissions may increase O_3 formation due to less organic nitrate formation whereas a large decrease in toluene emissions may decrease O_3 formation due to lower precursor levels). The DDM predictions of the VOC reactivity are only accurate for small perturbations and may not be representative of large perturbations. The accuracy of the DDM and OSAT predictions of VOC reactivity for large perturbations (e.g., 75% reduction in VOC emissions) was not evaluated in this project and is recommended for future investigation.

DDM and OSAT predict a strong daily variability for local and surrounding VOC groups in Atlanta and Chicago and for both the local and upwind VOC groups in New York City and Altoona.

T.3 Complementarity

The three probing techniques considered here provide results that are different because of the design of the individual techniques but can be seen as complementary if they are used and interpreted properly. We discuss below the complementarity of these three techniques to address source attribution, the relative importance of local chemistry and long-range transport, detailed chemical analysis, and the model responses to changes in emission levels.

Source Apportionment

Both OSAT (dircetly) and DDM (approximately through linear sensitivities) can attribute O_3 to source groups based on geographic area and emissions category, whereas PA provides no source category specific information. While OSAT attributes total O_3 concentration to all source groups, DDM provides first-order sensitivity of O_3 to all source groups. OSAT can track a larger number of source groups than DDM because OSAT uses reactivity-weighted tracers, whereas the number of source groups and geophysical regions treated with DDM is limited by the associated computational burden. OSAT results are naturally interpretable as source apportionments because they are based on the proportional contribution of emissions to the O_3 forming process; namely, the sum of O_3 contributions from all source groups always equals the predicted O_3 concentration. However, OSAT may overestimate the contribution of some sources (e.g., surface anthropogenic sources) and underestimate the contribution of other sources (e.g., biogenic sources) because it does not account for the titration/inhibition effect of NO_x (or VOC) (i.e., the negative sensitivity) on O_3 chemistry. On the other hand, DDM correctly accounts for the negative feedback, but DDM sensitivities cannot be interpreted as source apportionments because the sum of all first-order sensitivities will not account for all of the O_3 concentration (it usually accounts for 60-65% of the total O_3 concentration)**;** therefore, DDM provides source contribution to a fraction of the O_3 concentration (60-65%). Note that it is this fraction that will be mainly affected by small to moderate changes in emission levels. Although the source contributions expressed in terms of the percentage of the sum of the first-order sensitivity of O_3 predicted by DDM are not

equivalent to those expressed in terms of the percentage of total O_3 concentration predicted by OSAT, a qualitative comparison between the DDM and OSAT source contributions was conducted to provide the relative importance of all source groups.

The spatial distributions of O_3 sensitivities/contributions to/of total NO_x and VOC emissions from four different source categories predicted by DDM and OSAT are generally consistent. The predicted source contributions by DDM and OSAT are very similar in Atlanta, but somewhat different in New York City and Altoona and significantly different in Chicago. The major differences in the DDM and OSAT predictions are that DDM predicts negative source contributions whereas OSAT always predicts positive contributions. In particular, DDM predicts a negative contribution for on-road mobile source and a relatively smaller contribution of other surface and elevated anthropogenic sources than OSAT in Chicago. This results in a much higher contribution from biogenic emissions predicted by DDM than OSAT in Chicago; i.e., 71% of O_3 first-order sensitivity in DDM (which is equivalent to 43% of total O_3 concentration) vs. 33% of total O_3 concentration in OSAT. The significant differences in the DDM and OSAT predictions are due to the fact that OSAT does not account for the titration effect of NO_x, thus overestimating the contribution of surface anthropogenic sources and underestimating the contribution of biogenic sources.

The OSAT source contributions and the DDM sensitivities are clearly related for specific source groups at each receptor. Correlations were calculated for each source group between the OSAT contributions and the DDM sensitivities calculated for each grid cell of a receptor area (only grid cells with $[O_3] > 80$ ppb were included). The correlation between the DDM and OSAT results is generally good with R^2 values of 0.7-0.96 for most source groups in all receptor regions. However, poor correlation is found for the on-road mobile, other surface anthropogenic, and elevated anthropogenic NO_x emissions in Chicago, New York City, and Altoona where the titration/inhibition effect of NO_x is important (i.e., there are large negative sensitivities for those source groups). The overall DDM predictions are lower than the arithmetic average of the DDM and OSAT results for most source groups (e.g., other surface anthropogenic VOC emissions and NO_x emissions from all source categories) with negative fractional biases. Those low DDM values indicate either an underprediction of DDM or an overprediction of OSAT,

depending on whether there are large negative sensitivities. For some source groups at some receptors (e.g., other surface anthropogenic VOC emission in Atlanta, New York City, and Altoona) for which DDM predicts positive or small negative sensitivities, the low DDM values indicate an underprediction by DDM, which is due to the fact that the sum of O_3 sensitivities only accounts for 60-65% of total O_3 concentrations. For some source groups at some receptors (e.g., NO_x emissions from on-road mobile and other surface and elevated anthropogenic sources in Chicago) for which DDM predicts large negative sensitivities, the low DDM values indicate a significant overprediction by OSAT, which is due to the fact that OSAT does not account for the titration/inhibition effects of NO_x emissions from those source categories.

Relative Importance of Chemistry and Transport

All three probing tools can provide some information on the relative importance of photochemistry vs. transport, but PA results are at different time and spatial scales than those of OSAT and DDM and are thus not directly comparable to those of OSAT and DDM. Both OSAT and DDM can predict the relative importance of local sources vs. sources in upwind locations (i.e., local photochemistry vs. transport) and allow one to resolve the impacts of surface and elevated point source emissions in separate geographic regions. While both OSAT and DDM reflect the time history of the air parcel at the receptor, PA can only provide local and instantaneous relative importance of photochemistry and transport (horizontal and vertical) on O_3 formation at a specific grid cell.

The relative importance of chemistry and transport predicted by DDM and OSAT in each of the four receptor regions is generally consistent. Atlanta is mostly affected by local photochemistry. The local and surrounding sources in Atlanta are overwhelmingly more important than upwind sources, contributing to 90% of the O_3 sensitivity by DDM and 86% of the O_3 concentration by OSAT. New York City and Altoona are strongly influenced by long-range transport of pollutants. In New York City, the local/surrounding and upwind sources contribute to 40% and 52% of the O_3 sensitivity by DDM and 37% and 52% of the O_3 concentration by OSAT, respectively. In Altoona, the upwind emissions contribute to 57% of the O_3 sensitivity by DDM and 58% of the O_3

concentration by OSAT. Both transport and photochemistry could be important to O_3 formation in Chicago. DDM predicts that both surrounding and upwind emissions are the most important sources, contributing to 38% and 40% of the O_3 sensitivity, while OSAT predicts that the local, surrounding, and upwind emissions are the most important sources, contributing to 34%, 28% and 27% of the O_3 concentrations, respectively.

PA, on the other hand, provides the relative importance of various processes including chemistry, lateral boundary transport, top boundary transport, and deposition to the local and instantaneous O_3 production. Although the results from PA cannot be directly compared to those from DDM and OSAT, they are somewhat qualitatively consistent with those from DDM and OSAT. For example, PA predicted that the peak hourly O_3 formation was affected mostly by chemistry in Atlanta and Chicago and that lateral transport was relatively more important in New York City and Altoona, as compared to Atlanta and Chicago. As expected, PA also predicted results that were inconsistent with those from DDM and OSAT. For example, DDM and OSAT predicted that upwind emissions contributed to 40% of the total O_3 sensitivity and 27.5% of the total O_3 concentrations at the peak O_3 hour in Chicago on July 15, whereas PA predicted a negative net effect of lateral transport for this receptor. These differences are due to the fact that DDM and OSAT accounted for the time history of the air parcels whereas PA provided information on local and instantaneous O_3 formation.

Detailed Chemical Analysis

PA is the only tool that provides detailed chemical analysis among the three probing tools implemented in CAMx. The Integrated Reaction Rate (IRR) component of PA is designed to elucidate important chemical pathways and to identify key chemical characteristics. The chemical process analysis outputs in CAMx provide information on O_x and NO_x budget and radical initiation, propagation, and termination. This information is particularly useful for investigating mechanistic differences under different chemical regimes or between different mechanisms. It is also useful to assess the spatial and temporal variability in the sensitivity of O_x and O_3 production to precursors and to investigate the relationships between O_3 and its precursors. A detailed chemical analysis was conducted for the base case simulation with the EPA 2007 emission inventory.

Model Responses to Changes in Inputs

Both OSAT and DDM can be used to predict model responses to changes in input parameters or variables such as ICs, BCs, and emissions, whereas PA does not have this capability. However, there is a major difference in characterizing the model responses to perturbations in inputs between OSAT and DDM. DDM is more directly applicable to predicting the response to changes in emissions because the sensitivity coefficients directly address this issue. This information is particularly useful in developing emission strategies in many non-attainment areas in the U.S. The main limitation of DDM is that first-order sensitivities are only representative of small changes for non-linear systems, and are not expected to be accurate for large changes that require higher-order derivatives to characterize the model response.

OSAT is less applicable to quantitative prediction of the response to changes in emissions because OSAT does not calculate sensitivity coefficients and the extrapolation of the OSAT results to a different emission scenario involves some assumptions by the user. The most likely assumption that the user will make is linearity, i.e., that OSAT source contributions will scale proportionately with emissions. Our evaluation shows that applying linear scaling to the OSAT results is reasonably accurate for small perturbations in VOC emission levels but less accurate for both small and large perturbations in NO_x emissions (see more detailed results in the next section). Therefore, caution should be taken when using the OSAT results to extrapolate from a base simulation to an emission scenario with a perturbation in NO_x emissions.

T.4 Stretchability

The responses of the three probing tools to variations in emissions and local chemical conditions were evaluated by conducting 12 CAMx sensitivity runs with each tool for 25% and 75% reductions in anthropogenic emissions of NO_x only, and a 25% reduction in anthropogenic emissions of VOCs only. The stretchability of each tool was tested by (1) evaluating the accuracy of DDM and OSAT results under small and large perturbations; (2) evaluating the consistency in NO_x- vs. VOC-sensitivity of the O_3

chemistry by the three tools under different emission scenarios; and (3) evaluating the changes in chemical signatures for the four receptors under the 75% emission reduction scenario. The first test was conducted by comparing the O_3 concentrations calculated by the DDM sensitivities from the base simulation with the actual O_3 concentrations predicted from the sensitivity simulations with 25% and 75% emission reduction scenarios, and testing the validity of the OSAT source attribution results under different emission scenarios. Our stretchability test results for DDM and OSAT show that both DDM and OSAT predict accurate model responses under the 25% VOC emission reduction scenario. For the 25% NO_x emission reduction scenario, DDM predicts accurate model responses, whereas OSAT predicts inaccurate model responses due to the fact that OSAT does not account for the effect of NO_x titration on O_3 formation. For the 75% NO_x emission reduction scenario, both DDM and OSAT predict inaccurate model responses, with less errors in the OSAT predictions than the DDM predictions.

For DDM, we tested whether the sensitivity coefficients can be used to predict the change in O_3 concentrations due to changes in emissions. The DDM results from the base case were used to estimate the O_3 concentration for an emission control case. The estimated O_3 concentration was then compared to the O_3 concentration simulated with the emission change. For most fine grid cells in all receptors, the O_3 concentrations calculated with the DDM sensitivity coefficients are higher than the O_3 concentrations simulated with perturbed emission levels, with small percent differences (< 9.5%) for a 25% reduction in anthropogenic VOC or NO_x emissions but large percent differences (up to 98.2%) for a 75% reduction in anthropogenic NO_x emissions. The magnitudes of the percent differences in the calculated and the simulated O_3 concentrations indicate that the DDM sensitivities are reasonably accurate for a 25% emission reduction scenario, but inaccurate for a 75% emission reduction scenario.

For OSAT, we tested both the sensitivity of the source contributions to changes in emission levels and the ability of OSAT to predict model response. In particular, we evaluated the validity of applying linear scaling to the OSAT source attribution results under different emission scenarios. The spatial distributions of the O_3 contributions predicted by OSAT are very similar to the base case for the 25% emission reduction scenarios but are quite different from the base case for the 75% anthropogenic NO_x

emission reduction scenario. As compared to the base case, the differences in the percent contributions of different source categories in the four receptors are within 4% for the 25% emission reduction scenarios but within 11% for the 75% emission reduction scenario. Those results show that the OSAT source attribution results are relatively stable for emission scenarios with a small perturbation (e.g., a 25% reduction in anthropogenic NO_x and VOC emissions) but different (as expected) for emission scenarios with a large perturbation (e.g., a 75% emission reduction).

The OSAT results from the base case were used to estimate the O_3 concentration for an emission control case. The estimated O_3 concentration was then compared to the O_3 concentration simulated with the emission change. For most fine grid cells in all receptors, the O_3 concentrations calculated with the OSAT source contributions are lower than the O_3 concentrations simulated with perturbed emission levels, with small percent differences (< 9.1%) for a 25% reduction in anthropogenic VOC emissions but large percent differences for 25% and 75% reductions in anthropogenic NO_x emissions (up to -31.9% and -45.3%, respectively). The large percent differences for 25% or 75% reductions in anthropogenic NO_x emissions are due to the fact that OSAT does not account for the effect of NO_x titration on O_3 formation. The magnitudes of the percent differences in the calculated and the simulated O_3 concentrations indicate that applying linear scaling to the OSAT results is valid with small errors for a case with a 25% reduction in anthropogenic VOC emissions, but less accurate for cases with a 25% or 75% reduction in anthropogenic NO_x emissions.

For a 25% anthropogenic VOC or NO_x emission reduction scenario, both DDM and OSAT predict a NO_x-limited O_3 chemistry in Atlanta and Altoona for all five days, but their predictions in Chicago and New York City are quite different. In Chicago and New York City, DDM predicts a VOC-limited O_3 chemistry on most days, whereas OSAT predicts a NO_x-limited O_3 chemistry on most days. The large discrepancies in predicting NO_x- vs. VOC-limited fraction of O_3 concentration are due to the fact that OSAT does not account for the titration/inhibition effect of NO_x on O_3 chemistry. For a 75% anthropogenic NO_x emission reduction scenario, all three probing tools predict a NO_x-limited O_3 chemistry for all the four receptors for all five days. The NO_x-limited

fractions predicted by the three tools are similar in Atlanta but somewhat different in Chicago, New York City, and Altoona.

The O_3 chemistry changed from VOC-limited for the base emission case to NO_x-limited for a 75% anthropogenic NO_x emission reduction scenario for all days in Chicago and for some days in New York City. In addition, there are large differences in the NO_x-limited percentages predicted by the base emission and the 75% emission reduction scenarios in Atlanta and Altoona. Those changes and differences were caused by changes in the initiation, propagation, and termination of radical species and the subsequent changes in the mass budget of O_x and NO_x.

T.5 Comparison of the Results from CRC Projects A-29 and A-37

In a separate CRC project A-29, the results of DDM and the original version of OSAT were compared in terms of the ranking of the top 5 O_3 contributors, the correlation between the two sets of results, the relative importance of the source categories, and the spatial distributions of DDM sensitivities and OSAT source contributions for the Lake Michigan region for the O_3 episode of July 7-13, 1995 (Dunker et al., 2002b). The comparison between the results of DDM and the updated version of OSAT conducted in this project included all aforementioned components and was more comprehensive than that of CRC project A-29. The results from this project are generally consistent with those from CRC project A-29 in terms of the ranking of the top 5 O_3 contributors and the spatial distributions of DDM sensitivities and OSAT source contributions. There are three major differences in the results from the two projects:

- CRC Project A-29 reported that the original version of OSAT predicted a small and positive source contribution (0.3-2.6 ppb) for receptors where DDM predicted a large negative sensitivity (-33 ppb) to anthropogenic area-source NO_x emissions (e.g.,Chicago area). However, it was found in this project that in those regions where NO_x significantly inhibited O_3 formation (with negative sensitivities of -40 to -10 ppb), the updated version of OSAT

predicted much larger positive source contributions (10 to 25 ppb) than those reported in CRC Project A-29.

- A consistently good relation between the DDM sensitivities and OSAT source contributions for all the cases (with R^2 values of 0.8-0.98) was found in CRC Project A-29, whereas, in this project, poor correlation (with R^2 values as low as 0.02 to 0.33) was found for some source categories (e.g., on-road mobile, other surface anthropogenic, and elevated anthropogenic NO_x emissions) at some receptors (e.g., Chicago) where the titration/inhibition effect of NO_x is important (i.e., there are large negative sensitivities for those source groups).
- There are some inconsistencies or even conflicts regarding the relative importance of some source categories (e.g., biogenic VOC, elevated point-source NO_x emissions) predicted by DDM and OSAT between the two projects. For example, CRC project A-29 predicted that the original version of OSAT ascribes greater importance to biogenic VOC emissions than does DDM and DDM ascribes greater importance to point-source NO_x emissions than does OSAT. The relative importance of biogenic VOC and point-source NO_x emissions predicted by DDM and the updated version of OSAT in this project was just the opposite of that predicted from CRC project A-29, namely, DDM ascribes greater importance to biogenic VOC emissions than does OSAT and OSAT ascribes greater importance to point-source NO_x emissions than does DDM. Those inconsistencies indicate that the predicted relative importance of those source categories is sensitive to the selected locations of receptors and the episode simulated and may be different from case to case.

T.6 Computational/Implementation Requirements

The simulations with CAMx and PA impose minimal computational burden on the top of the base case simulation with CAMx only, whereas the simulations with CAMx and OSAT (or its associated techniques such as APCA and GOAT) and DDM require a significant increase in memory and CPU time. In particular, a single DDM run

to provide sensitivity information that is comparable to that from OSAT requires much more memory (about 2.3 GigaBytes vs. 325 MegaBytes) and CPU times (greater by a factor of 3-6) than the OSAT run and has to be split into several small runs.

The development and implementation of each of the three probing tools impose several challenges that are either common (e.g., accuracy, CPU cost, and interface) or unique (e.g., the size of the outputs for PA, the source-receptor relationships for OSAT, and the optimization of the efficiency and accuracy of the sensitivity calculation for DDM) to those tools.

1. INTRODUCTION

A number of probing techniques have been developed during the past several decades to (1) provide diagnostic analyses of air quality models in order to understand the internal processes that govern model performance and/or (2) provide information on the response of the model output (here, ozone, O_3, concentrations) to changes in model inputs (e.g., emissions of O_3 precursors). Providing insights into the model and the modeled processes, these tools enable a deeper understanding of the model dynamics than what the typical model outputs can elucidate (typical model outputs consist of model species concentrations and deposition fluxes as a function of time or location). Probing tools can be organized into two major groups:

- Mass balance analysis techniques
- Sensitivity analysis techniques

Mass balance analysis provides quantitative information on the contribution of the various processes (e.g., transport and chemical reactions) to the modeled ambient concentrations, whereas sensitivity analysis provides quantitative information on the response of these concentrations to changes in the air pollution system. Since O_3 concentrations are a non-linear function of their precursors, mass balance analysis and sensitivity analysis will provide different types of information on the air quality modeling system.

Mass balance techniques are appropriate for diagnostic evaluations of the air quality models (i.e., to identify which chemical transformation pathways and which physical transport processes govern O_3 concentrations). However, since mass balance analysis techniques cannot provide a quantitative measure of the response of O_3 concentrations to changes in emission levels for a non-linear air pollution system, it is not possible *a priori* to know how well a mass balance analysis technique can approximate that response. Mass balance analysis techniques are useful to identify which sources contribute to O_3 concentrations but are generally not accurate to characterize how these concentrations will respond to changes in emission levels (Seigneur et al., 1999).

Therefore, mass balance techniques should primarily be used as screening methods for source attribution.

Examples of mass balance analysis techniques include the Counter Species Method (CSM) (Leone and Seinfeld, 1984); the Ozone Assignment Method (OAM) (Bowman and Seinfeld, 1994a); the Geographic Ozone Assessment Technology (GOAT) (Yarwood et al., 1997); the Ozone Precursor Participation Assessment Technology (OPPAT) (Yarwood et al., 1997); the Threaded Source Apportionment Modeling System (TSAMS) (Deuel et al., 1997); the Process Analysis (PA, combining both the Integrated Process Rate Analysis (IPR) and the Integrated Reaction Rate Analysis (IRR), Tonnesen, 1990; 1995; Jang et al., 1995; Wang and Jeffries, 1999; Tonnesen and Dennis, 2000a, b); the original Ozone Source Apportionment Technology (OSAT) (Yarwood et al., 1996; 1997); and the Anthropogenic Precursor Culpability Assessment (APCA) (Yarwood et al., 1997). OSAT was recently modified to use information from a sensitivity analysis technique (DDM). However, it only uses DDM information to perform an attribution of O_3 production between NO_x and VOC and, consequently, it must still be viewed as a mass balance technique.

Many of the mass balance analysis techniques are designed to identify the origin of O_3 precursors and assign the O_3 being formed to its precursors. It must be noted that a source apportionment for O_3 is not unique. Different methods will likely produce different results because the formation of O_3 is a nonlinear function of emissions of its precursors. Therefore, some ambiguity must be expected when comparing different methods.

Among mass balance techniques, PA and OSAT are representative mass balance analysis techniques with several complementary features. PA is the most comprehensive mass balance analysis approach, providing information regarding the contribution of both chemical transformation and physical transport processes to pollutant concentrations. Figure 1-1 illustrates important components of the chemical processes that control the photochemical formation of O_3. These include the following: photolysis or decomposition reactions that produce new radicals, where the family of radical species is defined as HO_x=OH+HO_2+RO_2; a sequence of propagation reaction in which HO_x and NO_x catalyze the production of O_3; NO_x and HO_x termination reactions that reduce or

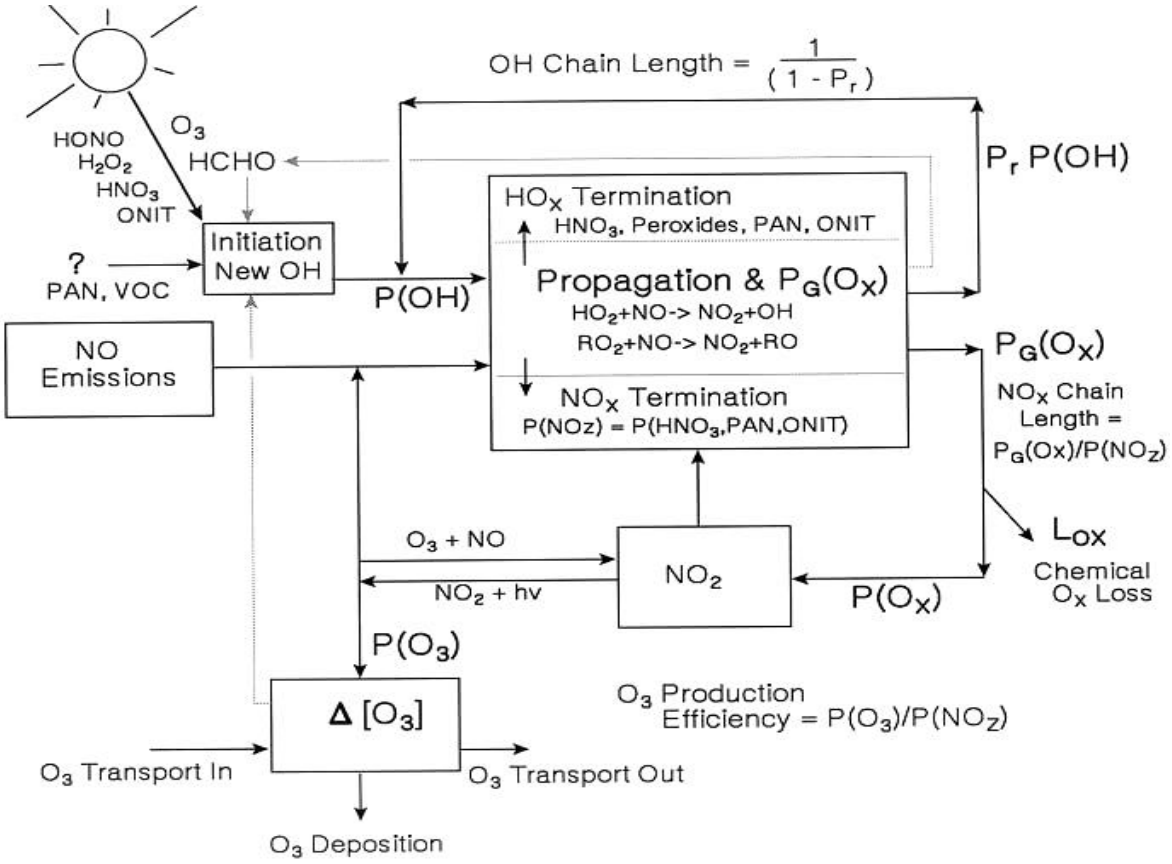

Figure 1-1. Process diagram illustrating important diagnostics for characterizing photochemical production of O_3.

stop the production of O_3; and the relationship between production of odd oxygen (O_x) (defined as $O_x = O_3 + NO_2 + O(^3P) + O(^1D) + 2\ NO_3 + 3\ N_2O_5 + PAN + HNO_4$) and O_3. Table 1-1 lists the chemical process analysis (CPA) outputs that are currently available in the CAMx model and that represent most of the processes illustrated in Figure 1-1. The CAMx model can be easily modified to include other model outputs as needed.

OSAT is a source apportionment approach, providing information on the sources that contribute to the concentration of O_3. OSAT also includes a methodology for diagnosing the temporal relationships between O_3 and emissions from groups of sources. OSAT uses multiple tracer species (called "O_3 reaction tracers") to track the fate of O_3 precursor emissions (VOC and NO_x) and the O_3 formation caused by these emissions within a simulation. The tracers operate as spectators to the normal CAMx calculations so that the underlying CAMx predicted relationships between emission groups (sources) and O_3 concentrations at specific locations (receptors) are not perturbed. A source group can be defined in terms of geographical area and/or emission category. All O_3 and precursor concentrations are attributed among the selected source groups at all times.

These two techniques are different in several aspects. First, OSAT is a method that runs forward in time with the host model. PA is a method for analyzing model results at fixed times, or if detailed information for each model time step is saved in a "history list", PA can be run backward in time by post-processing the history list (The history list method is extremely resource demanding for grid models and, therefore, is not being implemented for the CAMx version of PA). As a consequence of the forward methodology, OSAT can provide source apportionment information simultaneously for the whole grid system, whereas the application of PA to the whole grid system is largely limited by the computer storage space. Second, OSAT can predict the relative importance of local sources vs. sources in upwind locations to O_3 formation at a specific receptor, accounting for the time history of the air parcel. In contrast, PA provides the instantaneous relative importance of photochemistry, transport, and deposition to local O_3 formation occurring at that specific receptor. Third, OSAT cannot provide detailed chemical analysis, whereas PA can provide relative contributions of individual physical and chemical processes and chemical characteristics for pre-selected receptor/source

Table 1-1. Chemical process analysis outputs in CAMx for the CBM-IV mechanism.

O_x Budget
O_x Chemical Production
O_x Chemical Destruction
Radical Initiation
New OH from O^1D+H_2O
New OH from H_2O_2, HNO_3, HONO, PAA, OP1, OP2, O_3+HC (except isoprene)
New HO_2 from HCHO
New HO_2 Production (Total)
New RO_2 Production (Total)
New HO_x (including OH, HO_2 and RO_2) from isoprene
Radical Propagation
sum of OH+CO and OH+CH_4 reactions
OH+ISOP
isoprene reactions with O_3, NO_3 and O_3P
OH reacted with VOC
other OH propagation reactions (e.g., OH+SO_2)
Total HO_2 Production
Total RO_2 Production
NO_2 produced from reactions of HO_2
OH produced from reactions of HO_2
NO_2 produced from reactions of RO_2
Total OH production
Radical Termination
OH termination
HO_2 termination
RO_2 termination
NO_x Termination (or Production)
OH+NO_2 $\rightarrow$ HNO_3
NO_3+HC $\rightarrow$ HNO_3
N_2O_5+H_2O $\rightarrow$ 2 HNO_3
HNO_3 reacted (to produce NO_x)
net PAN Prod
net PAN Loss (source of NO_x and a radical)
production of organic nitrates

locations. Recognizing these differences in the two mass balance techniques, it is complementary to conduct a systematic assessment for both PA and OSAT.

To obtain quantitative information on the response of O_3 concentrations to changes in the emission levels, sensitivity analysis techniques must be used. That information can be used to understand which model parameters and input variables are the most influential for the model output. It can also be used in combination with specific perturbations in the model parameters or input variables to estimate the effect of those perturbations on the model output. Such perturbations can represent, for example, a change in emission levels for specific sources and pollutants or a measure of the uncertainty associated with the model parameters and input variables. Superior to mass balance techniques in that respect, sensitivity analysis techniques can represent the non-linear system. For example, a mass balance analysis technique may identify that NO_x emissions from a source category contribute to a high concentration of O_3. However, the changes in O_3 may not be proportional to the changes in NO_x emissions. This non-linearity can be characterized by the use of a sensitivity analysis technique.

Examples of sensitivity analysis techniques include the Decoupled Direct Method (DDM) (Dunker, 1981, 1984; Milford et al., 1992; Gao et al., 1995; and Yang et al., 1997); the Automatic Differentiation in FORTRAN (ADIFOR) (Carmichael et al., 1997; Zhang et al., 1998); the variational techniques (Koda et al., 1979; Gautier et al., 1985); the perturbation theory (Marchuk, 1975; Uliasz, 1983); the Green's function techniques (Dougherty et al., 1979; Demilrap and Rabitz, 1981; Cho et al., 1987; Vuilleumier et al., 1997); the indirect method (also known as the brute force method or single-perturbation method, e.g., Seigneur et al., 1981; Sillman et al., 1990; Milford et al., 1994); the Fourier amplitude sensitivity test method (Koda et al., 1979; Falls et al., 1979; Tilden and Seinfeld, 1982); and the stochastic methods (Costanza and Seinfeld, 1981; Shorter and Rabitz, 1997; Chen et al., 1997; Tatang et al., 1997; Pun, 1998).

To date, the only local sensitivity analysis technique that has been applied to 3-D air quality models is DDM. If the system is non-linear, sensitivities predicted by DDM are accurate for small changes (e.g., about 40% perturbations) but inaccurate for large changes (e.g., perturbations on the order of 40% or more) (Dunker et al., 2002a). The

quantitative definition of a small change depends on the non-linearity of the air pollution system and varies for each air pollution system.

The three probing tools that are evaluated here are the updated version of OSAT, DDM, and PA. Compared to the old version of OSAT, three major improvements have been made in the updated version of OSAT. First, the local sensitivity to VOC and NO_x calculated by DDM [instead of the ratio of the actual instantaneous production rates of H_2O_2 and HNO_3 ($P_{H_2O_2}/P_{HNO_3}$)] is used as an indicator of NO_x- or VOC-sensitive chemistry and ozone production is allocated in proportion to those DDM sensitivities in each grid cell at each time step. It is important to note, however, that there is a significant difference with the standard application of DDM. In the OSAT implementation, negative sensitivities that represent the fact that a reduction in a precursor (NO_x or VOC) leads to an increase in O_3, are not used. Instead, a negative sensitivity is interpreted as a zero contribution and O_3 production is attributed by default totally to the other precursor. Second, several chemical destruction pathways for O_3 (i.e., O^1D + water; HO_x + O_3; $O(^3P)$ + VOC; O_3 + VOC) are explicitly accounted for in calculating O_3 tracers. Third, the apportionment of VOC- sensitive ozone production has been modified to be based on maximum incremental reactivity (MIR) factors (instead of the reactivity of VOCs using OH rate constants). The MIR approach was developed by Carter (1994) to approximate the ozone forming potential of VOCs accounting for both kinetic and mechanistic reactivity effects. Compared to their earlier versions, the updated version of APCA incorporates the same improvements as the updated version of OSAT and the updated version GOAT incorporates the chemical destruction pathways for O_3. The three representative probing tools (i.e., OSAT, DDM, and PA) are now available within one modeling system, i.e., the Comprehensive Air Quality Model with extensions (CAMx). A detailed technical description of the three probing tools can be found in CAMx User's Guide (ENVIRON, 2000; Yarwood, 2001).

In this report, the three probing tools are evaluated for the July 7-15 1995 OTAG episode. The modeling domain and episode are described in Chapter 2. The selected receptors and their characteristics are provided in Chapter 3. The design of the base and sensitivity simulations and post-processing of the simulation results are described in

Chapters 4 and 5, respectively. A comprehensive evaluation of DDM, OSAT and PA is provided in Chapter 6.

2. MODELING DOMAIN AND EPISODE

The OTAG modeling domain was used as a test bed for these probing tools because it encompasses a range of atmospheric chemical and dynamic conditions (e.g., it includes cities that are either VOC- and NO_x-sensitive) and because it is probably the most widely used photochemical modeling database to date (e.g., it has been extensively studied by EPA, the States, and stakeholders). Figure 2-1 shows the OTAG modeling domain. The July 7-15, 1995 OTAG episode was simulated using CAMx with DDM, OSAT, and PA. A number of base case simulations with an EPA 2007 base emission scenario and sensitivity simulations with different emission scenarios were conducted for this episode. For applications of DDM and OSAT, the OTAG modeling domain was divided into 17 geographic source areas, as also shown in Figure 2-1. For each source area, three different emission categories (biogenic, surface anthropogenic, and elevated anthropogenic emissions) were considered in DDM base runs. To quantify the contribution of on-road mobile sources, the surface anthropogenic emission category was further split into two emission categories (on-road mobile and the other surface anthropogenic emissions) for the OSAT base run with 17 source areas and one DDM base run with one region-wide source area over the domain. A description of the base and sensitivity simulations is provided in Section 4.

The computational burden could be too significant to conduct all these simulations for the full duration of the episode and the complete geographic domain. This is particularly true for DDM simulations. We therefore applied two strategies to reduce the computational burden:

- Using a coarse grid for spin-up days.

  For the spin-up days of July 7-10, we ran CAMx with the coarse grid. This reduced CPU time by about 80% on these days while still providing good model spin-up. The fine grid was started on July 11 by initializing the fine grid cells with concentrations from their parent cells in the coarse grid. This capability is automatic in CAMx3, and has been used successfully in CRC

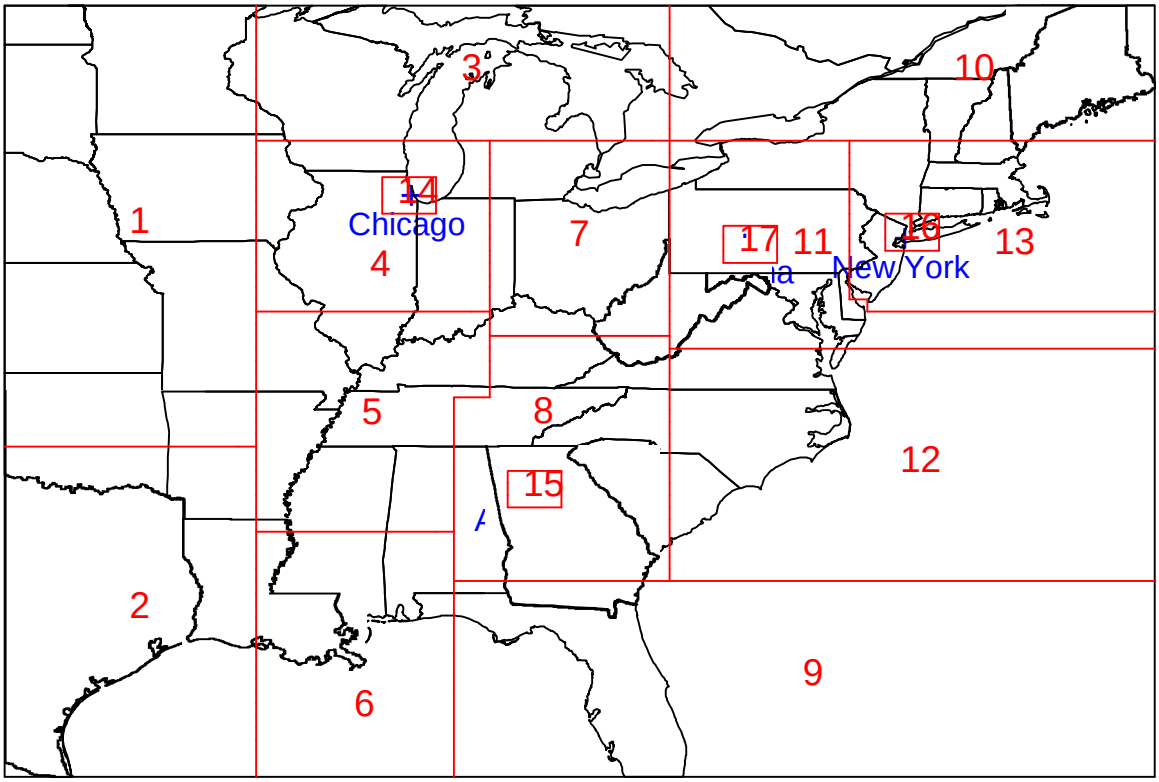

Figure 2-1. The geographic source areas for application of OSAT and DDM probing tools in the OTAG modeling domain.

project A-29 to evaluate the DDM results with the LADCO Grid M domain for the Midwest. The simulation stopped at the end of July 15. The 5-day simulation with a fine grid captured the heart of the episode (July 11-15) with the highest O_3 concentrations and provided several high O_3 days for analysis at each selected receptor.

- Conducting a species-breakout (i.e., VOC vs. NO_x) sensitivity calculation for subareas within the OTAG domain for the DDM simulations.
  We first conducted two base DDM simulations to calculate the sensitivity of O_3 concentrations to the emissions of VOC and NO_x from all three emission categories in a subarea that includes 11 source areas and covers the core of the OTAG modeling domain. We then conducted another base DDM simulation to obtain the sensitivity of O_3 concentrations to total precursor emissions (i.e., no VOC vs. NO_x breakout) for all three emission categories in the remaining 6 source areas along the boundary of the domain plus ICs and BCs. A detailed description for these DDM simulations is provided in Section 3.

These strategies permitted more complete testing and evaluation by allowing more simulations and focusing the analyses on high O_3 days.

The most current 2007 emission inventory available from EPA was used as the base emission scenario. 25% anthropogenic NO_x or VOC emission reduction scenarios and 75% anthropogenic NO_x emission reduction scenarios were simulated in the sensitivity study.

3. SELECTION OF RECEPTORS

Our rationale for selecting receptors is based on the need to cover a wide range of atmospheric conditions conducive to O_3 formation in the modeling domain. O_3 formation strongly depends on ambient meteorological and chemical conditions. Conditions with high O_3 precursor concentrations, high insolation, high stability, high RH, medium to high temperature, and low winds are likely conducive to O_3 formation. An additional consideration in selecting a rural site is that the selected rural site has been in attainment under the 1-hr O_3 National Ambient Air Quality Standard (NAAQS) but nonattainment under the 8-hr O_3 NAAQS in recent years. Chameides et al. (1997) have shown that the 8-hr O_3 NAAQS will increase the number of nonattainment rural sites from 6 to 41 out of the 85 sites from the Southern Oxidants Study Spatial Ozone Network (SOSSON) and the EPA Clean Air Status and Trends Network (CASTNet) in the eastern US. Analysis of CAMx simulation results at such a nonattainment rural receptor will provide useful information on governing processes in 8-hr O_3 concentrations and the most effective emission reduction strategies in nonattainment rural areas. Based on these considerations, we have selected four geophysical locations (receptors) for detailed assessments. These locations include three urban receptors (Atlanta, GA; Chicago, IL; and New York City, NY) and one rural receptor (Altoona, PA). Each of these regions exhibits a distinct O_3 air quality problem in terms of precursor concentrations, emissions, and meteorology.

Atlanta, GA presents a unique ambient condition representative of the southeastern U.S. The summer in this area is characterized by (1) a high frequency of air mass stagnation, warm temperatures, high humidities, and intense solar insolation; (2) a dense vegetation which, when coupled with the high summertime temperatures, results in large emissions of isoprene (that dominate VOC reactivity) and other natural hydrocarbons; and (3) an anthropogenic emission mix dominated by cities and large point sources (e.g., several power plants) located in rural areas (Cowling et al., 1998). The stagnant and hot summer climatology inhibits the dispersion of pollutants and favors the accumulation of O_3 precursors near the ground. The high biogenic emissions make the

O_3 formation generally NO_x-sensitive during summertime (Pun et al., 2001a). The VOC emission inventory reflects a different mix of anthropogenic/biogenic emissions.

Chicago, IL represents a case in the midwestern U.S. with a high temperature, a medium RH, and a VOC-sensitive chemistry in the summertime (Milford et al., 1994; Sillman, 1995; Pun et al., 2001a). Local sources such as fuel combustion and food/agriculture industries are major sources of O_3 precursors in this area.

New York City, NY represents a northeastern location, where the climatology is characterized by warm temperatures and high RH, coupled with pollutant transport along the axis of major source areas. It presents a fairly high ratio of VOC to NO_x emission rates among the areas considered here. The biogenic emissions are not as high as those in Atlanta but are higher than those in the other selected receptor areas. These features result in both NO_x-sensitive and VOC-sensitive chemistry in this region (Milford et al., 1989; Sillman, 1995; OTAG, 1998).

Altoona, PA is a rural site with a population of about 52,000. It is generally downwind of the Detroit, Chicago, and Ohio River Valley source areas while being upwind of New York City. During the 1995 OTAG episode, Altoona may be on the transport path between two of our selected urban receptors, Chicago and New York. Altoona has been in attainment of the 1-hr O_3 NAAQS (e.g., the 4^{th} highest 1-hr O_3 concentrations over three-year periods were 88-111 ppb during 1995-2000), however, it had an 8-hr O_3 problem (e.g., the 4^{th} highest 8-hr O_3 concentration was 90 ppb during 1995-1997) during the past few years.

The selected four receptors provide contrasts for NO_x vs. VOC sensitivity (e.g., Atlanta vs. Chicago), long range transport (LRT) of O_3 vs. dominant local sources (New York City/Altoona vs. Atlanta/Chicago), anthropogenic vs. biogenic sources (New York City/Chicago vs. Atlanta), and urban vs. rural areas (New York City/Chicago/Atlanta vs. Altoona).

4. DESIGN OF BASE AND SENSITIVITY SIMULATIONS

We conducted a number of base case and sensitivity simulations to evaluate the capabilities of the selected probing tools. The CBM-IV gas-phase mechanism was used in all CAMx base and sensitivity simulations. These simulations provided information on:

- Contributions from 17 geographic source areas (see the map in Figure 2-1)
- Contributions from 4 different emission categories (biogenic, on-road mobile, other surface anthropogenic, and elevated anthropogenic emissions) for the 17 source areas
- Region-wide contributions from 4 different emission categories (biogenic, on-road mobile, other surface anthropogenic, and elevated anthropogenic emissions)
- Contributions from initial conditions (ICs) and boundary conditions (BCs).
- Contributions of VOCs and NO_x emissions to O_3 formation
- Contributions of separate modeled processes to species concentrations
- Relative importance of different chemical processes in O_3 formation
- Sensitivity of O_3 formation and source apportionment to different emission reduction scenarios

The designed simulations are listed in Table 4-1, and discussed below. All these simulations were conducted over the OTAG domain with two grids: a fine grid with a horizontal resolution of 12 km x 12 km and a vertical resolution of 7 non-uniformly-space layers from ground level up to 4 km and a coarse grid with a horizontal resolution of 36 km x 36 km and a vertical resolution of 5 non-uniformly-space layers from ground level up to 4 km. Both grids were run in a single simulation with two-way nesting. The meteorological fields were obtained by running the Regional Atmospheric Modeling System (RAMS) simulations with three nested grids (108 km x 108 km, 36 km x 36 km, 12 km x 12 km). The RAMS simulations were nudged to observations using four-dimensional data assimilation (FDDA).

Table 4-1. Description of base and sensitivity simulations with CAMx and probing tools.

Simulation	Description
Base Case	
B1 [1]	OSAT with 17 source areas x 4 source categories plus ICs and BCs. O_3 attributed to VOC and NO_x in each source group.
B2 [2,3]	DDM with 11 source areas x 3 source categories.
B2N	O_3 sensitivity to NO_x from each source group.
B2V	O_3 sensitivity to VOC from each source group.
B3 [2, 4]	DDM with 6 source areas x 3 source categories plus ICs and BCs. O_3 sensitivity to all species from each source group.
B4 [2]	PA information extracted for 4 receptor regions (Atlanta, Chicago, New York, and Altoona) plus output of all gridded PA variables calculated within CAMx.
B5 [1]	APCA - Same configuration as B1.
B6 [1]	GOAT - Same configuration as B1.
B7 [1,5]	DDM with 1 source area x 4 source categories. O_3 sensitivity to VOC and NO_x from each source group.
25% Anthropogenic VOC Emissions Reduction	
S1 [1]	OSAT - Same configuration as B1
S2 [2, 3]	DDM with 11 source areas x 3 source categories.
S2N	O_3 sensitivity to NO_x from each source group.
S2V	O_3 sensitivity to VOC from each source group.
S3	PA - Same configuration as B4
25% Anthropogenic NO_x Emissions Reduction	
S4 [1]	OSAT - Same configuration as B1
S5 [2, 3]	DDM - Same configuration as S2
S5N	O_3 sensitivity to NO_x from each source group.
S5V	O_3 sensitivity to VOC from each source group.
S6	PA - Same configuration as B4
75% Anthropogenic NO_x Emissions Reduction	
S7 [1]	OSAT - Same configuration as B1
S8 [2, 3]	DDM - Same configuration as S2
S8N	O_3 sensitivity to NO_x from each source group.
S8V	O_3 sensitivity to VOC from each source group.
S9	PA - Same configuration as B4

1. The 17 source areas for B1, B5, B6, S1, S4, and S7 are shown in Figure 2-1. The 4 source categories for B1, B5, B6, B7, S1, S4, and S7 are biogenic (Bio), on-road mobile, other surface anthropogenic (anthro) and elevated anthropogenic emissions.
2. The 11 source areas for B2, S2, S5, and S8 are 4, 5, 7, 8, 11, 12, 13, 14, 15, 16, and 17 as shown in Figure 2-1. The 3 source categories for B2, B3, S2, S5, and S8 are biogenic, surface anthropogenic, and elevated emissions.
3. For DDM, sensitivity to VOC will be defined to include CO.
4. The 6 source areas for B3 are 1, 2, 3, 6, 9, and 10 as shown in Figure 2-1.
5. The 1 source area for B7 is the region-wide area as shown in Figure 2-1.

Base case simulations (B1-B7)

Eight base case simulations with the EPA 2007 base case emission scenario were conducted for the selected probing tools. In the single OSAT run (B1), four emission categories (biogenic, on-road mobile, other surface anthropogenic, and elevated anthropogenic emissions) from 17 source areas were included. B1 gives O_3 attributed to VOC and NO_x in each source group (a group is an area/category combination, so there are 4 x 17 = 68 groups in total) plus O_3 from ICs and BCs. The computational burden for this level of analysis is not great (see Table 6-50), and OSAT is generally applied with greater source category resolution. However, the design of the OSAT run is matched here to the level of analysis that is feasible with DDM.

A single DDM run to provide a comparable sensitivity information would require much more memory (about 2.3 GigaBytes vs. 325 MegaBytes) than the OSAT run and is not practical. However, three complementary DDM simulations (B2N, B2V, and B3) provide almost as much information, and are sufficient for this study. Simulations B2N and B2V provide sensitivity to NO_x and VOC, respectively, from three emission categories (biogenic, surface anthropogenic, and elevated anthropogenic emissions) in the 11 source areas that cover the core of the domain (i.e., source areas 4, 5, 7, 8, 11, 12, 13, 14, 15, 16, and 17). Simulation B3 supplements simulations B2N and B2V with sensitivity to total emissions (i.e., no VOC vs. NO_x breakout) for the three emission categories in the remaining 6 source areas along the boundary of the domain (i.e., source areas 1, 2, 3, 6, 9, and 10) plus ICs and BCs. The results from B3 are used to analyze distant vs. local O_3 production. Note that the surface anthropogenic sources used in DDM base simulations (B2N, B2V, and B3) include both the on-road and the other surface anthropogenic sources that are used in the OSAT base simulation (B1). Simulation B4 provides all available process analysis information for key receptor areas (process rates and reaction rates) plus gridded outputs of PA variables calculated within CAMx (OH chain length, etc.) for the entire domain. This level of process analysis imposes minimal computational burden on top of the base case simulation.

Simulations B5 and B6 provide the results from two alternate OSAT options called APCA and GOAT, thereby providing a comparison of these methods for the technical guidance document and journal article to be prepared in Task 4. APCA has been used extensively in prior CAMx studies, such as the assessment of the contribution of industrial and other source sectors to O_3 exceedances in the eastern U.S. (Morris et al., 1998). An interesting feature of GOAT is that it is directly equivalent to the way process analysis has been used previously to back-track through history lists to find the grid cell in which O_3 was formed by chemistry. This is the closest process analysis that has come to geographic O_3 source apportionment. GOAT does not require any information about O_3 precursors or VOC/NO_x sensitivity.

Simulation B7 provides the sensitivity of region-wide O_3 formation to region-wide VOC and NO_x from four emission categories (biogenic, on-road mobile, other surface anthropogenic, and elevated anthropogenic emissions) and region-wide source category contributions to O_3 formation at the selected receptors.

Sensitivity simulations (S1-S9)

A total of 12 sensitivity simulations (S1 through S9 with two separate runs for S2, S5, and S8) were conducted for the three probing tools (i.e., OSAT, DDM, and PA) with three different emission reduction scenarios:

- 25% reduction in anthropogenic VOC emissions
- 25% reduction in anthropogenic NO_x emissions
- 75% reduction in anthropogenic NO_x emissions

A 25% reduction in anthropogenic VOC or NO_x emissions represents a moderate level of perturbation. It is chosen mainly because DDM is a local sensitivity analysis method and it provides first-order sensitivity coefficients that are only accurate for small changes for a non-linear system of O_3 formation. A 75% reduction in anthropogenic NO_x emissions represents a high level of perturbation that will likely change the O_3 chemistry from VOC-limited to NO_x-limited regime at specific receptors. It therefore provides a

stretchability test for each probing tool for a large perturbation in emissions and possible changes in local chemical conditions. Both OSAT and DDM can be used to predict model responses to changes in input parameters or variables, whereas PA does not have this capability. Since both OSAT and DDM provide information local to the base case, extrapolation to a different emission scenario involves some assumptions by the user. The most likely assumption is linearity; i.e., that DDM first-order sensitivities will provide an adequate description and that OSAT source contributions will scale linearly with emissions. If the system is non-linear, sensitivities predicted by DDM are accurate for small changes (i.e., about 40% perturbations) but inaccurate for large changes (Dunker et al., 2002a). The range of perturbations for which the linear scaling of the OSAT results is valid will be determined in this project with the 25% and 75% emission reduction scenarios for the non-linear system of O_3 formation.

The configurations for the OSAT and PA sensitivity simulations were identical to the base cases because these simulations require relatively little CPU time. The configuration for DDM sensitivity simulations S2, S5, and S8 was the same as for simulation B2**.** Each of them was split into two separate runs: S2N, S2V, S5N, S5V, S8N, and S8V.

5. POST-PROCESSING OF THE SIMULATION RESULTS

The results from the aforementioned simulations were post-processed to produce graphics, tables, and charts that can be directly used for the systematic assessment of the probing tools and the preparation of the final report, guidance document, and journal article. The technical focus of the assessment was O_3 formation. The hourly results at the four selected receptors for several days with high O_3 concentrations were analyzed and interpreted. The detailed data output format and graphics and analyses are described below.

All three probing tools provided both gridded output files and receptor specific output files[1] from all simulations. The gridded output files from DDM and OSAT are extremely large and are generally post-processed in some form for display and analysis. In contrast, the receptor files are more compact and easy to work with, and provide an extremely rich database for analysis and interpretation.

The receptor regions selected for detailed analyses are Atlanta, Chicago, New York City, and Altoona. Consistent receptor definitions were used to output information from each probing tool. We defined several grid cells and grid cell combinations in each receptor region to capture both high emission density regions (downtown) and the downwind peak O_3 locations. In particular, we defined 9 aggregated coarse grid cells with a horizontal grid resolution of 36 km x 36 km for each receptor region. Each coarse grid cell is composed of 9 fine grid cells with a horizontal grid resolution of 12 km x 12 km. The CAMx standard results and the results from each probing tool were written in the output files for the 9 coarse grid cells and the 81 fine grid cells for each receptor region. The average concentrations, sensitivities, and the PA results were written out for major species including NO, NO_2, O_3, PAR, TOL, ETH, OLE, PAN, ISOP, XYL, FORM, ALD2, HNO_3, N_XO_Y (= NO_3 + 2 N_2O_5), NTR (i.e., organic nitrate), CO, H_2O_2, OH, and HO_2. The fine grid information was written into the fine grid output files, the coarse grid information was written into the coarse grid output files. In the areas covered by the fine grids, concentrations were aggregated to parent grid cells. Since the vertical

[1] DDM does not currently output a receptor file, but ENVIRON added this capability as part of this study. This was a simple modification.

resolutions of coarse and fine grid cells are different, the results obtained with the coarse and fine grid cells cannot be directly compared. We, therefore, focus our analyses on the results with the fine grid cells. In analyzing the results, we divided each receptor region into 9 subareas, each with 9 fine grid cells, as shown in Figure 5-1. For each receptor region, we used a two-step analysis approach. First, we analyzed the results for the 9 subareas by aggregating the results over the 9 fine grid cells in each of the 9 subareas for each receptor region. The average peak O_3 concentrations and corresponding O_3 sensitivities or O_3 contributions for the 9 subareas were calculated for high O_3 days. The dominant O_3 contributors and the emission characteristics in each subarea were identified and discussed. Second, we analyzed the results for the whole receptor region by aggregating the results over the 81 fine grid cells in each receptor region. The average peak O_3 concentrations and corresponding O_3 sensitivities or O_3 contributions for the whole receptor were calculated for high O_3 days. The dominant O_3 contributors in each receptor region were identified and discussed. The OSAT and DDM results for these grid cells were analyzed for the surface layer only and the PA results were analyzed for all 7 model layers to quantify the relative contributions of photochemistry and transport to local O_3 formation.

Receptor specific output files were extracted from the model standard output files for both the base case and emission reduction scenarios. Those receptor specific output files contain the model standard outputs such as O_3 and NO_x concentrations, O_3 contributions of VOCs and NO_x from emission source groups, and O_3 semi-normalized sensitivities to VOCs and NO_x emission source groups. Note that the source contributions from the on-road mobile source and the other surface anthropogenic source predicted by OSAT were combined into one surface anthropogenic source category to compare with the DDM results. The receptor specific outputs were directly used in the evaluation and further post-processed to calculate the O_3 productivities and the incremental reactivities of VOC source groups (see Section 6.1.3).

Scripts were developed by ENVIRON and AER to prepare a suite of "standard" displays and tables to serve as the starting point for the independent review and preparation of the guidance document, reports, and journal article. Examples of those preliminary displays and tables include:

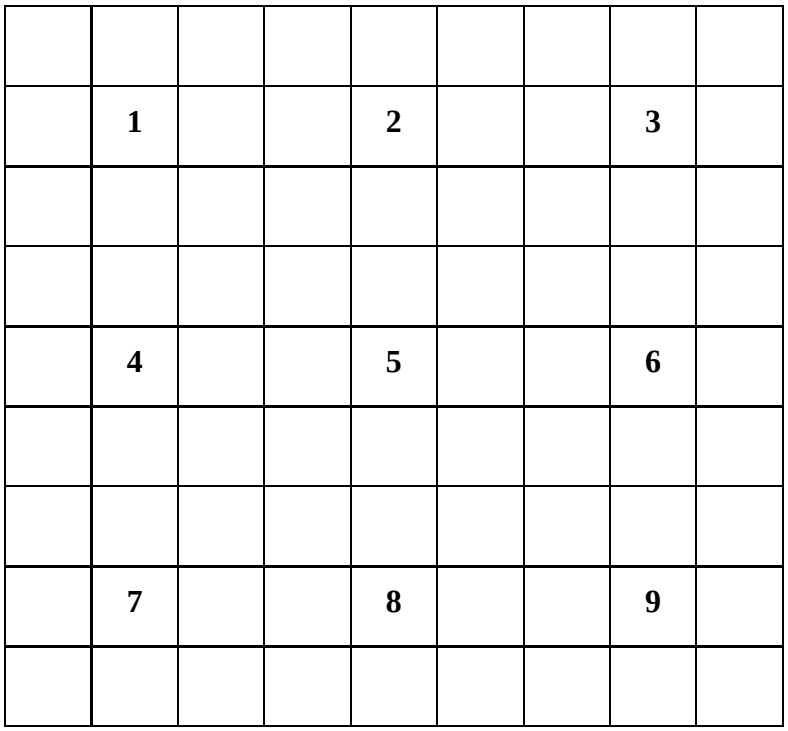

Figure 5-1. Nine subareas in the receptor region defined for data analyses. The subarea indices start from the NW corner of each receptor and proceed row-wise. Each subarea consists of 9 fine grid cells.

- Isopleth plots showing the total O_3 in mid-afternoon on high O_3 days, the contributions of separate source categories, geographic areas, VOCs and NO_x, and the semi-normalized sensitivities with respect to separate source categories, geographic areas, VOCs, and NO_x at the same time.

- Tables showing O_3 contributions and O_3 sensitivities by source category, source area, VOCs and NO_x for each receptor region. Tables were prepared for all hours and stratified by O_3 level (e.g., for hours with O_3 > 80 ppb) to differentiate source-receptor relationships according to O_3 level. Tables ranking the top 10 contributors for each receptor region and the top 2 contributors for each subarea for comparing rankings between DDM and OSAT.

- Tables showing the NO_x- vs. VOC-sensitivity of O_3 chemistry predicted by DDM, OSAT, and PA in the four selected receptor regions.

- Isopleth plots showing the changes in O_3 contributions and O_3 sensitivities for separate source categories, geographic areas, VOCs and NO_x between the base case and emission reduction scenarios in each receptor region.

- Tables summarizing the emissions of lumped VOCs and NO_x from each source group on each episode day.

- Time series plots of process contributions to O_3 at each receptor for high O_3 days.

- Isopleth plots of gridded chemical process analysis variables for several hours on high O_3 days. Isopleth plots may be zoomed in over the receptor areas if needed for clarity.

- Charts showing changes in process contributions to O_3 and process analysis variables between the base case and emission reduction scenarios at each receptor.

All model output files were archived so that they are available for later analysis. All isopleth plots were saved electronically in GIF format for easy distribution. All of the post-processing programs and scripts used to generate the plots and tables will be documented and delivered by ENVIRON as part of this study for use with the technical guidance document to be developed in Task 4.

6. EVALUATION OF DDM, OSAT, AND PA

We have developed the evaluation protocols to assess the performance of the three probing tools in Task 2. The probing tools are evaluated in terms of consistency, complementarity, stretchability, and computational/implementation requirements. The first component, consistency, refers to the ability of different probing techniques to provide consistent results for a specific application (e.g., O_3 sensitivity to NO_x or VOCs; relative reactivities of VOCs). Clearly, different probing techniques will by design provide results that differ quantitatively; however, it is important that those results be consistent qualitatively. If not, the reason for the inconsistency must be elucidated. The second component, complementarity, refers to the fact that some probing techniques can provide information that others cannot provide. The third component, stretchability, addresses the range over which a probing technique can be considered reliable. The fourth component, computational requirements, characterizes the practical aspects of the probing technique computations (e.g., a probing technique can in theory be able to provide very detailed and comprehensive information but it may not be feasible computationally). An overview of the components to be evaluated is provided in Figure 6-1. The theoretical bases of these four components of the assessment and the detailed evaluation of the three probing tools in terms of those components are provided below.

6.1 Consistency

Comparable information was extracted from the outputs of the three probing tools and relevant post-processing calculations were conducted. Consistency among the probing tools is evaluated for three important characteristics of O_3 formation for base simulations: (1) ranking of O_3 contributors; (2) NO_x- or VOC-sensitivity of O_3 chemistry; and (3) photochemical reactivity of lumped VOCs from separate source groups. The second characteristics (i.e., NO_x- or VOC-sensitivity of O_3 chemistry) is also evaluated for sensitivity simulations to check the consistency among these tools under different emission reduction scenarios (see section 6.3.2). The scientific rationale for using the

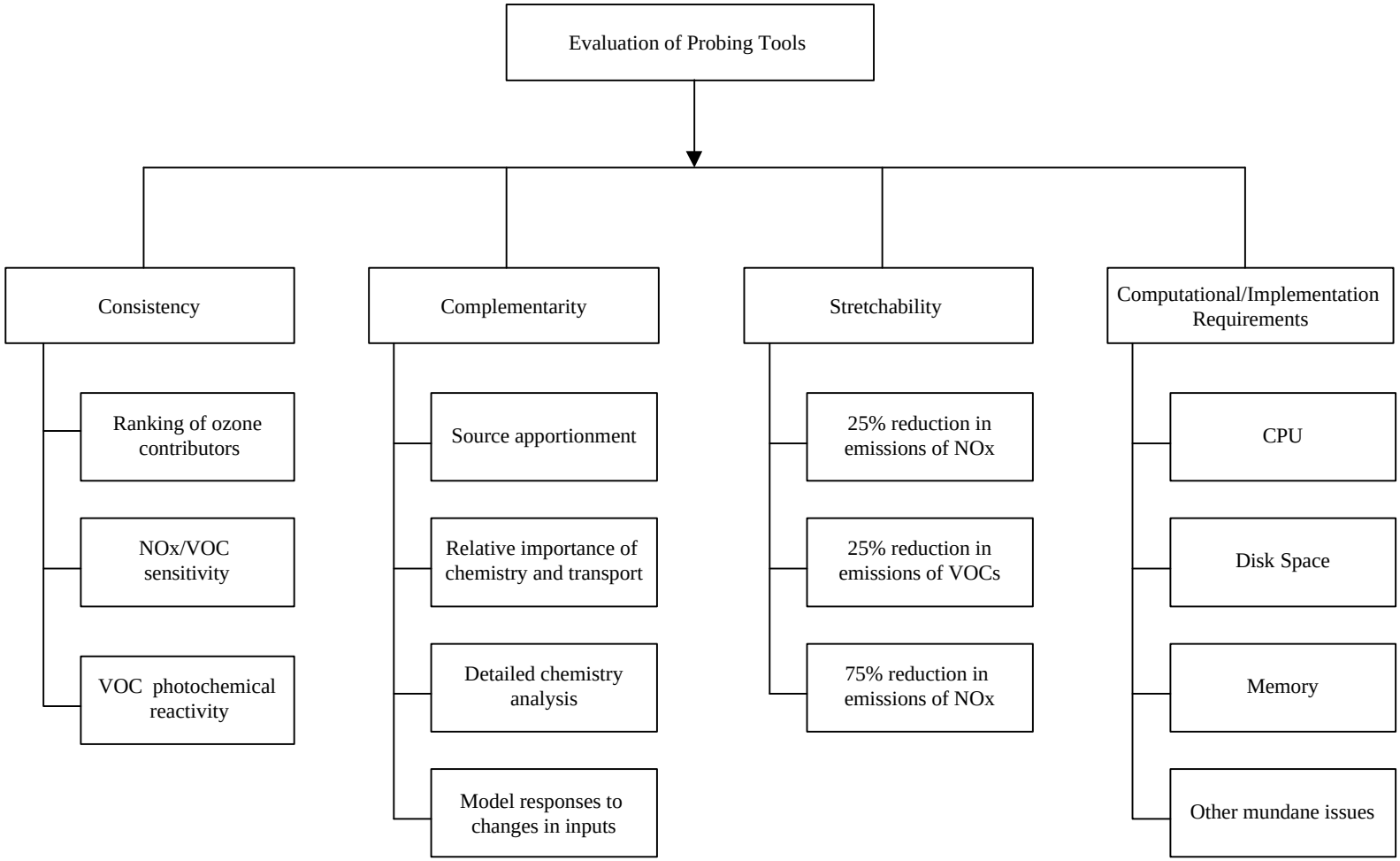

Figure 6-1. Overview of technical components for evaluation of probing tools.

three characteristics of O_3 formation as measures of consistency testing and their detailed evaluation are presented in detail below.

6.1.1 Ranking of O_3 Sensitivities and Contributions

While PA does not provide information on the O_3 contributors, DDM calculates the O_3 sensitivities with respect to VOC and NO_x emissions of different source groups and OSAT calculates O_3 contributions of those emission source groups. The ranking of those O_3 sensitivities or contributions provides information on which source group(s) has(have) the largest effects on O_3 formation in a particular receptor region and therefore is (are) of the most interest for designing O_3 control strategies. In comparing the DDM and OSAT rankings, we ranked the top 10 O_3 contributors by source area and by source group (i.e., the source areas or groups having either a large sensitivity or a large O_3 contribution) at each receptor for 6 stratified O_3 levels with O_3 concentration of < 80 ppb, 80-90 ppb, 90-100 ppb, 100-110 ppb, 110-120 ppb, and > 120 ppb using the DDM and OSAT predictions on July 11 to 15, 1995. Since the new National Ambient Air Quality Standard (NAAQS) for O_3 will use the 8-hr average O_3 concentration as a measure, the ranking is conducted for both the 1-hr and the 8-hr O_3 concentrations. The top 2 O_3 contributors by source area and by source group for the 6 stratified O_3 levels of 1-hr and 8-hr O_3 concentrations in the 9 subarea in each of the receptor regions are also identified.

Since a detailed ranking comparison between DDM and OSAT has not been conducted for the OTAG domain elsewhere, we will first analyze the ranking of O_3 sensitivities predicted by DDM, then compare the ranking of O_3 contributions predicted by OSAT to the DDM ranking. As shown in Table 4-1, the DDM base simulation predicting O_3 sensitivities of separate source groups was split into three runs: B2N, B2V, and B3 due to the computer memory constraints. Runs B2N and B2V provide sensitivity to NO_x and VOC emissions, respectively, from 3 source categories (i.e., biogenic, surface and elevated anthropogenic emissions) in 11 source areas (i.e., a total of 66 source groups) that covers the core of the domain (i.e., source areas 4, 5, 7, 8, 11, 12, 13, 14, 15, 16, and 17). Run B3 provides sensitivity to total emissions (i.e., no VOC vs. NO_x breakout) from the 3 source categories in 6 source areas (i.e., a total of 18 source groups)

that are located near the boundaries of the domain (i.e., source areas 1, 2, 3, 6, 9, and 10). On the other hand, the OSAT base simulation predicting O_3 contributions of NO_x and VOC emissions from 4 source categories (i.e., biogenic, on-road mobile, other surface and elevated anthropogenic emissions) in all 17 source areas (i.e., a total of 136 source groups) is conducted in just one run (i.e., B1). Therefore, the ranking comparison between DDM and OSAT should be compatible to the different DDM and OSAT configurations in those runs. The ranking is conducted by both source area and source group. To rank by source area, the sensitivities (or the O_3 contributions) to NO_x or VOC or total emissions from a particular source area are calculated by lumping O_3 sensitivities to all source categories for that source area. In comparing the DDM and OSAT rankings at each receptor, we first compare the O_3 sensitivities with respect to NO_x and VOC emissions from 33 source groups (i.e., DDM run B2 contains 3 source categories and 11 core source areas) to the O_3 contributions of NO_x and VOC emissions from the same 33 source groups (i.e., a subset of the results of OSAT run B1). We then compare the O_3 sensitivities with respect to total emissions from 18 source groups (i.e., DDM run B3 contains 3 source categories and 6 boundary source areas) to the O_3 contributions of total NO_x and VOC emissions from the same 18 source groups (i.e., another subset of the results of OSAT run B1). In those comparisons, the source contributions from the on-road mobile source and the other surface anthropogenic source from the OSAT run B1 are combined into one surface anthropogenic source category to compare with the DDM results. Since each receptor contains 81 fine grid cells and each subarea contains 9 fine grid cells, the O_3 concentrations and sensitivities (or the O_3 contributions) for the whole receptor and for each of the 9 subareas are obtained by averaging those over the 81 fine grid cells in the receptor and the 9 fine grid cells in each subarea, respectively. We provide below detailed analyses of the DDM ranking and the ranking comparison between DDM and OSAT.

6.1.1.1 Ranking of DDM Sensitivities with Respect to NO_x and VOC Emissions from 11 Core Source Areas

Note that absolute values of the sensitivity coefficients were used to rank the source areas and source groups. Therefore, this ranking reflects the influence of the sources, whether that influence is positive or negative.

Atlanta

Tables 6-1 and 6-2 show the top 10 O_3 sensitivities ranked by source area and by source group (out of 22 and 66 sensitivities, respectively) for the 6 stratified 1-hr and 8-hr O_3 levels, respectively, for the whole receptor region in Atlanta. In this receptor region, the high hourly O_3 concentrations (> 90 ppb) are most sensitive to changes in NO_x and VOC emissions from the local (i.e., source area 15) and surrounding sources (i.e., source area 8) that cover Georgia, southern Tennessee, eastern Alabama, western North Carolina and South Carolina. These results suggest that reduction in the local and surrounding emissions from those regions would be the most effective O_3 control strategy in Atlanta. The second most influential contributors to the high hourly O_3 concentrations are the VOC and NO_x emissions from the upwind source areas 5 and 12 for O_3 levels of 90-110 ppb and those from the upwind source areas 12 and 7 for O_3 levels of 110-120 ppb. The low O_3 concentrations (< 80 ppb) are mostly affected by NO_x transported from the surrounding region (i.e., source area 8) and the Atlantic coast (i.e., source area 12), and VOC emitted from the local sources (i.e., source area 15) and transported from the Atlantic coast and the surrounding region (i.e., source area 8). The dominant source categories for NO_x and VOC emissions from these source areas in Atlanta include the surface and elevated anthropogenic NO_x emissions and the biogenic VOC and NO_x emissions. A given emission reduction of NO_x or VOC in a specific source category may have different effects on O_3 concentrations in different concentration ranges. For example, reducing surface anthropogenic NO_x emissions from the local sources (i.e., source area 15) by 10% may reduce O_3 concentrations by 1.1, 1.5, 2.0, and 2.2 ppb for O_3 levels of 80-90, 90-100, 100-110, and 110-120 ppb, respectively, but it may potentially increase O_3 concentration by 0.08 ppb for O_3 levels of < 80 ppb. The small negative

Table 6-1. The top 10 O_3 sensitivities by source area and by source group for stratified 1-hr O_3 levels for the whole receptor region in Atlanta[1].

Rank	O_3 level, ppb									
	< 80		80-90		90-100		100-110		110-120	
	Sensitivity	Variable[2]	Sensitivity	Variable	Sensitivity	Variable	Sensitivity	Variable	Sensitivity	Variable
By source area[3]										
1	1.40E-02	8/NOX	1.70E-02	8/NOX	2.20E-02	15/NOX	2.90E-02	15/NOX	3.50E-02	15/NOX
2	3.30E-03	12/NOX	1.30E-02	15/NOX	1.80E-02	8/NOX	1.70E-02	8/NOX	1.60E-02	8/NOX
3	1.30E-03	15/VOC	4.60E-03	12/NOX	4.30E-03	15/VOC	5.20E-03	15/VOC	6.20E-03	15/VOC
4	1.30E-03	12/VOC	3.90E-03	15/VOC	2.90E-03	8/VOC	3.20E-03	8/VOC	4.00E-03	8/VOC
5	1.10E-03	8/VOC	3.60E-03	8/VOC	1.40E-03	5/VOC	1.90E-03	5/VOC	1.80E-03	12/VOC
6	9.10E-04	5/VOC	1.40E-03	12/VOC	1.30E-03	5/NOX	1.70E-03	5/NOX	1.40E-03	12/NOX
7	8.90E-04	5/NOX	8.60E-04	5/VOC	6.90E-04	12/NOX	5.60E-04	12/VOC	1.80E-04	7/NOX
8	-7.00E-04	15/NOX	7.00E-04	5/NOX	6.80E-04	12/VOC	5.00E-04	12/NOX	1.50E-04	7/VOC
9	2.00E-04	7/NOX	3.00E-04	7/NOX	1.70E-04	4/VOC	1.90E-04	4/VOC	8.40E-05	5/NOX
10	1.60E-04	4/NOX	2.00E-04	4/NOX	1.60E-04	4/NOX	1.60E-04	4/NOX	8.00E-05	5/VOC
By source group[4]										
1	8.00E-03	S-8/NOX	1.10E-02	S-8/NOX	1.50E-02	S-15/NOX	2.00E-02	S-15/NOX	2.20E-02	S-15/NOX
2	5.10E-03	E-8/NOX	1.10E-02	S-15/NOX	1.10E-02	S-8/NOX	1.00E-02	S-8/NOX	1.20E-02	E-15/NOX
3	1.50E-03	E-12/NOX	5.20E-03	E-8/NOX	6.00E-03	E-15/NOX	8.20E-03	E-15/NOX	9.50E-03	S-8/NOX
4	1.50E-03	S-12/NOX	3.70E-03	B-8/VOC	5.60E-03	E-8/NOX	5.40E-03	E-8/NOX	5.40E-03	B-15/VOC
5	1.30E-03	B-12/VOC	3.20E-03	B-15/VOC	3.60E-03	B-15/VOC	4.50E-03	B-15/VOC	4.90E-03	E-8/NOX
6	1.30E-03	B-8/VOC	2.30E-03	S-12/NOX	3.10E-03	B-8/VOC	3.40E-03	B-8/VOC	4.00E-03	B-8/VOC
7	1.00E-03	B-8/NOX	2.10E-03	E-15/NOX	1.40E-03	B-8/NOX	1.80E-03	B-5/VOC	1.60E-03	B-12/VOC
8	9.60E-04	B-15/VOC	1.80E-03	E-12/NOX	1.40E-03	B-5/VOC	1.30E-03	B-8/NOX	1.20E-03	B-8/NOX
9	8.50E-04	B-5/VOC	1.40E-03	B-12/VOC	7.00E-04	S-15/VOC	7.70E-04	S-5/NOX	7.60E-04	S-15/VOC
10	-8.00E-04	S-15/NOX	1.10E-03	B-8/NOX	6.40E-04	B-12/VOC	7.50E-04	E-5/NOX	6.60E-04	S-12/NOX

1. Data shown in the table were compiled for all hourly O_3 concentrations during the period of July 11-15, 1995.
2. Source area or source group/primary precursor.
3. The sensitivities by source area are calculated based on the lumped O_3 sensitivities to NO_x or VOC emissions from all three source categories for that source area from DDM Run B2, which calculates O_3 sensitivities to NO_x and VOC emissions from 11 core source areas.
4. Letters B, S, and E represent emissions from biogenic, surface anthropogenic, and elevated anthropogenic sources, respectively.

Table 6-2. The top 10 O_3 sensitivities by source area and by source group for stratified 8-hr O_3 levels for the whole receptor region in Atlanta[1].

Rank	O_3 level, ppb							
	< 80		80-90		90-100		100-110	
	Sensitivity	Variable[2]	Sensitivity	Variable	Sensitivity	Variable	Sensitivity	Variable
By source area[3]								
1	1.40E-02	8/NOX	2.10E-02	8/NOX	2.30E-02	15/NOX	2.90E-02	15/NOX
2	4.00E-03	12/NOX	1.30E-02	15/NOX	1.60E-02	8/NOX	1.60E-02	8/NOX
3	1.70E-03	15/VOC	4.60E-03	8/VOC	5.10E-03	15/VOC	5.30E-03	15/VOC
4	1.50E-03	8/VOC	3.50E-03	15/VOC	3.20E-03	8/VOC	3.00E-03	8/VOC
5	1.40E-03	12/VOC	1.70E-03	5/VOC	1.60E-03	5/VOC	1.10E-03	5/VOC
6	1.20E-03	15/NOX	1.40E-03	5/NOX	1.50E-03	5/NOX	1.00E-03	12/VOC
7	8.20E-04	5/VOC	2.40E-04	4/NOX	6.60E-04	12/VOC	1.00E-03	5/NOX
8	7.50E-04	5/NOX	2.40E-04	4/VOC	6.20E-04	12/NOX	9.20E-04	12/NOX
9	2.40E-04	7/NOX	2.00E-04	12/NOX	1.70E-04	4/VOC	1.30E-04	4/VOC
10	1.70E-04	4/NOX	1.80E-04	12/VOC	1.50E-04	4/NOX	1.20E-04	7/NOX
By source group[4]								
1	8.00E-03	S-8/NOX	1.30E-02	S-8/NOX	1.60E-02	S-15/NOX	1.90E-02	S-15/NOX
2	4.90E-03	E-8/NOX	9.80E-03	S-15/NOX	9.80E-03	S-8/NOX	9.80E-03	S-8/NOX
3	1.80E-03	S-12/NOX	6.40E-03	E-8/NOX	6.60E-03	E-15/NOX	8.90E-03	E-15/NOX
4	1.80E-03	E-12/NOX	5.00E-03	B-8/VOC	5.30E-03	E-8/NOX	5.20E-03	E-8/NOX
5	1.70E-03	B-8/VOC	2.90E-03	B-15/VOC	4.20E-03	B-15/VOC	4.50E-03	B-15/VOC
6	1.50E-03	B-12/VOC	2.50E-03	E-15/NOX	3.40E-03	B-8/VOC	3.20E-03	B-8/VOC
7	1.30E-03	B-15/VOC	1.50E-03	B-5/VOC	1.50E-03	B-5/VOC	1.30E-03	B-8/NOX
8	9.80E-04	B-8/NOX	1.40E-03	B-8/NOX	1.30E-03	B-8/NOX	1.00E-03	B-5/VOC
9	9.20E-04	S-15/NOX	6.80E-04	E-5/NOX	8.70E-04	S-15/VOC	9.60E-04	B-12/VOC
10	7.50E-04	B-5/VOC	5.80E-04	S-5/NOX	6.80E-04	S-5/NOX	7.60E-04	S-15/VOC

1. Data shown in the table were compiled for all hourly O_3 concentrations during the period of July 11-15, 1995.
2. Source area or source group/primary precursor.
3. The sensitivities by source area are calculated based on the lumped O_3 sensitivities to NO_x or VOC emissions from all three source categories for that source area from DDM Run B2, which calculates O_3 sensitivities to NO_x and VOC emissions from 11 core source areas.
4. Letters B, S, and E represent emissions from biogenic, surface anthropogenic, and elevated anthropogenic sources, respectively.

sensitivity to total local NO_x emissions for the low 1-hr O_3 level indicates that a decrease in the local NO_x emissions may increase O_3 concentrations in this concentration range. This is due to the so-called NO_x inhibition or titration effect.

The ranking by source area for the low 8-hr O_3 levels (< 80 ppb) is similar to that for the low 1-hr O_3 level in Atlanta, but the change in total NO_x emissions from the local sources (i.e., source area 15) has a larger (by 71%) and opposite effect (i.e., with a positive sensitivity) on the 8-hr O_3 than the 1-hr O_3. The ranking by source area for the high 8-hr O_3 concentrations of 90-100 ppb is identical to that for the 1-hr O_3 in the same range, and the magnitudes of sensitivities for both the 1-hr and 8-hr O_3 in this range are similar. For the high O_3 levels of 100-110 ppb, the changes in the VOC and NO_x emissions from source area 12 have a larger (by 79-84%) effect on the 8-hr O_3 than the 1-hr O_3, and those from source area 5 have a larger effect (by 70-73%) on the 1-hr O_3 than the 8-hr O_3. For the intermediate O_3 levels of 80-90 ppb, the ranking by source area is also different somewhat for the 1-hr and the 8-hr O_3 concentrations. The surface and elevated anthropogenic NO_x emissions, and the biogenic VOC emissions from the surrounding and local sources (i.e., S-8/NO_x, S-15/NO_x, E-8/NO_x, B-8/VOC, B-15/VOC, and E-15/NO_x) are the most influential contributors for both the 1-hr and 8-hr O_3 in this range. The surface/elevated anthropogenic NO_x and biogenic VOC emissions from source area 12 (i.e., S-12/NO_x, E-12/NO_x, and B-12/VOC) exhibit a much stronger (by a factor of 23 and 8, respectively) influence on the 1-hr O_3 concentrations than on the 8-hr O_3 concentrations (note that the three source groups are not in the top 10 list for the 8-hr O_3). The biogenic VOC and elevated/surface anthropogenic NO_x emissions from source area 5 (B-5/VOC, E-5/NO_x, and S-5/NO_x) exhibit a stronger (by a factor of 2) influence on the 8-hr O_3 concentrations than on the 1-hr O_3 concentrations (note that the three source groups are not in the top 10 list for the 1-hr O_3). In addition to the above differences between the 1-hr and 8-hr O_3 levels of 80-90 ppb, the NO_x emissions from source area 7 rank 9th for the 1-hr O_3 concentration but are not in the top 10 list for the 8-hr O_3 concentration, and the VOC emissions from source area 4 rank 8th for the 8-hr O_3 concentration but are not within the top 10 list for the 1-hr O_3 concentration. The differences in 1-hr and 8-hr O_3 sensitivities for O_3 levels of > 80 ppb imply that different emission control strategies for 1-hr and 8-hr O_3 compliance may be needed in Atlanta.

For example, a reduction of emissions from the source groups S-8/NO_x, E-8/NO_x, S-15/NO_x, and E-15/NO_x may reduce both the 1-hr and 8-hr O_3 concentrations of > 80 ppb, but a reduction in emissions from the source groups E-5/NO_x and S-5/NO_x may help reduce more 8-hr O_3 concentrations than 1-hr O_3 concentrations in the range of 80-90 ppb, and a reduction of emissions from the source groups S-12/NO_x and E-12/NO_x may help reduce more 1-hr O_3 concentrations than 8-hr O_3 concentrations in the same range.

Tables 6-3 and 6-4 show the top 2 most influential emissions to O_3 concentrations ranked by source area and by source group for the stratified 1-hr and 8-hr O_3 levels for the 9 subareas in Atlanta. The top 2 contributors for each stratified O_3 level for the whole receptor region are also listed for comparison. While the ranking by source area for individual subareas is generally consistent with that for the whole receptor region, the ranking by source group shows large differences among individual subareas and the whole receptor region. The local surface anthropogenic NO_x emissions (i.e., S-15/NO_x) rank 1st for the high 1-hr and 8-hr O_3 levels (> 90 ppb) in most subareas, and the surface anthropogenic NO_x emissions from the surrounding sources (i.e., S-8/NO_x) rank 1st for the intermediate and low 1-hr and 8-hr O_3 levels (< 90 ppb) in most subareas. The local biogenic VOC emissions (i.e., B-15/VOC) affect mostly the intermediate and high 1-hr O_3 concentrations in the center and central-west subareas of Atlanta (i.e., subareas 4 and 5) where the local biogenic VOC emissions are the largest among all subareas, but have less influence on the 8-hr O_3 concentrations (rank 4th or 5th, not shown). The local elevated anthropogenic NO_x emissions (i.e., E-15/NO_x) affect mostly the high 1-hr O_3 concentrations (> 90 ppb) in the northwest, central-north, central-east, and southeast subareas of Atlanta (subareas 1, 2, 6, and 9, respectively) and the high 8-hr O_3 concentrations (> 80 ppb) in the central-north and south-east subareas of Atlanta (subareas 2 and 9). This is consistent with the distribution of large point sources located in the northwest and southeast of metropolitan Atlanta area. The elevated anthropogenic NO_x emissions from the surrounding sources (i.e., E-8/NO_x) contribute mostly to the low 8-hr O_3 concentrations in all subareas and the low 1-hr O_3 concentrations in all subareas except for subareas 4 and 5.

Table 6-3. The top 2 contributors to O_3 formation by source area and by source group predicted by DDM for stratified 1-hr O_3 levels for 9 subareas in Atlanta[1].

O_3 level, ppb	Subarea									
	1	2	3	4	5	6	7	8	9	Whole receptor
By source area[2]										
< 80 ppb	8/NOX 12/NOX	8/NOX 12/NOX	8/NOX 12/NOX	8/NOX 15/NOX	8/NOX 15/NOX	8/NOX 12/NOX	8/NOX 12/NOX	8/NOX 12/NOX	8/NOX 12/NOX	8/NOX 12/NOX
80-90	15/NOX 8/NOX	8/NOX 15/NOX	8/NOX 15/NOX	8/NOX 15/VOC	8/NOX 15/NOX	8/NOX 15/NOX	15/NOX 8/NOX	8/NOX 15/NOX	15/NOX 8/NOX	8/NOX 15/NOX
90-100	15/NOX 8/NOX	15/NOX 8/NOX	N/A	8/NOX 15/NOX	8/NOX 15/NOX	15/NOX 8/NOX	15/NOX 8/NOX	15/NOX 8/NOX	15/NOX 8/NOX	15/NOX 8/NOX
100-110	15/NOX 8/NOX	15/NOX 8/NOX	N/A	15/NOX 8/NOX	15/NOX 8/NOX	N/A	15/NOX 8/NOX	15/NOX 8/NOX	15/NOX 8/NOX	15/NOX 8/NOX
110-120	N/A	N/A	N/A	15/NOX 8/NOX	15/NOX 8/NOX	15/NOX 8/NOX	15/NOX 8/NOX	15/NOX 8/NOX	15/NOX 8/NOX	15/NOX 8/NOX
> 120	N/A	N/A	N/A	15/NOX 15/VOC	15/NOX 15/VOC	15/NOX 8/NOX	15/NOX 8/NOX	15/NOX 8/NOX	15/NOX 8/NOX	N/A
By source group[3]										
< 80 ppb	S-8/NOX E-8/NOX	S-8/NOX E-8/NOX	S-8/NOX E-8/NOX	S-15/NOX S-8/NOX	S-8/NOX S-15/NOX	S-8/NOX E-8/NOX	S-8/NOX E-8/NOX	S-8/NOX E-8/NOX	S-8/NOX E-8/NOX	S-8/NOX E-8/NOX
80-90	S-15/NOX S-8/NOX	S-15/NOX S-8/NOX	S-8/NOX S-15/NOX	S-8/NOX B-8/VOC	S-8/NOX S-15/NOX	S-8/NOX S-15/NOX	S-15/NOX S-8/NOX	S-8/NOX S-15/NOX	S-15/NOX S-8/NOX	S-8/NOX S-15/NOX
90-100	S-15/NOX S-8/NOX	S-15/NOX E-15/NOX	N/A	S-8/NOX B-8/VOC	S-8/NOX S-15/NOX	S-15/NOX E-15/NOX	S-15/NOX S-8/NOX	S-15/NOX S-8/NOX	S-15/NOX E-15/NOX	S-15/NOX S-8/NOX
100-110	S-15/NOX E-15/NOX	S-15/NOX E-15/NOX	N/A	S-15/NOX B-15/VOC	S-15/NOX B-15/VOC	N/A	S-15/NOX S-8/NOX	S-15/NOX S-8/NOX	S-15/NOX E-15/NOX	S-15/NOX S-8/NOX
110-120	N/A	N/A	N/A	S-15/NOX B-15/VOC	S-15/NOX S-8/NOX	S-15/NOX E-15/NOX	S-15/NOX S-8/NOX	S-15/NOX S-8/NOX	S-15/NOX E-15/NOX	S-15/NOX E-15/NOX
> 120	N/A	N/A	N/A	S-15/NOX B-15/VOC	S-15/NOX B-15/VOC	S-15/NOX E-15/NOX	S-15/NOX E-15/NOX	S-15/NOX E-15/NOX	S-15/NOX E-15/NOX	N/A

1. Data shown in the table were compiled for all hourly O_3 concentrations during the period of July 11-15, 1995.
2. The sensitivities by source area are calculated based on the lumped O_3 sensitivities to NO_x or VOC emissions from all three source categories for that source area from DDM Run B2, which calculates O_3 sensitivities to NO_x and VOC emissions from 11 core source areas.
3. Letters B, S, and E represent emissions from biogenic, surface anthropogenic, and elevated anthropogenic sources, respectively.

Table 6-4. The top 2 contributors to O_3 formation by source area and by source group predicted by DDM for stratified 8-hr O_3 levels for 9 subareas in Atlanta[1].

O_3 level, ppb	Subarea									
	1	2	3	4	5	6	7	8	9	Whole receptor
By source area[2]										
< 80 ppb	8/NOX 12/NOX	8/NOX 15/NOX	8/NOX 15/NOX	8/NOX 12/NOX	8/NOX 12/NOX	8/NOX 12/NOX	8/NOX 12/NOX	8/NOX 12/NOX	8/NOX 15/NOX	8/NOX 12/NOX
80-90	8/NOX 15/NOX	15/NOX 8/NOX	N/A	8/NOX 15/NOX	8/NOX 15/NOX	15/NOX 8/NOX	8/NOX 15/NOX	8/NOX 15/NOX	15/NOX 8/NOX	8/NOX 15/NOX
90-100	15/NOX 8/NOX	15/NOX 8/NOX	N/A	8/NOX 15/NOX	8/NOX 15/NOX	15/NOX 8/NOX	8/NOX 15/NOX	15/NOX 8/NOX	15/NOX 8/NOX	15/NOX 8/NOX
100-110	15/NOX 8/NOX	N/A	N/A	15/NOX 8/NOX	15/NOX 8/NOX	N/A	15/NOX 8/NOX	15/NOX 8/NOX	15/NOX 8/NOX	15/NOX 8/NOX
110-120	N/A	N/A	N/A	8/NOX 15/NOX	15/NOX 8/NOX	15/NOX 8/NOX	8/NOX 15/NOX	15/NOX 8/NOX	15/NOX 8/NOX	N/A
> 120	N/A	N/A	N/A	15/NOX 8/NOX	15/NOX 8/NOX	N/A	15/NOX 8/NOX	15/NOX 8/NOX	N/A	N/A
By source group[3]										
< 80 ppb	S-8/NOX E-8/NOX	S-8/NOX E-8/NOX	S-8/NOX E-8/NOX	S-8/NOX E-8/NOX	S-8/NOX E-8/NOX	S-8/NOX E-8/NOX	S-8/NOX E-8/NOX	S-8/NOX E-8/NOX	S-8/NOX E-8/NOX	S-8/NOX E-8/NOX
80-90	S-8/NOX S-15/NOX	S-15/NOX S-8/NOX	N/A	S-8/NOX S-15/NOX	S-15/NOX S-8/NOX	S-15/NOX S-8/NOX	S-15/NOX S-8/NOX	S-8/NOX S-15/NOX	S-15/NOX E-15/NOX	S-8/NOX S-15/NOX
90-100	S-15/NOX S-8/NOX	S-15/NOX E-15/NOX	N/A	S-8/NOX S-15/NOX	S-8/NOX S-15/NOX	S-15/NOX E-15/NOX	S-8/NOX S-15/NOX	S-15/NOX S-8/NOX	S-15/NOX E-15/NOX	S-15/NOX S-8/NOX
100-110	S-15/NOX S-8/NOX	N/A	N/A	S-15/NOX S-8/NOX	S-15/NOX S-8/NOX	N/A	S-15/NOX S-8/NOX	S-15/NOX S-8/NOX	S-15/NOX E-15/NOX	S-15/NOX S-8/NOX
110-120	N/A	N/A	N/A	S-15/NOX S-8/NOX	S-15/NOX S-8/NOX	S-15/NOX S-8/NOX	S-8/NOX S-15/NOX	S-15/NOX S-8/NOX	S-15/NOX S-8/NOX	N/A
> 120	N/A	N/A	N/A	S-15/NOX S-8/NOX	S-15/NOX E-15/NOX	N/A	S-15/NOX S-8/NOX	S-15/NOX E-15/NOX	N/A	N/A

1. Data shown in the table were compiled for all hourly O_3 concentrations during the period of July 11-15, 1995.
2. The sensitivities by source area are calculated based on the lumped O_3 sensitivities to NOx or VOC emissions from all three source categories for that source area from DDM Run B2, which calculates O3 sensitivities to NOx and VOC emissions from 11 core source areas.
3. Letters B, S, and E represent emissions from biogenic, surface anthropogenic, and elevated anthropogenic sources, respectively.

Chicago

Similar ranking information for the 6 stratified 1-hr and 8-hr O_3 levels for the whole receptor region and individual subareas are shown in Tables 6-5 to 6-8 for Chicago. In Chicago, the hourly O_3 concentrations in all concentration ranges are most sensitive to changes in the NO_x and/or VOC emissions from the surrounding area (i.e., source area 4) and the local area (source area 14), with small differences in their ranking for different O_3 levels. This result suggests that high O_3 concentrations in Chicago are mainly influenced by the surrounding and local emissions from southern Wisconsin, Illinois and Indiana. The VOC and NO_x emissions from source area 5 (located south of Chicago) are the third most influential contributors for all O_3 levels. There are two noticeable differences in the effect of the local NO_x and VOC emissions on O_3 concentrations between Atlanta and Chicago. First, the sensitivity of O_3 to local NO_x emissions is positive in Atlanta (except for O_3 < 80 ppb) but negative in Chicago, indicating that decreasing the local NO_x emissions may decrease O_3 concentrations in Atlanta (except for O_3 < 80 ppb) but increase O_3 concentrations in Chicago. Second, both the local surface anthropogenic and biogenic VOC emissions (i.e., S-14/VOC and B-14/VOC) are important to O_3 formation in the intermediate and high O_3 levels (> 80 ppb) in Chicago, whereas the local biogenic VOC emissions (i.e., B-15/VOC) are more important to O_3 formation than the local surface anthropogenic VOC emissions (i.e., S-15/VOC) in Atlanta. The highest 1-hr O_3 concentrations (100-110 ppb) in Chicago are most sensitive to the biogenic VOC emissions from source area 5 (i.e., B-5/VOC) that covers southern Illinois and Indiana, southeastern Missouri, eastern Arkansas, northern Mississippi and Alabama, and western Kentucky and Tennessee. Since O_3 formation responds negatively to changes in the local NO_x emissions, a reduction of the surface/elevated anthropogenic NO_x emissions from the surrounding and upwind sources (i.e., S-4/NO_x, E-4/NO_x, and E-5/NO_x) and from the surface anthropogenic VOC emissions from the local and surrounding sources (i.e., S-14/VOC and S-4/VOC) appear to be the most effective O_3 control strategies for the Chicago area.

The top 10 most influential contributors by source area for the 8-hr O_3 concentrations in all O_3 levels (note that only the 1-hr O_3 concentrations reached the level of 100-110 ppb) in Chicago are the same as those for the 1-hr O_3 concentrations, with a

Table 6-5. The top 10 O_3 sensitivities by source area and by source group for stratified 1-hr O_3 levels for the whole receptor region in Chicago[1].

Rank	O_3 level, ppb							
	< 80		80-90		90-100		100-110	
	Sensitivity	Variable	Sensitivity	Variable	Sensitivity	Variable	Sensitivity	Variable
By source area[2]								
1	-1.30E-02	14/NOX	1.50E-02	4/NOX	1.70E-02	4/NOX	2.10E-02	4/NOX
2	7.50E-03	4/NOX	-1.30E-02	14/NOX	1.40E-02	14/VOC	1.30E-02	14/VOC
3	4.70E-03	4/VOC	1.20E-02	14/VOC	-1.10E-02	14/NOX	1.10E-02	5/VOC
4	4.70E-03	14/VOC	8.10E-03	4/VOC	7.40E-03	5/VOC	-9.20E-03	14/NOX
5	3.20E-03	5/VOC	7.10E-03	5/VOC	7.30E-03	4/VOC	4.80E-03	4/VOC
6	2.90E-03	5/NOX	3.40E-03	5/NOX	1.20E-03	5/NOX	2.50E-03	5/NOX
7	1.30E-05	8/VOC	6.00E-05	8/VOC	7.40E-05	8/VOC	6.30E-05	8/VOC
8	1.10E-05	8/NOX	5.10E-05	8/NOX	5.80E-05	8/NOX	4.90E-05	8/NOX
9	3.20E-06	15/NOX	1.50E-05	15/NOX	1.70E-05	15/NOX	1.40E-05	15/NOX
10	1.30E-06	7/VOC	5.80E-06	15/VOC	6.60E-06	15/VOC	5.40E-06	15/VOC
By source group[3]								
1	-9.60E-03	S-14/NOX	-1.10E-02	S-14/NOX	-1.00E-02	S-14/NOX	1.00E-02	B-5/VOC
2	3.80E-03	B-4/VOC	6.80E-03	B-4/VOC	7.40E-03	S-14/VOC	-8.70E-03	S-14/NOX
3	3.40E-03	S-4/NOX	6.70E-03	B-5/VOC	7.10E-03	B-5/VOC	7.20E-03	E-4/NOX
4	-3.20E-03	E-14/NOX	5.70E-03	B-14/VOC	6.70E-03	B-4/VOC	7.00E-03	B-4/NOX
5	3.00E-03	B-5/VOC	5.50E-03	S-14/VOC	6.20E-03	B-14/VOC	6.90E-03	S-4/NOX
6	2.60E-03	S-14/VOC	5.50E-03	S-4/NOX	6.00E-03	B-4/NOX	6.70E-03	B-14/VOC
7	2.20E-03	E-4/NOX	5.30E-03	B-4/NOX	5.90E-03	E-4/NOX	6.40E-03	S-14/VOC
8	2.00E-03	B-4/NOX	4.80E-03	E-4/NOX	5.50E-03	S-4/NOX	4.20E-03	B-4/VOC
9	1.90E-03	B-14/VOC	-2.70E-03	E-14/NOX	-1.40E-03	E-14/NOX	1.40E-03	E-5/NOX
10	1.40E-03	E-5/NOX	1.70E-03	E-5/NOX	6.40E-04	S-4/VOC	-8.20E-04	E-14/NOX

1. Data shown in the table were compiled for all hourly O_3 concentrations during the period of July 11-15, 1995.
2. The sensitivities by source area are calculated based on the lumped O_3 sensitivities to NOx or VOC emissions from all three source categories for that source area from DDM Run B2, which calculates O3 sensitivities to NOx and VOC emissions from 11 core source areas.
3. Letters B, S, and E represent emissions from biogenic, surface anthropogenic, and elevated anthropogenic sources, respectively.

Table 6-6. The top 10 O_3 sensitivities by source area and by source group for stratified 8-hr O_3 levels for the whole receptor region in Chicago[1].

Rank	O_3 level, ppb					
	< 80		80-90		90-100	
	Sensitivity	Variable	Sensitivity	Variable	Sensitivity	Variable
By source area[2]						
1	-1.30E-02	14/NOX	1.80E-02	4/NOX	1.80E-02	4/NOX
2	7.80E-03	4/NOX	-1.20E-02	14/NOX	1.30E-02	14/VOC
3	5.30E-03	14/VOC	1.00E-02	14/VOC	-1.20E-02	14/NOX
4	5.00E-03	4/VOC	7.00E-03	5/VOC	8.70E-03	5/VOC
5	3.50E-03	5/VOC	5.90E-03	4/VOC	6.20E-03	4/VOC
6	3.00E-03	5/NOX	2.00E-03	5/NOX	2.00E-03	5/NOX
7	4.60E-06	8/VOC	5.20E-05	8/VOC	7.70E-05	8/VOC
8	4.20E-06	8/NOX	4.20E-05	8/NOX	6.20E-05	8/NOX
9	1.30E-06	7/VOC	1.20E-05	15/NOX	1.80E-05	15/NOX
10	6.80E-07	15/NOX	4.90E-06	15/VOC	7.00E-06	15/VOC
By source group[3]						
1	-9.60E-03	S-14/NOX	-1.00E-02	S-14/NOX	-1.00E-02	S-14/NOX
2	4.10E-03	B-4/VOC	6.70E-03	B-5/VOC	8.30E-03	B-5/VOC
3	3.50E-03	S-4/NOX	5.90E-03	E-4/NOX	6.60E-03	S-14/VOC
4	-3.20E-03	E-14/NOX	5.90E-03	B-4/NOX	6.20E-03	B-4/NOX
5	3.20E-03	B-5/VOC	5.90E-03	S-4/NOX	6.20E-03	E-4/NOX
6	2.90E-03	S-14/VOC	5.40E-03	B-4/VOC	6.00E-03	S-4/NOX
7	2.30E-03	E-4/NOX	5.10E-03	S-14/VOC	6.00E-03	B-14/VOC
8	2.20E-03	B-14/VOC	4.90E-03	B-14/VOC	5.60E-03	B-4/VOC
9	2.00E-03	B-4/NOX	-1.60E-03	E-14/NOX	-1.70E-03	E-14/NOX
10	1.50E-03	E-5/NOX	9.30E-04	E-5/NOX	1.00E-03	E-5/NOX

1. Data shown in the table were compiled for all 8-hr O_3 concentrations during the period of July 11-15, 1995.
2. The sensitivities by source area are calculated based on the lumped O_3 sensitivities to NOx or VOC emissions from all three source categories for that source area from DDM Run B2, which calculates O3 sensitivities to NOx and VOC emissions from 11 core source areas.
3. Letters B, S, and E represent emissions from biogenic, surface anthropogenic, and elevated anthropogenic sources, respectively.

Table 6-7. The top 2 contributors to O_3 formation by source area and by source group predicted by DDM for stratified 1-hr O_3 levels for 9 subareas in Chicago[1].

O_3 level, ppb	Subarea									
	1	2	3	4	5	6	7	8	9	Whole receptor
By source area[2]										
< 80 ppb	14/NOX 4/NOX	14/NOX 4/NOX	14/NOX 4/NOX	14/NOX 4/NOX	14/NOX 4/NOX	14/NOX 4/NOX	4/NOX 14/NOX	14/NOX 4/NOX	14/NOX 4/NOX	14/NOX 4/NOX
80-90	4/NOX 14/VOC	14/NOX 14/VOC	14/NOX 4/VOC	4/NOX 5/VOC	14/NOX 14/VOC	4/NOX 14/NOX	4/NOX 5/VOC	4/NOX 5/VOC	4/NOX 5/VOC	4/NOX 14/NOX
90-100	4/NOX 5/VOC	14/VOC 14/NOX	14/NOX 14/VOC	4/NOX 5/VOC	14/NOX 14/VOC	14/NOX 14/VOC	4/NOX 5/VOC	4/NOX 5/VOC	4/NOX 14/VOC	4/NOX 14/VOC
100-110	N/A	14/VOC 14/NOX	14/NOX 14/VOC	4/NOX 5/VOC	14/NOX 4/NOX	14/NOX 14/VOC	4/NOX 5/VOC	N/A	N/A	4/NOX 14/VOC
110-120	N/A	14/VOC 14/NOX	14/VOC 5/VOC	N/A	N/A	14/VOC 4/NOX	N/A	N/A	N/A	N/A
> 120	N/A	14/VOC 14/NOX	14/VOC 14/NOX	N/A	N/A	14/VOC 4/VOC	N/A	N/A	N/A	N/A
By source group[3]										
< 80 ppb	S-14/NOX S-4/NOX	S-14/NOX B-4/VOC	S-14/NOX B-4/VOC	S-14/NOX S-4/NOX	S-14/NOX E-14/NOX	S-14/NOX B-4/VOC	S-4/NOX E-4/NOX	S-14/NOX S-4/NOX	S-14/NOX B-4/VOC	S-14/NOX B-4/VOC
80-90	B-4/NOX S-4/NOX	S-14/NOX B-14/VOC	S-14/NOX B-4/VOC	B-5/VOC S-4/NOX	S-14/NOX B-5/VOC	S-14/NOX B-4/VOC	E-4/NOX S-4/NOX	E-4/NOX S-4/NOX	S-4/NOX B-4/NOX	S-14/NOX B-4/VOC
90-100	B-4/NOX S-4/NOX	S-14/NOX S-14/VOC	S-14/NOX B-5/VOC	E-4/NOX B-4/NOX	S-14/NOX S-14/VOC	S-14/NOX B-5/VOC	E-4/NOX S-4/NOX	E-4/NOX S-4/NOX	B-5/VOC B-14/VOC	S-14/NOX S-14/VOC
100-110	N/A	S-14/NOX S-14/VOC	S-14/NOX B-4/VOC	E-4/NOX S-4/NOX	S-14/NOX B-5/VOC	S-14/NOX B-5/VOC	E-4/NOX S-4/NOX	N/A	N/A	B-5/VOC S-14/NOX
110-120	N/A	S-14/NOX B-5/VOC	B-5/VOC S-14/NOX	N/A	N/A	B-5/VOC S-14/NOX	N/A	N/A	N/A	N/A
> 120	N/A	S-14/VOC S-14/NOX	S-14/VOC S-14/NOX	N/A	N/A	S-14/VOC B-4/VOC	N/A	N/A	N/A	N/A

1. Data shown in the table were compiled for all hourly O_3 concentrations during the period of July 11-15, 1995.
2. The sensitivities by source area are calculated based on the lumped O_3 sensitivities to NOx or VOC emissions from all three source categories for that source area from DDM Run B2, which calculates O3 sensitivities to NOx and VOC emissions from 11 core source areas.
3. Letters B, S, and E represent emissions from biogenic, surface anthropogenic, and elevated anthropogenic sources, respectively.

Table 6-8. The top 2 contributors to O_3 formation by source area and by source group predicted by DDM for stratified 8-hr O_3 levels for 9 subareas in Chicago[1].

O_3 level, ppb	Subarea									
	1	2	3	4	5	6	7	8	9	Whole receptor
By source area[2]										
< 80 ppb	14/NOX 4/NOX	14/NOX 4/NOX	14/NOX 4/NOX	14/NOX 4/NOX	14/NOX 4/NOX	14/NOX 4/NOX	14/NOX 4/NOX	14/NOX 4/NOX	14/NOX 4/NOX	14/NOX 4/NOX
80-90	4/NOX 5/VOC	4/NOX 14/NOX	14/NOX 4/NOX	4/NOX 14/NOX	14/NOX 14/VOC	14/NOX 4/NOX	4/NOX 14/NOX	4/NOX 14/NOX	4/NOX 14/VOC	4/NOX 14/NOX
90-100	N/A	4/NOX 14/VOC	14/NOX 4/NOX	4/NOX 5/VOC	14/VOC 14/NOX	14/NOX 4/NOX	4/NOX 14/NOX	4/NOX 14/NOX	N/A	4/NOX 14/VOC
100-110	N/A	4/NOX 14/VOC	14/NOX 14/VOC	N/A	N/A	4/NOX 14/NOX	N/A	N/A	N/A	N/A
110-120	N/A	14/VOC 14/NOX	14/NOX 14/VOC	N/A	N/A	14/VOC 14/NOX	N/A	N/A	N/A	N/A
> 120	N/A	14/VOC 14/NOX	14/VOC 14/NOX	N/A	N/A	14/VOC 14/NOX	N/A	N/A	N/A	N/A
By source group[3]										
< 80 ppb	S-14/NOX S-4/NOX	S-14/NOX B-4/VOC	S-14/NOX B-4/VOC	S-14/NOX B-4/VOC	S-14/NOX B-4/VOC	S-14/NOX B-4/VOC	S-14/NOX B-4/VOC	S-14/NOX B-4/VOC	S-14/NOX B-4/VOC	S-14/NOX B-4/VOC
80-90	B-5/VOC B-4/NOX	S-14/NOX B-4/NOX	S-14/NOX B-4/VOC	S-14/NOX B-5/VOC	S-14/NOX B-5/VOC	S-14/NOX B-5/VOC	S-14/NOX B-5/VOC	S-14/NOX B-5/VOC	S-14/NOX B-5/VOC	S-14/NOX B-5/VOC
90-100	N/A	S-14/NOX B-5/VOC	S-14/NOX B-4/VOC	B-5/VOC S-14/NOX	S-14/NOX B-5/VOC	S-14/NOX B-5/VOC	B-5/VOC S-14/NOX	B-5/VOC S-14/NOX	N/A	S-14/NOX B-5/VOC
100-110	N/A	S-14/NOX B-5/VOC	S-14/NOX B-5/VOC	N/A	N/A	S-14/NOX B-5/VOC	N/A	N/A	N/A	N/A
110-120	N/A	S-14/VOC S-14/NOX	S-14/NOX B-5/VOC	N/A	N/A	S-14/NOX S-14/VOC	N/A	N/A	N/A	N/A
> 120	N/A	S-14/VOC S-14/NOX	S-14/NOX S-14/VOC	N/A	N/A	S-14/VOC S-14/NOX	N/A	N/A	N/A	N/A

1. Data shown in the table were compiled for all hourly O_3 concentrations during the period of July 11-15, 1995.
2. The sensitivities by source area are calculated based on the lumped O_3 sensitivities to NOx or VOC emissions from all three source categories for that source area from DDM Run B2, which calculates O3 sensitivities to NOx and VOC emissions from 11 core source areas.
3. Letters B, S, and E represent emissions from biogenic, surface anthropogenic, and elevated anthropogenic sources, respectively.

small difference in their rankings. The top 10 most influential contributors by source group for the 8-hr O_3 concentrations in the levels of 80-90 ppb and 90-100 ppb are quite similar to those for the 1-hr O_3 concentrations but with different rankings. For example, the surrounding elevated anthropogenic NO_x emission group (i.e., E-4/NO_x) ranks 3rd and 5th for the 8-hr O_3 levels of 80-90 ppb and 90-100 ppb respectively, and 8th and 7th for the same 1-hr O_3 levels, respectively. For the 8-hr O_3 levels of 80-90 ppb, the two most influential emissions are the local surface anthropogenic NO_x emissions (i.e., S-14/NO_x) and the upwind biogenic VOC emissions (i.e., B-5/VOC). O_3 formation responds negatively to changes in the local surface anthropogenic NO_x emissions and the upwind biogenic VOC emissions are uncontrollable. For the 8-hr O_3 levels of 90-100 ppb, the four most influential emissions are the local surface anthropogenic NO_x emissions (i.e., S-14/NO_x), the upwind biogenic VOC emissions (i.e., B-5/VOC), the local surface anthropogenic VOC emissions (i.e., S-14/VOC), and the surrounding biogenic NO_x emissions (i.e., B-4/NO_x). O_3 formation responds negatively to changes in the local surface anthropogenic NO_x emissions and the upwind/surrounding biogenic VOC emissions are uncontrollable. Therefore, a reduction of the surrounding elevated anthropogenic NO_x emissions may be a more effective strategy to reduce the 8-hr O_3 concentrations of > 80 ppb, but less effective for the reduction of the 1-hr O_3 levels of 80-100 ppb in Chicago. The order of controllable (i.e., anthropogenic) source groups in the top 10 contributors is E-4/NO_x, S-4/NO_x, S-14/VOC, E-5/NO_x, and E-14/NO_x for the highest 1-hr O_3 levels of 100-110 ppb and S-14/VOC, E-4/NO_x, S-4/NO_x, E-14/NO_x, and E-5/NO_x for the highest 8-hr O_3 level of 90-100 ppb. This indicates that different priorities in emission reductions may be needed to effectively reduce the maximum 1-hr or 8-hr O_3 concentrations in Chicago.

The effect of VOC on the intermediate and high 1-hr O_3 levels (> 80 ppb) and high 8-hr O_3 levels (> 100 ppb) is more noticeable in many subareas than for the whole receptor region in Chicago, as shown in Tables 6-7 and 6-8. The local VOC emissions (i.e., source area 14) rank either 1st or 2nd and are the dominant contributor for O_3 concentrations in downtown Chicago and along the Lake Michigan shore (i.e., subareas 2, 3, 5, and 6) (note that the local NO_x emissions 14/NO_x rank either 1st or 2nd in these subareas, but O_3 concentrations responds negatively to the changes in local NO_x

emissions). The 1-hr and 8-hr O_3 concentrations in other subareas (i.e., subareas 1, 4, 7, 8, and 9) are most sensitive to NO_x emissions from the surrounding sources (i.e., 4/NO_x) and/or the VOC emissions transported from the upwind source area 5 (i.e., 5/VOC). The highest 1-hr and 8-hr O_3 concentrations (> 120 ppb) occur only in subareas 2, 3, and 6 and are most sensitive to the local surface anthropogenic VOC emissions (i.e., S-14/VOC).

The relative importance of individual source categories is different in various subareas of Chicago. The O_3 formation (both 1-hr and 8-hr O_3 concentrations) in downtown and Lake Michigan shore areas (i.e., subareas 2, 3, 5, and 6) is most sensitive to the local surface anthropogenic NO_x emissions (i.e., S-14/NO_x), the local biogenic and surface anthropogenic VOC emissions (i.e., B-14/VOC and S-14/VOC), and the biogenic VOC emissions from the surrounding and upwind sources (i.e., B-4/VOC and B-5/VOC). In southwestern Chicago (i.e., subareas 4, 7, and 8), the 1-hr O_3 concentrations are affected by the elevated anthropogenic NO_x emissions from the point sources located southwest of Chicago (i.e., E-4/NO_x) and the surface anthropogenic NO_x emissions from the surrounding sources (i.e., S-4/NO_x), while the 8-hr O_3 concentrations are affected by the local surface anthropogenic NO_x emissions (i.e., S-14/NO_x) and biogenic VOC emissions from the surrounding and upwind sources (i.e., B-4/VOC and B-5/VOC). In northwestern Chicago (i.e., subarea 1), both the 1-hr and 8-hr O_3 concentrations are mainly affected by the biogenic and surface anthropogenic NO_x emissions from the surrounding sources (i.e., B-4/NO_x and S-4/NO_x), while the 8-hr O_3 concentrations are also affected by the biogenic VOC emissions from the upwind sources (i.e., B-5/VOC). In southeastern Chicago (i.e., subarea 9), the 1-hr O_3 concentrations are affected by the surface anthropogenic and biogenic NO_x emissions from the surrounding sources (i.e., S-4/NO_x and B-4/NO_x), and biogenic VOC emissions from the local, surrounding and upwind sources (i.e., B-14/VOC, B-4/VOC and B-5/VOC), while the 8-hr O_3 concentrations are affected by the local surface anthropogenic NO_x emissions (i.e., S-14/NO_x) and the biogenic VOC emissions from the surrounding and upwind sources (i.e., B-4/VOC and B-5/VOC).

New York City

Results for New York City are summarized in Tables 6-9 to 6-12.

Table 6-9. The top 10 O_3 sensitivities by source area and by source group for stratified 1-hr O_3 levels for the whole receptor region in New York City[1].

Rank	O_3 level, ppb									
	< 80		80-90		90-100		100-110		110-120	
	Sensitivity	Variable	Sensitivity	Variable	Sensitivity	Variable	Sensitivity	Variable	Sensitivity	Variable
By source area[2]										
1	-1.20E-02	16/NOX	9.50E-03	11/NOX	1.10E-02	11/NOX	1.10E-02	11/NOX	1.20E-02	13/NOX
2	8.00E-03	11/NOX	7.50E-03	11/VOC	7.70E-03	13/NOX	1.10E-02	13/NOX	1.00E-02	11/NOX
3	3.70E-03	11/VOC	-6.00E-03	16/NOX	6.60E-03	11/VOC	7.60E-03	11/VOC	7.50E-03	11/VOC
4	3.40E-03	12/NOX	5.10E-03	16/VOC	5.70E-03	16/VOC	6.90E-03	16/VOC	7.10E-03	16/VOC
5	3.30E-03	7/VOC	4.40E-03	13/NOX	3.30E-03	7/VOC	4.30E-03	7/VOC	7.10E-03	7/VOC
6	2.80E-03	16/VOC	3.80E-03	13/VOC	-3.30E-03	16/NOX	3.90E-03	13/VOC	6.20E-03	12/VOC
7	2.60E-03	7/NOX	3.40E-03	12/VOC	3.30E-03	13/VOC	3.80E-03	7/NOX	5.40E-03	7/NOX
8	1.80E-03	12/VOC	2.70E-03	7/VOC	3.20E-03	7/NOX	-3.20E-03	16/NOX	4.50E-03	13/VOC
9	1.40E-03	13/VOC	2.50E-03	7/NOX	1.70E-03	4/NOX	2.60E-03	12/VOC	-2.80E-03	16/NOX
10	7.20E-04	4/VOC	2.20E-03	12/NOX	1.50E-03	5/VOC	1.30E-03	4/NOX	1.60E-03	12/NOX
By source group[3]										
1	-9.80E-03	S-16/NOX	6.50E-03	B-11/VOC	5.70E-03	S-13/NOX	7.50E-03	S-13/NOX	8.40E-03	S-13/NOX
2	4.50E-03	S-11/NOX	5.40E-03	S-11/NOX	5.60E-03	S-11/NOX	6.60E-03	B-11/VOC	6.70E-03	B-11/VOC
3	3.10E-03	B-11/VOC	-5.30E-03	S-16/NOX	5.60E-03	B-11/VOC	5.70E-03	S-11/NOX	5.90E-03	B-7/VOC
4	2.90E-03	E-11/NOX	3.30E-03	S-13/NOX	4.00E-03	E-11/NOX	4.50E-03	E-11/NOX	5.70E-03	B-12/VOC
5	2.30E-03	B-7/VOC	3.20E-03	E-11/NOX	3.20E-03	B-16/VOC	3.90E-03	B-16/VOC	5.00E-03	S-11/NOX
6	1.90E-03	S-12/NOX	3.00E-03	B-12/VOC	-3.00E-03	S-16/NOX	3.30E-03	B-7/VOC	4.70E-03	E-11/NOX
7	-1.80E-03	E-16/NOX	2.80E-03	B-13/VOC	2.60E-03	B-13/VOC	2.90E-03	B-13/VOC	4.00E-03	B-16/VOC
8	1.80E-03	S-16/VOC	2.80E-03	B-16/VOC	2.50E-03	S-16/VOC	2.90E-03	S-16/VOC	3.20E-03	B-13/VOC
9	1.60E-03	B-12/VOC	2.20E-03	S-16/VOC	2.40E-03	B-7/VOC	-2.90E-03	S-16/NOX	3.20E-03	E-13/NOX
10	1.40E-03	E-7/NOX	1.90E-03	B-7/VOC	1.70E-03	E-13/NOX	2.60E-03	E-13/NOX	3.00E-03	S-16/VOC

1. Data shown in the table were compiled for all hourly O_3 concentrations during the period of July 11-15, 1995.
2. The sensitivities by source area are calculated based on the lumped O_3 sensitivities to NOx or VOC emissions from all three source categories for that source area from DDM Run B2, which calculates O3 sensitivities to NOx and VOC emissions from 11 core source areas.
3. Letters B, S, and E represent emissions from biogenic, surface anthropogenic, and elevated anthropogenic sources, respectively.

Table 6-10. The top 10 O_3 sensitivities by source area and by source group for stratified 8-hr O_3 levels for the whole receptor region in New York City[1].

Rank	O_3 level, ppb									
	< 80		80-90		90-100		100-110		110-120	
	Sensitivity	Variable	Sensitivity	Variable	Sensitivity	Variable	Sensitivity	Variable	Sensitivity	Variable
By source area[2]										
1	-1.10E-02	16/NOX	1.00E-02	11/NOX	1.10E-02	11/NOX	1.20E-02	11/NOX	1.10E-02	11/NOX
2	7.90E-03	11/NOX	6.30E-03	11/VOC	8.30E-03	13/NOX	1.00E-02	13/NOX	1.10E-02	13/NOX
3	4.10E-03	11/VOC	-5.80E-03	16/NOX	6.80E-03	11/VOC	7.20E-03	11/VOC	7.90E-03	11/VOC
4	3.50E-03	12/NOX	5.30E-03	13/NOX	5.70E-03	16/VOC	6.70E-03	7/VOC	6.90E-03	16/VOC
5	3.40E-03	7/VOC	4.90E-03	16/VOC	-3.80E-03	16/NOX	6.00E-03	16/VOC	6.80E-03	7/VOC
6	3.30E-03	16/VOC	3.50E-03	7/VOC	3.60E-03	7/VOC	5.70E-03	12/VOC	6.30E-03	12/VOC
7	2.70E-03	7/NOX	3.20E-03	7/NOX	3.30E-03	7/NOX	5.20E-03	7/NOX	5.20E-03	7/NOX
8	2.00E-03	12/VOC	2.80E-03	13/VOC	3.30E-03	13/VOC	-5.00E-03	16/NOX	4.60E-03	13/VOC
9	1.70E-03	13/VOC	2.10E-03	12/VOC	1.80E-03	12/VOC	4.10E-03	13/VOC	-4.30E-03	16/NOX
10	7.50E-04	4/VOC	1.50E-03	12/NOX	1.50E-03	4/NOX	2.10E-03	12/NOX	2.00E-03	12/NOX
By source group[3]										
1	-9.60E-03	S-16/NOX	5.60E-03	S-11/NOX	6.00E-03	S-13/NOX	7.30E-03	S-13/NOX	7.90E-03	S-13/NOX
2	4.40E-03	S-11/NOX	5.40E-03	B-11/VOC	5.80E-03	B-11/VOC	6.40E-03	B-11/VOC	7.10E-03	B-11/VOC
3	3.30E-03	B-11/VOC	-5.10E-03	S-16/NOX	5.70E-03	S-11/NOX	6.10E-03	S-11/NOX	5.90E-03	B-12/VOC
4	2.90E-03	E-11/NOX	4.00E-03	S-13/NOX	4.20E-03	E-11/NOX	5.80E-03	B-7/VOC	5.70E-03	B-7/VOC
5	2.40E-03	B-7/VOC	3.70E-03	E-11/NOX	-3.40E-03	S-16/NOX	5.30E-03	B-12/VOC	5.50E-03	S-11/NOX
6	2.10E-03	S-16/VOC	2.70E-03	B-16/VOC	3.20E-03	B-16/VOC	5.00E-03	E-11/NOX	4.80E-03	E-11/NOX
7	2.00E-03	S-12/NOX	2.60E-03	B-7/VOC	2.70E-03	B-7/VOC	-4.40E-03	S-16/NOX	4.00E-03	B-16/VOC
8	1.80E-03	B-12/VOC	2.20E-03	S-16/VOC	2.50E-03	B-13/VOC	3.50E-03	B-16/VOC	-3.70E-03	S-16/NOX
9	-1.80E-03	E-16/NOX	2.10E-03	B-13/VOC	2.40E-03	S-16/VOC	3.10E-03	B-13/VOC	3.40E-03	B-13/VOC
10	1.50E-03	E-7/NOX	1.90E-03	B-12/VOC	1.90E-03	E-13/NOX	3.00E-03	E-7/NOX	3.00E-03	E-13/NOX

1. Data shown in the table were compiled for all 8-hr O_3 concentrations during the period of July 11-15, 1995.
2. The sensitivities by source area are calculated based on the lumped O_3 sensitivities to NOx or VOC emissions from all three source categories for that source area from DDM Run B2, which calculates O3 sensitivities to NOx and VOC emissions from 11 core source areas.
3. Letters B, S, and E represent emissions from biogenic, surface anthropogenic, and elevated anthropogenic sources, respectively.

Table 6-11. The top 2 contributors to O_3 formation by source area and by source group predicted by DDM for stratified 1-hr O_3 levels for 9 subareas in New York City[1].

O_3 level, ppb	Subarea									
	1	2	3	4	5	6	7	8	9	Whole receptor
By source area[2]										
< 80 ppb	11/NOX 16/NOX	16/NOX 11/NOX	16/NOX 11/NOX	16/NOX 11/NOX	16/NOX 11/NOX	16/NOX 11/NOX	16/NOX 11/NOX	11/NOX 12/NOX	11/NOX 12/NOX	16/NOX 11/NOX
80-90	11/NOX 13/NOX	16/NOX 16/VOC	16/NOX 16/VOC	16/NOX 16/VOC	16/NOX 16/VOC	11/NOX 13/NOX	13/VOC 16/NOX	11/NOX 11/VOC	11/NOX 11/VOC	11/NOX 11/VOC
90-100	11/NOX 13/NOX	11/NOX 13/NOX	11/NOX 16/NOX	11/NOX 16/NOX	16/VOC 16/NOX	11/NOX 13/NOX	11/NOX 13/VOC	13/NOX 11/NOX	11/NOX 12/VOC	11/NOX 13/NOX
100-110	11/NOX 13/NOX	11/NOX 11/VOC	16/VOC 11/NOX	11/NOX 13/NOX	16/NOX 16/VOC	11/VOC 16/VOC	11/NOX 13/NOX	N/A	13/NOX 11/NOX	11/NOX 13/NOX
110-120	N/A	16/VOC 11/VOC	16/VOC 11/VOC	N/A	16/NOX 16/VOC	16/VOC 11/VOC	13/NOX 11/NOX	16/VOC 11/VOC	13/NOX 11/NOX	13/NOX 11/NOX
> 120	N/A	N/A	11/VOC 16/VOC	N/A	N/A	16/VOC 11/VOC	N/A	13/NOX 11/NOX	16/VOC 16/NOX	N/A
By source group[3]										
< 80 ppb	S-16/NOX S-11/NOX	S-16/NOX S-11/NOX	S-16/NOX S-11/NOX	S-16/NOX S-11/NOX	S-16/NOX S-11/NOX	S-16/NOX S-11/NOX	S-16/NOX S-11/NOX	S-11/NOX S-16/NOX	S-11/NOX S-12/NOX	S-16/NOX S-11/NOX
80-90	S-11/NOX E-11/NOX	S-16/NOX S-16/VOC	S-16/NOX B-11/VOC	S-16/NOX S-13/NOX	S-16/NOX B-16/VOC	S-11/NOX S-13/NOX	S-16/NOX B-11/VOC	S-11/NOX B-11/VOC	S-11/NOX B-11/VOC	B-11/VOC S-11/NOX
90-100	B-11/VOC S-11/NOX	S-11/NOX E-11/NOX	S-16/NOX B-11/VOC	S-16/NOX S-11/NOX	S-16/NOX B-16/VOC	B-11/VOC S-11/NOX	S-11/NOX B-11/VOC	S-13/NOX S-11/NOX	S-11/NOX B-12/VOC	S-13/NOX S-11/NOX
100-110	S-11/NOX B-11/VOC	B-11/VOC B-16/VOC	B-11/VOC S-16/NOX	S-11/NOX S-13/NOX	S-16/NOX B-11/VOC	B-11/VOC S-16/NOX	S-13/NOX S-11/NOX	N/A	S-13/NOX S-11/NOX	S-13/NOX B-11/VOC
110-120	N/A	B-11/VOC S-16/NOX	B-11/VOC B-16/VOC	N/A	S-16/NOX B-11/VOC	B-11/VOC B-16/VOC	S-13/NOX S-11/NOX	B-11/VOC B-13/VOC	S-13/NOX B-12/VOC	S-13/NOX B-11/VOC
> 120	N/A	N/A	B-11/VOC B-16/VOC	N/A	N/A	B-11/VOC S-16/VOC	N/A	S-13/NOX B-13/VOC	B-11/VOC S-16/NOX	N/A

1. Data shown in the table were compiled for all hourly O_3 concentrations during the period of July 11-15, 1995.
2. The sensitivities by source area are calculated based on the lumped O_3 sensitivities to NOx or VOC emissions from all three source categories for that source area from DDM Run B2, which calculates O3 sensitivities to NOx and VOC emissions from 11 core source areas.
3. Letters B, S, and E represent emissions from biogenic, surface anthropogenic, and elevated anthropogenic sources, respectively.

Table 6-12. The top 2 contributors to O_3 formation by source area and by source group predicted by DDM for stratified 8-hr O_3 levels for 9 subareas in New York City[1].

O_3 level, ppb	Subarea									
	1	2	3	4	5	6	7	8	9	Whole receptor
By source area[2]										
< 80 ppb	16/NOX 11/NOX	16/NOX 11/NOX	16/NOX 11/NOX	16/NOX 11/NOX	16/NOX 11/NOX	16/NOX 11/NOX	16/NOX 11/NOX	16/NOX 11/NOX	16/NOX 11/NOX	16/NOX 11/NOX
80-90	11/NOX 13/NOX	11/NOX 11/VOC	11/NOX 16/NOX	11/NOX 13/NOX	11/NOX 16/NOX	11/NOX 16/NOX	16/NOX 16/VOC	11/NOX 16/NOX	11/NOX 16/NOX	11/NOX 11/VOC
90-100	11/NOX 13/NOX	11/NOX 13/NOX	11/NOX 11/VOC	11/NOX 13/NOX	11/NOX 13/NOX	11/NOX 16/NOX	11/NOX 11/VOC	11/NOX 16/NOX	11/NOX 16/NOX	11/NOX 13/NOX
100-110	N/A	11/NOX 11/VOC	11/NOX 11/VOC	11/NOX 13/NOX	11/NOX 13/NOX	11/NOX 16/VOC	11/NOX 13/NOX	N/A	11/NOX 13/NOX	11/NOX 13/NOX
110-120	N/A	N/A	11/NOX 13/NOX	N/A	11/NOX 13/NOX	11/NOX 16/NOX	11/NOX 13/NOX	11/NOX 13/NOX	16/VOC 11/NOX	11/NOX 13/NOX
> 120	N/A	N/A	N/A	N/A	N/A	11/NOX 13/NOX	N/A	11/NOX 13/NOX	13/NOX 16/VOC	N/A
By source group[3]										
< 80 ppb	S-16/NOX S-11/NOX	S-16/NOX S-11/NOX	S-16/NOX S-11/NOX	S-16/NOX S-11/NOX	S-16/NOX S-11/NOX	S-16/NOX S-11/NOX	S-16/NOX S-11/NOX	S-16/NOX S-11/NOX	S-16/NOX S-11/NOX	S-16/NOX S-11/NOX
80-90	S-11/NOX E-11/NOX	S-11/NOX B-11/VOC	S-16/NOX S-11/NOX	S-11/NOX S-13/NOX	S-16/NOX S-11/NOX	S-16/NOX S-11/NOX	S-16/NOX B-11/VOC	S-16/NOX S-11/NOX	S-16/NOX S-11/NOX	S-11/NOX B-11/VOC
90-100	S-11/NOX B-11/VOC	S-11/NOX E-11/NOX	B-11/VOC S-11/NOX	S-11/NOX B-11/VOC	B-11/VOC S-13/NOX	S-16/NOX B-11/VOC	B-11/VOC S-16/NOX	S-16/NOX B-11/VOC	S-16/NOX S-11/NOX	S-13/NOX B-11/VOC
100-110	N/A	B-11/VOC S-11/NOX	B-11/VOC S-11/NOX	B-11/VOC S-11/NOX	B-11/VOC S-11/NOX	S-13/NOX B-11/VOC	B-11/VOC S-11/NOX	N/A	S-11/NOX S-13/NOX	S-13/NOX B-11/VOC
110-120	N/A	N/A	B-11/VOC S-11/NOX	N/A	B-11/VOC B-7//VOC	S-16/NOX B-11/VOC	B-11/VOC S-13/NOX	S-11/NOX S-13/NOX	S-13/NOX B-16/VOC	S-13/NOX B-11/VOC
> 120	N/A	N/A	N/A	N/A	N/A	B-11/VOC B-7/VOC	N/A	S-13/NOX B-11/VOC	S-13/NOX B-16/VOC	N/A

1. Data shown in the table were compiled for all hourly O_3 concentrations during the period of July 11-15, 1995.
2. The sensitivities by source area are calculated based on the lumped O_3 sensitivities to NOx or VOC emissions from all three source categories for that source area from DDM Run B2, which calculates O3 sensitivities to NOx and VOC emissions from 11 core source areas.
3. Letters B, S, and E represent emissions from biogenic, surface anthropogenic, and elevated anthropogenic sources, respectively.

and the VOC emissions from the local sources (i.e., source area 16). These results indicate that both the upwind (i.e., source area 11 that covers Pennsylvania, western New York, northeastern West Virginia, northern Virginia, and Maryland) and the local/surrounding emissions contribute mostly to the high O_3 concentrations in New York City. The VOC and NO_x emissions from the upwind Ohio River Valley (i.e., source area 7) and the VOC emissions from the surrounding sources are the next most important contributors to the high 1-hr O_3 concentrations. In addition, other most influential contributors include the local NO_x emissions for O_3 concentrations of 90-110 ppb and the VOC emissions from the Atlantic coast (source area 12) for O_3 concentrations > 110 ppb. Compared to Chicago, the high 1-hr O_3 concentrations show lower sensitivities to changes in the uncontrollable biogenic VOC emissions from the upwind, surrounding, and local sources in New York City (i.e., B-11/VOC, B-16/VOC, B-13/VOC for New York City in Table 6-9 vs. B-5/VOC, B-14/VOC, and B-4/VOC for Chicago in Table 6-5). Similar to Chicago, the sensitivities of O_3 to the local NO_x emission changes are negative, indicating that decreasing the local NO_x emissions may potentially increase O_3 in New York City. Therefore, a reduction of the surface/elevated anthropogenic NO_x emissions from the upwind and/or surrounding sources (i.e., S-11/NO_x, S-13/NO_x, E-11/NO_x, and E-13/NO_x) and the surface anthropogenic VOC emissions from the local sources (i.e., S-16/VOC) may be the most appropriate strategy for O_3 abatement in New York City. For the intermediate and low 1-hr O_3 levels (< 90 ppb), the NO_x and VOC emissions from the upwind and local sources (i.e., 11/NO_x, 11/VOC, 16/NO_x, and 16/VOC) are the most influential contributors. The NO_x and VOC emissions from the Atlantic coast (i.e., source area 12), the surrounding sources (i.e., source area 13), and the Ohio River valley (i.e., source area 7) may also affect O_3 formation in these O_3 levels. Reducing NO_x emissions from the surrounding area (i.e., 13/NO_x) can reduce more O_3 in the higher O_3 concentration ranges (e.g., a 10% reduction in NO_x emissions in source area 13 can reduce O_3 concentrations by 0.44, 0.77, 1.1, and 1.2 ppb for O_3 concentrations in the ranges of 80-90, 90-100, 100-110, and 110-120 ppb, respectively), but will slightly increase O_3 in the low O_3 concentration range (i.e., the sensitivity of O_3 formation to changes in the NO_x emissions in source area 13 is -2.4×10^{-4}, ranking 16^{th} for O_3 < 80 ppb).

The top 10 contributors by source area and source group for the 8-hr O_3 concentrations (see Table 6-10) are similar to those for the 1-hr O_3 in New York City, with small differences in their rankings for some O_3 levels. Compared to the high 1-hr O_3 (> 90 ppb), the biogenic VOC emissions from the Atlantic coast (i.e., source area 12) have a larger effect on the high 8-hr O_3 concentrations. The upwind biogenic VOC emissions (i.e., B-7/VOC) and the local surface anthropogenic NO_x emissions (i.e., S-16/NO_x, with negative influence) are generally more influential for the high 8-hr O_3 concentrations (> 80 ppb) than for the high 1-hr O_3 concentrations in the same ranges. However, those differences have little effect on the development of the O_3 control strategies for 1-hr and 8-hr O_3 concentrations because those source groups are either uncontrollable (i.e., biogenic) or causing an increased O_3 when controlled (i.e., with a negative sensitivity). Therefore, the emission control strategies developed for the 1-hr O_3 concentrations are generally applicable for the 8-hr O_3 concentrations in New York City.

The top 2 sensitivities of the intermediate and high 1-hr and 8-hr O_3 concentrations (> 80 ppb) in most subareas in New York City differ substantially from those in the whole receptor, as shown in Tables 6-11 and 6-12. For the O_3 levels of > 80 ppb, the 1-hr O_3 concentrations are most sensitive to the local NO_x and VOC emissions (i.e., 16/NO_x and 16/VOC) in downtown New York City (i.e., subarea 5), to the NO_x and VOC emissions from the local and upwind sources and the NO_x emissions from the surrounding sources (i.e., 16/NO_x, 16/VOC, 11/NO_x, 11/VOC, and 13/NO_x) in metropolitan New York City, Staten Island, and in the east of New York City (i.e., subareas 2, 3, 4, and 6), to the NO_x emissions from the upwind areas (i.e., 11/NO_x and 12/NO_x) and the NO_x and/or VOC emissions from the surrounding areas (13/NO_x and 13/VOC) and subareas of New York City (i.e., subareas 1, 7, 8, and 9). The highest 1-hr O_3 concentrations (> 120 ppb) occur only in subareas 3, 6, 8, and 9, with high sensitivities to the local and upwind VOC emissions in subareas 3 and 6, to the local and surrounding NO_x emissions in subarea 8, and to the local NO_x and VOC emissions in subarea 9. The ranking by source group shows that the surface anthropogenic NO_x emissions and biogenic VOC emissions are the most important contributors in many subareas, and the elevated anthropogenic NO_x emissions only affect the northwestern part of New York City (i.e., subareas 1 and 2).

The 8-hr O_3 concentrations over 80 ppb can occur in all subareas in New York City and its vicinity areas. Compared to the high 1-hr O_3 concentrations, the high 8-hr O_3 concentrations (> 80 ppb) in New York City are generally less sensitive to the local NO_x and VOC emissions (i.e., 16/NO_x and 16/VOC) but more sensitive to the NO_x and VOC emissions from the upwind sources (i.e., 11/NO_x and 11/VOC). For the 1-hr high O_3 concentrations, the surface anthropogenic NO_x emissions from the upwind, surrounding, and local sources (i.e., S-11/NO_x, S-13/NO_x, and S-16/NO_x) are the most important contributors to O_3 formation in subareas 4, 5, and 7, whereas for the high 8-hr O_3 concentrations, the biogenic VOC emissions from the upwind sources (i.e., B-11/VOC) are very important and rank even higher than those surface anthropogenic NO_x emissions for many high O_3 levels in those subareas.

Altoona:

Results for Altoona are presented in Tables 6-13 to 6-16.

In Altoona (see Table 6-13), all 1-hr O_3 concentrations are less than 120 ppb. The O_3 concentrations in all ranges are predominantly influenced by NO_x and/or VOC emissions from the surrounding (i.e., source areas 11) and upwind (i.e., source areas 7, 4, and 5) sources transported from Illinois, western Kentucky and Tennessee, eastern Missouri and Arkansas, and northern Mississippi to Pennsylvania. The O_3 contribution of the local NO_x emissions (i.e., source area 17) is relatively small, indicating that high O_3 concentrations in this receptor region are mainly caused by regional transport across several states upwind. The elevated/surface anthropogenic NO_x emissions and biogenic VOC emissions from the surrounding and upwind sources (e.g., E-11/NO_x, S-11/NO_x, E-7/NO_x, S-7/NO_x, B-7/VOC, B-5/VOC, B-11/VOC, B-8/VOC) are the major contributors to intermediate and high O_3 concentrations (> 80 ppb). The biogenic VOC emissions from source area 5 (i.e., B-5/VOC) and surface anthropogenic NO_x emissions from source area 4 (i.e., S-4/NO_x) show larger effect (by a factor of 3-6 and 2.6-4.0, respectively) on the intermediate and high O_3 concentrations than on the low O_3 concentrations.

Table 6-13. The top 10 O_3 sensitivities by source area and by source group for stratified 1-hr O_3 levels for the whole receptor region in Altoona[1].

Rank	O_3 level, ppb							
	< 80		80-90		90-100		100-110	
	Sensitivity	Variable	Sensitivity	Variable	Sensitivity	Variable	Sensitivity	Variable
By source area[2]								
1	6.20E-03	7/NOX	1.20E-02	11/NOX	1.20E-02	11/NOX	1.40E-02	11/NOX
2	4.80E-03	7/VOC	7.20E-03	7/NOX	7.70E-03	7/VOC	8.80E-03	7/NOX
3	2.50E-03	11/NOX	5.80E-03	7/VOC	7.50E-03	7/NOX	7.10E-03	5/VOC
4	1.60E-03	11/VOC	4.10E-03	4/NOX	5.40E-03	5/VOC	6.60E-03	4/NOX
5	1.60E-03	4/NOX	3.80E-03	5/VOC	4.50E-03	4/NOX	6.30E-03	7/VOC
6	1.30E-03	4/VOC	2.70E-03	11/VOC	3.70E-03	11/VOC	4.20E-03	11/VOC
7	1.20E-03	5/VOC	2.10E-03	17/NOX	3.10E-03	8/VOC	3.60E-03	5/NOX
8	6.10E-04	5/NOX	1.90E-03	4/VOC	2.80E-03	5/NOX	2.90E-03	8/VOC
9	5.70E-04	8/VOC	1.30E-03	5/NOX	2.60E-03	17/NOX	2.70E-03	4/VOC
10	5.40E-04	17/VOC	1.20E-03	8/VOC	2.00E-03	4/VOC	1.50E-03	17/NOX
By source group[3]								
1	3.30E-03	B-7/VOC	7.20E-03	E-11/NOX	7.80E-03	E-11/NOX	8.20E-03	E-11/NOX
2	3.00E-03	S-7/NOX	4.80E-03	B-7/VOC	6.80E-03	B-7/VOC	6.40E-03	B-5/VOC
3	2.60E-03	E-7/NOX	4.00E-03	S-11/NOX	4.80E-03	B-5/VOC	5.50E-03	B-7/VOC
4	1.50E-03	S-11/NOX	3.50E-03	E-7/NOX	4.20E-03	E-7/NOX	5.40E-03	S-11/NOX
5	1.30E-03	S-7/VOC	3.40E-03	B-5/VOC	3.90E-03	S-11/NOX	5.10E-03	E-7/NOX
6	1.00E-03	B-11/VOC	3.00E-03	S-7/NOX	2.90E-03	B-8/VOC	3.50E-03	B-11/VOC
7	1.00E-03	B-5/VOC	2.10E-03	B-11/VOC	2.80E-03	B-11/VOC	3.20E-03	S-7/NOX
8	8.90E-04	E-11/NOX	1.90E-03	S-4/NOX	2.70E-03	S-7/NOX	2.90E-03	S-4/NOX
9	6.90E-04	S-4/NOX	1.50E-03	B-4/VOC	2.30E-03	S-4/NOX	2.70E-03	B-8/VOC
10	6.30E-04	B-4/VOC	1.50E-03	S-17/NOX	1.80E-03	S-17/NOX	2.00E-03	B-4/VOC

1. Data shown in the table were compiled for all hourly O_3 concentrations during the period of July 11-15, 1995.
2. The sensitivities by source area are calculated based on the lumped O_3 sensitivities to NOx or VOC emissions from all three source categories for that source area from DDM Run B2, which calculates O3 sensitivities to NOx and VOC emissions from 11 core source areas.
3. Letters B, S, and E represent emissions from biogenic, surface anthropogenic, and elevated anthropogenic sources, respectively.

Table 6-14. The top 10 O_3 sensitivities by source area and by source group for stratified 8-hr O_3 levels for the whole receptor region in Altoona[1].

Rank	O_3 level, ppb					
	< 80		80-90		90-100	
	Sensitivity	Variable	Sensitivity	Variable	Sensitivity	Variable
By source area[2]						
1	6.10E-03	7/NOX	9.30E-03	11/NOX	1.20E-02	11/NOX
2	4.90E-03	7/VOC	7.20E-03	7/NOX	8.40E-03	7/NOX
3	3.20E-03	11/NOX	5.30E-03	7/VOC	7.30E-03	7/VOC
4	1.80E-03	11/VOC	4.90E-03	5/VOC	6.00E-03	5/VOC
5	1.40E-03	4/NOX	4.70E-03	4/NOX	5.20E-03	4/NOX
6	1.20E-03	4/VOC	2.30E-03	11/VOC	3.60E-03	11/VOC
7	1.10E-03	5/VOC	2.00E-03	4/VOC	3.20E-03	5/NOX
8	6.30E-04	17/VOC	1.90E-03	17/NOX	3.20E-03	8/VOC
9	5.90E-04	8/VOC	1.80E-03	5/NOX	2.20E-03	4/VOC
10	5.70E-04	5/NOX	1.70E-03	8/VOC	1.70E-03	17/NOX
By source group[3]						
1	3.40E-03	B-7/VOC	5.70E-03	E-11/NOX	7.00E-03	E-11/NOX
2	3.00E-03	S-7/NOX	4.60E-03	B-7/VOC	6.40E-03	B-7/VOC
3	2.60E-03	E-7/NOX	4.40E-03	B-5/VOC	5.30E-03	B-5/VOC
4	1.60E-03	S-11/NOX	3.30E-03	E-7/NOX	4.70E-03	E-7/NOX
5	1.40E-03	E-11/NOX	3.30E-03	S-11/NOX	4.20E-03	S-11/NOX
6	1.30E-03	S-7/VOC	3.10E-03	S-7/NOX	3.10E-03	S-7/NOX
7	1.20E-03	B-11/VOC	2.10E-03	S-4/NOX	2.90E-03	B-8/VOC
8	9.50E-04	B-5/VOC	1.80E-03	B-11/VOC	2.90E-03	B-11/VOC
9	6.30E-04	S-4/NOX	1.70E-03	B-4/VOC	2.50E-03	S-4/NOX
10	5.90E-04	B-4/VOC	1.60E-03	B-8/VOC	1.70E-03	E-5/NOX

1. Data shown in the table were compiled for all 8-hr O_3 concentrations during the period of July 11-15, 1995.
2. The sensitivities by source area are calculated based on the lumped O_3 sensitivities to NOx or VOC emissions from all three source categories for that source area from DDM Run B2, which calculates O3 sensitivities to NOx and VOC emissions from 11 core source areas.
3. Letters B, S, and E represent emissions from biogenic, surface anthropogenic, and elevated anthropogenic sources, respectively.

Table 6-15. The top 2 contributors to O_3 formation by source area and by source group predicted by DDM for stratified 1-hr O_3 levels for 9 subareas in Altoona[1].

O_3 level, ppb	Subarea									
	1	2	3	4	5	6	7	8	9	Whole receptor
By source area[2]										
< 80 ppb	7/NOX 7/VOC	7/NOX 7/VOC	7/NOX 11/NOX	7/NOX 7/VOC	7/NOX 7/VOC	7/NOX 11/NOX	7/NOX 7/VOC	7/NOX 11/NOX	11/NOX 7/NOX	7/NOX 7/VOC
80-90	7/NOX 7/VOC	11/NOX 7/NOX	11/NOX 7/NOX	7/VOC 7/NOX	11/NOX 7/NOX	7/NOX 11/NOX	11/NOX 7/VOC	11/NOX 7/NOX	11/NOX 7/NOX	11/NOX 7/NOX
90-100	11/NOX 7/NOX	11/NOX 7/VOC	11/NOX 7/NOX	11/NOX 7/VOC	11/NOX 7/VOC	11/NOX 7/NOX	11/NOX 7/NOX	11/NOX 7/NOX	11/NOX 7/VOC	11/NOX 7/VOC
100-110	7/VOC 11/VOC	N/A	N/A	11/VOC 7/VOC	11/NOX 7/VOC	11/NOX 7/VOC	11/NOX 7/NOX	11/NOX 7/NOX	11/NOX 7/VOC	11/NOX 7/NOX
110-120	N/A	N/A	N/A	11/NOX 11/VOC	N/A	N/A	11/NOX 7/NOX	N/A	N/A	N/A
> 120	N/A	N/A	N/A	N/A	N/A	N/A	N/A	N/A	N/A	N/A
By source group[3]										
< 80 ppb	S-7/NOX B-7/VOC	B-7/VOC S-7/NOX	B-7/VOC E-11/NOX	B-7/VOC E-11/NOX	B-7/VOC S-7/NOX	E-11/NOX B-7/VOC	E-7/NOX S-7/NOX	E-7/NOX B-7/VOC	E-11/NOX E-7/NOX	B-7/VOC S-7/NOX
80-90	B-7/VOC S-7/NOX	E-11/NOX B-7/VOC	E-11/NOX B-7/VOC	B-7/VOC B-11/VOC	E-11/NOX B-7/VOC	E-11/NOX B-7/VOC	B-7/VOC E-11/NOX	E-11/NOX B-7/VOC	E-11/NOX B-7/VOC	E-11/NOX B-7/VOC
90-100	B-7/VOC E-11/NOX	E-11/NOX B-7/VOC	E-11/NOX B-7/VOC	B-7/VOC B-11/VOC	B-7/VOC E-11/NOX	E-11/NOX B-7/VOC	B-5/VOC B-7/VOC	E-11/NOX B-7/VOC	E-11/NOX B-7/VOC	E-11/NOX B-7/VOC
100-110	B-7/VOC B-11/VOC	N/A	N/A	B-7/VOC B-11/VOC	E-11/NOX B-7/VOC	E-11/NOX B-7/VOC	E-11/NOX S-11/NOX	E-11/NOX S-11/NOX	E-11/NOX B-7/VOC	E-11/NOX B-5/VOC
110-120	N/A	N/A	N/A	E-11/NOX B-11/VOC	N/A	N/A	E-11/NOX S-11/NOX	N/A	N/A	N/A
> 120	N/A	N/A	N/A	N/A	N/A	N/A	N/A	N/A	N/A	N/A

1. Data shown in the table were compiled for all hourly O_3 concentrations during the period of July 11-15, 1995.
2. The sensitivities by source area are calculated based on the lumped O_3 sensitivities to NOx or VOC emissions from all three source categories for that source area from DDM Run B2, which calculates O3 sensitivities to NOx and VOC emissions from 11 core source areas.
3. Letters B, S, and E represent emissions from biogenic, surface anthropogenic, and elevated anthropogenic sources, respectively.

Table 6-16. The top 2 contributors to O_3 formation by source area and by source group predicted by DDM for stratified 8-hr O_3 levels for 9 subareas in Altoona[1].

O_3 level, ppb	Subarea									
	1	2	3	4	5	6	7	8	9	Whole receptor
By source area[2]										
< 80 ppb	7/NOX 7/VOC	7/NOX 7/VOC	7/NOX 7/VOC	7/NOX 7/VOC	7/NOX 7/VOC	7/NOX 7/VOC	7/NOX 7/VOC	7/NOX 7/VOC	7/NOX 7/VOC	7/NOX 7/VOC
80-90	11/NOX 7/NOX	7/NOX 11/NOX	11/NOX 7/NOX	11/NOX 7/NOX	7/NOX 11/NOX	7/NOX 7/VOC	7/NOX 11/NOX	7/NOX 11/NOX	11/NOX 7/NOX	11/NOX 7/NOX
90-100	11/NOX 7/VOC	11/NOX 7/VOC	N/A	11/NOX 7/NOX	7/VOC 7/NOX	11/NOX 7/NOX	11/NOX 7/NOX	11/NOX 7/NOX	11/NOX 7/NOX	11/NOX 7/NOX
100-110	N/A	N/A	N/A	11/NOX 7/VOC	11/NOX 7/NOX	N/A	11/NOX 7/NOX	N/A	N/A	N/A
110-120	N/A	N/A	N/A	N/A	N/A	N/A	11/NOX 4/NOX	N/A	N/A	N/A
> 120	N/A	N/A	N/A	N/A	N/A	N/A	N/A	N/A	N/A	N/A
By source group[3]										
< 80 ppb	B-7/VOC S-7/NOX	B-7/VOC S-7/NOX	B-7/VOC S-7/NOX	B-7/VOC S-7/NOX	B-7/VOC S-7/NOX	B-7/VOC S-7/NOX	B-7/VOC S-7/NOX	B-7/VOC S-7/NOX	B-7/VOC S-7/NOX	B-7/VOC S-7/NOX
80-90	B-7/VOC E-11/NOX	B-7/VOC E-11/NOX	B-7/VOC E-11/NOX	B-7/VOC E-11/NOX	B-7/VOC B-5/VOC	B-7/VOC B-5/VOC	B-7/VOC E-11/NOX	B-7/VOC B-5/VOC	E-11/NOX B-5/VOC	E-11/NOX B-7/VOC
90-100	B-7/VOC E-11/NOX	B-7/VOC E-11/NOX	N/A	E-11/NOX B-5/VOC	B-7/VOC B-5/VOC	B-7/VOC E-11/NOX	B-7/VOC E-11/NOX	E-11/NOX B-5/VOC	E-11/NOX B-5/VOC	E-11/NOX B-7/VOC
100-110	N/A	N/A	N/A	B-7/VOC E-11/NOX	B-7/VOC E-11/NOX	N/A	E-11/NOX B-5/VOC	N/A	N/A	N/A
110-120	N/A	N/A	N/A	N/A	N/A	N/A	E-11/NOX S-11/NOX	N/A	N/A	N/A
> 120	N/A	N/A	N/A	N/A	N/A	N/A	N/A	N/A	N/A	N/A

1. Data shown in the table were compiled for all hourly O_3 concentrations during the period of July 11-15, 1995.
2. The sensitivities by source area are calculated based on the lumped O_3 sensitivities to NOx or VOC emissions from all three source categories for that source area from DDM Run B2, which calculates O3 sensitivities to NOx and VOC emissions from 11 core source areas.
3. Letters B, S, and E represent emissions from biogenic, surface anthropogenic, and elevated anthropogenic sources, respectively.

While the 1-hr O_3 concentrations were in compliance with the previous 1-hr O_3 NAAQS, the 8-hr maximum O_3 concentrations exceeded the NAAQS of 80 ppb during the July 7-15 1995 high O_3 episode in Altoona, as shown in Tables 6-14 and 6-16. The top 10 most influential contributors for the 8-hr O_3 concentrations are the same as for the 1-hr O_3 concentrations, with small differences in their rankings. Compared to other urban receptors, the elevated anthropogenic NO_x emissions (e.g., E-11/NO_x and E-7/NO_x) play a more important role than the surface anthropogenic NO_x emissions (e.g., S-11/NO_x, S-7/NO_x) for O_3 > 80 ppb in Altoona. The elevated/surface anthropogenic NO_x emissions and biogenic VOC emissions are mainly responsible for this range of O_3 concentrations. Therefore, a reduction of the elevated and surface anthropogenic NO_x emissions from the upwind and surrounding sources (e.g., E-11/NO_x, E-7/NO_x, S-11/NO_x, S-7/NO_x) is the most effective control strategy for the maximum 8-hr O_3 concentration in Altoona.

As shown in Tables 6-15 and 6-16, the intermediate and high 1-hr and 8-hr O_3 concentrations (> 80 ppb) in most subareas in Altoona are most sensitive to the NO_x emissions from the surrounding sources (i.e., source area 11) and the NO_x or VOC emissions from the upwind sources (i.e., source area 7). The elevated anthropogenic NO_x emissions from the surrounding sources (i.e., E-11/NO_x) and the biogenic VOC emissions from the upwind and surrounding sources (i.e., B-7/VOC or B-11/VOC or B-5/VOC) affect both the 1-hr and 8-hr O_3 concentrations in all subareas. However, the elevated anthropogenic NO_x emissions from the surrounding sources are relatively more influential than the biogenic VOC emissions from the upwind sources for 1-hr O_3 concentrations but less influential for 8-hr O_3 concentrations in some subareas such as 2, 3, 5, and 6.

6.1.1.2 Comparison of the DDM and OSAT Rankings of O_3 Contributors from the 11 Core Source Areas

Figures 6-2 and 6-3 show a comparison of the DDM and OSAT rankings by source area and by source group for the 6 stratified 1-hr and 8-hr O_3 concentration levels at four receptors. The results are shown in terms of the number of source areas (or source

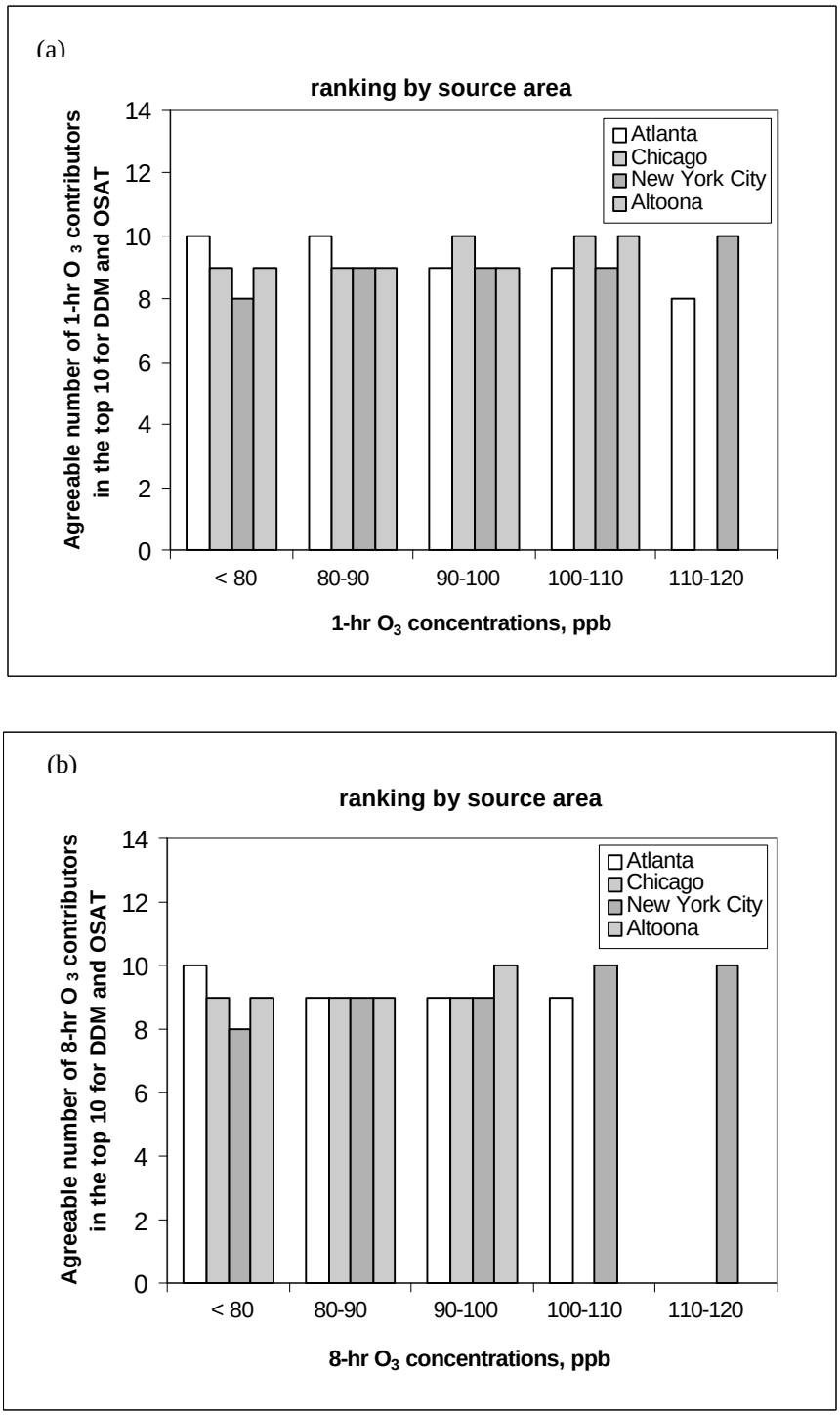

Figure 6-2. The agreeable number of O_3 contributors between the DDM and OSAT rankings by source area in the top 10 contributors for (a) 1-hr and (b) 8-hr stratified O_3 concentration levels at four receptors under the EPA 2007 base emission scenario (DDM base runs B2 and OSAT base run B1).

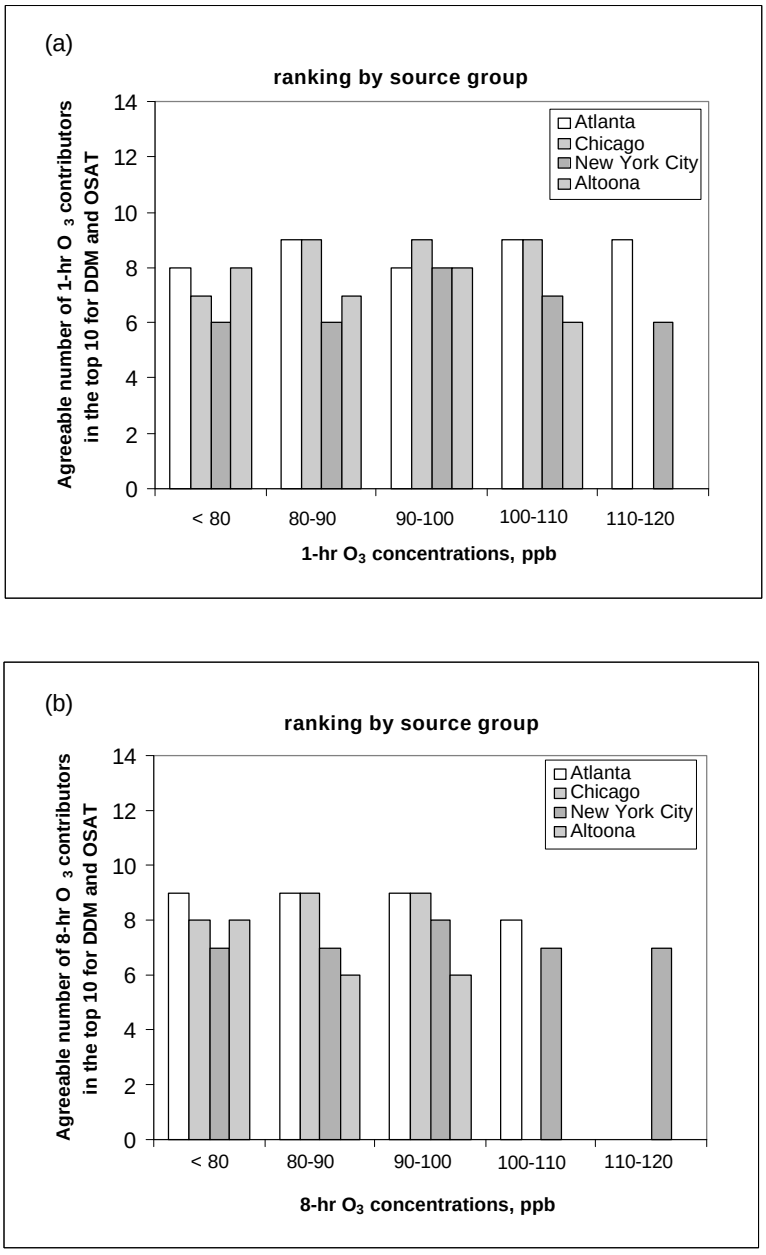

Figure 6-3. The agreeable number of O_3 contributors between the DDM and OSAT rankings by source group in the top 10 contributors for (a) 1-hr and (b) 8-hr stratified O_3 concentration levels at four receptors under the EPA 2007 base emission scenario (DDM base runs B2 and OSAT base run B1).

groups) that are listed among the top 10 contributors for both the DDM and OSAT analyses (i.e., a value of 10 shows that DDM and OSAT have the same top 10 contributors, although they could be ranked differently among them). Results are missing for some receptors for O_3 levels of 100-110 ppb and 110-120 ppb because the receptor-wide averaged 1-hr or 8-hr O_3 concentrations at those receptors are lower than 100 ppb. The rankings by both source area and source group at all receptors show a good agreement, with 8 to 10 of the top 10 contributors by source area and 6 to 9 of the top 10 contributors by source group. The level of agreement is about the same for all O_3 levels for each receptor, but the overall agreement is higher in Atlanta and Chicago and lower in New York City and Altoona. On average, DDM and OSAT agree well on the most important contributors on all O_3 levels, but disagree on about 8% of them by source area and 22% of them by source group. In a separate CRC project A-29, the top 5 source contributions predicted by the original version of OSAT and the top 5 sensitivities predicted by DDM were compared for six receptor regions in the Lake Michigan region for the O_3 episode of July 7-13, 1995 (Dunker et al., 2002b). They found that the OSAT and DDM results, on average, agreed on 4 of the top 5 contributors to O_3 concentrations for O_3 > 80 ppb. The results from this project are consistent with those of Dunker et al. (2002b).

Atlanta

Although DDM and OSAT agree well on the top 10 contributors, they predict different rankings for those contributors. Tables 6-17 to 6-20 show rankings for the stratified 1-hr and 8-hr O_3 levels predicted by OSAT for the whole receptor region and subareas in Atlanta (similar results were presented in Tables 6-1 to 6-4 for DDM). For the low 1-hr and 8-hr O_3 levels (< 80 ppb), OSAT gives greater importance to the local surface/elevated anthropogenic NO_x emissions (i.e., S-15/NO_x and E-15/NO_x) and the surrounding biogenic VOC emissions (i.e., B-8/VOC); and DDM gives greater importance to the upwind elevated/surface anthropogenic NO_x emissions (i.e., E-12/NO_x and S-12/NO_x) and the biogenic VOC emissions from the local and upwind sources (i.e., B-15/VOC, B-12/VOC, and B-5/VOC). For the 1-hr and 8-hr O_3 levels of 80-90 ppb, 90-100 ppb, and 100-110 ppb, DDM and OSAT give similar rankings, with slightly more weight to the biogenic VOC emissions from the source areas 5, 12 and 15 (i.e., B-5/VOC,

Table 6-17. The top 10 O_3 contributors by source area and by source group predicted by OSAT for stratified 1-hr O_3 levels for the whole receptor region in Atlanta[1].

Rank	O_3 level, ppb									
	< 80		80-90		90-100		100-110		110-120	
	Contribution	Variable	Contribution	Variable	Contribution	Variable	Contribution	Variable	Contribution	Variable
By source area[2]										
1	2.20E-02	8/NOx	2.90E-02	8/NOx	3.40E-02	15/NOx	4.40E-02	15/NOx	5.20E-02	15/NOx
2	7.00E-03	15/NOx	2.10E-02	15/NOx	3.20E-02	8/NOx	3.10E-02	8/NOx	3.10E-02	8/NOx
3	5.30E-03	12/NOx	7.50E-03	12/NOx	6.30E-03	8/VOC	6.60E-03	8/VOC	7.30E-03	8/VOC
4	3.30E-03	8/VOC	5.70E-03	8/VOC	5.70E-03	15/VOC	6.60E-03	15/VOC	7.30E-03	15/VOC
5	1.70E-03	5/NOx	4.20E-03	15/VOC	3.10E-03	5/NOx	4.10E-03	5/NOx	4.30E-03	12/NOx
6	1.60E-03	15/VOC	1.80E-03	5/NOx	1.90E-03	12/NOx	1.40E-03	12/NOx	1.00E-03	12/VOC
7	7.80E-04	12/VOC	1.20E-03	12/VOC	6.80E-04	5/VOC	9.70E-04	5/VOC	6.30E-04	5/NOx
8	3.80E-04	4/NOx	6.10E-04	4/NOx	4.80E-04	4/NOx	4.80E-04	4/NOx	4.60E-04	7/NOx
9	3.70E-04	5/VOC	6.00E-04	7/NOx	4.30E-04	12/VOC	3.50E-04	12/VOC	2.10E-04	11/NOx
10	3.60E-04	7/NOx	4.70E-04	5/VOC	2.90E-04	7/NOx	2.30E-04	7/NOx	1.60E-04	4/NOx
By source group[2,3]										
1	1.40E-02	S-8/NOx	1.90E-02	S-8/NOx	2.50E-02	S-15/NOx	3.20E-02	S-15/NOx	3.60E-02	S-15/NOx
2	6.30E-03	E-8/NOx	1.70E-02	S-15/NOx	2.00E-02	S-8/NOx	2.00E-02	S-8/NOx	2.00E-02	S-8/NOx
3	5.60E-03	S-15/NOx	7.70E-03	E-8/NOx	8.50E-03	E-15/NOx	1.10E-02	E-15/NOx	1.50E-02	E-15/NOx
4	2.90E-03	B-8/VOC	4.90E-03	B-8/VOC	8.10E-03	E-8/NOx	8.00E-03	E-8/NOx	8.60E-03	E-8/NOx
5	2.60E-03	S-12/NOx	3.90E-03	S-12/NOx	5.70E-03	B-8/VOC	6.00E-03	B-8/VOC	6.60E-03	B-8/VOC
6	2.10E-03	E-12/NOx	3.30E-03	E-15/NOx	4.10E-03	B-15/VOC	4.80E-03	B-15/VOC	5.40E-03	B-15/VOC
7	2.00E-03	B-8/NOx	3.00E-03	B-15/VOC	2.80E-03	B-8/NOx	2.70E-03	B-8/NOx	2.70E-03	B-8/NOx
8	1.20E-03	E-15/NOx	2.80E-03	E-12/NOx	1.50E-03	S-5/NOx	2.20E-03	S-5/NOx	2.10E-03	S-12/NOx
9	1.20E-03	B-15/VOC	2.30E-03	B-8/NOx	1.50E-03	S-15/VOC	1.80E-03	S-15/VOC	1.90E-03	S-15/VOC
10	8.20E-04	S-5/NOx	1.20E-03	S-15/VOC	1.20E-03	E-5/NOx	1.50E-03	E-5/NOx	1.70E-03	E-12/NOx

1. Data shown in the table were compiled for all hourly O_3 concentrations during the period of July 11-15, 1995.
2. The contributions by source area are calculated based on the lumped O_3 contributions to NOx or VOC emissions from all 4 source categories for that source area from OSAT Run B1. O3 contributions from the same 11 core source areas as DDM Run B2 are ranked.
3. Letters B, S, and E represent emissions from biogenic, surface anthropogenic (lumped on-road and other surface anthropogenic sources), and elevated anthropogenic sources, respectively.

Table 6-18. The top 10 O_3 contributors by source area and by source group predicted by OSAT for stratified 8-hr O_3 levels for the whole receptor region in Atlanta[1].

Rank	O_3 level, ppb							
	< 80		80-90		90-100		100-110	
	Contribution	Variable	Contribution	Variable	Contribution	Variable	Contribution	Variable
By source area[2]								
1	2.20E-02	8/NOx	3.50E-02	8/NOx	3.70E-02	15/NOx	4.40E-02	15/NOx
2	8.80E-03	15/NOx	2.20E-02	15/NOx	2.90E-02	8/NOx	3.00E-02	8/NOx
3	6.30E-03	12/NOx	6.00E-03	8/VOC	6.60E-03	8/VOC	6.80E-03	8/VOC
4	3.60E-03	8/VOC	4.00E-03	15/VOC	6.20E-03	15/VOC	6.60E-03	15/VOC
5	2.00E-03	15/VOC	3.10E-03	5/NOx	3.50E-03	5/NOx	2.60E-03	5/NOx
6	1.50E-03	5/NOx	8.20E-04	12/NOx	1.70E-03	12/NOx	2.60E-03	12/NOx
7	9.40E-04	12/VOC	7.60E-04	5/VOC	7.90E-04	5/VOC	6.10E-04	12/VOC
8	4.20E-04	7/NOx	7.40E-04	4/NOx	4.20E-04	4/NOx	5.90E-04	5/VOC
9	4.00E-04	4/NOx	3.00E-04	7/NOx	4.00E-04	12/VOC	3.40E-04	4/NOx
10	3.50E-04	5/VOC	2.60E-04	4/VOC	2.30E-04	7/NOx	3.20E-04	7/NOx
By source group[2,3]								
1	1.40E-02	S-8/NOx	2.30E-02	S-8/NOx	2.70E-02	S-15/NOx	3.10E-02	S-15/NOx
2	7.20E-03	S-15/NOx	1.80E-02	S-15/NOx	1.90E-02	S-8/NOx	2.00E-02	S-8/NOx
3	6.30E-03	E-8/NOx	8.80E-03	E-8/NOx	9.30E-03	E-15/NOx	1.20E-02	E-15/NOx
4	3.10E-03	B-8/VOC	5.30E-03	B-8/VOC	7.60E-03	E-8/NOx	8.10E-03	E-8/NOx
5	3.10E-03	S-12/NOx	4.00E-03	E-15/NOx	6.00E-03	B-8/VOC	6.20E-03	B-8/VOC
6	2.50E-03	E-12/NOx	2.90E-03	B-15/VOC	4.50E-03	B-15/VOC	4.80E-03	B-15/VOC
7	2.00E-03	B-8/NOx	2.90E-03	B-8/NOx	2.70E-03	B-8/NOx	2.70E-03	B-8/NOx
8	1.40E-03	B-15/VOC	1.50E-03	S-5/NOx	1.80E-03	S-5/NOx	1.80E-03	S-15/VOC
9	1.40E-03	E-15/NOx	1.30E-03	E-5/NOx	1.70E-03	S-15/VOC	1.40E-03	S-5/NOx
10	7.70E-04	B-12/VOC	1.00E-03	S-15/VOC	1.30E-03	E-5/NOx	1.30E-03	S-12/NOx

1. Data shown in the table were compiled for all hourly O_3 concentrations during the period of July 11-15, 1995.
2. The contributions by source area are calculated based on the lumped O_3 contributions to NOx or VOC emissions from all 4 source categories for that source area from OSAT Run B1. O3 contributions from the same 11 core source areas as DDM Run B2 are ranked.
3. Letters B, S, and E represent emissions from biogenic, surface anthropogenic (lumped on-road and other surface anthropogenic sources), and elevated anthropogenic sources, respectively.

Table 6-19. The top 2 contributors to O_3 concentrations by source area and by source group predicted by OSAT for stratified 1-hr O_3 levels for 9 subareas in Atlanta[1].

O_3 level, ppb	Subarea									
	1	2	3	4	5	6	7	8	9	Whole receptor
By source area[2]										
< 80 ppb	8/NOX 15/NOX	8/NOX 15/NOX	8/NOX 12/NOX	8/NOX 15/NOX	8/NOX 15/NOX	8/NOX 12/NOX	8/NOX 15/NOX	8/NOX 15/NOX	8/NOX 12/NOX	8/NOX 15/NOX
80-90	15/NOX 8/NOX	8/NOX 15/NOX	8/NOX 15/NOX	8/NOX 15/NOX	8/NOX 15/NOX	8/NOX 15/NOX	8/NOX 15/NOX	8/NOX 15/NOX	15/NOX 8/NOX	8/NOX 15/NOX
90-100	15/NOX 8/NOX	15/NOX 8/NOX	N/A	8/NOX 15/NOX	8/NOX 15/NOX	15/NOX 8/NOX	15/NOX 8/NOX	15/NOX 8/NOX	15/NOX 8/NOX	15/NOX 8/NOX
100-110	15/NOX 8/NOX	15/NOX 8/NOX	N/A	15/NOX 8/NOX	15/NOX 8/NOX	N/A	8/NOX 15/NOX	15/NOX 8/NOX	15/NOX 8/NOX	15/NOX 8/NOX
110-120	N/A	N/A	N/A	15/NOX 8/NOX	15/NOX 8/NOX	15/NOX 8/NOX	15/NOX 8/NOX	15/NOX 8/NOX	15/NOX 8/NOX	15/NOX 8/NOX
> 120	N/A	N/A	N/A	15/NOX 8/NOX	15/NOX 8/NOX	15/NOX 8/NOX	15/NOX 8/NOX	15/NOX 8/NOX	15/NOX 8/NOX	N/A
By source group[2,3]										
< 80 ppb	S-8/NOX E-8/NOX	S-8/NOX S-15/NOX	S-8/NOX E-8/NOX	S-8/NOX S-15/NOX	S-8/NOX E-8/NOX	S-8/NOX E-8/NOX	S-8/NOX E-8/NOX	S-8/NOX E-8/NOX	S-8/NOX E-8/NOX	S-8/NOX E-8/NOX
80-90	S-8/NOX S-15/NOX	S-15/NOX S-8/NOX	S-8/NOX S-15/NOX	S-8/NOX S-15/NOX	S-15/NOX S-8/NOX	S-8/NOX S-15/NOX	S-15/NOX S-8/NOX	S-8/NOX S-15/NOX	S-15/NOX S-8/NOX	S-8/NOX S-15/NOX
90-100	S-8/NOX S-15/NOX	S-15/NOX S-8/NOX	N/A	S-15/NOX S-8/NOX	S-15/NOX S-8/NOX	S-15/NOX S-8/NOX	S-15/NOX S-8/NOX	S-15/NOX S-8/NOX	S-15/NOX S-8/NOX	S-15/NOX S-8/NOX
100-110	S-15/NOX S-8/NOX	S-15/NOX S-8/NOX	N/A	S-15/NOX S-8/NOX	S-15/NOX S-8/NOX	N/A	S-15/NOX S-8/NOX	S-15/NOX S-8/NOX	S-15/NOX S-8/NOX	S-15/NOX S-8/NOX
110-120	N/A	N/A	N/A	S-15/NOX S-8/NOX	S-15/NOX S-8/NOX	S-15/NOX S-8/NOX	S-15/NOX S-8/NOX	S-15/NOX S-8/NOX	S-15/NOX S-8/NOX	S-15/NOX S-8/NOX
> 120	N/A	N/A	N/A	S-15/NOX S-8/NOX	S-15/NOX S-8/NOX	S-15/NOX E-15/NOX	S-15/NOX E-15/NOX	S-15/NOX E-15/NOX	S-15/NOX S-8/NOX	N/A

1. Data shown in the table were compiled for all hourly O_3 concentrations during the period of July 11-15, 1995.
2. The contributions by source area are calculated based on the lumped O_3 contributions to NOx or VOC emissions from all 4 source categories for that source area from OSAT Run B1. O3 contributions from the same 11 core source areas as DDM Run B2 are ranked.
3. Letters B, S, and E represent emissions from biogenic, surface anthropogenic (lumped on-road and other surface anthropogenic sources), and elevated anthropogenic sources, respectively.

Table 6-20. The top 2 contributors to O_3 concentration by source area and by source group predicted by OSAT for stratified 8-hr O_3 levels for 9 subareas in Atlanta[1].

O_3 level, ppb	Subarea									
	1	2	3	4	5	6	7	8	9	Whole receptor
By source area[2]										
< 80 ppb	8/NOX 15/NOX	8/NOX 15/NOX	8/NOX 15NOX	8/NOX 15/NOX	8/NOX 15/NOX	8/NOX 15/NOX	8/NOX 15/NOX	8/NOX 15/NOX	8/NOX 15/NOX	8/NOX 15/NOX
80-90	8/NOX 15/NOX	15/NOX 8/NOX	N/A	8/NOX 15/NOX	8/NOX 15/NOX	15/NOX 8/NOX	8/NOX 15/NOX	8/NOX 15/NOX	15/NOX 8/NOX	8/NOX 15/NOX
90-100	15/NOX 8/NOX	15/NOX 8/NOX	N/A	8/NOX 15/NOX	8/NOX 15/NOX	15/NOX 8/NOX	8/NOX 15/NOX	15/NOX 8/NOX	15/NOX 8/NOX	15/NOX 8/NOX
100-110	15/NOX 8/NOX	N/A	N/A	8/NOX 15/NOX	15/NOX 8/NOX	N/A	15/NOX 8/NOX	15/NOX 8/NOX	15/NOX 8/NOX	15/NOX 8/NOX
110-120	N/A	N/A	N/A	8/NOX 15/NOX	15/NOX 8/NOX	15/NOX 8/NOX	8/NOX 15/NOX	15/NOX 8/NOX	15/NOX 8/NOX	N/A
> 120	N/A	N/A	N/A	15/NOX 8/NOX	15/NOX 8/NOX	N/A	15/NOX 8/NOX	15/NOX 8/NOX	N/A	N/A
By source group[2,3]										
< 80 ppb	S-8/NOX S-15/NOX	S-8/NOX S-15/NOX	S-8/NOX S-15/NOX	S-8/NOX E-8/NOX	S-8/NOX S-15/NOX	S-8/NOX S-15/NOX	S-8/NOX E-8/NOX	S-8/NOX S-15/NOX	S-8/NOX S-15/NOX	S-8/NOX S-15/NOX
80-90	S-8/NOX S-15/NOX	S-8/NOX S-15/NOX	N/A	S-8/NOX S-15/NOX	S-15/NOX S-8/NOX	S-15/NOX S-8/NOX	S-15/NOX S-8/NOX	S-8/NOX S-15/NOX	S-15/NOX S-8/NOX	S-8/NOX S-15/NOX
90-100	S-15/NOX S-8/NOX	S-15/NOX S-8/NOX	N/A	S-8/NOX S-15/NOX	S-8/NOX S-15/NOX	S-15/NOX S-8/NOX	S-8/NOX S-15/NOX	S-15/NOX S-8/NOX	S-15/NOX S-8/NOX	S-15/NOX S-8/NOX
100-110	S-15/NOX S-8/NOX	N/A	N/A	S-15/NOX S-8/NOX	S-15/NOX S-8/NOX	N/A	S-15/NOX S-8/NOX	S-15/NOX S-8/NOX	S-15/NOX S-8/NOX	S-15/NOX S-8/NOX
110-120	N/A	N/A	N/A	S-15/NOX S-8/NOX	S-15/NOX S-8/NOX	N/A	S-15/NOX S-8/NOX	S-15/NOX S-8/NOX	S-15/NOX S-8/NOX	N/A
> 120	N/A	N/A	N/A	S-15/NOX S-8/NOX	S-15/NOX S-8/NOX	N/A	S-15/NOX S-8/NOX	S-15/NOX S-8/NOX	N/A	N/A

1. Data shown in the table were compiled for all hourly O_3 concentrations during the period of July 11-15, 1995.
2. The contributions by source area are calculated based on the lumped O_3 contributions to NOx or VOC emissions from all 4 source categories for that source area from OSAT Run B1. O3 contributions from the same 11 core source areas as DDM Run B2 are ranked.
3. Letters B, S, and E represent emissions from biogenic, surface anthropogenic (lumped on-road and other surface anthropogenic sources), and elevated anthropogenic sources, respectively.

B-12/VOC, and B-15/VOC) given by DDM and to the surface/elevated anthropogenic NO_x and surface anthropogenic VOC emissions from the source areas 5, 12, and 15 (i.e., S-5/NO_x, E-5/NO_x, S-12/NO_x, and S-15/VOC) given by OSAT. For the highest 1-hr O_3 levels of 110-120 ppb, OSAT gives greater importance to the NO_x emissions from the upwind sources (i.e., source areas 4 and 11); and DDM gives greater importance to the VOC emissions from the upwind sources (i.e., source areas 5 and 7). While the top 2 O_3 contributors for the 8-hr O_3 concentrations predicted by DDM and OSAT are quite similar, those for the 1-hr O_3 concentrations differ in many subareas in Atlanta, as shown in Tables 6-19 and 6-20. For example, the local and surrounding surface anthropogenic NO_x emissions (i.e., S-15/NO_x and S-8/NO_x) are the top 2 contributors for the 1-hr O_3 concentration levels of > 80 ppb for all subareas by OSAT but only for the subareas 3, 7, and 8 by DDM. DDM predicts both the local surface and elevated anthropogenic NO_x emissions (i.e., S-15/NO_x and E-15/NO_x) to be the top 2 contributors for some high O_3 levels (> 90 ppb) in some subareas (e.g., subareas 1, 2, 6, and 9) and the biogenic VOC emissions from the local and surrounding source areas (i.e., B-15/VOC and B-8/VOC) to be one of the top 2 contributors for some O_3 levels in subareas 4 and 5.

Chicago

Similar ranking information predicted by OSAT for the stratified 1-hr and 8-hr O_3 levels for the whole receptor area and individual subareas is shown in Tables 6-21 to 6-24 for Chicago (similar results were presented in Tables 6-5 to 6-8 for DDM). In Chicago, DDM predicts a negative sensitivity to the local NO_x emissions for all O_3 levels (i.e., S-14/NO_x and E-14/NO_x), whereas OSAT always predicts a positive O_3 contribution from the local NO_x emissions. Therefore, the OSAT ranking of O_3 contributors is not suitable for the development of O_3 control strategies in regions where there is a large titration or inhibition effect of NO_x on O_3 formation. For the low 1-hr and 8-hr O_3 levels (< 80 ppb), DDM gives more weight to the local surface/elevated anthropogenic NO_x emissions (i.e., S-14/NO_x and E-14/NO_x) and the upwind/local biogenic VOC emissions (i.e., B-5/VOC and B-14/VOC); OSAT gives more weight to the surrounding NO_x emissions from all source categories (i.e., S-4/NO_x, B-4/NO_x, and E-4/NO_x) and the surface/elevated anthropogenic NO_x emissions from the upwind sources (i.e., S-5/NO_x and E-5/NO_x). For the intermediate and high 1-hr and 8-hr O_3 levels (> 80 ppb), DDM gives more weight to

Table 6-21. The top 10 O_3 contributors by source area and by source group predicted by OSAT for stratified 1-hr O_3 levels for the whole receptor region in Chicago[1].

Rank	O_3 level, ppb							
	< 80		80-90		90-100		100-110	
	Contribution	Variable	Contribution	Variable	Contribution	Variable	Contribution	Variable
By source area[2]								
1	1.50E-02	4/NOx	2.70E-02	4/NOx	2.70E-02	4/NOx	3.30E-02	4/NOx
2	4.60E-03	5/NOx	8.20E-03	14/NOx	1.30E-02	14/NOx	1.30E-02	14/NOx
3	3.40E-03	4/VOC	7.50E-03	5/NOx	9.10E-03	14/VOC	9.10E-03	14/VOC
4	3.00E-03	14/VOC	7.10E-03	14/VOC	5.40E-03	5/VOC	6.90E-03	5/VOC
5	2.30E-03	14/NOx	6.10E-03	4/VOC	5.20E-03	5/NOx	6.70E-03	5/NOx
6	2.00E-03	5/VOC	4.70E-03	5/VOC	5.20E-03	4/VOC	4.20E-03	4/VOC
7	5.20E-05	8/NOx	2.10E-04	8/NOx	2.50E-04	8/NOx	2.20E-04	8/NOx
8	1.30E-05	8/VOC	5.20E-05	8/VOC	7.10E-05	8/VOC	6.00E-05	8/VOC
9	9.30E-06	15/NOx	4.40E-05	15/NOx	5.40E-05	15/NOx	4.70E-05	15/NOx
10	8.70E-06	7/NOx	1.30E-05	7/VOC	1.00E-05	15/VOC	8.90E-06	15/VOC
By source group[2,3]								
1	5.60E-03	S-4/NOx	9.70E-03	S-4/NOx	9.80E-03	B-4/NOx	1.20E-02	B-4/NOx
2	4.90E-03	B-4/NOx	9.40E-03	B-4/NOx	9.20E-03	S-4/NOx	1.20E-02	S-4/NOx
3	4.30E-03	E-4/NOx	7.90E-03	E-4/NOx	7.80E-03	E-4/NOx	9.20E-03	E-4/NOx
4	2.20E-03	S-14/VOC	4.40E-03	S-14/VOC	6.80E-03	S-14/NOx	7.00E-03	S-14/NOx
5	2.10E-03	B-4/VOC	4.10E-03	S-14/NOx	6.00E-03	S-14/VOC	6.10E-03	B-5/VOC
6	1.90E-03	S-5/NOx	4.10E-03	B-4/VOC	5.00E-03	E-14/NOx	5.80E-03	S-14/VOC
7	1.80E-03	E-5/NOx	4.00E-03	B-5/VOC	4.80E-03	B-5/VOC	5.20E-03	E-14/NOx
8	1.70E-03	E-5/VOC	3.40E-03	E-14/NOx	4.30E-03	B-4/VOC	3.30E-03	B-4/VOC
9	1.20E-03	S-14/NOx	3.20E-03	S-5/NOx	2.70E-03	B-14/VOC	3.00E-03	S-5/NOx
10	1.20E-03	S-4/VOC	2.70E-03	E-5/NOx	2.60E-03	S-5/NOx	2.90E-03	B-14/VOC

1. Data shown in the table were compiled for all hourly O_3 concentrations during the period of July 11-15, 1995.
2. The contributions by source area are calculated based on the lumped O_3 contributions to NOx or VOC emissions from all 4 source categories for that source area from OSAT Run B1. O_3 contributions from the same 11 core source areas as DDM Run B2 are ranked.
3. Letters B, S, and E represent emissions from biogenic, surface anthropogenic (lumped on-road and other surface anthropogenic sources), and elevated anthropogenic sources, respectively.

Table 6-22. The top 10 O_3 contributors by source area and by source group predicted by OSAT for stratified 8-hr O_3 levels for the whole receptor region in Chicago[1].

Rank	O_3 level, ppb					
	< 80		80-90		90-100	
	Contribution	Variable	Contribution	Variable	Contribution	Variable
By source area[2]						
1	1.50E-02	4/NOx	2.70E-02	4/NOx	2.90E-02	4/NOx
2	4.90E-03	5/NOx	9.30E-03	14/NOx	1.10E-02	14/NOx
3	3.70E-03	4/VOC	6.40E-03	14/VOC	8.40E-03	14/VOC
4	3.40E-03	14/VOC	5.80E-03	5/NOx	6.20E-03	5/NOx
5	2.60E-03	14/NOx	5.00E-03	5/VOC	5.70E-03	5/VOC
6	2.30E-03	5/VOC	4.10E-04	4/VOC	4.60E-03	4/VOC
7	3.30E-05	8/NOx	1.80E-04	8/NOx	2.60E-04	8/NOx
8	9.00E-06	7/NOx	5.50E-05	6/NOx	8.10E-05	6/NOx
9	8.90E-06	7/VOC	4.70E-05	8/VOC	7.10E-05	8/VOC
10	8.80E-06	8/VOC	3.70E-05	15/NOx	5.70E-05	15/NOx
By source group[2,3]						
1	5.90E-03	S-4/NOx	9.90E-03	B-4/NOx	1.10E-02	B-4/NOx
2	5.00E-03	B-4/NOx	9.50E-03	S-4/NOx	1.00E-02	S-4/NOx
3	4.50E-03	E-4/NOx	7.70E-03	E-4/NOx	8.10E-03	E-4/NOx
4	2.40E-03	S-14/VOC	4.90E-03	S-14/NOx	6.10E-03	S-14/NOx
5	2.30E-03	B-4/VOC	4.40E-03	B-5/VOC	5.40E-03	S-14/VOC
6	2.00E-03	S-5/NOx	4.10E-03	S-14/VOC	5.00E-03	B-5/VOC
7	2.00E-03	E-5/NOx	3.70E-03	E-14/NOx	4.50E-03	E-14/NOx
8	1.90E-03	B-5/VOC	3.40E-03	B-4/VOC	3.70E-03	B-4/VOC
9	1.40E-03	S-14/NOx	2.70E-03	S-5/NOx	2.90E-03	S-5/NOx
10	1.30E-03	S-4/VOC	2.10E-03	B-14/VOC	2.60E-03	B-14/VOC

1. Data shown in the table were compiled for all hourly O_3 concentrations during the period of July 11-15, 1995.
2. The contributions by source area are calculated based on the lumped O_3 contributions to NOx or VOC emissions from all 4 source categories for that source area from OSAT Run B1. O3 contributions from the same 11 core source areas as DDM Run B2 are ranked.
3. Letters B, S, and E represent emissions from biogenic, surface anthropogenic (lumped on-road and other surface anthropogenic sources), and elevated anthropogenic sources, respectively.

Table 6-23. The top 2 contributors to O_3 concentration by source area and by source group predicted by OSAT for stratified 1-hr O_3 levels for 9 subareas in Chicago[1].

O_3 level, ppb	Subarea									
	1	2	3	4	5	6	7	8	9	Whole receptor
By source area[2]										
< 80 ppb	4/NOX 14/VOC	4/NOX 14/VOC	4/NOX 4/VOC	4/NOX 5/NOX	4/NOX 5/NOX	4/NOX 5/NOX	4/NOX 5/NOX	4/NOX 5/NOX	4/NOX 5/NOX	4/NOX 5/NOX
80-90	4/NOX 14/NOX	4/NOX 14/VOC	4/NOX 4/VOC	4/NOX 5/NOX	4/NOX 14/NOX	4/NOX 4/VOC	4/NOX 5/NOX	4/NOX 14/NOX	4/NOX 14/NOX	4/NOX 14/NOX
90-100	4/NOX 14/NOX	4/NOX 14/NOX	4/NOX 4/VOC	4/NOX 14/NOX	4/NOX 14/NOX	4/NOX 14/VOC	4/NOX 5/NOX	4/NOX 5/NOX	4/NOX 14/NOX	4/NOX 14/NOX
100-110	N/A	4/NOX 14/VOC	4/NOX 14/VOC	4/NOX 14/NOX	4/NOX 14/NOX	4/NOX 14/VOC	4/NOX 5/NOX	N/A	N/A	4/NOX 14/NOX
110-120	N/A	4/NOX 14/VOC	4/NOX 14/NOX	N/A	N/A	4/NOX 14/NOX	N/A	N/A	N/A	N/A
> 120	N/A	14/VOC 14/NOX	14/NOX 14/VOC	N/A	N/A	14/NOX 14/VOC	N/A	N/A	N/A	N/A
By source group[3]										
< 80 ppb	S-4/NOX B-4/NOX	S-4/NOX B-4/NOX	S-4/NOX E-4/NOX	B-4/NOX S-4/NOX	S-4/NOX B-4/NOX	S-4/NOX E-4/NOX	S-4/NOX B-4/NOX	S-4/NOX B-4/NOX	S-4/NOX B-4/NOX	S-4/NOX B-4/NOX
80-90	B-4/NOX S-4/NOX	S-4/NOX B-4/NOX	S-14/VOC B-4/VOC	S-4/NOX B-4/NOX	B-4/NOX S-4/NOX	S-4/NOX E-4/NOX	S-4/NOX B-4/NOX	S-4/NOX B-4/NOX	B-4/NOX S-4/NOX	S-4/NOX B-4/NOX
90-100	B-4/NOX S-4/NOX	S-14/NOX S-14/VOC	S-4/NOX E-4/NOX	B-4/NOX S-4/NOX	B-4/NOX S-14/NOX	B-4/NOX S-4/NOX	S-4/NOX E-4/NOX	B-4/NOX S-4/NOX	B-4/NOX S-4/NOX	B-4/NOX S-4/NOX
100-110	N/A	S-14/VOC S-14/NOX	S-14/VOC B-4/VOC	B-4/NOX S-4/NOX	B-4/NOX S-4/NOX	S-4/NOX B-4/NOX	S-4/NOX B-4/NOX	N/A	N/A	B-4/NOX S-4/NOX
110-120	N/A	S-14/VOC S-14/NOX	S-14/NOX E-14/NOX	N/A	N/A	B-5/VOC E-14/VOC	N/A	N/A	N/A	N/A
> 120	N/A	S-14/VOC S-14/NOX	S-14/VOC S-14/NOX	N/A	N/A	S-14/VOC S-14/NOX	N/A	N/A	N/A	N/A

1. Data shown in the table were compiled for all hourly O_3 concentrations during the period of July 11-15, 1995.
2. The contributions by source area are calculated based on the lumped O_3 contributions to NOx or VOC emissions from all 4 source categories for that source area from OSAT Run B1. O3 contributions from the same 11 core source areas as DDM Run B2 are ranked.
3. Letters B, S, and E represent emissions from biogenic, surface anthropogenic (lumped on-road and other surface anthropogenic sources), and elevated anthropogenic sources, respectively.

Table 6-24. The top 2 contributors to O_3 concentration by source area and by source group predicted by OSAT for stratified 8-hr O_3 levels for 9 subareas in Chicago[1].

O_3 level, ppb	Subarea									
	1	2	3	4	5	6	7	8	9	Whole receptor
By source area[2]										
< 80 ppb	4/NOX 5/NOX	4/NOX 14/VOC	4/NOX 14/VOC	4/NOX 14/VOC	4/NOX 14/VOC	4/NOX 5/NOX	4/NOX 14/VOC	4/NOX 5/NOX	4/NOX 5/NOX	4/NOX 5/NOX
80-90	4/NOX 5/NOX	4/NOX 14/NOX	4/NOX 4/VOC	4/NOX 5/NOX	4/NOX 14/NOX	4/NOX 14/NOX	4/NOX 5/NOX	4/NOX 14/NOX	4/NOX 14/NOX	4/NOX 14/NOX
90-100	N/A	4/NOX 14/NOX	4/NOX 14/VOC	4/NOX 14/NOX	4/NOX 14/NOX	4/NOX 14/NOX	4/NOX 14/NOX	4/NOX 14/NOX	N/A	4/NOX 14/NOX
100-110	N/A	4/NOX 14/NOX	4/NOX 14/VOC	N/A	N/A	4/NOX 14/NOX	N/A	N/A	N/A	N/A
110-120	N/A	4/NOX 14/NOX	4/NOX 14/VOC	N/A	N/A	4/NOX 14/NOX	N/A	N/A	N/A	N/A
> 120	N/A	4/NOX 14/VOC	4/NOX 14/NOX	N/A	N/A	4/NOX 14/NOX	N/A	N/A	N/A	N/A
By source group[3]										
< 80 ppb	S-4/NOX B-4/NOX	S-4/NOX B-4/NOX	S-4/NOX B-4/NOX	S-4/NOX B-4/NOX	S-4/NOX B-4/NOX	S-4/NOX B-4/NOX	S-4/NOX B-4/NOX	S-4/NOX B-4/NOX	S-4/NOX B-4/NOX	S-4/NOX B-4/NOX
80-90	S-4/NOX B-4/NOX	B-4/NOX S-4/NOX	S-4/NOX B-4/NOX	B-4/NOX S-4/NOX	B-4/NOX S-4/NOX	B-4/NOX S-4/NOX	S-4/NOX B-4/NOX	B-4/NOX S-4/NOX	B-4/NOX S-4/NOX	B-4/NOX S-4/NOX
90-100		B-4/NOX S-4/NOX	B-4/NOX S-4/NOX	B-4/NOX S-4/NOX	B-4/NOX S-4/NOX	B-4/NOX S-4/NOX	B-4/NOX S-4/NOX	B-4/NOX S-4/NOX	N/A	B-4/NOX S-4/NOX
100-110	N/A	B-4/NOX S-4/NOX	B-4/NOX S-4/NOX	N/A	N/A	B-4/NOX S-4/NOX	N/A	N/A	N/A	N/A
110-120	N/A	S-14/VOC S-14/NOX	B-4/NOX S-4/NOX	N/A	N/A	B-4/NOX S-14/NOX	N/A	N/A	N/A	N/A
> 120	N/A	S-14/VOC S-14/NOX	S-14/VOC S-14/NOX	N/A	N/A	S-14/VOC S-14/NOX	N/A	N/A	N/A	N/A

1. Data shown in the table were compiled for all hourly O_3 concentrations during the period of July 11-15, 1995.
2. The contributions by source area are calculated based on the lumped O_3 contributions to NOx or VOC emissions from all 4 source categories for that source area from OSAT Run B1. O3 contributions from the same 11 core source areas as DDM Run B2 are ranked.
3. Letters B, S, and E represent emissions from biogenic, surface anthropogenic (lumped on-road and other surface anthropogenic sources), and elevated anthropogenic sources, respectively.

the local surface anthropogenic NO_x emissions (i.e., S-14/NO_x) and the biogenic VOC emissions from the local, surrounding and upwind sources (i.e., B-4/VOC, B-5/VOC, and B-14/VOC); OSAT gives more weight to the surrounding NO_x emissions from all source categories (i.e., S-4/NO_x, B-4/NO_x, and E-4/NO_x), the local elevated anthropogenic NO_x emissions (i.e., E-14/NO_x), and the upwind surface anthropogenic NO_x emissions (i.e., S-5/NO_x).

Significant differences exist in the top 2 contributors predicted by DDM and OSAT for all O_3 levels in all subareas of Chicago, as shown in Tables 6-23 and 6-24. For the low 1-hr and 8-hr O_3 concentrations, DDM predicts the local surface anthropogenic NO_x (i.e., S-14/NO_x) and the surrounding biogenic VOC (i.e., B-4/VOC) or the local elevated anthropogenic NO_x (i.e., E-14/NO_x) to be the top two contributors in subareas 2, 3, 5, 6, and 9; whereas OSAT predicts the surface anthropogenic and biogenic NO_x (i.e., S-4/NO_x and B-4/NO_x) or the elevated anthropogenic NO_x from surrounding sources (i.e., E-4/NO_x) to be the top two contributors in those subareas. For the 1-hr and 8-hr O_3 levels of 80-110 ppb, DDM predicts the local surface anthropogenic NO_x (i.e., S-14/NO_x) and/or upwind biogenic VOC (i.e., B-5/VOC) or the surrounding elevated anthropogenic NO_x (i.e., E-4/NO_x) to be one of the top two contributors in some subareas such as 3, 5, 6, and 9; whereas OSAT predicts the surface and/or elevated anthropogenic or biogenic NO_x emissions from the surrounding sources (i.e., S-4/NO_x and/or E-4/NO_x or B-4/NO_x) to be the top two contributors in those subareas. For the 1-hr high O_3 levels of > 110 ppb, in subareas 2 and 3, DDM predicts the upwind biogenic VOC (i.e., B-5/VOC) to be one of the top two contributors; whereas OSAT predicts either the local surface anthropogenic VOC emissions (S-14/VOC) or the local elevated anthropogenic NO_x (i.e., E-14/NO_x) to be one of the top two contributors. For subarea 6 in the same O_3 concentration range, DDM predicts either the local surface anthropogenic NO_x (i.e., S-14/NO_x) or the surrounding biogenic VOC (i.e., B-4/VOC) to be one of the top two contributors; whereas OSAT predicts either the local elevated anthropogenic VOC (i.e., E-14/VOC) or the surface anthropogenic NO_x (i.e., S-14/NO_x) to be one of the top two contributors. For the high 8-hr O_3 levels of 110-120 ppb, DDM predicts the local surface anthropogenic NO_x (i.e., S-14/NO_x) and the upwind biogenic VOC (B-5/VOC) to be the top two contributors for subarea 3; whereas OSAT predicts the surrounding biogenic and

surface anthropogenic NO_x (i.e., B-4/NO_x and S-4/NO_x) to be the top two contributors. In the subarea 6, DDM predicts the local surface anthropogenic VOC (S-14/VOC) to be one of the top two contributors; whereas OSAT predicts the surrounding biogenic NO_x (B-4/NO_x) to be one of the top 2 contributors.

New York City

Results for New York City are presented in Tables 6-25 to 6-28 (similar results were presented for DDM in Tables 6-9 to 6-12).

In New York City, DDM predicts a negative sensitivity to the local NO_x emissions for all O_3 levels (i.e., S-16/NO_x and E-16/NO_x); whereas OSAT always predicts a positive O_3 contribution from the local NO_x emissions. For the low1-hr and 8-hr O_3 levels (< 80 ppb), DDM gives more weight to the local surface/elevated anthropogenic NO_x (i.e., S-16/NO_x and E-16/NO_x) and the upwind biogenic VOC (i.e., B-7/VOC, B-11/VOC and B-12/VOC); OSAT gives more weight to the upwind elevated anthropogenic NO_x emissions (i.e., E-11/NO_x, E-7/NO_x, and E-12/NO_x) and the upwind/surrounding surface anthropogenic NO_x (i.e., S-12/NO_x, S-13/NO_x, and S-7/NO_x). For the 1-hr and 8-hr O_3 levels of 80-90 ppb, DDM gives more weight to the upwind/local biogenic VOC (i.e., B-11/VOC, B-12/VOC, B-7/VOC, and B-16/VOC) and the local surface anthropogenic NO_x emissions (i.e., S-16/NO_x); OSAT gives more weight to the surrounding/upwind surface anthropogenic NO_x (i.e., S-13/NO_x, S-7/NO_x, and S-12/NO_x) and the upwind/surrounding elevated anthropogenic NO_x (i.e., E-11/NO_x, E-13/NO_x, and E-7/NO_x). For the high 1-hr and 8-hr O_3 levels (> 90 ppb), DDM gives more weight to the upwind, local and surrounding biogenic VOC (i.e., B-11/VOC, B-7/VOC, B-16/VOC, and B-13/VOC); OSAT gives more weight to the local/upwind surface anthropogenic NO_x (i.e., S-16/NO_x and S-7/NO_x) and the upwind/surrounding elevated anthropogenic NO_x (i.e., E-11/NO_x, E-13/NO_x, and E-7/NO_x).

Significant differences exist in the top two contributors for all O_3 levels in all subareas in New York City, as shown in Tables 6-27 and 6-28. For the low 1-hr and 8-hr O_3 levels (< 80 ppb), DDM predicts the local and upwind surface anthropogenic NO_x (i.e., S-16/NO_x and S-11/NO_x) to be the top two contributors in most subareas; whereas OSAT predicts the upwind surface and elevated anthropogenic NO_x (i.e., S-11/NO_x and E-11/NO_x) to be the top two contributors in most subareas. For the higher 1-hr and 8-hr

Table 6-25. The top 10 O_3 contributors by source area and by source group predicted by OSAT for stratified 1-hr O_3 levels for the whole receptor region in New York City[1].

Rank	O_3 level, ppb									
	< 80		80-90		90-100		100-110		110-120	
	Contribution	Variable	Contribution	Variable	Contribution	Variable	Contribution	Variable	Contribution	Variable
By source area[2]										
1	1.20E-02	11/NOx	1.60E-02	11/NOx	1.70E-02	11/NOx	1.90E-02	11/NOx	1.80E-02	11/NOx
2	5.10E-03	12/NOx	1.00E-02	13/NOx	1.20E-02	13/NOx	1.50E-02	13/NOx	1.70E-02	13/NOx
3	4.30E-03	7/NOx	6.30E-03	11/VOC	8.30E-03	16/NOx	8.90E-03	16/NOx	1.30E-02	7/NOx
4	4.20E-03	13/NOx	5.80E-03	16/NOx	7.00E-03	7/NOx	8.50E-03	7/NOx	1.00E-02	16/NOx
5	3.80E-03	11/VOC	5.30E-03	7/NOx	6.30E-03	11/VOC	8.10E-03	11/VOC	8.70E-03	11/VOC
6	2.60E-03	7/VOC	4.10E-03	12/NOx	4.80E-03	4/NOx	5.70E-03	16/VOC	5.90E-03	12/NOx
7	2.10E-03	16/VOC	3.70E-03	4/NOx	4.60E-03	16/VOC	4.40E-03	13/VOC	5.80E-03	16/VOC
8	1.70E-03	13/VOC	3.60E-03	16/VOC	3.40E-03	13/VOC	3.90E-03	4/NOx	5.30E-03	12/VOC
9	1.60E-03	4/NOx	3.50E-03	13/VOC	2.80E-03	7/VOC	3.50E-03	7/VOC	5.20E-03	13/VOC
10	1.50E-03	16/NOx	2.20E-03	7/VOC	2.40E-03	12/NOx	3.50E-03	12/NOx	4.80E-03	7/VOC
By source group[2,3]										
1	6.50E-03	S-11/NOx	9.20E-03	S-11/NOx	9.40E-03	S-11/NOx	1.10E-02	S-13/NOx	1.20E-02	S-13/NOx
2	4.40E-03	E-11/NOx	7.30E-03	S-13/NOx	8.60E-03	S-13/NOx	9.90E-03	S-11/NOx	8.50E-03	S-16/NOx
3	2.90E-03	S-12/NOx	5.80E-03	E-11/NOx	6.80E-03	S-16/NOx	7.70E-03	E-11/NOx	8.50E-03	E-11/NOx
4	2.80E-03	S-13/NOx	5.00E-03	B-11/VOC	6.70E-03	E-11/NOx	7.40E-03	S-16/NOx	8.20E-03	S-11/NOx
5	2.70E-03	B-11/VOC	4.80E-03	S-16/NOx	4.70E-03	B-11/VOC	6.20E-03	B-11/VOC	7.30E-03	B-11/VOC
6	2.20E-03	E-7/NOx	2.70E-03	S-7/NOx	3.40E-03	S-7/NOx	3.90E-03	S-7/NOx	6.60E-03	E-7/NOx
7	1.80E-03	E-12/NOx	2.40E-03	S-12/NOx	2.80E-03	E-13/NOx	3.90E-03	E-7/NOx	5.10E-03	S-7/NOx
8	1.80E-03	S-7/NOx	2.40E-03	E-13/NOx	2.80E-03	E-7/NOx	3.90E-03	E-13/NOx	4.60E-03	E-13/NOx
9	1.60E-03	S-16/VOC	2.30E-03	B-13/VOC	2.70E-03	S-16/VOC	3.40E-03	S-16/VOC	4.30E-03	B-12/VOC
10	1.40E-03	S-7/VOC	2.10E-03	E-7/NOx	2.30E-03	B-13/VOC	2.90E-03	B-13/VOC	3.40E-03	S-12/NOx

1. Data shown in the table were compiled for all hourly O_3 concentrations during the period of July 11-15, 1995.
2. The contributions by source area are calculated based on the lumped O_3 contributions to NOx or VOC emissions from all 4 source categories for that source area from OSAT Run B1. O3 contributions from the same 11 core source areas as DDM Run B2 are ranked.
3. Letters B, S, and E represent emissions from biogenic, surface anthropogenic (lumped on-road and other surface anthropogenic sources), and elevated anthropogenic sources, respectively.

Table 6-26. The top 10 O_3 contributors by source area and by source group predicted by OSAT for stratified 8-hr O_3 levels for the whole receptor region in New York City[1].

Rank	O_3 level, ppb									
	< 80		80-90		90-100		100-110		110-120	
	Contribution	Variable	Contribution	Variable	Contribution	Variable	Contribution	Variable	Contribution	Variable
By source area[2]										
1	1.20E-02	11/Nox	1.70E-02	11/NOx	1.80E-02	11/NOx	2.00E-02	11/NOx	1.90E-02	11/NOx
2	5.40E-03	12/NOx	1.00E-02	13/NOx	1.30E-02	13/NOx	1.70E-02	13/NOx	1.70E-02	13/NOx
3	4.70E-03	13/NOx	6.50E-03	7/NOx	8.10E-03	16/NOx	1.20E-02	7/NOx	1.20E-02	7/NOx
4	4.60E-03	7/NOx	6.40E-03	16/NOx	7.20E-03	7/NOx	7.80E-03	11/VOC	8.70E-03	11/VOC
5	4.10E-03	11/VOC	5.90E-03	11/VOC	6.80E-03	11/VOC	7.70E-03	16/NOx	8.70E-03	16/NOx
6	2.70E-03	7/VOC	3.90E-03	16/VOC	4.70E-03	16/VOC	5.90E-03	12/NOx	6.10E-03	12/NOx
7	2.50E-03	16/VOC	3.90E-03	4/NOx	4.10E-03	4/NOx	4.60E-03	16/VOC	5.40E-03	16/VOC
8	2.00E-03	16/NOx	3.20E-03	12/NOx	3.70E-03	13/VOC	4.50E-03	12/VOC	5.10E-03	12/VOC
9	2.00E-03	13/VOC	3.20E-03	13/VOC	3.00E-03	7/VOC	4.50E-03	13/VOC	5.00E-03	13/VOC
10	1.60E-03	4/NOx	2.60E-03	7/VOC	3.00E-03	12/NOx	4.30E-03	7/VOC	4.40E-03	7/VOC
By source group[3]										
1	6.60E-03	S-11/NOx	8.90E-03	S-11/NOx	9.50E-03	S-11/NOx	1.20E-02	S-13/NOx	1.20E-02	S-13/NOx
2	4.60E-03	E-11/NOx	7.20E-03	S-13/NOx	9.10E-03	S-13/NOx	9.60E-03	S-11/NOx	9.10E-03	S-11/NOx
3	3.20E-03	S-13/NOx	6.20E-03	E-11/NOx	7.00E-03	E-11/NOx	8.60E-03	E-11/NOx	8.60E-03	E-11/NOx
4	3.10E-03	S-12/NOx	5.30E-03	S-16/NOx	6.70E-03	S-16/NOx	6.60E-03	S-16/NOx	7.40E-03	S-16/NOx
5	2.90E-03	B-11/VOC	4.50E-03	B-11/VOC	5.10E-03	B-11/VOC	6.50E-03	B-11/VOC	7.30E-03	B-11/VOC
6	2.30E-03	E-7/NOx	3.10E-03	S-7/NOx	3.50E-03	S-7/NOx	6.20E-03	E-7/NOx	6.30E-03	E-7/NOx
7	1.90E-03	S-7/NOx	2.80E-03	E-7/NOx	3.10E-03	E-7/NOx	4.80E-03	S-7/NOx	4.90E-03	S-7/NOx
8	1.90E-03	E-12/NOx	2.40E-03	E-13/NOx	3.10E-03	E-13/NOx	4.30E-03	E-13/NOx	4.60E-03	E-13/NOx
9	1.80E-03	S-16/VOC	2.30E-03	S-16/VOC	2.80E-03	S-16/VOC	3.60E-03	B-12/VOC	4.10E-03	B-12/VOC
10	1.60E-03	S-16/NOx	2.10E-03	B-13/VOC	2.40E-03	B-13/VOC	3.40E-03	S-12/NOx	3.50E-03	S-12/NOx

1. Data shown in the table were compiled for all hourly O_3 concentrations during the period of July 11-15, 1995.
2. The contributions by source area are calculated based on the lumped O_3 contributions to NOx or VOC emissions from all 4 source categories for that source area from OSAT Run B1. O3 contributions from the same 11 core source areas as DDM Run B2 are ranked.
3. Letters B, S, and E represent emissions from biogenic, surface anthropogenic (lumped on-road and other surface anthropogenic sources), and elevated anthropogenic sources, respectively.

Table 6-27. The top 2 contributors to O_3 concentrations by source area and by source group predicted by OSAT for stratified 1-hr O_3 levels for 9 subareas in New York City[1].

O_3 level, ppb	Subarea									
	1	2	3	4	5	6	7	8	9	Whole receptor
By source area[2]										
< 80 ppb	11/NOX 7/NOX	11/NOX 7/NOX	11/NOX 13/NOX	11/NOX 7/NOX	11/NOX 12/NOX	11/NOX 12/NOX	11/NOX 12/NOX	11/NOX 12/NOX	11/NOX 12/NOX	11/NOX 12/NOX
80-90	11/NOX 13/NOX	11/NOX 16/VOC	11/NOX 16/VOC	11/NOX 13/NOX	11/NOX 16/NOX	11/NOX 13/NOX	13/NOX 11/NOX	11/NOX 13/NOX	11/NOX 12/NOX	11/NOX 13/NOX
90-100	11/NOX 13/NOX	11/NOX 7/NOX	11/NOX 13/NOX	11/NOX 13/NOX	11/NOX 16/NOX	11/NOX 16/NOX	11/NOX 13/NOX	11/NOX 13/NOX	11/NOX 12/NOX	11/NOX 13/NOX
100-110	11/NOX 13/NOX	11/NOX 13/NOX	11/NOX 13/NOX	11/NOX 13/NOX	11/NOX 13/NOX	11/NOX 16/NOX	11/NOX 13/NOX	N/A	13/NOX 11/NOX	11/NOX 13/NOX
110-120	N/A	11/NOX 13/NOX	16/NOX 11/NOX	N/A	11/NOX 7/NOX	16/NOX 11/NOX	11/NOX 13/NOX	13/NOX 11/NOX	13/NOX 11/NOX	11/NOX 13/NOX
> 120	N/A	N/A	16/NOX 11/NOX	N/A	N/A	13/NOX 11/NOX	N/A	13/NOX 11/NOX	16/NOX 16/VOC	N/A
By source group[3]										
< 80 ppb	S-11/NOX E-11/NOX	S-11/NOX E-11/NOX	S-11/NOX E-11/NOX	S-11/NOX E-11/NOX	S-11/NOX E-11/NOX	S-11/NOX E-11/NOX	S-11/NOX E-11/NOX	S-11/NOX S-12/NOX	S-11/NOX S-12/NOX	S-11/NOX E-11/NOX
80-90	S-11/NOX E-11/NOX	S-11/NOX S-16/VOC	S-11/NOX S-16/VOC	S-13/NOX S-11/NOX	S-16/NOX S-11/NOX	S-11/NOX S-13/NOX	S-13/NOX B-11/VOC	S-11/NOX E-11/NOX	S-11/NOX E-11/NOX	S-11/NOX S-13/NOX
90-100	S-11/NOX E-11/NOX	S-11/NOX S-16/NOX	S-11/NOX S-13/NOX	S-11/NOX E-11/NOX	S-16/NOX S-13/NOX	S-16/NOX S-11/NOX	S-11/NOX S-13/NOX	S-11/NOX S-13/NOX	S-11/NOX E-11/NOX	S-11/NOX S-13/NOX
100-110	S-11/NOX S-13/NOX	S-11/NOX S-16/NOX	S-11/NOX S-13/NOX	S-11/NOX S-13/NOX	S-13/NOX S-11/NOX	S-16/NOX S-13/NOX	S-13/NOX S-11/NOX	N/A	S-13/NOX S-11/NOX	S-13/NOX S-11/NOX
110-120	N/A	S-11/NOX S-13/NOX	S-16/NOX S-11/NOX	N/A	B-11/VOC S-13/NOX	S-16/NOX S-13/NOX	S-13/NOX S-11/NOX	S-13/NOX S-16/NOX	S-13/NOX S-16/NOX	S-13/NOX S-11/NOX
> 120	N/A	N/A	S-16/NOX B-11/VOC	N/A	N/A	S-16/NOX S-13/NOX	N/A	S-13/NOX S-16/NOX	S-16/NOX S-13/NOX	N/A

1. Data shown in the table were compiled for all hourly O_3 concentrations during the period of July 11-15, 1995.
2. The contributions by source area are calculated based on the lumped O_3 contributions to NOx or VOC emissions from all 4 source categories for that source area from OSAT Run B1. O3 contributions from the same 11 core source areas as DDM Run B2 are ranked.
3. Letters B, S, and E represent emissions from biogenic, surface anthropogenic (lumped on-road and other surface anthropogenic sources), and elevated anthropogenic sources, respectively.

Table 6-28. The top 2 contributors to O_3 concentrations by source area and by source group predicted by OSAT for stratified 8-hr O_3 levels for 9 subareas in New York City[1].

O_3 level, ppb	Subarea									
	1	2	3	4	5	6	7	8	9	Whole receptor
By source area[2]										
< 80 ppb	11/NOX 13/NOX	11/NOX 7/NOX	11/NOX 13/NOX	11/NOX 7/NOX	11/NOX 13/NOX	11/NOX 13/NOX	11/NOX 7/NOX	11/NOX 12/NOX	11/NOX 12/NOX	11/NOX 12/NOX
80-90	11/NOX 13/NOX	11/NOX 13/NOX	11/NOX 13/NOX	11/NOX 13/NOX	11/NOX 13/NOX	11/NOX 13/NOX	11/NOX 13/NOX	11/NOX 13/NOX	11/NOX 13/NOX	11/NOX 13/NOX
90-100	11/NOX 13/NOX	11/NOX 13/NOX	11/NOX 13/NOX	11/NOX 13/NOX	11/NOX 13/NOX	11/NOX 13/NOX	11/NOX 13/NOX	11/NOX 13/NOX	11/NOX 13/NOX	11/NOX 13/NOX
100-110	N/A	11/NOX 13/NOX	11/NOX 13/NOX	11/NOX 13/NOX	11/NOX 13/NOX	11/NOX 16/NOX	11/NOX 13/NOX	N/A	11/NOX 13/NOX	11/NOX 13/NOX
110-120	N/A	N/A	11/NOX 13/NOX	N/A	11/NOX 7/NOX	11/NOX 13/NOX	11/NOX 13/NOX	11/NOX 13/NOX	16/NOX 13/NOX	11/NOX 13/NOX
> 120	N/A	N/A	N/A	N/A	N/A	11/NOX 13/NOX	N/A	11/NOX 13/NOX	16/NOX 13/NOX	N/A
By source group[3]										
< 80 ppb	S-11/NOX E-11/NOX	S-11/NOX E-11/NOX	S-11/NOX E-11/NOX	S-11/NOX E-11/NOX	S-11/NOX E-11/NOX	S-11/NOX E-11/NOX	S-11/NOX E-11/NOX	S-11/NOX E-11/NOX	S-11/NOX E-11/NOX	S-11/NOX E-11/NOX
80-90	S-11/NOX S-13/NOX	S-11/NOX E-11/NOX	S-11/NOX E-11/NOX	S-11/NOX S-13/NOX	S-11/NOX S-13/NOX	S-11/NOX E-11/NOX	S-11/NOX S-13/NOX	S-11/NOX E-11/NOX	S-11/NOX E-11/NOX	S-11/NOX S-13/NOX
90-100	S-11/NOX E-11/NOX	S-11/NOX S-13/NOX	S-11/NOX E-11/NOX	S-11/NOX E-11/NOX	S-11/NOX S-13/NOX	S-11/NOX S-13/NOX	S-11/NOX S-13/NOX	S-11/NOX E-11/NOX	S-11/NOX E-11/NOX	S-11/NOX S-13/NOX
100-110	N/A	S-11/NOX S-13/NOX	S-11/NOX E-11/NOX	S-11/NOX S-13/NOX	S-11/NOX S-13/NOX	S-16/NOX S-13/NOX	S-11/NOX S-13/NOX	N/A	S-13/NOX S-11/NOX	S-13/NOX S-11/NOX
110-120	N/A	N/A	S-11/NOX S-13/NOX	N/A	S-13/NOX S-11/NOX	S-11/NOX S-13/NOX	S-11/NOX S-13/NOX	S-13/NOX S-11/NOX	S-16/NOX S-13/NOX	S-13/NOX S-11/NOX
> 120	N/A	N/A	N/A	N/A	N/A	S-13/NOX S-11/NOX	N/A	S-13/NOX S-16/NOX	S-16/NOX S-13/NOX	N/A

1. Data shown in the table were compiled for all hourly O_3 concentrations during the period of July 11-15, 1995.
2. The contributions by source area are calculated based on the lumped O_3 contributions to NOx or VOC emissions from all 4 source categories for that source area from OSAT Run B1. O3 contributions from the same 11 core source areas as DDM Run B2 are ranked.
3. Letters B, S, and E represent emissions from biogenic, surface anthropogenic (lumped on-road and other surface anthropogenic sources), and elevated anthropogenic sources, respectively.

O_3 levels, the surface anthropogenic NO_x emissions from the upwind, local, and surrounding sources (i.e., S-11/NO_x, S-16/NO_x, and S-13/NO_x) are predicted to be one of the top two contributors for most O_3 concentration ranges for most subareas by OSAT but only for a few O_3 concentration ranges for subareas 4, 6, 7, 8, 9 by DDM. In addition, DDM predicts the biogenic VOC emissions from the local and upwind sources (i.e., B-11/VOC, B-16/VOC, and B-12/VOC or B-7/VOC) to be one of the top two contributors in many O_3 levels for many subareas in the New York City region.

Altoona

Results for Altoona are presented for OSAT in Tables 6-29 to 6-32. Similar results for DDM were presented in Tables 6-13 to 6-16.

In Altoona, for the 1-hr and 8-hr low O_3 levels (< 80 ppb), DDM gives greater importance to the upwind and surrounding biogenic VOC emissions (i.e., B-7/VOC, B-11/VOC, B-5/VOC, and B-4/VOC); OSAT gives greater importance to the upwind elevated anthropogenic NO_x emissions (i.e., E-7/NO_x, E-11/NO_x) and the local surface anthropogenic NO_x emissions (i.e., S-17/NO_x). For the 1-hr and 8-hr O_3 levels of 80-90 ppb, DDM gives more weight to the upwind and surrounding biogenic VOC emissions (i.e., B-7/VOC, B-5/VOC, B-11/VOC, and B-4/VOC); OSAT gives more weight to the upwind elevated/surface anthropogenic NO_x emissions (i.e., E-7/NO_x, S-7/NO_x, S-4/NO_x, and E-4/NO_x), the upwind elevated anthropogenic VOC (i.e., E-7/VOC), and the local surface anthropogenic NO_x emissions (i.e., S-17/NO_x). For the higher 1-hr O_3 levels of 90-100 and 100-110 ppb and 8-hr O_3 level of 90-100 ppb, DDM gives more weight to the upwind biogenic VOC emissions (i.e., B-7/VOC, B-5/VOC, B-11/VOC, and B-8/VOC); OSAT gives more weight to the upwind elevated/surface anthropogenic NO_x emissions (i.e., E-7/NO_x, S-7/NO_x, S-4/NO_x, E-4/NO_x, B-4/NO_x, S-5/NO_x, and E-5/NO_x) for the 1-hr and 8-hr O_3 concentrations and the local surface anthropogenic NO_x emissions (i.e., S-17/NO_x) for the 1-hr O_3 concentrations.

Similar to the other cases for urban receptors, significant differences exist between DDM and OSAT in the top two contributors for all O_3 levels in all subareas in Altoona, as shown in Tables 6-31 and 6-32. For the low 1-hr and 8-hr O_3 levels (< 80 ppb), for subareas where DDM predicts the upwind biogenic VOC emissions (i.e., B-7/VOC) to be one of the top two contributors, OSAT predicts either the upwind elevated

Table 6-29. The top 10 O_3 contributors by source area and by source group predicted by OSAT for stratified 1-hr O_3 levels for the whole receptor region in Altoona[1].

Rank	O_3 level, ppb							
	< 80		80-90		90-100		100-110	
	Contribution	Variable	Contribution	Variable	Contribution	Variable	Contribution	Variable
By source area[2]								
1	1.20E-02	7/NOx	1.70E-02	11/NOx	1.70E-02	11/NOx	2.10E-02	11/NOx
2	9.20E-03	11/NOx	1.40E-02	7/NOx	1.60E-02	7/NOx	1.70E-02	4/NOx
3	5.20E-03	7/VOC	9.80E-03	4/NOx	1.10E-02	4/NOx	1.50E-02	7/NOx
4	3.30E-03	4/NOx	5.80E-03	7/VOC	7.90E-03	7/VOC	9.20E-03	5/NOx
5	3.20E-03	11/VOC	4.30E-03	5/NOx	7.40E-03	5/NOx	5.60E-03	7/VOC
6	2.10E-03	17/NOx	4.30E-03	17/NOx	4.70E-03	17/NOx	4.30E-03	5/VOC
7	1.60E-03	4/VOC	3.60E-03	11/VOC	4.30E-03	11/VOC	4.20E-03	11/VOC
8	1.40E-03	5/NOx	2.20E-03	5/VOC	3.50E-03	5/VOC	3.70E-03	17/NOx
9	1.20E-03	17/VOC	1.70E-03	14/NOx	2.60E-03	8/VOC	2.10E-03	8/VOC
10	6.10E-04	5/VOC	1.60E-03	4/VOC	2.00E-03	8/NOx	2.10E-03	4/VOC
By source group[3]								
1	5.40E-03	E-7/NOx	1.10E-02	E-11/NOx	1.10E-02	E-11/NOx	1.30E-02	E-11/NOx
2	5.20E-03	E-11/NOx	6.60E-03	E-7/NOx	8.10E-03	E-7/NOx	8.30E-03	E-7/NOx
3	5.20E-03	S-7/NOx	6.10E-03	S-7/NOx	6.50E-03	B-7/VOC	8.00E-03	S-11/NOx
4	3.50E-03	S-11/NOx	5.80E-03	S-11/NOx	6.30E-03	S-7/NOx	7.30E-03	S-4/NOx
5	2.60E-03	B-7/VOC	4.40E-03	S-4/NOx	5.40E-03	S-11/NOx	6.20E-03	S-7/NOx
6	2.50E-03	S-7/VOC	4.20E-03	E-7/VOC	5.30E-03	S-4/NOx	4.90E-03	B-4/NOx
7	2.30E-03	B-11/VOC	2.90E-03	S-17/NOx	3.20E-03	S-17/NOx	4.40E-03	B-7/VOC
8	1.50E-03	S-4/NOx	2.80E-03	B-11/VOC	3.20E-03	B-11/VOC	4.10E-03	E-4/NOx
9	1.40E-03	S-17/NOx	2.70E-03	E-4/NOx	3.10E-03	S-5/NOx	3.90E-03	S-5/NOx
10	1.20E-03	S-4/VOC	2.70E-03	B-4/NOx	3.00E-03	B-4/NOx	3.70E-03	E-5/NOx

1. Data shown in the table were compiled for all hourly O_3 concentrations during the period of July 11-15, 1995.
2. The contributions by source area are calculated based on the lumped O_3 contributions to NOx or VOC emissions from all 4 source categories for that source area from OSAT Run B1. O3 contributions from the same 11 core source areas as DDM Run B2 are ranked.
3. Letters B, S, and E represent emissions from biogenic, surface anthropogenic (lumped on-road and other surface anthropogenic sources), and elevated anthropogenic sources, respectively.

Table 6-30. The top 10 O_3 contributors by source area and by source group predicted by OSAT for stratified 8-hr O_3 levels for the whole receptor region in Altoona[1].

Rank	O_3 level, ppb					
	< 80		80-90		90-100	
	Contribution	Variable	Contribution	Variable	Contribution	Variable
By source area[2]						
1	1.20E-02	7/NOx	1.50E-02	11/NOx	1.80E-02	11/NOx
2	9.90E-03	11/NOx	1.40E-02	7/NOx	1.60E-02	7/NOx
3	5.40E-03	7/VOC	1.10E-02	4/NOx	1.30E-02	4/NOx
4	3.40E-03	11/VOC	5.80E-03	5/NOx	8.00E-03	5/NOx
5	3.10E-03	4/NOx	5.20E-03	7/VOC	6.90E-03	7/VOC
6	2.40E-03	17/NOx	4.00E-03	17/NOx	4.00E-03	11/VOC
7	1.60E-03	4/VOC	3.00E-03	11/VOC	3.90E-03	17/NOx
8	1.30E-03	5/NOx	2.90E-03	5/VOC	3.70E-03	5/VOC
9	1.20E-03	17/VOC	1.70E-03	14/NOx	2.50E-03	8/VOC
10	5.80E-04	5/VOC	1.50E-03	4/VOC	1.90E-03	4/VOC
By source group[3]						
1	5.70E-03	E-11/NOx	9.10E-03	E-11/NOx	1.10E-02	E-11/NOx
2	5.50E-03	E-7/NOx	6.30E-03	E-7/NOx	8.40E-03	B-7/NOx
3	5.20E-03	S-7/NOx	6.10E-03	S-7/NOx	6.30E-03	S-7/NOx
4	3.60E-03	S-11/NOx	5.00E-03	S-4/NOx	6.10E-03	S-11/NOx
5	2.70E-03	B-7/VOC	4.80E-03	S-11/NOx	5.90E-03	S-4/NOx
6	2.60E-03	S-7/VOC	4.20E-03	B-7/VOC	5.70E-03	B-7/VOC
7	2.50E-03	B-11/VOC	3.10E-03	E-4/NOx	3.70E-03	B-4/NOx
8	1.60E-03	S-17/NOx	3.10E-03	B-4/NOx	3.40E-03	S-5/NOx
9	1.40E-03	S-4/NOx	2.70E-03	S-17/NOx	3.30E-03	E-5/NOx
10	1.20E-03	S-4/VOC	2.60E-03	S-5/NOx	3.30E-03	E-4/NOx

1. Data shown in the table were compiled for all hourly O_3 concentrations during the period of July 11-15, 1995.
2. The contributions by source area are calculated based on the lumped O_3 contributions to NOx or VOC emissions from all 4 source categories for that source area from OSAT Run B1. O3 contributions from the same 11 core source areas as DDM Run B2 are ranked.
3. Letters B, S, and E represent emissions from biogenic, surface anthropogenic (lumped on-road and other surface anthropogenic sources), and elevated anthropogenic sources, respectively.

Table 6-31. The top 2 contributors to O_3 concentration by source area and by source group predicted by OSAT for stratified 1-hr O_3 levels for 9 subareas in Altoona[1].

O_3 level, ppb	Subarea									
	1	2	3	4	5	6	7	8	9	Whole receptor
By source area[2]										
< 80 ppb	7/NOX 11/NOx	7/NOX 11/NOx	7/NOX 11/NOX	7/NOX 11/NOx	7/NOX 11/NOx	11/NOX 7/NOX	7/NOX 11/NOx	7/NOX 11/NOx	11/NOX 7/NOX	7/NOX 11/NOx
80-90	7/NOX 11/NOx	7/NOX 11/NOx	11/NOX 7/NOX	7/NOX 11/NOx	11/NOX 7/NOX	7/NOX 11/NOX	7/NOX 11/NOx	11/NOX 7/NOX	11/NOX 7/NOX	11/NOX 7/NOX
90-100	11/NOX 7/NOX	11/NOX 7/NOx	7/NOX 11/NOX	11/NOx 7/NOx	7/NOX 11/NOX	11/NOx 7/NOx	11/NOx 7/NOx	11/NOx 7/NOx	11/NOx 7/NOx	11/NOX 7/NOx
100-110	7/VOC 7/NOx	N/A	N/A	11/NOx 7/NOx	11/NOx 7/NOx	11/NOx 4/NOx	11/NOx 7/NOx	11/NOx 4/NOx	11/NOx 7/NOx	11/NOX 4/NOX
110-120	N/A	N/A	N/A	11/NOx 4/NOx	N/A	N/A	11/NOx 7/NOx	N/A	N/A	N/A
> 120	N/A	N/A	N/A	N/A	N/A	N/A	N/A	N/A	N/A	N/A
By source group[3]										
< 80 ppb	S-7/NOX E-7/NOx	S-7/NOx E-11/NOX	E-11/NOx S-7/NOX	E-7/NOx S-7/NOX	E-11/NOX E-7/NOX	E-11/NOX E-7/NOX	E-7/NOX S-7/NOX	E-11/NOX E-7/NOX	E-11/NOX E-7/NOX	E-7/NOx E-11/NOX
80-90	S-7/NOX E-7/NOX	E-11/NOX S-7/NOX	E-11/NOX E-7/NOX	E-11/NOX E-7/NOX	E-11/NOX E-7/NOX	E-11/NOX E-7/NOX	E-11/NOX E-7/NOX	E-11/NOX E-7/NOX	E-11/NOX E-7/NOX	E-11/NOX E-7/NOx
90-100	E-11/NOX E-7/NOX	E-11/NOX B-7/VOC	E-11/NOX E-7/NOX	E-11/NOX E-7/NOX	E-11/NOX B-7/VOC	E-11/NOX E-7/NOX	E-11/NOX E-7/NOX	E-11/NOX E-7/NOX	E-11/NOX S-11/NOX	E-11/NOX E-7/NOx
100-110	B-7/VOC E-7/NOx	N/A	N/A	E-11/NOx B-7/VOC	E-11/NOX E-7/NOX	E-11/NOX E-7/NOX	E-11/NOX E-7/NOX	E-11/NOX S-11/NOX	E-11/NOX S-11/NOX	E-11/NOX E-7/NOx
110-120	N/A	N/A	N/A	E-11/NOX E-7/NOX	N/A	N/A	E-11/NOX S-11/NOX	N/A	N/A	N/A
> 120	N/A	N/A	N/A	N/A	N/A	N/A	N/A	N/A	N/A	N/A

1. Data shown in the table were compiled for all hourly O_3 concentrations during the period of July 11-15, 1995.
2. The contributions by source area are calculated based on the lumped O_3 contributions to NOx or VOC emissions from all 4 source categories for that source area from OSAT Run B1. O3 contributions from the same 11 core source areas as DDM Run B2 are ranked.
3. Letters B, S, and E represent emissions from biogenic, surface anthropogenic (lumped on-road and other surface anthropogenic sources), and elevated anthropogenic sources, respectively.

Table 6-32. The top 2 contributors to O_3 concentration by source area and by source group predicted by OSAT for stratified 8-hr O_3 levels for 9 subareas in Altoona[1].

O_3 level, ppb	Subarea									
	1	2	3	4	5	6	7	8	9	Whole receptor
By source area[2]										
< 80 ppb	7/NOX 11/NOx	7/NOX 11/NOx	7/NOX 11/NOX	7/NOX 11/NOx	7/NOX 11/NOx	7/NOX 11/NOX	7/NOX 11/NOx	7/NOX 11/NOx	7/NOX 11/NOX	7/NOX 11/NOx
80-90	7/NOX 11/NOx	7/NOX 11/NOx	7/NOX 11/NOX	7/NOX 11/NOx	7/NOX 11/NOX	7/NOX 11/NOX	7/NOX 11/NOx	7/NOX 11/NOX	11/NOX 7/NOX	11/NOX 7/NOX
90-100	7/NOX 11/NOX	7/NOX 11/NOx	N/A	11/NOx 7/NOx	7/NOX 11/NOX	11/NOx 7/NOx	11/NOx 7/NOx	11/NOx 7/NOx	11/NOx 7/NOx	11/NOX 7/NOx
100-110	N/A	N/A	N/A	11/NOX 7/NOX	11/NOX 7/NOX	N/A	11/NOX 4/NOX	N/A	N/A	N/A
110-120	N/A	N/A	N/A	N/A	N/A	N/A	11/NOX 4/NOX	N/A	N/A	N/A
> 120	N/A	N/A	N/A	N/A	N/A	N/A	N/A	N/A	N/A	N/A
By source group[3]										
< 80 ppb	S-7/NOX E-7/NOx	S-7/NOx E-7/NOX	E-11/NOx S-7/NOX	S-7/NOx E-7/NOX	E-11/NOX S-7/NOX	E-11/NOX S-7/NOX	E-7/NOX E-11/NOX	E-11/NOX E-7/NOX	E-11/NOX E-7/NOX	E-11/NOx E-7/NOX
80-90	E-11/NOX E-7/NOX	E-11/NOX E-7/NOX	E-11/NOX E-7/NOX	E-11/NOX S-7/NOX	E-11/NOX S-7/NOX	E-7/NOX S-7/NOX	E-11/NOX E-7/NOX	E-11/NOX E-7/NOX	E-11/NOX E-7/NOX	E-11/NOX E-7/NOx
90-100	E-11/NOX E-7/NOX	E-11/NOX E-7/NOX	N/A	E-11/NOX S-7/NOX	E-11/NOX E-7/NOX	E-11/NOX E-7/NOX	E-11/NOX E-7/NOX	E-11/NOX E-7/NOX	E-11/NOX E-7/NOX	E-11/NOX E-7/NOx
100-110	N/A	N/A	N/A	E-11/NOX E-7/NOX	E-11/NOX E-7/NOX	N/A	E-11/NOX S-4/NOX	N/A	N/A	N/A
110-120	N/A	N/A	N/A	N/A	N/A	N/A	E-11/NOX S-11/NOX	N/A	N/A	N/A
> 120	N/A	N/A	N/A	N/A	N/A	N/A	N/A	N/A	N/A	N/A

1. Data shown in the table were compiled for all hourly O_3 concentrations during the period of July 11-15, 1995.
2. The contributions by source area are calculated based on the lumped O_3 contributions to NOx or VOC emissions from all 4 source categories for that source area from OSAT Run B1. O3 contributions from the same 11 core source areas as DDM Run B2 are ranked.
3. Letters B, S, and E represent emissions from biogenic, surface anthropogenic (lumped on-road and other surface anthropogenic sources), and elevated anthropogenic sources, respectively.

anthropogenic NO_x (i.e., E-7/NO_x or E-11/NO_x) or the surface anthropogenic NO_x emissions (i.e., S-7/NO_x) to be one of the top two contributors. For the intermediate and high 1-hr O_3 levels (> 80 ppb), DDM predicts the upwind biogenic VOC emissions (i.e., B-7/VOC and/or B-11/VOC) to be one of the top two contributors in many subareas; whereas OSAT predicts the upwind and surrounding elevated or surface anthropogenic NO_x emissions (i.e., E-7/NO_x or E-11/NO_x, or S-11/NO_x) to be one of the top two contributors. For the high 8-hr O_3 levels (> 80 ppb), DDM predicts the upwind biogenic VOC emissions (i.e., B-7/VOC and/or B-5/VOC) to be one of the top two contributors in many subareas; whereas OSAT predicts the upwind and surrounding elevated or surface anthropogenic NO_x emissions (i.e., E-7/NO_x or E-11/NO_x or S-7/NO_x) to be one of the top two contributors.

6.1.1.3 Ranking of DDM Sensitivities with Respect to Total NO_x and VOC Emissions from Six Boundary Source Areas

DDM run B3 provides O_3 sensitivity to total emissions (no NO_x vs. VOC breakout) from the remaining six source areas along the boundary of the domain (i.e., source areas 1, 2, 3, 6, 9, and 10). The effect of the total emissions from some of the six boundary source areas such as 1, 2, 3, and 9 on O_3 formation in the four receptors is either greater than or comparable to the effect of some source groups from the 11 core source areas. Tables 6-33 and 6-34 show the top two O_3 sensitivities by source area ranked only for the six boundary source areas for the stratified 1-hr and 8-hr O_3 levels at the four receptors. In Atlanta, the emissions from Florida (i.e., source area 9) are the most influential contributor for all 1-hr O_3 levels among the six boundary source areas and the emissions from Iowa, southern Minnesota, eastern South Dakota, and eastern Nebraska (i.e., source area 1) rank 2nd for all O_3 levels < 120 ppb. The O_3 sensitivities to emissions from source area 9 or 1 are generally lower by several orders of magnitudes than those to the total emissions from the local, surrounding or nearby upwind sources (e.g., source areas 15, 8, 5, and 12), but equivalent to that from the upwind sources (e.g., source area 4). For example, the O_3 sensitivities for the 1-hr O_3 levels of 100-110 ppb to the total NO_x and VOC emissions from source areas 15, 8, 5, 12, 4, 9, and 1 are 3.4 x10^{-2},

Table 6-33. The top 2 O_3 sensitivities by source area to the total NO_x and VOC emissions from the 6 boundary source areas predicted by DDM for stratified 1-hr O_3 levels in Atlanta, Chicago, New York City, and Altoona[1, 2].

O_3 level, ppb	Receptor							
	Atlanta		Chicago		New York City		Altoona	
	Sensitivity	Source area	Sensitivity	Source area	Sensitivity	Source area	Sensitivity	Source area
< 80 ppb	6.3E-4 3.0E-4	9 1	4.8E-3 1.0E-3	1 3	1.1E-3 6.1E-4	3 1	2.8E-3 1.0E-3	3 1
80-90	4.7E-4 3.1E-4	9 1	9.8E-3 1.6E-3	1 2	2.4E-3 2.2E-3	3 1	3.7E-3 7.1E-4	1 2
90-100	4.8E-4 2.3E-4	1 9	1.4E-2 2.8E-3	1 2	2.2E-3 2.2E-3	3 1	1.9E-3 1.6E-4	1 2
100-110	5.9E-4 1.9E-4	1 9	1.4E-2 1.9E-3	1 2	1.4E-3 1.3E-3	1 3	1.7E-3 1.5E-4	1 3
110-120	2.8E-4 5.7E-5	9 3	N/A	N/A	5.6E-4 2.4E-4	1 3	N/A	N/A
> 120	N/A	N/A	N/A	N/A	N/A	N/A	N/A	N/A

1. Data shown in the table were compiled for all hourly O_3 concentrations during the period of July 11-15, 1995.
2. The sensitivities by source area are calculated based on the lumped O_3 sensitivities to total NOx and VOC emissions from all three source categories for that source area from DDM Run B3, which calculates O3 sensitivities to total NOx and VOC emissions from 6 boundary source areas.

Table 6-34. The top 2 O_3 sensitivities by source area to the total NO_x and VOC emissions from the 6 boundary source areas predicted by DDM for stratified 8-hr O_3 levels in Atlanta, Chicago, New York City, and Altoona[1, 2].

O_3 level, ppb	Receptor							
	Atlanta		Chicago		New York City		Altoona	
	Sensitivity	Source area	Sensitivity	Source area	Sensitivity	Source area	Sensitivity	Source area
< 80	6.6E-4 2.8E-4	9 1	5.1E-3 1.1E-3	1 3	1.0E-3 5.3E-4	3 1	2.9E-3 9.9E-4	3 1
80-90	5.4E-4 2.0E-4	1 9	1.2E-2 2.4E-3	1 2	1.9E-3 1.9E-3	3 1	4.0E-3 7.8E-4	1 2
90-100	5.4E-4 2.4E-4	1 9	1.3E-2 2.2E-3	1 2	1.8E-3 1.8E-3	3 1	1.6E-3 1.2E-4	1 3
100-110	3.5E-4 2.4E-4	1 9	N/A	N/A	5.4E-3 2.3E-3	1 3	N/A	N/A
110-120	N/A	N/A	N/A	N/A	5.4E-4 2.4E-4	1 3	N/A	N/A
> 120	N/A	N/A	N/A	N/A	N/A	N/A	N/A	N/A

1. Data shown in the table were compiled for all hourly O_3 concentrations during the period of July 11-15, 1995.
2. The sensitivities by source area are calculated based on the lumped O_3 sensitivities to total NOx and VOC emissions from all three source categories for that source area from DDM Run B3, which calculates O3 sensitivities to total NOx and VOC emissions from 6 boundary source areas.

2.0×10^{-2}, 3.6×10^{-3}, 1.1×10^{-3}, 3.5×10^{-4}, 1.9×10^{-4}, and 5.9×10^{-4}, respectively. This indicates that O_3 formation in Atlanta is largely affected by the local and surrounding sources.

The intermediate and high 1-hr O_3 concentrations in Chicago are quite sensitive to the total emissions from source areas 1 and 2. The O_3 sensitivity for the O_3 levels of 100-110 ppb to the total emissions from source area 1 is 1.4×10^{-2}, which is comparable to that for the surrounding and upwind sources (i.e., source areas 4 and 5) (2.6×10^{-2} and 1.4×10^{-2}, respectively). The O_3 sensitivity for the O_3 levels of 100-110 ppb to the total NO_x and VOC emissions from source area 2 (1.9×10^{-3}) is lower by one order of magnitude than that from the source areas 4 and 5, but comparable to that for the local or upwind sources (e.g., source area 14) (3.8×10^{-3}) and larger than that from the source areas 8 and 15 (1.1×10^{-4} and 1.9×10^{-5}, respectively). This indicates that the across-state transport plays a certain role in contributing to the high 1-hr O_3 concentrations in Chicago.

O_3 concentrations in New York City are sensitive to the total emissions from the source areas 1 and 3 that cover Iowa, southern Minnesota, eastern South Dakota, eastern Nebraska, Wisconsin, and Michigan. The O_3 sensitivities to the total emissions from source areas 1 or 3 are lower by one order of magnitude than those for the surrounding or nearby upwind sources (e.g., source areas 11, 13, and 7), but comparable to those for the local or upwind sources (e.g., source areas 16, 12, and 4). For example, the O_3 sensitivities for the 1-hr O_3 levels of 100-110 ppb to the total NO_x and VOC emissions from the source areas 11, 13, 7, 16, 12, 4, 1, and 3 are 1.9×10^{-2}, 1.5×10^{-2}, 8.1×10^{-3}, 3.7×10^{-3}, 3.9×10^{-3}, 2.5×10^{-3}, 1.4×10^{-3}, and 1.3×10^{-3}, respectively. This indicates that long-range transport may also play an important role in O_3 formation in New York City.

In Altoona, the low O_3 concentrations are sensitive to the total emissions from source areas 1 and 3, and the intermediate and high O_3 concentrations are sensitive to the total emissions from source area 1. For example, the O_3 sensitivity for the O_3 levels of 100-110 ppb to the total NO_x and VOC emissions from source area 1 is 1.7×10^{-3}, which is lower by one order of magnitude than that of the surrounding or upwind emissions (i.e., source areas 11, 7, 5, and 4), but comparable to that of the upwind or local emissions (i.e., source areas 8 and 17) (3.0×10^{-3} and 1.3×10^{-3}). This also indicates that long-range transport can play an important role in O_3 formation in Altoona.

The effect of the six boundary source areas on the 8-hr O_3 concentrations at the four receptor areas is almost identical to that for the 1-hr O_3 concentrations at all receptors, as shown in Table 6-34. This suggests that these source areas contribute mostly to the "background" O_3 levels and little to the "peak" O_3 concentrations.

6.1.1.4 Comparison of the DDM and OSAT Rankings of O_3 Contributors from the Six Boundary Source Areas

Tables 6-35 and 6-36 show the top two O_3 contributors from OSAT by source area ranked only for the six boundary source areas for the stratified 1-hr and 8-hr O_3 levels at the four receptors. The results of OSAT are very similar to those of DDM with differences for a few O_3 levels in Atlanta, New York City, and Altoona. In Atlanta, DDM predicts that the total emissions from source areas 9 and 3 are the top two contributors for the 1-hr O_3 levels of 110-120 ppb; whereas OSAT predicts that the total emissions from source areas 9 and 1 are the top two contributors for this range of O_3 concentrations. For the 8-hr O_3 levels of 90-100 and 100-110 ppb in Atlanta, both DDM and OSAT predict that the total emissions from source areas 9 and 1 are the top two contributors but with a different ranking. In New York City, DDM predicts that the total emissions from source area 3 are more influential to the 1-hr and 8-hr O_3 concentrations in the ranges of 80-90 ppb and 90-100 ppb than those from source area 1; whereas OSAT predicts an opposite order of influences of the total emissions from source areas 3 and 1. For O_3 levels of 90-100 ppb in Altoona, DDM predicts that the total emissions from source areas 1 and 2 are the top two contributors; whereas OSAT predicts that the total emissions from source areas 1 and 3 are the top two contributors.

6.1.2 NO_x- or VOC-sensitivity

Several approaches have been developed to determine the NO_x- or VOC-sensitivity of O_3. These approaches include (1) the use of an O_3 isopleth diagram generated as a function of NO_x and VOC emissions; (2) the sensitivity analysis of 3-D photochemical models using the indirect method or other sensitivity analysis tools such

Table 6-35. The top 2 O_3 contributors by source area from the total NO_x and VOC emissions from the 6 boundary source areas predicted by OSAT for stratified 1-hr O_3 levels in Atlanta, Chicago, New York City, and Altoona[1, 2].

O_3 level, ppb	Receptor							
	Atlanta		Chicago		New York City		Altoona	
	Contribution	Source area	Contribution	Source area	Contribution	Source area	Contribution	Source area
< 80 ppb	1.7E-3	9	6.3E-3	1	1.4E-3	3	3.6E-3	3
	4.8E-4	1	1.1E-3	3	1.0E-3	1	1.8E-3	1
80-90	1.5E-3	9	1.2E-2	1	4.0E-3	1	6.1E-3	1
	6.2E-4	1	1.8E-3	2	3.5E-3	3	8.5E-4	2
90-100	9.4E-4	9	1.9E-2	1	4.1E-3	1	3.9E-3	1
	8.1E-4	1	3.3E-3	2	3.5E-3	3	3.0E-4	3
100-110	1.0E-3	1	1.9E-2	1	2.8E-3	1	4.3E-3	1
	8.4E-4	9	2.4E-3	2	2.2E-3	3	3.3E-4	3
110-120	1.2E-3	9	N/A	N/A	1.4E-3	1	N/A	N/A
	1.3E-4	1			5.5E-4	3		
> 120	N/A	N/A	N/A	N/A	N/A	N/A	N/A	N/A

1. Data shown in the table were compiled for all hourly O_3 concentrations during the period of July 11-15, 1995.
2. The contributions by source area are calculated based on the lumped O_3 contributions to total NOx and VOC emissions from all 4 source categories for that source area from OSAT run B1. O3 contributions from the same 6 boundary source areas as DDM Run B3 are ranked.

Table 6-36. The top 2 O_3 contributors by source area from the total NO_x and VOC emissions from the 6 boundary source areas predicted by OSAT for stratified 8-hr O_3 levels in Atlanta, Chicago, New York City, and Altoona[1, 2].

O_3 level, ppb	Receptor							
	Atlanta		Chicago		New York City		Altoona	
	Contribution	Source area	Contribution	Source area	Contribution	Source area	Contribution	Source area
< 80	1.8E-3 4.6E-4	9 1	6.8E-3 1.1E-3	1 3	1.4E-3 9.7E-4	3 1	3.7E-3 1.7E-3	3 1
80-90	9.5E-4 7.7E-4	1 9	1.6E-2 2.8E-3	1 2	3.4E-3 2.8E-3	1 3	6.7E-3 9.4E-4	1 2
90-100	9.8E-4 8.6E-4	9 1	1.7E-2 2.7E-3	1 2	3.4E-3 2.9E-3	1 3	3.6E-3 3.0E-4	1 3
100-110	1.0E-3 6.3E-4	9 1	N/A	N/A	1.3E-3 5.0E-4	1 3	N/A	N/A
110-120	N/A	N/A	N/A	N/A	1.3E-3 5.3E-4	1 3	N/A	N/A
> 120	N/A	N/A	N/A	N/A	N/A	N/A	N/A	N/A

1. Data shown in the table were compiled for all hourly O_3 concentrations during the period of July 11-15, 1995.
2. The contributions by source area are calculated based on the lumped O_3 contributions to total NOx and VOC emissions from all 4 source categories for that source area from OSAT run B1. O3 contributions from the same 6 boundary source areas as DDM Run B3 are ranked.

as DDM; (3) the use of measurable photochemical indicators such as NO_y, $O_3/(NO_y-NO_x)$ (also referred to as O_3/NO_z), O_3/H_2O_2, $HCHO/NO_x$, $HCHO/NO_y$, and H_2O_2/HNO_3 (Trainer et al., 1993; Milford et al., 1994; Sillman, 1995; Tonnesen and Dennis, 2000b) or the extent parameters of atmospheric chemical reactions (Chang et al., 1997; Blanchard et al., 1999) (Note that these are indicators of the sensitivity of peak O_3 concentrations to VOCs and NO_x); (4) the use of dominant reactions for different chemical regimes (e.g., VOC- vs. NO_x-limited regimes) and (5) the use of differences in O_3 concentrations between weekdays and weekends (Pun et al., 2001a). These approaches can be generally classified into two major groups in terms of their treatment in the trajectory of the air parcels:

- Approach that accounts for the history of the air parcels and determines the NO_x- or VOC-sensitivity of peak O_3 formation based on the integrated concentrations of indicator species or integrated first-order sensitivities over the course of the day (i.e., O_3 that has been formed). Examples include those used in DDM, OSAT, and Sillman (1995);
- Approach that does not account for the history of the air parcels and determines the NO_x- or VOC-sensitivity of local O_3 formation based on the local and instantaneous concentrations of indicator species or extent parameters (i.e., O_3 that is to be formed). Examples include those used in Chang et al. (1997) and Blanchard et al. (1999). The approach used for PA also falls into this category (see below).

Some of these approaches and their derivatives have been used in the three probing tools to determine NO_x or VOC sensitivity of O_3 production. We provide below a description of the approach used in each of the three probing tools and the intercomparison of NO_x or VOC sensitivity of O_3 production estimated from the three probing tools.

DDM

DDM predicts the responses of O_3 to the changes in NO_x and VOC emissions by computing first-order sensitivities in a 3-D air quality model. The local, time-dependent sensitivity of species concentration (i.e., O_3) with respect to a given model parameter or input variable can be calculated as the partial derivative of the species concentrations with respect to the parameter or variable:

$$S_{ij}(t) = \frac{\partial C_i(t)}{\partial x_j} \quad (1)$$

where C_i is the time-varying concentration of species i, and x_j represents an input parameter or variable such as emission or initial concentration of NO_x.

The sensitivities of species concentrations with respect to different model parameters and inputs may have different units and their magnitudes can vary dramatically in space and time. To compare sensitivities with dependent and independent variables of different orders of magnitude and/or different units, semi-normalized local sensitivities or normalized local sensitivities (i.e., dimensionless sensitivities) are typically used. The semi-normalized first-order sensitivities can be calculated as:

$$S_{ij}^{*}(t) = X_j \frac{\partial C_i(t)}{\partial x_j} = X_j \frac{\partial C_i(t)}{\partial (e_j X_j)} = \frac{\partial C_i(t)}{\partial e_j} \quad (2)$$

Given a parameter x_j, its variation is defined as $_{xj} = e_{jXj}$, where $_{Xj}$ is the unperturbed parameter, which can vary in time and space; e_j represents a scaling variable with a nominal value of 1. Given the unperturbed parameter $_{Xj}$ and unperturbed species concentration C_i, the normalized first-order sensitivities can be calculated as:

$$S_{ij}^{\circ}(t) = \frac{X_j}{C_i}\frac{\partial C_i(t)}{\partial x_j} = \frac{\partial \ln C_i}{\partial \ln x_j} \quad (3)$$

The dimensionless sensitivities are sometimes referred to as elasticities and actually correspond to the original direct method (Lange, 1942). The signs of $S_{ij}^{*}(t)$ and $S_{ij}^{\circ}(t)$ give the direction of the response of $C_i(t)$ to the relative variation of x_j. The positive values indicate that $C_i(t)$ increases with the increase in $_{xj}$, while the negative values mean a decrease in $C_i(t)$ when increasing x_j.

The normalized or semi-normalized first-order sensitivities have been widely used to interpret sensitivity simulation results (e.g., Samuelson, 1983; Gao et al., 1995; Yang et al., 1997; Zhang et al., 1998; Lohman et al., 2000). While the semi-normalized sensitivities are typically used to compare the response of the concentration of the same species such as O_3 to changes in different model parameters/input variables, the normalized sensitivities are used to compare the responses of the concentrations of different species such as O_3 and NO_2 to changes in the same model parameter/input variable.

DDM calculates the semi-normalized sensitivities as defined in Equation (2). Since we are interested in the sensitivity of O_3 to changes in the emissions of NO_x or VOCs, the semi-normalized sensitivities of DDM will be sufficient for this part of the evaluation and no further post-processing will be needed. In this project, the semi-normalized first-order sensitivities of DDM were evaluated against the OSAT results in terms of the NO_x- and VOC-sensitivity of O_3 production. One limitation in the DDM sensitivities is that the local first-order sensitivities are only representative of small perturbations (i.e., perturbations small enough to be represented by first-order derivatives). For the non-linear system of O_3 formation, sensitivities predicted by DDM are expected to be accurate for small changes (i.e., about 40% perturbations) but inaccurate for large changes (Dunker et al., 2002a).

OSAT

The old version of OSAT uses the actual instantaneous production rates of H_2O_2 and HNO_3 ($P_{H_2O_2}/P_{HNO_3}$) as an indicator of NO_x- or VOC-sensitive chemistry. A value of 0.35 for $P_{H_2O_2}/P_{HNO_3}$ was selected as the transition threshold between NO_x- and VOC-sensitive conditions (Sillman, 1995). The use of P_{H2O2}/P_{HNO3} as an indicator of NO_x- or

VOC-sensitive chemistry is technically sound, but it differs somewhat from the original approach of Sillman (1995). Sillman (1995) obtained a criterion for the transition point between NO_x- or VOC-sensitive chemistry in terms of photochemical production rates of H_2O_2, ROOH, and HNO_3. However, he calculated the values of the indicator and determined its transition point based on the ratios of H_2O_2 and HNO_3 concentrations at the time of peak O_3, which are integrated values over the course of the day, rather than the instantaneous production rates ($P_{H_2O_2}/P_{HNO_3}$). There are two major limitations for the approach used in the old version of OSAT. First, the atmosphere is assumed to be either NO_x- or VOC-limited; however, it can be in a regime that is neither NO_x-nor VOC-limited, and the dual approach of NO_x and VOC limitations will not characterize well such cases. Second, the value of the $P_{H_2O_2}/P_{HNO_3}$ ratio to characterize the NO_x- or VOC-limited states of the air mass is not a universal number and involves some uncertainties (e.g., Sillman et al., 1997; Kumar and Lurmann, 1997). Tonnesen and Dennis (2000a) found that a value of 0.06 to 0.07 is a more accurate threshold by using a simple trajectory model with the RADM2 photochemical mechanism. STI conducted a peer-review of OSAT and suggested changing the threshold from 0.35 to a value between 0.05 and 0.2 (Kumar and Lurmann, 1997). However, such a change only causes a small shift (5-10%) in O_3 formed under VOC-sensitive conditions to that under NO_x-sensitive conditions (Yarwood and Morris, 1997). In addition, Dunker et al. (2002a) evaluated the appropriateness of the use of 0.35 as the transition point between NO_x- and VOC-sensitive chemistry by comparing the $P_{H_2O_2}/P_{HNO_3}$ approach used in the original version of OSAT in CRC Project A-29 and the DDM sensitivity approach used in the updated version of OSAT in this project. They found that the use of $P_{H_2O_2}/P_{HNO_3}$ =0.35 as the transition point gave very good agreement with the local DDM sensitivities to NO_x and VOC emissions.

In the updated version of OSAT, the local sensitivity to VOC and NO_x emission groups calculated by DDM is used as an indicator of NO_x- or VOC-sensitive chemistry and ozone production is then allocated in proportion to those DDM sensitivities in each grid cell at each time step. The apportionment of ozone production into VOC- and NO_x-sensitive portions is performed by defining:

$$F_{VOC} = \left[\frac{\partial O_3}{\partial VOC} + \left| \frac{\partial O_3}{\partial VOC} \right| \right] \Big/ \left[\frac{\partial O_3}{\partial VOC} + \left| \frac{\partial O_3}{\partial VOC} \right| + \frac{\partial O_3}{\partial NO_x} + \left| \frac{\partial O_3}{\partial NO_x} \right| \right]$$

$$F_{NOx} = \left[\frac{\partial O_3}{\partial NO_x} + \left| \frac{\partial O_3}{\partial NO_x} \right| \right] \Big/ \left[\frac{\partial O_3}{\partial VOC} + \left| \frac{\partial O_3}{\partial VOC} \right| + \frac{\partial O_3}{\partial NO_x} + \left| \frac{\partial O_3}{\partial NO_x} \right| \right] \qquad (4)$$

to be the VOC- and NO_x-sensitive fractions. Equation (4) is used because the sensitivity to NO_x (and occasionally to VOC) can be negative, and in such cases all ozone production is allocated to the species with the positive sensitivity. When both sensitivities are positive, O_3 production is allocated in proportion to the VOC and NO_x sensitivities.

OSAT then estimates the fractions of O_3 transported to the receptor that were formed en-route under VOC- or NO_x-limited conditions using O_3 reaction tracers O_3V_i and O_3N_i:

$$O_3V_i = O_3V_i + \Delta O_3V \times \left(\frac{V_i \times MIR_i}{\sum (V_i \times MIR_i)} \right) \qquad (5)$$

$$O_3N_i = O_3N_i + \Delta O_3N \times \left(\frac{N_i}{\sum N_i} \right) \qquad (6)$$

where O_3V_i and O_3N_i are the tracers of O_3 formation under VOC-limited and NO_x-limited conditions, respectively, attributed to source group *i*. ΔO_3V and ΔO_3N are the ozone production allocated to the VOC and NO_x sensitivities (i.e., $\Delta O_3V = \Delta O_3 \times F_{VOC}$ and $\Delta O_3N = \Delta O_3 \times F_{NOx}$). N_i and V_i are the NO_x tracer and VOC tracer for source group *i* and can be calculated as:

$$V_i = V_i + \Delta VOC \times \left(\frac{V_i \times kOH_i}{\sum (V_i \times kOH_i)} \right) \qquad (7)$$

$$N_i = N_i + \Delta NO_x \times \left(\frac{N_i}{\sum N_i} \right) \qquad (8)$$

where VOC and NO_x are the changes in the predicted VOC and NO_x concentrations between two consecutive time steps, kOH_i is the reaction rate constant of the VOC source group *i* with the OH radical. The relative magnitudes of O_3 reaction tracers O_3V_i and O_3N_i indicate whether O_3 concentrations at the receptor will respond more to reductions in VOCs or NO_x precursor emissions.

The use of DDM sensitivities as an indicator of NO_x- or VOC-sensitive chemistry overcomes the aforementioned shortcomings for the original $P_{H_2O_2}/P_{HNO_3}$ approach. However, this use of DDM is approximate since DDM does not apply, in theory, to the whole O_3 amount but only to the fraction explained by the first-order derivatives. In addition, the negative sensitivity to NO_x or VOC (i.e., the titration or inhibition effect of NO_x or VOC) is not accounted for (in such cases F_{NOx} or $F_{VOC} = 0$) in the allocation of O_3 production in OSAT. These limitations may cause inaccuracies in determining the NO_x- or VOC-sensitive chemistry by the use of O_3V_i and O_3N_i.

PA

The IRR component of PA can be used to elucidate important chemical pathways and to determine important characteristics of different chemical mechanisms. This is particularly useful for investigating mechanistic differences under different chemical regimes (e.g., VOC vs. NO_x limiting conditions), because the dominant reactions are different for NO_x- and VOC-sensitive regimes. PA has been mainly used as an explanatory tool to gain an understanding of some of the important processes in the model such as the mass budgets of HO_x, NO_y, and O_3. In this project, we explore the use of CPA outputs in CAMx to determine whether the system is the NO_x- vs. VOC-limited for a specific receptor. One of the process analysis outputs in the CAMx CPA file is the hourly rate of O_x production. Additional outputs include the rate of termination of HO_2+HO_2 to produce H_2O_2, and the rate of termination of $OH+NO_2$ to produce HNO_3. The ratio of the production rates of $P(H_2O_2)/P(HNO_3)$ is useful as an indicator of $P(O_3)$ and P(Ox) sensitivity to VOC and NO_x (Sillman, 1995; Tonnesen and Dennis, 2000a).

There is uncertainty in the particular value of $P(H_2O_2)/P(HNO_3)$ that demarks the transition from VOC sensitive to NO_x sensitive conditions. For example, Sillman (1995)

found that a ratio of $P(H_2O_2)/P(HNO_3)$ = 0.35 indicated conditions of equal O_3 concentration sensitivity to VOC and NO_x. In later results, Sillman (1995) revised the value to 0.2. Tonnesen and Dennis (2000a) evaluated $P(O_x)$ sensitivity to precursor emissions and found that the value of $P(H_2O_2)/P(HNO_3)$ that demarked the transition was not constant and varied as a function of the O_3 concentration. They found that this ratio ranged between 0.06 to 0.20 for conditions associated with a ridgeline of $P(O_x)$ production defined as:

$$dP(O_x)/dE_{NOx} = 0 \qquad (9)$$

where E_{NOx} represents emissions of NO_x.

Because the CAMx CPA file includes the hourly rates of $P(O_x)$, $P(H_2O_2)$ and $P(HNO_3)$, the ratio of $P(H_2O_2)/P(HNO_3)$ can be used to classify the hourly $P(O_x)$ as either VOC sensitive or NOx sensitive. Because of the uncertainty in the indicator ratio, a three-way classification scheme is used here:

- $P(H_2O_2)/P(HNO_3) < 0.06$ implies radical-limited (VOC-sensitive) conditions.
- $P(H_2O_2)/P(HNO_3)$ between 0.06 to 0.20 implies ridgeline conditions for $P(O_x)$, i.e., approximately equally sensitive to VOC and NO_x changes.
- $P(H_2O_2)/P(HNO_3) > 0.20$ implies NO_x-limited (NO_x-sensitive) conditions.

Normally, a CAMx post processing program is used to extract nested CPA domains from a single output file that contains the CPA data for all nested grids. For this project, the extraction program was modified to also calculate the $P(O_x)$ sensitivity to VOC and NO_x as a separate output. Note that this is one example of post-processing the CPA output, and there may be other post-processing analyses that can provide information about the photochemical system. For example, it may be possible to attribute O_x or O_3 production to the individual VOC species. This calculation was routinely performed using the process analysis output in trajectory models and box models. It has

not been performed in a grid model because of the complexity of the bookkeeping required to attribute organic intermediates to their parent species. However, such analyses could be considered in the future, and if feasible this would be a complementary analysis to the DDM and OSAT results that are presented in this report.

This approach has several limitations. First, as discussed above, the value of the $P_{H_2O_2}/P_{HNO_3}$ ratio to characterize the NO_x- or VOC- limited states of the air mass is not a universal number and involves some uncertainties (e.g., Sillman et al., 1997; Kumar and Lurmann, 1997). Second, since PA cannot be used to predict the response of O_3 concentrations to the changes in model input variables, this approach can only provide the NO_x- vs. VOC-sensitivity of the local O_3 production in a very qualitative sense. Third, since PA does not account for the history of the air parcels, the estimated NO_x- vs. VOC-sensitivity only reflects that for the local instantaneous O_3 production in a specific grid cell. This approach is thus similar to the extent parameter approach used in Chang et al. (1997) and Blanchard et al. (1999). As in the case of the modified OSAT approach, it would be useful to apply the DDM results for $P(O_x)$ to provide a more robust estimate of the $P(O_x)$ sensitivity in future studies.

Intercomparison

As shown above, each of the three probing tools provides information that can be used to directly or indirectly determine the NO_x or VOC sensitivity of peak O_3 concentrations at a particular receptor. However, the sensitivity of peak O_3 concentrations estimated by these tools is different, due to different characteristics of each tool and different quantity/approach used by these tools. In the following sections, we compare the NO_x or VOC sensitivity of O_3 chemistry predicted by or derived from the three probing tools. For DDM, the O_3 sensitivities to the total VOC and total NO_x emissions are calculated using the results of DDM run B7, in which DDM provides the local sensitivity to the domain-wide VOC and NO_x emissions from 4 source categories (i.e., biogenic, on-road mobile, other surface anthropogenic, and elevated anthropogenic emissions). We first calculate the averaged hourly O_3 concentrations for the 9 subareas and the whole receptor region to determine the peak O_3 hour for those subareas and the

whole receptor. Note that the peak O_3 hour may be different for each subarea and for the whole receptor region. For each subarea, the sensitivities to the VOC and NO_x emissions from the 4 source categories in its 9 fine grid cells are lumped to obtain the sensitivities to the total VOC and total NO_x emissions in those fine grid cells at the peak O_3 hour of the subarea and the averaged O_3 sensitivities to the total VOC and NO_x emissions for the subarea are then obtained by taking an average of the sensitivities to total VOC and total NO_x emissions over the 9 fine grid cells. A similar approach is used to obtain the averaged O_3 sensitivities to the total VOC and NO_x emissions for the whole receptor region. For OSAT, we use the results from the OSAT run B1, which provides the O_3 contributions of the VOC and NO_x emissions from a total of 68 source groups (17 source areas x 4 source categories). For each subarea, the O_3 contributions attributed to the VOC and NO_x emissions from 68 source groups in its 9 fine grid cells are lumped to obtain the contributions of the total VOC and total NO_x emissions in those fine grid cells at the peak O_3 hour of the subarea and the averaged O_3 contributions of the total VOC and NO_x emissions for the subarea are then obtained by taking an average of the contributions of the total VOC and total NO_x emissions over the 9 fine grid cells. A similar approach is used to obtain the averaged O_3 contributions attributed to the total VOC and NO_x emissions for the whole receptor region. For PA, we use the results from the PA run B4, which provides O_x production under NO_x-sensitive, VOC-sensitive, and ridgeline (i.e., equally-sensitive) conditions. The amount of $P(O_x)$ that was formed under each of these conditions for the four receptor regions for each day from July 11 to July 15 were summed as a total $P(O_x)$ for each day up to 16:00 EST. The totals were calculated for all grid cells in each of the receptor regions and for layers 1 to 4. The total O_x production in units of ppb was divided by the total number of grid cells to calculate the average $P(O_x)$ for each receptor region.

Recognizing the limitations of the approach used in each tool, we can only conduct such comparisons qualitatively. If large discrepancies exist among the results predicted by the three probing tools (e.g., for a given receptor, one tool predicts a VOC-limited chemistry, and the other predicts a NO_x-limited chemistry), we will use the results from both the CAMx base simulation and the sensitivity simulation with a 25% reduction in anthropogenic NO_x or VOC emissions to verify the accuracy of the probing tools.

Since the sensitivity simulations with a 25% emission reduction are only for the reductions of anthropogenic NO_x or VOC emissions (instead of the reductions of the total NO_x or VOC emissions from all source categories), the brute-force sensitivity coefficients calculated using results from the base and the sensitivity simulations (i.e., the change in O_3 concentrations divided by the change in anthropogenic VOC or NO_x emissions) cannot be directly used to verify the sensitivity to the total VOC or NO_x emissions obtained from the base simulations of DDM. However, we can compare O_3 concentrations predicted with the DDM sensitivities from the base simulations against the actual O_3 concentrations obtained from the 25% emission reduction scenarios. The O_3 concentrations and the DDM sensitivities from the base simulation can be used to predict the resulting O_3 concentration for an emission reduction scenario as follows:

$$C_{l=-d} = C_{l=0} - S_{l=0} \cdot d \tag{10}$$

where $C_{\lambda=0}$ and $C_{\lambda=-\delta}$ are the concentrations of O_3 obtained from the base simulation and the simulation with 25% reductions in anthropogenic emissions, respectively; $S_{\lambda=0}$ is the sensitivity of O_3 with respect to changes in the anthropogenic VOC or NO_x emissions calculated from the base simulation (note that the sensitivity with respect to changes in biogenic VOC or NO_x emissions should be excluded); δ is the perturbation in parameter λ (i.e., 0.25, respectively). $C_{\lambda=-\delta}$ can then be compared to the O_3 concentrations obtained from the 25% anthropogenic emission reduction scenarios. Such a comparison will help indirectly evaluate the accuracy of DDM sensitivities predicted in the base run B7. Large discrepancies between $C_{\lambda=-\delta}$ and the actual O_3 concentrations obtained by altering emissions indicate that the DDM sensitivities are inaccurate for a perturbation of δ in VOC or NO_x emissions. This approach is also used later in section 6.3, where we test the stretchability of DDM under a 75% reduction of anthropogenic NO_x emissions and the ability of OSAT to predict model responses under all emission reduction scenarios. For DDM test, $C_{\lambda=-\delta}$ is first calculated using Equation (10) with δ = 0.75 and then will be compared to O_3 concentrations obtained from the 75% anthropogenic emission reduction scenario (i.e., DDM run S8). For OSAT test, $S_{\lambda=0}$ is the O_3 source contribution of the anthropogenic VOC or NO_x emissions calculated from the base simulation (note that the

source contributions of biogenic VOC or NO_x emissions should be excluded). $C_{\lambda=-\delta}$ is first calculated using Equation (10) with $\delta = 0.25$ or 0.75 and then will be compared to O_3 concentrations obtained from the 25% or 75% anthropogenic emission reduction scenario (i.e., OSAT runs S1, S4, and S7). This information helps evaluate the accuracy of DDM sensitivities and OSAT source contributions for a range of perturbations in VOC or NO_x emissions. It also helps verify which tool(s) provide(s) accurate information in terms of NO_x or VOC-sensitivity under the base emission scenario. The likely causes for the inconsistency among the three tools will be analyzed.

In the following section, the spatial distribution of the predicted NO_x- or VOC-sensitivity by the three probing tools will first be compared. The consistency in NO_x or VOC sensitivity predicted by the three tools for the four selected receptor regions (i.e., Atlanta, Chicago, New York City, and Altoona) will then be tested in detail.

6.1.2.1 Spatial Distribution of NO_x- or VOC-Sensitivity of O_3 Chemistry

Figures 6-4 to 6-8 show the spatial distribution of the differences in the O_3 sensitivities to the total NO_x and VOC emissions predicted by DDM at 2 p.m. on July 11-15, the differences in the O_3 contributions from the total NO_x and VOC emissions predicted by OSAT at 2 p.m. on July 11-15, and the differences in the accumulative daily total O_x (i.e., odd oxygen = $O_3 + NO_2 + O(^3P) + O(^1D) + 2\ NO_3 + 3\ N_2O_5 + PAN + HNO_4$) production under NO_x- and VOC-limited conditions on July 11-15 predicted by PA. While the DDM and OSAT results are plotted for the whole simulation domain by combining both coarse- and fine grid results, the PA results are only plotted for the fine grid domain, which is smaller than the whole simulation domain. A positive value in Figures 6-4 to 6-8 indicates that O_3 formation is NO_x-limited, and a negative value indicates that O_3 formation is VOC-limited.

On July 11, DDM predicts a VOC-limited O_3 chemistry in a number of regions including Minneapolis, MN and the vicinity area in its northwest, the southwestern coastal area of Lake Michigan, Chicago, IL, the western portion of Lake Erie and its coastal area, Pittsburgh, PA and its vicinity area, New York City, NY and its vicinity area, Boston, MA and its vicinity area, Indianapolis, IN and its vicinity area, the

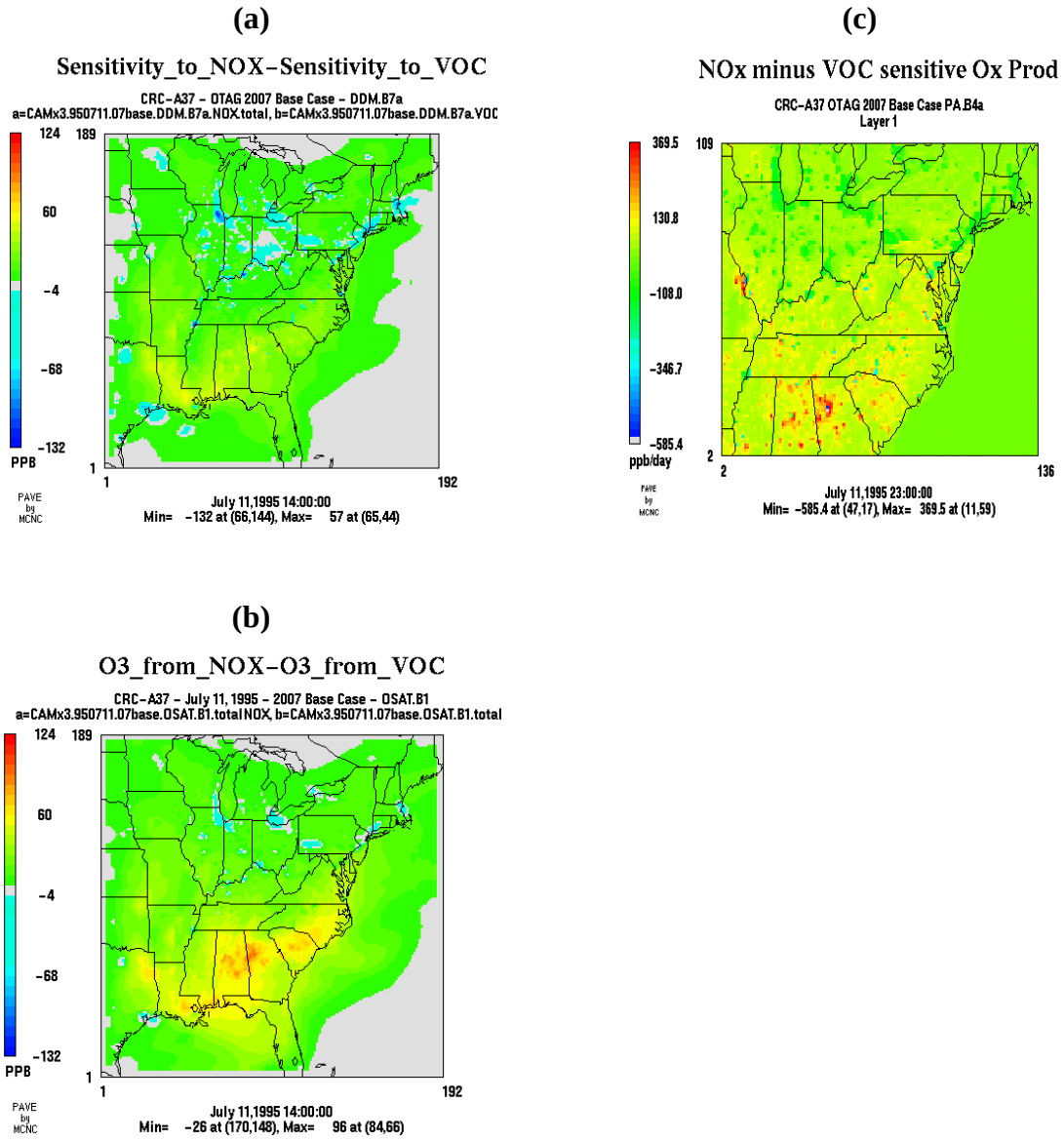

Figure 6-4. The spatial distribution of the differences in (a) the O_3 sensitivities to total NO_x and VOC predicted by DDM at 2 p.m. on July 11, (b) the O_3 contributions from total NO_x and VOC predicted by OSAT at 2 p.m. on July 11, and (c) the accumulative daily total O_x production under NO_x- and VOC-limited conditions predicted by PA on July 11. All results were obtained under the EPA 2007 base emission scenario (DDM base run B7, OSAT base run B1, and PA base run B4).

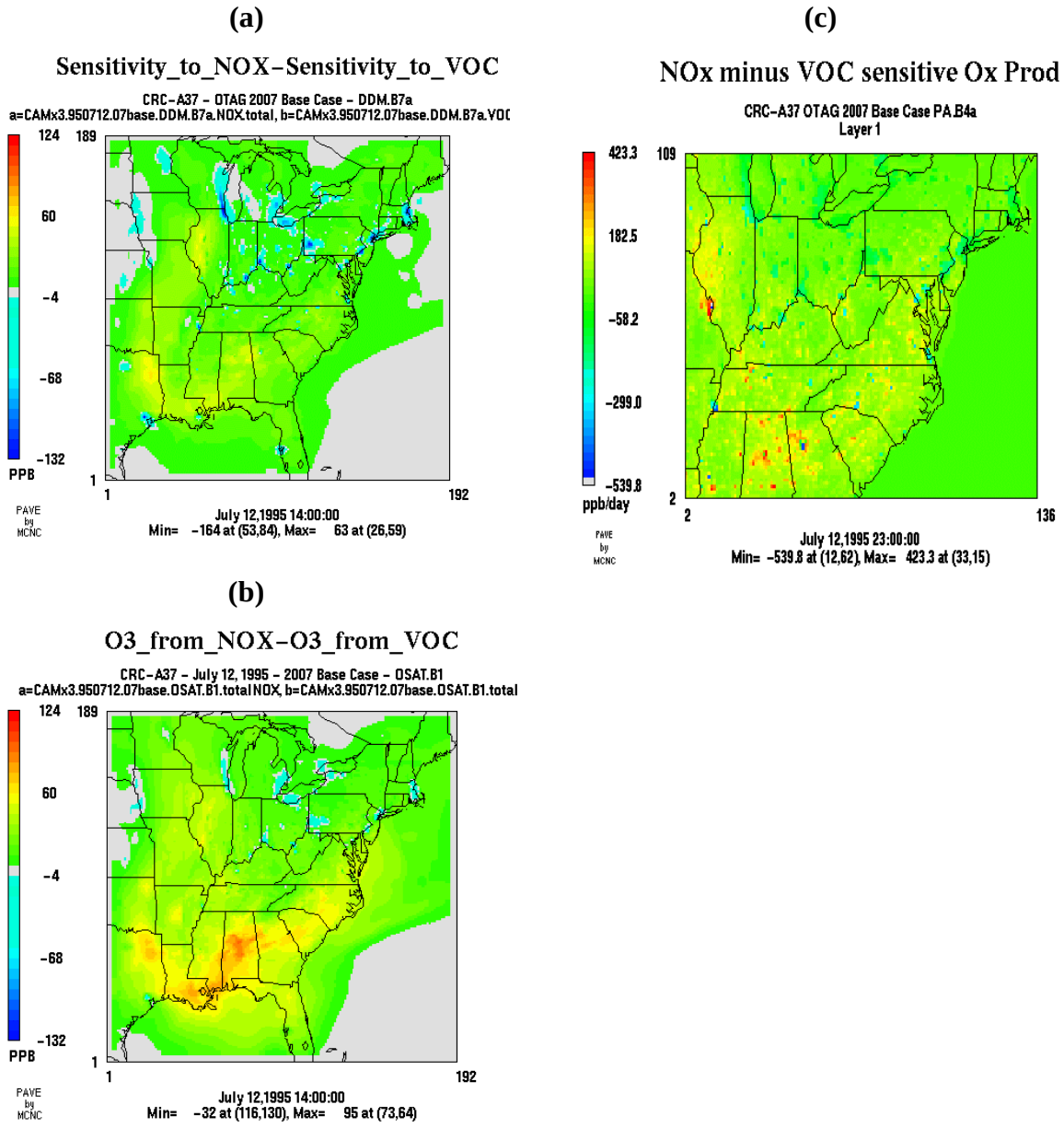

Figure 6-5. The spatial distribution of the differences in (a) the O_3 sensitivities to total NO_x and VOC predicted by DDM at 2 p.m. on July 12, (b) the O_3 contributions from total NO_x and VOC predicted by OSAT at 2 p.m. on July 12, and (c) the accumulative daily total O_x production under NO_x- and VOC-limited conditions predicted by PA on July 12. All results were obtained under the EPA 2007 base emission scenario (DDM base run B7, OSAT base run B1, and PA base run B4).

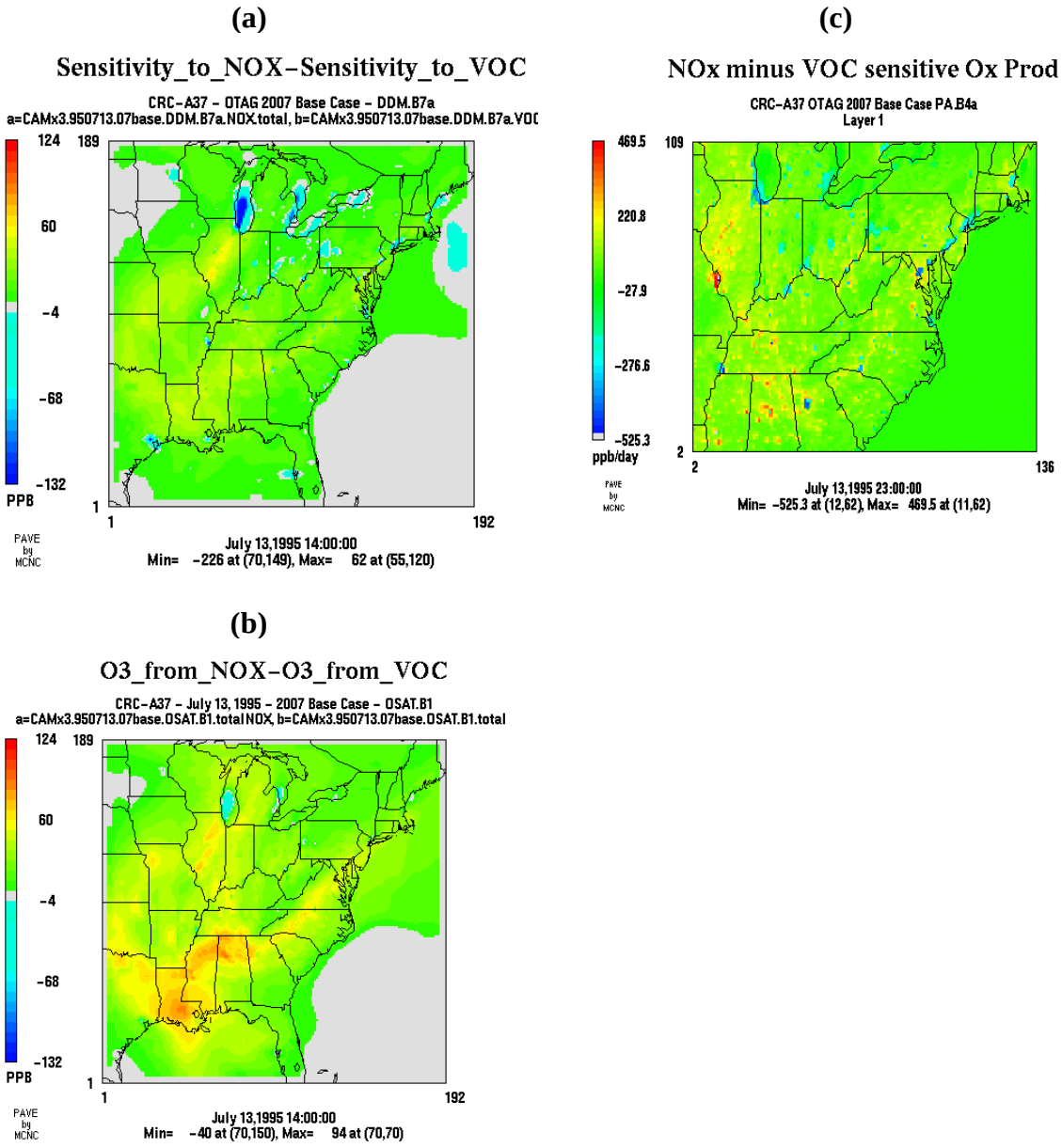

Figure 6-6. The spatial distribution of the differences in (a) the O_3 sensitivities to total NO_x and VOC predicted by DDM at 2 p.m. on July 13, (b) the O_3 contributions from total NO_x and VOC predicted by OSAT at 2 p.m. on July 13, and (c) the accumulative daily total O_x production under NO_x- and VOC-limited conditions predicted by PA on July 13. All results were obtained under the EPA 2007 base emission scenario (DDM base run B7, OSAT base run B1, and PA base run B4).

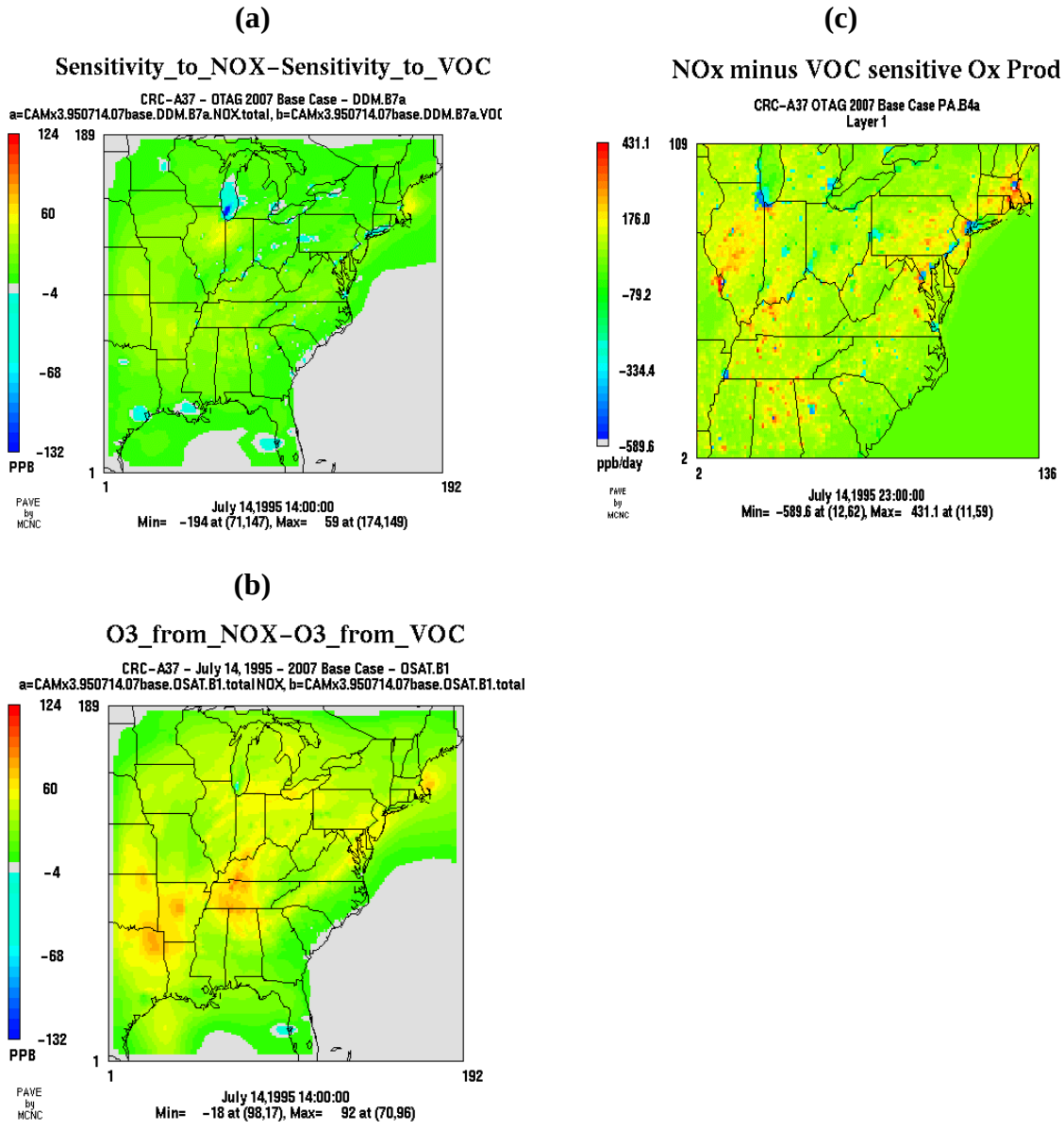

Figure 6-7. The spatial distribution of the differences in (a) the O_3 sensitivities to total NO_x and VOC predicted by DDM at 2 p.m. on July 14, (b) the O_3 contributions from total NO_x and VOC predicted by OSAT at 2 p.m. on July 14, and (c) the accumulative daily total O_x production under NO_x- and VOC-limited conditions predicted by PA on July 14. All results were obtained under the EPA 2007 base emission scenario (DDM base run B7, OSAT base run B1, and PA base run B4).

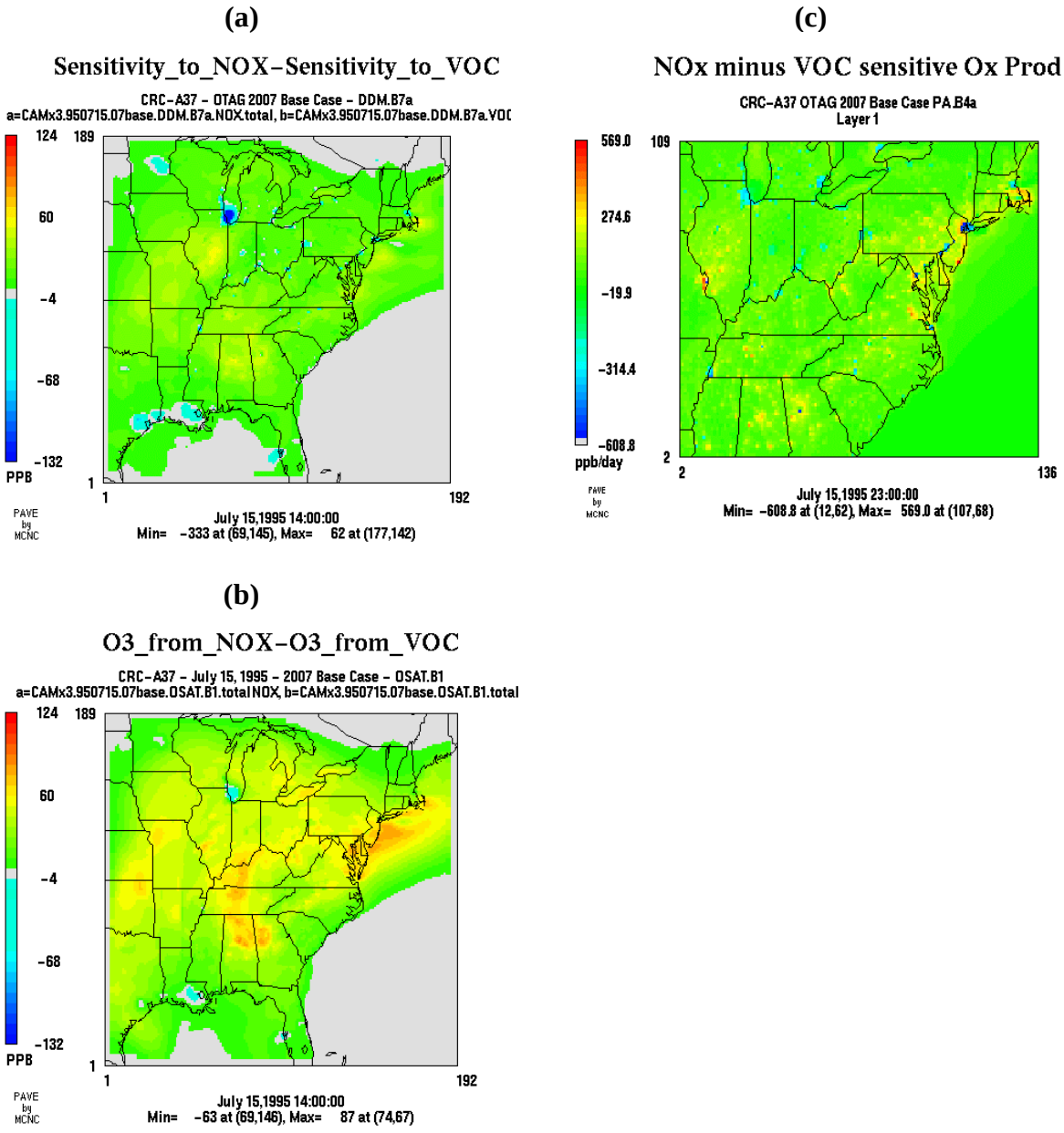

Figure 6-8. The spatial distribution of the differences in (a) the O_3 sensitivities to total NO_x and VOC predicted by DDM at 2 p.m. on July 15, (b) the O_3 contributions from total NO_x and VOC predicted by OSAT at 2 p.m. on July 15, and (c) the accumulative daily total O_x production under NO_x- and VOC-limited conditions predicted by PA on July 15. All results were obtained under the EPA 2007 base emission scenario (DDM base run B7, OSAT base run B1, and PA base run B4).

southwestern portion of the state of Ohio, Houston, TX and its vicinity area, and a number of locations in the states of Kentucky, Illinois, Indiana, and Pennsylvania. O_3 production is NO_x-limited in the other regions. The VOC-limited regions predicted by OSAT are quite similar to those predicted by DDM, but the VOC-limited areas in those regions are smaller than those predicted by DDM. Both DDM and OSAT predict that O_3 formation is predominantly NO_x-limited in the regions in the southern domain. PA predicts that more O_x production is VOC-limited in the southwestern coastal area of Lake Michigan, Chicago, the western portion of Lake Erie and its coastal area, Pittsburgh and its vicinity area, New York City and its vicinity area, Boston and its vicinity area, Indianapolis and its vicinity area, and a number of locations in the states of Kentucky, Illinois, Indiana, and Pennsylvania.

On July 12, DDM predicts that the VOC-limited regions in the southwestern coastal area of Lake Michigan extend north into a larger area. Some areas in southeastern Michigan, the western and the southern coastal areas of Lake Ontario, and Tampa, FL became VOC-limited regions. The VOC-limited regions in the southwestern portion of the state of Ohio (except for Cincinnati and its vicinity area) became NO_x-limited. Other VOC-limited regions remained similar to those on July 11. Similar changes from NO_x-limited to VOC-limited conditions were predicted by OSAT along the western coastal area of Lake Michigan and the western and the southern coastal areas of Lake Ontario. OSAT predicts that more O_3 is produced under NO_x-limited conditions in Chicago, which is different from July 11. The VOC-limited regions predicted by PA are quite similar to those on July 11.

On July 13, DDM predicts that more O_3 is produced under the VOC-limited conditions over a large area of Lake Michigan and Chicago, a small portion in southern Lake Huron, Lake Erie, Lake Ontario, Pittsburgh, PA and its vicinity area, Boston, MA, New York City, NY, Indianapolis, IN, Cincinnati, OH and its vicinity area, Columbus, OH, Houston, TX and its vicinity area, and Tampa, FL. OSAT predicts that more O_3 is produced under VOC-limited conditions over some areas of Lake Michigan and Lake Huron but more O_3 is produced under NO_x-limited conditions in Chicago, IL, Pittsburgh, PA, Boston, MA, New York City, NY, Memphis, TN, Houston, TX and Tampa, FL. The VOC-limited regions predicted by PA are quite similar to those predicted by DDM. It

predicts that more O_x production is VOC-limited in a large area over Lake Michigan and Chicago, IL, a small portion in southern Lake Huron and its southern coastal areas in the eastern Michigan, Indianapolis, IN, Louisville, KY, Columbus, OH, Cincinnati, OH, Pittsburgh, PA and its vicinity area, Boston, MA, New York City, NY, Memphis, TN, and Atlanta, GA.

On July 14, DDM predicts that more O_3 is produced under VOC-limited conditions in Minneapolis, MN and its vicinity area, over a large area of Lake Michigan and Chicago, IL, Pittsburgh, PA and its vicinity area, Boston, MA, New York City, NY, Indianapolis, IN, Cincinnati, OH, Columbus, OH, Houston, TX and its vicinity area, Baton Rough, LA, and Tampa, FL. OSAT predicts that more O_3 is produced under NO_x-limited conditions in all those regions except for a small area over southern Lake Michigan and Tampa, FL. The VOC-limited regions predicted by PA are quite similar to those on July 13.

On July 15, the VOC-limited regions predicted by DDM are similar to those on July 14 but the VOC-limited region extends further northwest of Minneapolis, MN and northeast of Houston, TX. OSAT predicts that more O_3 is produced under VOC-limited conditions in the southwestern portion of Lake Michigan, Baton Rouge, LA and Tampa, FL but more O_3 is produced under NO_x-limited conditions in all other major cities including Chicago, IL, Boston, MA and New York City, NY. The VOC-limited regions predicted by PA are also similar to those on July 13.

Detailed predictions of the NO_x- vs. VOC-limited O_3 production by each tool and possible causes for their discrepancies at the four receptors are provided in the section below.

6.1.2.2 Comparison of the NO_x- or VOC-Sensitivity Predicted at Four Receptors by DDM and OSAT

Tables 6-37 to 6-40 show the NO_x- vs. VOC-sensitivity of O_3 chemistry at the hour of peak O_3 on July 11-15 in the 9 subareas in Atlanta, Chicago, New York City, and Altoona, respectively, predicted by DDM and OSAT under the EPA 2007 base emission scenario. The NO_x- or VOC-limited fraction of O_3 concentrations is calculated using the

Table 6-37. NO_x- vs. VOC-limited O_3 concentration in 9 subareas in Atlanta predicted by DDM and OSAT under the EPA 2007 base emission scenario.

Date	Subarea	DDM Prediction				OSAT Prediction			
		Sensitivities of O_3		O_3 concentration		Contributions to O_3		O_3 Concentration	
		NO_x	VOC	NO_x-limited, %	VOC-limited, %	NO_x	VOC	NO_x-limited, %	VOC-limited, %
950711	1	4.7E-02	1.4E-02	77.0	23.0	8.0E-02	1.7E-02	82.5	17.5
	2	4.0E-02	4.4E-03	90.1	9.9	6.8E-02	7.4E-03	90.2	9.8
	3	3.6E-02	3.5E-03	91.1	8.9	6.0E-02	5.0E-03	92.4	7.6
	4	6.5E-02	2.5E-02	72.2	27.8	1.2E-01	2.7E-02	80.8	19.2
	5	5.3E-02	2.2E-02	70.7	29.3	9.3E-02	2.5E-02	79.1	20.9
	6	4.1E-02	5.7E-03	87.8	12.2	7.1E-02	5.1E-03	93.4	6.6
	7	7.4E-02	2.7E-02	73.3	26.7	1.3E-01	2.9E-02	82.2	17.8
	8	5.6E-02	1.4E-02	80.0	20.0	9.6E-02	1.6E-02	85.7	14.3
	9	3.8E-02	6.5E-03	85.4	14.6	6.9E-02	4.3E-03	94.1	5.9
950712	1	4.3E-02	1.0E-02	81.1	18.9	6.8E-02	1.3E-02	84.2	15.8
	2	3.5E-02	7.2E-03	82.9	17.1	6.2E-02	7.5E-03	89.1	10.9
	3	3.6E-02	9.4E-03	79.3	20.7	6.5E-02	8.0E-03	89.0	11.0
	4	5.2E-02	2.8E-02	65.0	35.0	9.4E-02	2.9E-02	76.5	23.5
	5	3.5E-02	1.8E-02	66.0	34.0	6.8E-02	1.6E-02	80.5	19.5
	6	3.5E-02	8.9E-03	79.7	20.3	6.4E-02	6.5E-03	90.8	9.2
	7	5.5E-02	1.1E-02	83.3	16.7	8.5E-02	1.9E-02	81.8	18.2
	8	3.8E-02	8.6E-03	81.5	18.5	6.6E-02	8.7E-03	88.4	11.6
	9	3.4E-02	8.3E-03	80.4	19.6	6.5E-02	5.5E-03	92.2	7.8
950713	1	5.0E-02	1.2E-02	80.6	19.4	8.2E-02	1.5E-02	84.6	15.4
	2	4.0E-02	7.1E-03	84.9	15.1	6.7E-02	7.7E-03	89.8	10.2
	3	3.5E-02	5.4E-03	86.6	13.4	6.0E-02	5.8E-03	91.1	8.9
	4	4.9E-02	2.3E-02	68.1	31.9	8.6E-02	2.6E-02	76.9	23.1
	5	3.3E-02	1.3E-02	71.7	28.3	6.2E-02	1.5E-02	80.1	19.9
	6	3.2E-02	2.8E-03	92.0	8.0	5.5E-02	5.8E-03	90.4	9.6
	7	4.0E-02	1.1E-02	78.4	21.6	6.7E-02	1.4E-02	82.6	17.4
	8	3.2E-02	7.2E-03	81.6	18.4	5.7E-02	8.9E-03	86.5	13.5
	9	2.8E-02	3.9E-03	87.8	12.2	5.1E-02	4.8E-03	91.4	8.6
950714	1	5.2E-02	1.4E-02	78.8	21.2	8.2E-02	1.8E-02	82.4	17.6
	2	4.0E-02	5.7E-03	87.5	12.5	6.3E-02	8.3E-03	88.4	11.6
	3	3.1E-02	3.7E-03	89.3	10.7	4.9E-02	4.4E-03	91.9	8.1
	4	5.4E-02	3.1E-02	63.5	36.5	9.4E-02	3.5E-02	72.9	27.1
	5	3.2E-02	1.9E-02	62.7	37.3	6.0E-02	2.1E-02	74.2	25.8
	6	2.7E-02	3.0E-03	90.0	10.0	4.2E-02	4.7E-03	89.8	10.2
	7	4.6E-02	1.2E-02	79.3	20.7	7.0E-02	1.8E-02	79.7	20.3
	8	3.1E-02	6.7E-03	82.2	17.8	4.7E-02	9.7E-03	83.0	17.0
	9	2.5E-02	6.6E-03	79.1	20.9	3.7E-02	7.7E-03	82.6	17.4
950715	1	4.8E-02	1.0E-02	82.8	17.2	8.2E-02	1.4E-02	85.0	15.0
	2	5.0E-02	7.9E-03	86.4	13.6	8.3E-02	1.3E-02	86.4	13.6
	3	4.5E-02	2.6E-03	94.5	5.5	7.1E-02	8.4E-03	89.4	10.6
	4	5.1E-02	1.4E-02	78.5	21.5	8.7E-02	2.0E-02	81.5	18.5
	5	6.3E-02	3.5E-02	64.3	35.7	1.2E-01	3.7E-02	76.4	23.6
	6	6.0E-02	1.7E-02	77.9	22.1	1.1E-01	2.2E-02	82.7	17.3
	7	5.3E-02	1.0E-02	84.1	15.9	8.9E-02	1.5E-02	85.5	14.5
	8	6.4E-02	1.9E-02	77.1	22.9	1.1E-01	2.6E-02	81.3	18.7
	9	5.9E-02	1.2E-02	83.1	16.9	1.0E-01	1.9E-02	84.2	15.8

1. The O_3 concentration is considered as 100% VOC-limited if the sensitivity of O_3 to NO_x emissions is negative, and vice versa.

Table 6-38. NO_x- vs. VOC-limited O_3 concentration in 9 subareas in Chicago predicted by DDM and OSAT under the EPA 2007 base emission scenario.

Date	Subarea	DDM Prediction				OSAT Prediction			
		Sensitivities of O_3		O_3 concentration[1]		Contributions to O_3		O_3 Concentration	
		NO_x	VOC	NO_x-limited, %	VOC-limited, %	NO_x	VOC	NO_x-limited, %	VOC-limited, %
950711	1	-1.5E-02	4.5E-02	0.0	100.0	2.6E-02	3.6E-02	41.5	58.5
	2	1.1E-02	1.5E-02	42.3	57.7	2.8E-02	2.2E-02	56.2	43.8
	3	1.9E-02	8.3E-03	69.6	30.4	3.1E-02	1.7E-02	64.3	35.7
	4	-4.5E-02	6.1E-02	0.0	100.0	2.0E-02	3.7E-02	34.8	65.2
	5	-3.4E-02	3.7E-02	0.0	100.0	1.8E-02	2.4E-02	43.2	56.8
	6	1.7E-02	1.2E-02	58.6	41.4	3.0E-02	2.2E-02	57.1	42.9
	7	-7.7E-03	2.5E-02	0.0	100.0	2.4E-02	2.3E-02	50.8	49.2
	8	-3.9E-02	4.9E-02	0.0	100.0	1.9E-02	3.2E-02	36.9	63.1
	9	-3.4E-02	4.4E-02	0.0	100.0	1.9E-02	3.3E-02	36.4	63.6
950712	1	1.5E-02	3.6E-02	29.4	70.6	5.3E-02	2.9E-02	64.6	35.4
	2	-2.7E-02	5.9E-02	0.0	100.0	3.9E-02	3.5E-02	53.3	46.7
	3	1.6E-02	3.7E-02	30.2	69.8	5.3E-02	3.6E-02	59.2	40.8
	4	2.0E-02	2.6E-02	43.5	56.5	5.3E-02	2.1E-02	71.5	28.5
	5	-9.1E-03	3.8E-02	0.0	100.0	4.2E-02	2.2E-02	65.8	34.2
	6	4.4E-03	3.9E-02	10.1	89.9	4.5E-02	3.2E-02	58.6	41.4
	7	2.3E-02	1.8E-02	56.1	43.9	4.9E-02	1.6E-02	75.9	24.1
	8	2.3E-02	1.9E-02	54.8	45.2	4.9E-02	1.6E-02	74.7	25.3
	9	1.5E-02	2.3E-02	39.5	60.5	4.4E-02	2.0E-02	69.2	30.8
950713	1	3.7E-02	1.6E-02	69.8	30.2	6.7E-02	1.2E-02	85.2	14.8
	2	-9.8E-03	7.6E-02	0.0	100.0	6.6E-02	4.4E-02	60.3	39.7
	3	4.4E-03	8.0E-02	5.2	94.8	7.9E-02	5.6E-02	58.2	41.8
	4	4.3E-02	1.7E-02	71.7	28.3	7.7E-02	1.3E-02	85.8	14.2
	5	1.4E-02	4.1E-02	25.5	74.5	7.3E-02	2.1E-02	78.1	21.9
	6	1.4E-02	5.4E-02	20.6	79.4	7.3E-02	3.7E-02	66.5	33.5
	7	4.7E-02	1.7E-02	73.4	26.6	8.5E-02	1.1E-02	88.2	11.8
	8	4.8E-02	1.2E-02	80.0	20.0	7.9E-02	1.2E-02	86.9	13.1
	9	3.7E-02	1.5E-02	71.2	28.8	7.1E-02	1.3E-02	84.2	15.8
950714	1	3.5E-02	8.4E-03	80.6	19.4	5.9E-02	7.5E-03	88.7	11.3
	2	6.9E-03	5.2E-02	11.7	88.3	6.0E-02	3.6E-02	62.4	37.6
	3	-2.7E-02	1.2E-01	0.0	100.0	7.7E-02	7.7E-02	50.1	49.9
	4	3.7E-02	6.0E-03	86.0	14.0	5.9E-02	1.2E-02	83.6	16.4
	5	-1.7E-03	5.1E-02	-3.4	103.4	5.9E-02	3.0E-02	66.5	33.5
	6	6.9E-03	6.7E-02	9.3	90.7	7.2E-02	4.9E-02	59.5	40.5
	7	4.0E-02	8.1E-03	83.2	16.8	6.7E-02	7.6E-03	89.8	10.2
	8	4.1E-02	7.8E-03	84.0	16.0	6.7E-02	9.5E-03	87.5	12.5
	9	3.5E-02	1.2E-02	74.5	25.5	6.4E-02	1.8E-02	78.4	21.6
950715	1	1.5E-02	3.2E-02	31.9	68.1	5.4E-02	2.1E-02	71.8	28.2
	2	-3.1E-02	1.1E-01	0.0	100.0	5.7E-02	7.4E-02	43.4	56.6
	3	1.0E-02	7.2E-02	12.2	87.8	6.4E-02	6.7E-02	48.9	51.1
	4	2.6E-02	1.8E-02	59.1	40.9	5.6E-02	1.2E-02	82.4	17.6
	5	-4.9E-02	9.3E-02	0.0	100.0	4.9E-02	4.4E-02	52.8	47.2
	6	5.0E-03	7.7E-02	6.1	93.9	6.8E-02	6.2E-02	52.5	47.5
	7	3.4E-02	1.4E-02	70.8	29.2	6.4E-02	8.6E-03	88.1	11.9
	8	2.6E-02	2.2E-02	54.2	45.8	5.9E-02	1.6E-02	78.4	21.6
	9	1.9E-02	3.4E-02	35.8	64.2	6.1E-02	2.4E-02	71.5	28.5

1. The O_3 concentration is considered as 100% VOC-limited if the sensitivity of O_3 to NO_x emissions is negative, and vice versa.

Table 6-39. NO_x- vs. VOC-limited O_3 concentration in 9 subareas in New York City predicted by DDM and OSAT under the EPA 2007 base emission scenario.

Date	Subarea	DDM Prediction				OSAT Prediction			
		Sensitivities of O_3		O_3 concentration[1]		Contributions to O_3		O_3 Concentration	
		NO_x	VOC	NO_x-limited, %	VOC-limited, %	NO_x	VOC	NO_x-limited, %	VOC-limited, %
950711	1	1.7E-02	2.0E-02	45.9	54.1	3.8E-02	2.6E-02	59.2	40.8
	2	-1.4E-02	4.9E-02	0.0	100.0	3.3E-02	3.9E-02	45.9	54.1
	3	-1.7E-02	5.1E-02	0.0	100.0	3.2E-02	4.1E-02	43.9	56.1
	4	-6.8E-03	3.8E-02	0.0	100.0	3.5E-02	3.3E-02	51.5	48.5
	5	-1.2E-02	3.8E-02	0.0	100.0	3.3E-02	2.8E-02	54.0	46.0
	6	7.7E-03	2.2E-02	25.9	74.1	3.5E-02	2.4E-02	59.7	40.3
	7	1.1E-02	3.5E-02	23.9	76.1	4.3E-02	3.7E-02	54.0	46.0
	8	2.4E-02	1.3E-02	64.9	35.1	4.2E-02	2.0E-02	68.1	31.9
	9	2.0E-02	8.1E-03	71.2	28.8	3.7E-02	1.2E-02	75.8	24.2
950712	1	1.4E-02	2.4E-02	36.8	63.2	3.9E-02	2.5E-02	61.3	38.7
	2	-8.1E-03	4.3E-02	0.0	100.0	3.3E-02	3.5E-02	48.5	51.5
	3	4.8E-03	3.3E-02	12.7	87.3	3.7E-02	3.2E-02	53.8	46.2
	4	-6.1E-03	4.3E-02	0.0	100.0	3.8E-02	3.4E-02	53.3	46.7
	5	-2.6E-02	5.0E-02	0.0	100.0	3.2E-02	3.1E-02	51.1	48.9
	6	9.2E-03	2.4E-02	27.7	72.3	3.7E-02	2.6E-02	58.5	41.5
	7	1.2E-02	3.6E-02	25.0	75.0	4.5E-02	3.7E-02	54.4	45.6
	8	1.9E-02	1.8E-02	51.4	48.6	4.2E-02	2.1E-02	66.7	33.3
	9	2.1E-02	1.3E-02	61.8	38.2	4.3E-02	1.3E-02	77.4	22.6
950713	1	3.4E-02	2.1E-02	61.8	38.2	6.3E-02	2.5E-02	71.3	28.7
	2	1.9E-02	4.5E-02	29.7	70.3	6.3E-02	4.5E-02	58.6	41.4
	3	3.1E-02	3.8E-02	44.9	55.1	6.6E-02	4.5E-02	59.8	40.2
	4	2.4E-02	3.2E-02	42.9	57.1	6.2E-02	3.4E-02	64.3	35.7
	5	1.5E-02	3.8E-02	28.3	71.7	6.1E-02	3.5E-02	63.4	36.6
	6	3.0E-02	2.1E-02	58.8	41.2	6.0E-02	2.7E-02	69.3	30.7
	7	4.3E-02	2.6E-02	62.3	37.7	7.7E-02	3.2E-02	70.9	29.1
	8	3.6E-02	1.6E-02	69.2	30.8	6.2E-02	2.2E-02	74.3	25.7
	9	2.6E-02	1.7E-02	60.5	39.5	5.5E-02	1.6E-02	78.0	22.0
950714	1	3.4E-02	1.3E-02	72.3	27.7	5.9E-02	2.1E-02	74.0	26.0
	2	3.4E-02	2.5E-02	57.6	42.4	6.5E-02	3.0E-02	68.5	31.5
	3	1.5E-02	5.7E-02	20.8	79.2	6.1E-02	5.4E-02	52.8	47.2
	4	2.7E-02	3.2E-02	45.8	54.2	6.5E-02	3.1E-02	67.6	32.4
	5	-3.3E-03	6.2E-02	0.0	100.0	6.1E-02	4.6E-02	56.9	43.1
	6	2.1E-02	6.3E-02	25.0	75.0	7.7E-02	5.9E-02	56.7	43.3
	7	4.0E-02	3.0E-02	57.1	42.9	8.2E-02	2.6E-02	76.3	23.7
	8	4.2E-02	3.5E-02	54.5	45.5	7.9E-02	4.2E-02	65.4	34.6
	9	4.2E-02	2.2E-02	65.6	34.4	7.0E-02	3.4E-02	67.6	32.4
950715	1	3.0E-02	9.3E-03	76.3	23.7	5.6E-02	8.6E-03	86.7	13.3
	2	3.3E-02	1.2E-02	73.3	26.7	6.1E-02	1.2E-02	83.1	16.9
	3	3.8E-02	1.4E-02	73.1	26.9	6.5E-02	1.4E-02	82.5	17.5
	4	3.1E-02	2.1E-02	59.6	40.4	6.7E-02	1.8E-02	78.6	21.4
	5	1.4E-02	4.4E-02	24.1	75.9	6.6E-02	3.3E-02	66.3	33.7
	6	3.2E-02	4.3E-02	42.7	57.3	7.6E-02	4.3E-02	63.9	36.1
	7	3.3E-02	3.7E-02	47.1	52.9	7.7E-02	3.3E-02	69.7	30.3
	8	2.5E-02	5.8E-02	30.1	69.9	8.3E-02	5.1E-02	61.8	38.2
	9	3.9E-02	6.0E-02	39.4	60.6	9.5E-02	6.1E-02	60.9	39.1

1. The O_3 concentration is considered as 100% VOC-limited if the sensitivity of O_3 to NO_x emissions is negative, and vice versa.

Table 6-40. NO_x- vs. VOC-limited O_3 concentration in 9 subareas in Altoona predicted by DDM and OSAT under the EPA 2007 base emission scenario.

Date	Subarea	DDM Prediction				OSAT Prediction			
		Sensitivities of O_3		O_3 concentration[1]		Contributions to O_3		O_3 Concentration	
		NO_x	VOC	NO_x-limited, %	VOC-limited, %	NO_x	VOC	NO_x-limited, %	VOC-limited, %
950711	1	1.7E-02	1.2E-02	58.6	41.4	2.9E-02	2.0E-02	59.4	40.6
	2	4.6E-03	2.2E-02	17.3	82.7	3.1E-02	2.5E-02	55.5	44.5
	3	6.8E-03	2.0E-02	25.4	74.6	3.2E-02	2.4E-02	57.1	42.9
	4	1.0E-02	2.2E-02	31.3	68.8	3.0E-02	2.8E-02	51.4	48.6
	5	2.2E-02	1.4E-02	61.1	38.9	3.3E-02	2.4E-02	58.4	41.6
	6	1.1E-02	1.9E-02	36.7	63.3	2.9E-02	2.5E-02	53.6	46.4
	7	-5.3E-03	3.9E-02	0.0	100.0	2.9E-02	4.0E-02	42.3	57.7
	8	1.5E-02	2.7E-02	35.7	64.3	3.7E-02	3.5E-02	51.5	48.5
	9	2.6E-02	1.3E-02	66.7	33.3	3.8E-02	2.5E-02	60.9	39.1
950712	1	1.7E-02	6.1E-03	73.6	26.4	2.5E-02	1.1E-02	69.6	30.4
	2	1.5E-02	3.7E-03	80.2	19.8	2.1E-02	8.7E-03	71.0	29.0
	3	2.0E-02	2.2E-03	90.1	9.9	2.6E-02	6.3E-03	80.3	19.7
	4	-1.3E-03	3.1E-02	0.0	100.0	2.4E-02	3.1E-02	43.9	56.1
	5	1.4E-02	1.8E-02	43.8	56.3	2.9E-02	2.4E-02	55.1	44.9
	6	2.0E-02	4.5E-03	81.6	18.4	2.9E-02	1.3E-02	68.8	31.3
	7	1.6E-02	2.4E-02	40.0	60.0	3.4E-02	3.2E-02	51.2	48.8
	8	2.5E-02	1.4E-02	64.1	35.9	3.7E-02	2.3E-02	61.8	38.2
	9	2.4E-02	6.5E-03	78.7	21.3	3.6E-02	1.4E-02	71.5	28.5
950713	1	2.8E-02	2.7E-02	50.9	49.1	5.4E-02	3.0E-02	64.2	35.8
	2	2.9E-02	2.3E-02	55.8	44.2	5.4E-02	2.6E-02	67.2	32.8
	3	2.8E-02	1.6E-02	63.6	36.4	4.9E-02	2.0E-02	70.9	29.1
	4	2.6E-02	2.4E-02	52.0	48.0	4.9E-02	2.8E-02	63.7	36.3
	5	3.0E-02	1.5E-02	66.7	33.3	5.0E-02	1.9E-02	72.0	28.0
	6	2.7E-02	8.9E-03	75.2	24.8	4.6E-02	1.4E-02	76.5	23.5
	7	3.2E-02	1.6E-02	66.7	33.3	5.7E-02	1.8E-02	75.8	24.2
	8	3.1E-02	8.7E-03	78.1	21.9	5.1E-02	1.4E-02	78.6	21.4
	9	2.8E-02	5.2E-03	84.3	15.7	4.6E-02	1.1E-02	80.8	19.2
950714	1	1.4E-02	4.7E-02	23.0	77.0	4.7E-02	4.6E-02	50.8	49.2
	2	2.7E-02	2.9E-02	48.2	51.8	5.2E-02	3.5E-02	59.6	40.4
	3	3.0E-02	2.1E-02	58.8	41.2	5.8E-02	2.4E-02	70.6	29.4
	4	3.7E-02	3.3E-02	52.9	47.1	7.5E-02	2.9E-02	72.1	27.9
	5	3.8E-02	2.7E-02	58.5	41.5	7.4E-02	2.4E-02	75.9	24.1
	6	3.7E-02	2.3E-02	61.7	38.3	7.1E-02	2.1E-02	77.3	22.7
	7	3.8E-02	3.0E-02	55.9	44.1	7.8E-02	2.4E-02	76.6	23.4
	8	3.8E-02	2.8E-02	57.6	42.4	7.7E-02	2.3E-02	76.9	23.1
	9	3.7E-02	2.3E-02	61.7	38.3	7.3E-02	2.0E-02	78.2	21.8
950715	1	3.1E-02	2.4E-02	56.4	43.6	6.1E-02	2.4E-02	71.6	28.4
	2	3.1E-02	1.7E-02	64.6	35.4	6.0E-02	1.5E-02	80.1	19.9
	3	3.0E-02	1.4E-02	68.2	31.8	6.1E-02	1.1E-02	85.2	14.8
	4	9.0E-03	5.3E-02	14.5	85.5	5.4E-02	4.5E-02	54.7	45.3
	5	3.2E-02	2.4E-02	57.1	42.9	6.2E-02	2.4E-02	71.8	28.2
	6	3.0E-02	1.5E-02	66.7	33.3	6.2E-02	1.4E-02	81.2	18.8
	7	4.5E-02	2.8E-02	61.6	38.4	8.6E-02	2.3E-02	79.2	20.8
	8	4.1E-02	2.0E-02	67.2	32.8	7.5E-02	1.7E-02	81.3	18.7
	9	3.2E-02	1.7E-02	65.3	34.7	6.4E-02	1.7E-02	79.6	20.4

1. The O_3 concentration is considered as 100% VOC-limited if the sensitivity of O_3 to NO_x emissions is negative, and vice versa.

sensitivity to NO_x (or VOC) emissions or the O_3 contribution from NO_x (or VOC) emissions divided by the total sensitivity or total O_3 contribution. Both DDM and OSAT predict a NO_x-limited chemistry in Atlanta for all 9 subareas for all five days. However, their predictions are different for some subareas in the other three receptors for some days, with largest discrepancies for subareas in Chicago and New York City. For example, DDM predicts a VOC-limited O_3 chemistry in 3, 7, and 7 out of the 9 subareas in Altoona, Chicago, and New York City, respectively on July 12, whereas OSAT predicts a VOC-limited O_3 chemistry in 1, 0, and 1 out of 9 subareas on the same day at the three receptors, respectively. The predicted fractions of O_3 formed under VOC-limited conditions from DDM and OSAT are also significantly different. For example, DDM predicts a 100% VOC-limited O_3 formation but OSAT predicts a 51.5% VOC-limited O_3 formation in subarea 2 in New York City on July 12.

Table 6-41 shows the NO_x- vs. VOC-sensitivity of O_3 chemistry at the hour of peak O_3 on July 11-15 for the whole receptor region at the four receptors predicted by DDM and OSAT under the EPA 2007 base emission scenario. Those results were obtained by averaging the O_3 sensitivities/contributions for the 81 fine grid cells at the peak O_3 hour for the whole receptor predicted by DDM run B7 and OSAT run B1. Note that the sum of all O_3 sensitivities/contributions over the 9 subareas shown in Tables 6-37 to 6-40 may be different from those for the whole receptor, since the peak O_3 hour for the whole receptor may be different from those for each subarea in the receptor region. Both DDM and OSAT predict a NO_x-limited O_3 chemistry for the whole receptor region in Atlanta and Altoona for all five days, but their predictions in Chicago and New York City are quite different. In Chicago, DDM predicts a VOC-limited O_3 chemistry for all five days, with 58-100% of O_3 formed under VOC-limited conditions, whereas OSAT predicts that O_3 chemistry is VOC-limited on July 11 only and NO_x-limited on July 12-15, with only 25-52% of O_3 formed under VOC-limited conditions. In New York City, DDM predicts a VOC-limited O_3 chemistry for all days except for July 13, with 48-90% of O_3 formed under VOC-limited conditions, whereas OSAT predicts a NO_x-limited O_3 chemistry for all five days, with only 31-44% of O_3 formed under VOC-limited conditions. The VOC-limited (or NO_x-limited) percentages predicted by DDM and OSAT differ by 4-9% in Atlanta, 33-50% in Chicago and 15-48% in New York City, and 4-20% in Altoona.

Table 6-41. NO_x- vs. VOC-limited O_3 concentration at four receptors predicted by DDM and OSAT under the EPA 2007 base emission scenario.

Date	Receptor	DDM Prediction				OSAT Prediction			
		Sensitivities of O_3		O_3 concentration [1]		Contributions to O_3		O_3 Concentration	
		NO_x	VOC	NO_x-limited, %	VOC-limited, %	NO_x	VOC	NO_x-limited, %	VOC-limited, %
950711	Atlanta	4.9E-02	1.3E-02	79.0	21.0	8.6E-02	1.5E-02	85.5	14.5
	Chicago	-1.3E-02	3.1E-02	0.0	100.0	2.4E-02	2.6E-02	47.8	52.2
	New York	3.4E-03	3.0E-02	10.2	89.8	3.6E-02	2.8E-02	56.2	43.8
	Altoona	1.8E-02	1.6E-02	52.9	47.1	3.4E-02	2.3E-02	59.5	40.5
950712	Atlanta	4.0E-02	1.2E-02	76.9	23.1	7.0E-02	1.2E-02	85.9	14.1
	Chicago	1.0E-02	3.1E-02	24.4	75.6	4.8E-02	2.4E-02	67.2	32.8
	New York	3.4E-03	3.1E-02	9.9	90.1	3.7E-02	2.8E-02	57.5	42.5
	Altoona	1.6E-02	1.2E-02	57.1	42.9	2.9E-02	1.8E-02	61.6	38.4
950713	Atlanta	3.6E-02	1.0E-02	78.3	21.7	6.3E-02	1.0E-02	85.9	14.1
	Chicago	2.6E-02	3.6E-02	41.9	58.1	7.4E-02	2.4E-02	75.4	24.6
	New York	2.9E-02	2.7E-02	51.8	48.2	6.2E-02	3.1E-02	66.7	33.3
	Altoona	2.9E-02	1.6E-02	64.4	35.6	5.0E-02	2.0E-02	71.7	28.3
950714	Atlanta	3.7E-02	1.1E-02	77.1	22.9	6.0E-02	1.3E-02	81.9	18.1
	Chicago	1.9E-02	3.4E-02	35.8	64.2	6.2E-02	2.6E-02	70.3	29.7
	New York	2.6E-02	3.8E-02	40.6	59.4	6.7E-02	3.7E-02	64.2	35.8
	Altoona	3.6E-02	2.4E-02	60.0	40.0	7.2E-02	2.1E-02	77.9	22.1
950715	Atlanta	5.3E-02	1.3E-02	80.3	19.7	9.1E-02	1.7E-02	84.7	15.3
	Chicago	6.7E-03	5.1E-02	11.6	88.4	5.8E-02	3.6E-02	61.9	38.1
	New York	2.7E-02	3.6E-02	42.9	57.1	6.9E-02	3.1E-02	69.3	30.7
	Altoona	2.8E-02	2.5E-02	52.8	47.2	6.1E-02	2.2E-02	73.2	26.8

1. The O_3 concentration is considered as 100% VOC-limited if the sensitivity of O_3 to NO_x emissions is negative, and vice versa.

Since there are large discrepancies between the DDM and OSAT predictions, we used the indirect method [i.e., Equation (10)] to calculate the anticipated O_3 concentrations with a 25% reduction in anthropogenic VOC or NO_x emissions, and then compared them with those actually predicted from the DDM sensitivity simulation runs S2 and S5. Such a calculation was done for all the 81 fine grid cells in each receptor region. The results show that the O_3 concentrations calculated using the DDM sensitivity coefficients are lower for most fine grid cells in all receptor regions than the O_3 concentrations simulated with the 25% emission reductions in anthropogenic VOC or NO_x, but with small percentage differences (< -9%). The detailed results are shown and analyzed in section 6.3.1.1. This indirectly verifies that the DDM sensitivities predicted under the base emission scenario are reasonably accurate. Since there are large discrepancies between the OSAT and DDM predictions, the NO_x- or VOC-sensitivity of O_3 chemistry predicted by OSAT may not always be accurate.

The large discrepancies between the DDM and OSAT results occur for all cases when the averaged DDM O_3 sensitivities to the NO_x (or VOC) emissions in a subarea or a whole receptor region are negative or cases when the averaged O_3 sensitivities to the NO_x (or VOC) emissions in a subarea or the whole receptor are positive but O_3 sensitivities to the NO_x (or VOC) emissions in some grid cells in that subarea or some subareas of that receptor are negative. A negative O_3 sensitivity to the NO_x (or VOC) emissions indicates that O_3 concentrations decrease with increased NO_x (or VOC) emissions due to the effect of NO_x (or VOC) titration/inhibition on O_3 chemistry. The discrepancies between DDM and OSAT predictions on the NO_x- vs. VOC-limited O_3 chemistry are due primarily to the fact that the NO_x (or VOC) inhibition is accounted for by DDM but not accounted for by OSAT. As shown in Equation (4), all ozone production is allocated to the species with the positive sensitivity when the sensitivity to NO_x (or VOC) is negative by OSAT. This equation can be modified to account for negative contributions (corresponding to negative sensitivities of DDM that are currently set to zero in the current OSAT formulation) as follows:

$$F_{VOC} = \left[\frac{\partial O_3}{\partial VOC}\right] \Big/ \left[\frac{\partial O_3}{\partial VOC} + \frac{\partial O_3}{\partial NO_x}\right]$$

$$F_{Nox} = \left[\frac{\partial O_3}{\partial NO_x}\right] \Big/ \left[\frac{\partial O_3}{\partial VOC} + \frac{\partial O_3}{\partial NO_x}\right] \quad (11)$$

Alternative formulations would need to be tested for special cases where $\partial O_3/\partial VOC$ and $\partial O_3/\partial NO_x$ are equal or very close in magnitude but opposite in sign and where the net O_3 production equals zero or is very small.

The reason for the differences between the DDM and OSAT predictions is demonstrated in Table 6-42, which shows the O_3 sensitivities/contributions to/of NO_x and VOC emissions from the 6 most influential source areas at the peak O_3 hour in New York City. The NO_x and/or VOC emissions from the 6 most influential source areas are among the top 10 most influential contributors by source area for the 1-hr O_3 concentrations in New York City, as shown in Table 6-9. The sensitivities to the NO_x and VOC emissions from the 6 source areas shown in Table 6-42 are calculated using the results of DDM run B2 and OSAT run B1, which provide the local sensitivities to the NO_x and VOC emissions and the O_3 contributions of NO_x and VOC emissions from individual source groups. The NO_x- and VOC-limited fractions calculated using the sensitivities/contributions to/of NO_x and VOC emissions from the 6 most influential source areas shown in Table 6-42 are quite consistent (within 5%) with those in Table 6-41, which shows the lumped O_3 sensitivity to the total NO_x or total VOC emissions from the region-wide sources from DDM run B7 and the total lumped O_3 contributions of total NO_x or total VOC emissions from all 68 source groups (17 source areas x 4 source categories) from OSAT run B1. For instance, the VOC-limited fractions calculated using values for the 6 major source areas and all source categories from DDM run B2 are 92%, 92%, 50%, 58%, and 53% in New York City on July 11-15, respectively. For comparison, the corresponding VOC-limited fractions calculated using values of region-wide emissions and all source categories from DDM run B7 are 90%, 90%, 48%, 59%, and 57%, respectively. The VOC-limited fractions calculated using values for the 6 major source areas and all source categories from OSAT RUN B1 are 43%, 42%, 32%,

Table 6-42. O_3 sensitivities to contributions of NO_x and VOC emissions from 6 most influential source areas at peak hourly O_3 time in New York City[1].

Date	Tool	Species	***O_3 sensitivities/contributions***						***Total***	VOC-limited O_3, %
			Area 11	Area 13	Area 16	Area 7	Area 12	Area 4		
950711	DDM	NO_x	4.3E-03	3.0E-03	-1.3E-02	3.5E-03	3.9E-03	6.3E-04	2.3E-03	
		VOC	7.6E-03	4.1E-03	6.9E-03	6.2E-03	2.4E-03	1.1E-03	2.8E-02	92.4
	OSAT	NO_x	1.0E-02	6.5E-03	2.2E-03	7.0E-03	6.3E-03	1.7E-03	3.4E-02	
		VOC	7.2E-03	3.8E-03	5.1E-03	5.8E-03	2.2E-03	1.7E-03	2.6E-02	43.4
950712	DDM	NO_x	4.0E-03	4.3E-03	-1.1E-02	2.2E-03	2.5E-03	3.4E-04	2.3E-03	
		VOC	4.0E-03	4.8E-03	1.4E-02	3.2E-03	1.9E-03	8.5E-04	2.9E-02	92.5
	OSAT	NO_x	8.1E-03	7.6E-03	9.2E-03	4.0E-03	4.6E-03	9.8E-04	3.4E-02	
		VOC	3.4E-03	4.5E-03	1.2E-02	3.2E-03	1.1E-03	1.1E-03	2.5E-02	42.3
950713	DDM	NO_x	1.2E-02	1.4E-02	-2.7E-03	2.1E-03	1.1E-03	3.4E-04	2.7E-02	
		VOC	9.4E-03	4.0E-03	7.5E-03	3.3E-03	1.3E-03	9.0E-04	2.6E-02	49.6
	OSAT	NO_x	2.4E-02	1.7E-02	7.9E-03	5.1E-03	3.3E-03	1.1E-03	5.8E-02	
		VOC	1.1E-02	5.4E-03	5.3E-03	3.7E-03	1.3E-03	1.3E-03	2.8E-02	32.4
950714	DDM	NO_x	9.2E-03	1.2E-02	-2.7E-03	5.2E-03	1.6E-03	7.2E-04	2.6E-02	
		VOC	8.6E-03	5.0E-03	7.5E-03	6.9E-03	7.3E-03	9.6E-04	3.6E-02	58.2
	OSAT	NO_x	1.7E-02	1.6E-02	9.9E-03	1.2E-02	6.4E-03	2.2E-03	6.4E-02	
		VOC	1.0E-02	6.0E-03	6.5E-03	4.8E-03	6.4E-03	1.2E-03	3.5E-02	35.5
950715	DDM	NO_x	3.8E-03	7.4E-03	2.8E-03	4.3E-03	-1.1E-07	3.5E-03	2.2E-02	
		VOC	5.2E-03	3.2E-03	1.1E-02	2.6E-03	8.9E-07	2.2E-03	2.4E-02	52.6
	OSAT	NO_x	7.3E-03	1.0E-02	1.7E-02	9.1E-03	9.8E-06	1.0E-02	5.3E-02	
		VOC	5.6E-03	3.7E-03	9.9E-03	2.6E-03	1.5E-05	1.7E-03	2.4E-02	30.6

1. Data were compiled using OSAT run B1 by lumping O3 sensitivities/contributions to/of NOx and VOC emissions from four source categories for each source area. The values shown are for the whole receptor area of New York City (averaged over 81 fine grid cells within the receptor area).

35%, and 31% in New York City on July 11-15, respectively. For comparison, the corresponding VOC-limited fractions calculated by lumping values from 17 source areas and 4 source categories from the same OSAT run are 44%, 42%, 33%, 36%, and 31%, respectively.

As shown in Table 6-42, the O_3 sensitivities in New York City to NO_x emissions from the upwind and surrounding areas (i.e., source areas 7, 11, 13, 12, and 4) are all positive on July 11, with a lumped value of 1.5×10^{-2}. This positive sensitivity is largely offset by a negative O_3 sensitivity to the NO_x emissions from the local sources (i.e., source area 16) of -1.3×10^{-2}, resulting in a net O_3 sensitivity of 2.3×10^{-3} to the total NO_x emissions from all 6 major source areas. This O_3 sensitivity to the total NO_x emissions is smaller by one order of magnitude than that to the total VOC emissions from the 6 major source areas. As a result, DDM predicts that O_3 chemistry in New York City is 92% VOC-limited on July 11, 1995. On the other hand, OSAT allocates O_3 production into the NO_x- or VOC-sensitive portions according to the NO_x and VOC sensitivities predicted by DDM. However, for cases where the sensitivity to NO_x (or VOC) is negative, all O_3 production is allocated to the species with the positive sensitivity. As a result of this rule of apportionment and an aggregating of O_3 sensitivities of 81 fine grid cells in a receptor region (O_3 sensitivity to the NO_x emissions from the source area 16 may be either positive or negative in those fine grid cells), OSAT predicts a positive O_3 contribution from the local NO_x emissions in New York City on July 11, with a lumped O_3 contribution of 34 ppb from the total NO_x emissions from the 6 major source areas. Therefore, OSAT predicts that O_3 chemistry in New York City is 58% NO_x-limited and 43% VOC-limited on July 11. The case on July 12 is very similar to that on July 11, with a large discrepancy (with a difference of 49% or greater) in the predicted VOC-limited fractions between DDM and OSAT (92% vs. 42%). On July 13, the negative O_3 sensitivity to the local NO_x emissions is much smaller than the lumped positive sensitivity from other upwind and surrounding sources, resulting in a net sensitivity to the total NO_x emissions that is slightly greater than that to the total VOC emissions from the 6 major areas. Therefore, DDM predicts a 50% NO_x-limited and 50% VOC-limited O_3 chemistry in New York City on July 13. In this case, the difference in predicted VOC-limited fractions between DDM and OSAT is smaller than those for the previous two

days, but it is still quite significant (17%). On July 14, DDM also predicts a small negative sensitivity to the local NO_x emissions, but the net sensitivity to the total NO_x emissions from the 6 major source areas is smaller than that to the total VOC emissions, resulting in a 58% VOC-limited O_3 chemistry, whereas OSAT predicts a 35% VOC-limited O_3 chemistry, with a difference of 23% between DDM and OSAT. On July 15, the O_3 sensitivity to the local NO_x emissions is positive, but it is smaller by a factor of 4 than that to the local VOC emissions due likely to the aggregating of negative sensitivities to the local NO_x emissions in some grid cells in the receptor region. In this case, DDM predicts a 53% VOC-limited O_3 chemistry and OSAT predicts a 31% VOC-limited O_3 chemistry, with a difference of 22% between DDM and OSAT.

The above analyses show that whether O_3 chemistry is NO_x- or. VOC-limited depends on the magnitude of the effect of NO_x titration and inhibition in a receptor region where the NO_x titration/inhibition likely occurs and its importance relative to the positive effect of VOC emissions on O_3 formation. The degree of discrepancies in predicting NO_x- or VOC-limited O_3 chemistry between DDM and OSAT largely depends on whether and how much O_3 is NO_x- or VOC-limited. Figure 6-9 shows a correlation between the degree of VOC-limited O_3 predicted by DDM and the differences in the predicted VOC-limited fractions by DDM and OSAT in New York City. The four O_3 chemistry regimes predicted by DDM are 70% or more NO_x-limited (i.e., 30% or less VOC-limited) (Regime I), 50-70% NO_x-limited (i.e., 30-50% VOC-limited) (Regime II), 50-80% VOC-limited (Regime III), and 80% or more VOC-limited (Regime IV). The corresponding percent differences in the VOC-limited fractions predicted by DDM and OSAT are within 3%, 11-24%, 14-30%, and 30-60% for Regimes I, II, III, and IV, respectively. The correlation shown in Figure 6-9 generally exists for all the four receptors, although such a correlation can be slightly different for a different receptor because of different source-receptor relationships. The correlation plot provides the range of discrepancies that likely occurs between DDM and OSAT predictions, given the VOC-limited fractions predicted by DDM. For instance, DDM predicts that the O_3 production due to the emissions from the source area 7 is 57-64% VOC-limited on July 11-14 (i.e., in Regime III) and 38% VOC-limited on July 15 (Regime II) in New York City. The anticipated percent differences in the predicted VOC-limited fractions between

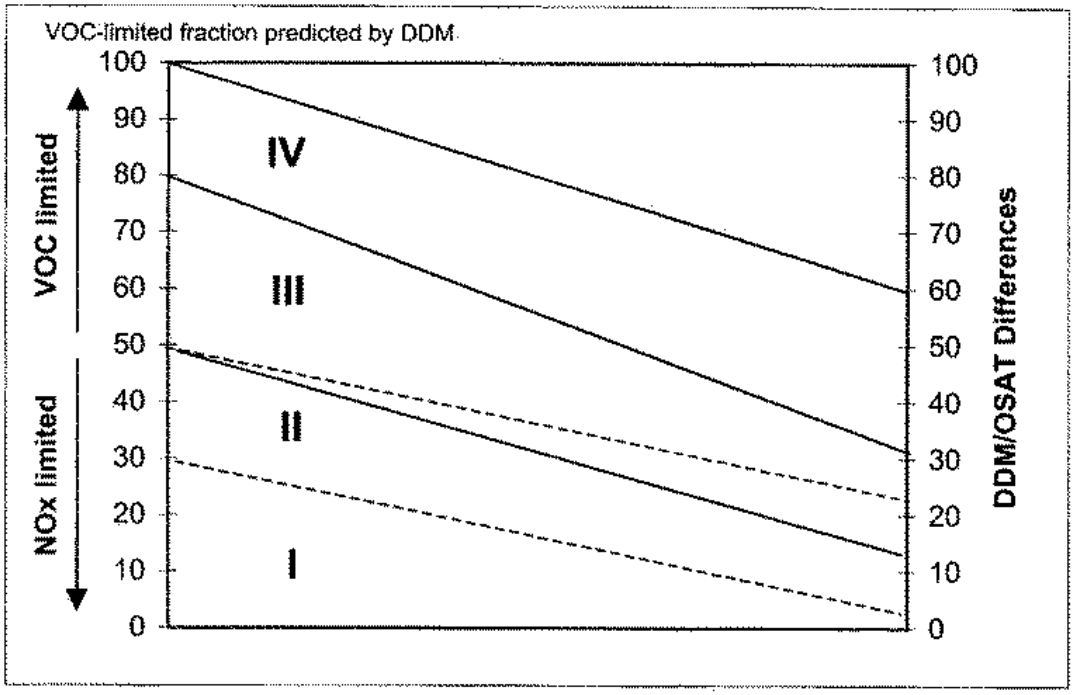

Figure 6-9. A correlation between the VOC-limited fractions of O_3 concentrations predicted by DDM and the differences in the predicted VOC-limited fractions of O_3 concentrations by DDM and OSAT in New York City under the EPA 2007 base emission scenario (DDM base run B2 and OSAT base run B1).

DDM and OSAT are in the range of 11-30%, according to Figure 6-9. OSAT predicts that O_3 production due to the emissions from the source area 7 is 22-45% VOC-limited in New York City on July 11-15. Therefore, the actual differences between the DDM and OSAT predictions range from 15% to 29%. Given the fact that the source area 7 is located upwind of New York City, those differences are quite significant. This large discrepancy is likely because the NO_x emitted from Ohio River valley in the source area 7 is transported to New York City, contributing to the NO_x titration in some grid cells in New York City and this NO_x titration/inhibition effect is not accounted for by OSAT (despite the fact that the aggregated O_3 sensitivities in New York City to the NO_x emissions from the source area 7 are positive, as shown in Table 6-42).

The results from the DDM and OSAT simulations with the EPA 2007 base emissions show that differences in predicting NO_x vs. VOC-sensitive O_3 chemistry by DDM and OSAT are small (within 10%) (e.g., in Atlanta) when O_3 chemistry is 70% or more NO_x-limited, but are significant when O_3 chemistry is 30% or more VOC-limited (i.e., in Chicago and New York City). In section 6.3.2, we will show that O_3 chemistry is predominantly NO_x-limited in the four receptor regions under a 75% anthropogenic NO_x emission reduction scenario and the differences in predicting NO_x- vs. VOC-sensitive O_3 chemistry by DDM and OSAT are much smaller than those under the base emission scenario.

6.1.2.3 Comparison of NO_x- or VOC-sensitivity Predicted at the Four Receptors by PA, DDM, and OSAT

Table 6-43 shows the average total amount of $P(O_x)$ summed for each day up to 16:00 EST for the four receptor regions predicted by PA. The NO_x-sensitive or VOC-sensitive or equally-sensitive percentages of the O_x production are also shown. The totals of NO_x- and VOC-sensitive $P(O_x)$ were calculated for all grid cells in each of the receptor regions and for layers 1 to 4. For an approximate comparison to OSAT and DDM results (see Table 6-41), the VOC-sensitive and equal sensitivity $P(O_x)$ can be summed in Table 6-43. Treating the sum of these two terms is consistent with the approach used previously by Sillman (1995) and in an earlier version of OSAT. However, because of

Table 6-43. O_x production sensitivity to precursors at four receptors predicted by PA under the EPA 2007 base emission scenario. The sensitivity was determined using the ratio of $P(H_2O_2)/P(HNO_3)$.

Date	Receptor	PA Prediction						
		O_x concentration, ppb/day				Percentage in O_x concentration		
		NO_x-sensitive	Equally sensitive	VOC-sensitive	Total concentration	NO_x-sensitive, %	Equally sensitive	VOC-sensitive, %
950711	Atlanta	166	12	23	201	82.6	6.0	11.4
	Chicago	15	7	59	81	18.5	8.6	72.8
	New York	13	8	47	68	19.1	11.8	69.1
	Altoona	55	9	21	85	64.7	10.6	24.7
950712	Atlanta	144	14	26	184	78.3	7.6	14.1
	Chicago	37	11	64	112	33.0	9.8	57.1
	New York	25	11	50	86	29.0	12.8	58.1
	Altoona	54	5	9	68	79.4	7.4	13.2
950713	Atlanta	128	17	24	169	75.7	10.1	14.2
	Chicago	92	28	80	200	46.0	14.0	40.0
	New York	70	20	64	154	45.5	13.0	41.6
	Altoona	78	4	12	94	83.0	4.3	12.8
950714	Atlanta	131	17	30	178	73.6	9.5	16.9
	Chicago	121	37	97	255	47.5	14.5	38.0
	New York	132	27	90	249	53.0	10.8	36.1
	Altoona	119	8	9	136	87.5	5.9	6.6
950715	Atlanta	165	11	25	201	82.1	5.5	12.4
	Chicago	73	23	87	183	40.0	12.6	47.5
	New York	161	24	73	258	62.4	9.3	28.4
	Altoona	109	6	8	123	88.6	4.9	6.5

the uncertainty in the transition from VOC-sensitive to NO_x-sensitive conditions, the appropriateness of summing these two terms should be evaluated in future work. A more robust estimate of the $P(O_x)$ sensitivity can be obtained by applying the DDM results for $P(O_x)$ in PA.

All three tools predicted a predominantly NO_x-sensitive O_3 chemistry for all the five days in Atlanta and Altoona. The NO_x-sensitive fractions predicted by the three tools are similar for Atlanta but quite different for Altoona. For example, the predicted NO_x-sensitive fractions are 80.3% by DDM, 84.7% by OSAT, and 82.1% by PA in Atlanta and 52.8% by DDM, 73.2% by OSAT, and 88.6% by PA in Altoona on July 15. The predictions of the three tools are significantly different in Chicago and New York City. In Chicago, DDM predicted a VOC-sensitive O_3 chemistry for all five days and OSAT predicted a VOC-sensitive O_3 chemistry on July 11 only. For comparison, PA predicted a VOC-sensitive O_3 chemistry for all five days when the VOC-sensitive and equally-sensitive $P(O_x)$ are summed together but only for July 11 and July 12 when only the VOC-sensitive $P(O_x)$ is accounted for. The amount of O_x production under VOC-sensitive and NO_x-sensitive conditions was comparable on July 13-15 in Chicago, indicating a borderline condition in Chicago region. In New York City, DDM predicted a VOC-sensitive O_3 chemistry for all days except July 13; OSAT predicted a NO_x-sensitive O_3 chemistry for all the five days; and PA predicted a VOC-sensitive O_3 chemistry for July 11, 12, and 13 when the VOC-sensitive and equally-sensitive $P(O_x)$ are summed together but only for July 11 and July 12 when only the VOC-sensitive $P(O_x)$ is considered.

As discussed in Section 6.1.2.2, the differences between DDM and OSAT were due primarily to the fact that the NO_x (or VOC) inhibition is accounted for by DDM but not accounted for by OSAT. It is expected that PA predicted results that were consistent with those of DDM and OSAT in Atlanta and Altoona, because the effect of NO_x titration on O_3 formation was relatively small at both locations and the local emissions dominated O_3 chemistry in Atlanta. The large differences between the PA and DDM results in Chicago and New York City are due to the fact that the historical transport along the air parcel back trajectory, which contributed to O_3 production at those locations, was

accounted for by DDM, whereas the PA results described only the local chemical production of O_x within the receptor region.

The values in Tables 6-41 and 6-43 provide an average O_3 or O_x sensitivity for the 81 grid cells in each receptor region, but they do not adequately capture the heterogeneity of VOC- and NO_x-sensitive regimes within the receptor domains. As shown in Tables 6-37 to 6-40, the sensitivity of O_3 production predicted by DDM exhibits large spatial variabilities for Chicago, New York City, and Altoona for all the five days, and the sensitivity of O_3 production predicted by OSAT exhibits some spatial variabilities for some days for Chicago, New York City, and Altoona. Both DDM and OSAT predicted that a NO_x-sensitive O_3 chemistry dominated all the 9 subareas in Atlanta. As a qualitative comparison, the spatial variability in the sensitivity of O_x production predicted by PA for each of the receptor regions is shown in Figures 6-10 to 6-13 for July 14 (note that the plot domains for Atlanta, New York City, and Altoona receptors are slightly larger than the receptor domain, the plot domain for Chicago corresponds exactly to the receptor domain). For a qualitative comparison, the VOC sensitive and equal sensitivity $P(O_x)$ are included together in the top plots in Figures 6-10 to 6-13. Those figures represent total $P(O_x)$ for July 14 and therefore they do not show the temporal variability in the $P(O_x)$ sensitivity during the course of the day. However, this temporal variability can be analyzed using PAVE to visualize the processed CPA output file. As shown in Figures 6-10 to 6-13, there is a considerable variability in VOC- or NO_x-sensitive condition among the grid cells in the receptor domains for Chicago, Atlanta and New York. In each case, there are grid cells for which $P(O_x)$ is exclusively VOC-sensitive that are adjacent to grid cells in which P(Ox) is largely NO_x-sensitive. The sensitivity of peak O_x concentrations estimated by PA could be quite different from those estimated by OSAT and DDM because PA, by design, only gives local information in a specific grid cell and does not account for the history of air parcels. For example, PA estimated a NO_x-limited local O_x formation in subareas 1 and 2 in Altoona on July 14 (see Figure 6-13), whereas DDM estimated a VOC-limited integrated O_3 formation in the same subareas on the same day (see Table 6-40), because O_3 in those subareas may be transported from upwind locations where O_3 formation is VOC-limited.

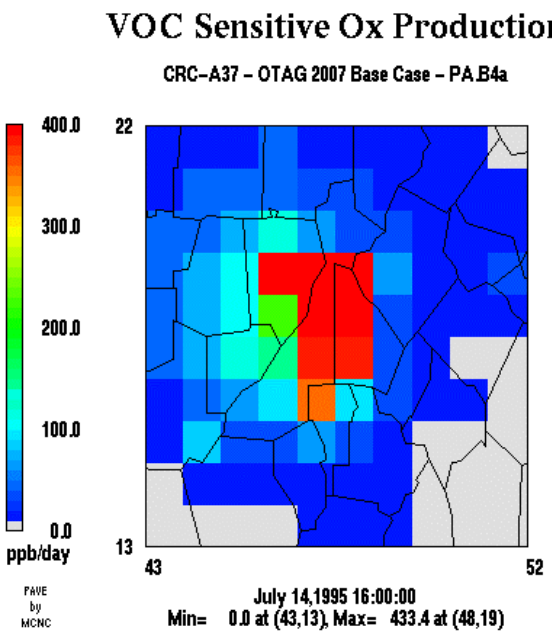

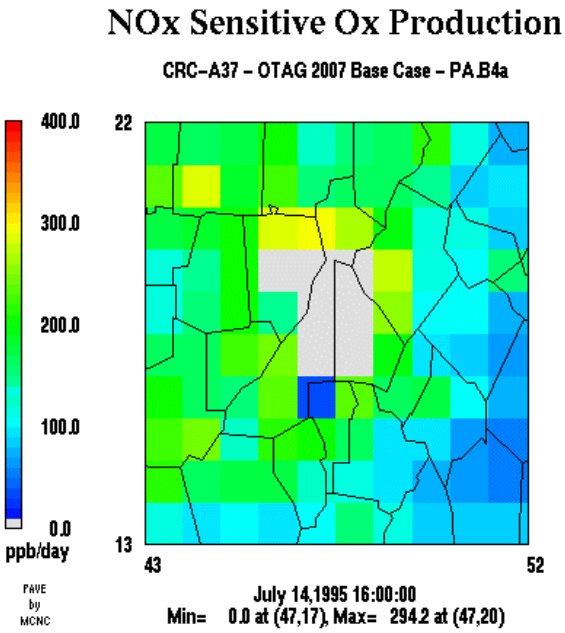

Figure 6-10. The receptor average O_x production in VOC-sensitive (top) and NO_x-sensitive (bottom) regimes for layers 1 to 4 in Atlanta on July 14 (a total O_x production up to 16:00 EST) under the EPA 2007 base emission scenario (PA base run B4). The VOC-sensitive plot includes O_x produced for equally-sensitive conditions.

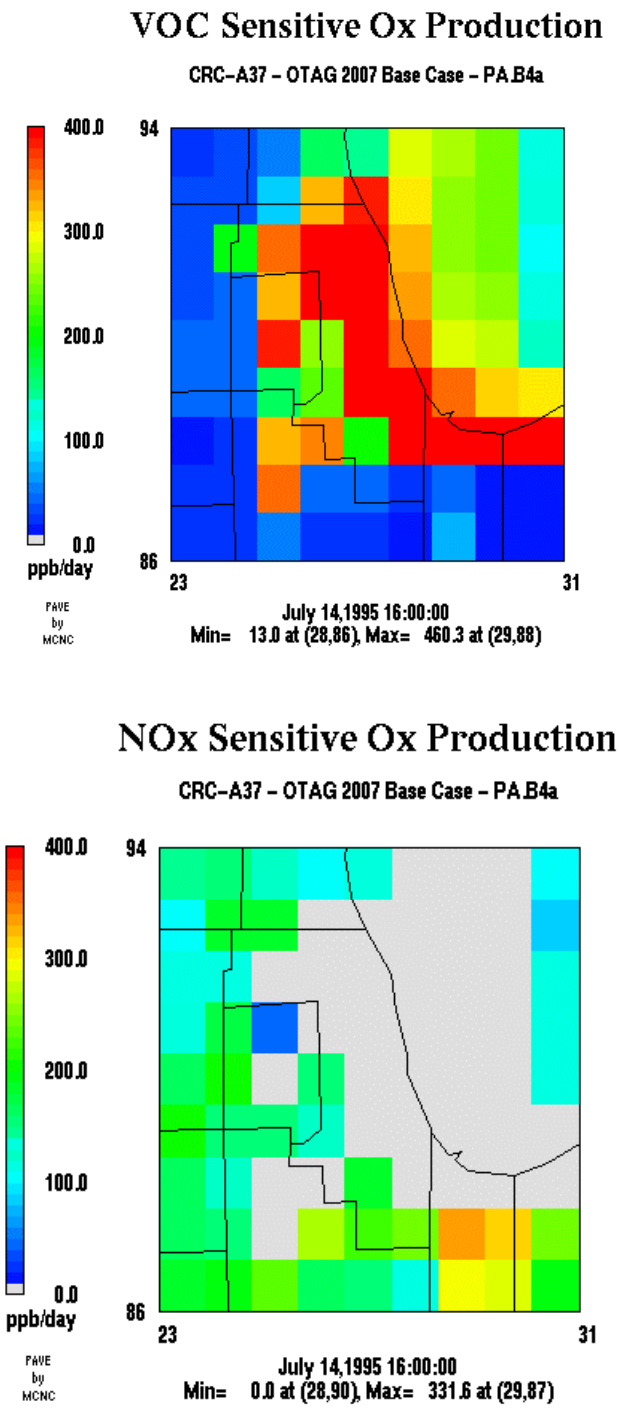

Figure 6-11. The receptor average O_x production in VOC-sensitive (top) and NO_x-sensitive (bottom) regimes for layers 1 to 4 in Chicago on July 14 (a total O_x production up to 16:00 EST) under the EPA 2007 base emission scenario (PA base run B4). The VOC-sensitive plot includes O_x produced for equally-sensitive conditions.

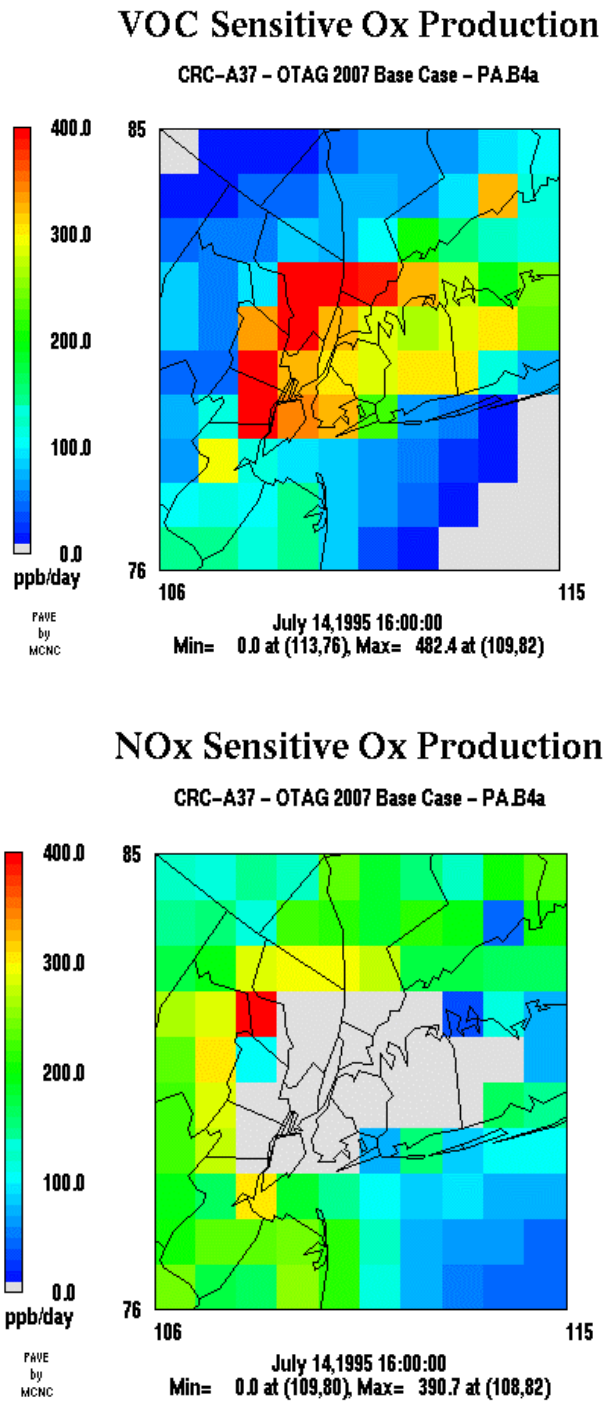

Figure 6-12. The receptor average O_x production in VOC-sensitive (top) and NO_x-sensitive (bottom) regimes for layers 1 to 4 in New York City on July 14 (a total O_x production up to 16:00 EST) under the EPA 2007 base emission scenario (PA base run B4). The VOC-sensitive plot includes O_x produced for equally-sensitive conditions.

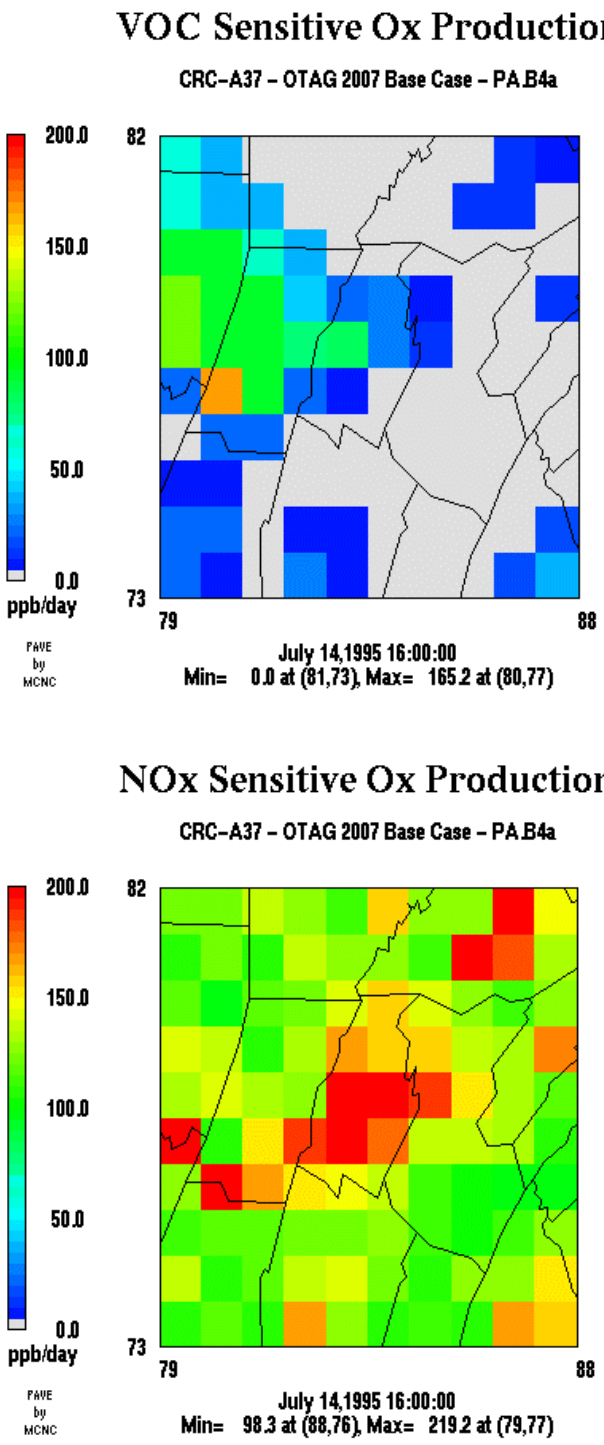

Figure 6-13. The receptor average O_x production in VOC-sensitive (top) and NO_x-sensitive (bottom) regimes for layers 1 to 4 in Altoona on July 14 (a total O_x production up to 16:00 EST) under the EPA 2007 base emission scenario (PA base run B4). The VOC-sensitive plot includes O_x produced for equally-sensitive conditions.

The analysis of $P(O_x)$ represents local chemical production in the receptor region. By contrast, DDM and OSAT represent the sensitivity of the O_3 concentration. The DDM and OSAT results are therefore more appropriate for assessing the sensitivity of O_3 to precursor emission reductions. However, the process analysis output may be useful for fine-tuning the control strategy. For example, the process analysis indicates grid cells where control of radical sources would be most effective for reducing $P(O_x)$. The IRR and IPR analysis in CAMx could be used to determine which species contributed to radical sources in those grid cells. For example, the IPR analysis could be used to evaluate transport of HCHO and O_3 into the receptor region, and the IRR analysis could be used to determine which VOC contributed to the production of HCHO and other carbonyls.

6.1.3 Photochemical reactivity of VOCs

VOCs exhibit a range of reactivities with respect to O_3 formation because different VOCs react at different rates for their photolysis and chemical reactions with OH radicals, NO_3 radicals, and O_3. The O_3-forming capability of individual VOC species can be measured by two approaches: the O_3 productivity approach and the incremental reactivity approach (Carter and Atkinson, 1987; Milford et al., 1992; Bowman and Seinfeld, 1994a, 1994b). The O_3 productivity is defined as the amount of O_3 formed per VOC available for reaction (Bowman and Seinfeld, 1994a and 1994b):

$$P_j = \frac{R_j}{[VOC_j]} \tag{12}$$

$$R_j = ([O_3]_j)_{peak} - ([O_3]_j)_{t=0}$$

or

$$R_j = ([O_3]_j - [NO]_j)_{peak} - ([O_3]_j - [NO]_j)_{t=0} \quad (13)$$

where P_j is the O_3 productivity of VOC species *j*, R_j is the change in the quantity $[O_3]$ or $([O_3]$-$[NO])$ in ppb attributable to VOC species *j*, $[VOC_j]$ is the concentration of VOC species *j* in ppbC initially present and emitted, and $[O_3]_j$ and $[NO]_j$ are the concentrations of O_3 and NO that are attributable to VOC species *j* initially and at the time of peak O_3 concentration. Note that both the quantities $[O_3]$ and $([O_3]$-$[NO])$ can be used to define the O_3 productivity of VOCs. The O_3 productivity approach traces O_3 (or other products) and the reaction pathways of a mechanism and attributes the amount of O_3 formed back to the original VOC precursors.

The incremental reactivity is defined as the change in peak O_3 concentrations due to the additional or incremental organics (Carter and Atkinson, 1989):

$$IR_i = \frac{\Delta_i R}{\Delta[VOC_i]} \quad (14)$$

where IR_i is the incremental reactivity of VOC species *i*, *R* is the maximum change of the quantity $[O_3]$ or $([O_3]$-$[NO])$ in ppb from their initial value at the beginning of the simulation, the Ä$_i$ operator represents the change from a base case scenario as a result of an incremental change in VOC species *i*. Ä$[VOC_i]$ is the incremental change in the concentration of VOC species *i*. In the incremental reactivity approach, a small amount of an individual organic is added to a base case mixture, either in a smog chamber or in a chemical mechanism, and the change in peak O_3 concentrations due to the additional or incremented organic is simulated. The incremental reactivity approach can only be used to determine the O_3-forming capability of individual VOC species for small perturbations.

Equations (12) and (14) can also be applied to calculate the O_3 productivity and the incremental reactivity of the emission of lumped VOCs from a specific source category or group. In this case, the denominators, $[VOC_j]$ and Ä$[VOC_i]$, represent the emission of lumped VOCs from source category *j* (or group *j*) and the incremental change

in the emission of source category *i*, respectively. Their units should be in moles C hr^{-1} or grams C hr^{-1}.

Two of the three probing tools (OSAT and DDM) can provide some information on the reactivities of several VOC source groups that to some extent can be compared. OSAT attributes the amount of O_3 formed on a specific day to the emissions of several VOC source groups (e.g., biogenic, on-road mobile, other surface anthropogenic, and elevated anthropogenic VOCs) from that day and all previous days. This information can be used to calculate the O_3 productivity of the VOC source groups at the time of peak O_3 concentration as shown in Equation (12). Since the effects of the emissions of previous days on the O_3 concentrations on a specific day vary from one receptor to another receptor, we use the daily emission of a VOC source group to calculate the O_3 productivity of that source group at the time of peak O_3 concentration for that day. DDM can provide the incremental reactivity of these VOC source groups at the time of peak O_3 concentration, because the instantaneous sensitivity coefficient at the time of the peak O_3 shown in Equation (1) is equivalent to the incremental reactivity as defined above (Milford et al., 1992). The DDM semi-normalized sensitivity of O_3 to the emission of a VOC source group divided by the daily emission of that VOC source group gives the incremental reactivity of that VOC source group for that day. Although the daily emission was used in the above calculations, the daily O_3 productivity and the daily incremental reactivity of a VOC source group reflect the effects of multi-day emissions (except for the first day), since the O_3 contributions predicted by OSAT and the sensitivities of O_3 predicted by DDM for a specific day reflect the effects of the emissions from all previous days for a multi-day simulation. Note that the current implementation of DDM in CAMx can provide the sensitivities of O_3 with respect to changes in both single- and multi-day emissions. However, the simulations for this project were not set up to provide the sensitivities of O_3 with respect to changes in single-day emissions.

PA as implemented in CAMx, on the other hand, provides neither the incremental reactivity nor the O_3 productivity of VOC species or source groups. This is because (1) PA does not predict the response of O_3 concentrations to changes in the concentrations of VOCs; (2) it is very difficult to get a complete accounting of the O_3 productivity for a

particular VOC in a grid model since most VOCs use a common set of intermediate reaction products, and it is prohibitively expensive to trace the fate of a VOC and its intermediate products for all grid cells. This can be done in a trajectory model, but transport complicates the problem in a grid model, and we would need an extensive system of tracers to track the reactions of the individual VOCs and their products. On the other hand, PA can be used in a complementary fashion with OSAT and DDM to provide information that can be used to characterize the O_3 formation efficiency of the system. For example, the OH chain length and the NO chain length are two important parameters to determine the O_3 forming efficiency of the system. The OH chain length is defined to be the total number of OH radicals reacted divided by the number of new OH radicals (Tonnesen and Jeffries, 1994). It corresponds to the average number of times each new OH is cycled until it is removed from the system. Similarly, the NO chain length is the average number of times each newly emitted NO is cycled before being converted into non-reactive products. The longer these chain lengths, the greater the potential for O_3 formation per unit of NO_x emissions.

Since PA does not provide information that can be directly comparable to those from OSAT or DDM, we evaluate the consistency in the O_3 productivity of VOC source groups derived from OSAT and the incremental reactivity of VOC source groups derived from DDM in this section. This evaluation was performed in terms of the relative reactivity of these VOC source groups. We provide below a description of the relevant information that can be obtained from DDM and OSAT and the intercomparison of the incremental reactivity obtained from the DDM results and the O_3 productivity obtained from the OSAT results.

DDM

DDM can provide the changes in O_3 concentrations due to the changes in the emissions and initial concentrations of individual or lumped VOCs. The first-order derivative of the quantity $[O_3]$ to the change in the emission of a specific VOC source group is equivalent to the incremental reactivity of that VOC source group. In the DDM base and sensitivity simulations, the semi-normalized sensitivity coefficients of O_3 to

three VOC source groups (i.e., biogenic, surface anthropogenic, and elevated anthropogenic emissions), $\partial[O_3]/\partial\varepsilon_i$, where *i* represents different VOC source groups and ε_i represents a scaling variable with a nominal value of 1 in the emission of VOC source group *i*, are calculated. Given these semi-normalized sensitivities and the corresponding daily emissions of that VOC source group, the daily incremental reactivity of VOC source group *i* at the time of peak O_3 concentration, $\partial([O_3])/\partial[VOC_i]$, can be calculated as follows:

$$\frac{\Delta_i([O_3])}{\Delta_i[VOC_i]} = \frac{\partial[O_3]}{\partial[VOC_i]} = \frac{\frac{\partial[O_3]}{\partial e_i}}{[VOC_i]} \qquad (15)$$

The incremental reactivity can also be expressed in terms of ($[O_3]$-[NO]) as follows:

$$\frac{\Delta_i([O_3]-[NO])}{\Delta_i[VOC_i]} = \frac{\partial[O_3]}{\partial[VOC_i]} - \frac{\partial[NO]}{\partial[VOC_i]} = \frac{\frac{\partial[O_3]}{\partial e_i} - \frac{\partial[NO]}{\partial e_i}}{[VOC_i]} - \qquad (16)$$

Since OSAT attributes the amount of O_3 formed to emission source groups, we calculate incremental reactivities of VOC species in terms of O_3 concentration alone from DDM, then compare them with the O_3 productivity derived from the OSAT results.

Equations (15) and (16) provide the incremental reactivity of VOC source group *i*, as defined in Equation (14). The daily incremental reactivity of VOC source groups at the time of the peak O_3 concentration was calculated for five high O_3 days (i.e., July 11-15, 1995). By comparing the relative magnitude of incremental reactivities for the emissions of VOCs for different source categories in the same or different geographic area at the time of the peak O_3 concentration, we can distinguish the differences in the reactivity of VOCs from different source groups.

OSAT

OSAT attributes O_3 formation to VOC emissions as a lumped species (i.e., using a single reactivity weighted tracer) for different source categories that likely have different reactivities. In theory, OSAT could be modified to attribute O_3 formation to the emissions of each CBM-IV speciated VOC from different source groups. However, this would significantly increase the number of source groups and tracers such that resource requirements would be comparable to DDM, in which case DDM may be a preferable approach. Using a single reactive weighted tracer allows OSAT to efficiently track many separate source groups, but it may not distinguish reactivity differences very well depending upon how source groups are defined. For OSAT base and sensitivity simulations, VOC emissions are divided into four source categories: biogenic, on-road mobile, other surface and elevated anthropogenic sources. The biogenic VOC (BVOCs) emissions are treated as a separate source category because these BVOCs have significantly higher reactivity than anthropogenic VOCs.

The daily O_3 productivity of VOC groups at the time of peak O_3 concentration can be calculated for several high O_3 days based on Equation (12), given the corresponding daily emissions of lumped VOCs from each of the source groups. Note that the calculation of R_j in Equation (12) requires the concentration of O_3 that is attributable to VOC source group *j* initially (i.e., at the reference time) and at the time of peak O_3 concentration for a specific day. Since the air parcel trajectory at the time of peak O_3 may be different from anytime before the peak O_3 hour, the daily O_3 productivity of VOC groups at the time of peak O_3 concentration may be sensitive to the changes in air parcel trajectories during the period of midnight to the peak O_3 time. We evaluate this sensitivity by selecting two different reference times: one at midnight and one at 6 a.m. to calculate R_j for various VOC source groups.

Intercomparison

Since OSAT and DDM provide reactivity information that to some extent can be compared and PA does not provide such information, we evaluate the consistency

between the OSAT results and the DDM results. Since the O_3 productivity derived from OSAT and the incremental reactivity calculated by DDM are two different quantities, we evaluate the consistency in the two quantities in a qualitative sense; namely, we use these two quantities to rank the relative importance of VOC source categories from different source areas and compare the rankings qualitatively.

To characterize reactivity of different VOC groups at the four receptors, we calculate the daily O_3 productivity and the daily incremental reactivity of lumped VOCs at the time of the peak O_3 concentration from three source categories (biogenic sources, surface anthropogenic sources, and elevated anthropogenic sources, denoted by "B", "S", and "E", respectively) from 11 core source areas (a total of 33 source groups) in the OTAG domain using the results of OSAT run B1 and DDM run B2 (see Figure 2-1). No calculation is done for the VOC emissions from the 6 boundary source areas because there is no VOC vs. NO_x breakout in the DDM base run B3. Note that the surface anthropogenic sources are split into two source categories (i.e., on-road mobile and other surface anthropogenic sources) in OSAT run B1. In analyzing the O_3 productivity of VOCs, we combine the source contributions from on-road mobile and other surface anthropogenic source categories to obtain the source contribution of one surface anthropogenic source category from the OSAT run B1 to match that calculated from the DDM run B2. The incremental reactivities or the O_3 productivities of various VOC source groups are calculated for the whole receptor region by taking an average of the values over the 81 fine grid cells. The relative reactivities of VOC source groups are ranked based on their O_3 productivities derived from the OSAT results and their incremental reactivities calculated from the DDM results at the peak O_3 hour for July 11-15. The two sets of rankings of the relative reactivities are compared qualitatively and the relative importance of VOC source groups is discussed below.

6.1.3.1 Comparison Between the Incremental Reactivity from DDM and the O_3 Productivity from OSAT

Figures 6-14 to 6-17 show the top 5 incremental reactivities and top 5 O_3 productivities of VOC emission groups derived from the DDM and OSAT predictions at

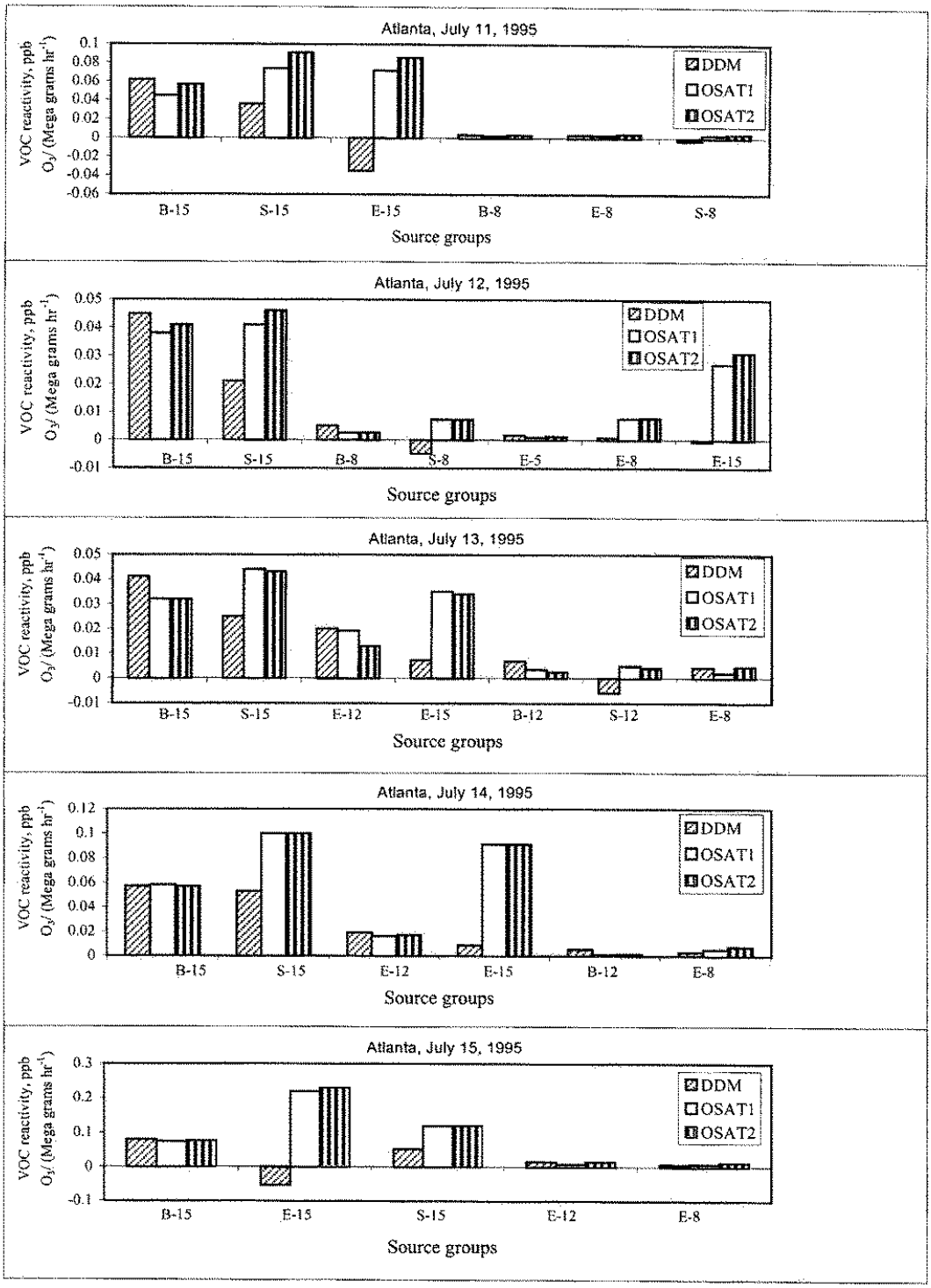

Figure 6-14. The top 5 incremental reactivities and O_3 productivities of VOC emission groups derived from the DDM and OSAT results at the time of peak O_3 concentration on July 11-15, 1995 in Atlanta under the EPA 2007 base emission scenario (DDM base run B2 and OSAT base run B1).

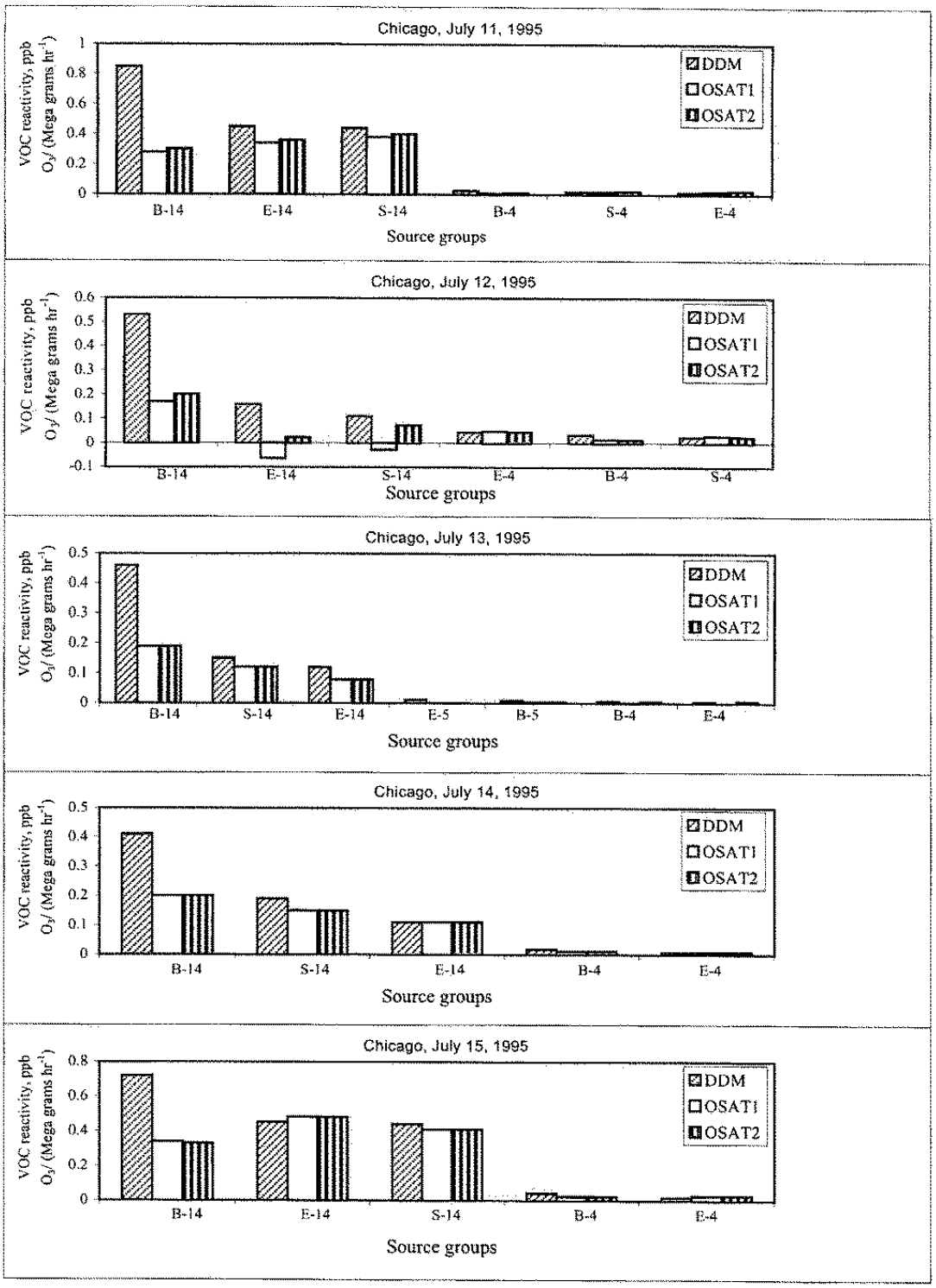

Figure 6-15. The top 5 incremental reactivities and O_3 productivities of VOC emission groups derived from the DDM and OSAT results at the time of peak O_3 concentration on July 11-15, 1995 in Chicago under the EPA 2007 base emission scenario (DDM base run B2 and OSAT base run B1).

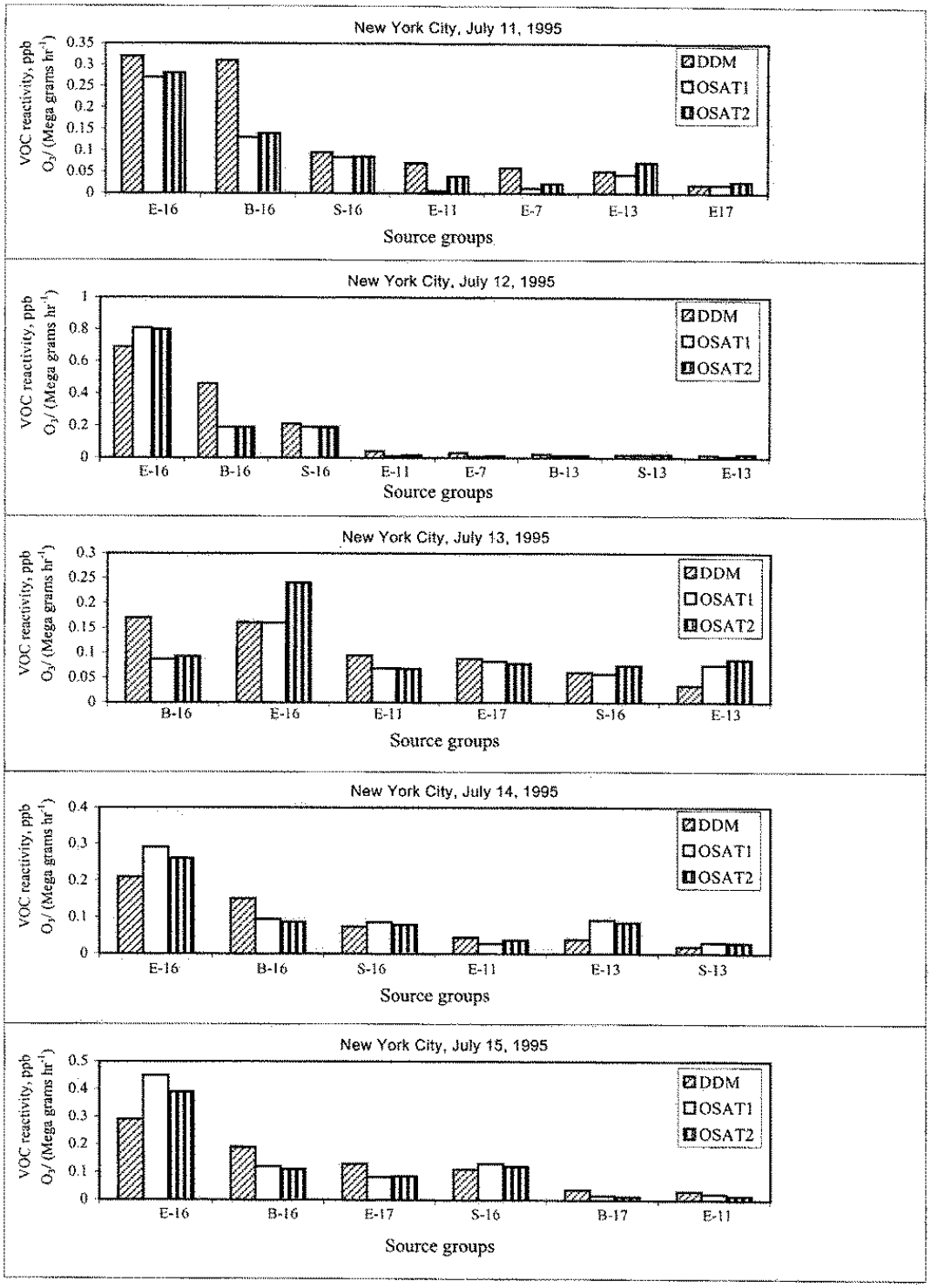

Figure 6-16. The top 5 incremental reactivities and O_3 productivities of VOC emission groups derived from the DDM and OSAT results at the time of peak O_3 concentration on July 11-15, 1995 in New York City under the EPA 2007 base emission scenario (DDM base run B2 and OSAT base run B1).

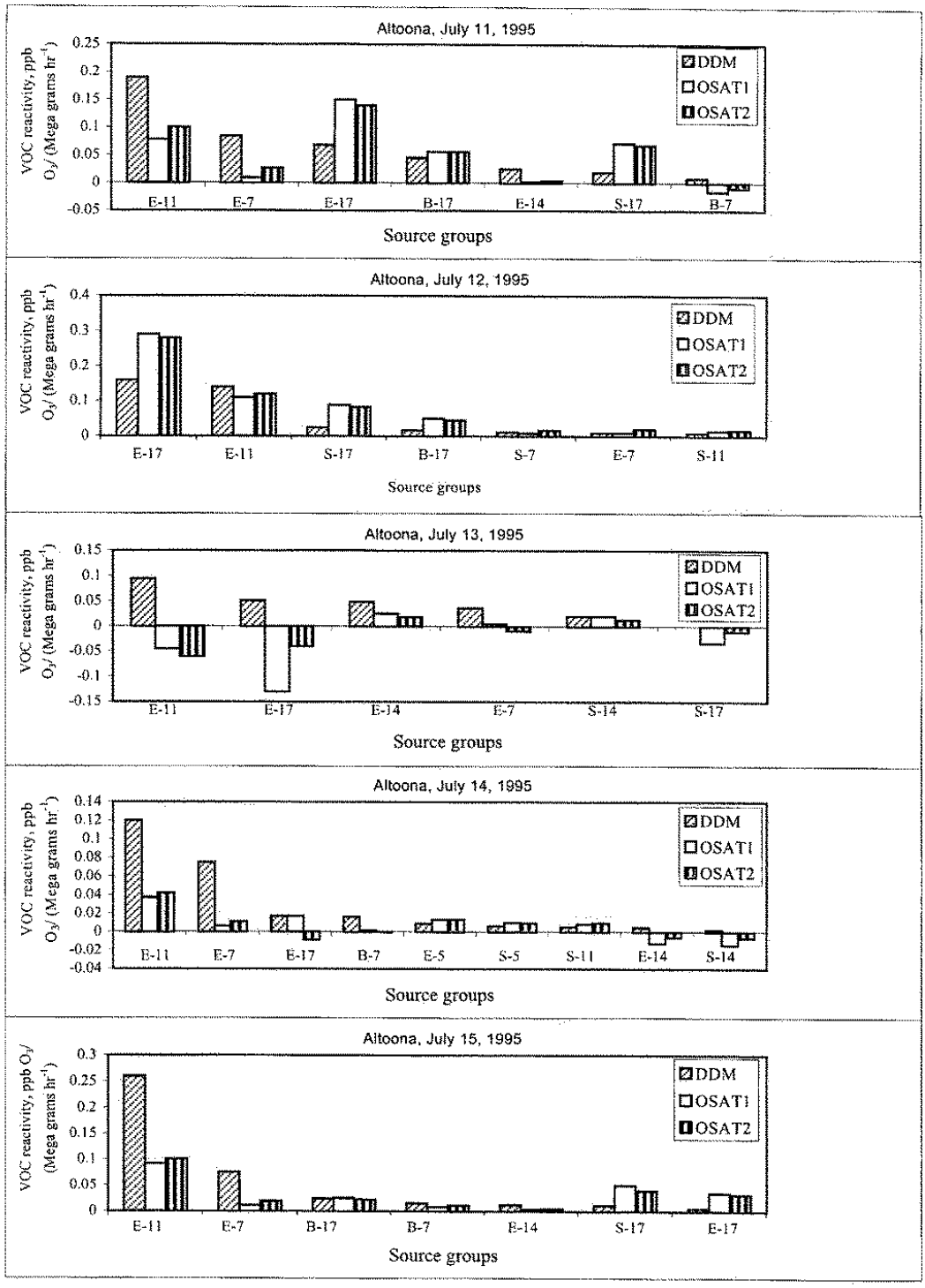

Figure 6-17. The top 5 incremental reactivities and O_3 productivities of VOC emission groups derived from the DDM and OSAT results at the time of peak O_3 concentration on July 11-15, 1995 in Altoona under the EPA 2007 base emission scenario (DDM base run B2 and OSAT base run B1).

the time of peak O_3 concentration on July 11-15, 1995 in Atlanta, Chicago, New York City, and Altoona, respectively. OSAT1 and OSAT2 represent the O_3 productivities calculated using the O_3 concentrations at midnight and at 6 a.m., respectively, as a reference time. Since many of the VOC emission groups having the incremental reactivities or the O_3 productivities in the top 5 list are the same, the number of emission groups shown in those plots may vary from 5 to 9, depending on how many VOC emission groups are different in the top 5 lists of the DDM and OSAT predictions.

Atlanta

In Atlanta, the OSAT results using different reference times are very similar, indicating that the air parcel trajectories are similar between midnight and 6 a.m. Both DDM and OSAT predict large positive reactivities (> 0.005 ppb O_3 /(Mega grams C hr^{-1})) for the local biogenic and surface anthropogenic VOC emissions (i.e., B-15 and S-15) on all days and the local and upwind elevated anthropogenic emissions (i.e., E-15 and/or E-12) on July 11-14, indicating that those VOC emission groups are the most reactive groups. However, DDM predicts that the local biogenic emission group B-15 has the largest incremental reactivity, whereas OSAT predicts that either the local surface or elevated anthropogenic emission group (i.e., S-15 or E-15) has the largest O_3 productivity. In addition, DDM and OSAT predict reactivities that differ significantly in the mathematical signs and/or magnitude for some emission groups such as the local elevated anthropogenic emissions (i.e., E-15) on all five days and the surrounding surface anthropogenic, biogenic, and elevated anthropogenic emissions (i.e., S-8, B-8, and E-8) and the upwind surface anthropogenic and biogenic emissions (i.e., S-12 and B-12) on some days. For example, DDM predicts a large negative reactivity for E-15 on July 11 and 15, for S-8 on July 12, and for S-12 on July 13, whereas OSAT predicts a large positive reactivity for those VOC source groups on those days. Although an increase in most VOC species can always increase O_3 production, some anthropogenic VOC species such as xylenes, toluene, acetaldehyde and higher molecular aldehydes (ALD2), and a few biogenic VOC species such as olefins may inhibit O_3 formation (Milford et al., 1992; Pun et al., 2001b). For example, ALD2 acts as a PAN precursor via the following reactions:

$$R1 \qquad ALD2 + OH \rightarrow C2O3$$

$$R2 \qquad C2O3 + NO2 \leftrightarrow PAN$$

The reversible reaction of R2, i.e., the thermal decomposition of PAN into C2O3 and NO2, is highly temperature-dependent. At the lower temperatures of the middle and upper troposphere, PAN is relatively stable and acts as a reservoir for NO_x. When an air mass containing PAN is transported into warmer regions, PAN decomposes, releasing both NO_2 and C2O3 radicals. If sufficient NO is present, C2O3 reacts with NO to regenerate NO_2 via:

$$R3 \qquad C2O3 + NO \rightarrow FORM + NO2 + HO2 + XO2$$

Under low-NO_x condition even at high temperatures, however, the formation of PAN dominates its decomposition, tying up significant amounts of NO_x (Finlayson-Pitts and Pitts, 2000). Under such conditions, ALD2 always have a negative influence on O_3 formation because they act as a sink for O_3-precursor NO_2 via the reactions R1 and R2. The negative reactivities of ALD2 under low-NO_x conditions or the smog chamber conditions with higher reactive organics to NO_x ratio have been reported by Carter and Atkinson (1989), Milford et al. (1992), and Carmichael et al. (1997). The reactivity of a VOC emission group is negative if emissions of VOC species having negative reactivities dominate emissions of other VOC species in that group. The discrepancy between the DDM and OSAT predictions is due to the fact that the inhibition effect of some VOC emission groups in O_3 formation was accounted for by DDM but not by OSAT. The reactivity of VOC source groups may vary in magnitudes and mathematical signs with the levels of perturbations in VOC emissions (e.g., a small decrease in toluene emissions may increase O_3 formation due to less organic nitrate formation whereas a large decrease in toluene emissions may decrease O_3 formation due to lower precursor levels). The DDM predictions of the VOC reactivity are only accurate for small perturbations and may not be representative of large perturbations. The accuracy of the DDM and OSAT

predictions of VOC reactivity for large perturbations (e.g., 75% reduction in VOC emissions) was not evaluated in this project and is recommended for future investigation.

DDM and OSAT predict a strong daily variability for E-15 and B-15 on all five days and for B-8 and S-8 on July 11-12. For example, the VOC reactivities for E-15 are -3.5 x 10^{-2}, -5.6 x 10^{-4}, 7.2 x 10^{-3}, 8.0 x 10^{-3}, -5.4 x 10^{-2} ppb O_3/(Mega grams C hr^{-1}) and the O_3 productivities (with a reference time of 6 a. m.) for E-15 are 8.6 x 10^{-2}, 3.1 x 10^{-2}, 3.4 x 10^{-2}, 9.1 x 10^{-2}, and 2.3 x 10^{-1} ppb O_3/(Mega grams C hr^{-1}) for July 11-15, respectively.

Chicago

In Chicago, DDM predicts very small negative reactivities (< -2 x $^{10-4}$ ppb O_3/(Mega grams C hr^{-1})) for a few emission groups such as E-15, E-7, and S-7 (not shown). Interestingly, OSAT also predicts negative O_3 productivities for the local elevated and surface anthropogenic emissions (i.e., E-14 and S-14) on July 12 with a reference time of midnight (i.e., OSAT1). The O_3 productivities of VOC source groups E-14 and S-14 change from negative to positive values when the reference time changes from midnight to 6 a.m., indicating that the air parcel trajectory changed significantly in Chicago between midnight and 6 a.m. on July 12. The OSAT results using different reference times are quite consistent on the other days. Both DDM and OSAT predict that the local biogenic, elevated anthropogenic, and surface anthropogenic VOC emissions are the top three most reactive emission groups (i.e., B-14, E-14, and S-14) on all days except July 12 and the surrounding or upwind biogenic, elevated anthropogenic, and surface anthropogenic emissions (B-4, S-4, E-4, E-5, and B-5) are the next most reactive groups on all five days. DDM predicts that the local biogenic emission group (i.e., B-14) has the largest incremental reactivity while OSAT predicts that the local biogenic, or elevated or surface anthropogenic emission group (i.e., B-14, or E-14, or S-14) has the largest O_3 productivity. A strong daily variability is predicted for B-14 by DDM, and E-14 and S-14 by both DDM and OSAT.

New York City

In New York City, the OSAT results using different reference times are generally consistent, indicating that the air parcel trajectories are similar between midnight and the peak hourly O_3 time. Both DDM and OSAT predict positive reactivities for the top 5

emission groups on all five days, but their rankings and magnitudes are somewhat different. On July 11, DDM and OSAT predict that the local elevated anthropogenic, biogenic and surface anthropogenic emission groups (i.e., E-16, B-16, and S-16) are the 1st, 2nd, and 3rd, respectively, most reactive emission groups. OSAT predicts that the surrounding elevated anthropogenic emission group (i.e., E-13) is more reactive than the upwind elevated anthropogenic emission groups (i.e., E-11 and E-7) on July 11; whereas DDM predicts the opposite results. On July 12, the top three most reactive emission groups and their relative rankings are the same as those on July 11. On July 13, DDM and OSAT predict the same emission groups in the top five list, but with different rankings and magnitudes. For example, the emission groups B-16 and E-13 rank 1st and 6th by DDM but 2nd and 3rd or 4th (depending on the reference time) by OSAT, respectively. On July 14, the ranking for E-13 by OSAT is higher than that by DDM (3rd vs. 5th). On July 15, the ranking for S-16 by OSAT is higher than that by DDM (2nd vs. 4th). A strong daily variability is predicted for B-16 and S-16 by DDM and for E-16, E-11, E-7, E-13 and E-17 by both DDM and OSAT.

Altoona

In Altoona, DDM predicts small negative reactivities [$< -3 \times 10^{-3}$ ppb O_3/(Mega grams C hr^{-1})] for the local surface anthropogenic emission group S-17 on July 13 (too small to be seen) and for the local surface and elevated anthropogenic emission groups S-17 and B-17 on July 14 (not shown). OSAT predicts large negative O_3 productivities for the local elevated/surface anthropogenic emissions and the surrounding elevated anthropogenic emissions (i.e., E-11, E-17, S-17) on July 13 and the upwind surface/elevated anthropogenic emissions (i.e., E-14 and S-14) and the local elevated anthropogenic emissions (i.e., E-17, with a reference time of 6 a.m. only) on July 14. Those negative O_3 productivities indicate that the air parcel trajectory changed significantly between midnight and the peak hourly O_3 time. Thus, the calculated O_3 productivities using Equation (12) on July 13-14 may not be as accurate as for the other days when the air parcel trajectory is similar between the reference time and the peak hourly O_3 time. On July 11, DDM predicts the elevated anthropogenic VOC emissions from the surrounding (E-11), upwind (E-7), and local sources (E-17) to be the top 1st, 2nd, and 3rd most reactive VOC source groups; whereas OSAT predicts the local elevated

anthropogenic VOC emissions (E-17), the upwind elevated emissions (E-11), and the local surface anthropogenic VOC emission group (S-17) to be the 1st, 2nd, and 3rd most reactive groups, respectively. On July 12, the top five incremental reactivities and O_3 productivities predicted by DDM and OSAT and their relative rankings are quite similar. On July 15, the ranking for E-7 by DDM is higher than that by OSAT (2nd vs. 5th), and the ranking for S-17 and E-17 by OSAT is higher than that by DDM (2nd and 3rd vs. 6th and 7th). Both DDM and OSAT predict a strong daily variability for VOC emission groups E-11, E-7, E-17, B-17, E-14, and S-17 in Altoona.

6.2 Complementarity

As shown above, the three probing tools can provide information that is to some extent comparable. They also provide several different types of information that are complementary. Table 6-44 summarizes the technical capabilities of the three probing tools as implemented in CAMx. It is clear that these tools are complementary and each has its own strengths and weaknesses. The complementary features of these probing tools and their strengths and weaknesses are identified, analyzed, and compared in detail in this section. Those features are demonstrated through insightful analyses of O_3 formation for relevant receptors. The differences in the applications/functions of the probing tools and our evaluations are described below.

6.2.1 Source Apportionment

Both OSAT and DDM can attribute O_3 to source groups based on geographic area and emissions category, whereas PA provides no source category specific information. While OSAT attributes total O_3 concentration to all source groups, DDM provides first-order sensitivity of O_3 to all source groups. OSAT can track a larger number of source groups than DDM because OSAT uses reactive weighted tracers; the number of source groups and geophysical regions treated with DDM is limited by the associated computational burden. OSAT results are naturally interpretable as source apportionments because they are based on the proportional contribution of emissions to the O_3 forming

Table 6-44. The technical capabilities of DDM, OSAT, and PA implemented in CAMx.

Tools	Ranking of O_3 contributors	NO_x or VOC sensitivity	Photochemical reactivity	Source apportionment	Relative importance of chemistry and transport	Detailed chemical analysis	Model responses to changes in emissions, ICs, and BCs
DDM	✓	✓	✓	✓[1]	✓[2]	×[3]	✓[4]
OSAT	✓	✓[5]	✓	✓	✓[2]	×	✓[4]
PA	×	✓[5]	×	×	✓[2]	✓	×

[1] Both OSAT and DDM can attribute O_3 to geophysical source groups. While OSAT is designed to track relatively large number of source groups from many geophysical regions, the number of source groups and geophysical regions is limited by the computational burden when DDM is used to obtain such information.

[2.] Both OSAT and DDM can predict the relative importance of local sources vs. sources in upwind locations (i.e., photochemistry vs. transport). PA can only provide the local and instantaneous relative importance of photochemistry, transport (horizontal and vertical), and deposition in a specific grid cell, but it will be computationally expensive to trace O_3 production in the grid cell back to the upwind sources of the precursors.

[3] The current implementation of DDM does not allow calculations of sensitivities of model predictions to chemical rate constants and product yields.

[4] Since both OSAT and DDM provide information local to the base case, extrapolation to a different emission scenario involves some assumptions by the user. The most likely assumption is linearity, i.e., that DDM first-order sensitivities will provide an adequate description and that OSAT source contributions will scale linearly with emissions. For the non-linear system of O_3 formation in this work, sensitivities predicted by DDM are accurate for small changes (i.e., about 40% perturbations) but inaccurate for large changes. The linear scaling of OSAT results is valid for small changes in VOC emissions but inaccurate for small or large changes in NO_x emissions (see Section 6.3.1).

[5] OSAT uses the DDM sensitivities to determine whether the O_3 formation is NO_x-or VOC-sensitive, however, it does not account for the titration/inhibition effect of NO_x (or VOC) on O_3 chemistry (i.e., the negative sensitivities). PA cannot characterize well the transition regime because the dominant reactions are not well defined in the transition regime.

process; namely, the sum of O_3 contributions from all source groups always equals the predicted O_3 concentration. On the other hand, DDM correctly accounts for the negative sensitivities, but DDM sensitivities cannot be strictly interpreted as source apportionments because the sum of all first-order sensitivities will not account for all of the O_3 concentration (it usually accounts for 60-65% of the total O_3 concentration), therefore, DDM provides source contributions to a fraction of the O_3 concentration (60-65%). Note that it is this fraction that will be mainly affected by small to moderate changes in emission levels. Although the source contributions expressed in terms of the percentage of the sum of the first-order sensitivities of O_3 predicted by DDM are not equivalent to those expressed in terms of the percentage of total O_3 concentration predicted by OSAT, a qualitative comparison between the DDM and OSAT source contributions was conducted to provide the relative importance of all source groups. Nevertheless, there should be a clear relationship between OSAT source contributions and DDM sensitivities for specific source area/source category groups.

Below we first analyze the spatial distributions of O_3 sensitivities/contributions to/of total NO_x and VOC emissions from four different source categories: biogenic, on-road mobile, other surface anthropogenic, and elevated sources under the EPA 2007 base emission scenario. The O_3 sensitivities/contributions to/of total NO_x and VOC emissions from the four different source categories, ICs, and BCs are then analyzed and compared in detail for each receptor region. Finally, the inter-correlation between DDM sensitivities and OSAT source contributions are quantified and discussed.

6.2.1.1 Domain-wide O_3 Sensitivities and Source Contributions from Four Source Categories

The domain-wide O_3 sensitivities/contributions to/of various source categories can be obtained directly from the DDM base run B7 and indirectly from the OSAT base run B1 by lumping source category contributions of 17 source areas. Figures 6-18 and 6-19 show the spatial distributions of O_3 sensitivities/contributions to/of the VOC and NO_x emissions from four source categories predicted by DDM and OSAT at 2 p.m. on July 15 under the EPA 2007 base emission scenario. The spatial distributions of DDM

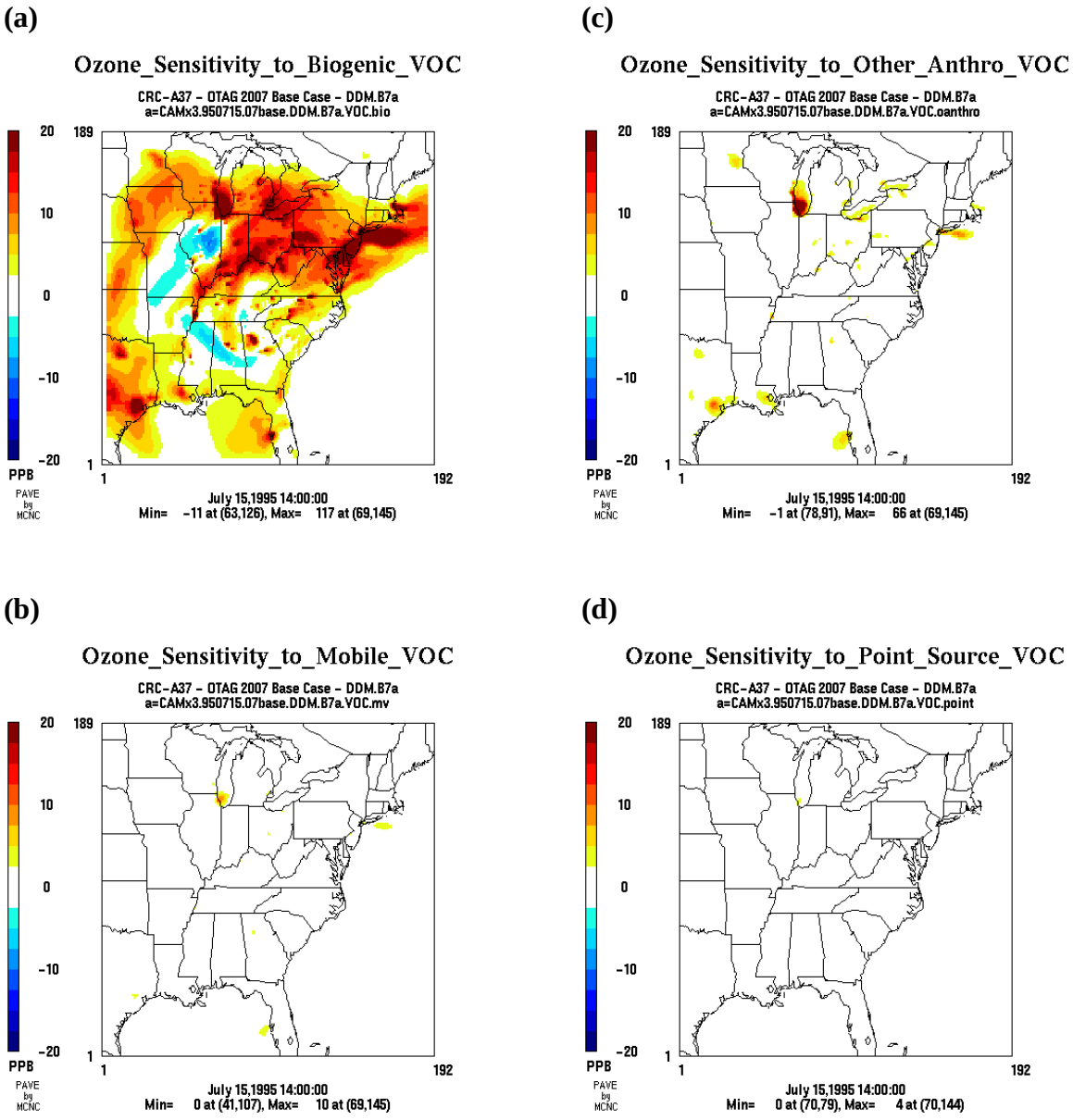

Figure 6-18. The spatial distribution of O_3 sensitivities predicted by DDM at 2 p.m. on July 15 under the EPA 2007 base emission scenario (DDM base run B7) for emissions from (a) biogenic VOC, (b) on-road mobile VOC, (c) other surface anthropogenic VOC, and (d) elevated anthropogenic VOC, (e) biogenic NO_x, (f) on-road mobile NO_x, (g) other surface anthropogenic NO_x, and (h) elevated anthropogenic NO_x.

(e)

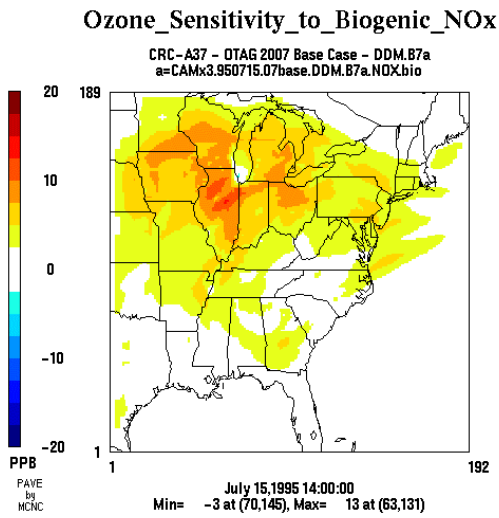

(g)

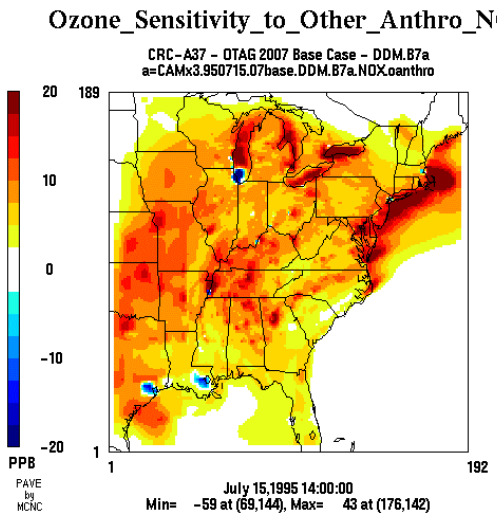

(f)

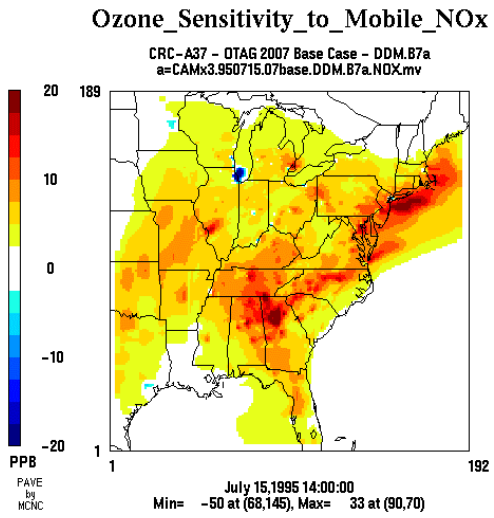

(h)

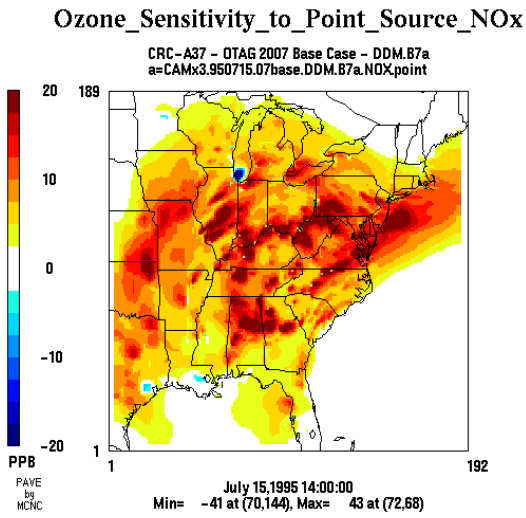

Figure 6-18. (Continued).

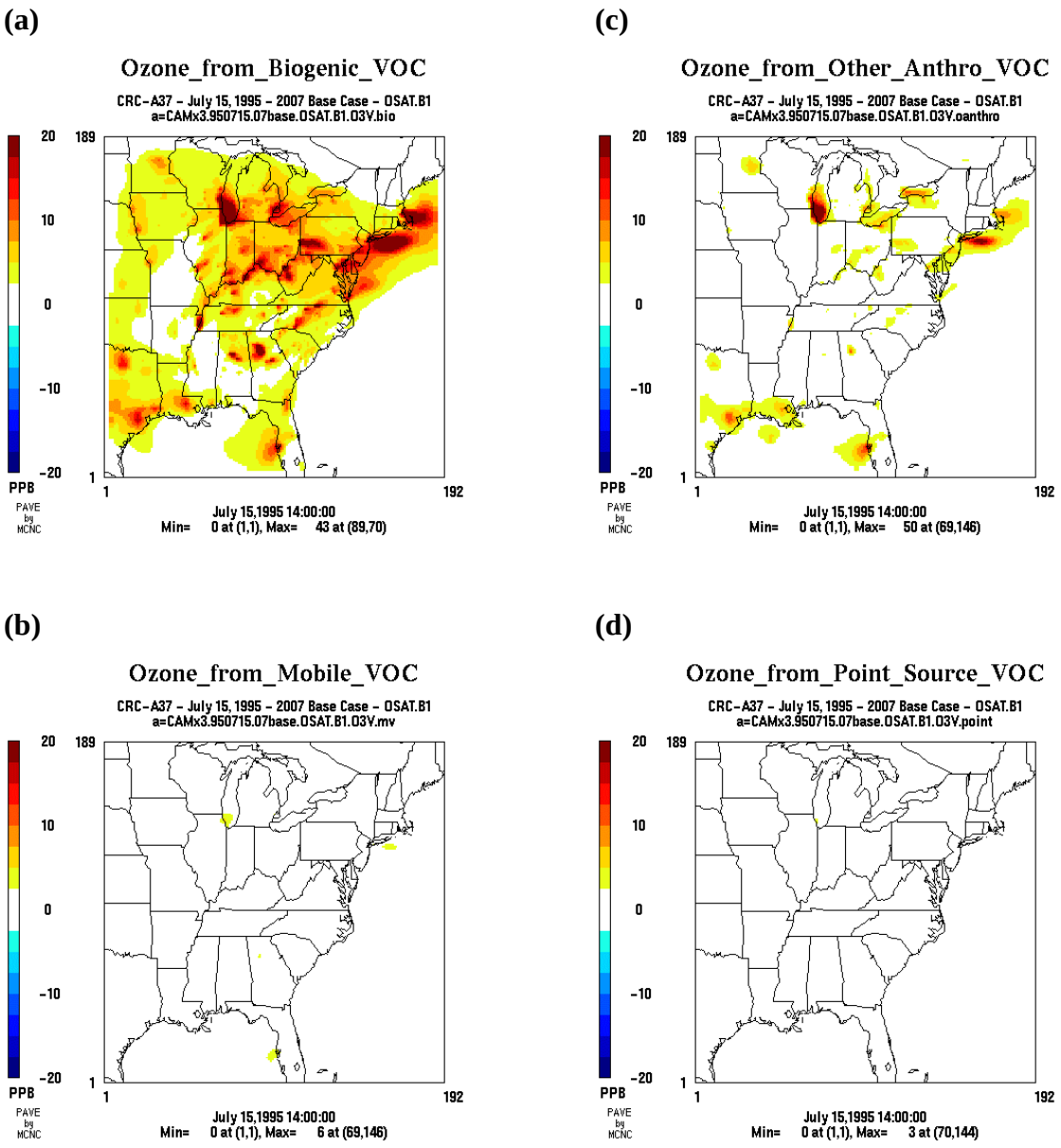

Figure 6-19. The spatial distribution of O_3 contributions predicted by OSAT at 2 p.m. on July 15 under the EPA 2007 base emission scenario (OSAT base run B1) for emissions from (a) biogenic VOC, (b) on-road mobile VOC, (c) other surface anthropogenic VOC, and (d) elevated anthropogenic VOC, (e) biogenic NO_x, (f) on-road mobile NO_x, (g) other surface anthropogenic NO_x, and (h) elevated anthropogenic NO_x.

(e)

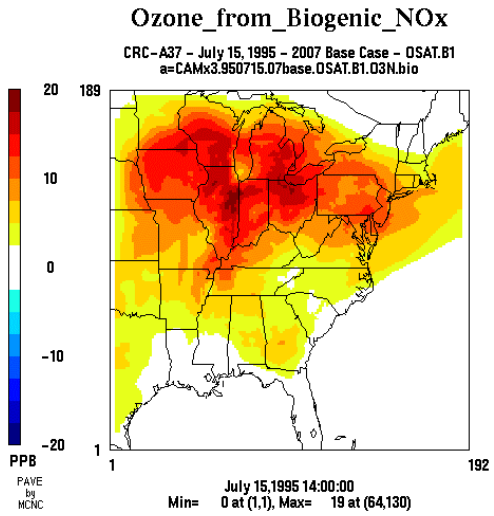

(g)

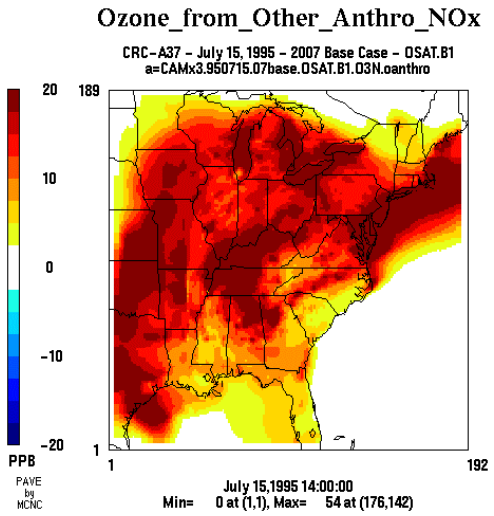

(f)

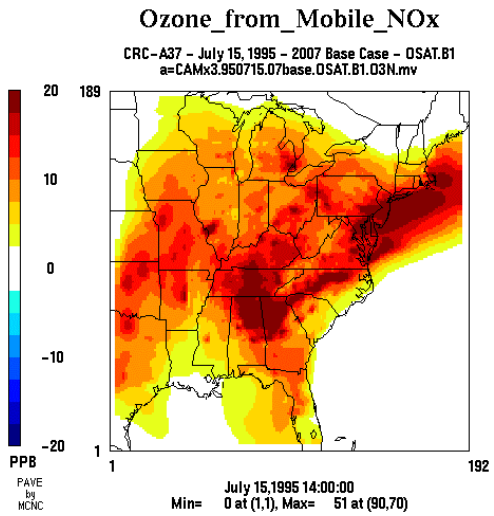

(h)

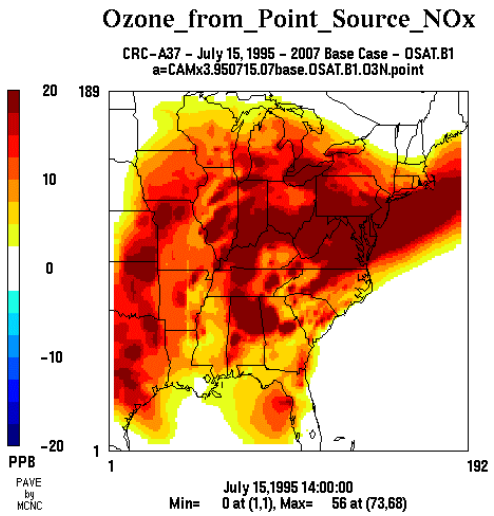

Figure 6-19. (Continued).

sensitivities and OSAT source contributions for all source categories are generally consistent, although the magnitudes of DDM sensitivities and OSAT source contributions differ for biogenic VOC and NO_x emissions from all source categories. Both DDM and OSAT predict that the other surface anthropogenic NO_x emissions are most important in many areas in the OTAG domain including areas over the four easternmost Great Lakes (i.e., Lake Michigan, Lake Huron, Lake Erie, and Lake Ontario), the northeastern coastal areas, and a large area over the State of Kentucky, the State of Tennessee, and eastern Kansas, Oklahoma and Texas. The elevated anthropogenic NO_x emissions are the most important source in many urban areas along the Ohio River (e.g., Louisville, KY, Cincinnati, OH, Charleston, WV, and Pittsburgh, PA); southern Illinois; Nashville, TN and its vicinity area; and several cities and their vicinity areas in eastern Virginia, northern Alabama, and northern Georgia. The on-road mobile NO_x emissions are the most important source in Atlanta, GA and its vicinity area and over some of the Atlantic area in the east of New Bedford and Boston, MA and in the south of New York City. It is also important in St. Louis, MO, Nashville, TN, Baltimore, MD and their vicinity areas. The biogenic NO_x emissions are the most important source in northern Illinois and Ohio, southern Minnesota and Wisconsin area, and southeastern Michigan. It is also important in many states in the northern part of the domain. Among all source categories, both DDM and OSAT predict that the biogenic VOC emissions are the most important source and the other surface anthropogenic VOC emissions are the second most important source. The mobile and elevated VOC emissions are not important for most areas in the OTAG domain. The biogenic VOC emissions play an important role in many areas in the entire domain with exceptions in some areas in several states including Illinois, Missouri, Arkansas, Mississippi, Alabama, Georgia, and Tennessee where the DDM sensitivities are negative and the OSAT source contributions are zero. The other surface anthropogenic VOC emissions are most important in the southern Lake Michigan and Chicago area. It is also important in areas over Lake Erie, Lake Ontario, south of Long Island, and Houston, TX.

There are three major differences between the DDM and the OSAT predictions. First, DDM predicts negative source contributions for a few areas where OSAT always predicts positive contributions. For example, DDM predicts negative contributions for

NO_x emissions from the elevated anthropogenic, the on-road mobile, and the other surface anthropogenic sources for the southern Lake Michigan and Chicago area. Second, the magnitudes of OSAT source contributions and DDM sensitivities for biogenic VOC emissions and NO_x emissions from all source categories are quite different. The DDM sensitivities for biogenic VOC emissions are larger than OSAT source contributions for biogenic VOC emissions in many areas in the domain. The OSAT source contributions for NO_x emissions from all source categories are much larger than the corresponding DDM sensitivities for NO_x emissions in many areas in the entire domain. Third, the relative importance of various source groups predicted by DDM and OSAT is different in some locations. For example, in Atlanta, DDM predicts that the mobile NO_x emissions and the biogenic VOC emissions are the most important sources, followed by the elevated NO_x emissions, the other surface anthropogenic NO_x and VOC emissions and the mobile VOC emissions. The sensitivities to the elevated VOC emissions and the biogenic NO_x emissions are zero in Atlanta. By comparison, OSAT predicts that the NO_x emissions from mobile, other surface anthropogenic, and elevated sources and the biogenic VOC emissions are the most important sources, followed by the other surface anthropogenic VOC emissions, the biogenic NO_x emissions and the mobile VOC emissions. The source contribution of the elevated VOC emissions is zero in Atlanta.

In a separate CRC project A-29, the spatial distributions of the sensitivities and source contributions for different emission categories, source regions and boundaries were compared in the Lake Michigan region for the O_3 episode of July 7-13, 1995 (Dunker et al., 2002b). We found that the spatial distributions of the sensitivities and source contributions were similar in all cases. DDM predicted a large negative sensitivity (-33 ppb) to anthropogenic area-source NO_x emissions in the Chicago area, whereas OSAT predicted a small and positive source contribution (0.3-2.6 ppb) from the same emission category. The general consistency between DDM sensitivities and OSAT source contributions was also observed in this project. However, in regions where NO_x significantly inhibited O_3 formation such as in the southern Lake Michigan and Chicago area, OSAT predicted much larger positive source contributions in this project than those reported by Dunker et al. (2002b). For example, in this project, for the southern Lake

Michigan and northeastern Chicago area, DDM predicted sensitivities of O_3 concentration to the elevated point NO_x emissions to be -40 to -10 ppb, whereas OSAT predicted a source contribution of 10-25 ppb from the same sources.

6.2.1.2 Receptor-Wide O_3 Sensitivities and Source Contributions from Four Source Categories

Figures 6-20 and 6-21 show the O_3 contributions of total VOC and NO_x emissions from four source categories, ICs, and BCs in percentage predicted by DDM and OSAT, respectively, at 3 p.m. on July 15 under the EPA 2007 base emission scenario. While the sum of the OSAT O_3 contributions gives the total O_3 concentration, the sum of the DDM sensitivities is only the 60-65% of the total O_3 concentrations in those receptor regions. Therefore, DDM provides source contribution to a fraction of the O_3 concentration (60-65%). Note that it is this fraction that will be mainly affected by small to moderate changes in emission levels. The predicted contributions by DDM and OSAT are very similar in Atlanta, but somewhat different in New York City and Altoona and significantly different in Chicago. In Atlanta, both DDM and OSAT predict that the on-road mobile emissions are the most important source, followed by the elevated anthropogenic sources, the other surface anthropogenic sources, the biogenic sources, BCs, and ICs. In New York City and Altoona, the contributions of the total surface anthropogenic sources (i.e., the sum of contributions of the on-road mobile and the other surface anthropogenic sources) predicted by DDM are lower by 8-9% than those predicted by OSAT, and the contributions of the biogenic sources predicted by DDM are higher by 10-15% than those of OSAT. This is because OSAT does not account for the titration effect of NO_x, thus overestimating the contributions of the surface anthropogenic sources and underestimating the contributions of the biogenic sources. In Chicago, the overestimation of the contribution of the anthropogenic sources including the on-road mobile and the other surface and elevated anthropogenic sources (and thus the underestimation of the contribution of the biogenic sources) by OSAT is much more significant than in New York City and Altoona, because of a large titration/inhibition effect of NO_x on O_3 formation at this receptor. DDM predicts that the contributions of

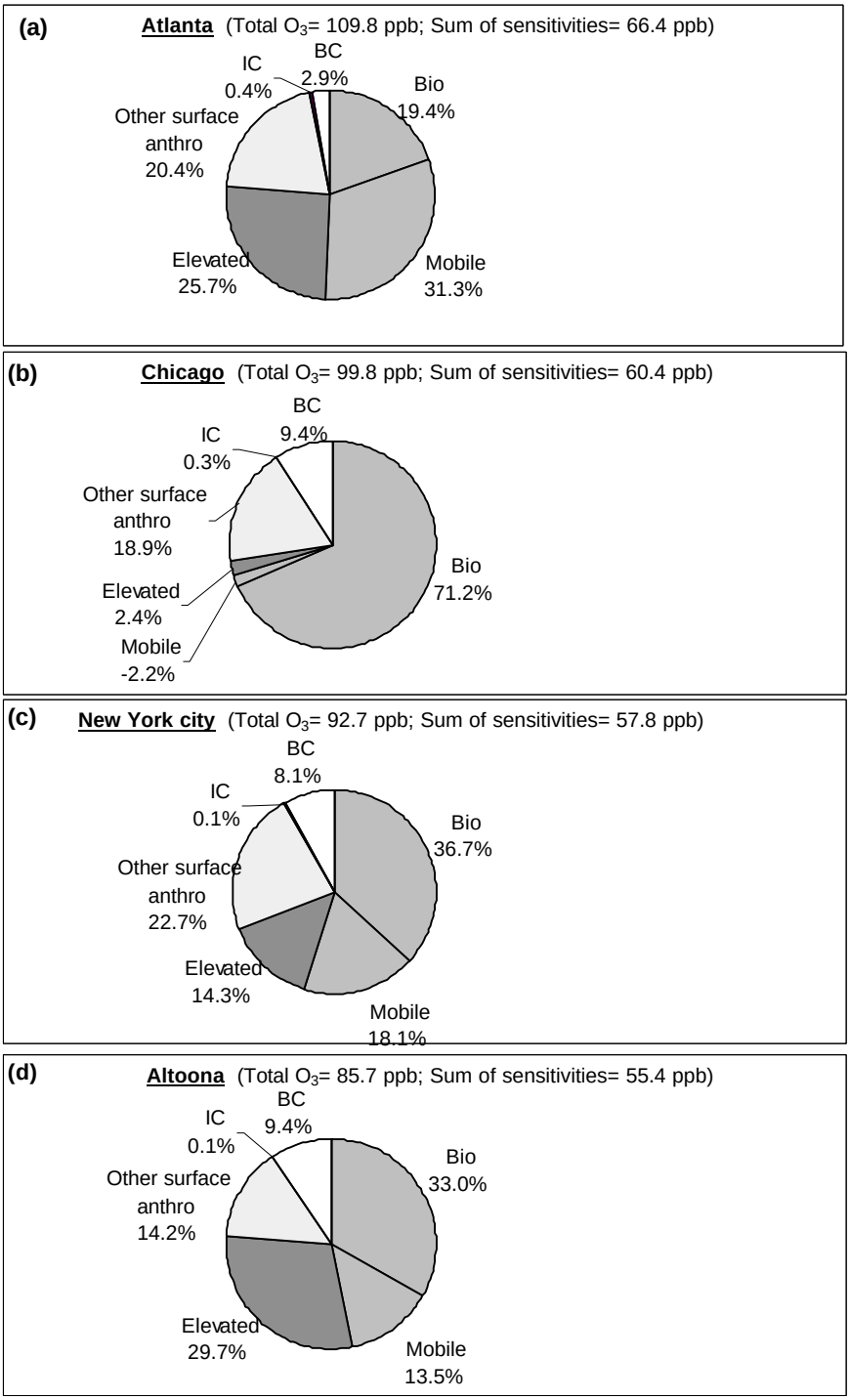

Figure 6-20. The O_3 sensitivities to total NO_x and VOC emissions from four source categories, ICs, and BCs predicted by DDM at 3 p.m. on July 15 under the EPA 2007 base emission scenario (DDM base run B7) in (a) Atlanta, (b) Chicago, (c) New York City, and (d) Altoona.

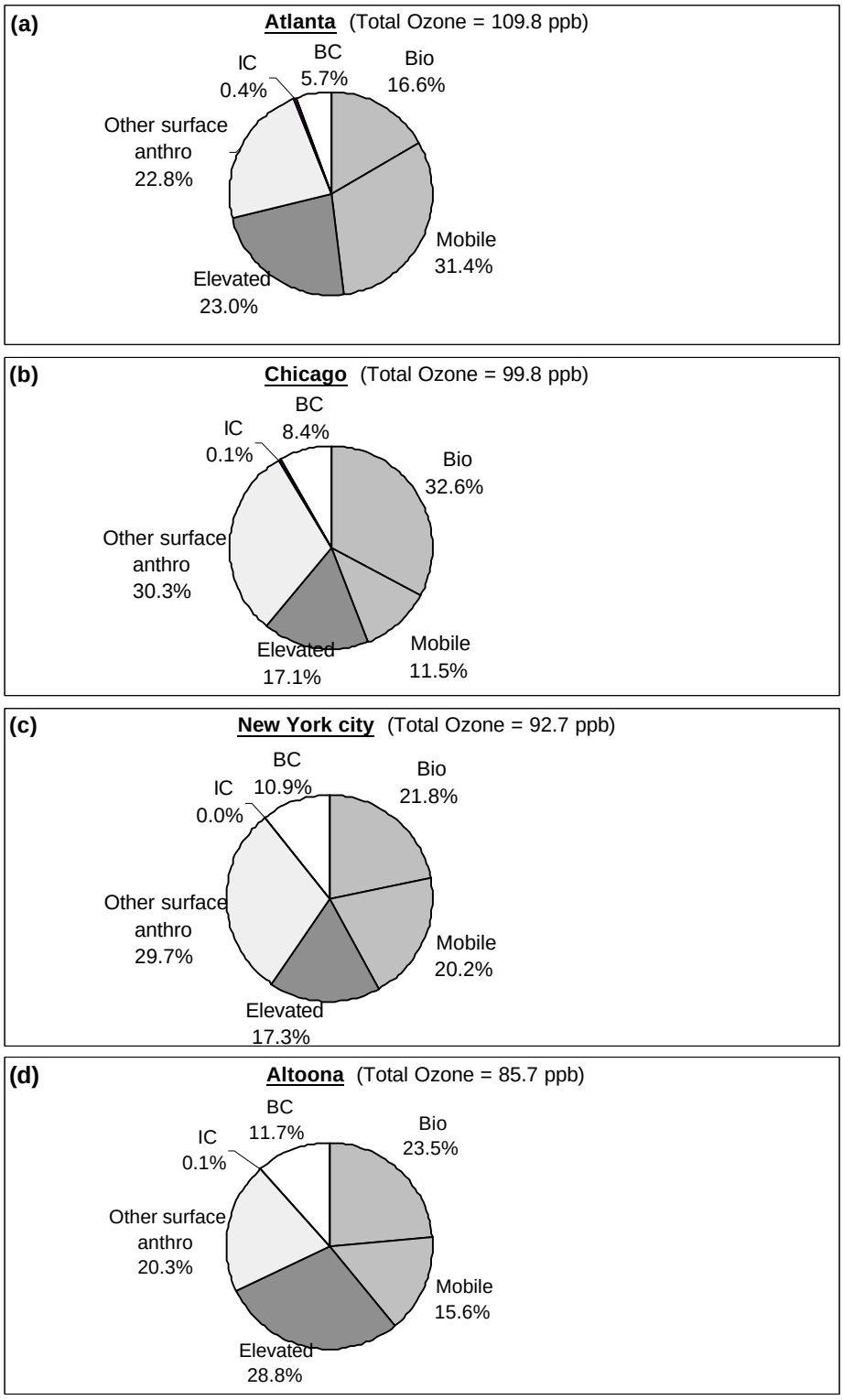

Figure 6-21. The O_3 contributions of total NO_x and VOC emissions from four source categories, ICs, and BCs predicted by OSAT at 3 p.m. on July 15 under the EPA 2007 base emission scenario (OSAT base run B1) in (a) Atlanta, (b) Chicago, (c) New York City, and (d) Altoona.

the biogenic, on-road mobile, other surface and elevated anthropogenic sources to be 71%, -2%, 19%, and 2%, respectively. For comparison, OSAT predicts the contributions of those source categories to be 33%, 11.5%, 30%, and 17%, respectively. Considering the fact that the sum of DDM sensitivities only explains about 61% of the total O_3 concentration in Chicago, the 71% of 60.4 ppb O_3 by the biogenic sources is equivalent to 43% of total O_3 concentration (99.8 ppb), implying that the contribution of the biogenic emissions (mostly VOCs) to the total O_3 concentration predicted by DDM is at least 43% and could be higher if higher-order sensitivities were calculated in DDM. Under a separate CRC Project (A-23), Pun et al. (2001c) found that the contributions of the biogenic emissions to O_3 production range from 22% to 34% in urban areas in the eastern U.S. While the DDM and OSAT results obtained in Atlanta and New York City are generally consistent with those of Pun et al. (2001c), the contributions of the biogenic sources to the O_3 production predicted by DDM in Chicago are much higher than the upper bound value of Pun et al. (2001c). The high contribution of the biogenic sources in Chicago is not surprising, however, given the fact that the anthropogenic NO_x emissions severely inhibit O_3 formation in Chicago.

While the contributions of ICs to the total O_3 sensitivity or concentration predicted by DDM and OSAT for all receptors are very small (< 0.4%), the contributions of BCs predicted by DDM and OSAT are in the range of 3-9% and 6-12%, respectively. In this project, however, we do not intend to compare the contributions of ICs and BCs predicted by DDM and OSAT, because DDM and OSAT treat ICs and BCs somewhat differently. For example, OSAT does not attribute O_3 to PAN or other NO_x carriers that enter the domain via initial or boundary concentrations. The boundary concentrations of PAN were found to have a noticeable impact on O_3 formation in CRC Project A-29 (Dunker, 2001). In addition, we do not intend to address the importance of initial and boundary concentrations of VOC, NO_x and O_3 on O_3 formation in this project, because the DDM simulations conducted in this project only provide the contributions of the lumped ICs and BCs of all species (i.e., no VOC vs. NO_x breakout) to O_3 concentrations, which is insufficient to investigate the importance of ICs and BCs of VOC, NO_x and O_3 to O_3 formation.

DDM and OSAT can also attribute O_3 concentrations to emissions from different source regions. This information is very useful to analyze the relative importance of the local vs. upwind sources (i.e., local photochemistry vs. transport) and allow one to resolve the impacts of the surface and elevated point source emissions in separate geographic regions. The O_3 contributions of emissions by separate geographic regions and their relative importance will be discussed in detail in Section 6.2.2.

6.2.1.3 The Relationship Between DDM Sensitivities and OSAT Source Contributions

Figures 6-22 to 6-29 show the DDM sensitivities versus the OSAT source contributions of the VOC and NO_x emissions from four source categories (a total of 8 source groups) in four receptor regions. The data shown in the plots only include the DDM and OSAT results for all fine grid cells (each receptor contains 81 fine grid cells) with an O_3 concentration > 80 ppb at 3 p.m. on July 11-15. Thus, the number of points varies for each receptor, depending on how many grid cells have O_3 > 80 ppb at 3 p.m. on each day (the maximum point is 405 (= 81 x 5), if all 81 fine grid cells have O_3 > 80 ppb at 3 p.m. on all five days). The degree of correlation between two variables can be evaluated using a number of statistics such as normalized bias, fractional bias, and fractional gross error (Seigneur et al., 2000). Since the normalized bias tends to give more weight to overpredictions than underpredictions, we use the fractional bias to evaluate the agreement between the magnitudes of the DDM and the OSAT results in this project. The fractional bias normalizes the bias by the arithmetic average of the DDM and OSAT results, thus giving equal weight to overpredictions and underpredictions. It is defined as:

$$B_F = \frac{1}{N}\sum_{i=1}^{N}\left[2 \bullet \frac{D_i - O_i}{D_i + O_i}\right] \qquad (16)$$

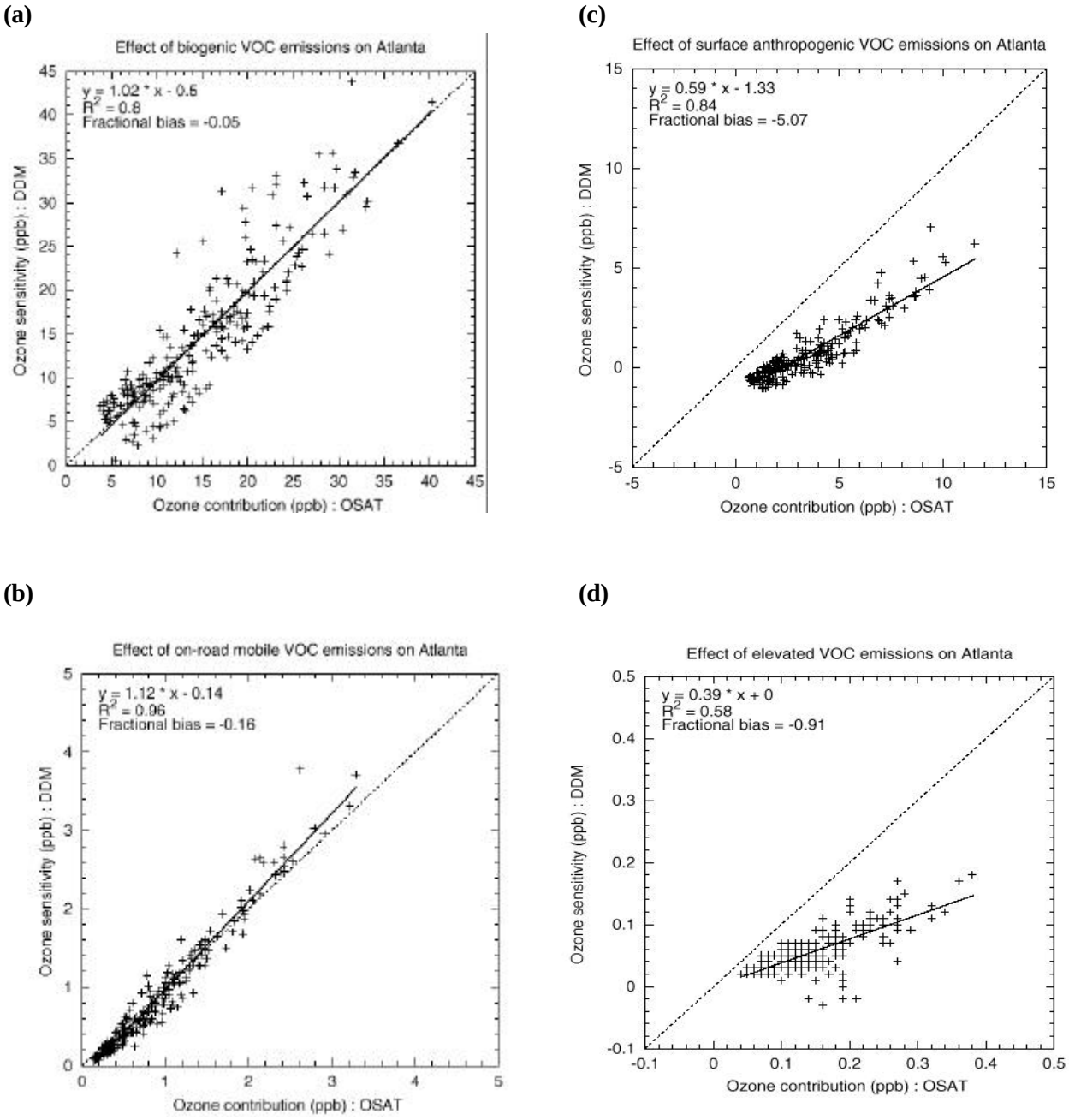

Figure 6-22. The DDM sensitivities versus the OSAT source contributions of VOC emissions from (a) biogenic, (b) on-road mobile, (c) other surface anthropogenic, and (d) elevated anthropogenic sources in Atlanta. The data shown only include the DDM and OSAT results for all fine grid cells with an O_3 concentration > 80 ppb at 3 p.m. on July 11-15 under the EPA 2007 base emission scenario (DDM base run B7 and OSAT base run B1).

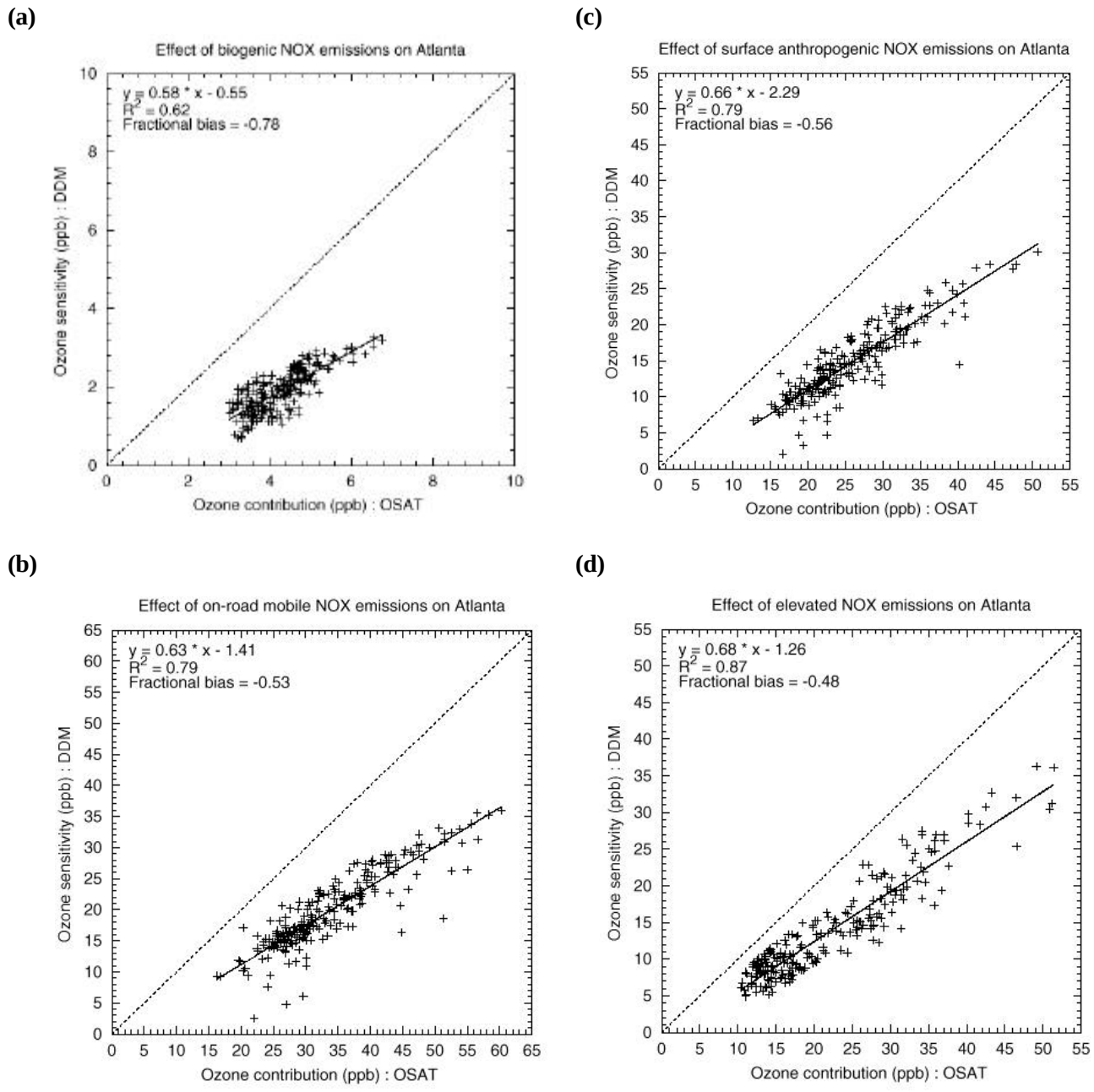

Figure 6-23. The DDM sensitivities versus the OSAT source contributions of NO_x emissions from (a) biogenic, (b) on-road mobile, (c) other surface anthropogenic, and (d) elevated anthropogenic sources in Atlanta. The data shown only include the DDM and OSAT results for all fine grid cells with an O_3 concentration > 80 ppb at 3 p.m. on July 11-15 under the EPA 2007 base emission scenario (DDM base run B7 and OSAT base run B1).

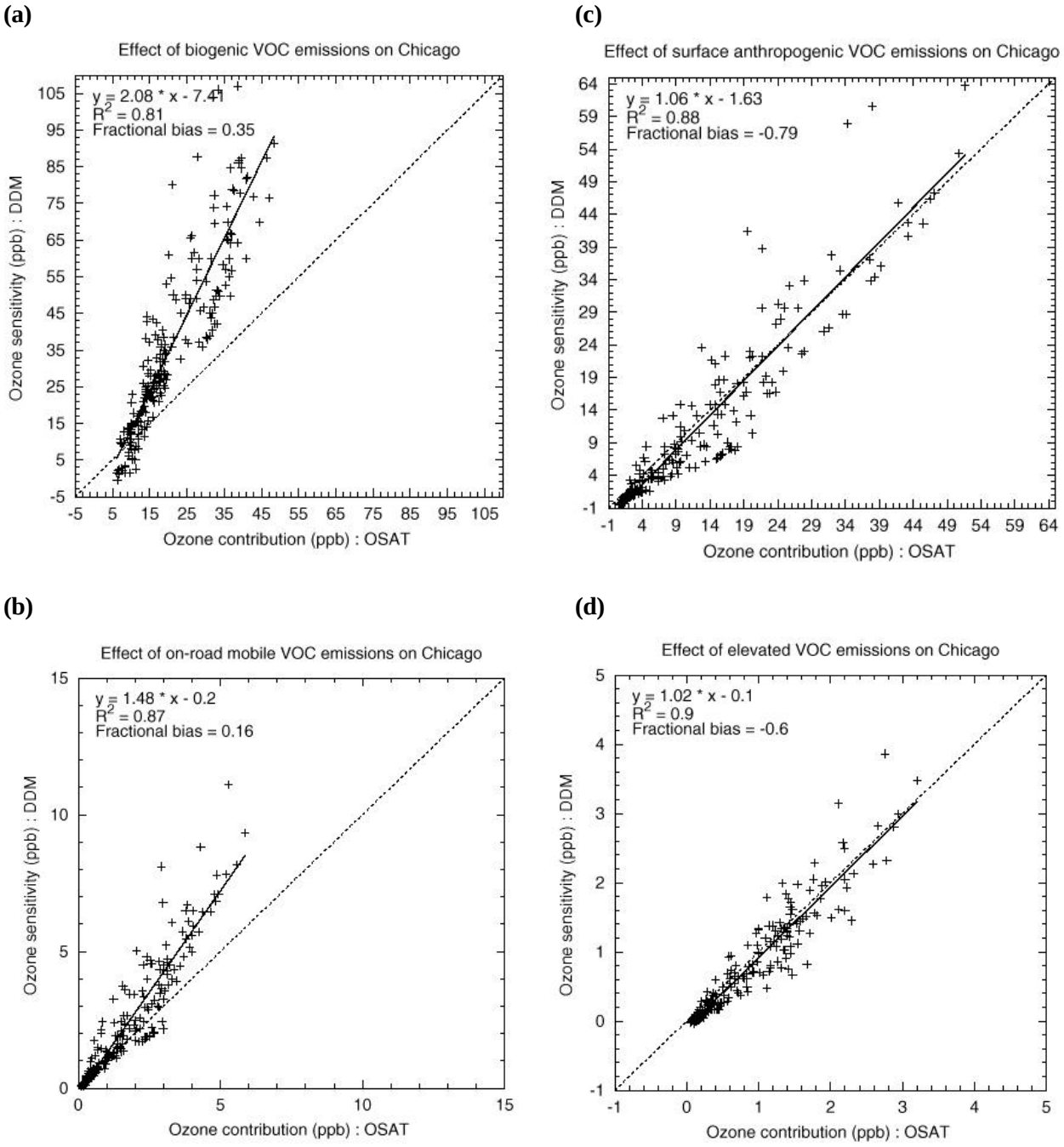

Figure 6-24. The DDM sensitivities versus the OSAT source contributions of VOC emissions from (a) biogenic, (b) on-road mobile, (c) other surface anthropogenic, and (d) elevated anthropogenic sources in Chicago. The data shown only include the DDM and OSAT results for all fine grid cells with an O_3 concentration > 80 ppb at 3 p.m. on July 11-15 under the EPA 2007 base emission scenario (DDM base run B7 and OSAT base run B1).

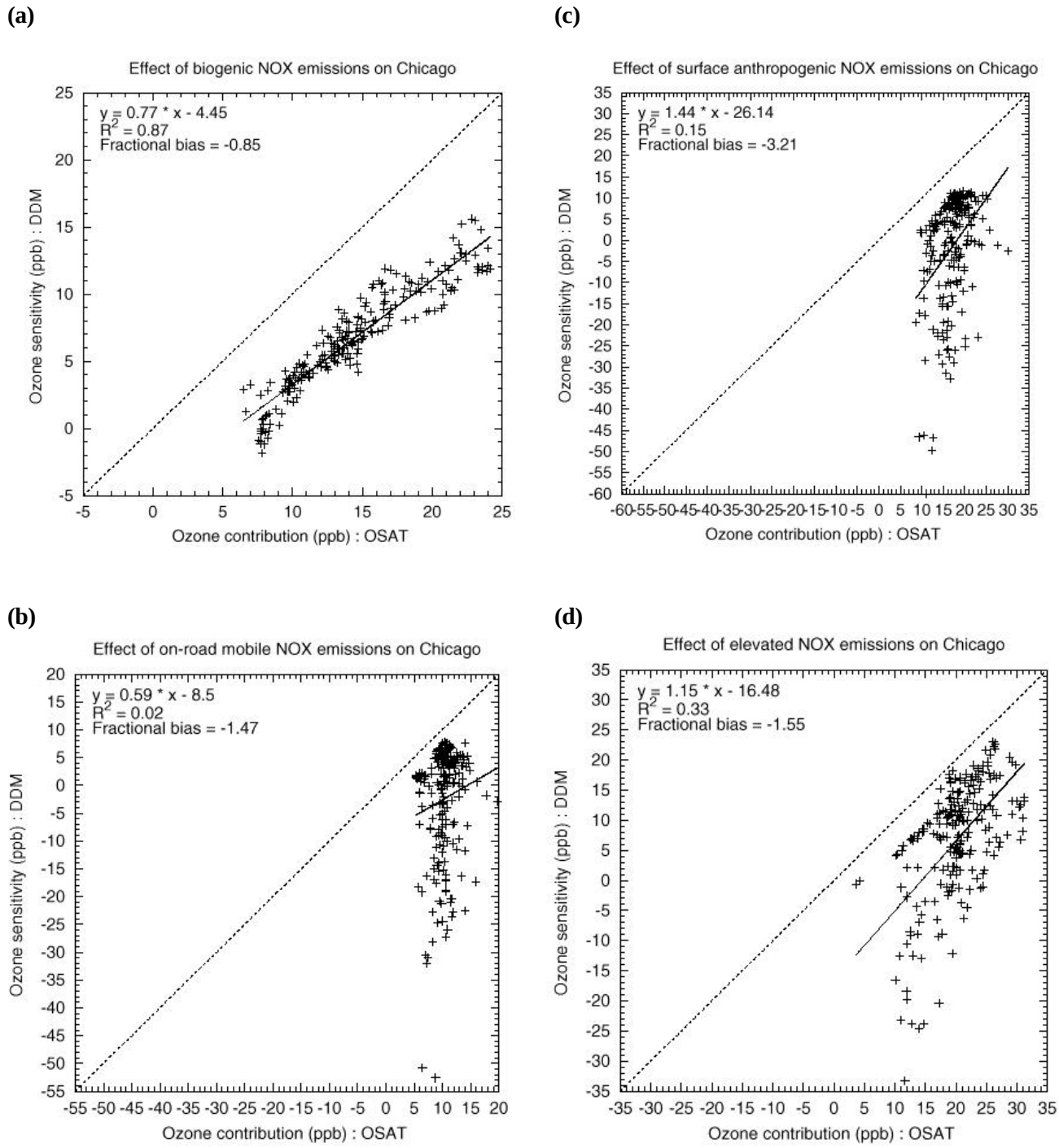

Figure 6-25. The DDM sensitivities versus the OSAT source contributions of NO_x emissions from (a) biogenic, (b) on-road mobile, (c) other surface anthropogenic, and (d) elevated anthropogenic sources in Chicago. The data shown only include the DDM and OSAT results for all fine grid cells with an O_3 concentration > 80 ppb at 3 p.m. on July 11-15 under the EPA 2007 base emission scenario (DDM base run B7 and OSAT base run B1).

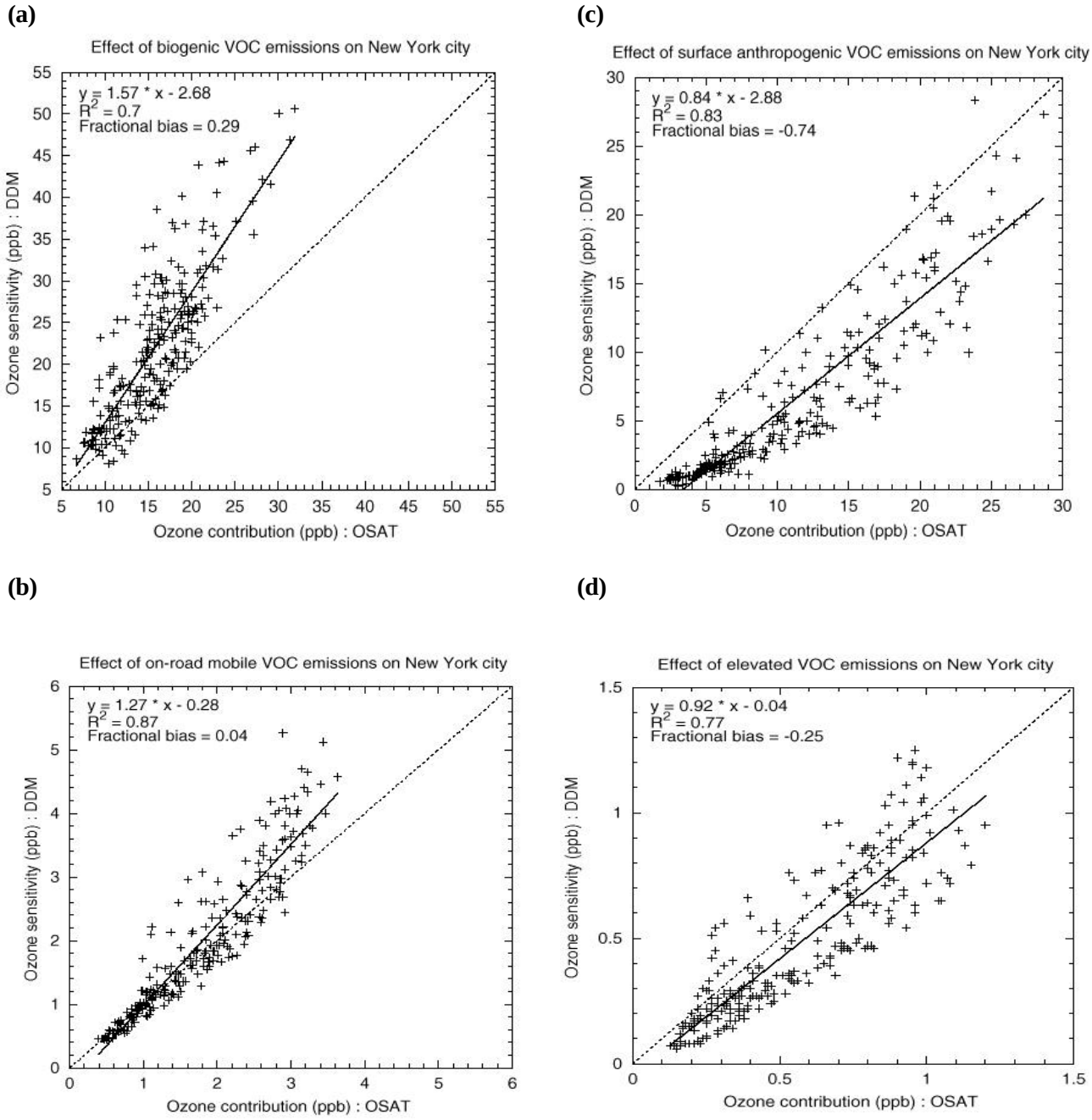

Figure 6-26. The DDM sensitivities versus the OSAT source contributions of VOC emissions from (a) biogenic, (b) on-road mobile, (c) other surface anthropogenic, and (d) elevated anthropogenic sources in New York City. The data shown only include the DDM and OSAT results for all fine grid cells with an O_3 concentration > 80 ppb at 3 p.m. on July 11-15 under the EPA 2007 base emission scenario (DDM base run B7 and OSAT base run B1).

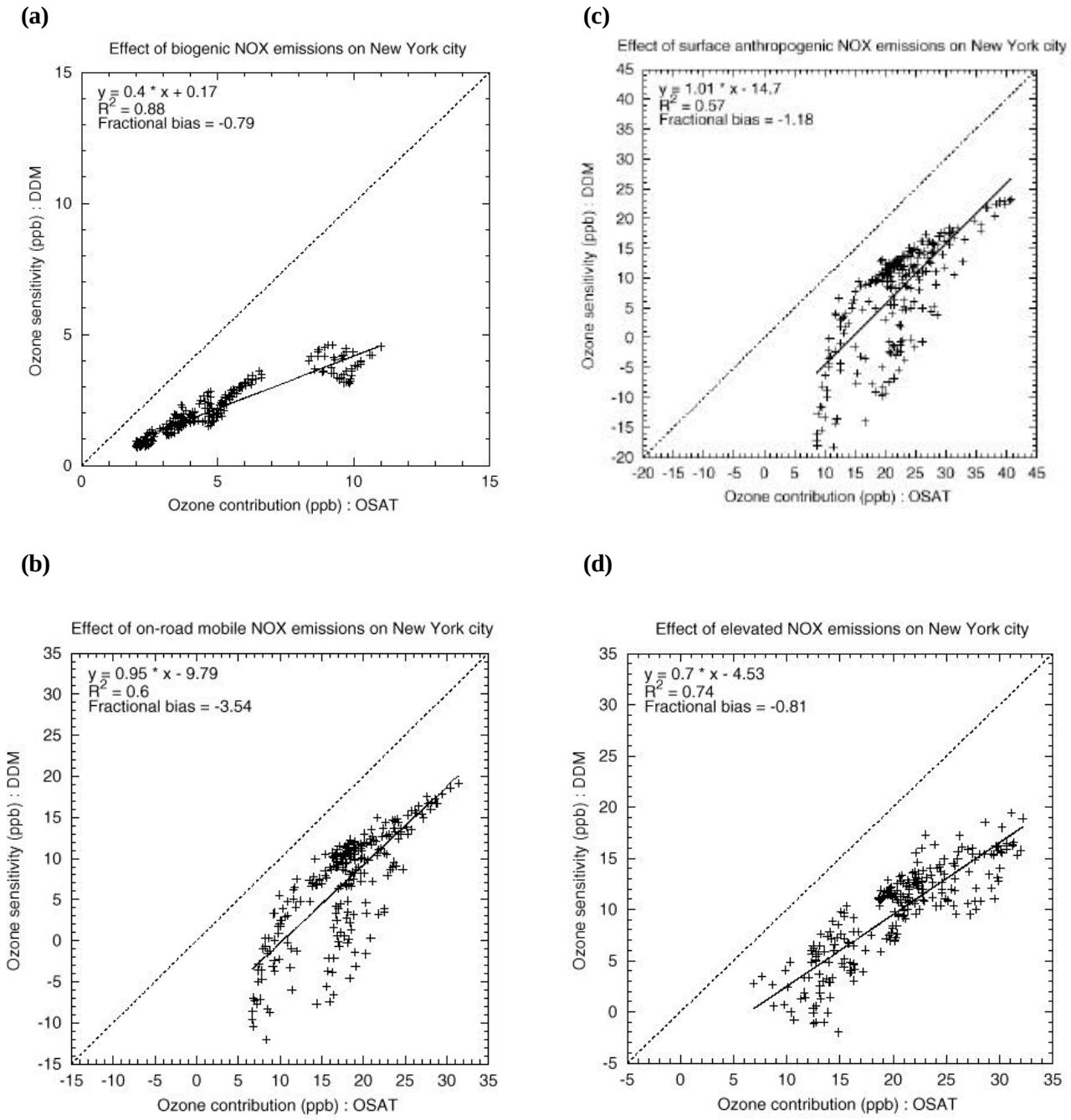

Figure 6-27. The DDM sensitivities versus the OSAT source contributions of NO_x emissions from (a) biogenic, (b) on-road mobile, (c) other surface anthropogenic, and (d) elevated anthropogenic sources in New York City. The data shown only include the DDM and OSAT results for all fine grid cells with an O_3 concentration > 80 ppb at 3 p.m. on July 11-15 under the EPA 2007 base emission scenario (DDM base run B7 and OSAT base run B1).

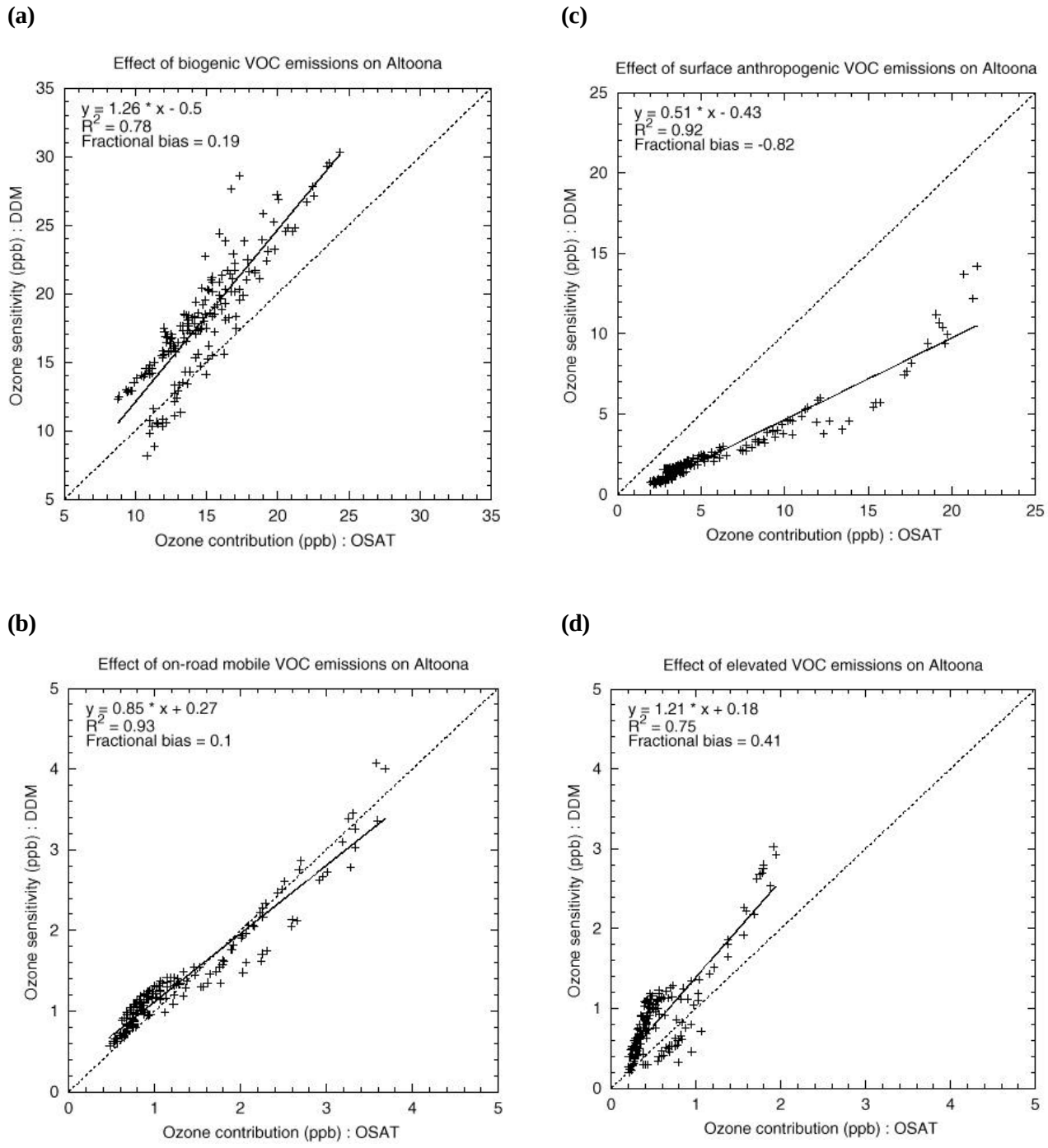

Figure 6-28. The DDM sensitivities versus the OSAT source contributions of VOC emissions from (a) biogenic, (b) on-road mobile, (c) other surface anthropogenic, and (d) elevated anthropogenic sources in Altoona. The data shown only include the DDM and OSAT results for all fine grid cells with an O_3 concentration > 80 ppb at 3 p.m. on July 11-15 under the EPA 2007 base emission scenario (DDM base run B7 and OSAT base run B1).

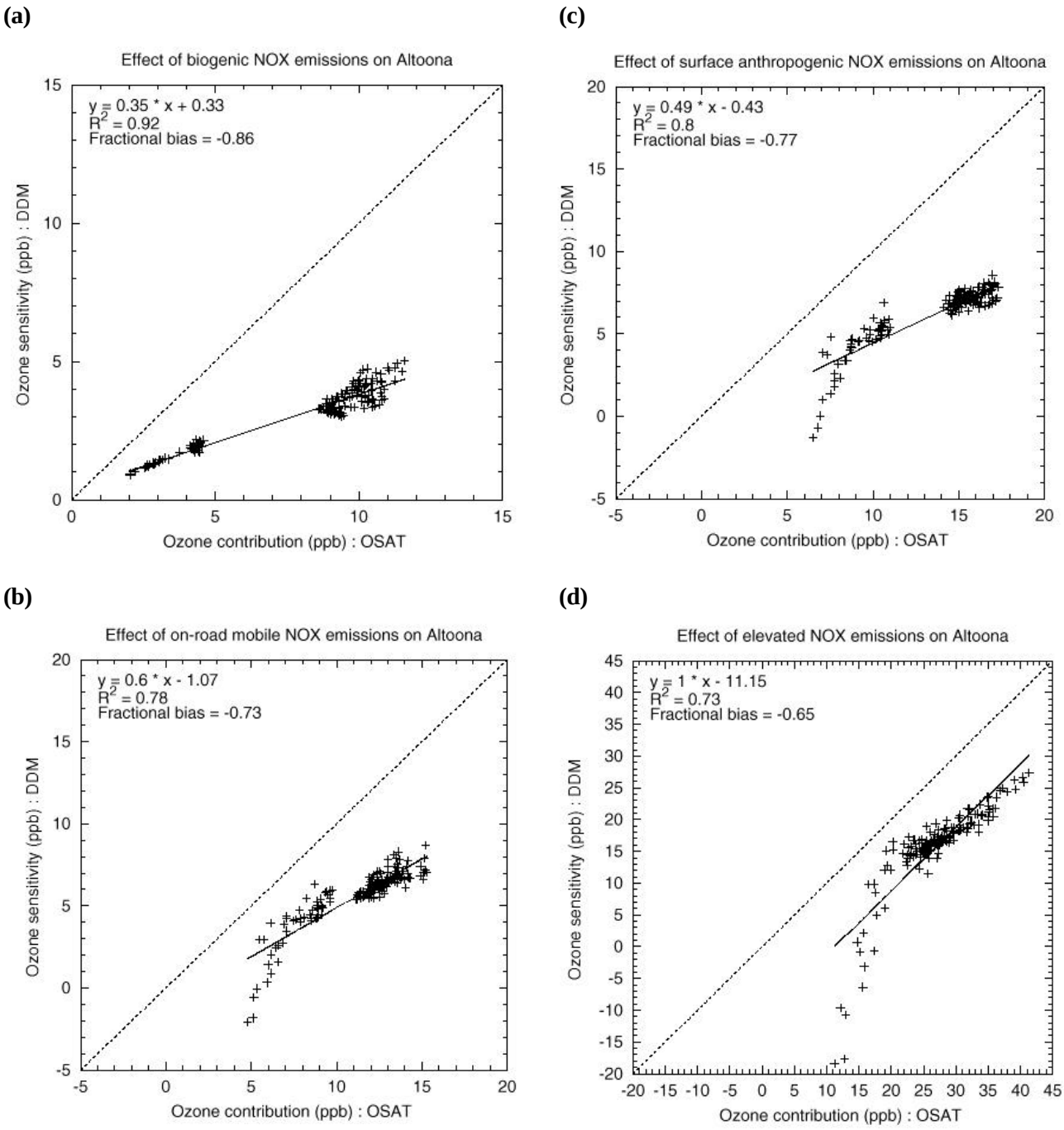

Figure 6-29. The DDM sensitivities versus the OSAT source contributions of NO_x emissions from (a) biogenic, (b) on-road mobile, (c) other surface anthropogenic, and (d) elevated anthropogenic sources in Altoona. The data shown only include the DDM and OSAT results for all fine grid cells with an O_3 concentration > 80 ppb at 3 p.m. on July 11-15 under the EPA 2007 base emission scenario (DDM base run B7 and OSAT base run B1).

where N is the total number of fine grid cells having O_3 > 80 ppb at 3 p.m. on each day for each receptor. D_i and O_i are the sensitivities predicted by DDM and the O_3 contributions predicted by OSAT, respectively. A positive fractional bias indicates that most DDM sensitivities are greater than the arithmetic average of the DDM and OSAT results. The greater the absolute fractional bias is, the larger the degree of disagreement in the magnitudes of D_i and O_i. We also use the coefficient of determination (R^2) to evaluate the degree of correlation between the DDM and OSAT results. In Dunker et al. (2002b), the regression slope is used to evaluate the correlation between the DDM and OSAT results. The use of regression slopes, however, can not always accurately determine the agreement (or the disagreement) between the magnitudes of the DDM and OSAT results, because DDM may give underpredictions at most points but still have a regression slope greater than 1 (or vice versa). Although this was not the case in the CRC Project A-29 (Dunker, private communication, 2002), such cases indeed occur in all the four receptor regions in this project and will be discussed in detail below.

Atlanta

In Atlanta (see Figures 6-22 and 6-23), the correlation between the DDM and OSAT results is quite good with R^2 values of 0.79-0.96 for all VOC and NO_x source groups except for the elevated anthropogenic VOC and the biogenic NO_x emissions. The fractional biases for all source groups are negative with values ranging from -5.07 to -0.05. The regression slopes for all source groups except for the biogenic and on-road mobile VOC emissions are less than 1. The negative biases indicate that the overall DDM predictions are lower than the arithmetic average of the DDM and OSAT results. The lower DDM values indicate either an underprediction of DDM or an overprediction of OSAT, depending on whether there are large negative sensitivities. DDM predicts positive sensitivities to the VOC and NO_x emissions from all source groups in most fine grid cells and small negative sensitivities (> -2.0) in some fine grid cells, indicating that the titration/inhibition effect of NO_x or VOC on O_3 concentrations is small or negligible in Atlanta. For the other surface and elevated anthropogenic VOC emissions and the NO_x emissions from all source categories, the significant lower DDM values (i.e., the large negative fractional biases) indicate a significant underprediction of DDM for those groups. This is due to the fact that the sum of the O_3 sensitivities only accounts for 60-

65% of the total O_3 concentrations in Atlanta. OSAT ascribes much greater importance to those source groups than DDM in Atlanta. For the biogenic and on-road mobile VOC emissions, the slopes that are slightly greater than 1 and the small negative fractional biases indicate a good agreement between the DDM and OSAT results.

Chicago

In Chicago (see Figures 6-24 and 6-25), the correlation between the DDM and OSAT results is also quite good, with R^2 values of 0.81-0.9 for the VOC emissions from all source categories and the biogenic NO_x emissions. However, poor correlation is found for the on-road mobile, other surface anthropogenic, and elevated anthropogenic NO_x emissions, with R^2 values of 0.02, 0.15, and 0.33, respectively. The regression slopes are all greater than 1 but the corresponding fractional biases are all negative for the elevated and other surface anthropogenic VOC and NO_x emissions. The fractional biases are also negative for the NO_x emissions from the biogenic and the on-road mobile sources. Those negative fractional biases indicate that the overall DDM predictions are lower than the arithmetic average of the DDM and OSAT results for those emission groups. The use of slope alone may lead to an opposite conclusion for those emission groups with a slope of greater than 1 but a negative fractional bias. The large negative sensitivities predicted by DDM for the on-road mobile, other surface anthropogenic, and elevated anthropogenic NO_x emissions from the local sources (i.e., the titration effect) strongly offset positive sensitivities of those NO_x emissions from other source areas, causing significantly lower sensitivities than the contributions predicted by OSAT for those NO_x emission groups.

Therefore, the lower DDM values indicate a significant overprediction of OSAT for those emissions groups (rather than an underprediction of DDM, as was the case in Atlanta), due to the fact that OSAT does not account for the titration/inhibition effect of NO_x on O_3 chemistry. For the biogenic NO_x emission group, DDM predicts either positive or small negative sensitivities, indicating that the effect of biogenic NO_x titration on O_3 formation is negligible. In such a case, it is likely that DDM underpredicts the source contribution of biogenic NO_x emissions. Although the biogenic NO_x contributions predicted by OSAT are higher than the arithmetic average of the DDM and OSAT results, OSAT may still underpredict the true source contribution of the biogenic NO_x

emission group since it significantly overpredicts the contributions of all other NO_x emission groups. For the biogenic and on-road mobile VOC emission groups, OSAT significantly underpredicts their contributions. For the elevated and other surface anthropogenic VOC emissions, DDM and OSAT show relatively good agreement.

New York City

In New York City (see Figures 6-26 and 6-27), the correlation between the DDM and OSAT results is good with R^2 values of 0.7-0.87 for all VOC and NO_x source groups except for the on-road mobile and other surface anthropogenic NO_x emissions. Greater importance is given to the biogenic and on-road mobile VOC emissions by DDM and to the other surface anthropogenic VOC and NO_x emissions and the biogenic, on-road mobile and elevated anthropogenic NO_x emissions by OSAT. DDM and OSAT show relatively good agreement for the elevated anthropogenic VOC emissions. DDM predicts positive sensitivities to the VOC emissions from all source categories and the biogenic NO_x emissions in all fine grid cells and some large (up to -19) negative sensitivities to the NO_x emissions from on-road mobile and other surface and elevated anthropogenic sources in some fine grid cells. The significant underpredictions of DDM for the other surface anthropogenic VOC emission and biogenic NO_x emissions are due to the fact that the sum of the O_3 sensitivities only accounts for 60-65% of the total O_3 concentrations. The significant overpredictions of OSAT for the NO_x emissions from the on-road mobile and other surface and elevated anthropogenic sources occur because OSAT does not account for the titration effects of the NO_x emissions from those source categories in New York City.

Altoona

In Altoona (see Figures 6-28 and 6-29), the correlation between the DDM and OSAT results is quite good with R^2 values of 0.75-0.93 for all VOC and NO_x source categories. DDM gives greater importance to the biogenic, on-road mobile, and elevated anthropogenic VOC emissions, and OSAT gives greater importance to the other surface anthropogenic VOC emissions and the NO_x emissions from all the four source categories. Note that the fractional bias is positive (= 0.1) but the regression slope is less than 1 (=0.85) for the on-road mobile VOC emissions. The small positive fractional bias indicates that the overall DDM predictions are slightly higher than the arithmetic average

of the DDM and OSAT results for the on-road mobile VOC emissions. The use of slope alone may lead to an opposite conclusion for the on-road mobile VOC emissions. As for to New York City, DDM predicts positive sensitivities to VOC emissions from all source categories and the biogenic NO_x emissions in all fine grid cells and some negative sensitivities (up to -19) to the NO_x emissions from the on-road mobile and other surface and elevated anthropogenic sources in some fine grid cells. The significant underpredictions of DDM for the other surface anthropogenic VOC emissions and the NO_x emissions from the biogenic, on-road mobile, and other surface anthropogenic sources are due to the fact that the sum of the O_3 sensitivities only accounts for 60-65% of the total O_3 concentrations. The significant overpredictions of OSAT for the NO_x emissions from the elevated anthropogenic sources are because OSAT does not account for the titration/inhibition effects of the elevated anthropogenic NO_x emissions in Altoona.

6.2.1.4 Comparisons with OSAT-DDM Relationship Predicted by CRC Project A-29

Dunker et al. (2002b) investigated the relationship between the sensitivities from DDM and the source contributions from OSAT in the CRC project A-29. They found a consistently good relation between the DDM and OSAT results for all the cases, with R^2 values of 0.8-0.98. For comparison, the correlation between the DDM and OSAT results obtained here is generally good with R^2 values of 0.7 – 0.96 for most source groups for all receptor regions evaluated in this project. However, poor correlation (with R^2 values as low as 0.02 to 0.33) is found for the on-road mobile, other surface anthropogenic, and elevated anthropogenic NO_x emissions in Chicago, New York City, and Altoona where the titration/inhibition effect of NO_x is important (i.e., there are large negative sensitivities for those source groups).

Some disagreements were found between the DDM and OSAT results on the relative importance of source categories by Dunker at al. (2002b) and in this project. For example, Dunker et al. (2002b) reported that the OSAT results ascribe greater importance to biogenic VOC and NO_x emissions, anthropogenic area-source NO_x emissions, and VOC and NO_x boundary conditions than do the DDM sensitivities. The DDM

sensitivities ascribe greater importance to anthropogenic area-source VOC emissions and point-source VOC and NO_x emissions than do the OSAT source contributions. For comparison, it is found in this project that OSAT results ascribe much greater importance to the NO_x emissions from all source categories for all the four receptors and to the other surface anthropogenic VOC emissions for all receptors except for Chicago than do the DDM sensitivities, whereas DDM sensitivities ascribe much greater importance to the biogenic VOC emissions at all receptors except for Atlanta and to on-road mobile VOC emission groups in Chicago and New York City.

It is noted that there are some inconsistencies or even conflicts regarding the relative importance of some source categories (e.g., biogenic VOC, elevated point-source NO_x emissions) predicted by DDM and OSAT between the two projects. Several important factors may be responsible for the inconsistencies between the results in Projects A-29 and A-37. First, the versions of OSAT used in the two projects are substantially different (see Chapter 1 for major differences between the original and the updated versions of OSAT). Second, Project A-37 used an emission inventory for 2007 whereas Project A-29 used an inventory for 1995. These inventories could be quite different both in absolute amount of emissions and in the relative proportions of mobile, point-source, other anthropogenic, and biogenic emissions. Furthermore, the results were analyzed differently in the two projects. For example, for the scatter plots in Project A-29, sensitivities and source contributions were averaged across receptor regions but not across geographic source regions. In the scatter plots in this poject (e.g., Figures 6-22 to 6-29), sensitivities and source contributions were plotted for individual grid cells in the receptor regions, but there was only one geographic source region. The different averaging procedures employed in the two studies may affect the comparison between DDM and OSAT. Nevertherless, The inconsistencies in the results in Projects A-29 and A-37 indicate that the predicted contributions and relative importance of the source categories are sensitive to the selected locations of receptors and the episode simulated and may be different from case to case.

6.2.2 Relative Importance of Chemistry and Transport

All three probing tools can provide some information on the relative importance of photochemistry vs. transport, but PA results are at different time and spatial scales to OSAT and DDM and are thus not comparable to those of OSAT and DDM. Both OSAT and DDM can predict the relative importance of local sources vs. sources in upwind locations (i.e., local photochemistry vs. transport) and allow one to resolve the impacts of surface and elevated point source emissions in separate geographic regions. While both OSAT and DDM reflect the time history of the air parcel at the receptor, PA can only provide the local and instantaneous relative importance of photochemistry and transport (horizontal and vertical) on O_3 formation at a specific grid cell.

The relative importance of chemistry and transport in the four receptor regions are quite different. For example, Atlanta is mostly affected by the local and surrounding emissions, whereas New York City and Altoona are strongly influenced by long range transport of pollutants. The relative importance of chemistry and transport in the four receptor regions is analyzed and discussed in detail below.

Figures 6-30 to 6-33 show the O_3 sensitivities/contributions to/of total VOC and NO_x emissions from 17 source areas, ICs, and BCs predicted by DDM and OSAT at 3 p.m. on July 15 under the EPA 2007 base emission scenario in the four receptor regions. Contributions of individual source groups predicted by DDM and OSAT are shown in Figures 6-34 to 6-41 for those receptors.

Atlanta

In Atlanta (see Figure 6-30), both DDM and OSAT predict that the local and surrounding sources (i.e., source areas 15 and 8) are overwhelmingly more important than the upwind sources, contributing to 90% of the total O_3 sensitivity by DDM and 86% of the total O_3 concentration by OSAT. The total emissions from the upwind source area 12 and boundary conditions only contribute to 5% and 3% of the total O_3 sensitivity by DDM and 5% and 6% of the total O_3 concentration by OSAT. The individual contribution of the other upwind sources such as the emissions from the source areas 9, 7, and 5 to the total O_3 concentration is less than 1.2%. This indicates that O_3 concentrations in Atlanta are mainly affected by local photochemistry. As shown in

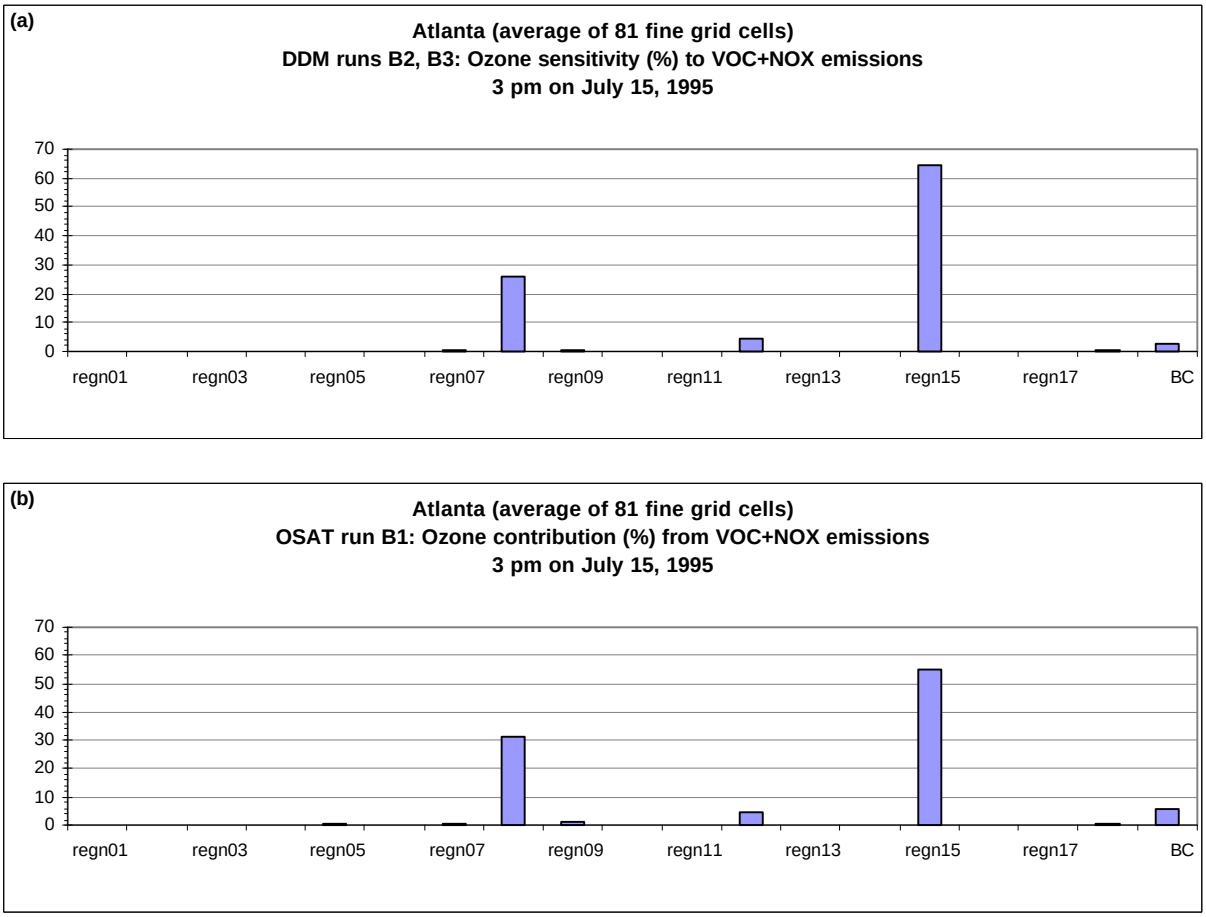

Figure 6-30. The (a) O_3 sensitivities to total NO_x and VOC emissions from 17 source areas, ICs, and BCs predicted by DDM and (b) O_3 contributions of total NO_x and VOC emissions from 17 source areas, ICs, and BCs predicted by OSAT at 3 p.m. on July 15 under the EPA 2007 base emission scenario (DDM base runs B2 and B3 and OSAT base run B1) in Atlanta.

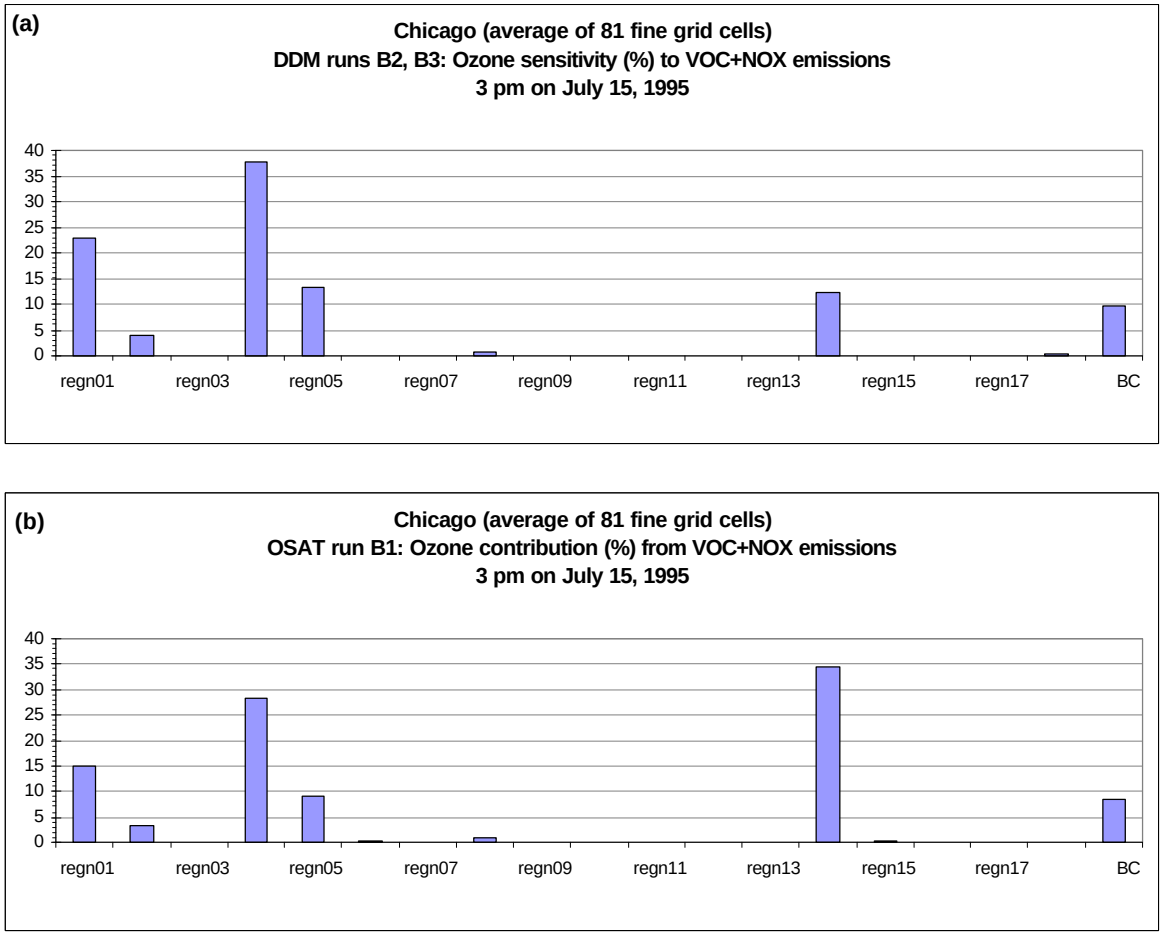

Figure 6-31. The (a) O_3 sensitivities to total NO_x and VOC emissions from 17 source areas, ICs, and BCs predicted by DDM and (b) O_3 contributions of total NO_x and VOC emissions from 17 source areas, ICs, and BCs predicted by OSAT at 3 p.m. on July 15 under the EPA 2007 base emission scenario (DDM base runs B2 and B3 and OSAT base run B1) in Chicago.

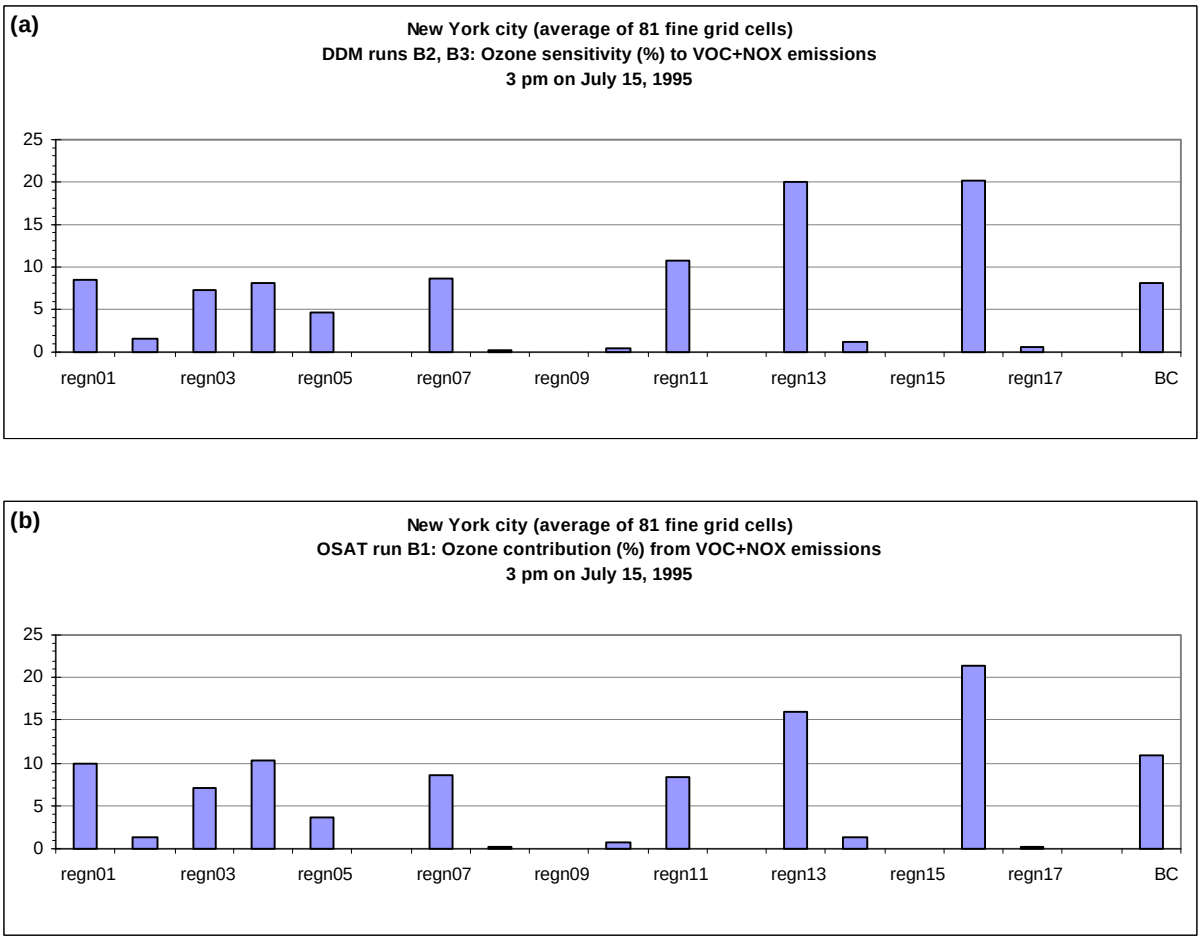

Figure 6-32. The (a) O_3 sensitivities to total NO_x and VOC emissions from 17 source areas, ICs, and BCs predicted by DDM and (b) O_3 contributions of total NO_x and VOC emissions from 17 source areas, ICs, and BCs predicted by OSAT at 3 p.m. on July 15 under the EPA 2007 base emission scenario (DDM base runs B2 and B3 and OSAT base run B1) in New York City.

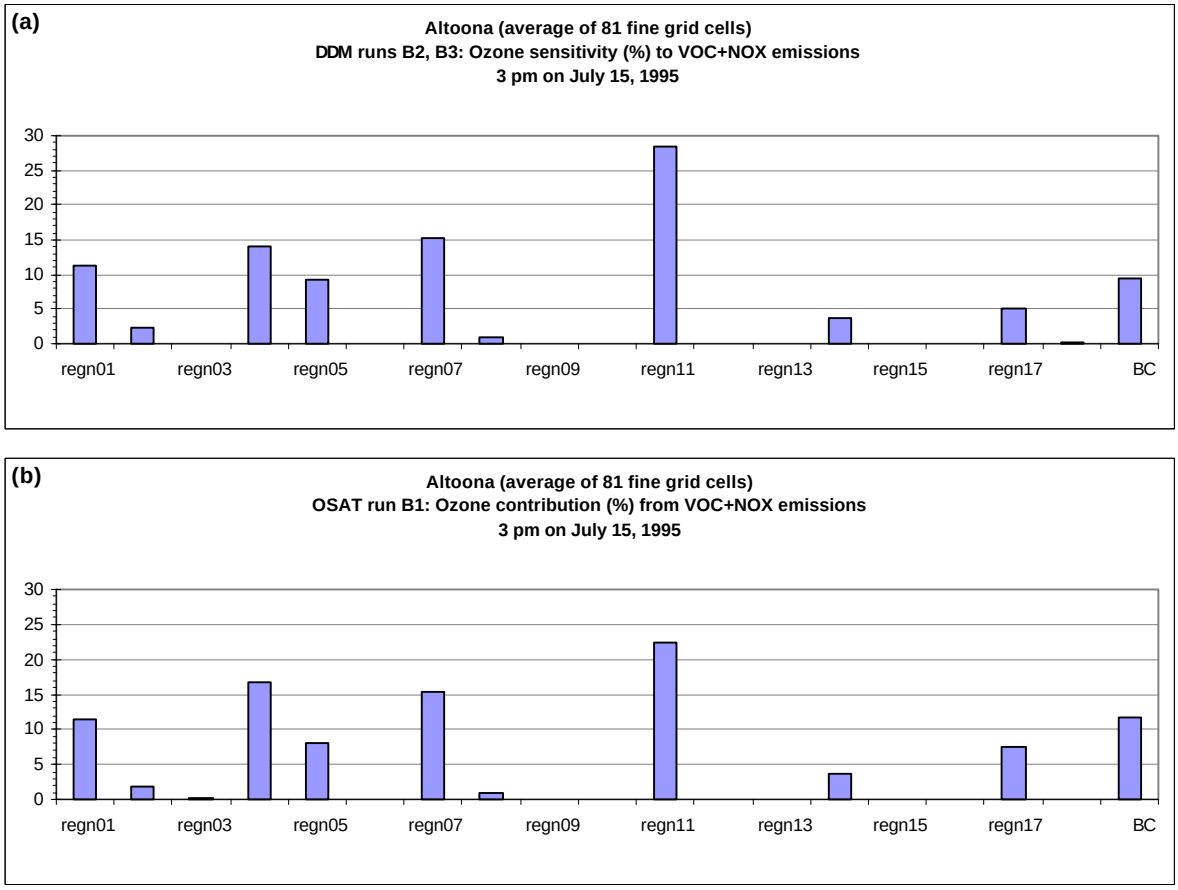

Figure 6-33. The (a) O_3 sensitivities to total NO_x and VOC emissions from 17 source areas, ICs, and BCs predicted by DDM and (b) O_3 contributions of total NO_x and VOC emissions from 17 source areas, ICs, and BCs predicted by OSAT at 3 p.m. on July 15 under the EPA 2007 base emission scenario (DDM base runs B2 and B3 and OSAT base run B1) in Altoona.

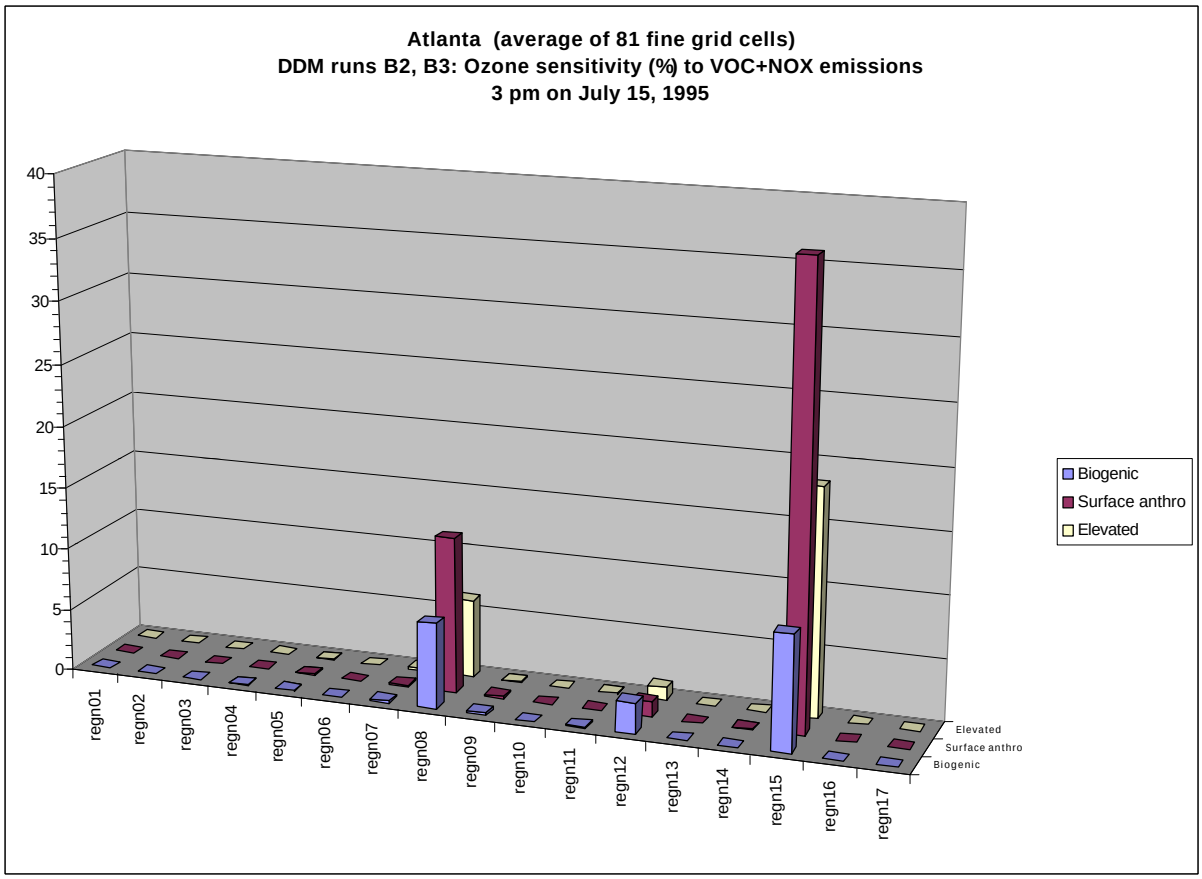

Figure 6-34. The O_3 sensitivities to total NO_x and VOC emissions from 3 source categories and 17 source areas predicted by DDM at 3 p.m. on July 15 under the EPA 2007 base emission scenario (DDM base runs B2 and B3) in Atlanta.

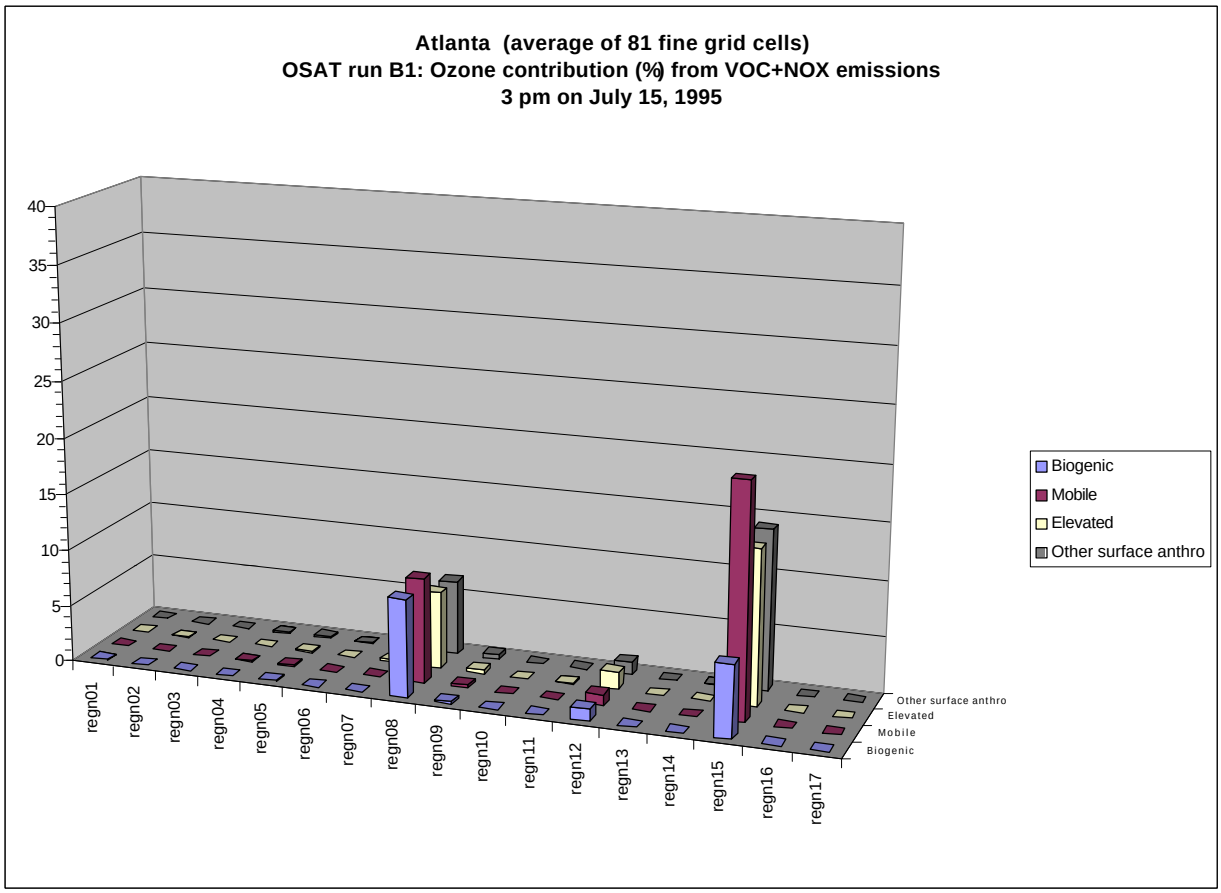

Figure 6-35. The O_3 contributions of total NO_x and VOC emissions from 3 source categories and 17 source areas predicted by OSAT at 3 p.m. on July 15 under the EPA 2007 base emission scenario (OSAT base run B1) in Atlanta.

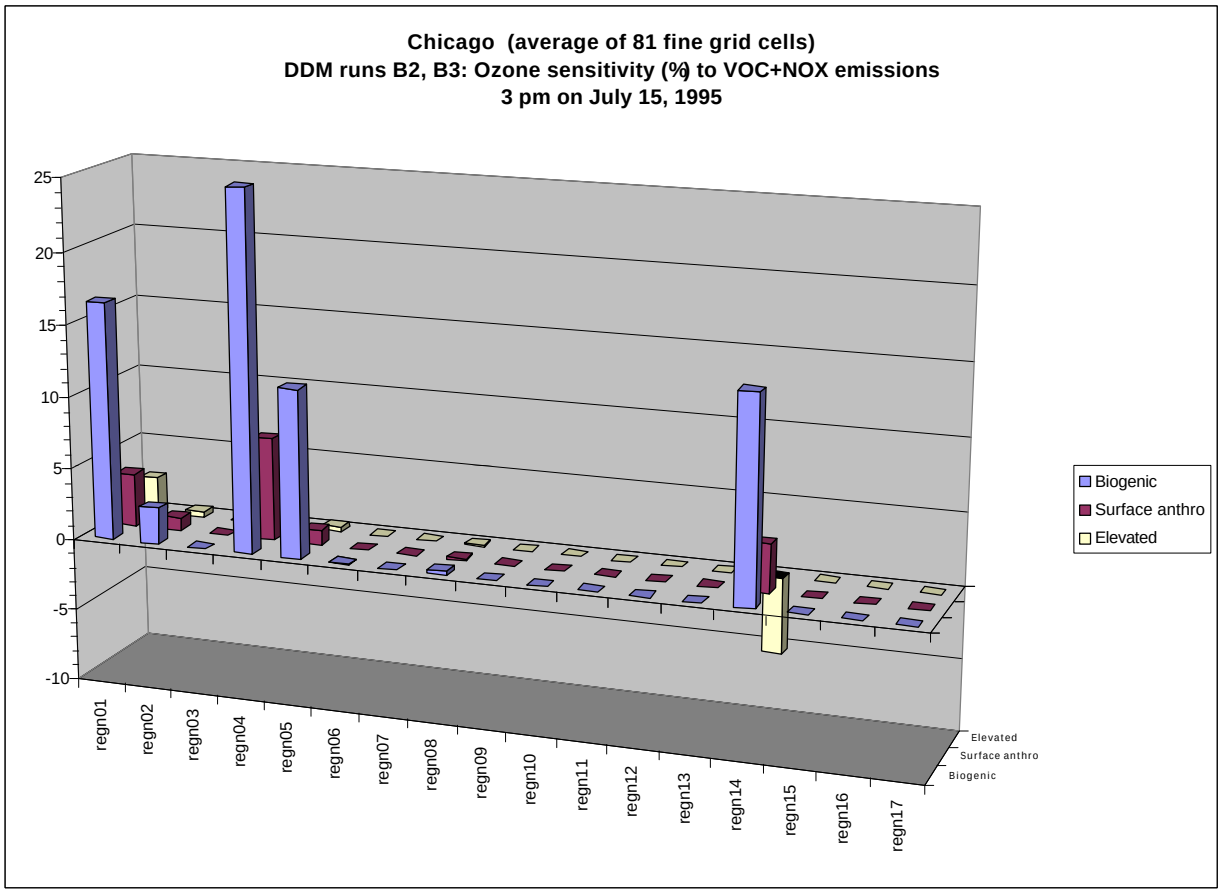

Figure 6-36. The O_3 sensitivities to total NO_x and VOC emissions from 3 source categories and 17 source areas predicted by DDM at 3 p.m. on July 15 under the EPA 2007 base emission scenario (DDM base runs B2 and B3) in Chicago.

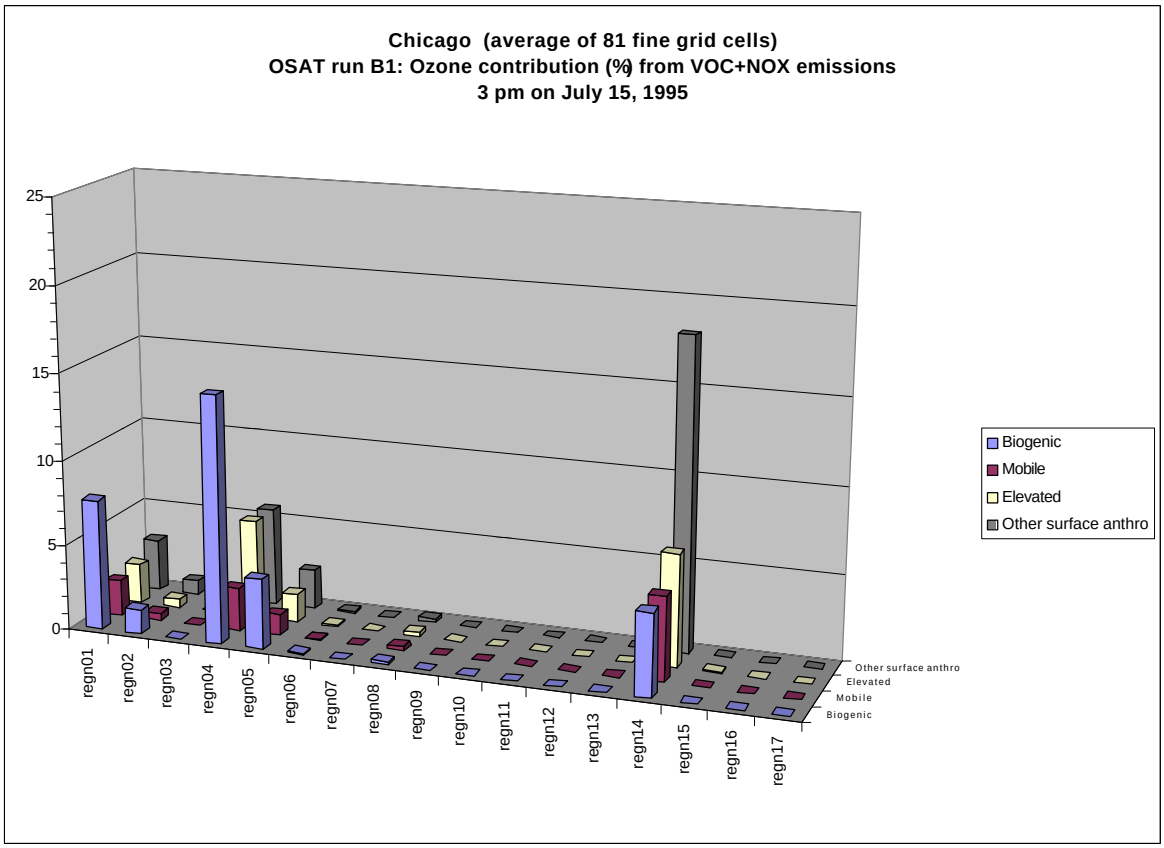

Figure 6-37. The O_3 contributions of total NO_x and VOC emissions from 3 source categories and 17 source areas predicted by OSAT at 3 p.m. on July 15 under the EPA 2007 base emission scenario (OSAT base run B1) in Chicago.

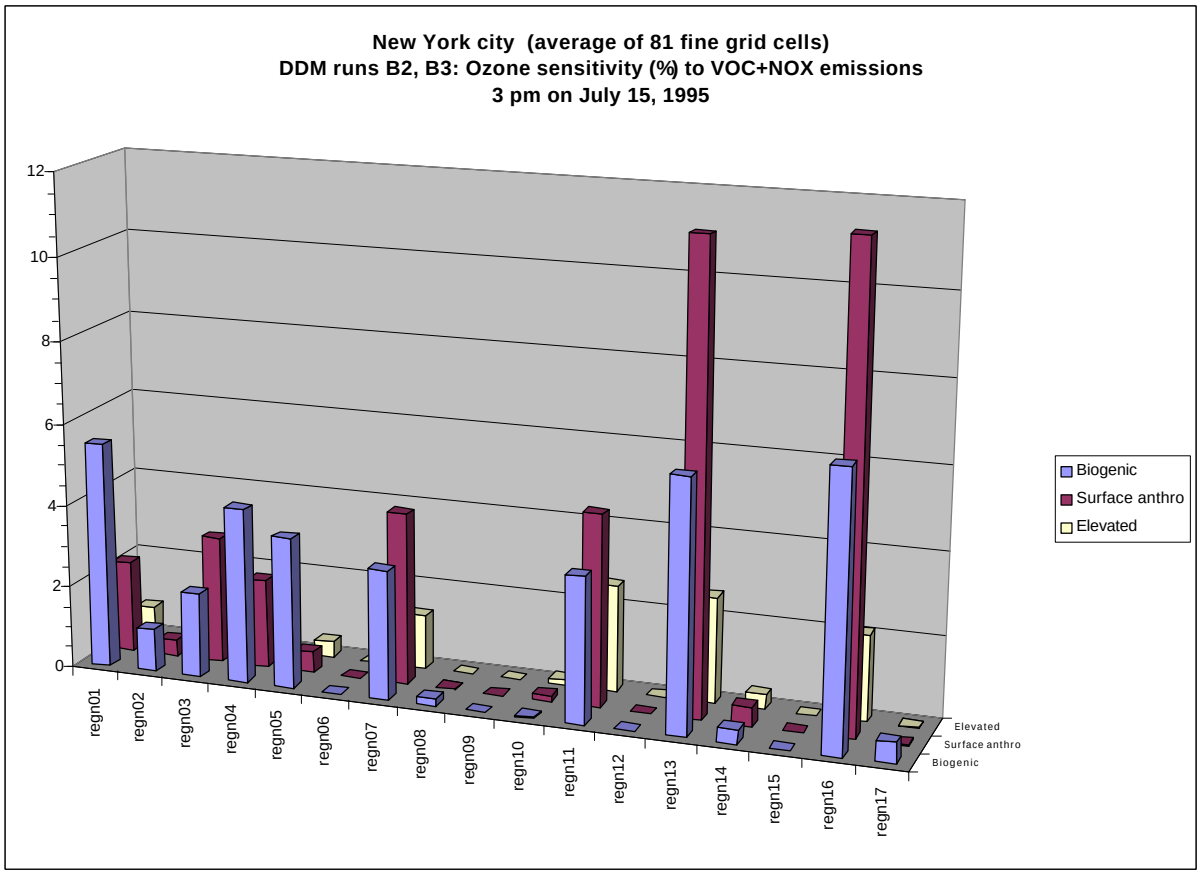

Figure 6-38. The O_3 sensitivities to total NO_x and VOC emissions from 3 source categories and 17 source areas predicted by DDM at 3 p.m. on July 15 under the EPA 2007 base emission scenario (DDM base runs B2 and B3) in New York City.

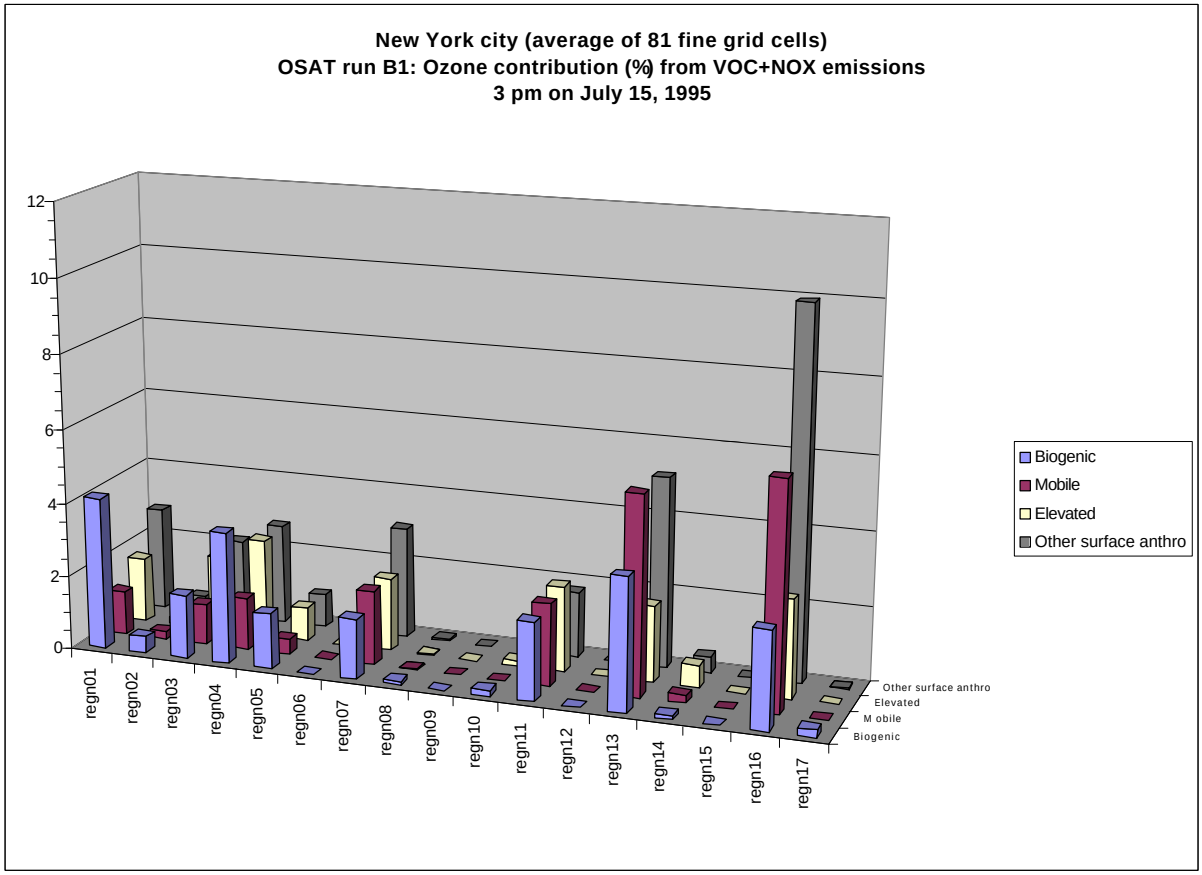

Figure 6-39. The O_3 contributions of total NO_x and VOC emissions from 3 source categories and 17 source areas predicted by OSAT at 3 p.m. on July 15 under the EPA 2007 base emission scenario (OSAT base run B1) in New York City.

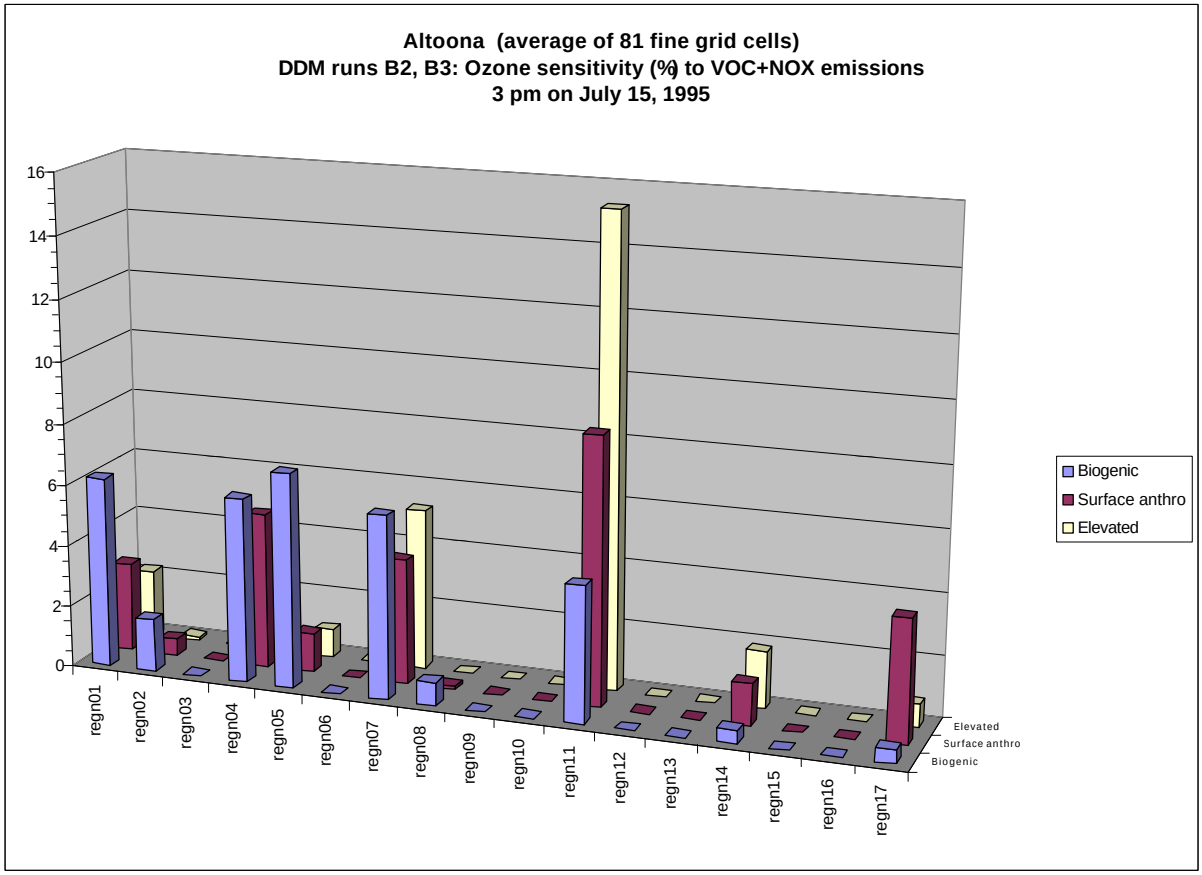

Figure 6-40. The O_3 sensitivities to total NO_x and VOC emissions from 3 source categories and 17 source areas predicted by DDM at 3 p.m. on July 15 under the EPA 2007 base emission scenario (DDM base runs B2 and B3) in Altoona.

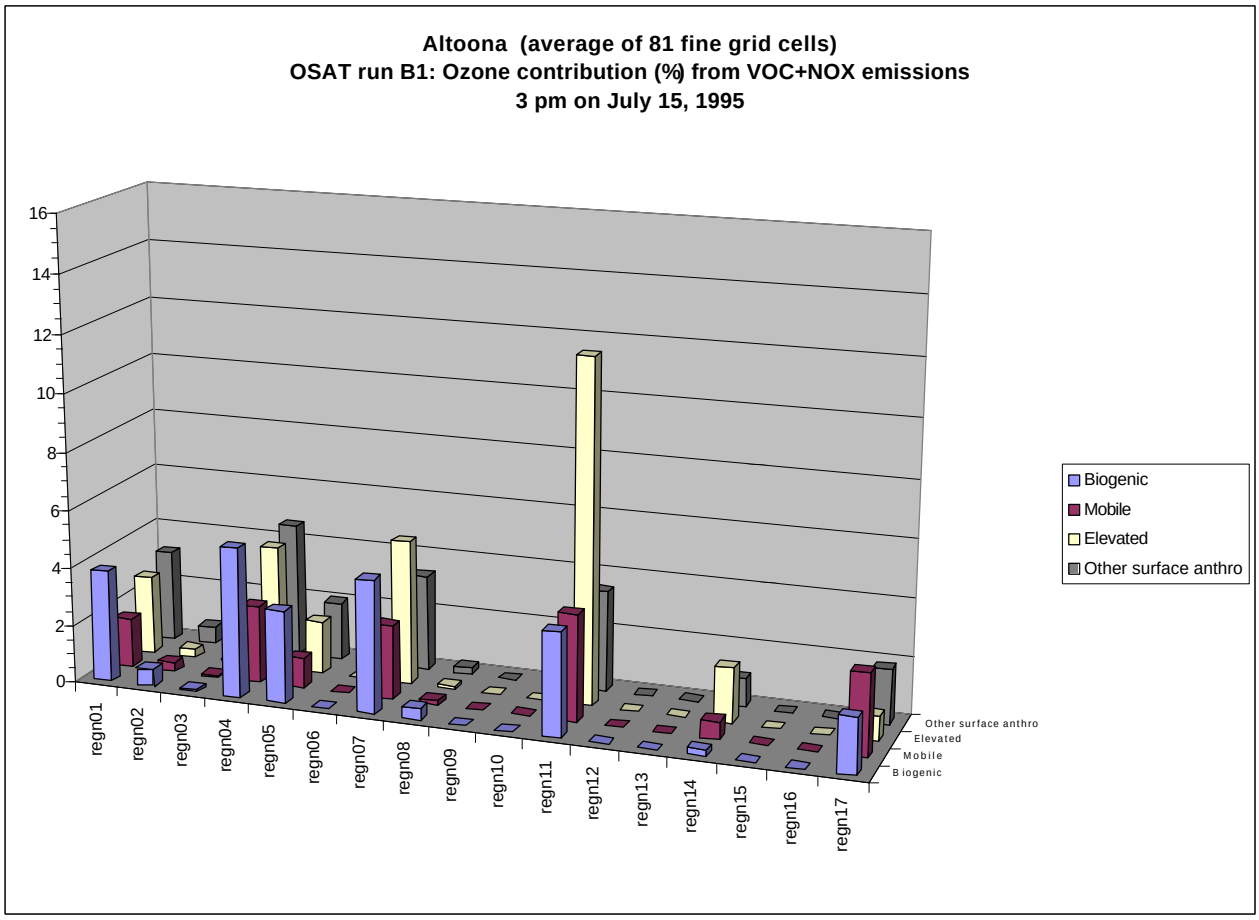

Figure 6-41. The O_3 contributions of total NO_x and VOC emissions from 3 source categories and 17 source areas predicted by OSAT at 3 p.m. on July 15 under the EPA 2007 base emission scenario (OSAT base run B1) in Altoona.

Figures 6-34 and 6-35, for the local sources (i.e., source area 15), DDM predicts that the biogenic, surface anthropogenic, and elevated anthropogenic emissions contribute 9%, 37%, and 18% of the total O_3 sensitivity, respectively, and OSAT predicts that their contributions to the total O_3 concentration are 6%, 35% (21% from the on-road mobile sources, and 14% from the other surface anthropogenic sources), and 14%, respectively. For the surrounding sources (i.e., source area 8), DDM predicts that the biogenic, surface anthropogenic, and elevated anthropogenic emissions contribute to 7%, 13%, 6% of the total O_3 sensitivity, respectively, and OSAT predicts their contributions to the total O_3 concentration are 9%, 16% (9% from the on-road mobile sources, and 7% from the other surface anthropogenic sources), and 7%, respectively.

Chicago

In Chicago (see Figure 6-31), DDM predicts that both the surrounding (i.e., source area 4) and the upwind (i.e., source areas 1, 5, and 2) emissions are the most important sources, contributing to 38% and 40% of the total O_3 sensitivity. The secondary contributors include the local emissions (i.e., source area 14) and BCs, contributing to 12% and 9.5% of the total O_3 sensitivity, respectively. Whereas OSAT predicts that the local and surrounding emissions (i.e., source areas 14 and 4) and the upwind emissions (i.e., source areas 1, 5, and 2) are the most important sources, contributing 34%, 28% and 27.5% of the total O_3 concentrations, respectively. Those predictions indicate that both transport and photochemistry could be important to O_3 formation in Chicago. BCs are the secondary contributor in this receptor, contributing 9.5% of the total O_3 sensitivity by DDM and 8% of the total O_3 concentration by OSAT. The significant differences in the contributions from the local and surrounding emissions predicted by DDM and OSAT can also be seen in Figures 6-36 and 6-37. For the local sources, DDM predicts that the biogenic, surface anthropogenic, and elevated anthropogenic emissions contribute 14%, 3%, and -5% of the total O_3 sensitivity, respectively, and OSAT predicts their contributions to the total O_3 concentration are 5%, 23% (5% from the on-road mobile sources, and 18% from the other surface anthropogenic sources), and 6.5% of the total O_3 concentration, respectively. The small contributions from the surface anthropogenic emissions and the negative contributions from the elevated anthropogenic emissions predicted by DDM are due to the fact that

DDM accounts for the large titration/inhibition effect of NO_x on O_3 chemistry. By contrast, OSAT overestimates the contributions from the surface and elevated anthropogenic emissions because the titration/inhibition effect of NO_x was not taken into account by OSAT. For the surrounding sources, DDM predicts that the biogenic, surface anthropogenic, and elevated anthropogenic emissions contribute 26%, 7%, 4% of the total O_3 sensitivity, respectively, and OSAT predicts their contributions to the total O_3 concentration are 14%, 8% (2% from the on-road mobile sources, and 6% from the other surface anthropogenic sources), and 6%, respectively. In Chicago, DDM predicts that the biogenic emissions are the most important sources for all source areas, contributing 71% of the total O_3 sensitivity. This is quite different from Atlanta where the surface anthropogenic emissions are the most important sources, contributing to 51% of the total O_3 sensitivity by DDM.

New York City

In New York City (see Figure 6-32), the source contributions by source area predicted by DDM and OSAT are quite similar. The local and surrounding sources only account for 40.2% of the total O_3 sensitivity by DDM and 37% of the total O_3 concentration by OSAT. The contributions from all upwind sources and BCs are 52% and 8% of the total O_3 sensitivity by DDM and 52% and 11% of the total O_3 concentration by OSAT, respectively. Therefore, O_3 formation in New York City is strongly affected by long-range transport of air pollutants from upwind regions. The most important upwind sources include the emissions from the source areas 4, 1, 7, 11, and 3, contributing 8%, 8%, 9%, 11%, and 7% of the total O_3 sensitivity by DDM and 10%, 10%, 9%, 8%, and 7% of the total O_3 concentration by OSAT, respectively. Both DDM and OSAT predict that the surface anthropogenic emissions are the most important source category for the local and surrounding sources, accounting for 11.5% and 11% of the total O_3 sensitivity by DDM and 16% and 10.5% of the total O_3 concentration by OSAT, respectively (see Figures 6-38 and 6-39). DDM predicts a lower contribution of the local surface anthropogenic emissions than OSAT because DDM accounts for the titration/inhibition effect of NO_x on O_3 chemistry whereas OSAT does not account for this effect. The contributions of the local and surrounding biogenic emissions predicted by DDM are higher than those by OSAT (7% vs. 3% for the local biogenic sources and

6% vs. 4% for the surrounding biogenic sources). The most important source category is different for different upwind sources. For example, both DDM and OSAT predict that the biogenic sources are the most important source category for the source areas 1 and 5, and the surface anthropogenic sources are the most important source category for the source areas 7 and 3, and 11. For the source area 4, the most important source category is the biogenic sources by DDM and the surface anthropogenic sources by OSAT.

Altoona

In Altoona (see Figure 6-33), both DDM and OSAT predict that the upwind emissions (e.g., source areas 1, 2, 4, 5, 7, and 14) are the most important sources, contributing to 57% of the total O_3 sensitivity by DDM and 58% of the total O_3 concentration by OSAT. This indicates that O_3 formation in Altoona is also strongly affected by long-range transport of pollutants from upwind regions. The contribution of the local and surrounding sources (i.e., source areas 17 and 11) is 34% by DDM and 30% by OSAT. The contribution of BCs is only 9.5% by DDM and 12% by OSAT. The most important upwind sources include the emissions from the source areas 4, 7, 1, and 5, contributing 14%, 15%, 11%, and 9% of the total O_3 sensitivity by DDM and 17%, 15%, 11.5%, and 8% of the total O_3 concentrations by OSAT, respectively. For the local sources, the surface anthropogenic emissions are the most important sources, contributing 4% of the total O_3 sensitivity by DDM and 5% of the total O_3 concentration by OSAT, as shown in Figures 6-40 and 6-41. For the surrounding sources, the elevated anthropogenic emissions are the most important sources, contributing to 15% of the total O_3 sensitivity by DDM and 12% of the total O_3 concentration by OSAT. DDM predicts that the biogenic emissions are the most important source category for major upwind emissions, whereas OSAT predicts that the surface anthropogenic (on-road mobile + other surface anthropogenic) emissions are the most important source category for major upwind emissions (except for source area 5, where the biogenic emissions are the most important source category).

Figures 6-42 To 6-45 show hourly O_3 change from different processes as a function of time in the four receptors predicted by the IPR component of PA. In Atlanta (see Figure 6-42), chemistry was the most important process to the local and instantaneous O_3 production at the peak O_3 hour, followed by lateral boundary transport,

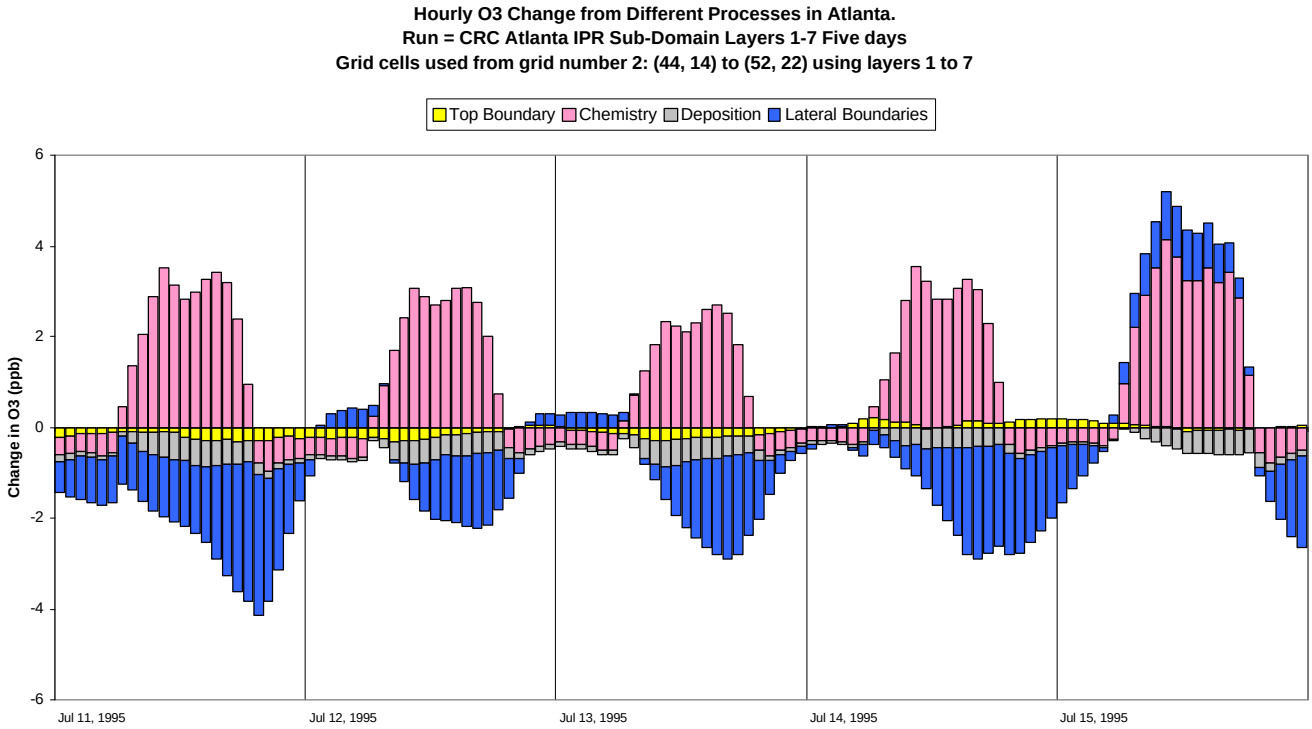

Figure 6-42. The change in hourly O_3 concentration in ppb caused by different processes as a function of time in Atlanta. The data shown were obtained by taking an average over the 81 fine grid cells for layers 1 to 7 in the receptor region. Lateral boundary inflow/outflow has been aggregated to a single net term.

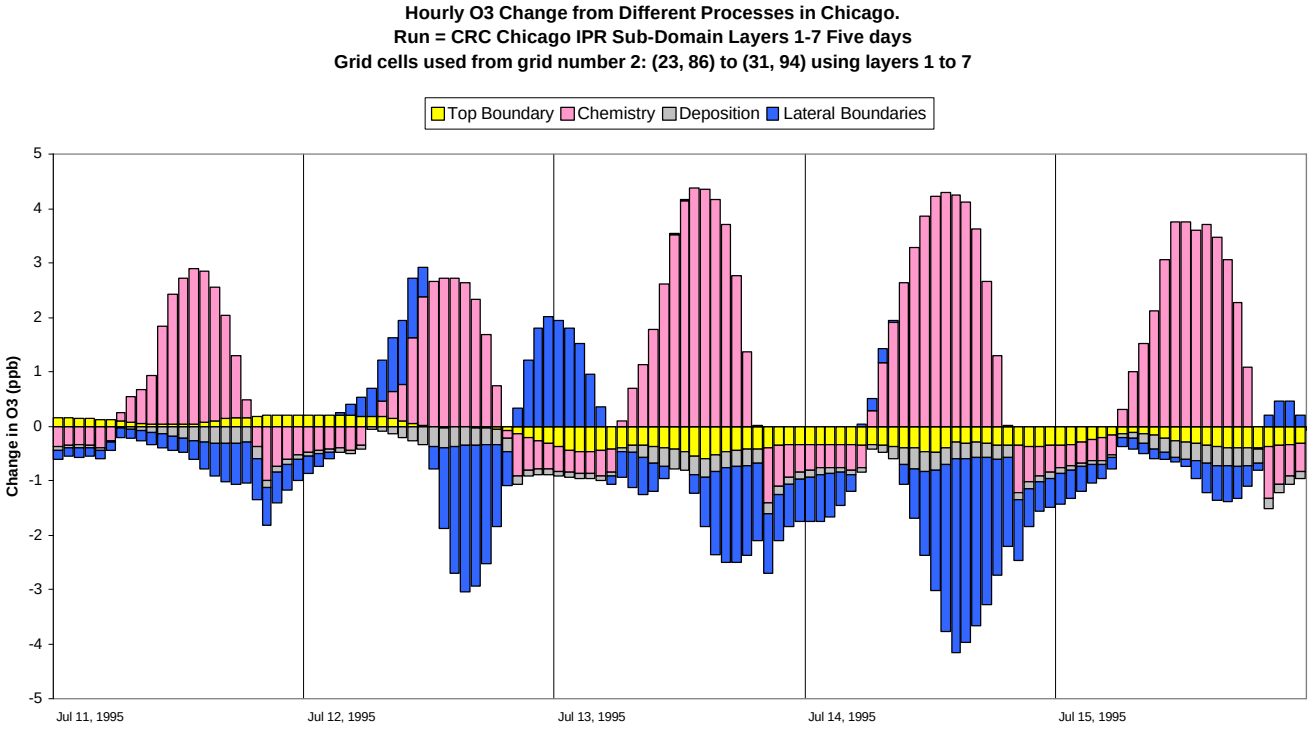

Figure 6-43. The change in hourly O_3 concentration in ppb caused by different processes as a function of time in Chicago. The data shown were obtained by taking an average over the 81 fine grid cells for layers 1 to 7 in the receptor region. Lateral boundary inflow/outflow has been aggregated to a single net term.

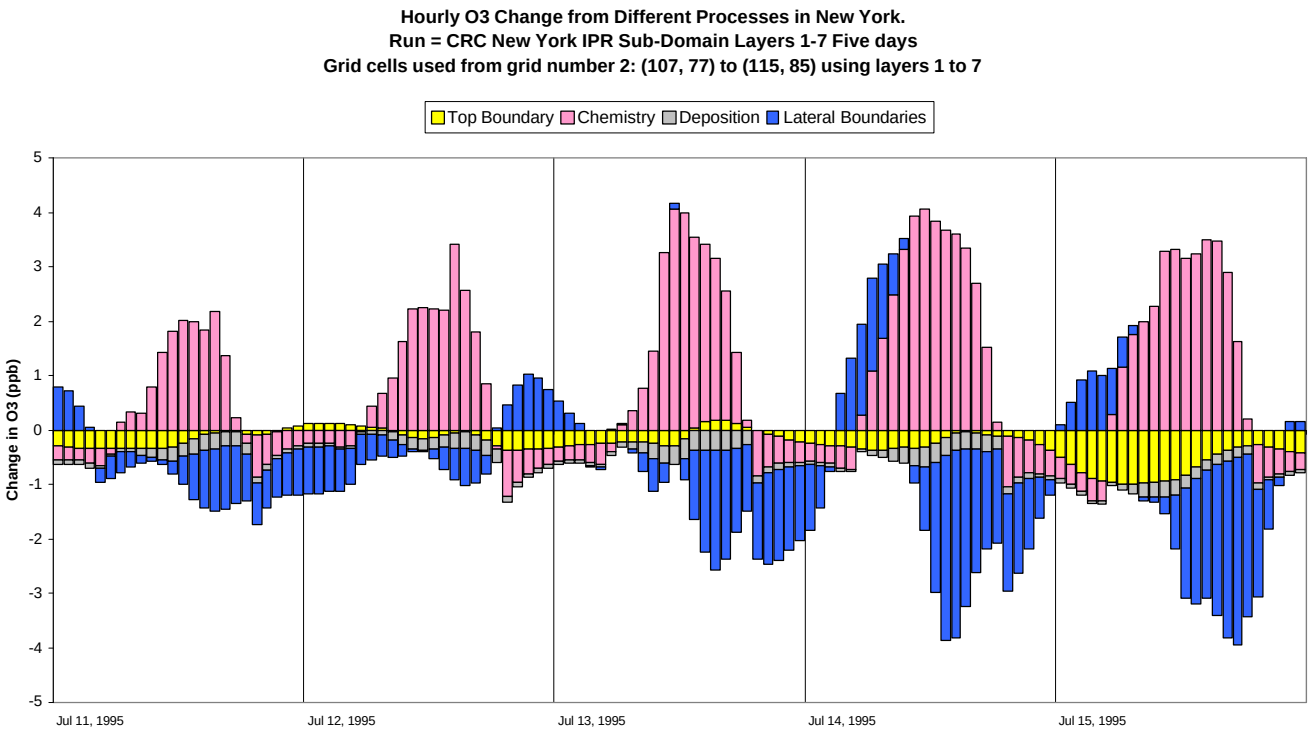

Figure 6-44. The change in hourly O_3 concentration in ppb caused by different processes as a function of time in New York City. The data shown were obtained by taking an average over the 81 fine grid cells for layers 1 to 7 in the receptor region. Lateral boundary inflow/outflow has been aggregated to a single net term.

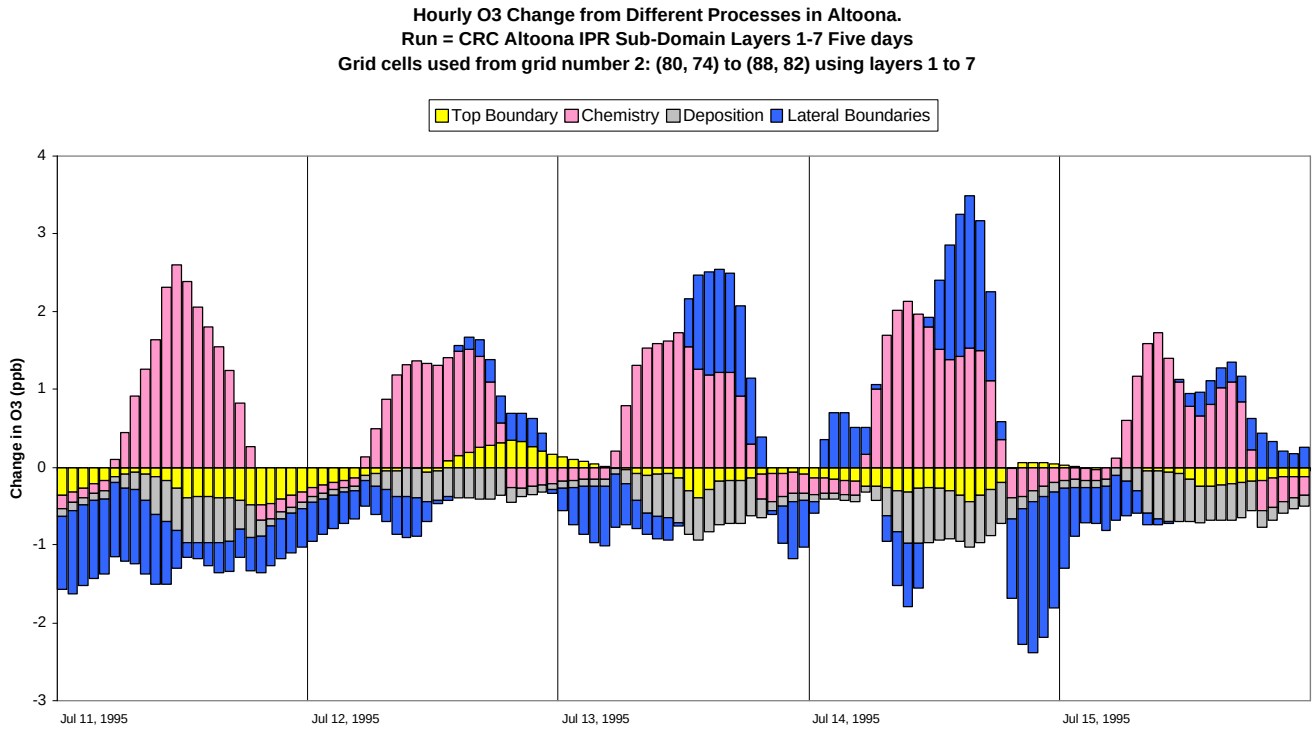

Figure 6-45. The change in hourly O_3 concentration in ppb caused by different processes as a function of time in Altoona. The data shown were obtained by taking an average over the 81 fine grid cells for layers 1 to 7 in the receptor region. Lateral boundary inflow/outflow has been aggregated to a single net term.

deposition, and top boundary transport. The latter two processes only contributed to a small change (< -0.6 and -0.3 ppb, respectively) in peak hourly O_3 concentration. The net effect of lateral boundary transport on peak hourly O_3 concentrations is negative on July 11-14 and positive on July 15.

In Chicago (see Figure 6-43), chemistry was the predominant process to the local and instantaneous O_3 production at the peak O_3 hour. The second important process was lateral boundary transport on July 11, 12 and 14 and deposition July 13. The contributions of lateral boundary transport, top boundary transport, and deposition to changes in peak hourly O_3 concentration were almost equal (-0.3 ppb) on July 15. The lateral boundary transport was more important on July 14 than the other days. All processes except for chemistry decreased the peak hourly O_3 concentrations on the five days.

In New York City (see Figure 6-44), chemistry is the predominant process to changes in peak hourly O_3 concentrations on July 11, 12, 13, and 15. Chemistry and lateral boundary transport were almost equally important on July 14, but their effect was just the opposite, with a contribution of 4.3 ppb and -3.0 ppb to the peak hourly O_3 concentration, respectively.

In Altoona (see Figure 6-45), the most important process to the peak hourly O_3 formation was chemistry on July 11, 12, and 15 and lateral boundary transport on July 13 and 14. Lateral boundary transport had a positive effect on O_3 concentrations (i.e., increased the peak hourly O_3 concentrations) on July 12-15, which was different from that in other urban receptors (except for Atlanta on July 15). In addition, the relative importance of deposition was greater in Altoona than in other urban receptors.

Although the results from PA cannot be directly compared to those from DDM and OSAT, the PA results indicated the relative importance of chemistry and transport that were somewhat qualitatively consistent with those from DDM and OSAT. For example, for July 15, PA predicted that the peak hourly O_3 formation was affected mostly by chemistry in Atlanta and Chicago and that lateral transport was relatively more important in New York City and Altoona, as compared to Atlanta and Chicago. As expected, PA also predicted results that were inconsistent with those from DDM and OSAT. For example, DDM and OSAT predicted that upwind emissions contributed to

40% of the total O_3 sensitivity and 27.5% of the total O_3 concentrations at the peak O_3 hour in Chicago on July 15, whereas PA predicted a negative net effect of lateral transport for this receptor. These differences are due to the fact that DDM and OSAT accounted for the time history of the air parcels whereas PA provided information on local and instantaneous O_3 formation.

6.2.3 Detailed Chemical Analysis

OSAT is not designed to provide detailed chemical analysis. While DDM has the capability to characterize the chemistry of the system, the current implementation of DDM does not allow calculations of sensitivities of model predictions to chemical rate constants and product yields. The IRR component of PA is designed to elucidate important chemical pathways and to identify key chemical characteristics. This is particularly useful for investigating mechanistic differences under different chemical regimes or between different mechanisms. It is also useful to investigate the relationships between O_3 and its precursors. Below we provide a detailed chemical analysis for the base case simulation with EPA 2007 emission inventory. The goal of this section was to provide a somewhat qualitative analysis and comparison of the O_3 production for the model episode and to suggest additional analysis that should be performed. Most likely this analysis will initially be performed interactively working with the model output and with various visualization and analysis tools. Eventually, as more experience is gained in analyzing the CPA, IPR and IRR outputs in grid models, it is expected that tools will be developed to automate these types of analyses.

A standard set of CPA output is shown in Figures 6-46 to 6-58. These include a subset of outputs listed in Table 1-1 that are generally useful in characterizing a model simulation. Plots are shown for both July 11 and July 14 to compare and contrast differences in the photochemistry for these two days. Figures 6-46 shows O_x production and confirms that the differences in O_3 on these two days are largely due to differences in photochemical activity. That is, differences in transported O_3 can be ruled out as an alternative explanation for the low large differences in O_3 in the northern part of the domain on July 14 and 15. Figure 6-46 is also useful for identifying the particular grid

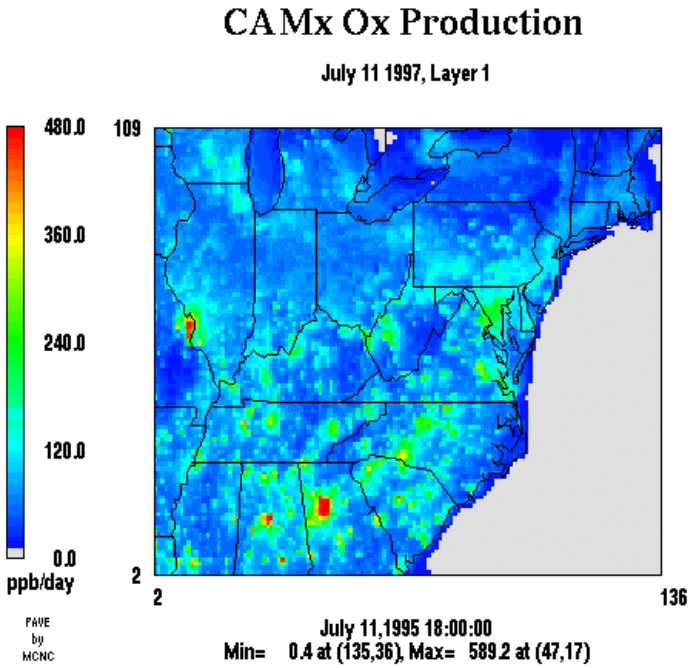

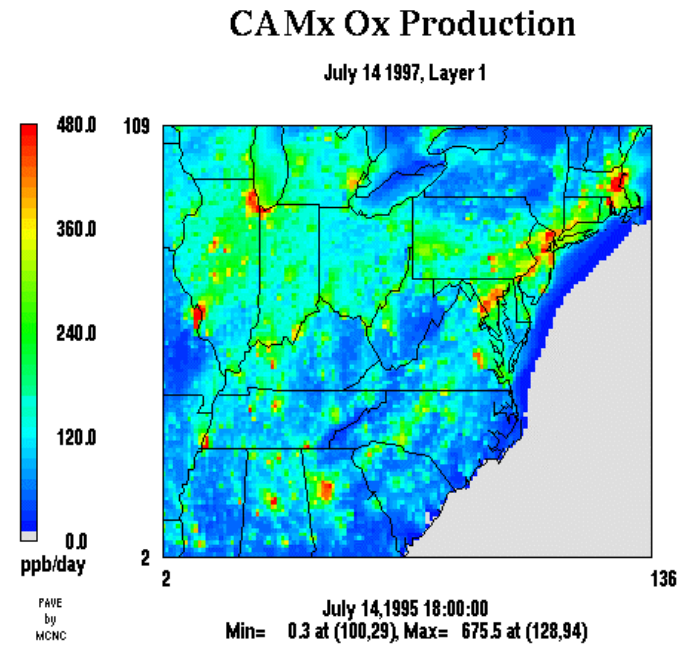

Figure 6-46. The daily O_x production predicted by PA under the EPA 2007 base emission scenario (PA base run B4) on July 11 (top) and July 14 (bottom).

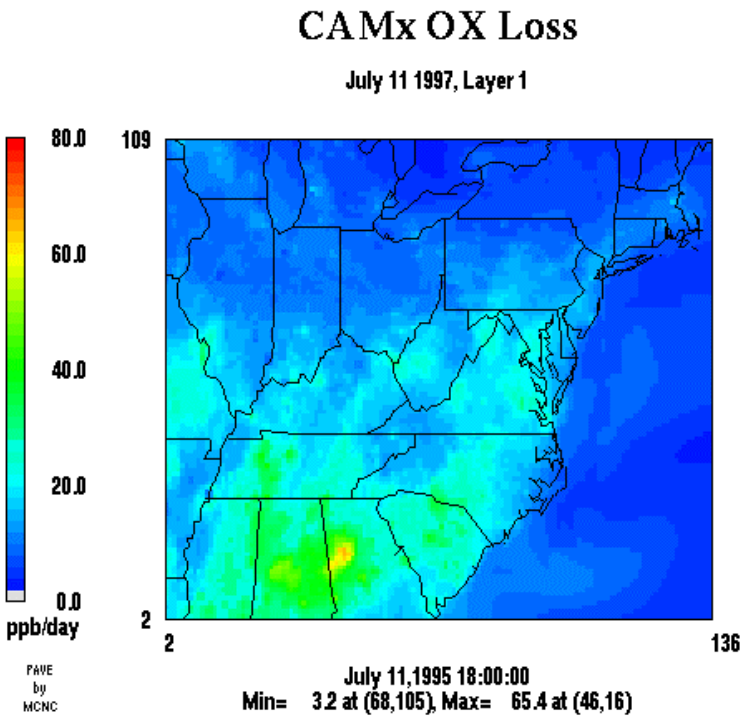

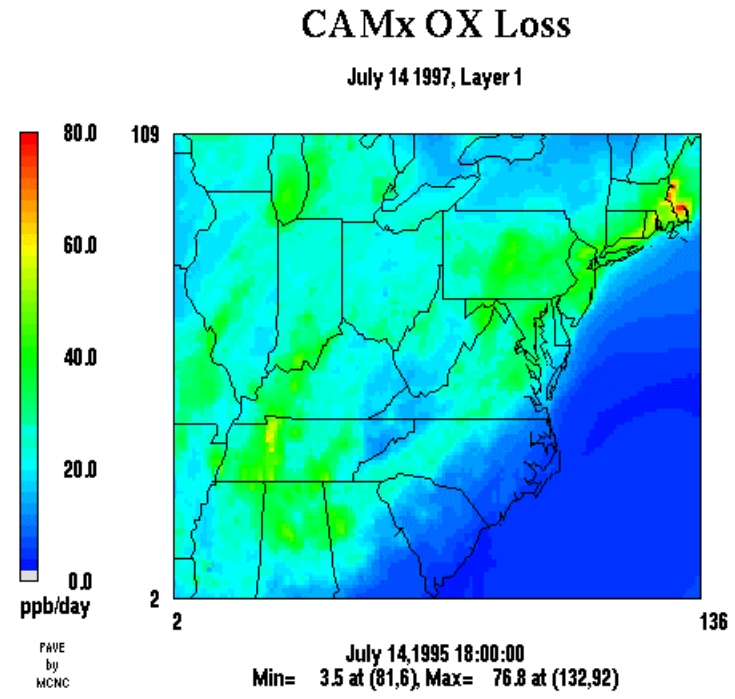

Figure 6-47. The daily O_x photochemical destruction predicted by PA under the EPA 2007 base emission scenario (PA base run B4) on July 11 (top) and July 14 (bottom).

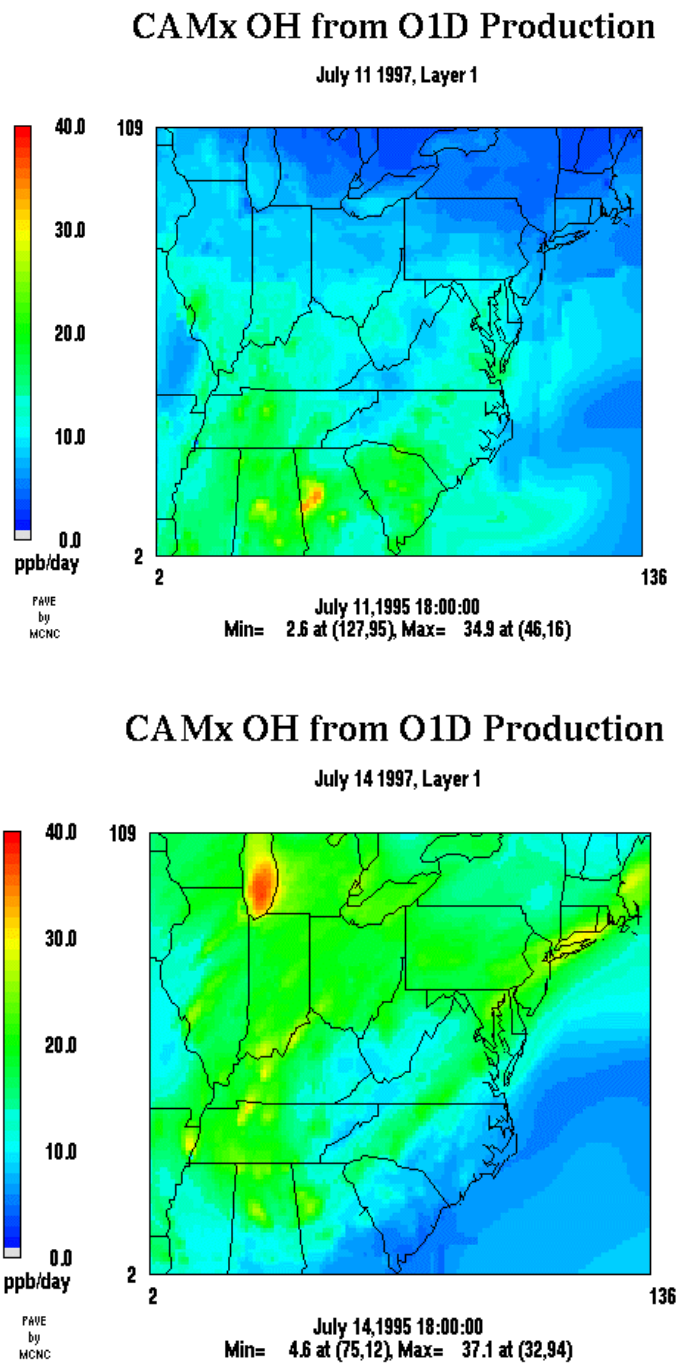

Figure 6-48. The daily OH initiation from O^1D predicted by PA under the EPA 2007 base emission scenario (PA base run B4) on July 11 (top) and July 14 (bottom).

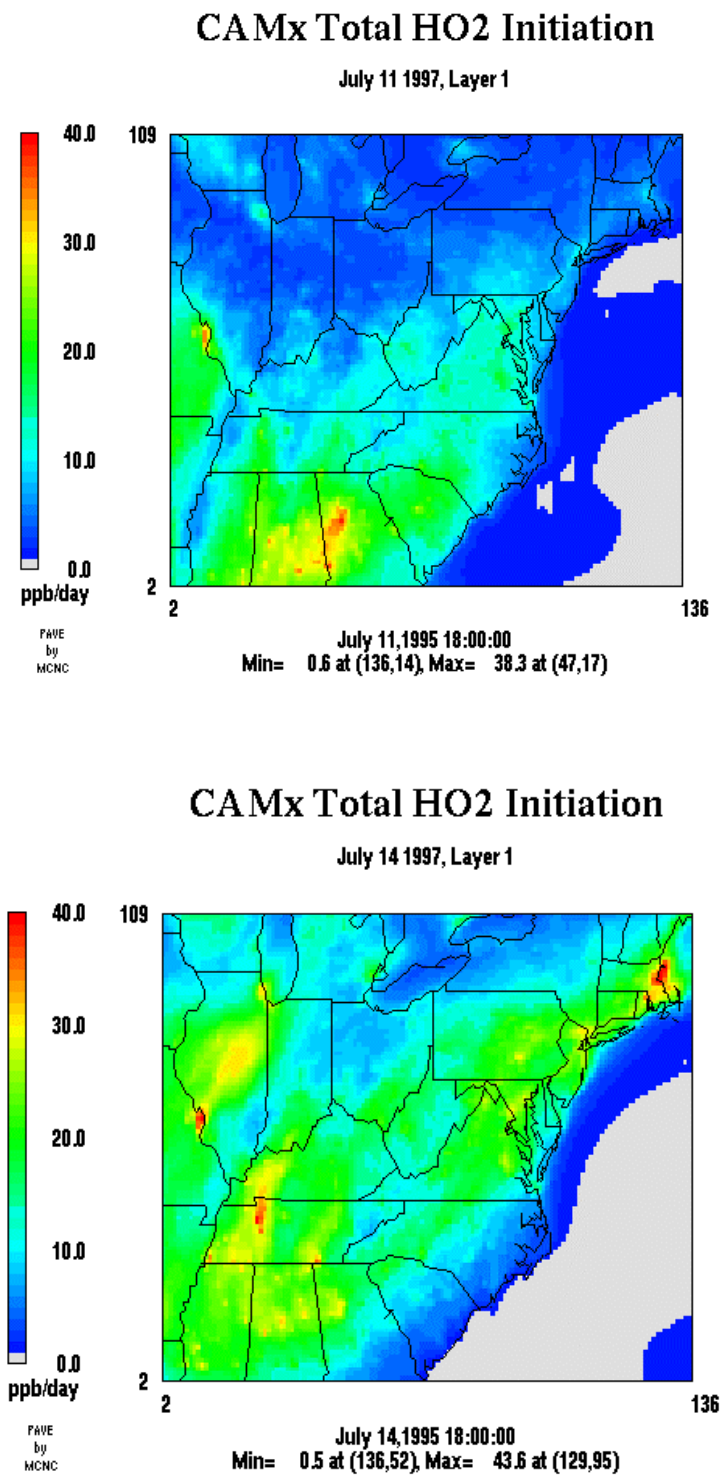

Figure 6-49. The daily HO_2 initiation predicted by PA under the EPA 2007 base emission scenario (PA base run B4) on July 11 (top) and July 14 (bottom).

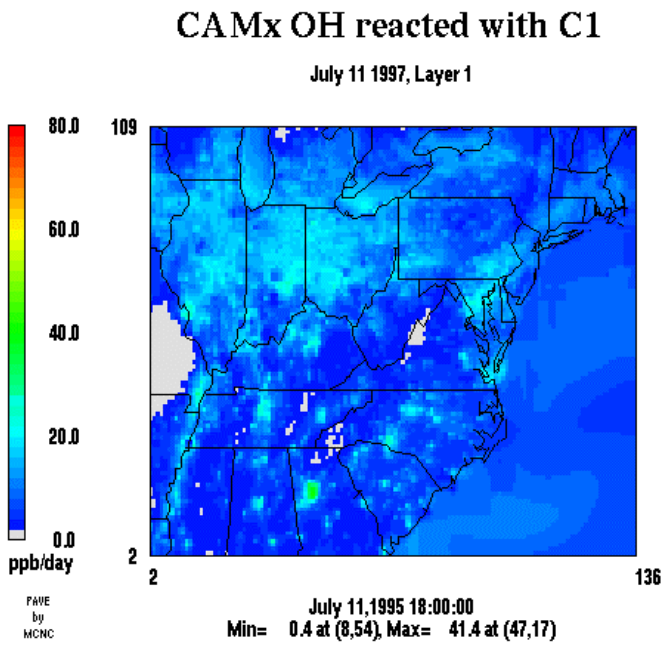

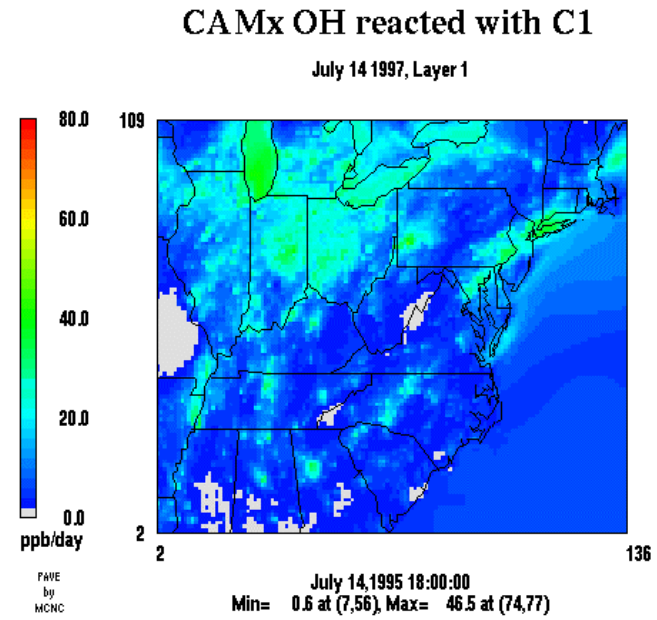

Figure 6-50. The daily OH reacted with CO and CH_4 predicted by PA under the EPA 2007 base emission scenario (PA base run B4) on July 11 (top) and July 14 (bottom).

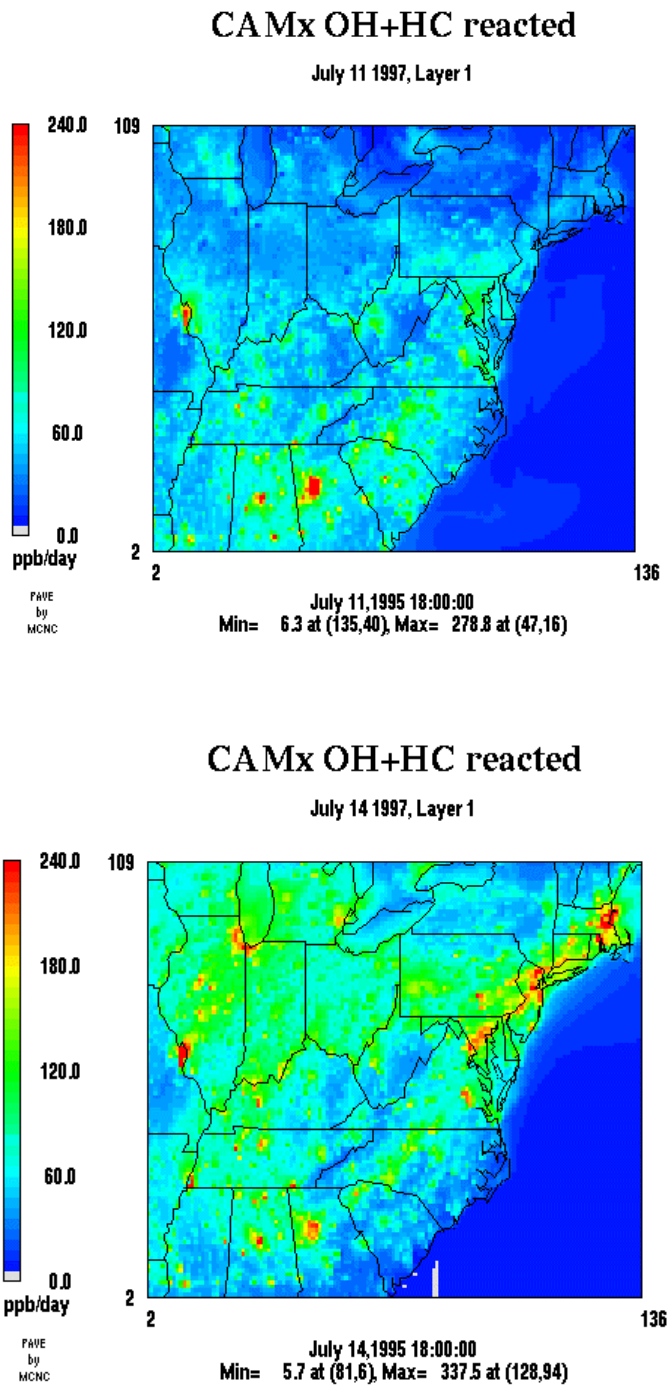

Figure 6-51. The daily OH reacted with all VOC species including CO and CH_4 but excluding biogenic VOC predicted by PA under the EPA 2007 base emission scenario (PA base run B4) on July 11 (top) and July 14 (bottom).

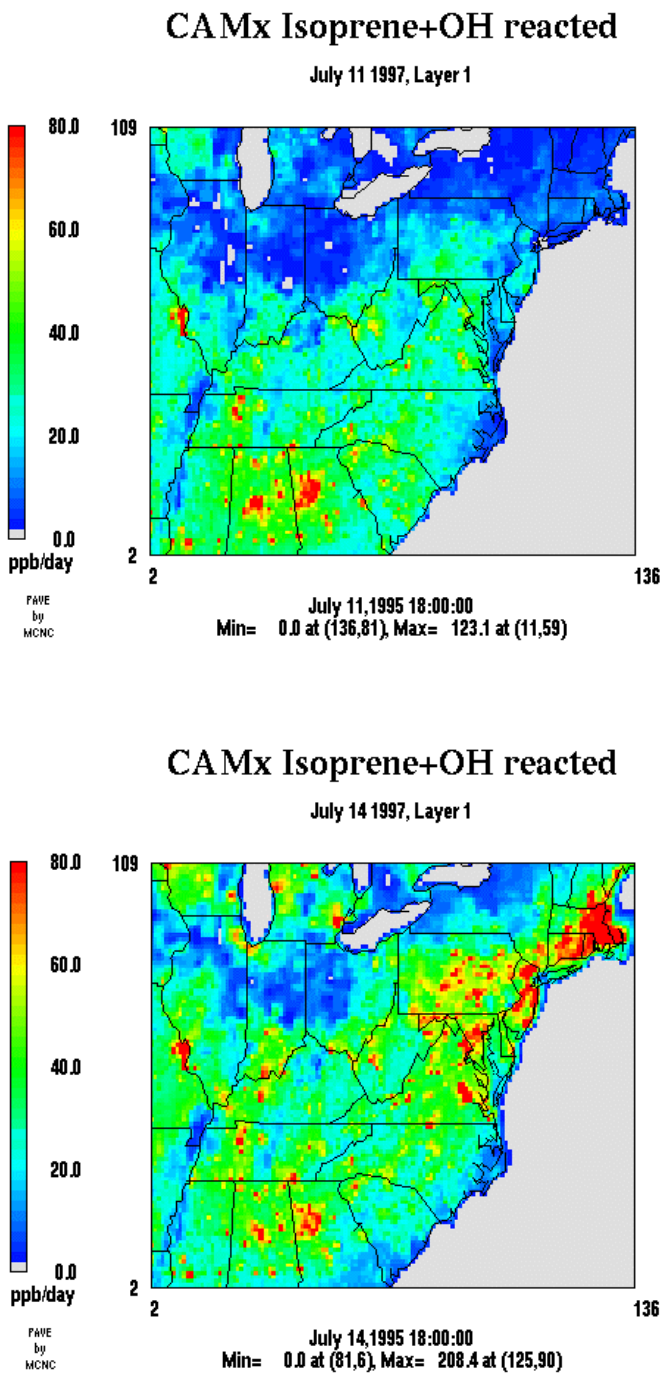

Figure 6-52. The daily OH reacted with isoprene predicted by PA under the EPA 2007 base emission scenario (PA base run B4) on July 11 (top) and July 14 (bottom).

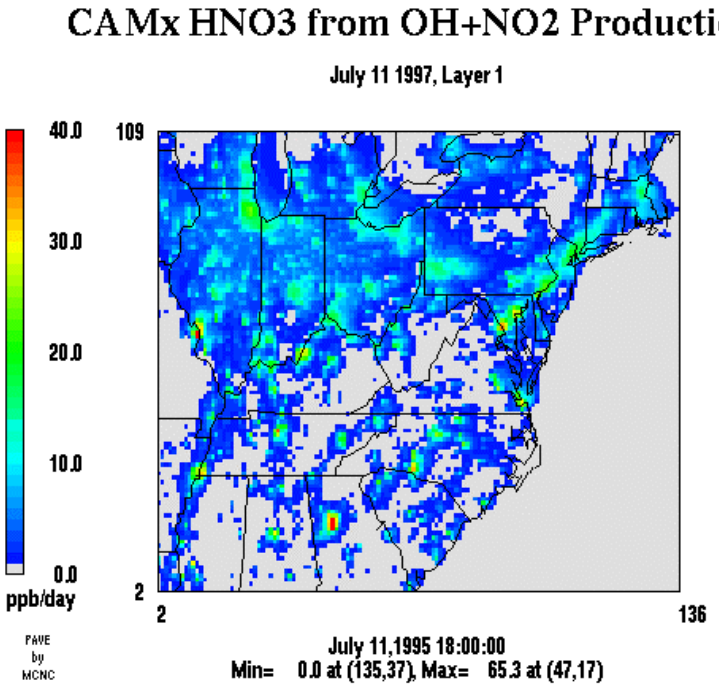

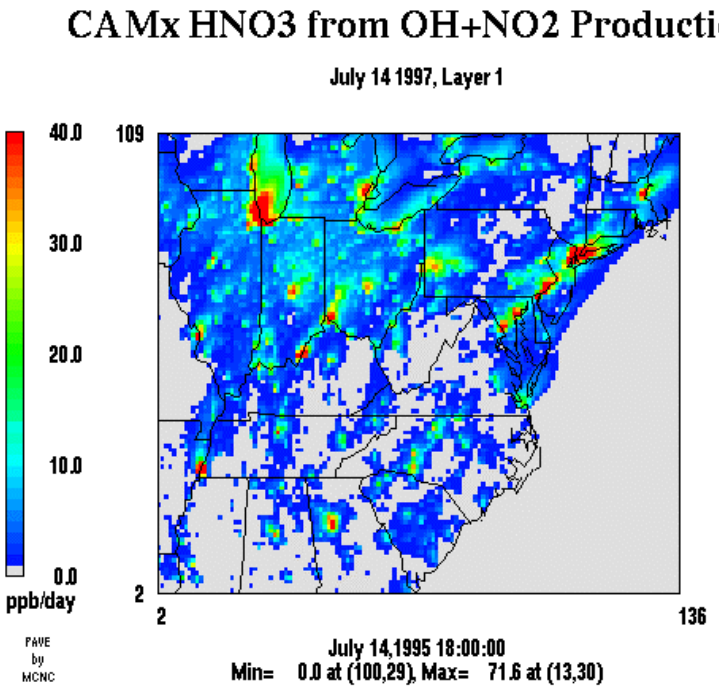

Figure 6-53. The daily HNO_3 production from $OH+NO_2$ predicted by PA under the EPA 2007 base emission scenario (PA base run B4) on July 11 (top) and July 14 (bottom).

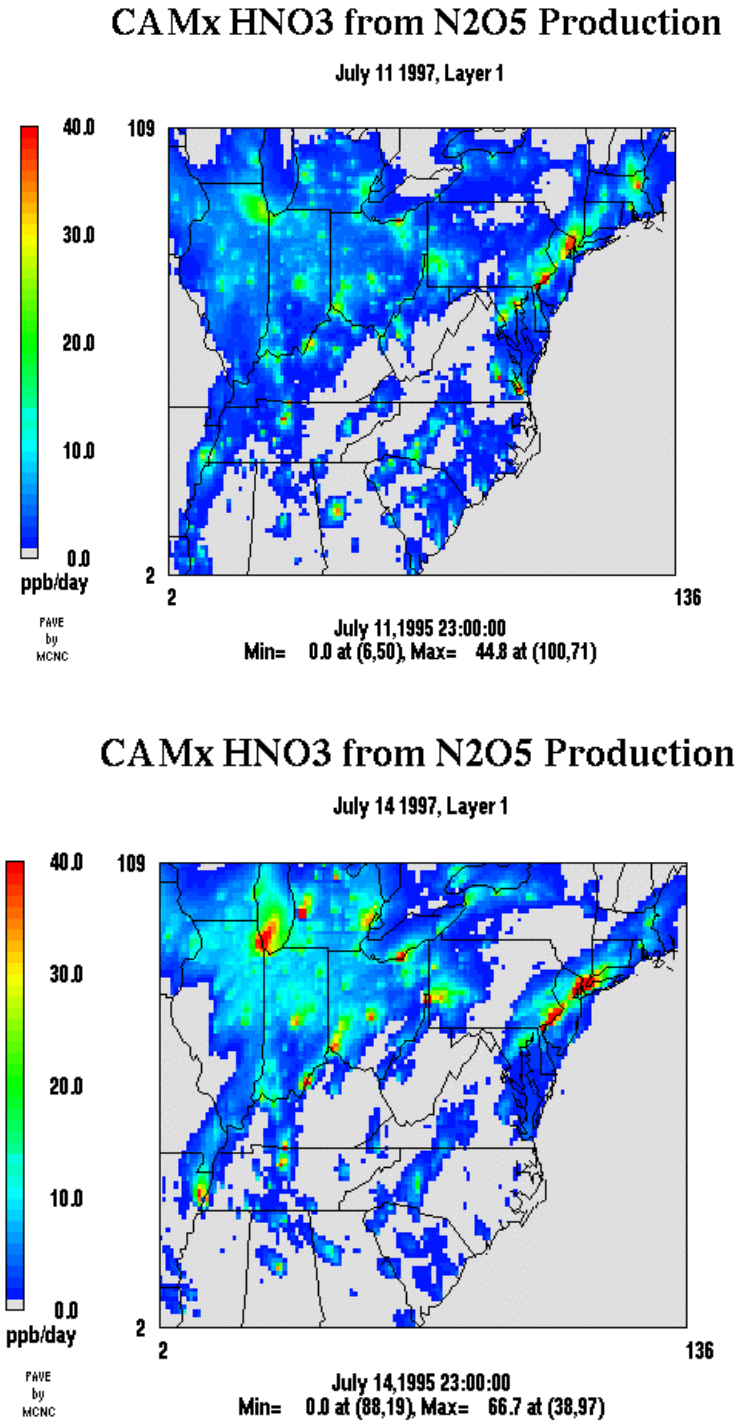

Figure 6-54. The daily HNO_3 production from N_2O_5 predicted by PA under the EPA 2007 base emission scenario (PA base run B4) on July 11 (top) and July 14 (bottom).

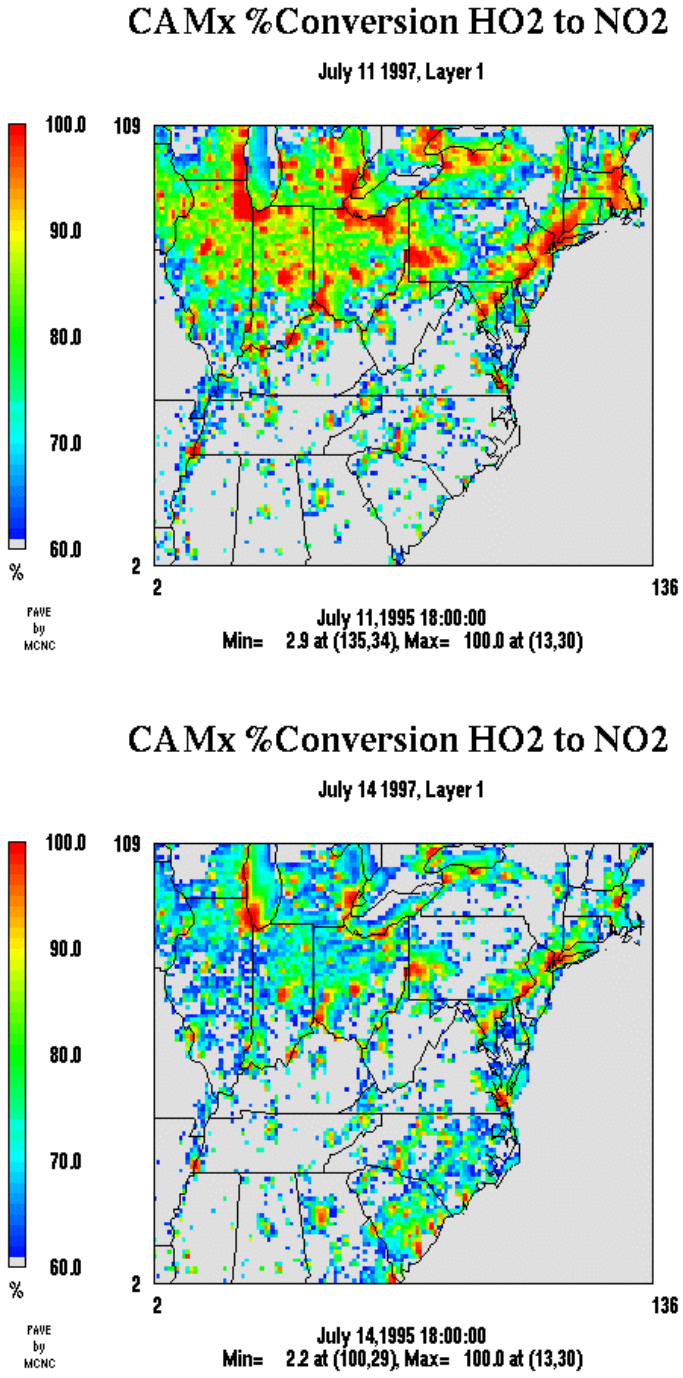

Figure 6-55. The percent conversion of HO_2 to NO predicted by PA under the EPA 2007 base emission scenario (PA base run B4) on July 11 (top) and July 14 (bottom).

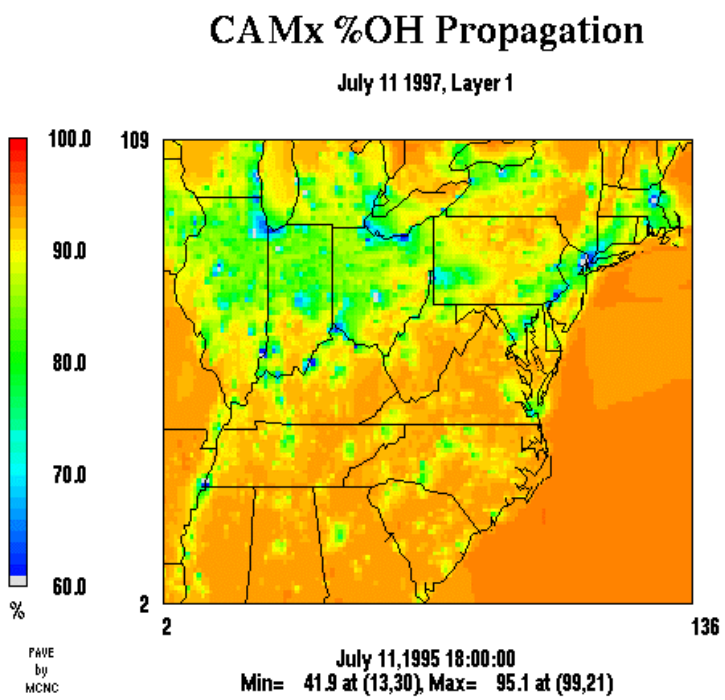

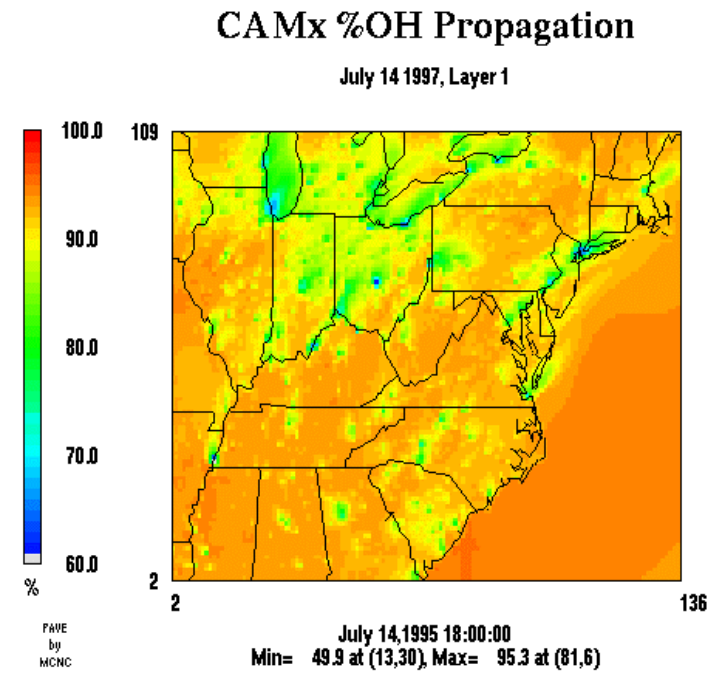

Figure 6-56. The percent of OH reacting in radical propagation reactions predicted by PA under the EPA 2007 base emission scenario (PA base run B4) on July 11 (top) and July 14 (bottom).

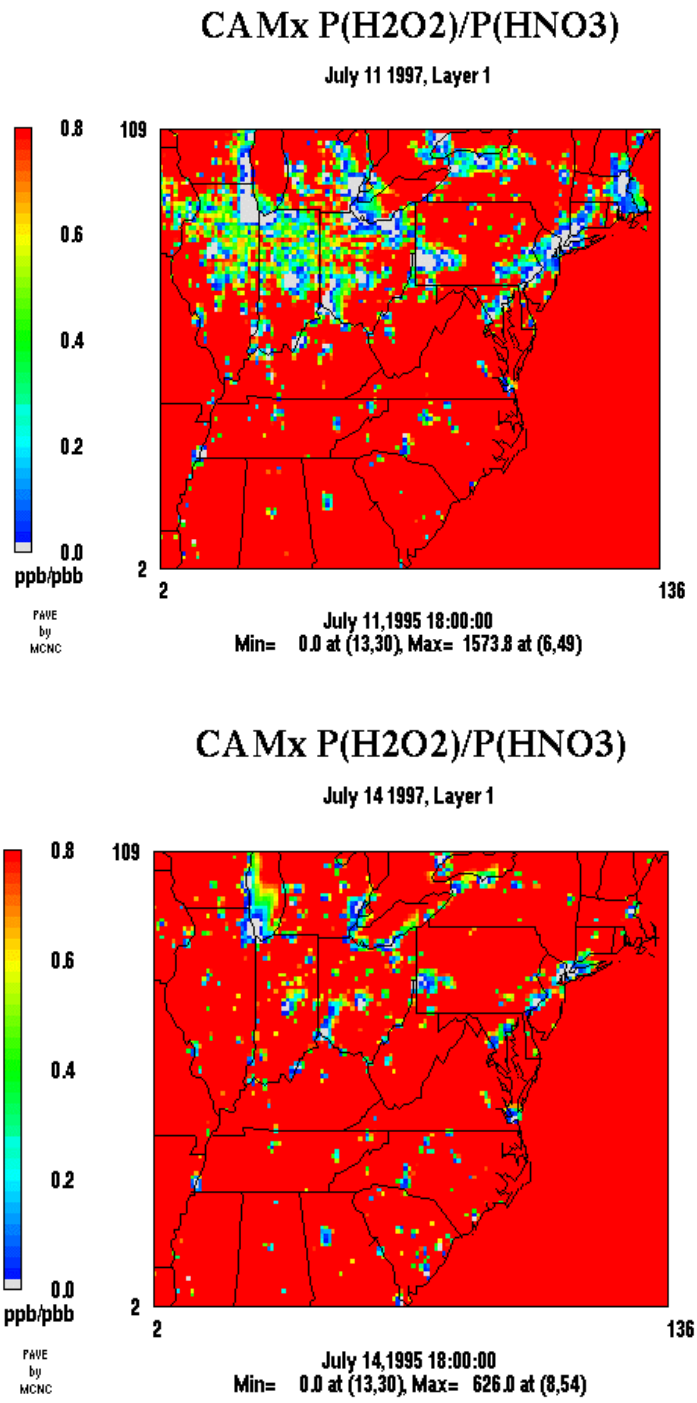

Figure 6-57. The indicator ratio of $P(H_2O_2)/P(HNO_3)$ predicted by PA under the EPA 2007 base emission scenario (PA base run B4) on July 11 (top) and July 14 (bottom).

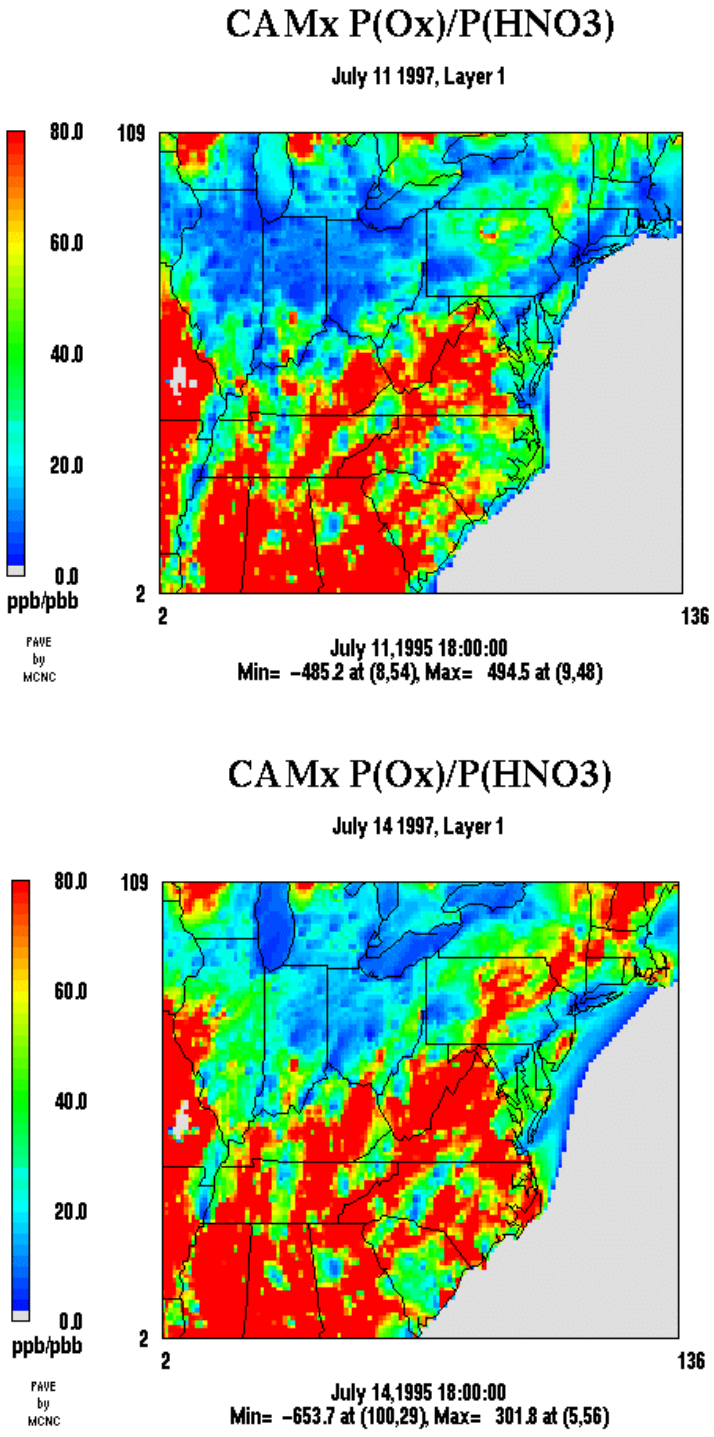

Figure 6-58. The production efficiency of O_x per NO_x converted to HNO_3 predicted by PA under the EPA 2007 base emission scenario (PA base run B4) on July 11 (top) and July 14 (bottom).

cells in which O_x production occurred on each day. If these plots are analyzed interactively in PAVE it is also possible to identify the temporal differences in O_x production.

Figure 6-47 shows the destruction of O_x by photochemical reactions for each day, where O_x destruction reactions include, e.g.:

$$NO_3 + hv = NO + NO_2$$
$$OH + O_3 = HO_2$$
$$O^1D + H_2O = 2\ OH$$

The ratio of Figure 6-46 to Figure 6-47 provides a qualitative estimate of the chemical lifetime of O_x and when combined with an analysis of other loss processes (e.g., deposition and transport) it can be used to estimate the influence of regional transport of O_3. The difference of Figure 6-46 and Figure 6-47 is the net production of O_x, and this is equal to the sum of the production of O_3 and the amount of NO emissions oxidized. Typically, the amount of O_x destruction by photochemical reactions is on the order of 10% of the O_x production. Figure 6-48 shows the sources of OH radical initiation from the reaction of O^1D with H_2O, and Figure 6-49 shows the total initiation of HO_2 from all sources including photolysis of HCHO and aldehydes and decomposition of aromatic decay products. Production of new HO_2 radicals results directly from the emissions and reactions of VOC, so a comparison of new HO_2 initiation versus OH initiation can be used to quantify the importance of VOC versus O_3 in initiating the chain propagation reactions that produce O_3. The CAMx source code can be easily modified to produce more detailed information on the contribution of individual VOC species to radical initiation. These outputs would not be useful for directly estimating O_3 sensitivity to individual VOC, however, it would be useful for explaining why certain VOC are more reactive than others.

Figure 6-50 shows the amount of OH that reacted with CO and CH_4. Figure 6-51 shows the amount of OH reacted with all VOC (including CO and CH_4), and Figure 6-52 shows the amount of OH reacted with isoprene. The plots of OH reacted with isoprene are an approximate indicator of the contribution of isoprene to O_3 production, and Figure

6-52 shows explicitly the importance of isoprene especially in the southern and northeastern US. Figure 6-52 can be compared with the DDM and OSAT plots (see Figures 6-18 and 6-19) which show that O_3 has low sensitivity to isoprene in the rural areas, and that most of the O_3 production in rural areas is attributed to NO_x by OSAT. Thus, the CPA results showing the mass of isoprene reacted provides information not available by DDM and OSAT. The DDM sensitivity of O_3 to isoprene for urban areas can be explained by a combination of direct isoprene chemistry (e.g., isoprene reacted southwest of Chicago and New York) and indirect isoprene chemistry that produces HCHO and O_3 in rural areas which are subsequently transported and act as radical precursors in urban areas. The CPA and IPR output can be used to provide a quantitative analysis of this contribution, however, this would be a time intensive analysis to perform and is beyond the scope of the current project.

Figure 6-53 shows the amount of NO_x converted to HNO_3 by the $OH+NO_2$ reaction. Figure 6-54 shows the amount of NO_x converted to HNO_3 by the nighttime N_2O_5 chemistry. Conversion of NO_x to inert HNO_3 is a key process in the model because, as discussed below, much of the domain is NO_x-limited. Conversion of NO_x to HNO_3 in the nighttime chemistry can substantially affect the NO_x budget and make it unavailable to participate in daytime O_3 production chemistry. This can affect model predicted O_3 concentrations and the sensitivity of O_3 to VOC and NO_x. Comparisons of Figures 6-53 and 6-54 show that approximately equal amounts of NO_x were converted to HNO_3 in the nighttime chemistry. This is substantially different from previous simulations of the Regional Acid Deposition Model (RADM) for a July, 1988 model scenario in which approximately 30% of NO_x was converted to HNO_3 by nighttime N_2O_5 chemistry (Tonnesen and Dennis, unpublished results) and for the CMAQ model in which 18% of HNO_3 production occurred in the nighttime N_2O_5 chemistry (Tonnesen, 2001). The large differences in the nighttime HNO_3 production predicted by different models indicate that the N_2O_5 kinetics is an area of large uncertainty and should be subject to further study.

Figures 6-55, 6-56, and 6-57 show indicators of O_x production sensitivity to VOC and NO_x (see Tonnesen and Dennis, 2000a,b for derivation of indicators based on radical propagation chemistry). In Figure 6-55, areas in red or yellow indicate radical-limited conditions in which O_x production was sensitive to VOC and was inhibited by increasing

NO_x. In Figures 6-56 and 6-57 areas of gray and dark blue indicate these radical-limited conditions. Figures 6-55 to 6-57 are useful for assessing the spatial and temporal variability in the sensitivity of O_x and O_3 production to precursors. These indicators were evaluated in Section 6.1.2.3 to assess the sensitivity of O_x production to precursors in the receptor regions.

Figure 6-58 shows the net production efficiency of O_x per NO_x converted to HNO_3 ($P(O_x)/P(HNO_3)$). This can be thought of as the NO_x chain length and is closely related to the O_3 production efficiency per NO_x. Comparisons of $P(O_x)/P(HNO_3)$ in the base case and in the sensitivity cases with NO_x emission reductions may be useful for understanding the unresponsiveness of the system to NO_x reductions, i.e., the increasing O_x production efficiency at decreasing NO_x conditions can provide an explanation for the "piston effect" whereby it becomes increasingly difficult to obtain further O_3 reductions. The analysis of $P(O_x)/P(HNO_3)$ and its response to precursor controls provides fundamental information that can be used to assess the feasibility of attaining an air quality standard using a particular control strategy. The information can be obtained from DDM by calculating sensitivities for the base case and cases with reduced emissions, i.e., an approach analogous to that described for PA. Further evaluation may be required to determine if this type of information is accessible in OSAT.

6.2.4 Model Responses to Changes in ICs, BCs, and Emissions

Both OSAT and DDM can be used to predict model responses to changes in input parameters or variables such as ICs, BCs, and emissions, whereas PA does not have this capability. However, there is a major difference in characterizing the model responses to perturbations in inputs between OSAT and DDM. DDM is more directly applicable to predicting the response to changes in emissions because the sensitivity coefficients directly address this issue. This information is particularly useful in developing emission control strategies for many non-attainment areas. The main limitation is the range of validity of the first-order sensitivities obtained from the base case. First-order sensitivities are expected to accurately predict responses to changes in model inputs for cases where the relationship between model output and input is linear. If that relationship

is not linear (i.e., a non-linear system such as O_3 chemistry), first-order sensitivities are only representative of small changes (i.e., about 40% change, perturbations small enough to be represented by first-order derivatives, Dunker et al., 2002b), but are not expected to be accurate for large changes that span significant non-linearity in model response (e.g., in the chemistry or transport algorithms). The limitation of DDM predictions under large emission perturbations will be discussed in detail in Section 6.3.

OSAT is less applicable to quantitative prediction of the response to changes in emissions because OSAT does not calculate sensitivity coefficients and the extrapolation of the OSAT results to a different emission scenario involves some assumptions by the user. The most likely assumption that the user will make is linearity, i.e., that OSAT source contributions will scale proportionately with emissions. As shown in Section 6.3.1, applying linear scaling to the OSAT results is reasonably accurate for small perturbations in VOC emission levels (e.g., the errors are less than 10% for a 25% reduction in VOC emissions) but less accurate for both small and large perturbations in NO_x emissions (e.g., the errors are up to -31.9% and -45.3% for a 25% or 75% reduction in NO_x emissions, respectively). Therefore, caution should be taken when using the OSAT results to extrapolate from a base simulation to an emission scenario with a perturbation in NO_x emissions.

6.2.5 Other differences among the three probing tools

In addition to the aforementioned complementarity, there are other important differences among the three probing techniques that are worth mentioning:

- OSAT gives information on O_3 only, whereas DDM and PA give information on all modeled species.
- OSAT requires subdividing the modeling domain and the emissions so that sources with widely disparate VOC reactivity are not lumped together. DDM allows any grouping or lumping of emissions by source, geographic area, or type (VOC or NO_x). For example, you can calculate the sensitivity to mobile source emissions in the entire eastern U.S. without subdividing the modeling

domain. This is useful because to answer some questions you do not need detailed partitioning of sources by geographic area. Also, DDM allows anywhere from one to a large number of sensitivities to be calculated so that the number of sensitivities can be tailored closely to the questions being asked.

- DDM can provide information on the effects of changing the spatial or diurnal distribution of emissions (and other inputs) whereas OSAT and PA cannot.

6.3 Stretchability

The range of conditions for a valid application has been tested and identified for some of the probing tools by the original developers or earlier users. For example, the accuracy of DDM is confined to small perturbations. It has been shown to be accurate for perturbations of up to 40% perturbation (Dunker et al., 2002b). However, this range of accuracy will vary for different simulations. OSAT has also been tested under a variety of conditions (Yarwood et al., 1996, Morris et al., 1998; EPA, 1998). In this project, the responses of the three probing tools to variations in emissions and local chemical conditions are evaluated by conducting 12 CAMx sensitivity runs for 25% and 75% reductions in anthropogenic emissions of NO_x only, and a 25% reduction in emissions of VOCs only.

These sensitivity simulations allow us to (1) test the stretchability of each tool for a moderate level of perturbations (i.e., 25% emission reduction) and from one chemical regime to another chemical regime (i.e., a 75% reduction in anthropogenic emissions of NO_x will likely change the O_3 chemistry from VOC-limited to NO_x-limited regime in some receptor regions such as Chicago); (2) evaluate the consistency of these probing tools under several different emission scenarios.

In the following sections, we first evaluate the accuracy of DDM and OSAT results under small and large perturbations. This is conducted by (1) comparing the O_3 concentrations calculated by the DDM sensitivities from the base simulation according to Equation (10) with the actual O_3 concentrations predicted from the sensitivity simulations with 25% and 75% emission reduction scenarios; and (2) testing the validity of the OSAT

source attribution results under different emission scenarios. In particular, we evaluate the validity of applying linear scaling to the OSAT source contributions under different emission scenarios. We then evaluate the consistency in NO_x- vs. VOC-sensitivity of the O_3 chemistry predicted by the three tools under different emission scenarios. Finally, we evaluate the changes in the chemical signatures for the four receptors for the 75% emission reduction scenario. These evaluations help verify the accuracy, robustness, and reliability of these tools under atmospheric conditions that are representative of future emission scenarios. Limitations in the application of each tool are also identified.

6.3.1 Accuracy of DDM and OSAT Results under Small and Large Perturbations

6.3.1.1 O_3 Concentrations Predicted by the DDM Sensitivities under Different Emission Scenarios

For DDM, we tested whether the sensitivity coefficients can be used to predict the change in O_3 concentrations due to changes in emissions. Since the O_3 concentrations as a function of time are the regular outputs for these CAMx simulations with probing tools, we can compare O_3 concentrations calculated with the DDM sensitivities from the base simulation using Equation (10) against the actual O_3 concentrations predicted from the 25% and 75% emission reduction scenarios. This is valuable because sensitivities are normally applied to predict concentrations for scenarios with altered inputs.

Figures 6-59 to 6-62 show the percent differences and absolute differences in the calculated O_3 concentrations based on Equation (10) using the O_3 concentrations and sensitivities predicted from the DDM base run B7 and the simulated O_3 concentrations from the sensitivity simulations S2, S5, and S9 in all 81 fine grid cells in the four receptor regions. The percent differences are calculated in terms of (calculated O_3 – simulated O_3) * 100 / simulated O_3, and the absolute differences are calculated in terms of (calculated O_3 – simulated O_3). The calculated O_3 concentrations for most fine grid cells in all receptors are higher than the simulated O_3 concentrations, with small percent differences (< 9.5%) for a 25% reduction in anthropogenic VOC or NO_x emissions but large percent differences (up to 98.2%) for a 75% reduction in anthropogenic NO_x emissions. It is

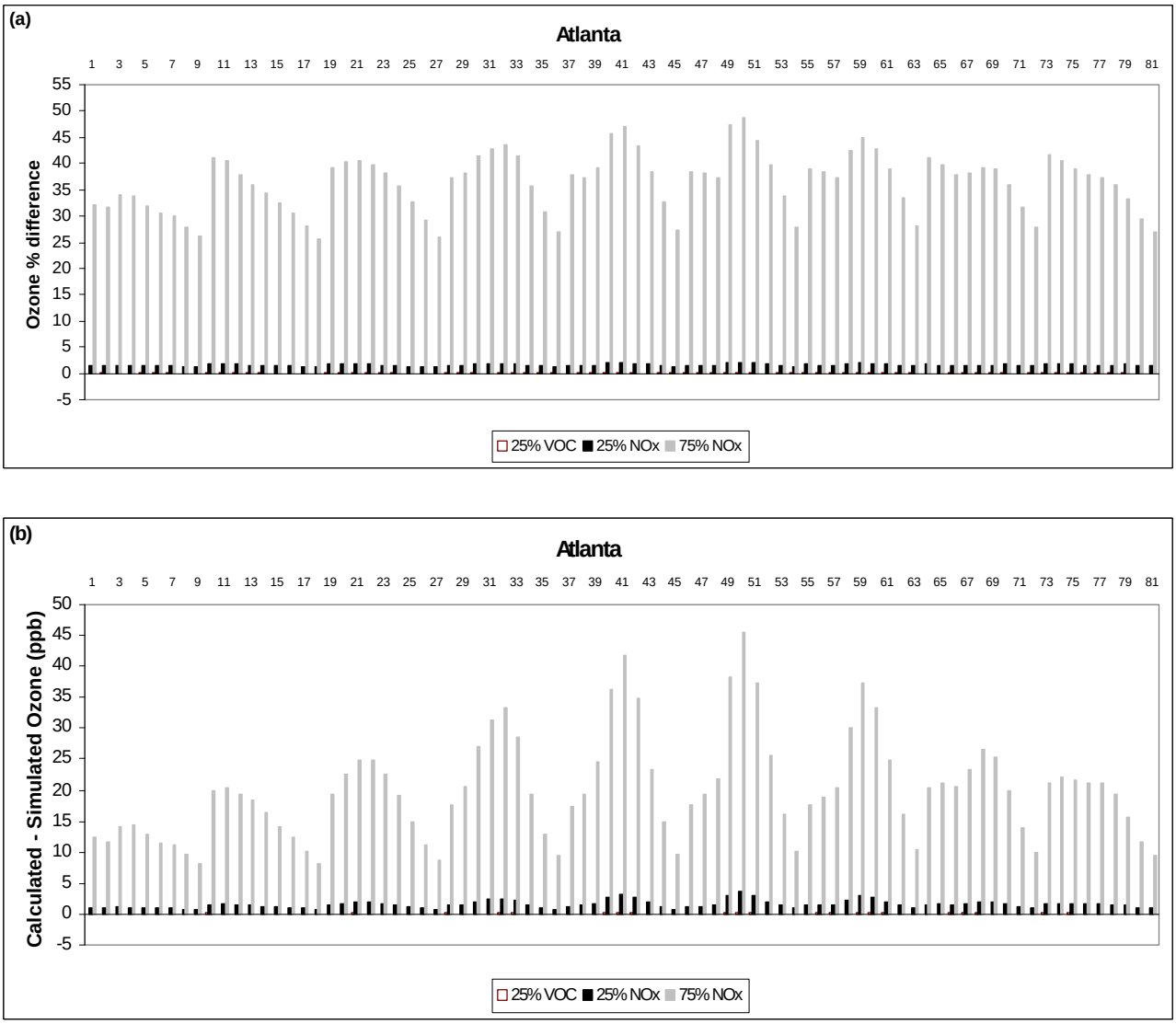

Figure 6-59. (a) The percent differences and (b) absolute differences in the calculated O_3 concentrations using the O_3 concentrations and sensitivities predicted from DDM base run B7 and the simulated O_3 concentrations from DDM sensitivity runs S2, S5, and S8 in all 81 fine grid cells in Atlanta at 3 p.m. on July 15, 1995. Labels on the x-axis correspond to fine grid cell indices for each receptor starting from the NW corner and proceeding row-wise.

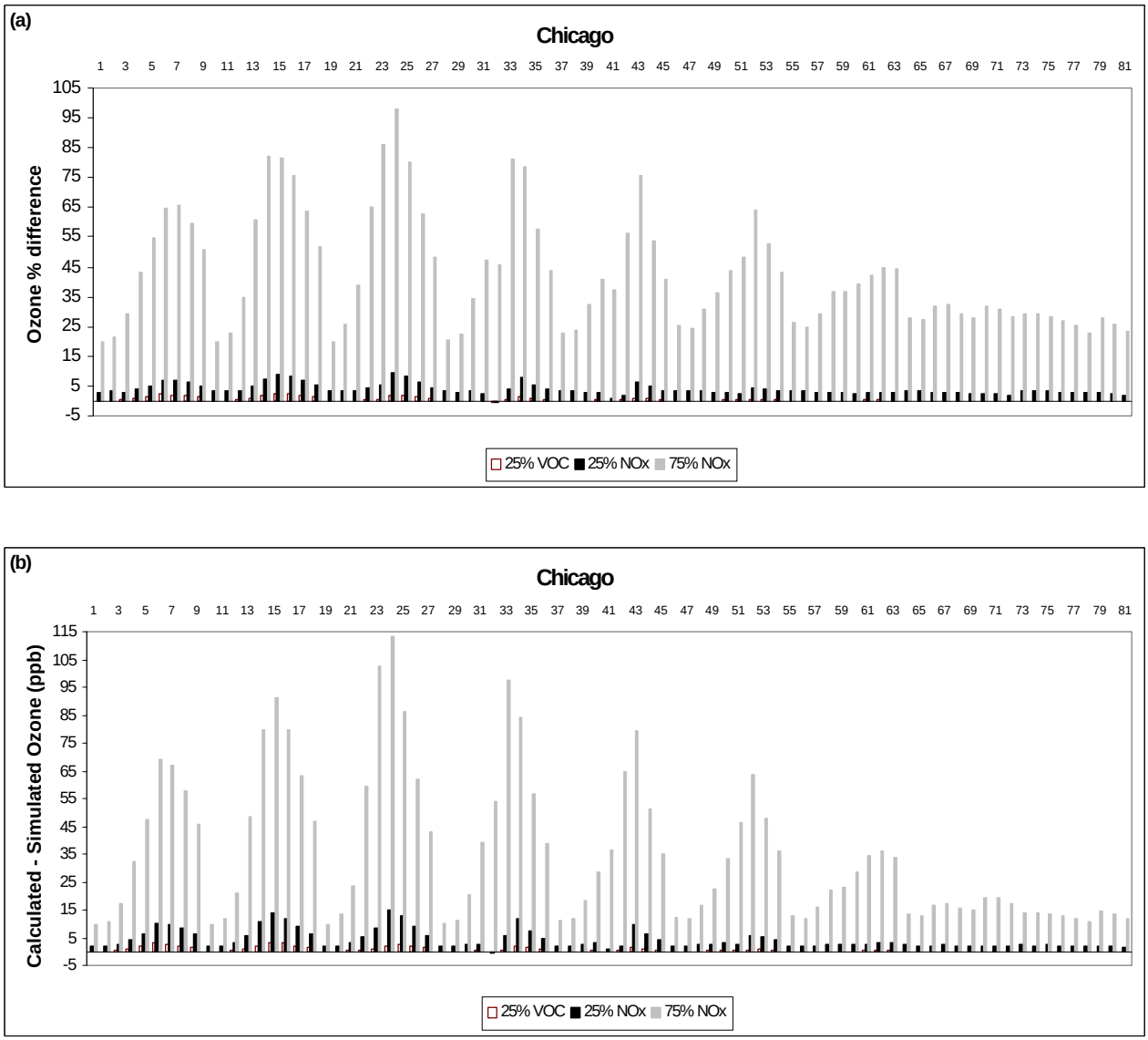

Figure 6-60. (a) The percent differences and (b) absolute differences in the calculated O_3 concentrations using the O_3 concentrations and sensitivities predicted from DDM base run B7 and the simulated O_3 concentrations from DDM sensitivity runs S2, S5, and S8 in all 81 fine grid cells in Chicago at 3 p.m. on July 15, 1995. Labels on the x-axis correspond to fine grid cell indices for each receptor starting from the NW corner and proceeding row-wise.

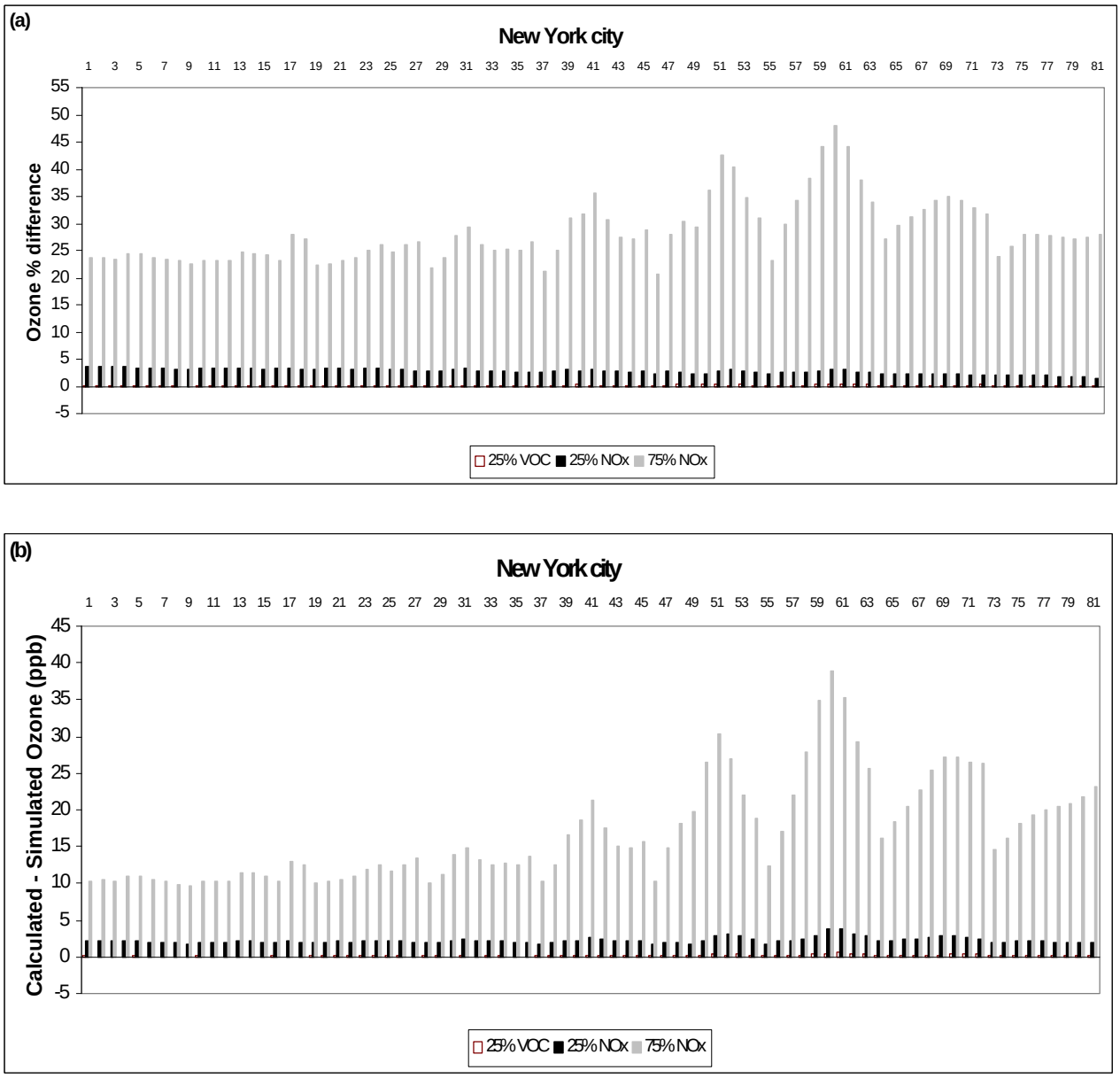

Figure 6-61. (a) The percent differences and (b) absolute differences in the calculated O_3 concentrations using the O_3 concentrations and sensitivities predicted from DDM base run B7 and the simulated O_3 concentrations from DDM sensitivity runs S2, S5, and S8 in all 81 fine grid cells in New York City at 3 p.m. on July 15, 1995. Labels on the x-axis correspond to fine grid cell indices for each receptor starting from the NW corner and proceeding row-wise.

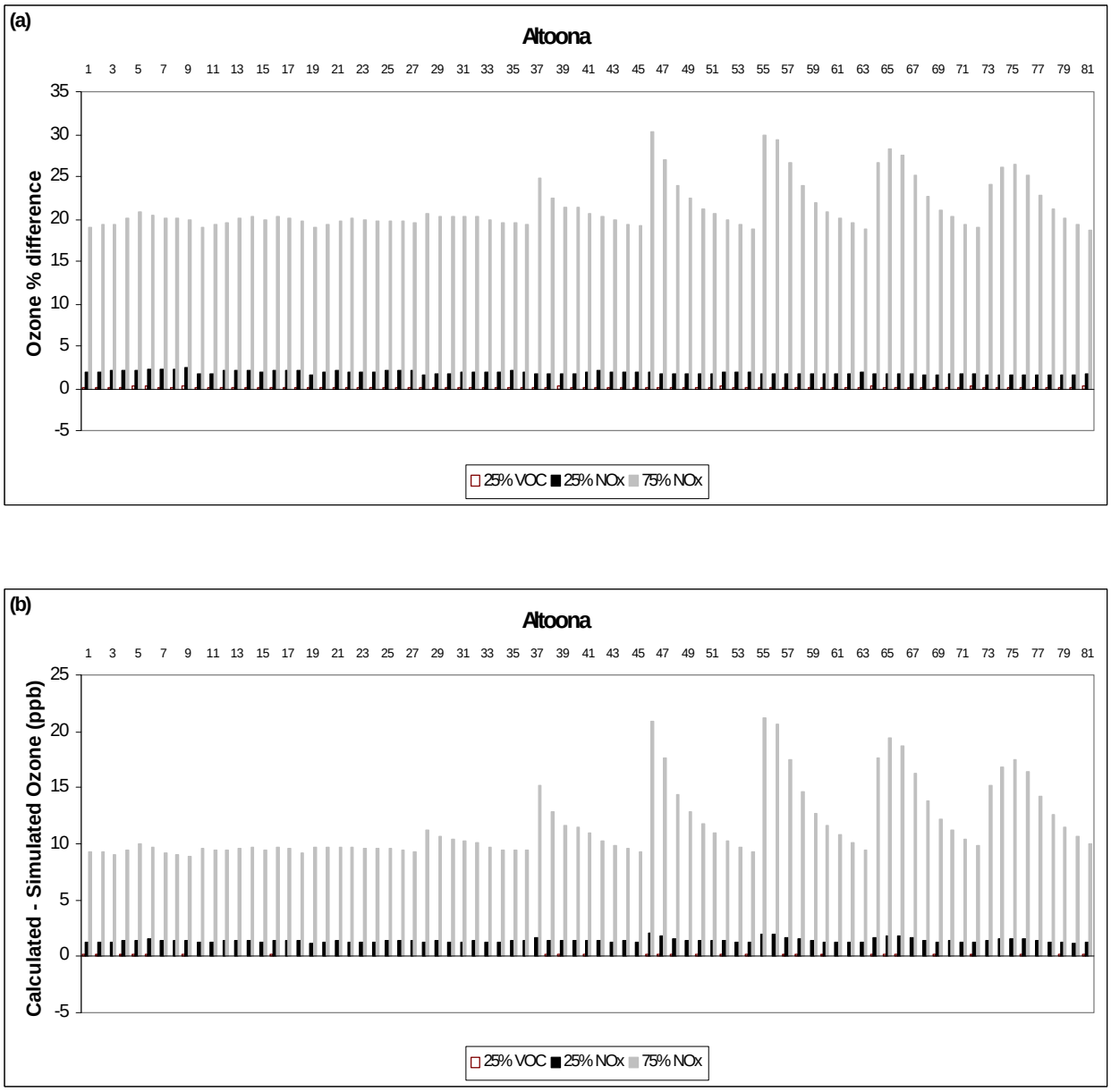

Figure 6-62. (a) The percent differences and (b) absolute differences in the calculated O_3 concentrations using the O_3 concentrations and sensitivities predicted from DDM base run B7 and the simulated O_3 concentrations from DDM sensitivity runs S2, S5, and S8 in all 81 fine grid cells in Altoona at 3 p.m. on July 15, 1995. Labels on the x-axis correspond to fine grid cell indices for each receptor starting from the NW corner and proceeding row-wise.

noted that large percent differences (> 45%) always occurred for grid cells with high O_3 concentrations (> 80 ppb) in all the four receptor regions for a 75% reduction in anthropogenic NO_x emissions. In particular, those large percent differences are always associated with large negative sensitivity coefficients predicted by DDM in Chicago. For example, for the 24th grid cell in Chicago, the simulated O_3 concentrations at 3 pm on July 15 for the base emission and a 75% reduction in anthropogenic NO_x emissions scenarios are 147.5 ppb and 115.7 ppb, respectively. The predicted sensitivity of O_3 to changes in anthropogenic NO_x emissions is -109.1 ppb, resulting in a calculated O_3 concentration of 229.3 ppb according to Equation (10) and a percent difference of 98.2% between the calculated and simulated O_3 for a 75% reduction in anthropogenic NO_x emissions.

For a 25% reduction in anthropogenic VOC emissions, the percent differences in the calculated and simulated O_3 concentrations range from -0.1% to 0.2% in Atlanta, -0.3% to 2.4% in Chicago, -0.1% to 0.4% in New York City, and 0.03% to 0.2% in Altoona, with an average difference of 0.06%, 0.5%, 0.2%, and 0.1%, respectively. The absolute differences in the calculated and simulated O_3 concentrations range from -0.07 to 0.3 ppb in Atlanta, -0.2 to 3.2 ppb in Chicago, -0.05 to 0.5 ppb in New York City, and 0.02 to 0.2 ppb in Altoona, with an average absolute difference of 0.07, 0.6, 0.2, and 0.1 ppb, respectively. For a 25% reduction in anthropogenic NO_x emissions, the differences in the simulated and calculated O_3 concentrations range from 1.1% to 2.2% in Atlanta, -0.5% to 9.5% in Chicago, 1.5% to 3.7% in New York City, and 1.5% to 2.4% in Altoona, with an average difference of 1.6%, 3.9%, 2.8%, and 1.8%, respectively. The absolute differences in the calculated and simulated O_3 concentrations range from 0.6 to 3.6 ppb in Atlanta, -0.5 to 15.2 ppb in Chicago, 1.7 to 3.8 ppb in New York City, and 1.2 to 2.1 ppb in Altoona, with an average absolute difference of 1.6, 4.2, 2.3, and 1.4 ppb, respectively. For a 75% reduction in anthropogenic NO_x emissions, the differences in the simulated and calculated O_3 range from 25.6% to 48.7% in Atlanta, 19.7% to 98.2% in Chicago, 20.6% to 48.0% in New York City, and 18.6% to 30.2% in Altoona, with an average difference of 25.6%, 42.5%, 28.4%, and 21.4%, respectively. The absolute differences in the calculated and simulated O_3 concentrations range from 8.3 to 45.5 ppb in Atlanta, 9.5 to 113.6 ppb in Chicago, 9.6 to 38.9 ppb in New York City, and 8.9 to 21.1 ppb in

Altoona, with an average absolute difference of 20.0, 35.1, 16.9, and 11.7 ppb, respectively. The magnitudes of the percent and absolute differences in the calculated and the simulated O_3 concentrations indicate that the DDM sensitivities are accurate for a 25% emission reduction scenario, but inaccurate for a 75% emission reduction scenario.

6.3.1.2 Validity of the OSAT Source Attribution Results under Different Emission Scenarios

For OSAT, we first tested whether the source contributions vary significantly as emission levels change by comparing the spatial distribution and receptor-average of source contributions predicted from sensitivity simulations with the base simulation. We then tested the ability of OSAT to predict model response to evaluate the validity of applying linear scaling to the OSAT source attribution results under different emission scenarios.

Figures 6-63 to 6-65 show the spatial distributions of the O_3 contributions of the VOC and NO_x emissions from four source categories predicted by OSAT at 2 p.m. on July 15, 1995 under different emission scenarios with a 25% reduction of anthropogenic VOC emissions, a 25% reduction of anthropogenic NO_x emissions, and a 75% reduction of anthropogenic NO_x emissions, respectively. Compared to Figure 6-19, the spatial distribution of the OSAT source apportionment under the 25% reduction of anthropogenic VOC and NO_x emission scenarios are quite similar to that under the EPA 2007 base emission scenario. However, the spatial distribution of the OSAT source apportionment under the 75% reduction of anthropogenic NO_x emission scenario is quite different from that under the base emission scenario. In particular, the source contributions of VOC emissions from biogenic, on-road mobile and other surface anthropogenic sources are much smaller than those for the base emission scenario (note that the source contributions of VOC emissions from elevated sources are zero for both the base emission and the 75% NO_x emission reduction scenarios). Those differences are caused by several factors. First, the total O_3 concentrations predicted under the 75% reduction of anthropogenic NO_x emission scenario is much lower than those under the base emission scenario. Second, the O_3 chemistry for the entire domain is predominantly

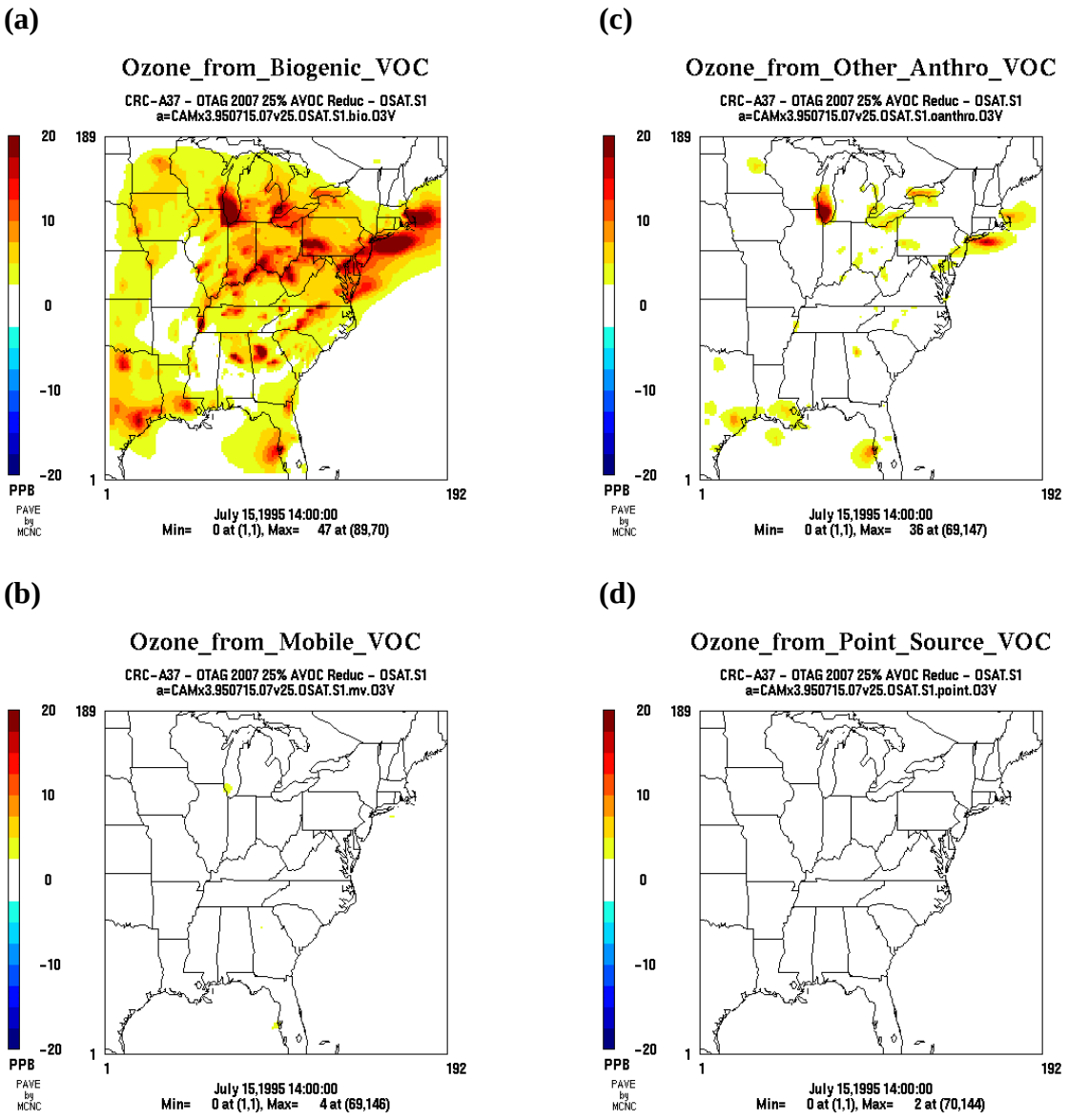

Figure 6-63. The spatial distribution of O_3 contributions predicted by OSAT at 2 p.m. on July 15 under the 25% anthropogenic VOC emissions reduction scenario (DDM sensitivity run S1) for emissions from (a) biogenic VOC, (b) on-road mobile VOC, (c) other surface anthropogenic VOC, and (d) elevated anthropogenic VOC, (e) biogenic NO_x, (f) on-road mobile NO_x, (g) other surface anthropogenic NO_x, and (h) elevated anthropogenic NO_x.

(e)

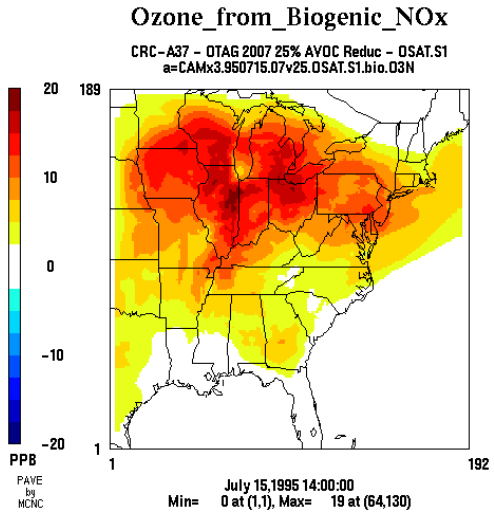

(g)

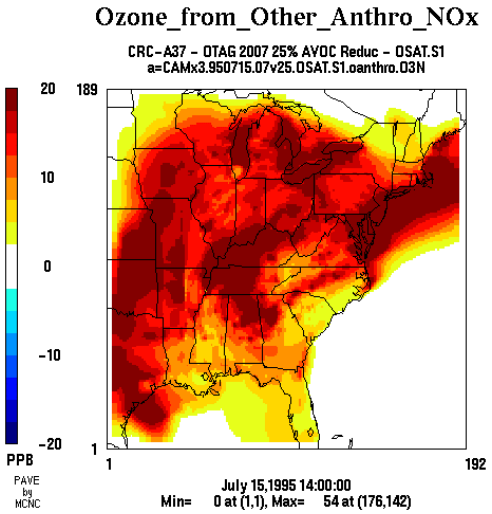

(f)

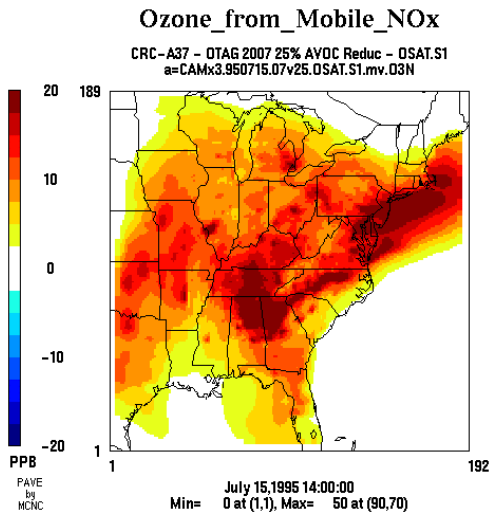

(h)

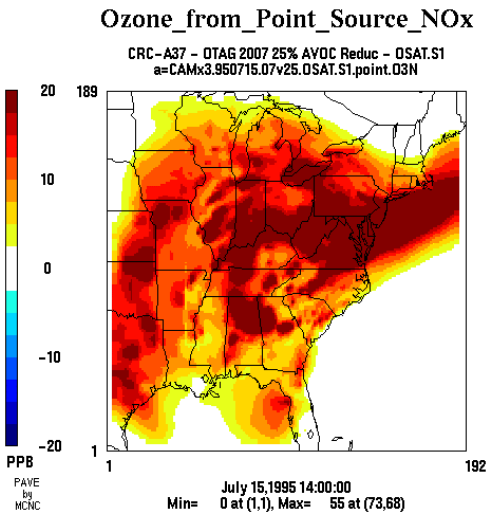

Figure 6-63. (Continued).

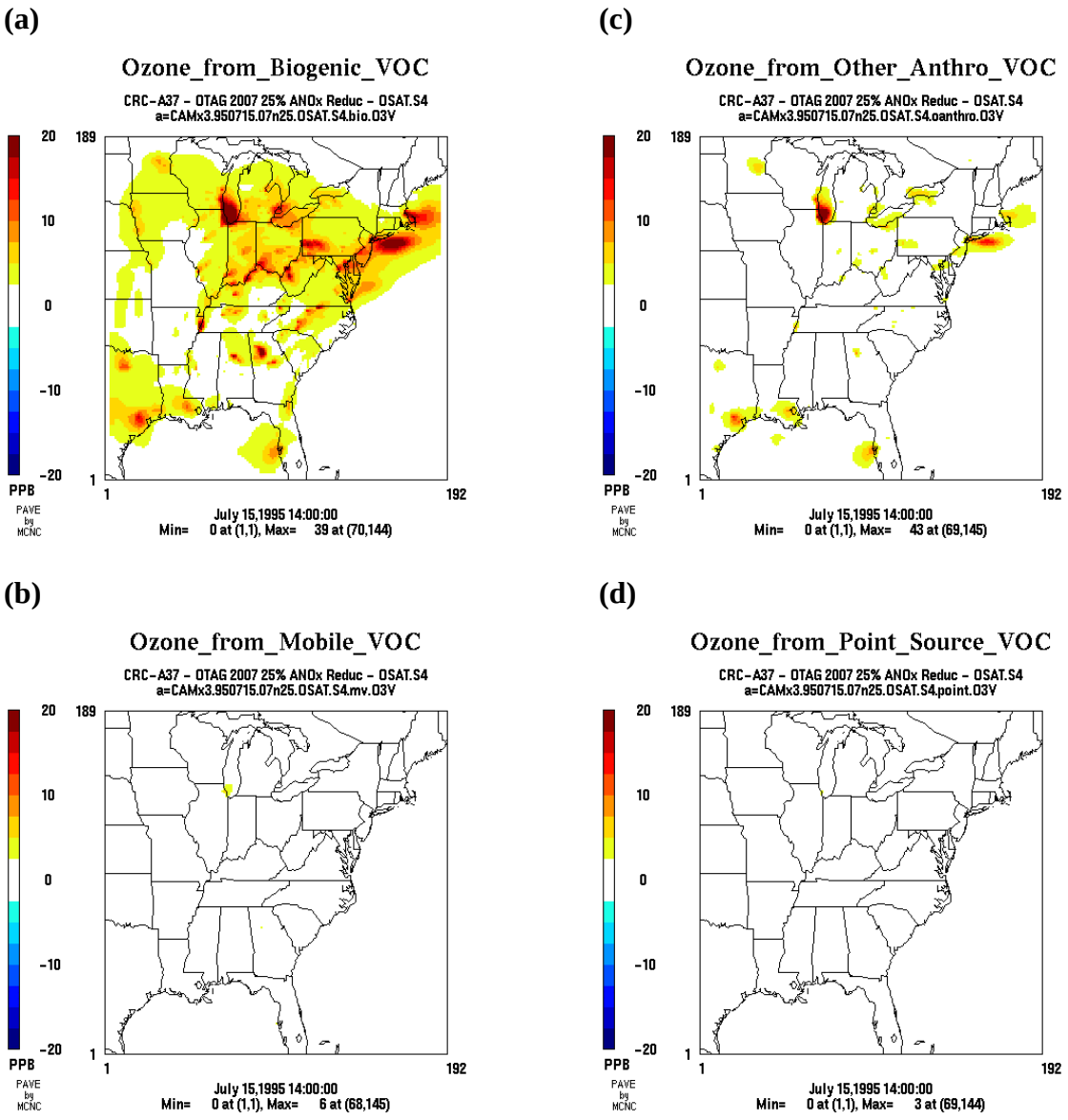

Figure 6-64. The spatial distribution of O_3 contributions predicted by OSAT at 2 p.m. on July 15 under the 25% anthropogenic NO_x emissions reduction scenario (DDM sensitivity run S4) for emissions from (a) biogenic VOC, (b) on-road mobile VOC, (c) other surface anthropogenic VOC, and (d) elevated anthropogenic VOC, (e) biogenic NO_x, (f) on-road mobile NO_x, (g) other surface anthropogenic NO_x, and (h) elevated anthropogenic NO_x.

(e)

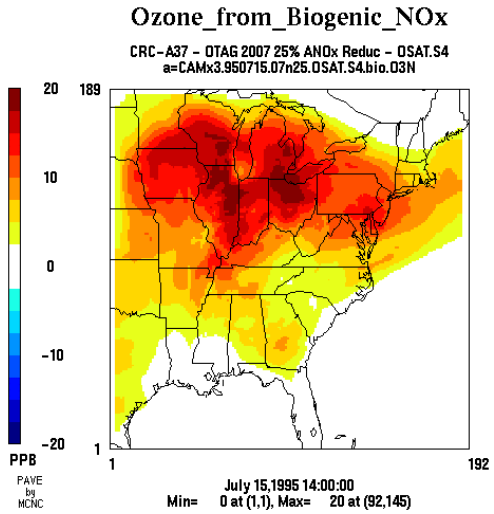

(g)

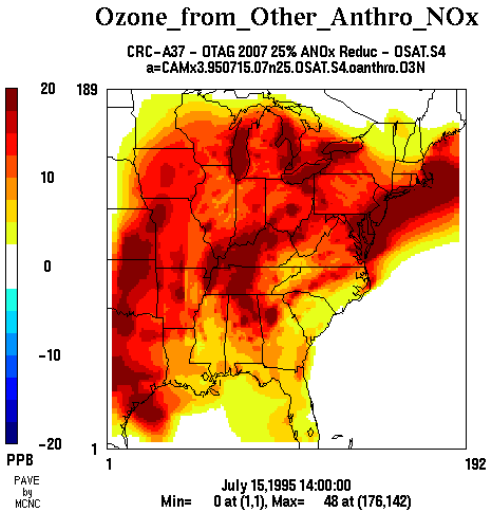

(f)

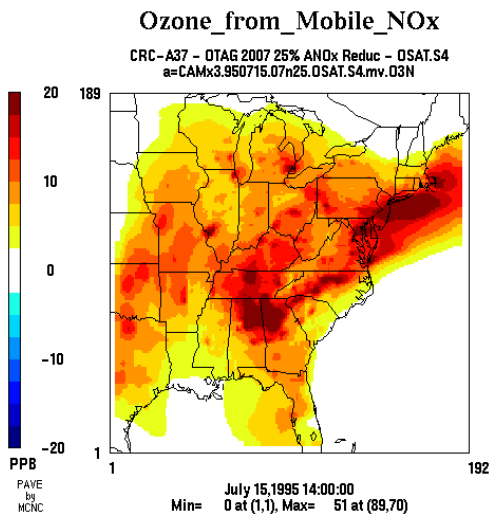

(h)

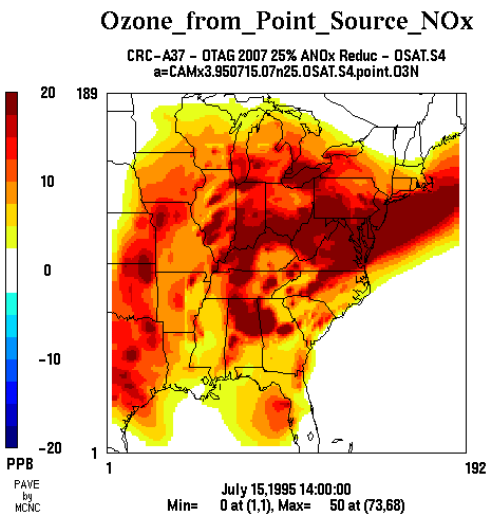

Figure 6-64. (Continued).

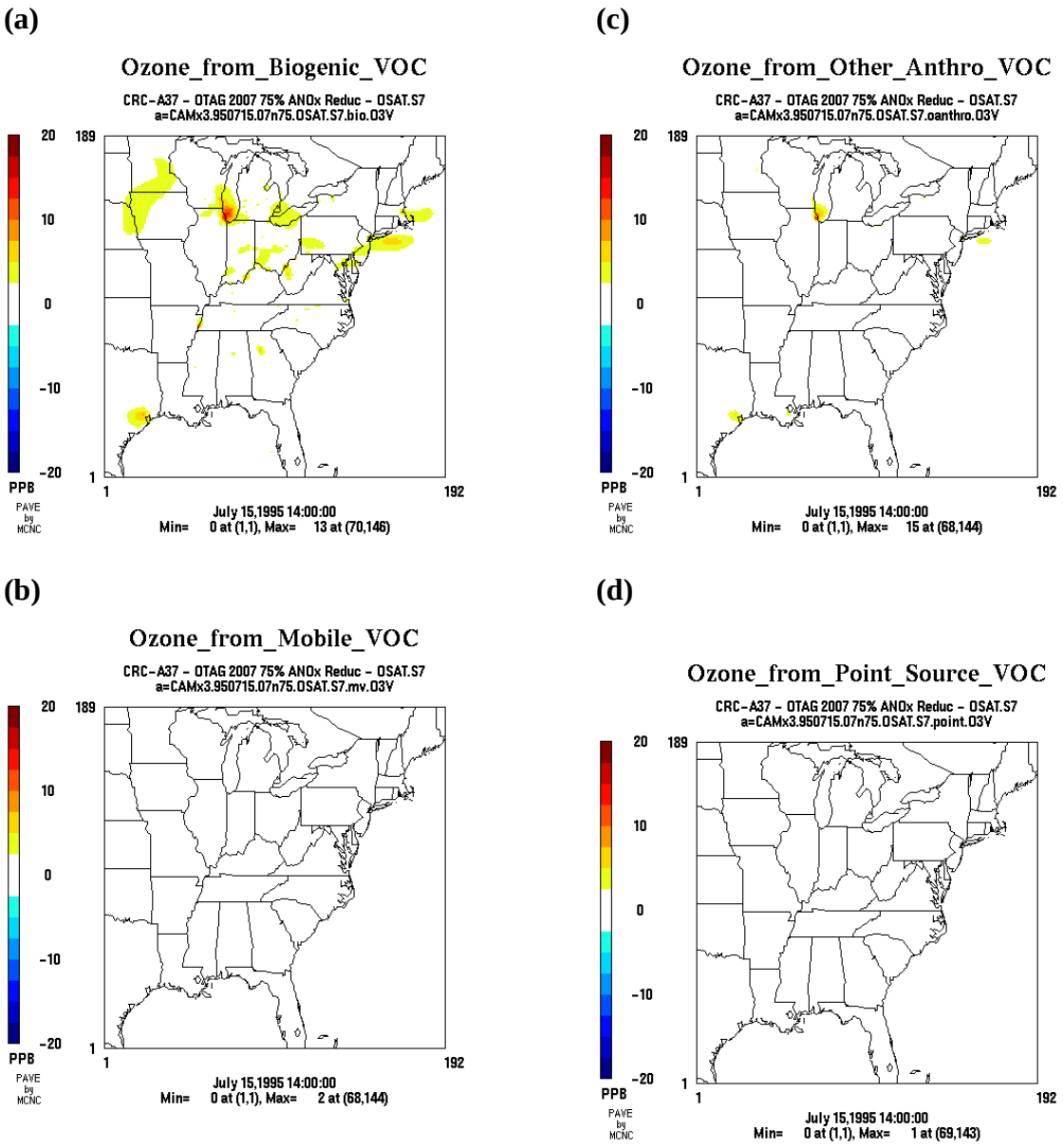

Figure 6-65. The spatial distribution of O_3 contributions predicted by OSAT at 2 p.m. on July 15 under the 75% anthropogenic NO_x emissions reduction scenario (DDM sensitivity run S7) for emissions from (a) biogenic VOC, (b) on-road mobile VOC, (c) other surface anthropogenic VOC, and (d) elevated anthropogenic VOC, (e) biogenic NO_x, (f) on-road mobile NO_x, (g) other surface anthropogenic NO_x, and (h) elevated anthropogenic NO_x.

(e)

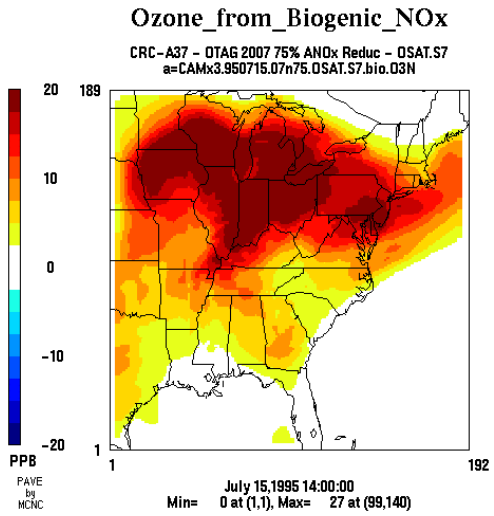

(g)

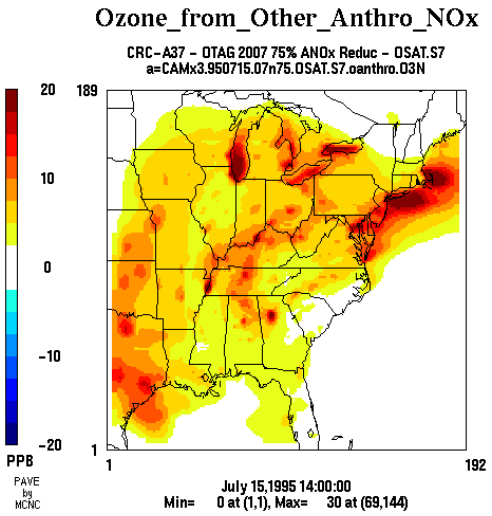

(f)

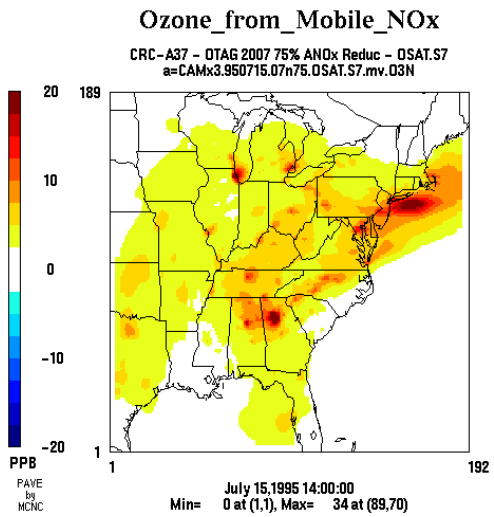

(h)

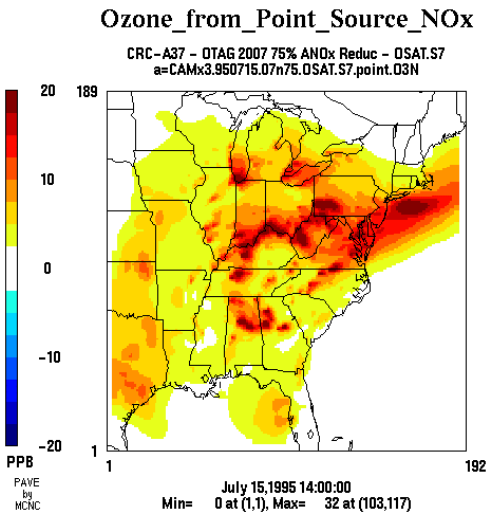

Figure 6-65. (Continued).

NO_x-limited for the 75% NO_x emission reduction scenario, as compared to the base emission scenario for which the O_3 chemistry in some big cities is VOC-limited. Third, the source apportionment of the total O_3 concentration to the VOC and NO_x emissions from the four source categories under a 75% emission reduction scenario is different from that under the base emission scenario. For example, while the total O_3 concentrations predicted under the 75% emission reduction scenario are lower than the values under the base emission scenario in the northeastern corner of the State of Pennsylvania, the contributions of biogenic NO_x emissions in ppb to the total O_3 concentration are higher under the 75% emission reduction scenario than those under the base emission scenario, indicating that the percent contributions of the biogenic emissions to the total O_3 concentrations are also higher in this region for the 75% NO_x emission reduction scenario than for the base emission scenario.

Figures 6-66 to 6-68 show the O_3 contributions of the total VOC and NO_x emissions from four source categories, ICs, and BCs predicted by OSAT at 3 p.m. for the four receptors on July 15 under a 25% anthropogenic VOC emission reduction, a 25% anthropogenic NO_x emission reduction, and a 75% anthropogenic NO_x emission reduction scenarios, respectively. The source contributions predicted under the 25% anthropogenic VOC or NO_x emission reduction scenarios are similar to those under the EPA 2007 base emission scenario (see Figure 6-21), with a range of differences of 0-3.6% in the contributions of various sources, ICs, and BCs at the four receptors. However, the differences in the source contributions between the base and the 75% anthropogenic NO_x reduction emission scenario can be as high as 10.5%. For example, in Altoona, the contribution of the biogenic sources predicted under the 75% anthropogenic NO_x emission reduction scenario is higher by 10.5% than that under the base emission scenario, and those of the on-road mobile, other surface anthropogenic, elevated sources are lower by 4%, 7%, and 5%, respectively, than those under the base emission scenarios. Under all different emission scenarios, the contributions of ICs to the total O_3 concentration is very small (0-0.4%).

To test the ability of OSAT to predict model responses, we compare O_3 concentrations calculated with the OSAT source contributions from the base simulation using Equation (10) against the actual O_3 concentrations predicted from the 25% and

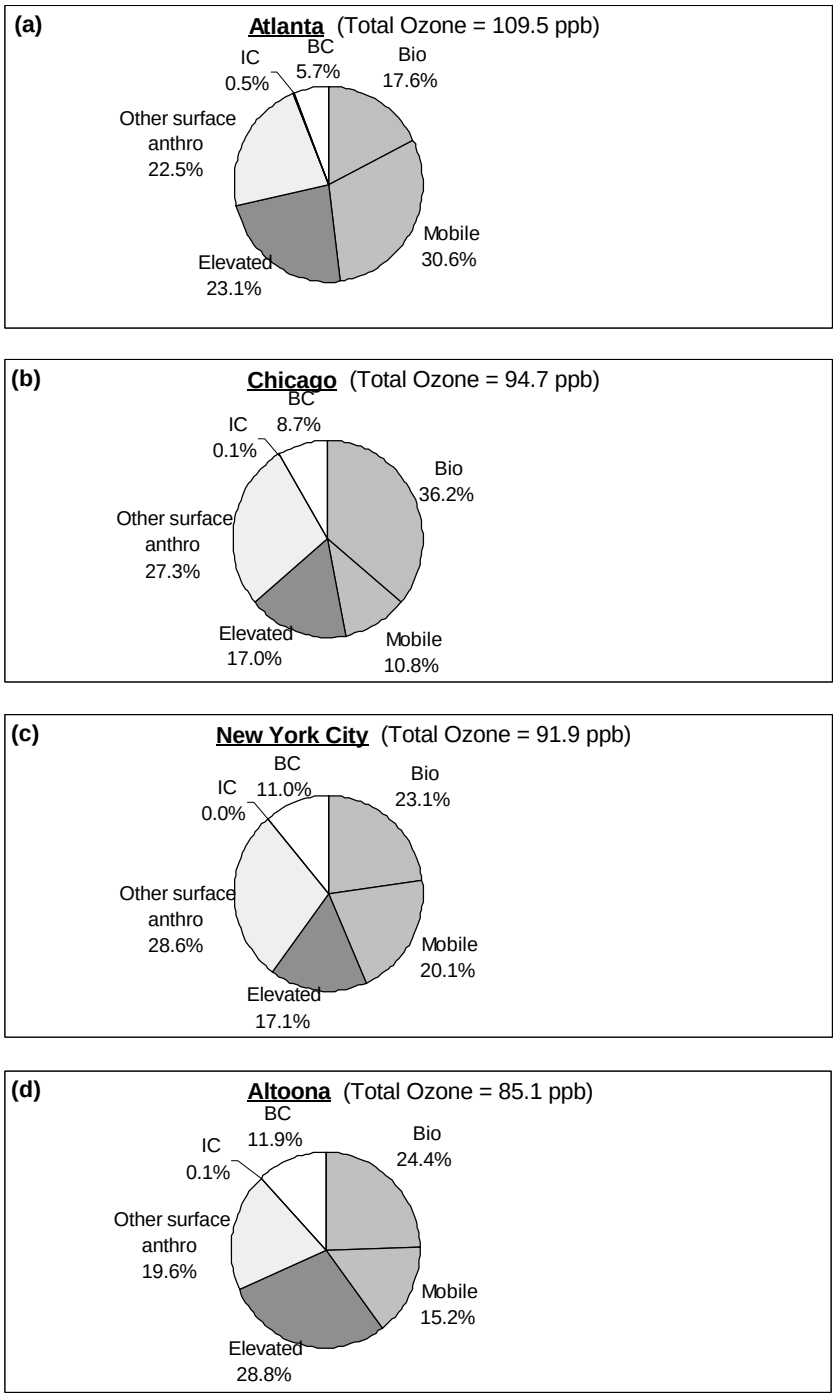

Figure 6-66. The O_3 contributions of total NO_x and VOC emissions from four source categories, ICs, and BCs predicted by OSAT at 3 p.m. on July 15 under the 25% anthropogenic VOC emissions reduction scenario (OSAT sensitivity run S1) in (a) Atlanta, (b) Chicago, (c) New York City, and (d) Altoona.

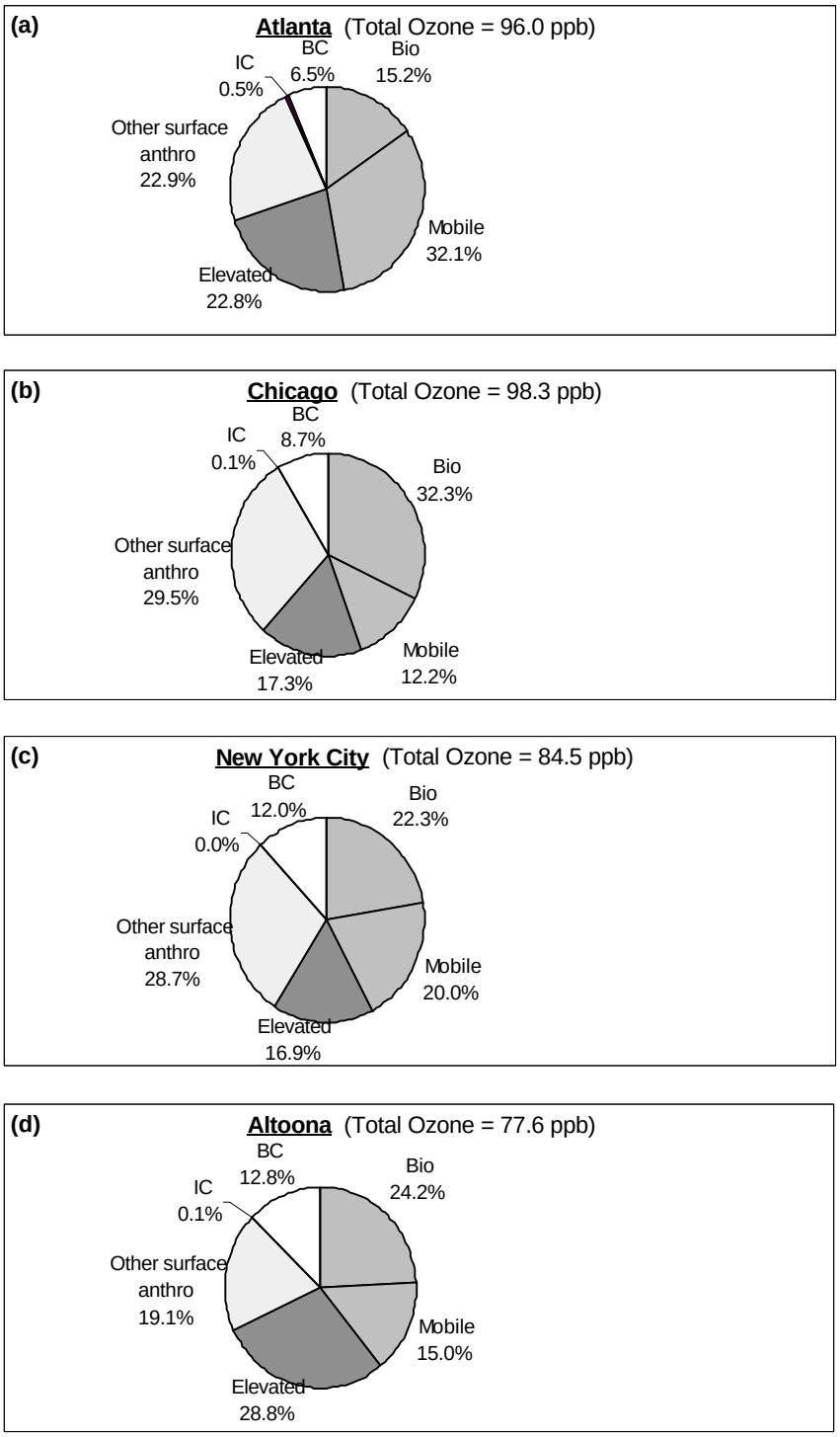

Figure 6-67 The O_3 contributions of total NO_x and VOC emissions from four source categories, ICs, and BCs predicted by OSAT at 3 p.m. on July 15 under the 25% anthropogenic NO_x emissions reduction scenario (OSAT sensitivity run S4) in (a) Atlanta, (b) Chicago, (c) New York City, and (d) Altoona.

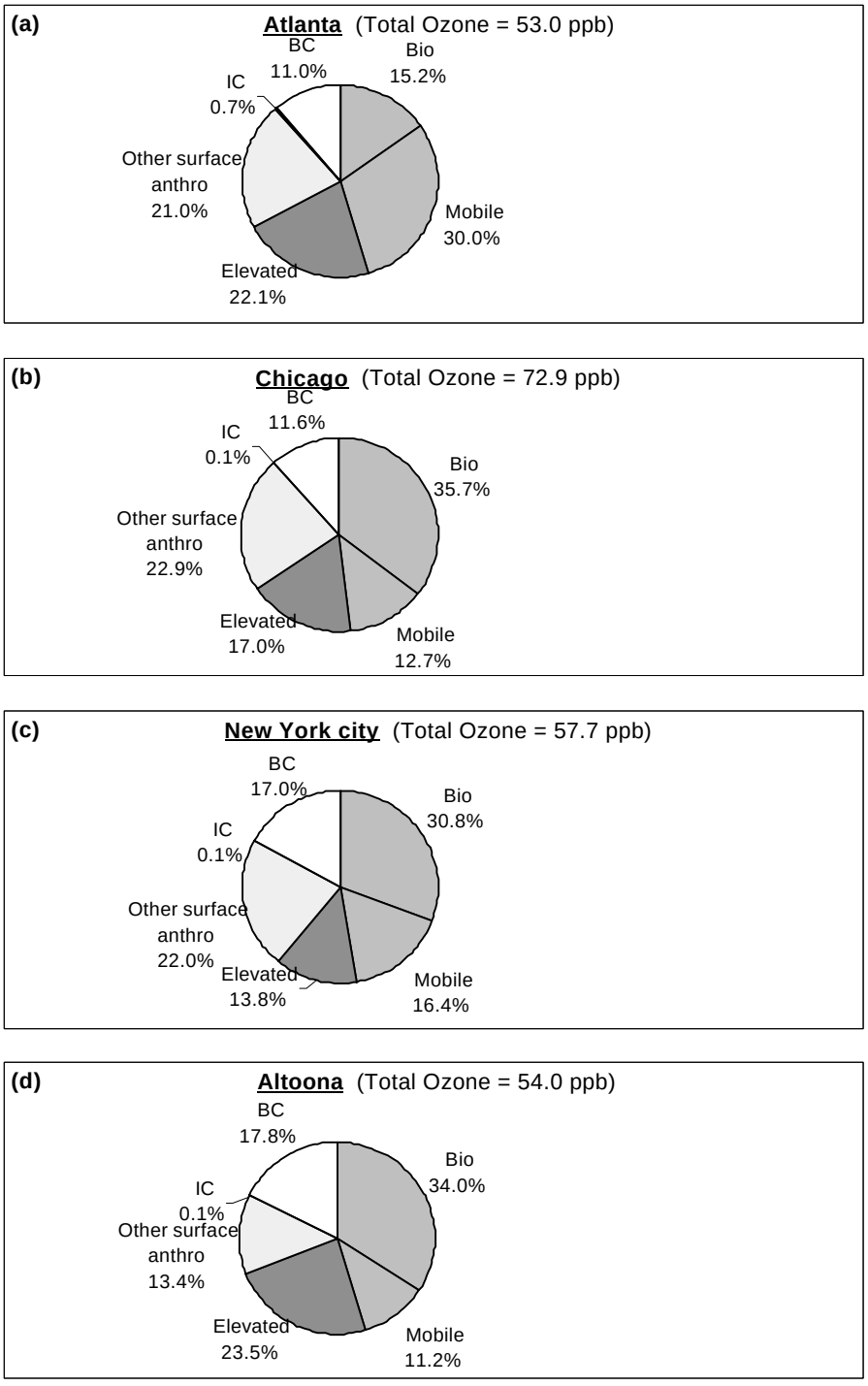

Figure 6-68. The O_3 contributions of total NO_x and VOC emissions from four source categories, ICs, and BCs predicted by OSAT at 3 p.m. on July 15 under the 75% anthropogenic NO_x emissions reduction scenario (OSAT sensitivity run S7) in (a) Atlanta, (b) Chicago, (c) New York City, and (d) Altoona.

75% emission reduction scenarios. Figures 6-69 to 6-72 show the percent differences and absolute differences in the calculated O_3 concentrations based on Equation (10) using the O_3 concentrations and source contributions predicted from the OSAT base run B1 and the simulated O_3 concentrations from the sensitivity simulations S1, S4, and S7 in all 81 fine grid cells in the four receptor regions. The percent differences are calculated in terms of (calculated O_3 – simulated O_3) * 100 / simulated O_3, and the absolute differences are calculated in terms of (calculated O_3 – simulated O_3). The calculated O_3 concentrations for most fine grid cells in all receptors are lower than the simulated O_3 concentrations, with small percent differences (< 9.1%) for a 25% reduction in anthropogenic VOC emissions but large percent differences for 25% and 75% reductions in anthropogenic NO_x emissions (up to -31.9% and -45.3%, respectively). The large percent differences for 25% or 75% reductions in anthropogenic NO_x emissions are due to the fact that OSAT does not account for the effect of NO_x titration on O_3 formation. For some grid cells in Atlanta, Chicago and New York City, the percent differences for the 25% NO_x emission reduction scenario are even higher than those for the 75% NO_x emission reduction scenario. This indicates that neglecting the effect of NO_x inhibition/titration of O_3 has less impact on the O_3 predictions of OSAT for the 75% NO_x emission reduction scenario than for the 25% NO_x emission reduction scenario in those grid cells, as O_3 chemistry changes from VOC-limited to NO_x-limited in Chicago or from NO_x-limited to more NO_x-limited in Atlanta and New York City when the anthropogenic NO_x emission reduction percentage changes from 25% to 75% (see Tables 6-46 and 6-47 in Section 6.3.2).

For a 25% reduction in anthropogenic VOC emissions, the percent differences in the calculated and simulated O_3 concentrations range from -0.7% to -0.3% in Atlanta, -1.1% to 9.1% in Chicago, -1.1% to 0.2% in New York City, and -0.6% to -0.1% in Altoona, with an average difference of -0.5%, 0.7%, -0.5%, and -0.3%, respectively. The absolute differences in the calculated and simulated O_3 concentrations range from -1.0 to -0.3 ppb in Atlanta, -0.9 to 7.5 ppb in Chicago, -1.7 to 0.2 ppb in New York City, and -0.6 to -0.07 ppb in Altoona, with an average absolute difference of -0.5, 0.7, -0.5, and -0.3 ppb, respectively. For a 25% reduction in anthropogenic NO_x emissions, the differences in the simulated and calculated O_3 range from -8.6% to -5.5% in Atlanta,

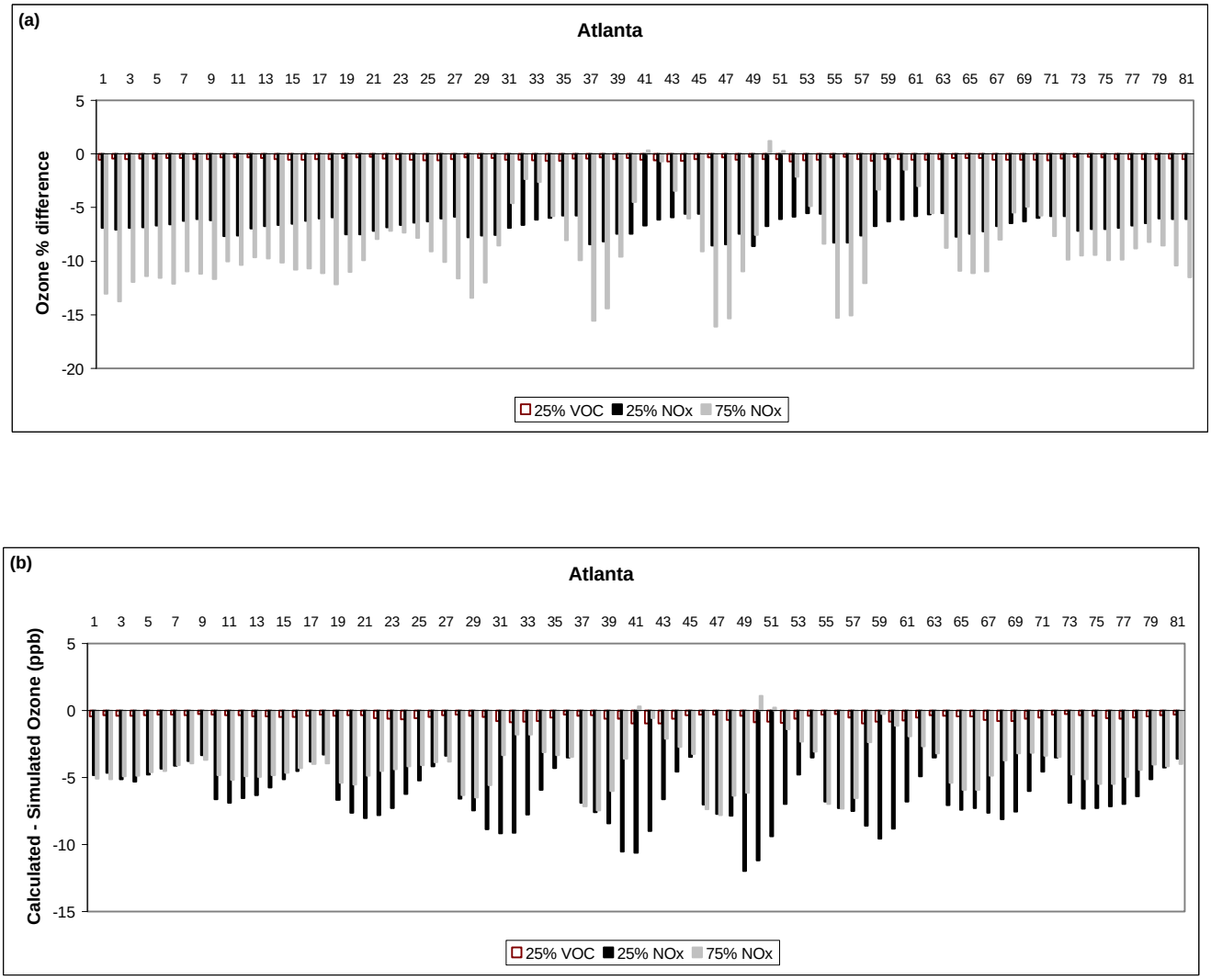

Figure 6-69. (a) The percent differences and (b) absolute differences in the calculated O_3 concentrations using the O_3 concentrations and source contributions predicted from OSAT base run B1 and the simulated O_3 concentrations from OSAT sensitivity runs S1, S4, and S7 in all 81 fine grid cells in Atlanta at 3 p.m. on July 15, 1995. Labels on the x-axis correspond to fine grid cell indices for each receptor starting from the NW corner and proceeding row-wise.

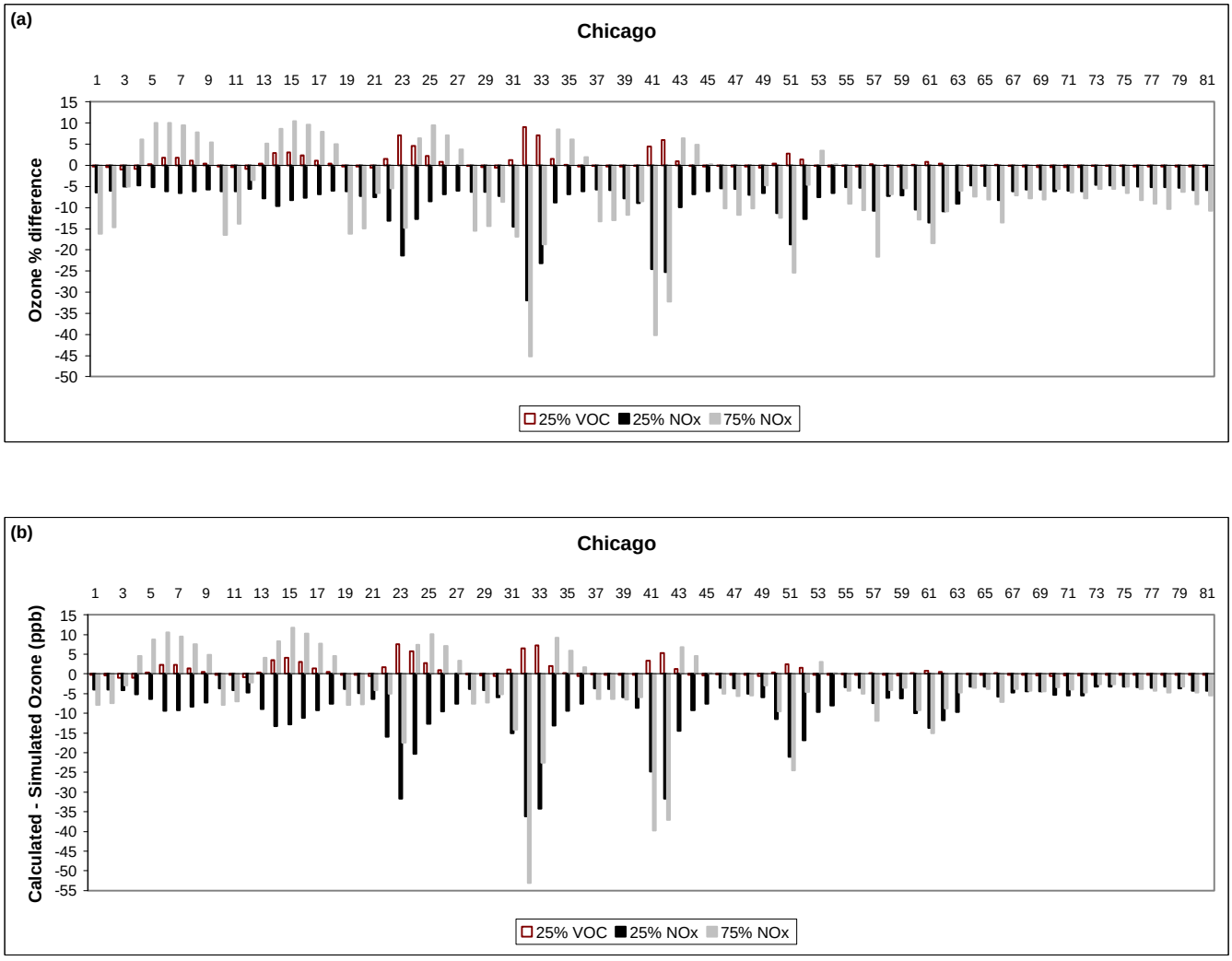

Figure 6-70. (a) The percent differences and (b) absolute differences in the calculated O_3 concentrations using the O_3 concentrations and source contributions predicted from OSAT base run B1 and the simulated O_3 concentrations from OSAT sensitivity runs S1, S4, and S7 in all 81 fine grid cells in Chicago at 3 p.m. on July 15, 1995. Labels on the x-axis correspond to fine grid cell indices for each receptor starting from the NW corner and proceeding row-wise.

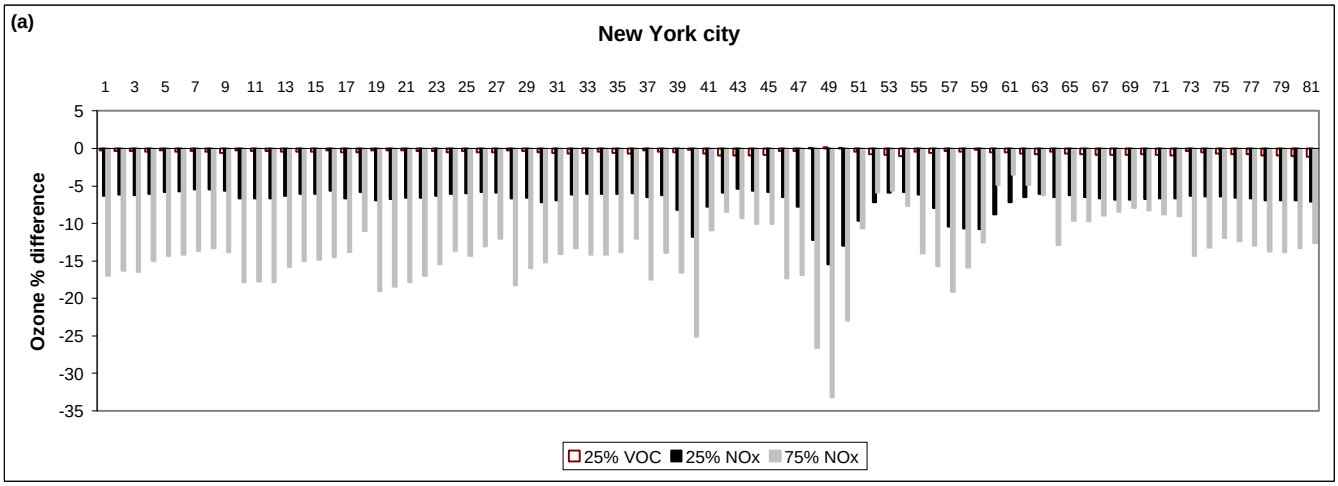

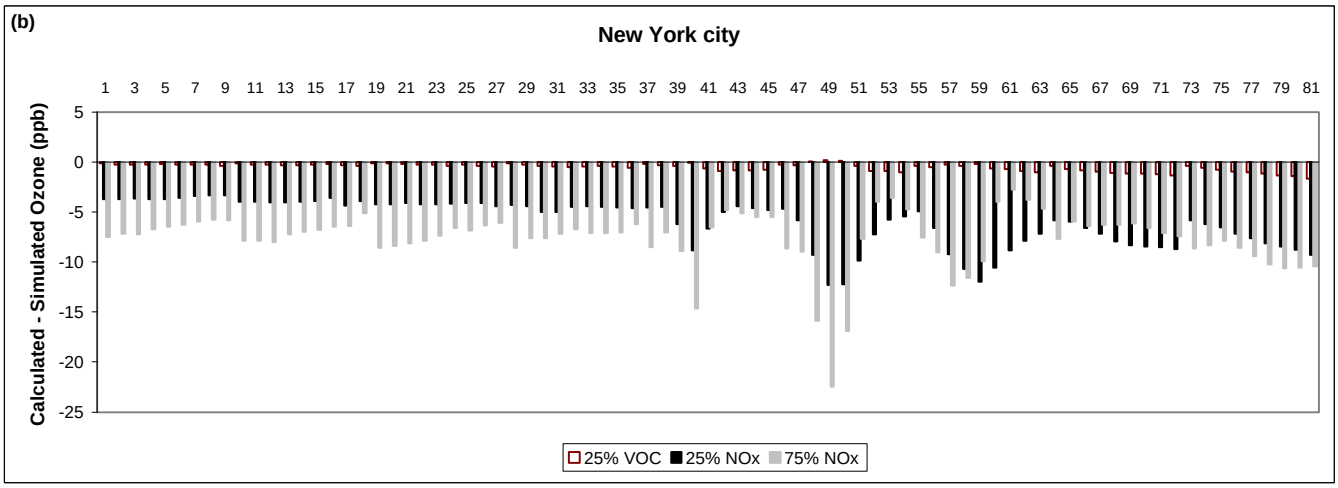

Figure 6-71. (a) The percent differences and (b) absolute differences in the calculated O_3 concentrations using the O_3 concentrations and source contributions predicted from OSAT base run B1 and the simulated O_3 concentrations from OSAT sensitivity runs S1, S4, and S7 in all 81 fine grid cells in New York City at 3 p.m. on July 15, 1995. Labels on the x-axis correspond to fine grid cell indices for each receptor starting from the NW corner and proceeding row-wise.

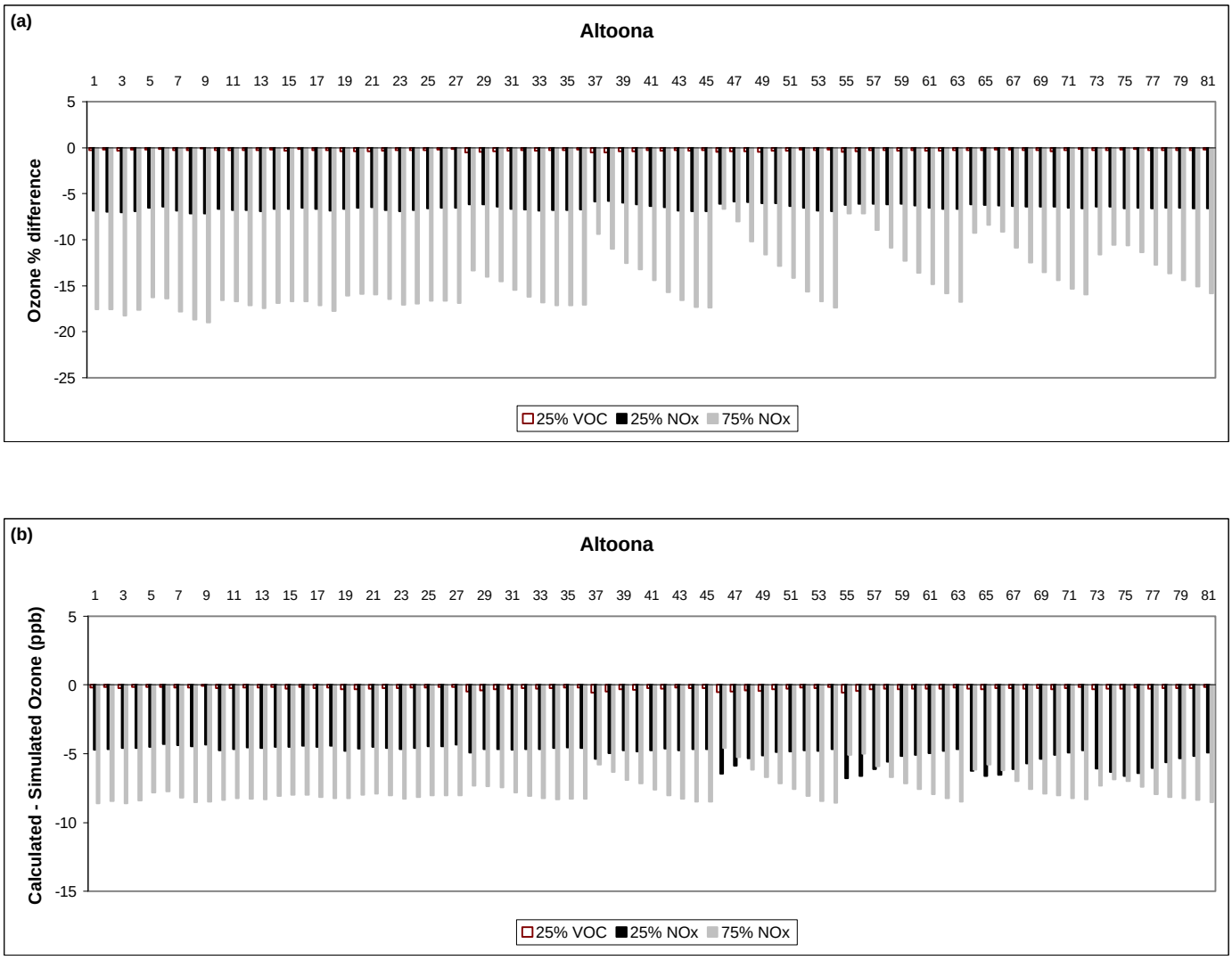

Figure 6-72. (a) The percent differences and (b) absolute differences in the calculated O_3 concentrations using the O_3 concentrations and source contributions predicted from OSAT base run B1 and the simulated O_3 concentrations from OSAT sensitivity runs S1, S4, and S7 in all 81 fine grid cells in Altoona at 3 p.m. on July 15, 1995. Labels on the x-axis correspond to fine grid cell indices for each receptor starting from the NW corner and proceeding row-wise.

-31.9% to -4.6% in Chicago, -15.5% to -5.4% in New York City, and -7.2% to -5.8% in Altoona, with an average difference of -6.7%, -8.4%, -7.0%, and -6.5%, respectively. The absolute differences in the calculated and simulated O_3 concentrations range from -12.0 to -3.3 ppb in Atlanta, -36.2 to -3.2 ppb in Chicago, -12.3 to -3.3 ppb in New York City, and -6.8 to -4.3 ppb in Altoona, with an average absolute difference of -6.5, -8.8, -6.0, and -5.0 ppb, respectively.

For a 75% reduction in anthropogenic NO_x emissions, the differences in the simulated and calculated O_3 range from -16.1% to 1.2% in Atlanta, -45.3% to 10.5% in Chicago, -33.2% to -3.5% in New York City, and -19.0% to -6.7% in Altoona, with an average difference of -8.7%, -6.6%, -13.7%, and -14.5%, respectively. The absolute differences in the calculated and simulated O_3 concentrations range from -7.8 to 1.1 ppb in Atlanta, -53.1 to 11.7 ppb in Chicago, -22.4 to -2.8 ppb in New York City, and -8.6 to -4.6 ppb in Altoona, with an average absolute difference of -4.2, -4.1, -7.7, and -7.6 ppb, respectively.

The magnitudes of the percent and absolute differences in the calculated and the simulated O_3 concentrations indicate that applying linear scaling to the OSAT results is reasonably accurate for a case with a 25% reduction in anthropogenic VOC emissions, but less accurate for cases with a 25% or 75% reduction in anthropogenic NO_x emissions.

6.3.2 Consistency in Predicting NO_x- vs. VOC-sensitivity under Different Emission Reduction Scenarios

Tables 6-45 to 6-47 show the predicted NO_x- vs. VOC-sensitivity of O_3 formation at the hour of peak O_3 concentration on July 11-15 in the four receptor regions predicted by DDM and OSAT for a 25% reduction in anthropogenic VOC emissions, a 25% reduction in anthropogenic NO_x emissions, and a 75% reduction in anthropogenic NO_x emissions, respectively. Those results were obtained by averaging the O_3 sensitivities/contributions for the 81 fine grid cells at the peak O_3 hour for the whole receptor predicted by DDM sensitivity runs S2, S5, and S8 and OSAT sensitivity runs S1, S4, and S7. For a 25% anthropogenic VOC or NO_x emission reduction scenario, both DDM and OSAT predict a NO_x-limited O_3 chemistry in Atlanta and Altoona for all five

Table 6-45. NO_x- vs. VOC-limited O_3 concentration at four receptors predicted by DDM and OSAT under 25% anthropogenic VOC emission reduction scenario.

Date	Receptor	DDM Prediction				OSAT Prediction			
		Sensitivities of O_3		O_3 concentration [1]		Contributions to O_3		O_3 Concentration	
		NO_x	VOC	NO_x-limited, %	VOC-limited, %	NO_x	VOC	NO_x-limited, %	VOC-limited, %
950711	Atlanta	4.9E-02	1.4E-02	78.3	21.7	8.6E-02	1.5E-02	85.2	14.8
	Chicago	-1.7E-02	2.3E-02	0.0	100.0	2.3E-02	2.4E-02	49.0	51.0
	New York	1.4E-03	2.8E-02	4.6	95.4	3.5E-02	2.7E-02	56.1	43.9
	Altoona	1.2E-02	1.2E-02	50.6	49.4	3.2E-02	2.3E-02	58.3	41.7
950712	Atlanta	3.9E-02	1.3E-02	75.2	24.8	7.0E-02	1.2E-02	85.7	14.3
	Chicago	8.3E-03	2.8E-02	23.0	77.0	4.7E-02	2.3E-02	67.1	32.9
	New York	5.2E-05	2.9E-02	0.2	99.8	3.5E-02	2.6E-02	57.4	42.6
	Altoona	1.3E-02	8.9E-03	59.5	40.5	2.7E-02	1.8E-02	60.6	39.4
950713	Atlanta	3.5E-02	1.1E-02	76.5	23.5	6.3E-02	1.1E-02	85.7	14.3
	Chicago	1.9E-02	2.5E-02	42.4	57.6	7.3E-02	2.3E-02	75.7	24.3
	New York	2.5E-02	2.7E-02	48.8	51.2	6.0E-02	3.1E-02	65.7	34.3
	Altoona	2.7E-02	1.4E-02	65.1	34.9	4.9E-02	2.0E-02	71.5	28.5
950714	Atlanta	3.5E-02	1.1E-02	76.1	23.9	5.9E-02	1.3E-02	81.5	18.5
	Chicago	8.3E-03	2.4E-02	25.4	74.6	6.1E-02	2.5E-02	70.7	29.3
	New York	2.3E-02	3.9E-02	37.6	62.4	6.5E-02	3.7E-02	63.5	36.5
	Altoona	3.4E-02	2.4E-02	59.1	40.9	7.1E-02	2.1E-02	77.4	22.6
950715	Atlanta	5.2E-02	1.4E-02	78.7	21.3	9.0E-02	1.7E-02	84.3	15.7
	Chicago	9.3E-04	3.9E-02	2.4	97.6	5.8E-02	3.2E-02	64.1	35.9
	New York	2.1E-02	3.4E-02	38.0	62.0	6.7E-02	3.1E-02	68.8	31.2
	Altoona	2.5E-02	2.2E-02	53.5	46.5	6.1E-02	2.2E-02	73.0	27.0

1. The O_3 concentration is considered as 100% VOC-limited if the sensitivity of O_3 to NO_x emissions is negative, and vice versa.

Table 6-46. NO_x- vs. VOC-limited O_3 concentration at four receptors predicted by DDM and OSAT under 25% anthropogenic NO_x emission reduction scenario.

Date	Receptor	DDM Prediction				OSAT Prediction			
		Sensitivities of O_3		O_3 concentration [1]		Contributions to O_3		O_3 Concentration	
		NO_x	VOC	NO_x-limited, %	VOC-limited, %	NO_x	VOC	NO_x-limited, %	VOC-limited, %
950711	Atlanta	4.7E-02	5.6E-03	89.5	10.5	7.8E-02	9.9E-03	88.8	11.2
	Chicago	-8.5E-03	2.5E-02	0.0	100.0	2.6E-02	2.6E-02	50.4	49.6
	New York	1.2E-02	2.2E-02	35.2	64.8	3.9E-02	2.4E-02	61.8	38.2
	Altoona	1.6E-02	9.0E-03	64.7	35.3	3.3E-02	1.8E-02	64.2	35.8
950712	Atlanta	3.9E-02	6.0E-03	86.6	13.4	6.3E-02	8.0E-03	88.6	11.4
	Chicago	1.5E-02	2.4E-02	38.3	61.7	4.9E-02	2.1E-02	70.0	30.0
	New York	1.0E-02	2.3E-02	30.4	69.6	3.9E-02	2.4E-02	61.8	38.2
	Altoona	1.6E-02	5.8E-03	72.9	27.1	2.8E-02	1.4E-02	67.2	32.8
950713	Atlanta	3.4E-02	5.5E-03	86.1	13.9	5.7E-02	7.4E-03	88.5	11.5
	Chicago	2.6E-02	2.0E-02	57.2	42.8	7.2E-02	2.0E-02	77.9	22.1
	New York	3.2E-02	1.8E-02	64.2	35.8	6.1E-02	2.4E-02	71.7	28.3
	Altoona	2.7E-02	1.0E-02	72.4	27.6	4.7E-02	1.4E-02	76.5	23.5
950714	Atlanta	3.5E-02	5.3E-03	87.0	13.0	5.4E-02	9.3E-03	85.2	14.8
	Chicago	1.9E-02	2.0E-02	48.8	51.2	6.1E-02	2.4E-02	72.0	28.0
	New York	2.9E-02	3.1E-02	48.6	51.4	6.4E-02	3.4E-02	65.3	34.7
	Altoona	3.4E-02	1.9E-02	64.8	35.2	6.8E-02	1.5E-02	82.2	17.8
950715	Atlanta	5.1E-02	4.8E-03	91.4	8.6	8.2E-02	1.1E-02	87.7	12.3
	Chicago	2.0E-02	2.8E-02	41.5	58.5	6.2E-02	2.9E-02	67.8	32.2
	New York	3.0E-02	2.2E-02	57.9	42.1	6.9E-02	2.4E-02	74.5	25.5
	Altoona	2.8E-02	1.6E-02	63.5	36.5	6.0E-02	1.6E-02	78.8	21.2

1. The O_3 concentration is considered as 100% VOC-limited if the sensitivity of O_3 to NO_x emissions is negative, and vice versa.

Table 6-47. NO_x- vs. VOC-limited O_3 concentration at four receptors predicted by DDM and OSAT under 75% anthropogenic NO_x emission reduction scenario.

Date	Receptor	DDM Prediction				OSAT Prediction			
		Sensitivities of O_3		O_3 concentration [1]		Contributions to O_3		O_3 Concentration	
		NO_x	VOC	NO_x-limited, %	VOC-limited, %	NO_x	VOC	NO_x-limited, %	VOC-limited, %
950711	Atlanta	3.4E-02	-7.9E-03	100	0.0	4.5E-02	1.9E-03	95.9	4.1
	Chicago	1.7E-02	7.3E-03	69.9	30.1	3.1E-02	1.4E-02	69.2	30.8
	New York	2.3E-02	2.4E-03	90.6	9.4	3.4E-02	8.3E-03	80.3	19.7
	Altoona	1.4E-02	5.9E-03	70.9	29.1	2.7E-02	9.4E-03	74.2	25.8
950712	Atlanta	2.8E-02	-5.0E-03	100	0.0	3.6E-02	1.6E-03	95.9	4.1
	Chicago	2.5E-02	8.1E-03	75.6	24.4	4.4E-02	1.1E-02	80.6	19.4
	New York	2.3E-02	3.0E-03	88.3	11.7	3.4E-02	8.4E-03	80.0	20.0
	Altoona	1.4E-02	-6.9E-05	100	0.0	2.1E-02	4.1E-03	83.6	16.4
950713	Atlanta	2.6E-02	-4.6E-03	100	0.0	3.4E-02	1.5E-03	95.8	4.2
	Chicago	3.6E-02	1.9E-03	94.8	5.2	5.9E-02	7.3E-03	89.0	11.0
	New York	2.6E-02	7.4E-03	77.9	22.1	4.4E-02	1.2E-02	77.9	22.1
	Altoona	2.2E-02	1.5E-03	93.5	6.5	3.4E-02	4.1E-03	89.1	10.9
950714	Atlanta	2.4E-02	-2.8E-03	100	0.0	3.1E-02	2.0E-03	94.0	6.0
	Chicago	3.3E-02	8.0E-04	97.7	2.3	5.3E-02	8.5E-03	86.2	13.8
	New York	3.8E-02	-1.2E-03	100	0.0	5.2E-02	8.7E-03	85.7	14.3
	Altoona	3.0E-02	3.8E-03	88.8	11.2	5.1E-02	3.7E-03	93.2	6.8
950715	Atlanta	3.6E-02	-8.6E-03	100	0.0	4.8E-02	2.0E-03	95.9	4.1
	Chicago	3.3E-02	5.6E-03	85.4	14.6	5.7E-02	9.0E-03	86.3	13.7
	New York	3.2E-02	3.5E-03	90.2	9.8	5.5E-02	7.6E-03	87.8	12.2
	Altoona	2.5E-02	4.9E-03	83.4	16.6	4.7E-02	4.2E-03	91.8	8.2

1. The O_3 concentration is considered as 100% VOC-limited if the sensitivity of O_3 to NO_x emissions is negative, and vice versa.

days, but their predictions in Chicago and New York City are quite different. While the VOC-limited fractions predicted by DDM and OSAT are similar (< 10.5%) in Atlanta, they are quite different (up to 20%) in Altoona. For a 25% anthropogenic VOC emission reduction scenario, DDM predicts a VOC-limited O_3 chemistry for all five days, with 58-100% of the O_3 concentration under VOC-limited conditions in Chicago, whereas OSAT predicts that the O_3 chemistry is VOC-limited on July 11 only and NO_x-limited on July 12-15, with only 24-51% of the O_3 concentration formed under VOC-limited conditions. In New York City, DDM predicts a VOC-limited O_3 chemistry for all days, with 51-99.8% of the O_3 concentration under VOC-limited conditions, whereas OSAT predicts that a NO_x-limited O_3 chemistry for all five days, with only 31-44% of the O_3 concentration formed under VOC-limited conditions. In Altoona, the predicted VOC-limited fractions are 35-49% by DDM and 23-42% by OSAT. For a 25% anthropogenic NO_x emission reduction scenario, DDM predicts a VOC-limited O_3 chemistry for all five days except July 13, with 43-100% of the O_3 concentration under VOC-limited conditions in Chicago, whereas OSAT predicts that the O_3 chemistry is NO_x-limited for all five days, with only 22-50% of the O_3 concentration formed under VOC-limited conditions. In New York City, DDM predicts a VOC-limited O_3 chemistry on July 11, 12, and 14 and a NO_x-limited O_3 chemistry on July13 and 15, with 36-70% of the O_3 concentration under VOC-limited conditions. On the other hand, OSAT predicts a NO_x-limited O_3 chemistry for all five days, with only 25.5-38% of the O_3 concentration formed under VOC-limited conditions. In Altoona, the predicted VOC-limited fractions are 27-36.5% by DDM and 18-36% by OSAT. As discussed in Section 6.1.2, the large discrepancies in predicting NO_x- vs. VOC-limited fraction of the O_3 formation in Chicago, New York City, and Altoona are due to the fact that OSAT does not account for the titration/inhibition effect of NO_x on O_3 chemistry.

For a 75% anthropogenic NO_x emission reduction scenario, both DDM and OSAT predict a NO_x-limited O_3 chemistry for all the four receptors for all five days. The percent differences in the NO_x-limited O_3 fractions range from 4% to 6% in Atlanta, 0.7% to 11.5% in Chicago, 0%-14% in New York City, and 3% to 16% in Altoona. This confirms our early observation that the DDM and OSAT predictions of NO_x- vs. VOC-

sensitivity of O_3 chemistry are in closer agreement under NO_x-limited conditions than under VOC-limited conditions.

Table 6-48 shows the average total amount of $P(O_x)$ summed for each day up to 16:00 EST for the four receptor regions predicted by PA for a 75% reduction in anthropogenic NO_x emissions (PA sensitivity run S9). The NO_x-sensitive or VOC-sensitive or equally-sensitive percentages of the O_x production are also shown. The totals were calculated for all grid cells in each of the receptor regions and for layers 1 to 4. As shown in Table 6-48, all three tools predicted a NO_x-sensitive O_3 chemistry for all the four receptors for all the five days. Those results are consistent with those of DDM and OSAT as shown in Table 6-47. The NO_x-sensitive fractions predicted by the tools are similar for Atlanta but quite different for the other receptors. As discussed in Section 6.1.2.2, the differences between DDM and OSAT predictions are due to the fact that the NO_x or VOC inhibition was accounted for by DDM but not by OSAT. The differences between PA and DDM/OSAT predictions are due to the fact that the time history of air parcels was accounted by DDM/OSAT but not by PA.

Figures 6-73 to 6-75 show the O_x productions in VOC- and NO_x-sensitive regimes predicted by PA under a 75% NO_x emission reduction scenario (i.e., PA sensitivity run S9) in Atlanta, Chicago, and New York City, respectively. Those figures can be compared to Figures 6-10 To 6-12 in section 6.1.2.3 to indicate whether there was a regime change for the O_x production when the anthropogenic NO_x emissions were reduced by 75%. In Atlanta, all grid cells except for some grid cells in the central subarea are in the NO_x-limited regime under the 2007 base case emission scenario. Those VOC-limited grid cells were changed to be NO_x-limited under a 75% NO_x emission reduction scenario. Similar changes occurred in Chicago and New York City between the base case and the S9 sensitivity runs for most VOC-limited grid cells, but some VOC-limited grid cells in the central subareas in Chicago and New York City remained unchanged. In the next section, we will use Chicago as an example to demonstrate how the chemical signatures were changed when the O_3 chemistry regime changed from VOC-limited to NO_x-limited.

Table 6-48. O_x production sensitivity to precursors at four receptors predicted by PA under 75% anthropogenic NO_x emission reduction scenario. The sensitivity was determined using the ratio of $P(H_2O_2)/P(HNO_3)$.

Date	Receptor	PA Prediction						
		O_x concentration, ppb/day				Percentage in O_x concentration		
		NO_x-sensitive	Equally sensitive	VOC-sensitive	Total concentration	NO_x-sensitive, %	Equally sensitive	VOC-sensitive, %
950711	Atlanta	95	1	2	98	96.9	1.0	2.0
	Chicago	61	11	19	91	67.0	12.1	20.9
	New York	45	9	12	66	68.2	13.6	18.2
	Altoona	42	2	2	46	91.3	4.3	4.3
950712	Atlanta	85	1	2	88	96.6	1.1	2.3
	Chicago	78	11	17	106	73.6	10.4	16.0
	New York	54	6	13	73	74.0	8.2	17.8
	Altoona	34	1	0	35	97.1	2.9	0.0
950713	Atlanta	79	1	2	82	96.3	1.2	2.4
	Chicago	133	8	13	154	86.4	5.2	8.4
	New York	86	8	11	105	81.9	7.6	10.5
	Altoona	48	0.3	0.4	48.7	98.6	0.6	0.8
950714	Atlanta	82	2	4	88	93.2	2.3	4.5
	Chicago	165	9	11	185	89.2	4.9	5.9
	New York	133	9	12	154	86.4	5.8	7.8
	Altoona	69	0.1	0	69.1	99.9	0.1	0.0
950715	Atlanta	93	2	3	98	94.9	2.0	3.1
	Chicago	123	9	13	145	84.8	6.2	9.0
	New York	130	3	6	139	93.5	2.2	4.3
	Altoona	64	0.3	0.1	64.4	99.4	0.5	0.2

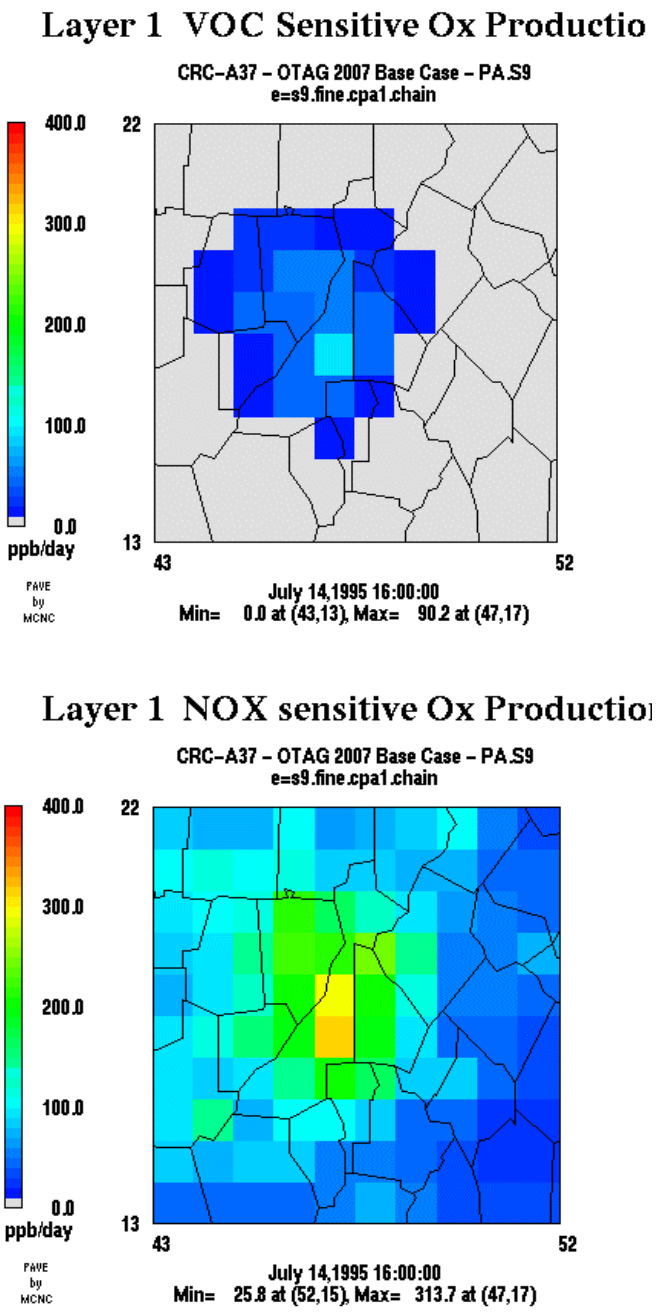

Figure 6-73. The receptor average O_x production in VOC-sensitive (top) and NO_x-sensitive (bottom) regimes for layers 1 to 4 in Atlanta on July 14 (a total O_x production up to 16:00 EST) under 75% anthropogenic NO_x emission reduction scenario (PA sensitivity run S9). The VOC-sensitive plot includes O_x produced for equally-sensitive conditions.

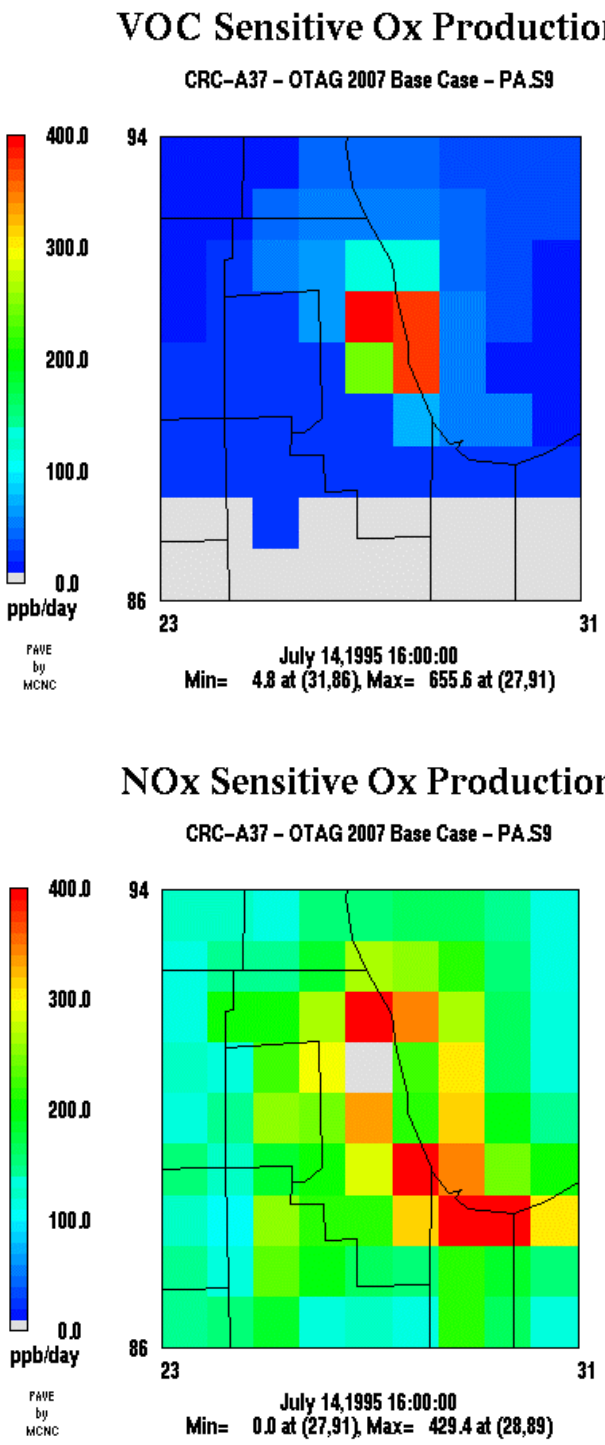

Figure 6-74. The receptor average O_x production in VOC-sensitive (top) and NO_x-sensitive (bottom) regimes for layers 1 to 4 in Chicago on July 14 (a total O_x production up to 16:00 EST) under 75% anthropogenic NO_x emission reduction scenario (PA sensitivity run S9). The VOC-sensitive plot includes O_x produced for equally-sensitive conditions.

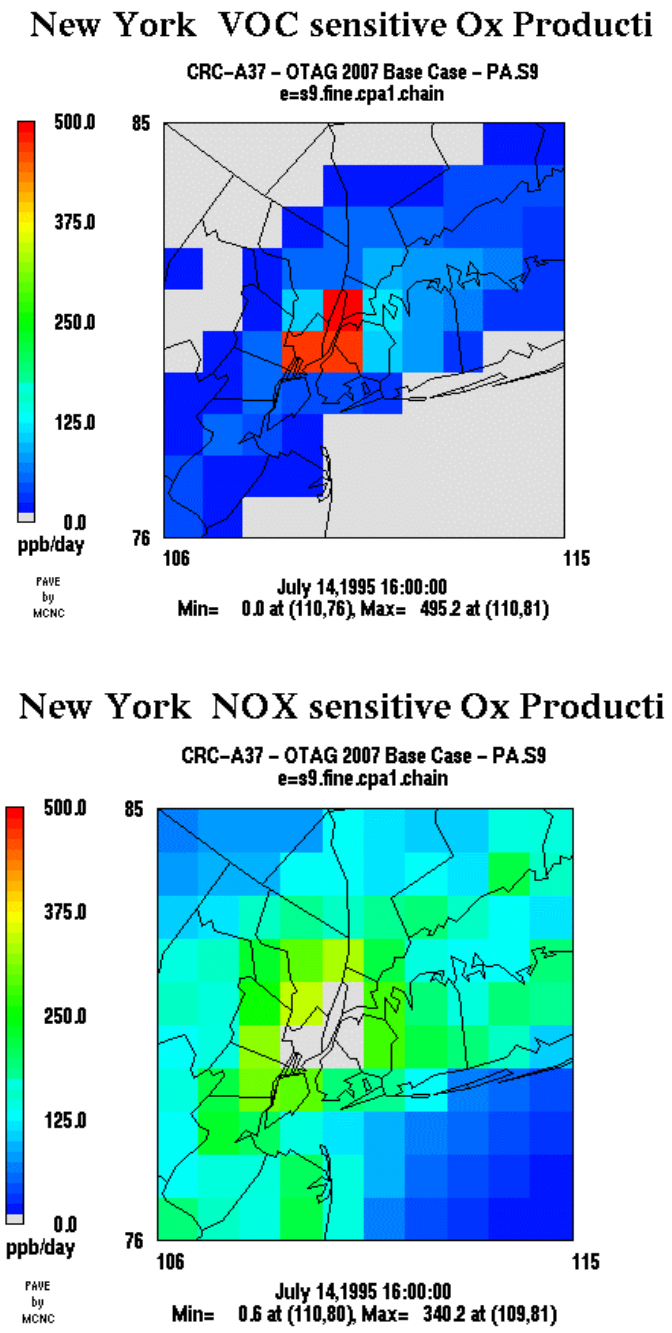

Figure 6-75. The receptor average O_x production in VOC-sensitive (top) and NO_x-sensitive (bottom) regimes for layers 1 to 4 in New York City on July 14 (a total O_x production up to 16:00 EST) under 75% anthropogenic NO_x emission reduction scenario (PA sensitivity run S9). The VOC-sensitive plot includes O_x produced for equally-sensitive conditions.

6.3.3 Changes in Chemical Signatures in the Four Receptors under a 75% Reduction in Anthropogenic NO_x Emissions

As shown in section 6.3.2, DDM predicted that the O_3 chemistry changed from VOC-limited to NO_x-limited for all five days in Chicago and for four days in New York City for a 75% anthropogenic NO_x emission reduction scenario. In addition, there are large differences in the NO_x-limited percentages predicted by the base emission and the 75% emission reduction scenarios in Atlanta and Altoona. A detailed analysis of CPA outputs can provide useful information to understand the chemistry that caused those changes and differences in the four receptor regions. Table 6-49 summarizes the CPA outputs for the EPA 2007 base emission (i.e., PA run B4) and 75% NO_x emissions reduction scenarios (i.e., PA run S9) for the four receptors on July 14 when high O_3 conditions occurred throughout the model domain. The CPA output for 81 fine-grid cells was totaled and averaged for each of the four receptor regions. Table 6-49 also shows the percent differences for each CPA parameter between the PA runs B4 and S9. A detailed analysis of the CPA outputs in the four receptor regions is provided below.

The first row of Table 6-49 show total O_x production. It's interesting to note that total photochemical reactivity, as measured by O_x production, was greatest for Chicago and New York with approximately 250 ppb of O_x production. By contrast, there was 178 ppb of O_x production in the Atlanta region and 136 ppb of O_x production in the Altoona region. The relatively small difference between Atlanta and Altoona reflects the averaging over the 81 fine-grid cells included in each receptor region. Differences for the peak cells in each receptor region would be larger (see Figures 6-10 to 6-13 for B4 run and Figures 6-73 to 6-75 for S9 run). In the 2007 base case for Atlanta and Altoona, most of the O_x was produced in NO_x sensitive conditions, while for New York City and Chicago, approximately half of the O_x was produced in regimes that were either VOC-sensitive or equally-sensitive to VOC and NO_x. Therefore, as one would expect, the reductions in O_x production for the 75% NO_x control are largest in Atlanta and Altoona (51% and 49% in total O_x production, respectively). The reductions in total O_x production are smaller in Chicago and New York City (27% and 38%, respectively). For

Table 6-49. Process analysis outputs at four receptors on July 14 under the EPA 2007 base emission scenario (PA base run B4) and the 75% anthropogenic NO_x emission reduction scenario (PA sensitivity run S9).

Row	PA Outputs	Atlanta			Chicago			New York City			Altoona		
		B4	S9	S9-B4, %	B4	S9	S9-B4, %	B4	S9	S9-B4, %	B4	S9	S9-B4, %
1	Total OxProd	178.5	87.76	-50.8	254.71	185.32	-27.2	249.47	155.13	-37.8	136.23	69.24	-49.2
2	O_xP_VOC	30	3.82	-87.3	96.55	10.85	-88.8	90.45	12.47	-86.2	9.02	0	-100.0
3	O_xP_equal	17.41	2.08	-88.1	36.95	9.01	-75.6	27.31	9.34	-65.8	8.3	0.12	-98.6
4	O_xP_NOx	131.08	81.86	-37.5	121.2	165.46	36.5	131.71	133.31	1.2	118.91	69.13	-41.9
5	O_xLoss	23.67	13.86	-41.4	29.27	20.51	-29.9	32.37	21.65	-33.1	28.78	18.95	-34.2
6	newOH_O^1D	18.03	9.76	-45.9	25.59	16.98	-33.6	26.43	16.56	-37.3	20.93	12.97	-38.0
7	newOHother	1.43	1.2	-16.1	1.31	0.77	-41.2	1.45	1.19	-17.9	1.86	1.66	-10.8
8	nwHO_2_HCHO	12.82	11.02	-14.0	14.51	17.83	22.9	15.23	15.83	3.9	11.66	11.13	-4.5
9	newHO_2tot	19.21	16.04	-16.5	19.48	25.56	31.2	21.57	23.42	8.6	16.96	16.09	-5.1
10	newRO_2tot	4.3	3.61	-16.0	4.98	6.38	28.1	5.51	5.32	-3.4	5.17	5.05	-2.3
11	nHOx_isop	3.93	3.01	-23.4	0.92	1.95	112.0	2.22	3.3	48.6	4.69	4.17	-11.1
12	OHwCO_CH_4	12.64	5.03	-60.2	27.39	14.87	-45.7	26.89	14.42	-46.4	11.24	4.64	-58.7
13	ISOPwOH	35.27	23.95	-32.1	15.07	15.68	4.0	25.18	21.97	-12.7	37.25	25.63	-31.2
14	OH+VOC	54.64	26.35	-51.8	94.16	77.55	-17.6	86.7	59.91	-30.9	39.08	20.07	-48.6
15	OHw_all_HC	102.55	55.33	-46.0	136.62	108.1	-20.9	138.77	96.3	-30.6	87.57	50.34	-42.5
16	OHpropmisc	2.15	0.75	-65.1	7.18	3.73	-48.1	3.29	1.79	-45.6	1.59	0.8	-49.7
17	HO_2TotProd	117.78	69.22	-41.2	157.35	131.34	-16.5	156.55	115.6	-26.2	102.32	66.25	-35.3
18	RO_2TotProd	24.78	13.83	-44.2	35.62	35.11	-1.4	34.21	26.31	-23.1	19.36	12.75	-34.1
19	HO_2_to_NO_2	83.71	38.69	-53.8	131.27	85.98	-34.5	126.97	73.39	-42.2	61.05	28.11	-54.0
20	HO_2_to_OH	93.02	46.21	-50.3	140.61	98.94	-29.6	135.95	84.2	-38.1	71.66	37.32	-47.9
21	RO_2_to_NO_2	90.93	47.1	-48.2	118.68	96.43	-18.7	117.46	78.77	-32.9	71.83	39.49	-45.0
22	OH_reacted	116.95	59.92	-48.8	172.16	120.21	-30.2	169.03	105.83	-37.4	98.64	54.65	-44.6
23	OHterm	12.25	3.83	-68.7	28.36	8.37	-70.5	26.98	7.74	-71.3	9.49	3.51	-63.0
24	HO_2term	25.84	24.16	-6.5	17.62	34.4	95.2	21.47	32.99	53.7	31.92	30.38	-4.8
25	RO_2term	4.89	2.62	-46.4	5.38	6.92	28.6	6.52	5.77	-11.5	3.52	1.89	-46.3
26	HCHOp_isop	26.45	18.48	-30.1	11.89	14.2	19.4	19.54	17.91	-8.3	28.48	20.33	-28.6
27	HCHOp_Tot	54.33	34.82	-35.9	53.42	50.76	-5.0	57.21	45.99	-19.6	49.22	34.16	-30.6
28	HNO_3_$OHNO_2$	6.9	0.81	-88.3	21.77	3.88	-82.2	20.18	3.21	-84.1	4.41	0.5	-88.7
29	HNO_3_NO_3HC	0.3	0.1	-66.7	1.42	0.94	-33.8	1.43	0.59	-58.7	0.27	0.06	-77.8

Table 6-49. (continued).

Row	PA Outputs	Atlanta			Chicago			New York City			Altoona		
		B4	S9	S9-B4, %	B4	S9	S9-B4, %	B4	S9	S9-B4, %	B4	S9	S9-B4, %
30	HNO_3_N_2O_5	0.64	0.02	-96.9	7.64	2.05	-73.2	5.59	0.45	-91.9	1.57	0.07	-95.5
31	HNO_3reacte	0.08	0.01	-87.5	0.28	0.04	-85.7	0.33	0.03	-90.9	0.18	0.01	-94.4
32	PANprodNet	4.32	2.19	-49.3	4.4	5.93	34.8	5.69	4.99	-12.3	3	1.42	-52.7
33	PANlossNet	0.87	0.6	-31.0	1.41	0.54	-61.7	1.12	0.37	-67.0	1.25	1.31	4.8
34	RNO_3_prod	5.54	2.53	-54.3	5.67	3.86	-31.9	6.53	4.62	-29.2	4.24	2.27	-46.5
35	OH Chain Length	2.7	2.0	-28.1	3.4	2.4	-27.8	3.1	2.3	-26.0	2.2	1.5	-30.4
36	$P(O_x)/P(NO_z)$	9.24	14.66	58.6	5.75	10.25	78.3	5.72	9.92	73.4	8.91	16.76	88.1
37	%HO_2 Propagation	71%	56%		83%	65%		81%	63%		60%	42%	
38	%OH Propagation	90%	94%		84%	93%		84%	93%		90%	94%	
39	Prop Product	64%	52%		70%	61%		68%	59%		54%	40%	

all four receptor regions, the O_x production in the NO_x control case occurred almost primarily under NO_x-sensitive conditions.

Radical initiation is the key chemical process that limits O_3 formation for VOC-sensitive conditions. The major sources of radical initiation are reaction of O^1D with H_2O (row 6), photolysis of HO_2 (row 8), and total photolysis of carbonyls including HCHO (row 9). The change in radical initiation from O^1D is closely related to the change in O_3 concentration and this is an important feedback effect in O_3 photochemistry. Row 6 shows reduction of 34% to 46% in OH initiation for the receptor regions.

The responses to the 75% NO_x reduction differed, however, in the initiation of radicals from carbonyls (shown in rows 8 and 9). There were reductions in the carbonyl initiation for Atlanta and Altoona and increases in Chicago and New York. Precursors of HO_2 radical initiation include VOC emissions and the oxidation products of VOC. The total mass of VOC is unchanged in the NO_x control simulation, but the amount of VOC oxidized can either increase or decrease in response to the NO_x control. Rows 12 to 15 show the change in the various organic species reacted in each receptor region; there were larger percent decreases in VOC reacted for Atlanta and Altoona than in Chicago and New York City. The NO_x reduction also affected the OH concentration which in turn affected the competition between photolysis and OH attack on the carbonyl species. The change in OH concentration can be approximately inferred from the change in the amount of CO and CH_4 reacted, where these are shown in row 12. There were large reduction in OH concentration so that a larger fraction of the carbonyls photolyzed. The net result of these processes was an increase in HO_2 initiation from carbonyls in Chicago and New York City.

Even with the increase in HO_2 initiation in Chicago and New York City, the large reduction in OH initiation from O^1D (row 6) and the reduction in the OH chain length (row 35) contributed to less total production of OH (row 22) in all four receptor regions for the 75% NO_x reduction case.

The results in rows 2 and 4 of Table 6-49 show that, on average, O_x production is mostly NO_x-limited (i.e., NO_x-sensitive) in each of the receptor regions for the 2007 base case. The only exception is Chicago which is, on average, borderline between NO_x-sensitive and VOC-sensitive. As discussed above, there is considerable heterogeneity

among the grid cells within each receptor region, so it would be incorrect to conclude that NO_x controls would be more effective than VOC controls. Nonetheless, it is interesting to consider the O_x production efficiency per NO_x converted to NO_z for each of the receptor regions. To the extent that the individual grid cells are NO_x-limited, the $P(O_x)/P(NO_z)$ will determine the amount of O_x produced. The change in this ratio from the base case to the NO_x control case is also a useful feedback effect in the photochemical system that makes O_3 unresponsive to precursor reduction. For example, increasing values of $P(O_x)/P(NO_z)$ in the control case tend to "buffer" the system by allowing more O_3 to be produced with a smaller mass of NO_x emissions. This is one of the key feedback effects that contribute to the "piston effect". The values of $P(O_x)/P(NO_z)$ are shown in row 36 in Table 6-49. For Atlanta, this ratio increased from 9.2 in the base case to 14.7 ppb/ppb in the 75% NO_x control case. For Altoona, it increased from 8.9 to 16.8 ppb/ppb. For both New York City and Chicago, it increased from 5.7 to about 10 ppb/ppb. Thus, in terms of the average chemistry over the entire receptor region, New York City and Chicago in the 75% NO_x control case were quite similar to that of Atlanta and Altoona in the base case.

Rows 28 through 34 provide detailed information on the NO_y budget. It is especially noteworthy that there were large reductions in HNO_3 production by each of the main pathways in the 75% NO_x control case compared to the base case. In the control case, production of PAN was the largest sink for NO_x. Except for Chicago, production of organic nitrates was a large sink for NO_x than was the production of HNO_3. The large reduction in HNO_3 production in the control case is largely responsible for the higher $P(O_x)/P(NO_z)$ in the control cases. The PAN and RNO_3 also act as a reservoir of reactive NO_x that can be transported for 100s of km, so this will continue to contribute to regional O_3 production in the control case. That is, the NO_x controls were effective for reducing O_3 production near the source region, but they may provide less benefit for reducing O_3 production in the rural regions where transported NO_x is of great importance.

The contribution of biogenic and anthropogenic VOC for each receptor region can be estimated qualitatively by comparing the amount of CO, CH_4, VOC, and isoprene reacted in each receptor region. These values are listed in rows 12 through 15. Note that these values are calculated on a ppbV basis, and that if the VOC were weighted by their

carbon number, the contribution of isoprene would be even larger than shown in row 13. Moreover, some of the VOC reacted is actually HCHO, ALD2, and other organic intermediate species that were produced from isoprene decay. Therefore, row 13 is an underestimate of the contribution of isoprene in these grid cells. Also note that Table 6-49 shows only the direct contribution of isoprene that reacted in the receptor region. Reactions of isoprene upwind of the receptor also contribute to transported O_3 and HCHO. Because these species are radical precursors, O_3 production in the receptor regions for Chicago and New York City should be especially sensitive to any changes in upwind isoprene emissions, which is consistent with the DDM and OSAT results. However, the PA outputs cannot be used to quantify the contribution of isoprene to HCHO and O_3 production, so the PA results provide only an approximate indication of the importance of isoprene.

While the comparison of the average PA values for the receptor region may provide some insight into the overall chemistry, it is important to consider the heterogeneity within each receptor region. As shown previously in Section 6.3.2 (Figures 6-74 and 6-75), there is one grid cell in Chicago and three grid cells in New York that continue to be exclusively VOC-sensitive even in the 75% NO_x control case. Therefore, targeted VOC controls could be very useful for reducing O_x and O_3 production in those areas.

6.4 Computational/Implementation Requirements

The CPU and memories required for the CAMx simulations with each probing tool are shown in Table 6-50. Overall, those simulations needed 38 CPU days, with 28 of these devoted to the DDM simulations. Careful design of the DDM simulations was the dominant factor in managing the overall CPU requirement for the project. A simulation of CAMx with no probing tool took 4.4 CPU hours. The simulations with CAMx and PA increased the memory by 67% but only increased the computational burden by 23%. This is because that the PA runs in this project provided process rates and reaction rates for only 4 receptor regions plus gridded outputs of Chemical Process Analysis calculated within CAMx (e.g., OH Chain length, etc.) for the entire domain. The outputs of process

Table 6-50. The memory and computational requirements for CAMx base model and CAMx with a probing tool.

Model	Run Name	Memory (Mbytes)	Run Time [1] (CPU hour)
CAMx		85	4.4
CAMx+PA	B4,S3,S6,S9	142	5.4
CAMx+OSAT	B1,S1,S4,S7	324	29.3
CAMx+APCA	B5	324	30.9
CAMx+GOAT	B6	178	15.4
CAMx+DDM	B7	284	24.8
CAMx+DDM	B3	541	53.7
CAMx+DDM[2]	B2N,B2V S2N,S2V S5N,S5V S8N,S8V	820	79.8

1. The runtimes are for a 1 GHz Pentium III workstation running Linux and using the Portland Group FORTRAN77 compiler.
2. Note that B2, S2, S5 and S8 were split to separate VOC and NO_x runs.

rates and reaction rates for a larger region may take more memory and CPU time. The simulations with CAMx and OSAT or its associated techniques such as APCA and GOAT increased the memory and the CPU time by a factor of 3.8 and 3.5-7.0, respectively. The simulations with CAMx and DDM imposed the largest computational burden among all those tools, increasing the memory and the CPU time by a factor of 3.3-9.6 and 5.6-18.1, respectively. A single DDM run to provide sensitivity information that is comparable to that from OSAT would require much more memory (about 2.3 GigaBytes) than the OSAT run and is not practical. Therefore, the DDM base run B2 and sensitivity runs S2, S5, and S8 were split to separate VOC and NOx runs (i.e., B2N, B2V, S2N, S2V, S5N, S5V, S8N, and S8V) to keep the run size under 1 Gbyte RAM.

There are several challenges in developing and implementing the three probing tools. For PA, the challenges include:

- Extracting accurate process rate information for every process that affects model-predicted concentrations. The PA algorithms must be accurate to provide a useful description of how the model-predictions were obtained;
- Implementing the PA algorithms without changing the results from the underlying model;
- Providing a flexible interface for specifying what PA information to extract so that the volume of output is not overwhelming.

For OSAT, the challenges include:

- Accounting not only for the presence of O_3 precursors from a given source region at a given receptor location, but also accurately estimating the cumulative contribution to O_3 production of those precursors while they were en-route to the receptor;
- Ensuring compatibility with the underlying air quality model formulation so that derived source-receptor relationships will be consistent with model response to emission changes;

- Providing sufficient spatial and temporal resolution while managing, within practical constraints, the computer resources required to run the software tool.

For DDM, the challenges include:

- Ensuring accuracy by using consistent numerical methods and the same time steps for the concentrations and sensitivities;
- Optimizing the efficiency of the sensitivity coefficient calculations without compromising accuracy;
- Proving a flexible User Interface that allows calculation of sensitivities to all sources and precursors;
- Ensuring that the DDM algorithms have minimal impact on computer resource requirements (memory and CPU time) when the DDM is not being used.

Note that each probing tool cannot be used at the same time as the other two probing tools because PA, OSAT, and DDM share internal data structures to minimize the total memory resources required by CAMx. The O_3 sensitivities to VOC and NO_x calculated from DDM are used in OSAT to allocate O_3 production into VOC- and NO_x-sensitive portions. Those sensitivities are calculated within the OSAT option and no separate DDM run is needed.

7. REFERENCES

Blanchard, C.L., F.W. Lurmann, P.M. Roth, H.E. Jeffries, M. Korc, 1999, The use of ambient data to corroborate analyses of ozone control strategies, *Atmos. Environ.* **33**, 369-381.

Bowman, F.M. and J.H. Seinfeld, 1994a, Ozone productivity of atmospheric organics, *J. Geophys. Res.*, **99**, 5309-5324.

Bowman, F.M. and J.H. Seinfeld, 1994b, Fundamental basis of incremental reactivities of organic in ozone formation in VOC/NO_x mixtures, *Atmos. Environ.* **28**, 3359-3368.

Carmichael, G.R., A. Sandu and F.A. Potra, 1997, Sensitivity analysis for atmospheric chemistry models via automatic differentiation, *Atmos. Environ.* **31**, 475-489.

Carter, W.P.L, 1994, Calculation of Reactivity Scales Using an Updated Carbon Bond IV Mechanism, Auto/Oil Air Quality Improvement Research Program Report available from the Coordinating Research Council, 3650 Mansell Road, Alpharetta, GA, 30022.

Carter, W.P.L. and Atkinson R.J., 1987, An experimental study of incremental hydrocarbon reactivity. *Environ. Sci. Technol.*, **21**, 670-679.

Carter, W.P. L. and R. J. Atkinson, 1989, Computer modeling study of incremental hydrocarbon reactivity, Environ. Sci. Technol., **23**, 864-880.

Chang, T.Y., D.P. Chock, B.I. Nance, and S.L. Winkler, 1997, A photochemical extent parameter to aid ozone air quality management, *Atmos. Environ.* **31**, 2787-2794.

Chameides, W.L., R.D. Saylor, and E.B. Cowling, 1997, Ozone pollution in the rural united states and the new NAAQS, *Science*, **276**, 916.

Chen, L., H. Rabitz, D.B. Considine, C.H. Jackman and J.A. Shorter, 1997, Chemical reaction rate sensitivity and uncertainty in a two-dimensional middle atmospheric ozone model, *J. Geophys. Res.*, **102**, 16201-16214.

Cho, S.Y., G.R. Carmichael and H. Rabitz, 1987, Sensitivity analysis of the atmospheric reaction – diffusion equation, *Atmos. Environ.*, **12**, 2589-2598.

Costanza, V. and Seinfeld J.H., 1981, Stochastic sensitivity analysis in chemical kinetics, *J. Chem. Phys.*, **74**, 3852-3858.

Cowling, E.B., W.L. Chameides, C.S. Kiang, F.C. Fehsenfeld and J.F. Meagher, 1998, Introduction to special section: Southern Oxidants study Nashville/Middle Tennessee Ozone Study, *J. Geophys. Res.*, **103**, 22209-22212.

Demilrap, M. and Rabitz H., 1981, Chemical kinetic functional sensitivity analysis: Elementary sensitivities, *J. Chem. Phys*, **74**, 3362-3375.

Deuel, H.P., R.E. Looker and P.D. Guthrie, 1997, A UAM-V based threaded source-apportionment modeling system, *90th Annual Meeting of the Air & Waste Management Association*, June 8-13, 1997, Toronto, Ontario, Canada.

Dougherty, E. P., J.T. Kwang, and H. Rabitz, 1979, Further developments and applications of the Green's function method of sensitivity analysis in chemical kinetics, *J. Chem. Phys.*, **71**, 1794-1808.

Dunker, A.M., 1980, The response of an atmospheric reaction-transport model to changes in input functions, *Atmos. Environ.*, **14**, 671-679.

Dunker, A.M., 1981, Efficient calculations of sensitivity coefficients for complex atmospheric models, *Atmos. Environ*. **15**, 1155-1161.

Dunker, A.M., 1984, The decoupled direct method for calculating sensitivity coefficients in chemical kinetics, *J. Chem. Phys.*, **81**, 2385.

Dunker, A., G. Yarwood, J.P. Ortmann and G.M. Wilson, 2002a, The decoupled direct method for sensitivity analysis in a three-dimensional air quality model – Implementation, accuracy and efficiency, *Environ. Sci. Technol.*, **36**, 2965-2976.

Dunker, A., G. Yarwood, J.P. Ortmann and G.M. Wilson, 2002b, A comparison of source apportionment and source sensitivity of ozone in a three-dimensional air quality model, *Environ. Sci. Technol.*, **36**, 2953-2964.

Dunker, A.M., 2001, Private communication.

Dunker, A.M., 2002, Private communication.

EPA, 1998, Atmospheric Observations: Helping Build the Scientific Basis for Decisions related to Airborne Particulate Matter, Report of the PM Measurements Research Workshop, Chapel Hill, North Carolina, 22-23, July 1998.

ENVIRON, 2000, User's Guide - Comprehensive Air Quality Model with Extensions (CAMx) Version 3.00, ENVIRON International Corporation, 101 Rowland Way, Suite 220, Navato, CA 94945.

Falls, A.H., McRae, G.J., Seinfeld, J.H., 1979, Sensitivity and uncertainty of reaction mechanisms for photochemical air pollution, *Intern. J. Chem. Kinet*., **11**, 1137-1162.

Finlayson-Pitts, B.J. and J.N. Pitts, 2000, Chemistry of the Upper and Lower Atmosphere, Academic Press, San Diego, CA.

Gao, D., W.R. Stockwell and J.B. Milford, 1995, First-order sensitivity and uncertainty analysis for a regional-scale gas-phase chemical kinetic mechanism, *J. Geophys. Res.*, **100**, 23153.

Gautier, O., R.W. Carr and C. Seigneur, 1985, Variational sensitivity analysis of a photochemical smog mechanism, *Int. J. Chem. Kinet.*, **17**, 1347-1364.

Jang, J.C.C., Jeffries, H.E. and G.S. Tonnesen, 1995, Sensitivity of ozone to model grid resolution -- II: Detailed process analysis for ozone chemistry. *Atmospheric Environment* **29**, 3101-3114.

Koda, M., A.H. Dogru, and J.H. Seinfeld, 1979, Sensitivity analysis of partial differential equations with application to reaction and diffusion processes, *J. Comput. Phys*., **30**, 259-282.

Kumar, N. and F.W. Lurmann, 1997, Peer review of ENVIRON's ozone source apportionment technology and CAMx air quality model, Report STI-996203-1732-RFR, prepared for the Ohio Environmental Protection Agency Division of Air Pollution Control, Columbus, Ohio.

Lange, O, 1942, Theoretical derivation of elasticities of demand and supply; the direct method, *Econometrica*, **10**, 193-241.

Leone, J.A. and J.H. Seinfeld, 1984, Analysis of the characteristics of complex chemical reaction mechanisms, *Environ. Sci. Technol*., **18**, 280-287.

Lohman, K., P. Pai, C. Seigneur, L. Levin, 2000, Sensitivity analysis of mercury human exposure, *Sci. Total Environ.*, **259**, 3-11.

Marchuk, G.I., 1975: Formulation of the theory of perturbations for complicated models, *Appl. Math. & Optimization*, **2**, 1-33.

Milford, J.B., D. Gao, A.G. Russell and G.J. McRae, 1992: Use of sensitivity analysis to compare chemical mechanisms for air quality modeling, *Environ. Sci. Technol.*, **26**, 1179-1189.

Milford, J.B., D. Gao, S. Sillman, P. Blossey, and A.G. Russell, 1994, Total reactive nitrogen (NO_y) as an indicator of the sensitivity of ozone to reductions in hydrocarbon and NO_x emissions, *J. Geophys. Res.*, **99**, 3533-3542.

Milford, J.B., A.G. Russell, and G.J. McRae, 1989, A new approach to photochemical pollution control: Implications of spatial patterns in pollutant responses to reductions in nitrogen oxides and reactive organic gas emissions, *Environ. Sci. Technol.*, **23**, 1290-1301.

Morris, R.E., G. Wilson, E. Tai, and J. Hower, 1998, Assessment of the Contribution of Industrial and Other Source Sectors to Ozone Exceedances in the Eastern U.S. Final Report. Prepared for Ohio Environmental Protection Agency.

OTAG Technical Supporting Document, http://www.epa.gov.ttn/rto/otag/finalrpt, 1998.

Pun, B.K., 1998, Treatment of Uncertainties in Atmospheric Chemical Systems: A Combined Modeling and Experimental Approach, Ph.D. Thesis, Massachusetts Institute of Technology, Cambridge, MA.

Pun, B.K., C. Seigneur, and W. White, 2001a, Weekday/weekend ozone differences and emissions of NO_x and VOC in three cities, presented at the 11th CRC On-Road Vehicle Emissions Worshop, San Diego, CA, March 26-28.

Pun, B. K., S.-Y. Wu, and C. Seigneur, 2001b, Contribution of biogenic emissions to the formation of ozone and particulate matter: modeling studies in the Nashville, Tennessee and Northeast, final report for CRC project A-23, Document Number CP051-01-1, September.

Pun, B. K., S.-Y. Wu, and C. Seigneur, 2001c, Contribution of biogenic emissions to the formation of ozone and particulate matter in the Eastern United States, Environ. Sci. and Technology (submitted), December.

Samuelson, P.A. 1983, Foundations of economic analysis. Cambridge, Massachusetts: Harvard University Press, 1983.

Seigneur, C., B. Pun, and Y. Zhang, 1999, Review of methods for source apportionment in three-dimensional air quality models for particulate matter, EPRI, TR-112070, EPRI, Palo Alto, CA.

Seigneur, C., B. Pun, and P. Pai, 2000, Guidance for the performance evaluation of three-dimensional air quality modeling systems for particulate matter and visibility, *J. Air Waste Manage. Assoc*., **50**, 588-599.

Seigneur, C., T.W. Tesche, P.M. Roth and L.E. Reid, 1981, Sensitivity of a complex urban air quality model to input data, *J. Appl. Met*., **20**, 1020-1040.

Shorter, J.A. and H.A. Rabitz, 1997, Risk analysis by the Guided Monte Carlo technique, *J. Statist. Comput. Simul.*, **57**, 321-336.

Sillman, S., J.A. Logan, and S. C. Wofsy, 1990, The sensitivity of ozone to nitrogen oxides and hydrocarbons in regional ozone episodes, *J. Geophys. Res*., **95**, 1837-1851.

Sillman, S., 1995, The use of NO_y, H_2O_2, and HNO_3 as indicators for ozone-NO_x-hydrocarbon sensitivity in urban locations, *J. Geophys. Res*., **100**, 14175-14188.

Sillman, S., D. He, C. Cardelino, and R.E. Imhoff, 1997, The use of photochemical indicators to evaluate ozone-NO_x-hydrocarbon sensitivity: Case studies from Atlanta, New York, and Los Angeles, *J. Air Waste Manag. Assoc.*, **47**, 1030-1040.

Tatang, M.A., W. Pan, R.G., Prinn and G.J. McRae, 1997, An efficient method for parametric uncertainty analysis of numerical geophysical models, *J. Geophy. Res*. **102**, 21925-21932.

Tilden, J.W. and J.H. Seinfeld, 1982, Sensitivity analysis of a mathematical model for photochemical air pollution, *Atmos. Environ.*, **16**, 1357-1364.

Tonnesen, G.S., 1990, Integrated Reaction Rate Analysis of Ozone Production in a Photochemical Oxidant Model. Master of Science Thesis in Environmental Engineering, University of North Carolina, Chapel Hill, NC, December, 1990.

Tonnesen, G.S., 1995, Development and application of a process analysis method for photochemical oxidant models, Ph.D. Dissertation in Environmental Engineering, University of North Carolina, Chapel Hill, NC, May, 1995.

Tonnesen, G.S., 2001, Evaluation of the budgets of odd nitrogen compounds using Eulerian photochemical air quality models, Interim Report submitted to the American Chemistry Council, January.

Tonnesen, G.S. and R.L. Dennis, 2000a, Analysis of radical propagation efficiency to assess ozone sensitivity to hydrocarbons and NO_x 1. Local indicators of instantaneous odd oxygen production sensitivity, *J. Geophys. Res.*, **105**, 9213-9225.

Tonnesen, G.S. and R.L. Dennis, 2000b, Analysis of radical propagation efficiency to assess ozone sensitivity to hydrocarbons and NO_x 2. Long-lived species as indicators of ozone concentration sensitivity, *J. Geophys. Res.*, **105**, 9227-9241.

Tonnesen, G.S. and H.E. Jeffries, 1994. Inhibition of odd oxygen production in the Carbon Bond Four and the Generic Reaction Set mechanisms, *Atmos. Environ.*, **28**, 1339-1349.

Trainer, M., D.D. Parrish, M.P. Buhr, R.B. Norton, F.C. Fehsenfeld, K.G. Anlauf, J.W. Bottenheim, Y.Z. Tang, H.A. Wiebe, J.M. Roberts, R.L. Tanner, L. Newman, V.C. Bowersox, J.F. Meagher, K.J. Olszyna, M.O. Rodgers, T.Wang, H.Berresheim, K.L. Demerjian, and U.K. Roychowdhury, 1993, Correlation of ozone with NO_y in photochemically aged air, *J. Geophys. Res*., **98**, 2917-2925.

Uliasz, M., 1983, Application of the perturbation theory to the sensitivity analysis of an air pollution model, *Z. Meteor*., **33**, 355-362.

Vuilleumier, L., R.A. Harley and N.J. Brown, 1997, First- and second-order sensitivity analysis of a photochemically reactive system (a Green's function approach), *Environ. Sci. Technol*., **31**, 1206-1217.

Wang, Z. and H.E. Jeffries, 1999, Integrated Process Rate Analysis Method - Process Analysis - Components and Implementation, to be submitted to *J. Geophys. Res.*

Yang, Y.J., J.G. Wilkinson and A.G. Russell, 1997, Fast direct sensitivity analysis of multidimensional photochemical models, *Environ. Sci. Technol*., **31**, 2859-2868.

Yarwood, G., R.E. Morris, M. A. Yocke, H. Hogo, and T. Chico, 1996, Development of a Methodology for Source Apportionment of Ozone Concentration Estimates from a Photochemical Grid Model. Presented at the 89th AWMA Annual Meeting, Nashville TN, June 23-28 and Development of a Methodology to Assess Geographic and Temporal Ozone Control Strategies for the South Coast Air Basin. Prepared for South Coast Air Quality Management District, Diamond Bar, CA.

Yarwood, G. and R.E. Morris, 1997, Description of CAMx source attribution algorithms, Memorandum to the EPA Source Attribution Workshop Peer Review Panel.

Yarwood, G., G. Wilson, R.E. Morris and M.A. Yocke, 1997, User's Guide to the Ozone Tool: Ozone Source Apportionment Technology for UAM-IV, Report prepared for the South Coast Air Quality Management District, Diamond Bar, California.

Yarwood, G., Memorandum on the updated OSAT, ENVIRON, Novato, CA, Nov., 2001

Zhang, Y., C.H. Bischof, R.C. Easter, and P.-T. Wu, 1998, Sensitivity analysis of a mixed-phase chemical mechanism using Automatic differentiation, *J. Geophys. Res.*, **103**, 18953-18979.